

### EDITORIAL

The editors and publishers consider that the experimental section of the *Journal of Polymer Science*—Part B: Polymer Letters—has been quite successful because of the wide variety of interesting and timely communications which have been submitted and published during the past year. We are anxious to maintain and improve the quality of the communications and therefore have the following suggestions to the authors: Communications will be judged according to their scientific worth and timeliness and, if in the editors' opinion they do not reach a certain level of novelty and timeliness they will be automatically classified as a "Note" and published in the *Journal of Polymer Science Part A: General Papers*, as such. Communications for Polymer Letters should not exceed a word limit of 1000 words and should be written concisely with as much key experimental data as possible presented to prove the important conclusions. The editors have agreed to insist in this minimum in order to give ample opportunity for everyone to publish. These new procedures will go into effect immediately in the next forthcoming issues.

## A Poly(ethylene Oxide)-Mercuric Chloride Complex

AVROM A. BLUMBERG\* and SIDNEY S. POLLACK, *Mellon Institute, Pittsburgh, Pennsylvania*, and C. A. J. HOEVE, *National Bureau of Standards, Washington, D. C.*

### Synopsis

Oriented poly(ethylene oxide) fibers form a complex with mercuric chloride, with the empirical formula  $(\text{CH}_2\text{CH}_2\text{O})_n \cdot \text{HgCl}_2$ . Tentatively the unit cell of the complex is orthorhombic with dimensions 13.5, 17.1, and 11.6 Å. (*c*, the fiber axis). In spite of a major change in the unit cell, fiber orientation is maintained. The infrared spectrum of the complex is more detailed than that of the polymer alone, a fact consistent with a change from *trans* to *gauche* state of one O-C bond.

Complex formation between polymers and low molecular weight compounds has been observed in several cases. We wish to report here on a surprising observation: during complex formation of crystalline, oriented poly(ethylene oxide) the chain orientation is preserved although the packing of chains in the crystalline lattice is drastically changed.

Recently stable complexes of poly(ethylene oxide), P(EO), with urea and thiourea have been reported.<sup>1</sup> Dioxanate-metal halide compounds, especially between 1,4-dioxane and mercuric chloride are known.<sup>2,3</sup> Because 1,4-dioxane is the cyclic dimer of ethylene oxide, the existence of a complex of P(EO) and mercuric chloride was suspected.

High molecular weight polymer (Polyox WSR 301, Carbide and Carbon Chemicals Company) as a powder was pressed into pellets under vacuum, at 120°C. These were then forced through a die at the same temperature. The extruded ribbon was elongated, at 64°C., for one week. The fibers so formed were highly oriented as judged by x-ray diffraction patterns and polarized light examinations. After exposure to saturated dry ether solutions of mercuric chloride at room temperature for 45 days and drying in vacuum, the fibers were still highly oriented, despite large changes in unit cell dimensions as reported below.

Although P(EO) is flexible, the complex is rigid and brittle. Where the former is quite soluble in water, the latter is insoluble. However, the compound may be dissolved in an aqueous cyanide solution. There is no measurable difference in the viscosity of aqueous P(EO) solutions before and after complex formation, which indicates no measurable chain scission.

\* Present address: Department of Chemistry, De Paul University, 1036 W. Belden Ave., Chicago, Illinois 60614.

TABLE I  
Infrared Absorption of Films of Poly(ethylene Oxide) with and without Mercuric Chloride

Wave number, $\text{cm.}^{-1}$	
P(EO)	P(EO) on long exposure to mercuric chloride
	~815 sh
845 $\pm$ 1 m	832 $\pm$ 1 m
	856 $\pm$ 1 mw
	872 $\pm$ 1 mw
	890 $\pm$ 1 mw
	924 $\pm$ 1 m
937 $\pm$ 1 sh	
949 $\pm$ 2 sh	942 $\pm$ 1 m
964 $\pm$ 1 m	
1002 $\pm$ 1 sh	
	1014 $\pm$ 1 ms
1030 $\pm$ 1 sh	1029 $\pm$ 1 m, sh
	1046 $\pm$ 1 ms
1062 $\pm$ 3 m	
	1081 $\pm$ 1 s
1104 $\pm$ 1 s	1104 $\pm$ 1 s
1106 $\pm$ 1 s	
	1126 $\pm$ 1 sh
	1136 $\pm$ 1 sh
1151 $\pm$ 3 m	1154 $\pm$ 1 sh
1244 $\pm$ 2 mw	1243 $\pm$ 1 m
1264 $\pm$ 2 sh	1265 $\pm$ 1 w
1281 $\pm$ 3 m	1284 $\pm$ 1 vw
	1309 $\pm$ 2 mw
	1324 $\pm$ 2 w
1345 $\pm$ 3 m	1346 $\pm$ 2 mw
	1354 $\pm$ 2 w
1363 $\pm$ 3 w	
	1384 $\pm$ 3 vw
	1408 $\pm$ 3 vw
1417 $\pm$ 3 vw	
1422 $\pm$ 2 vw	
1434 $\pm$ 2 vw	
	1442 $\pm$ 3 m
1458 $\pm$ 2 sh	
	1466 $\pm$ 3 mw
1470 $\pm$ 2 m	
1742 $\pm$ 5 w	
2720 $\pm$ 8 sh	
2750 $\pm$ 8 sh	
	2880 $\pm$ 8 sh
2900 $\pm$ 14 ms	
	2930 $\pm$ 8 ms

The structure of crystalline P(EO) has been investigated by Walter and Reding,<sup>4</sup> Fraser and Kilb,<sup>5</sup> Miyazawa, Fukushima, and Ideguchi,<sup>6</sup> Richards and Hughes,<sup>7</sup> and us, with essentially the same results. The unit cell is

monoclinic, and contains 28 monomer units, in four helices each with two turns. The unit cell dimensions are  $a = 8.02$  Å,  $b = 13.4$  Å,  $c = 19.25$  Å (fiber axis),  $\beta = 126^\circ 52'$ . The calculated specific gravity is 1.23, whereas the measured density is approximately 1.20.

Tentatively the unit cell of the P(EO)-mercuric chloride complex is orthorhombic with dimensions  $a = 13.5$  Å,  $b = 17.1$  Å,  $c = 11.6$  Å (fiber axis). By chemical analysis the empirical formula is  $(\text{CH}_2\text{CH}_2\text{O})_4 \cdot \text{HgCl}_2$ . The specific gravity calculated based on 32 ethylene oxide and eight mercuric chloride units is 2.21; the measured value is in the range 2.08–2.12. The polymer also forms a complex with cadmium chloride. The diffraction pattern of this complex is isomorphous to that of P(EO)-mercuric chloride.

Films for infrared spectroscopy were prepared by coating glass slides with thin layers of dilute P(EO)-benzene solutions, drying, peeling the polymer from the glass, and exposing the films to mercuric chloride-ether solutions for 54 hr. The films were about  $15 \mu$  thick. Infrared spectra were obtained by using a Beckmann IR-4 spectrophotometer.

From the structure of crystalline P(EO) the rotation angles about the C—C and C—O bonds were in the *gauche* and *trans* states, respectively. The infrared spectrum of the polymer-salt compound has more detail than that of the polymer alone, (see Table I) suggesting that more rotational states are present in the former than in the latter. This increase in number is compatible with a change from *trans* to *gauche* state of one of the C—O bonds per unit of ethylene oxide. This suggestion is also compatible with a shortening of the unit cell along the *c*-axis. Further investigation of this complex is underway.

Support of this investigation by the Office of Naval Research is acknowledged with gratitude.

## References

1. Bailey, F. E., Jr., and H. G. France, *J. Polymer Sci.*, **49**, 397 (1961).
2. Laurent, P. A., and E. Arsenio, *Bull. Soc. Chim. France*, **1958**, 618.
3. Hendra, P. J., and D. B. Powell, *J. Chem. Soc.*, **1960**, 5105.
4. Walter, E. R., and F. Reding, paper presented at 133rd American Chemical Society Meeting, San Francisco, April 1958.
5. Price, F. P., and R. Killb, *J. Polymer Sci.*, **57**, 395 (1962).
6. Miyazawa, T., K. Fukushima, and Y. Ideguchi, *J. Chem. Phys.*, **37**, 2764 (1962).
7. Richards, J. R., Doctoral Dissertation, Chemistry Department, University of Pennsylvania, Philadelphia, Pa.

## Résumé

Des fibres orientées d'oxyde de polyéthylène forment un complexe avec le chlorure mercurique de formule empirique  $(\text{CH}_2\text{CH}_2\text{O})_4 \cdot \text{HgCl}_2$ . Expérimentalement on trouve que la cellule unitaire du complexe est orthorhombique et de dimensions 13.5, 17.1 et 11.6 Å (C, l'axe de la fibre). En dépit d'un grand changement dans la cellule unitaire, l'orientation de la fibre est maintenue. Le spectre infrarouge du complexe est plus détaillé que celui du polymère seul, fait en rapport avec le changement de la position *trans* à la position *gauche* d'une des liaisons O—C.

### Zusammenfassung

Orientierte Polyäthylenoxydfasern bilden mit Quecksilber(II)-chlorid einen Komplex mit der empirischen Formel  $(\text{CH}_2\text{CH}_2\text{O})_4 \cdot \text{HgCl}_2$ . Wie aus vorläufigen Untersuchungen hervorgeht, hat der Komplex eine orthorhombische Elementarzelle mit den Dimensionen 13,5, 17,1 und 11,6 Å (C ist die Faserachse). Trotz einer grösseren Veränderung der Elementarzelle bleibt die Faserorientierung erhalten. Das IR-Spektrum des Komplexes weist mehr Einzelheiten auf als dasjenige des Polymeren allein. Dies lässt sich durch einen Übergang einer O—C-Bindung von trans- in "gauche"-Stellung erklären.

Received May 15, 1963

## Kinetics of the $\gamma$ -Radiation-Induced Polymerization of Ethylene in Alkyl Chlorides

RICHARD H. WILEY, N. T. LIPSCOMB, and C. F. PARRISH,  
*Department of Chemistry, College of Arts and Sciences, University of Louisville,  
Louisville, Kentucky,* and J. E. GUILLET, *Tennessee Eastman Company,  
Kingsport, Tennessee*

### Synopsis

A study has been made of the kinetics and mechanism of the liquid-phase,  $\gamma$ -radiation-induced, alkyl chloride solution polymerization of ethylene. The  $\gamma$ -radiation was provided by a  $4.07 \times 10^5$  r/hr.  $\text{Co}^{60}$  source. The kinetics of these polymerizations were studied up to 10% conversion and over the temperature range 0 to  $-25^\circ\text{C}$ . Three solvents (*n*-propyl chloride, *iso*-propyl chloride, and *tert*-butyl chloride) were used with concentrations of ethylene ranging from 6.76 to 8.89 moles/l. Two different grades of ethylene were used: the first contained an upper limit of 1000 ppm of oxygen, the second 60 ppm. The ethylene containing only 60 ppm of oxygen was found to give a smaller induction period, and faster rate of polymerization than the ethylene containing 1000 ppm. Activation energies of 5.0 kcal./mole for the reaction in *n*-propyl chloride and 7.4 kcal./mole for the reaction in *tert*-butyl chloride were observed for the temperature range studied. These values were higher than the 4.4 kcal./mole obtained for the bulk polymerization of ethylene in this temperature range. The order of the reaction with respect to ethylene concentration in *n*-propyl chloride at  $0^\circ\text{C}$ . was found to be 1.41. Although the heterogeneity of the system is a complicating factor, this rate expression agrees well with the general scheme proposed for other heterogeneous polymerizations. Molecular weight information which shows an increase in molecular weight with increasing temperature leads to the conclusion that a termination step involving weakly reactive solvent radicals may be important.

Previous studies of the kinetics of the  $\gamma$ -radiation-induced polymerization of ethylene<sup>1-5</sup> have been made at temperatures from  $-40$  to  $237^\circ\text{C}$ . and usually in the gas phase. The rate expressions obtained in these investigations have been difficult to explain by a simple kinetic scheme. This investigation seeks to add to the present fund of knowledge by obtaining rate data for the polymerization of ethylene in alkyl chloride solutions over a temperature range of  $-25$  to  $0^\circ\text{C}$ . These solvents were selected because of the interesting radiation-induced isomerization reactions observed with *n*-propyl chloride.

A modification of the usual initiation step for a  $\gamma$ -radiation-induced free radical polymerization is necessary for the reaction in solution. Since the interaction of  $\gamma$ -rays with matter is proportional to the electron density of the media, the rate of formation of free radicals must include the solvent

TABLE I  
Primary Reactions of Ethylene Polymerization in Solution

Reaction	Equation	Rate expression
1a. Primary initiation	$M + \text{Radiation} \xrightarrow{k_{1a}} R\cdot$	$\frac{d[R\cdot]}{dt} = k_{1a}[I][M] + k_{1b}[I][S]$
1b. Primary initiation	$S + \text{Radiation} \xrightarrow{k_{1b}} R\cdot$	
2. Chain initiation	$M + R\cdot \xrightarrow{k_2} RM\cdot$	$-\frac{d[R\cdot]}{dt} = k_2[R\cdot][M]$
3. Chain propagation	$RM_n\cdot + M \xrightarrow{k_3} RM_{n+1}\cdot$	$-\frac{d[M]}{dt} = k_3[RM\cdot][M]$
4. Transfer to monomer	$RM_n\cdot + M \xrightarrow{k_4} RM_nH + M\cdot$	$-\frac{d[RM\cdot]}{dt} = k_4[RM\cdot][M]$
5. Transfer to solvent	$RM_n\cdot + S \xrightarrow{k_5} RM_nH + S\cdot$	$-\frac{d[RM\cdot]}{dt} = k_5[RM\cdot][S]$
6. Transfer to polymer	$RM_n\cdot + P \xrightarrow{k_6} RM_nH + P\cdot$	$-\frac{d[RM\cdot]}{dt} = k_6[RM\cdot][P]$
7. Mutual termination	$RM_n\cdot + RM_m\cdot \xrightarrow{k_7} RM_{n+m}R$ <p style="text-align: center;">or</p> $RM_{m-1}\cdot + CH=CH_2 \rightarrow RM_mH + \cdot$	$-\frac{d[RM\cdot]}{dt} = 2k_7[RM\cdot]^2$
8. Primary radical termination	$RM_n\cdot + R\cdot \xrightarrow{k_8} RM_nR$	$-\frac{d[RM\cdot]}{dt} = k_8[RM\cdot][R\cdot]$

concentration as well as the monomer concentration. The important steps in ethylene polymerization, incorporating this factor, are summarized (Table I).

The usual kinetic scheme for a free radical polymerization, assuming a steady state of free radicals and a mutual termination step (reaction 7, Table 1), leads to the following rate of polymerization.

$$-\frac{d[M]}{dt} = k_3 \left( \frac{k_{1a}}{k_{1b}} \right)^{1/2} I^{1/2} [M] \left( [M]^{1/2} + \frac{k_{1b}}{k_{1a}} [S] \right) = \frac{d[P]}{dt}$$

To obtain this expression it is also necessary to neglect the loss of monomer due to primary initiation (reaction 1) and transfer to monomer (reaction 4). This is acceptable in situations involving reasonably long polymer chains. This rate expression indicates that the rate dependence on the power of the monomer concentration will lie between 1 and 1.5, being governed by the ratio  $k_{1b}/k_{1a}$ .

In the case of high radiation intensities, termination may occur by interaction of primary radicals with the polymer radicals (reaction 8). This would be quite likely to occur in a heterogeneous media. The growing radicals may be occluded in solid particles and could be terminated only by primary radicals which are small enough to diffuse through the polymer to reach the active ends.<sup>6</sup> If the radicals are sufficiently buried they may remain untermiated, which would result in a pseudo first-order termination.<sup>7</sup> It has been shown that either of these mechanisms could increase the monomer concentration exponent to an upper limit of 2. Therefore, depending upon the contributions of these factors the monomer concentration exponent should fall between 1 and 2.

### Effect of Concentration

The rate of polymerization in alkyl chloride solutions is higher than the rate in bulk under identical conditions.<sup>8</sup> If changes in reactivity of the radicals are not significant, the different rates result from changes in the rates of initiation or termination steps. Several factors are involved here; they are: electron density of the solution, transfer to solvent, reactivity of solvent radicals, and homogeneity of the reaction.

Figure 1 shows the variation of the rate of polymerization of ethylene with respect to monomer concentration, and the rates obtained are listed in Table II. These data were subjected to regression analysis with the use of the equation:

$$\log (\text{rate}) = a + b \log [M]$$

where  $[M]$  is the monomer concentration. The analysis yielded a value for the exponent of the ethylene concentration of  $1.41 \pm 0.05$  which is within the limits predicted by the kinetic scheme.

TABLE II  
Rate of Polymerization of Ethylene in *n*-Propyl Chloride at 0°C.

Ethylene concn., moles/l. <sup>a</sup>	Rate, moles/l. hr.	Electron density (total)
6.76	2.24	0.392
7.99	2.88	0.354
8.50	2.99	0.335
8.79	3.19	0.325

<sup>a</sup> Ethylene contained an upper limit of 1000 ppm of oxygen.

An induction period of 1.5 hr. was noted for the polymerization in *n*-propyl chloride. The induction period remained essentially the same when isopropyl chloride and *tert*-butyl chloride were used. Ethylene containing less oxygen (60 ppm instead of 1000 ppm) gave an induction period of 0.9 hr. Oxygen has been shown to be an effective inhibitor in the gas phase polymerization as is consistent with this decreased induction period.



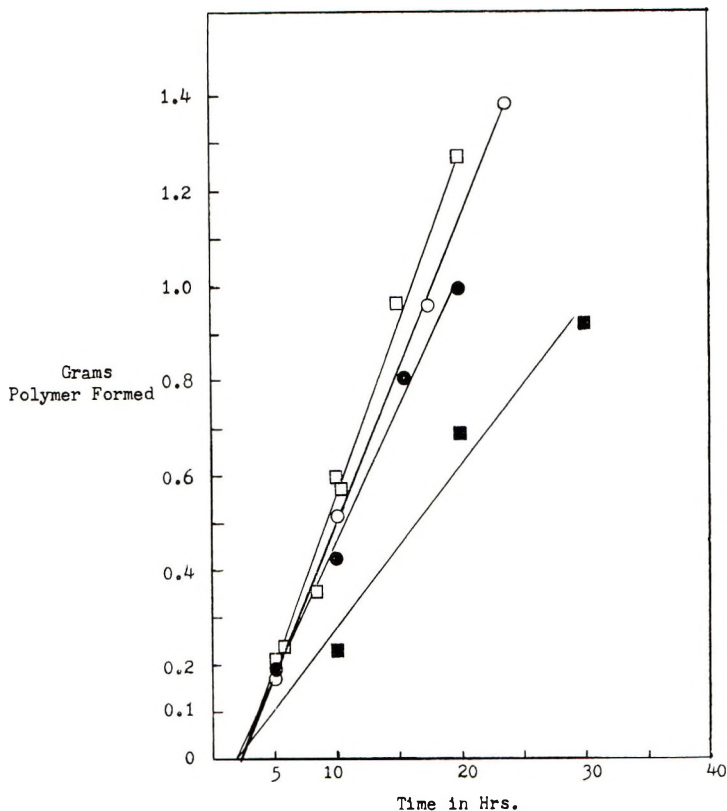


Fig. 1. Rate of polymerization of ethylene as a function of concentration at 0°C. in *n*-propyl chloride: (■) 8.79 moles/l.; (●) 8.5 moles/l.; (○) 7.99 moles/l.; (□) 6.76 moles/l.

### Effect of Solvent

Participation by the solvent in the polymerization process is established by the presence of 0.9 chlorine atoms per chain. This is equivalent to approximately one solvent molecule per chain and is consistent with a mechanism in which the solvent is active in the initiation or termination steps.

Variation of the rate of polymerization with respect to structure of the alkyl chloride is shown in Table III. There are three factors which may cause this change in rate. First, there is a change in the electron density of the irradiated solution. This means that there should be more or less primary radicals produced for a given volume of solution. Secondly, there is a change in the rate of transfer with the solvent, and finally, the solvent radicals may have different reactivities.

It would seem evident that the primary factor is the change in the electron density of the irradiated solution. Thus, *tert*-butyl chloride, having the highest electron density of the three, gives the highest rate. This is consistent with a change in the rate of initiation.

The variation of rate caused by transfer to solvent is usually negligible, and molecular weight data for the present series of polymers show that solvent transfer does not occur with great frequency. Thus, the molecular weight for polymers prepared in the three chlorides is within the range of 1100–2650. There would also be an effect on the rate caused by the relative reactivities of the different solvent primary radicals. The rate of

TABLE III  
Rates of Polymerization of Ethylene in Various Solvents

Solvent	Temp., °C.	Rate, moles/l. hr. × 10 <sup>2</sup>	Ethylene concn., moles/l.	Electron density	O <sub>2</sub> concn., ppm
<i>n</i> -PrCl	0	2.88	7.99	0.354	1000
<i>i</i> -PrCl	0	2.45	7.99	0.354	1000
<i>t</i> -BuCl	0	3.56	7.99	0.367	1000
<i>n</i> -PrCl	-25	1.37	9.01	0.390	1000
<i>t</i> -BuCl	-20	1.68	8.89	0.416	60
<i>n</i> -PrCl	0	3.17	7.99	0.354	60
<i>t</i> -BuCl	0	4.23	7.99	0.367	60

polymerization in *tert*-butyl chloride seems to be more rapid than can be accounted for on the basis of its increased electron density. This indicates that it may produce a more reactive radical or it may be less subject to transfer or termination by solvent radicals may be less rapid.

### Effect of Additives

Oxygen effects at different concentrations are of considerable interest. Oxygen has been demonstrated to interfere with the polymerization in small concentrations.<sup>9</sup> A series of reactions was carried out using ethylene having an oxygen content of 60 ppm (Table III). For *n*-propyl chloride and *tert*-butyl chloride the rates were, respectively, 3.17 moles/l. hr. and 4.23 moles/l. hr., and the induction period was cut to 0.9 hr. This compares to values of 2.88 moles/l. hr. and 3.56 moles/l. hr., and an induction period of 1.5 hr. for ethylene used previously (1000 ppm upper limit). This information indicates that oxygen not only inhibits ethylene polymerization but may act as a retarder as well and also that within the range of 60–1000 ppm there is unexpectedly only a 10–15% decrease.

Two other additives which have characteristic effects on free radical reactions were used in this study also. Iodine, when added to a run, produces an increase in the induction period proportional to the amount of iodine used. After this induction period the reaction proceeded at the same rate as without the additive. Diphenylamine showed an entirely different effect. There was no change in the induction period but a large decrease in the rate of polymerization. Both these effects have previously been found to be associated with free radical reactions.

### Activation Energy

Table III also shows the variation of the rate of polymerization with temperature. From the Arrhenius equation an activation energy for the reaction in *tert*-butyl chloride of 7.4 kcal./mole and for *n*-propyl chloride 5.0 kcal./mole may be obtained. This is somewhat higher than the value of 4.4 kcal./mole<sup>5</sup> reported for polymerization of liquid ethylene in bulk in the temperature range 0 to  $-40^{\circ}\text{C}$ . In the case of  $\gamma$ -ray initiation the activation energy is usually equated to the difference between the activation energies for propagation and termination, since the initiation step is assumed to require no activation energy. It seems unlikely that the presence of a solvent would decrease the activation energy for termination.<sup>10</sup> Therefore, it appears that the action of the solvent is to increase the activation energy of the propagation step.

### Molecular Weights

The kinetic chain length for a vinyl polymerization is usually considered to be given by the ratio of the rate of propagation to the rate of initiation.<sup>5</sup> Assumption of a steady state of radical concentration and a mutual termination step (reaction 7) establishes a direct relation between the chain length and the square root of the monomer concentration. It is necessary to assume for this relationship that no chain transfer occurs. In actual fact, the molecular weight of polyethylene has been considered to be controlled largely by chain transfer reactions<sup>11</sup> (reactions 4, 5, 6). Table IV shows the variation of the molecular weight with respect to concentration, dose, solvent, and temperature for the polymers obtained in this study.

TABLE IV  
Molecular Weight of Polyethylene

Solvent	Temp., $^{\circ}\text{C}$ .	Dose, rep $\times 10^{-6}$	Ethylene concn., moles/l. <sup>a</sup>	Molecular weight
<i>n</i> -PrCl	0	1.95	8.50	1860
<i>n</i> -PrCl	0	3.89	8.50	2356
<i>n</i> -PrCl	0	6.67	8.50	1952
<i>n</i> -PrCl	0	9.20	8.50	1596
<i>n</i> -PrCl	0	3.85	8.79	2299
<i>n</i> -PrCl	0	4.03	7.99	1521
<i>n</i> -PrCl	0	3.97	6.76	1178
<i>n</i> -PrCl	0	6.43	7.99	1860
<i>n</i> -PrCl	$-25$	5.97	8.89	1264
<i>i</i> -PrCl	0	5.62	7.99	1785
<i>t</i> -BuCl	0	5.39	7.99	2637

<sup>a</sup> Ethylene contained an upper limit of 1000 ppm oxygen.

The variation of molecular weight with total dose in *n*-propyl chloride is of interest. The molecular weight of the polymer quickly passes through a maximum then decreases as the total dose increases (Table IV). This

decrease is often a characteristic of radiation-induced polymerizations and is usually explained as polymer degradation. The initial increase is probably a post induction period effect in which impurities that reduce the molecular weight are being consumed.

The variation of the molecular weight with respect to concentration at approximately  $4 \times 10^6$  rep shows a much greater increase of molecular weight with increasing concentration than can be explained by a mutual termination mechanism. Over the concentration range studied the molecular weight seems to be roughly proportional to the concentration of ethylene to the third power. This deviation from the square root relationship indicates that the solvent does participate in the termination step in this system.

The relation between temperature of polymerization and the molecular weight depends on the difference in activation energies for the transfer and propagation reactions if termination of the growing chains is primarily by chain transfer. In most polymerizations the activation energy for chain transfer is greater than for propagation. This has been shown to be true for ethylene in bulk in the liquid state. This would result in a molecular weight decrease as the temperature is increased. In the present investigation the converse is true as seen in the data given in Table IV. Since a solvent transfer mechanism would involve a high frequency factor, a high molecular weight polymer could not be obtained if the activation energy for transfer was less than for propagation. This can be accounted for by postulating a termination of the growing chain by primary solvent radicals which do not readily initiate chains.

### Experimental

The irradiation facility used in these experiments is similar to that described previously,<sup>12</sup> and the dosimetry technique, using ferrous ion has likewise been described.<sup>13</sup> Two different grades of ethylene were used in these investigations. Both were obtained from the Tennessee Eastman Company. The first grade, which was used in most irradiations, was the same grade used in the polymerization of ethylene in the liquid phase<sup>5</sup> and had an upper limit oxygen content of 1000 ppm. The second grade containing 99.955% ethylene, 0.027% nitrogen, 0.012% methane, and 0.006% oxygen was used in the remaining determinations. A restudy of the bulk polymerization of ethylene using this second grade is now under way. The solvents were dried over calcium chloride and then fractionated through a 3-ft., insulated, helices-packed column.

The pressure chamber has been described previously,<sup>5</sup> and was slightly modified by the addition of a sample cell, which was a stainless steel vessel containing 25 ml. of solvent that snugly fitted the inside of the pressure chamber. The procedure for charging the vessel was as follows. The entire pressure system was charged with prepurified nitrogen to 300 psi and bled to the atmosphere. This was repeated five times. The valve between the radiation chamber and the measuring system was closed.

The measuring system was charged to the desired pressure of ethylene and allowed to come to thermal equilibrium. The coolant was pumped directly through the Dry Ice bath and the valve between the measuring system and irradiation chamber was opened. Ethylene was allowed to condense into the radiation chamber until the pressure of the system reached a predetermined value. The valve between the pressure system and the radiation chamber was then closed and the pump stopped. The heated was turned on and the cooling system was changed to circulate from the automatically controlled system. From the known volume of the measuring system and compressibility data the mass of ethylene was determined. Chlorine analyses (Micro Tech Laboratory) gave values of 0.8 and 1.0 for different samples of polymer prepared in *n*-propyl chloride having molecular weights of 1178 and 1596, respectively.

Each rate given in Table II and III was determined from the slope and intercept of the line obtained by a least squares analysis of from four to seven yield determinations at times of 5–33 hr. and the temperatures stated.

This research was supported in part by the Atomic Energy Commission under Contract No. AT-(40-1)-2055 between the Atomic Energy Commission and the University of Louisville. The authors wish to thank the Tennessee Eastman Company, and especially Dr. C. A. Glover who furnished the molecular weight data.

### References

1. Collinson, E., and A. J. Swallow, *Chem. Revs.*, **56**, 486 (1956).
2. Hayward, J. C., Jr., Doctoral Dissertation, Yale University, New Haven, Conn., 1955. Atomic Energy Commission Report NYO-3313, OTS, Dept. of Commerce, Washington 25, D. C.
3. Martin, J. J., and L. C. Anderson, Progress Report, Project 1943: 4-60P, Engineering Research Institute, University of Michigan, Ann Arbor, 1954; J. G. Lewis, J. J. Martin, and L. C. Anderson, *Chem. Eng. Progr.*, **50**, 249 (1954).
4. Laird, R. K., A. G. Morrell, and L. Seed, *Discussions Faraday Soc.*, No. **22**, 126 (1956).
5. Wiley, R. H., N. T. Lipscomb, F. J. Johnston, and J. E. Guillet, *J. Polymer Sci.*, **57**, 867 (1962).
6. Durup, H., and M. Magat, *J. Polymer Sci.*, **18**, 586 (1955).
7. Thomas, W. M., Jr., and J. J. Pellon, *J. Polymer Sci.*, **13**, 329 (1954).
8. Medvedev, S. S., A. Dabkin, and P. M. Khomikovski, International Conference of High Energy Sources of Radiation, Warsaw (Sept. 1959) AEC-tr-3894.
9. Storch, H. H., *J. Am. Chem. Soc.*, **57**, 2598 (1935).
10. Melville, H. W., and G. M. Burnett, *J. Polymer Sci.*, **13**, 417 (1954).
11. Flory, P. J., *J. Am. Chem. Soc.*, **59**, 241 (1937).
12. Burton, M., J. A. Ghormley, and C. J. Hochanadel, *Nucleonics*, **13**, No. 10, 74 (1955).
13. Weiss, J., A. O. Allen, and H. A. Schwartz, *Proc. Intern. Conf. Peaceful Uses of Atomic Energy*, Vol. 14, United Nations, New York, 1956, p. 179.

### Résumé

Une étude a été faite de la cinétique et du mécanisme en phase liquide de la polymérisation de l'éthylène en solution dans le chlorure d'alcoyle, induite par rayonnement gamma. Le rayonnement gamma était fourni par une source en cobalt 60 de  $4.07 \times 10^6$

r/hr. La cinétique de ces polymérisations a été étudiée jusqu'à 10% de conversion et dans un domaine de températures de 0 à  $-25^{\circ}\text{C}$ . Trois solvants (le chlorure de *n*-propyle, le chlorure d'isopropyle et le chlorure de *t*-butyle) ont été employés avec des concentrations en éthylène allant de 6.76 à 8.89 moles par litre. Deux échantillons différents d'éthylène ont été employés: le premier contenant une limite supérieure de 1.000 ppm en oxygène, le second 60 ppm. L'éthylène contenant seulement 60 ppm d'oxygène donne une période d'induction plus courte et une vitesse de polymérisation plus élevée que l'éthylène contenant 1.000 ppm. Des énergies d'activation de 5.0 kcal/mole pour la réaction dans le chlorure de *t*-butyle ont été observées dans le domaine de température envisagé. Ces valeurs sont plus élevées que les 4.4 kcal/mole obtenues pour la polymérisation en émulsion de l'éthylène dans ce domaine de température. L'ordre de la réaction en fonction de la concentration en éthylène dans le chlorure de *n*-(propyle est de 1.41 à  $0^{\circ}\text{C}$ . Bien que l'hétérogénéité du système soit un facteur complexe, cette valeur de la vitesse est en bon accord avec le schéma général proposé pour d'autres polymérisations hétérogènes. Des données sur le poids moléculaire indiquent une augmentation du poids moléculaire avec l'augmentation de la température et mènent à la conclusion qu'une étape de terminaison impliquant des radicaux de solvant faiblement réactionnels peut être importante.

### Zusammenfassung

Kinetik und Mechanismus der in flüssiger Phase durch  $\gamma$ -Strahlung gestarteten Polymerisation von Äthylen in Alkylchloridlösung wurden untersucht. Die  $\gamma$ -Strahlung wurde von einer Kobalt-60-Quelle von  $4.07 \cdot 10^6$  r/Std. geliefert. Die Kinetik dieser Polymerisation wurde bis zu Umsätzen von 10% und im Temperaturbereich von  $0^{\circ}$  bis  $-25^{\circ}\text{C}$  untersucht. Es wurden drei Lösungsmittel (*n*-Propylchlorid, *i*-Propylchlorid und *t*-Butylchlorid) verwendet und die Äthylenkonzentration lag zwischen 6,76 und 8,89 Mol pro Liter. Die eine der beiden verwendeten Äthylensorten enthielt 1000 ppm Sauerstoff, die andere 60 ppm. Bei dem nur 60 ppm enthaltenden Äthylen war die Induktionsperiode kürzer und die Polymerisationsgeschwindigkeit grösser als bei dem Äthylen mit 1000 ppm Sauerstoff. In dem untersuchten Temperaturbereich war die Aktivierungsenergie der Reaktion in *n*-Propylchlorid 5,0, in *t*-Butylchlorid 7,4 kcal/Mol. Diese Werte sind höher als der für die Polymerisation von Äthylen in Substanz im gleichen Temperaturbereich bestimmte Wert von 4,4 kcal/Mol. Die Reaktion in *n*-Propylchlorid bei  $0^{\circ}\text{C}$  ist bezüglich der Äthylenkonzentration von der Ordnung 1,41. Obwohl die Reaktion durch die Heterogenität des Systems kompliziert wird, steht dieser Ausdruck für die Geschwindigkeit in gutem Einklang mit dem für andere heterogene Polymerisationen vorgeschlagenen allgemeinen Schema. Molekulargewichtsdaten, die eine Zunahme des Molekulargewichts mit steigender Temperatur erkennen lassen, führen zu dem Schluss, dass eine Abbruchsreaktion unter Beteiligung wenig reaktionsfähiger Lösungsmittelradikale von Bedeutung sein dürfte.

Received February 4, 1963

Revised May 13, 1963

## Rubber Elasticity of Preswollen Polymer Networks: Lightly Crosslinked Vinyl-Divinyl Systems\*

M. C. SHEN† and A. V. TOBOLSKY, *Frick Chemical Laboratory, Princeton University, Princeton, New Jersey*

### Synopsis

The rubber elasticity of lightly crosslinked, preswollen polymers is studied by both stress-relaxation and torsion measurements. The equation of state of rubber elasticity is applied to evaluate their front factors. It is found that both elastic moduli and front factors decrease linearly as the diluent content increases. This relationship is independent of the type of crosslink and the diluent used. Properties of deswollen polymer networks are also investigated. No significant change in front factor is apparent before and after deswelling. All these observations are attributed to the network topology. One factor is that effective chemical crosslinks may be decreased by the formation of intramolecular loops. Also, trapped entanglements become less significant at higher diluent concentrations.

### INTRODUCTION

The pronounced effects that diluents have on the viscoelastic properties of network polymers are quite well known. Generally speaking, two means are available to incorporate diluents into network polymers. One may either form the polymer network first, and then introduce the diluent into it (postswelling); or form the network in the presence of the diluent (preswelling). The effects of postswelling have been discussed in the literature. Moduli of postswollen rubbers have been found to be approximately inversely proportional to the five-thirds power of the swelling volume ratio in a given diluent.<sup>1</sup> However, similar studies of preswollen rubbers have received little attention.

Most of the experiments in the literature on preswollen rubbers do not deal with effects of diluents on mechanical properties of polymer networks. Hermanns<sup>2,3</sup> investigated its effects on the entropy of crosslinking and deformation; Rijke and Prins<sup>4</sup> reported on the swelling of cellulose acetate networks obtained by crosslinking in solution; and Alfrey and Lloyd<sup>5,6</sup> studied the equilibrium post-swelling of preswollen network polymers. In a previous communication<sup>7</sup> we have presented preliminary results on the

\* This article is based on part of a dissertation submitted by M. C. Shen for the partial fulfillment of the requirements for the degree of Doctor of Philosophy at Princeton University.

†Harvard Chemistry Fellow, 1961-1962.

rubber elasticity of preswollen systems. In this paper, we shall further treat the rubber elasticity of some lightly crosslinked, preswollen polymer networks; that of highly crosslinked ones will be discussed in a forthcoming paper.

### THEORETICAL CONSIDERATION

In a previous paper from this laboratory, the following equation was discussed:<sup>8</sup>

$$F = \Phi NkT (\alpha - 1/\alpha^2) \quad (1)$$

where  $F$  is force per cross sectional area,  $N$  is the number of network chains per cubic centimeter,  $k$  is the Boltzmann constant,  $T$  is absolute temperature,  $\alpha$  is relative extension, and  $\Phi$  is the front factor relating distances between network junctures in the networks and in free space. This equation was derived for polymer networks formed in the bulk state. However, samples investigated in this paper are all polymer networks formed in the presence of diluents. Here we have replaced part of the monomer by an inert diluent, maintaining constant concentration of crosslinking agent (in moles per cubic centimeter), then polymerized it under the same conditions as the ones in bulk.

In deriving eq. (1) the configurational free energy is calculated by assuming that the number of conformations of an isolated chain consistent with an end-to-end distance is the Gaussian expression. If this assumption is valid for networks formed in the "dry" state, the same should also hold for networks formed in the presence of diluents. This concept has been amply discussed by Hermans.<sup>2,3</sup> There is no difference in the arguments leading to eq. (1) between the bulk and preswollen systems. As long as the diluent content is not so high as to cause the network chains to be strained (and therefore no longer Gaussian), one may expect that eq. (1) will be applicable to preswollen polymer networks. On employing the Flory-Rehner tetrahedron model<sup>9</sup> as a physical model, it is easy to see that the presence of diluents probably causes the network elements to be less interpenetrating. For a very lightly crosslinked system, in our case only 0.05%, the chains are sufficiently long so that they are Gaussian up to fairly high diluent contents. Therefore eq. (1) may be used to evaluate the effects of preswelling on rubber elasticity.

Equation (1) was derived for simple tension measurements. If instead shear moduli were measured by torsion, the following equation could be used:

$$G = \Phi NkT \quad (2)$$

where  $G$  is the shear modulus.

In evaluating the front factors, the number of chains is calculated on the basis of the amount of crosslinking agent added:

$$N = zceN_A \quad (3)$$



where  $c$  is the number of moles of crosslinking per cubic centimeter of rubber,  $e$  is the crosslinking efficiency,  $N_{A_0}$  is Avogadro's number, and  $z$  depends on the functionality of the crosslink. For a tetrafunctional crosslink, the  $z$  value is 2, since each network chain is shared by two crosslinks. According to Loshaek and Fox,<sup>10</sup> the crosslinking efficiency is unity at very low concentrations of crosslinks. (By crosslinking efficiency we mean the fraction of the second double bonds of the divinyl molecules that have reacted.) However, no experimental confirmation is possible, since the method of measurement is not accurate in this region. We prefer to leave  $e$  unspecified, although in a forthcoming paper it will be shown that  $e$  is quite close to unity at all crosslink concentrations where it can be measured. The front factors are therefore evaluated by the following equations:

$$\Phi e = F/2cRT(\alpha - 1/\alpha^2) \quad (4a)$$

for measurements made by the stress-relaxation balance, and

$$\Phi e = G/2cRT \quad (4b)$$

for those by the Gehman apparatus. Here  $R$  is the gas constant.

## EXPERIMENTAL METHODS

Monomers ethyl, *n*-butyl, and *n*-octyl acrylates, ethylene glycol dimethacrylate (EGDM) and tetraethylene glycol dimethacrylate (TEGDM) were obtained from the Borden Chemical Company; dimethyl phthalate (DMP), dioctyl phthalate (DOP), dimethyl adipate (DMA), and dioctyl adipate (DOA) from Eastman Chemical Company were used as diluents. Photopolymerizations were carried out between Pyrex glass plates for 48 hr. in front of a G.E. RS sunlamp. Benzoin (Matheson) was used as the photosensitizer. Care was taken to insure a complete polymerization. Any unreacted monomer was removed by storing in a vacuum oven at room temperature for 10–15 days. In all cases the weight loss was only a fraction of 1%, indicating essentially complete conversions.

Densities were determined by displacement measurements. Volume contractions upon polymerization were thus found so as to calculate crosslinker concentrations per unit volume of polymer.

Two types of modulus measurements were made in order to countercheck each other. The Young's moduli were measured by the stress-relaxation balance,<sup>11</sup> and the 10-sec. shear moduli by a modified Gehman apparatus.<sup>12</sup> The results are found to be in good agreement, employing the relationship  $E = 3G$ .

The deswelling of some of the preswollen samples was carried out by heating in a vacuum oven at 100°C. for approximately one week.

## RESULTS

## Effect of Preswelling on Front Factors

We have already reported previously<sup>7</sup> that the presence of preswollen diluents reduces the front factors of a series of polyacrylates. The relationship between  $\phi_e$  and per cent diluent by volume is linear within experimental error. The decrease is more pronounced for lower acrylates than for higher acrylates. One of the polymers (poly-*n*-butyl acrylate) was preswollen by four different diluents: dimethyl phthalate, dioctyl phthalate, dimethyl adipate, and dioctyl adipate. From the data it is clear that the variation of front factors is independent of the diluent used.

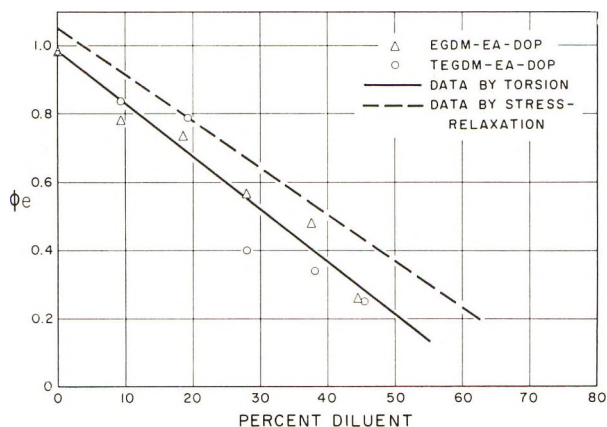


Fig. 1. Front factors  $\phi_e$  of crosslinked poly(ethyl acrylate) preswollen with dioctyl phthalate vs. per cent diluent by volume: (O) systems crosslinked by ethylene glycol dimethacrylate; ( $\Delta$ ) systems crosslinked by tetraethylene glycol dimethacrylate; (—) best straight line through the experimental points; (---) data of Tobolsky et al.<sup>7</sup>

In order to investigate the role of the type of crosslink on the preswollen polymer networks, we measured front factors of preswollen poly(ethyl acrylate) crosslinked to 0.05% by ethylene glycol dimethacrylate and tetraethylene glycol dimethacrylate respectively. The results are shown in Figure 1. Here all experimental points fall on the same straight line, indicating that the type of crosslink used has no effect on the front factors of preswollen systems. The results obtained here (solid line) are compared with those reported earlier<sup>7</sup> (dotted line). A slight deviation is observed. This deviation, however, is not surprising in view of the fact that the modulus here is determined by torsion instead of stress relaxation; and that  $\phi_e$  is evaluated at 153°C. rather than 60°C.

## Effect of Preswelling on Elastic Moduli

We have also determined the Young's moduli by the stress-relaxation balance on a variety of polymer-diluent systems. Three polyacrylates:

TABLE I  
Comparison of Shear Moduli and Front Factors of Preswollen and Deswollen Polymer Networks

Polymer	%Diluent (dimethyl phthalate)	Preswollen networks			Deswollen networks		
		$c \times 10^5$ , mole/cc.	$G \times 10^{-6}$ , dynes/cm. <sup>2</sup>	$\Phi_e$	$c \times 10^5$ , mole/cc.	$G \times 10^{-6}$ , dynes/cm. <sup>2</sup>	$\Phi_e$
Poly(ethyl acrylate)	0	2.50	1.85	0.98	(2.50)	(1.85)	(0.98)
	12.9	2.68	1.48	0.81	3.76	1.58	0.76
	23.0	2.97	1.40	0.68	4.82	1.70	0.63
	35.6	3.04	1.02	0.51	5.49	1.45	0.47
	46.7	2.79	0.78	0.44	5.95	1.25	0.38
Poly( <i>n</i> -butyl acrylate)	0	2.57	1.03	0.67	(2.57)	(1.03)	(0.67)
	11.3	2.68	0.88	0.55	3.21	0.92	0.51
	19.4	2.85	0.82	0.49	3.83	0.95	0.45
	32.7	2.90	0.63	0.37	4.65	0.80	0.34
	40.8	2.58	0.45	0.30	4.74	0.63	0.24
	51.8	2.82	0.24	0.16	5.60	0.38	0.12

ethyl (PEA), *n*-butyl (PBA), and *n*-octyl (POA) crosslinked by TEGDM were preswollen by dioctyl phthalate. Three additional diluents: dimethyl phthalate, dimethyl adipate, and dioctyl adipate were used for

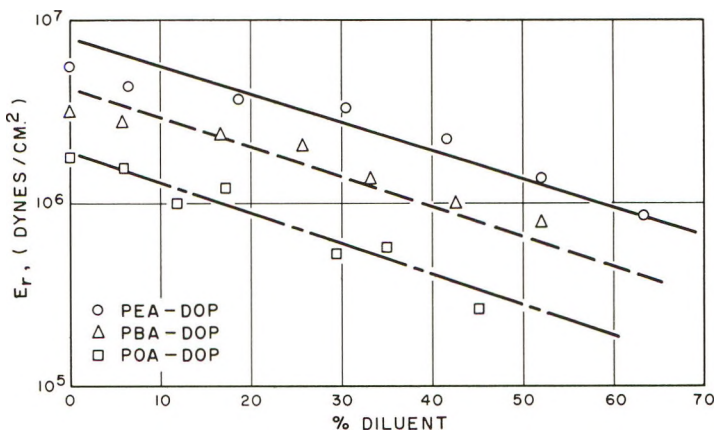


Fig. 2. Young's moduli of poly(ethyl acrylate) (PEA), poly(*n*-butyl acrylate) (PBA), and poly(*n*-octyl acrylate) (POA) preswollen by dioctyl phthalate (DOP) vs. per cent diluent by volume.

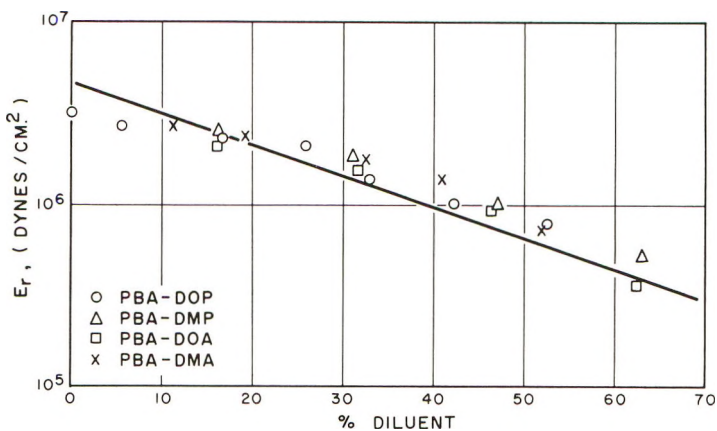


Fig. 3. Young's moduli of poly(*n*-butyl acrylate) (PBA) preswollen with dioctyl phthalate (DOP), dimethyl phthalate (DMP), dioctyl adipate (DOA), and dimethyl adipate (DMA) vs. per cent diluent by volume.

PBA. Figures 2 and 3 show that Young's moduli decrease linearly as solvent contents increase. It is interesting to note that slopes of decrease are practically the same for all systems involved. Here again the effect is independent of the diluent used. The scattering of data may be partially attributed to the fluctuation of the degree of crosslinking.

### Deswollen Network Polymers

To isolate further the role of diluents on network polymers, we evaluated two series of polymers: poly(ethyl acrylate) and poly(*n*-butyl acrylate) preswollen by dimethyl phthalate. Shear moduli were measured while they were preswollen and after their diluents were removed by evacuation. Values of  $\phi_e$  were also calculated on the basis of the new crosslink concentration. Results are summarized in Table I. The front factors remain essentially unchanged before and after deswelling, and definitely lower than that of corresponding polymers prepared without solvent.

### DISCUSSION

Throughout this paper we have tacitly assumed that all the reacted second double bonds of the divinyl compound are effective as intermolecular network junctures. This is, however, not quite the case. First of all, we have neglected those crosslinks that unite two points of the same linear molecule. The formation of intramolecular linkages leads to loops or rings rather than an infinite network. An approximate statistical calculation showed that the relative number of such linkages is comparatively small in the absence of diluents, but that it increases rapidly with dilution.<sup>13</sup> These ring formations reduce the number of effective intermolecular chemical crosslinks in the network. The effect of these "wastage reactions" has already been pointed out in our previous communication.<sup>7</sup> Staverman<sup>14</sup> has long ago studied its role in the entropy of high polymer solutions. Recently Kuhn and Balmer<sup>15</sup> in investigating the viscosity of dilute polymer solutions have also shown that intramolecular ring formation becomes more important as polymer concentration decreases.

Secondly, the contribution of physical crosslinks due to chain entanglements should be taken into account. Mullins<sup>16</sup> showed that, for natural rubber vulcanized in bulk, chain entanglements are responsible for at least half of the total number of crosslinks. As we mentioned earlier, the presence of diluents during the network formation gives rise to less network interpenetration and less trapped entanglements. Studies in the retardation spectra of solutions of linear polymers<sup>17-19</sup> revealed that the degree of chain entanglements is inversely proportional to the concentration of polymer per unit volume of solution. One may therefore expect that physical crosslinks contribute less to the total stress as diluent content increases.

Both of the preceding two factors cited arise during the formation of the network. After the network is formed, the presence or absence of diluent has no effect on the topology of the network or on the front factor. Our data on deswollen polymers illustrate this point very well. Of great importance is the complicated topological pattern the network chains assume. Once the network is formed, its topology is essentially unaffected by subsequent deformations. This was also pointed out by Alfrey and Lloyd<sup>5,6</sup> in their studies of swelling equilibria of preswollen network polymers.

Other considerations, such as differences in chain conformation in pre-swollen versus nonswollen networks may also effect the absolute magnitudes of the front factors.<sup>8</sup>

It is possible that the low front factors we had previously observed<sup>8</sup> in networks of acrylates and methacrylates with long alkyl side chains may in part be due to the same considerations as discussed in this paper for preswollen networks. In other words, the long side chains may act in part as internal diluent.

### References

1. Flory, P. J., *Chem. Revs.*, **35**, 51 (1944).
2. Hermanns, J. J., *Trans. Faraday Soc.*, **43**, 591 (1947).
3. Hermanns, J. J., paper presented at the meeting of American Chemical Society, St. Louis, March, 1961.
4. Rijke, A. M., and W. Prins, paper presented at the 139th meeting of the American Chemical Society, St. Louis, March 1961.
5. Alfrey, T., Jr., and W. G. Lloyd, *J. Polymer Sci.*, **62**, 159 (1962).
6. Lloyd, W. G., and T. Alfrey, Jr., *J. Polymer Sci.*, **62**, 301 (1962).
7. Tobolsky, A. V., D. W. Carlson, N. Indictor, and M. C. Shen, *J. Polymer Sci.*, **61**, 523 (1962).
8. Tobolsky, A. V., D. W. Carlson, and N. Indictor, *J. Polymer Sci.*, **54**, 175 (1961).
9. Flory, P. J., and J. Rehner, Jr., *J. Chem. Phys.*, **11**, 512 (1943).
10. Loshaek, S., and T. G. Fox, *J. Am. Chem. Soc.*, **75**, 3544 (1953).
11. Tobolsky, A. V., *Properties and Structure of Polymers*, Wiley, New York, 1960.
12. ASTM Standards Designation D1053-58 (1958).
13. Flory, P. J., and J. Rehner, Jr., *J. Chem. Phys.*, **11**, 521 (1943).
14. Staverman, A. J., *Rec. Trav. Chim.*, **69**, 163 (1950).
15. Kuhn, W., and G. Balmer, *J. Polymer Sci.*, **57**, 311 (1962).
16. Mullins, L., *J. Appl. Polymer Sci.*, **2**, 1 (1959).
17. Saunders, P. R., and J. D. Ferry, *J. Colloid Sci.*, **14**, 239 (1959).
18. DeWitt, T. W., H. Markovitz, F. J. Padden, Jr., and L. J. Zapas, *J. Colloid Sci.*, **10**, 174 (1955).
19. Ferry, J. D., L. Jordan, W. W. Evans, and M. F. Johnson, *J. Polymer Sci.*, **14**, 161 (1954).

### Résumé

L'élasticité caoutchouteuse de polymères préalablement gonflés et légèrement pontés est étudiée à la fois par relaxation de la tension et par des mesures de torsion. L'équation d'état de l'élasticité du caoutchouc est appliquée pour évaluer leurs facteurs de front. On a trouvé que le module d'élasticité et les facteurs de front décroissent linéairement quand le contenu en diluant augmente. Cette relation est indépendante du type de pontage et du diluant employé. Les propriétés des réseaux de polymères dégonflés sont également envisagées. Un changement suffisant dans le facteur du front avant et après dégonflement n'a pu être observé. Toutes ces observations sont attribuées à la topologie du réseau. Les pontages chimiquement actifs peuvent être diminués par formation de ponts intramoléculaires. De même des enchevêtrements piégés deviennent moins importantes pour des plus grandes concentrations en diluant.

### Zusammenfassung

Die Kautschukelastizität schwach vernetzter, vorgequollener Polymerer wurde sowohl durch Spannungsrelaxations- als auch durch Torsionsmessungen untersucht. Zur Bestimmung des Frontfaktors dieser Polymeren wurde die Zustandsgleichung der

Kautschukelastizität angewandt. Sowohl der Elastizitätsmodul als auch der Frontfaktor nehmen mit steigendem Gehalt an Verdünnungsmittel linear ab. Diese Beziehung ist von der Art der Vernetzung und vom verwendeten Verdünnungsmittel unabhängig. Weiters wurden die Eigenschaften des entquollenen Polymernetzwerkes untersucht. Der Frontfaktor ist offenbar vor und nach der Entquellung im wesentlichen gleich. Alle diese experimentellen Befunde lassen sich auf die Topologie des Netzwerkes zurückführen. Ein wesentlicher Umstand besteht darin, dass die effektive chemische Vernetzung durch Bildung intramolekularer Schlingen herabgesetzt werden kann. Ebenso verlieren eingeschlossene Verschlingungen bei höheren Konzentrationen des Verdünnungsmittels an Bedeutung.

Received May 17, 1963

## Preparation and Polymerization of Vinyl Esters of Cyclic and Polychloro Fatty Acids\*

C. S. MARVEL and J. C. HILL,† *Department of Chemistry, University of Arizona, Tucson, Arizona*, and J. C. COWAN, J. P. FRIEDRICH, and J. L. O'DONNELL, *Northern Utilization Research and Development Division, U. S. Department of Agriculture, Peoria, Illinois*

### Synopsis

Homopolymers and vinyl chloride copolymers have been prepared from the vinyl esters of mixed hydrogenated cyclized linolenic acid, 9,10-dichlorostearic acid, 9,10,12,13-tetrachlorostearic acid, 13,14-dichlorobehenic acid, 9(10)-phenylstearic acid and technical behenic acid. Vinyl 13,14-dichlorobehenate (29%)–vinyl chloride (71%) gave a copolymer with a brittle temperature of  $-2^{\circ}\text{C}$ . All of the other copolymers with vinyl chloride had brittle temperatures of  $16^{\circ}\text{C}$ . or higher and behaved more like rigid plastics.

There are numerous esters that are effective external plasticizers for polyvinyl chloride. Some work has been done to see if copolymerization of a vinyl ester with vinyl chloride would result in a permanently plasticized copolymer. For example, Port and co-workers have copolymerized vinyl chloride and vinyl esters of straight chain fatty acids.<sup>1</sup> They observed that as the chain length of the acid increased the degree of plasticization increased. Copolymers of vinyl chloride and vinyl acetate were rigid plastics, while copolymers of vinyl chloride and vinyl stearate were flexible plastics.

Vinyl esters with the general structure of effective external plasticizers have been copolymerized with vinyl chloride with the hope that a permanently plasticized copolymer would be achieved.<sup>2</sup> For example, since di-2-ethylhexyl phthalate is known to be a good plasticizer for polyvinyl chloride, vinyl 2-ethylhexyl phthalate was prepared and copolymerized with vinyl chloride. This copolymer and others of this type were somewhat more flexible than polyvinyl chloride, but the improvement was not enough to be useful.

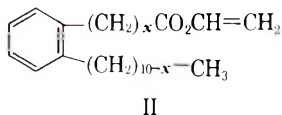
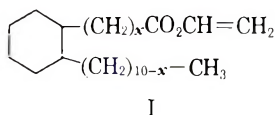
In this work, vinyl esters of cyclized linolenic acid (CAL) and its hydrogenation product (HCAL) were prepared. Studies on hydrogenation of

\* Presented in part at the 141st National Meeting of the American Chemical Society, Washington, D. C., March, 1962.

† This is a partial report of work done under contract with four Utilization Research and Development Divisions, Agricultural Research Service, U. S. Department of Agriculture, and authorized by the Research and Marketing Act. The contract was supervised by J. C. Cowan of the Northern Division.



small amounts of cyclized lineolenic acid using palladium-on-charcoal as a catalyst showed that the cyclic acid absorbed hydrogen readily to give the hydrogenated product. However, in the preparation of the larger amounts of materials which were used in these polymerization studies, hydrogenation proceeded slowly. The carbon and hydrogen analysis of the homopolymer (A-25, see Table I) indicated a low hydrogen content. A gas-liquid chromatograph established the presence of approximately 60% of aromatic derivatives. The presence of both aromatic and hydrogenated cyclic products was verified by ultraviolet and infrared spectra. Thus, the vinyl ester of hydrogenated cyclic acid used in these studies consists of approximately 60% of the benzene derivative (II) and 40% of the cyclohexane derivative (I).



The vinyl esters of the unsaturated cyclic acids (CAL) would not be polymerized by free radical initiation. The vinyl esters of the mixed reduced acids (HCAL) were homopolymerized and were copolymerized with vinyl chloride. Of special interest were the low temperature properties of the esters. They have a very low pour point, about  $-45^{\circ}\text{C}.$ , and become a clear glass when cooled further, but fail to crystallize even at  $-70^{\circ}\text{C}.$  It was of interest to see if the vinyl esters of these acids with good low temperature characteristics would impart internal plasticization to vinyl chloride copolymers.

The vinyl esters used in this study were the esters of the mixed hydrogenated cyclic acids (HCAL), structures I + II; of 9,10-dichlorostearic acid, III; of 9,10,12,13-tetrachlorostearic acid, IV; of 13,14-dichlorobehenic acid, V; of a mixture of straight chain fatty acids ( $\text{C}_{22}$ , 78%;  $\text{C}_{20}$ , 10%;  $\text{C}_{18}$ , 7%; and  $\text{C}_{16}$ , 1%), VI; and of 9(10)-phenylstearic acid, VII. Their copolymers with vinyl chloride were evaluated to see if internal plasticization occurred. The polychloro esters might also be expected to function as flame retardants.

### ESTER SYNTHESIS

Cyclic fatty acids were prepared by alkali cyclization and hydrogenation as described by Scholfield and Cowan<sup>3</sup> and Friedrich, et al.<sup>4</sup> Properties of the cyclic (CAL) and hydrocyclic (HCAL) fatty acids from linseed oil and their vinyl esters vary somewhat depending on the conditions of preparation and isolation.

The polychloro fatty acids were prepared by the addition of chlorine to the corresponding unsaturated fatty acids in either methylene chloride or chloroform at reduced temperatures.<sup>5,6</sup> A technical sample of behenic acid which contained approximately 78% of  $\text{C}_{22}$  acid, 10%  $\text{C}_{20}$  acid, 7% of  $\text{C}_{18}$  acid, and 1% of  $\text{C}_{16}$  acid was used to make one of the vinyl ester samples.

The phenylstearic acid which was used in this experiment was a mixture of the 9- and 10-phenyl isomers prepared from oleic acid by the method of Stirton et al.<sup>7</sup> We are indebted to Dr. W. C. Ault of the Eastern Utilization Research and Development Division, USDA, for this sample.

Vinyl esters were prepared by acid-ester interchange reaction of vinyl acetate with mercuric acetate and sulfuric acid as a catalyst.<sup>8</sup> One sample of vinyl esters of HCAL was prepared by direct reaction of the acid with acetylene under pressure with zinc stearate as catalyst. Vinyl esters of HCAL may have structures other than I + II present, but the main variation is probably in the number of CH<sub>2</sub> groups between the ring and the ester and methyl group.

### POLYMERIZATION

All of the vinyl esters except those of the unsaturated cyclic acids (CAL) homopolymerized readily in bulk when 2,2'-azobisisobutyronitrile (AIBN)

TABLE I  
Homopolymerization of Vinyl Esters

Vinyl ester of	Expt.	Time, hr.	Conversion, %	Softening range, °C.	Inherent viscosity <sup>a</sup>
Cyclized linolenic acid (CAL)		40	0	—	—
Hydrogenated cyclic acid (HCAL, I + II)	A-25 <sup>b</sup>	22	50	<25	0.168
9,10-Dichlorostearic acid (III) <sup>c</sup>	A-62	6	85	<25	0.125
9,10-Dichlorostearic acid (III) <sup>d</sup>	A-63 <sup>e</sup>	6	90	<25	0.141
9,10,12,13-Tetrachlorostearic acid (IV)	A-58 <sup>f</sup>	6	90	76-83	0.183
13,14-Dichlorobehenic acid (V)	A-72 <sup>g</sup>	6	81.5	<25	0.153
Technical behenic acid (VI)	A-94 <sup>h</sup>	6	82.5	62.5-63.5	0.239
9(10)-Phenylstearic acid (VII)	A-99 <sup>i</sup>	6	81.5	<25	0.104

<sup>a</sup> Measured at a concentration of 0.20 g. polymer in 100 ml. of benzene at 30°C.

<sup>b</sup> Anal. Calcd. for C<sub>20</sub>H<sub>36</sub>O<sub>2</sub>: C, 77.86%; H, 11.76%. Found: C, 78.22%; H, 10.55%. (If the assumption is made that HCAL is 60% aromatic, the calculated hy-

TABLE II. Copolymerization Experiments with Vinyl Chloride and Vinyl Esters

	Vinyl ester of acid	Vinyl ester, g.	Vinyl chloride, g.	Conversion, %	Softening range, °C. <sup>a</sup>	Inherent viscosity <sup>b</sup>	Cl, % <sup>c</sup>	Ester incorporated, % <sup>d</sup>
A-31°	I + II	2	18	90	79-110	0.94	54.23	4.42
A-28°	I + II	4	16	90	77-103	0.96	50.61	10.80
A-34°	I + II	4	16	88	78-102	0.95	49.76	12.29
A-36°	I + II	4	16	85	77-104	0.96	49.50	12.75
A-30°	I + II	6	14	85	70-93	0.93	46.28	18.43
A-47	I + II	8	12	69.5	63-84	1.17	43.36	23.58
A-48°	I + II	10	10	57	55-77	1.10	38.29	32.52
A-46	I + II	16.63	3.37	29	<25	0.73	26.13	53.95
A-78°	I + II	10	10	55	57-79	1.22	39.57	30.26
A-79°	I + II	10	10	57.5	57-79	1.11	40.38	28.83
A-49	III <sup>f</sup>	2	18	86.5	79-105	0.88	55.01	4.55
A-50	III <sup>f</sup>	4	16	78.5	69-91	0.84	54.08	7.00
A-44	III <sup>f</sup>	6	14	80.1	53-85	0.76	50.02	15.62
A-45°	III <sup>f</sup>	8	12	70.1	54-78	0.77	49.16	19.94
A-51°	III <sup>f</sup>	10	10	60.5	50-69	0.69	44.35	32.59
A-80°	III <sup>f</sup>	10	10	53	53-76	0.72	45.83	28.69
A-81°	III <sup>f</sup>	10	10	53.5	53-76	0.70	45.98	28.32
A-82°	III <sup>f</sup>	10	10	55	53-76	0.70	46.14	27.88
A-67	III <sup>g</sup>	0.5	4.5	79.4	83-113	0.94	54.43	6.08
A-68	III <sup>g</sup>	1.0	4.0	69	70-100	0.88	52.55	11.02
A-69	III <sup>g</sup>	1.5	3.5	68.1	65-85	0.82	51.41	14.02
A-70	III <sup>g</sup>	2.0	3.0	62.4	58-80	0.74	48.60	21.41
A-71	III <sup>g</sup>	2.5	2.5	54	50-73	0.70	45.62	29.25
A-73	IV	0.5	4.5	77	89-113	0.89	54.90	7.32
A-74	IV	1.0	4.0	75	84-106	0.84	54.02	10.71
A-75	IV	1.5	3.5	69.4	74-99	0.78	52.50	16.88
A-76	IV	2.0	3.0	61	70-95	0.73	50.81	23.60
A-77	IV	2.5	2.5	52.2	64-84	0.62	50.35	25.43
A-92°	IV	10	10	50.5	80-95	0.74	51.01	23.31
A-93°	IV	10	10	51.5	80-95	0.75	49.44	29.05
A-53	V	0.5	4.5	78	74-110	0.96	55.12	4.12
A-54	V	1.0	4.0	70	67-98	0.94	51.71	12.78
A-55	V	1.5	3.5	66	65-95	0.83	51.00	14.58
A-56	V	2.0	3.0	52	62-92	0.73	50.36	16.21
A-57°	V	2.5	2.5	50	50-75	0.62	44.21	31.83
A-87°	V	10	10	48.8	53-77	0.69	45.67	28.12
A-89°	V	10	10	57	53-77	0.75	44.42	31.29
A-95°	VI	10	10	51.5	69-81	0.80	43.06	24.21
A-96°	VI	10	10	52.5	69-81	0.79	43.27	23.84
A-97°	VI	10	10	48.0	70-83	0.77	43.84	22.50
A-100	VII	0.5	4.5	76	86-102	0.98	53.12	6.41
A-101	VII	1.0	4.0	56	84-100	0.93	52.36	7.75
A-102	VII	1.5	3.5	38	81-98	0.85	50.00	11.93

<sup>a</sup> Measured on a Kofler micro melting point apparatus.

<sup>b</sup> The inherent viscosities were measured at a concentration of 0.2 g. of polymer in 100 ml. of tetrahydrofuran at 30°C.

<sup>c</sup> Chlorine analyses were performed by the Micro-Tech Laboratories, Skokie, Illinois.

<sup>d</sup> The amount of vinyl ester in the copolymer was calculated from the chlorine analysis.

<sup>e</sup> Samples were used in the evaluation tests.

<sup>f</sup> Prepared from Emersol 233, a technical oleic acid.

<sup>g</sup> Prepared from pure oleic acid.

was used as the initiator. Conversions ranged from 50 to 90%. The homopolymers were soluble in benzene and insoluble in methanol. They were syrupy, thick liquids except for polyvinyl tetrachlorostearate, which melted at 76–83°C., and the polymer of the vinyl ester of the technical behenic acid, which melted at 62.5–63.5°C. Attempts to homopolymerize these monomers by emulsion and suspension techniques gave low conversions and inherent viscosities similar to those obtained from bulk polymerization. Data are given in Table I.

Copolymers of each vinyl ester with vinyl chloride were prepared in an emulsion system. The polymerization bottles were charged with the vinyl ester in amounts of 10, 20, 30, 40, and 50 wt.-% of the total monomer charge. As the ester content of the charge increased, the percentage conversion to polymer and the softening range of the isolated copolymer decreased. Conversions ranged from 29 to 90%. The inherent viscosities of the copolymers ranged from 0.62 to 1.22. The initial softening points ranged from 50 to 89°C. All the copolymers were soluble in tetrahydrofuran and insoluble in methanol. The unpolymerized vinyl esters were soluble in both methanol and tetrahydrofuran, so this pair of liquids provided a suitable reprecipitation system. The percentage conversion was calculated from the weight of dry polymer remaining after sufficient reprecipitations to remove unchanged vinyl ester. Data on copolymers are given in Table II.

## EVALUATION

We are indebted to Dr. L. P. Witnauer, Eastern Utilization Research and Development Division, USDA, for this evaluation of the mixed polymers (Table III). The methods used are those reported earlier.<sup>1</sup>

A slight plasticization was imparted by the vinyl esters of the mixed reduced acids, I + II, but the polymers probably still fall in the rigid plastic class. The brittle temperatures are similar to those of vinyl pelargonate–vinyl chloride copolymers with the same compositions.

Vinyl dichlorostearate, III, appears to be a better internal plasticizer than the vinyl ester of mixed hydrogenated cyclic acid (I + II). The copolymer, designated DS-50, could be milled at 150°F. and has a lower brittle temperature than HP-50. However, that temperature is higher than the brittle temperature of the vinyl chloride–vinyl stearate copolymer.

Dykstra copolymerized vinyl 4-ketostearate, vinyl 9(10)-ketostearate, vinyl 12-ketostearate with vinyl chloride.<sup>2b</sup> The vinyl 9(10)-ketostearate and vinyl 12-ketostearate had higher brittle temperatures than vinyl stearate–vinyl chloride copolymers of similar composition.

If motion of the side chain is an important factor in plasticization, then side chains with polar substituents should be less effective than straight hydrocarbon chains. If the side chains facilitate motion of neighboring polymer segments, then polar substituents might reduce the effectiveness of the internal plasticizer.

The copolymer of vinyl chloride and vinyl tetrachlorostearate, IV, TS-50, was much more brittle than DS-50.

The copolymer prepared with vinyl dichlorobehenate, V, designated DB-50, had a brittle temperature of  $-2^{\circ}\text{C}$ . The internal plasticity as indicated by the brittle temperature is greater than that in the vinyl chloride-vinyl stearate copolymer.

The vinyl ester of technical behenic acid, VI, gave a copolymer (HB-50) of very low tensile strength and with a brittle temperature of  $28^{\circ}\text{C}$ .

TABLE III  
Mechanical Properties of Copolymers

Sample	Vinyl ester of acid	Composition of sample <sup>a</sup>	Ester, wt.-%	Mill temp., $^{\circ}\text{F}$ .	Elongation, %	Tensile strength, psi	Brittle temp., $^{\circ}\text{C}$ . <sup>b</sup>
HP-20 <sup>c</sup>	I + II	A-28, 34, 36	12.32	270	30	7100	54
HP-30	I + II	A-30	18.95	270	15	3000	38
HP-50 <sup>c</sup>	I + II	A-48, 78, 79	31.29	260	15	1700	25
DS-50 <sup>c,d</sup>	III	A-51, 80, 81, 82	28.45	150	65 <sup>e</sup>	3230	16
TS-50 <sup>c,d</sup>	IV	A-92, 93	26.68	240	10	820	47
DB-50 <sup>c,d</sup>	V	A-87, 89	29.71	200	25	2600	-2
HB-50 <sup>c,d</sup>	VI	A-95, 96, 97	23.42	210	10	470	28
VCl-VS	Stearic		30.00	170	170 <sup>e</sup>	2810 <sup>f</sup>	6
Geon-101	—	g	100.00	320+	30	7300	72
Modified Geon-101	—	h		320	350	2830	-30

<sup>a</sup> See Table II.

<sup>b</sup> The brittle temperature given is the temperature at which the torsional modulus attains a value of 135,000 psi.

<sup>c</sup> Samples blended to obtain enough sample for testing.

<sup>d</sup> Sample gave an opaque sheet; all others were transparent.

<sup>e</sup> Specimen necked down indicating orientation.

<sup>f</sup> This value is the yield point. Break load is lower.

<sup>g</sup> Geon-101 is a technical sample of polyvinyl chloride.

<sup>h</sup> Geon-101 containing 35% di-2-ethylhexylphthalate.

The copolymers of vinyl phenylstearate (VII) and vinyl chloride were rigid plastics at room temperature and the mechanical properties were not determined.

As the ester content of the charge and the resulting copolymer increases, the tensile strength of the polymer decreases. The strength of HP-50 dropped to nearly one-half the strength of HP-30 and one-fourth the strength of HP-20. The inherent viscosities of these copolymers changed only slightly as the ester content increased, so presumably the copolymers had about the same average molecular weights. The decrease in the tensile strength is probably due to an increase in the heterogeneity of the copolymer as the ester content of the charge and the copolymer increases. Table IV shows the results of fractional precipitation of a 6-g. sample of a copoly-

TABLE IV  
Fractional Precipitation

Fraction	Methanol added, ml.	Weight polymer, g.	Inherent viscosity	Softening range, °C.	Cl, %	Ester content, %
200 ml. THF	0	6.0	1.17	75-90	43.36	23.58
1	200	3.42	1.97	76-95	44.34	21.85
2	300	1.88	0.50	68-86	42.64	24.85
3	From remaining solution	0.68	0.21	63-76	42.02	25.94

mer of the vinyl ester of the mixed hydrocyclic acids and vinyl chloride which contained 23.58% of ester.

Fraction precipitation of a sample of HP-50 gave fractions which had an inherent viscosity spread of 0.3-2.3. The heterogeneity is probably due to the differences in the monomer reactivity ratios.<sup>9</sup> It could also be due, in part, to the emulsion system used.

## EXPERIMENTAL

### Preparation of Fatty Vinyl Esters

**Vinyl 9(10)-Phenylstearate.** The vinylation of 9(10)-phenylstearic acid was carried out by the vinyl interchange procedure of Adelman.<sup>8</sup>

To a 1-l., three-necked flask equipped with a mechanical stirrer, condenser with calcium chloride drying tube, and thermometer were charged 50 g. of 9(10)-phenylstearic acid, 670 ml. of vinyl acetate (Matheson, Coleman and Bell, stabilized), 4.0 g. of mercuric acetate, and 0.2 g. of Copper Resinate (Harshaw Chemical Company). This mixture was stirred at room temperature until a clear solution was obtained. The system was swept with nitrogen gas and 0.50 ml. of concentrated sulfuric acid was added. The reaction mixture was stirred and the temperature was maintained at 38-45°C. for 60 hr. Then 2.0 g. of sodium acetate was added with stirring to the reaction mixture. Most of the unchanged vinyl acetate was removed at reduced pressure. The remaining oil was dissolved in 700 ml. of ether. The ether solution was washed twice with 500 ml. portions of dilute aqueous sodium chloride solution and then with 500 ml. of 1% potassium carbonate solution. The ether layer was washed again with 500 ml. of dilute aqueous sodium chloride solution and then dried over anhydrous sodium sulfate. The ether solution was stripped of solvent leaving 39.5 g. of oil.

A 19.5 g. portion of the oil was placed on a column of 238 g. of alumina. Elution with 5:1 cyclohexane-ether gave 4.85 g. of vinyl 9(10)-phenylstearate. The remaining 20 g. of oil was distilled in the presence of clean copper wire and Copper Resinate (Harshaw Chemical Company). The

TABLE V  
Vinyl Esters of Fatty Acids

Acid used	Acid, °C.	$\eta_{sp}^{30}$ of vinyl ester	Analyses of esters							
			Calculated			Found				
			C, %	H, %	Cl, %	C, %	H, %	Cl, %		
Cyclic fatty (CAL)	< -45	1.4882								
Mixed hydro-cyclic fatty (HCAL)	< -45	1.4714								
9(10)-Phenyl-stearic	<25	1.4749	80.77	10.92		80.95	10.86			
Technical behenic										
9,10-dichloro-stearic	36.5-37.5	1.4682	63.31	9.57	18.69	78.25	12.64	18.69	9.61	18.60
9,10,12,13-Tetrachloro-stearic	126-127	(m.p. 74-75)	53.58	7.64	31.64	53.51	7.82	31.64	7.82	31.50
13,14-Dichloro-obeheic	44.5-45.5	1.4678	66.19	10.18	16.28	66.04	10.19	16.28	10.19	15.92

main fraction distilled at 169–171°C. (0.05 mm. Hg). The yield of ester was 13.60 g.

ANAL. Calcd. for  $C_{26}H_{42}O_2$ : C, 80.77%; H, 10.92%. Found: C, 80.95%, H, 10.86%.

The total yield by chromatography and distillation was 18.95 g. (35% of the theoretical yield).

**Vinyl Esters of the Unsaturated Cyclic Acids and the Hydrogenated Cyclic Acids.** CAL was prepared by the method of Friedrich, et al.<sup>4</sup> and hydrogenated by their procedure to give HCAL. Both acids were reacted with vinyl acetate according to the method of Adelman.<sup>8</sup> Crude reaction products were stripped of vinyl acetate, diluted with 2.5 parts of petroleum ether (pentane–hexane) and passed through an alumina column to remove fatty acid. HCAL esters were distilled under reduced pressure, b.p. 135–150°C. at 0.1 mm. (acid value = 15). Esters were redissolved in petroleum ether and passed through an alumina column, and the petroleum ether was removed *in vacuo*. A direct vinylation was effected as follows. HCAL (136.1 g.) and zinc stearate (8.3 g.) were charged into a 300-ml. autoclave with stirrer. The mixture was heated to 165°C. after being flushed with acetylene gas. Acetylene pressure was increased to 500 psig. After 5 hr. the product had an acid value of 6, and further reaction did not decrease this value in another hour. The crude product was refined with alumina.

**Dichlorobehenic Acid.** A chlorine solution in methylene chloride was added slowly with stirring to a solution of erucic acid (98% pure) in methylene chloride at –20°C. Sufficient chlorine to saturate 95% of the acid was used. The crude dichlorobehenic acid was recrystallized from heptane; neutralization equivalent calculated 409.5, found, 410. The properties of the vinyl esters are summarized in Table V.

### Homopolymerization

The homopolymerizations were carried out in a 100 mm. × 28 mm. tube connected by ground glass joints to a stopcock. In each experiment 20 mg. of 2,2'-azobisisobutyronitrile and 2.0 g. of the vinyl ester were weighed into the tube. The system was flushed with nitrogen and evacuated to 0.025 mm. The stopcock was closed and the lower half of the tube immersed in an oil bath at 90°C. for the time indicated in Table I. After the tube and contents had cooled to room temperature, the contents were dissolved in 10 ml. of benzene, and the solution was poured into 50 ml. of methanol. The polymer was separated and the purification procedure repeated until all of the unchanged monomer was removed from the polymer.

### Copolymerization

The general procedure followed in these experiments was to charge a 4-oz. polymerization bottle with vinyl ester monomer, water (38 ml.), Triton X-301 (Rohm and Haas, sodium alkylaryl polyether sulfate, 20% aqueous



dispersion) (3.0 g.), sodium chloride (0.6 g.) and potassium persulfate solution (4 ml. of a 2.5% aqueous solution). The bottle was cooled in a Dry Ice-acetone bath. An excess of liquid vinyl chloride was added and the bottle allowed to warm up so vinyl chloride distilled out of the bottle until the desired weight remained. The bottle was capped, allowed to warm up to room temperature, placed in a 50°C. bath, and tumbled for 65 hr. The bottle was removed, cooled, and opened. The latex was coagulated by a sodium chloride-sulfuric acid-water solution. The polymer was collected on a filter, washed well with water and then methanol. A 10% solution of the polymer in tetrahydrofuran was prepared, poured into excess methanol, and stirred in a Waring Blendor. The polymer was washed well with methanol, and dried under reduced pressure. The results are collected in Table II.

In some of the experiments a 2-oz. polymerization bottle was used and the recipe described was reduced by 75%.

### References

1. Port, W. S., E. F. Jordan, Jr., W. E. Palm, L. P. Witnauer, J. E. Hansen, and D. Swern, *Ind. Eng. Chem.*, **47**, 472 (1955).
2. (a) C. S. Marvel, Y. Shimuro, and F. C. Magne, *J. Polymer Sci.*, **45**, 13 (1960); (b) C. S. Marvel, T. K. Dykstra and F. C. Magne, *J. Polymer Sci.*, **62**, 369 (1962).
3. Scholfield, C. R., and J. C. Cowan, *J. Am. Oil Chemists' Soc.*, **36**, 631 (1959).
4. Friedrich, J. P., H. M. Teeter, J. C. Cowan, and G. E. McManis, *J. Am. Oil Chemists' Soc.*, **38**, 329 (1961).
5. Lyness, W. I., and F. W. Quackenbush, *J. Am. Oil Chemists' Soc.*, **32**, 520 (1955).
6. Teeter, H. M., and J. E. Jackson, *J. Am. Oil Chemists' Soc.*, **26**, 535 (1949).
7. Stirton, A. J., B. B. Schaeffer, A. A. Stawitzke, J. K. Weil, and W. C. Ault, *J. Am. Oil Chemists' Soc.*, **25**, 365 (1948).
8. Adelman, R. L., *J. Org. Chem.*, **14**, 1057 (1949).
9. Marvel, C. S., and W. G. DePierri, *J. Polymer Sci.*, **27**, 39 (1958).

### Résumé

Des homopolymères et des copolymères avec le chlorure de vinyle ont été préparés à partir des esters vinyliques du mélange hydrogéné et cyclisé des acides linoléique, 9,10-dichlorostéarique, 8,10,12,13-tétrachlorostéarique, 13,14-dichlorobehénique, 9(10)-phényle stéarique et behénique technique. Le 1 >, 14-dichlorobehénate de vinyle (29%) chlorure de vinyle (71%) fournit un copolymère présentant une température de cassure de -2°C. Tous les autres copolymères avec le chlorure de vinyle possédant des températures de cassure de 16°C ou plus et se comportent comme des plastiques beaucoup plus rigides.

### Zusammenfassung

Aus den Vinylestern von gemischt hydrolysiertes zyklisierte Linolensäure, 9,10-Dichlorstearinsäure, 9,10,12,13-Tetrachlorstearinsäure, 13,14-Dichlorbehensäure, 9-(10)-Phenylstearinsäure und technischer Behensäure wurden Homopolymere und Vinylchlorid-Copolymere hergestellt. Ein aus Vinyl-13,14-dichlorbehenat (29%) und Vinylchlorid (71%) hergestelltes Copolymeres besass einen Sprödigkeitspunkt von -2°C. Alle anderen Vinylchloridcopolymeren hatten Sprödigkeitspunkte von 16°C und darüber und waren in ihrem Verhalten starren Kunststoffen ähnlich.

Received April 12, 1963

Revised May 17, 1963

## Cationic Polymerization of 9-Vinylanthracene\*

R. H. MICHEL, *Film Department, E. I. du Pont de Nemours & Company, Inc., Buffalo, New York*

### Synopsis

9-Vinylanthracene has been polymerized in a wide variety of cationic systems. Under these conditions of polymerization, the vinyl group and the center ring of the anthracene nucleus act as a 1,3,5-triene system. Evidence for the structure of the product was obtained from infrared, ultraviolet, and particularly nuclear magnetic resonance spectroscopy. In the presence of trifluoroacetic acid, poly-9-vinylanthracene was converted to poly-9,10-dimethyleneanthracene.

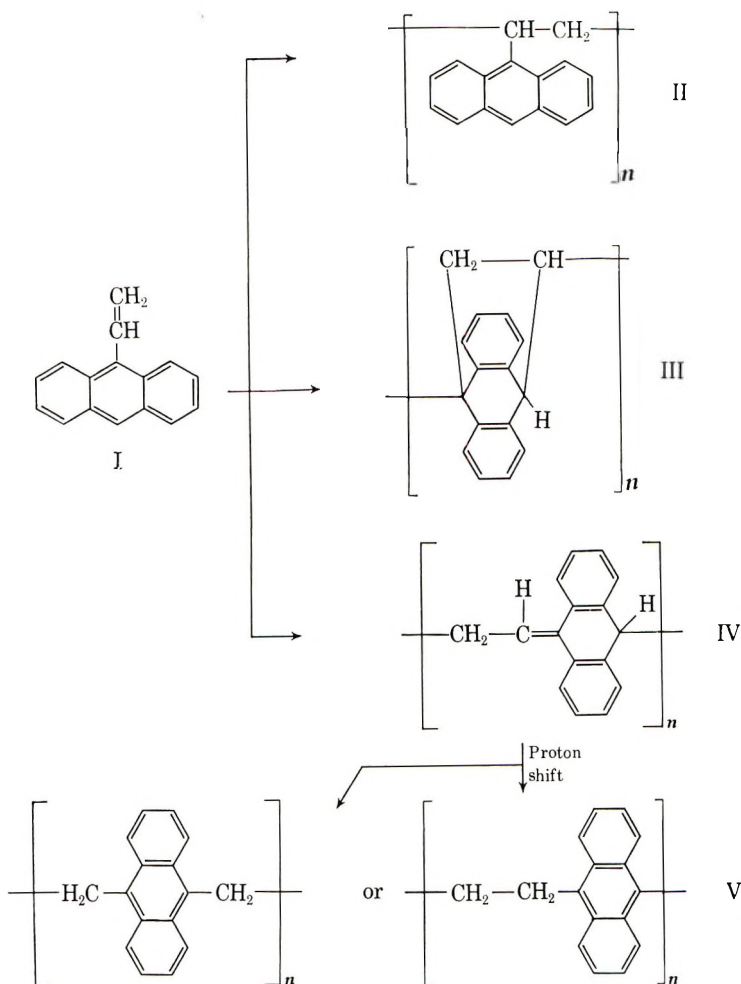
### INTRODUCTION

Bergmann and Katz<sup>1</sup> reported that the cationic polymerization of 9-vinylanthracene (I) yielded a normal vinyl type polymer (II) and that free radical copolymerization with styrene gave an anthracene group-containing polymer. The free radical homopolymerization was reported to be very slow, and the products were not completely characterized. Cherkasov and Voldaikina<sup>2</sup> examined the styrene copolymer in greater detail and found that it has a complex structure due to reactions involving the anthracene nucleus. Natta and co-workers<sup>3</sup> reported coordination polymerization studies on a large series of vinyl aromatic monomers including 9-vinylanthracene. However, such polymerization systems were not effective with 9-vinylanthracene.

Our work in this area was stimulated by some interesting possibilities in the polymerization of 9-vinylanthracene. Aside from the normal vinyl polymerization, 9-vinylanthracene might polymerize by repeated addition

If the polymerization of 9-vinylanthracene proceeded by the latter route, it would yield a product which could be converted by a simple proton shift to the *p*-xylylene-like aromatic polymer, poly-9,10-dimethyleneanthracene (V). Polymers with this structure have been of interest for

\* We have just recently become aware of the work of Inoue et al., *J. Chem. Soc. Japan, Ind. Chem. Sect.*, **65**(8), 1286 (1962), which describes the cationic polymerization of 9-vinylanthracene. Two types of products were described by these workers—a soluble one which appears from its properties to be identical to the polytriene form prepared by us and an insoluble one which Inoue believes to be crosslinked material.



some time because of their high melting points. Indeed, 9,10-dimethyleneanthracene polymer has been prepared by various condensation reactions by a number of workers, including Marvel<sup>4</sup> and more recently Golden.<sup>5</sup> However, the insolubility of this polymer appears to make the preparation of high molecular weight polymer by these direct methods impossible.

## RESULTS AND DISCUSSION

### I. Polymerization of 9-Vinylanthracene

We were initially unaware of the work of Natta regarding the coordination polymerization of 9-vinylanthracene. Consequently we attempted polymerization with 1:1 mole ratios of titanium tetrachloride-triisobutylaluminum at room temperature in heptane. Polymers with molecular weights of 1000 to 2000 were obtained. However, it was soon learned that the triisobutyl aluminum was superfluous and that the polymerization was cationic.

In the hope of obtaining higher molecular weight products at lower temperatures, we investigated a number of solvents and found several in which 9-vinylanthracene was soluble at temperatures from  $-74$  to  $-130^{\circ}\text{C}$ . The solvents which were examined included heptane, toluene, methylene chloride, carbon disulfide and dichlorofluoromethane. Carbon disulfide and the chlorinated hydrocarbons were most satisfactory. The cationic initiators used were titanium tetrachloride, stannic chloride, and borontrifluoride.

The data in Table IV of the Experimental Section show the effect of polymerization temperature on the molecular weight of the products. The highest measured molecular weight was 8800, ( $\eta = 0.04$ ). However, polymer prepared in Freon 21 (du Pont trademark) at  $-130^{\circ}\text{C}$ . having an inherent viscosity of 0.22 is undoubtedly of considerably higher molecular weight. Temperature, solvent type, solvent purity, as well as initiator type and concentration were widely examined. No better results were obtained.

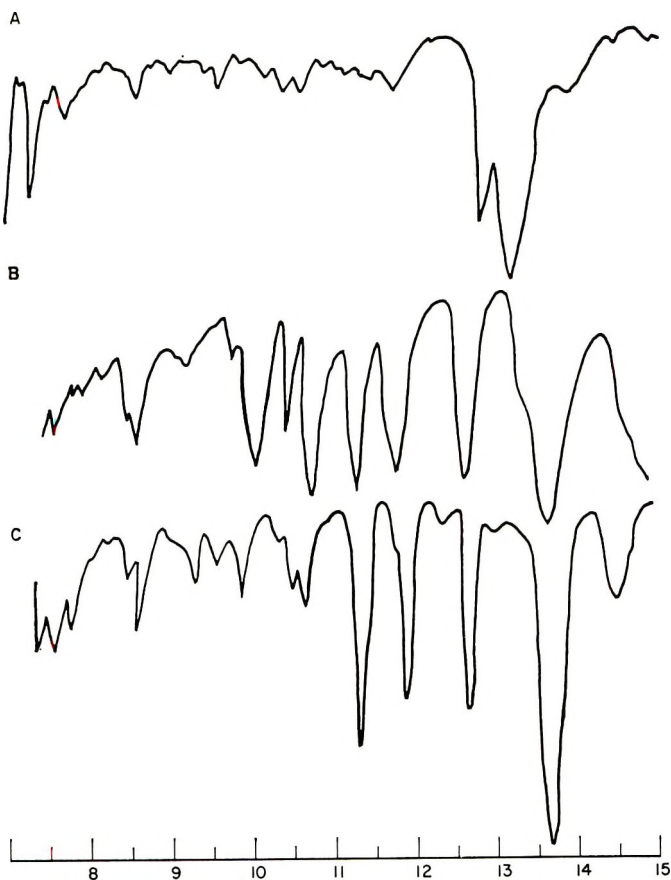


Fig. 1. Infrared spectra (in Nujol mull) of: (A) poly-9-vinylanthracene; (B) 9-vinylanthracene; (C) 9-ethylanthracene.

## II. Structure of Poly-9-vinylanthracene

When the infrared spectrum of cationic poly-9-vinylanthracene was examined, it became apparent that this was not the normal vinyl polymer. Figure 1 compares the infrared spectra of 9-ethylanthracene, the model compound for poly-9-vinylanthracene by normal vinyl polymerization, of 9-vinylanthracene, and of the polymer. Both 9-ethylanthracene and 9-vinylanthracene have a strong band at  $\sim 13.7 \mu$ , not at  $13.2 \mu$  as the polymer has.

Examination of the ultraviolet spectrum of the polymer showed that it

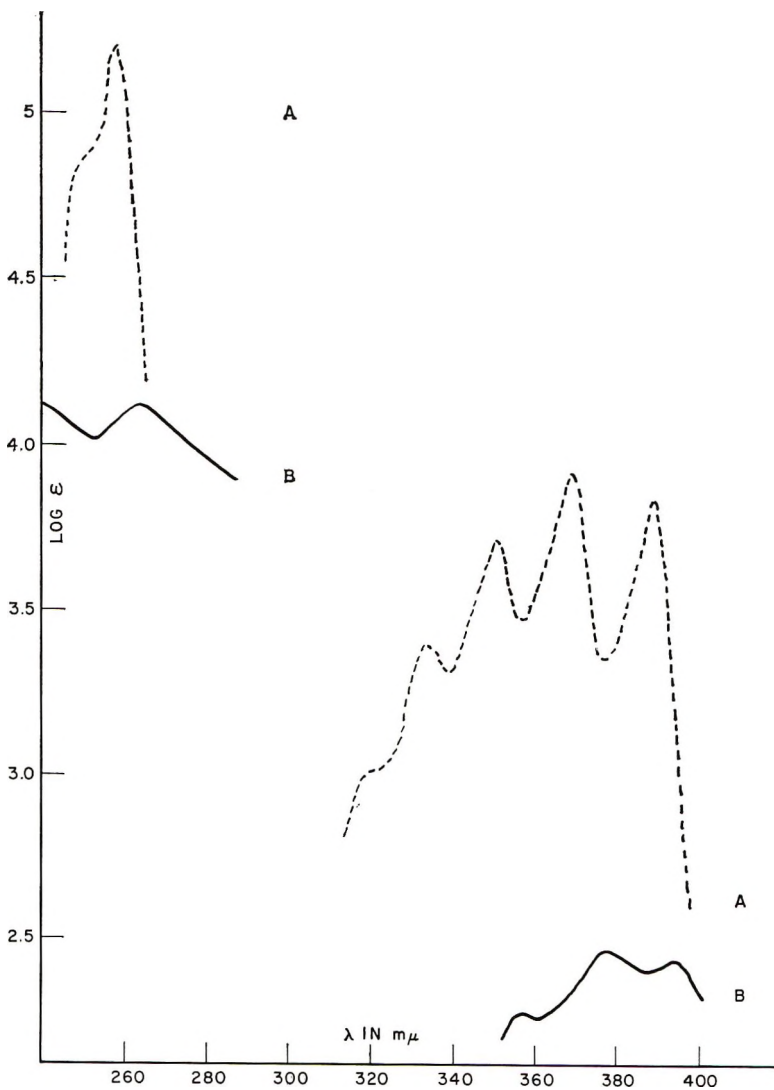


Fig. 2. Ultraviolet spectra (in methylene chloride) of: (A) 9-ethylanthracene; (B) poly-9-vinylanthracene.

TABLE I  
Ultraviolet Extinction Coefficients

	$\lambda_{\max}$ $\sim 370 \text{ m}\mu$	$\lambda_{\max}$ $\sim 260 \text{ m}\mu$
9-Ethylanthracene, $\epsilon_{\max}$	8,400	157,000
Poly-9-vinylanthracene, $\epsilon^*_{\max}$ <sup>a</sup>		
$\eta_{\text{inh}} = 0.03$	2,800	35,000
$\eta_{\text{inh}} = 0.1$	290	13,500

<sup>a</sup>  $\epsilon^*_{\max} = \text{Optical density} \times \text{molecular weight of monomer/grams of polymer per liter.}$

had the qualitative spectrum of an anthracene derivative. However, quantitative considerations indicated that the anthracene structure is a minor constituent of this material. Less strongly absorbing material makes up a larger portion of the polymer. Figure 2 compares the ultraviolet spectra of 9-ethylanthracene and the polymer. Table I compares the extinction coefficients of 9-ethylanthracene and of this polymer. Note the decrease in extinction coefficient on going from the model compound to polymeric material and the further decrease in extinction coefficient with increasing molecular weight. This indicates that the anthracene structure is present either as an endgroup or as a chain abnormality which becomes rarer under conditions where higher polymer forms. Such an abnormality could be due to ordinary vinyl polymerization. Evidence for this interpretation is provided by the infrared spectra in Figure 3 which indicates that the 9-alkylanthracene characteristics decrease as the molecular weight increases. Note the disappearance of the band at  $13.8 \mu$  in higher polymers.

The above results suggest strongly that the major portion of the polymer has a dihydroanthracene structure. However, to be certain of the struc-

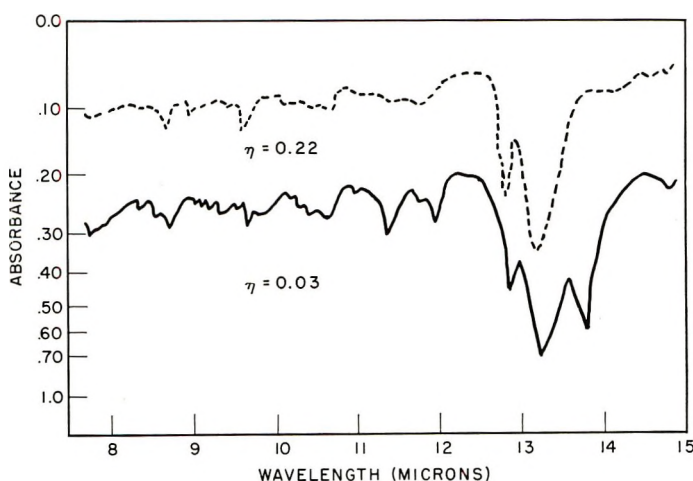


Fig. 3. Effect of molecular weight on infrared spectra of polymer.

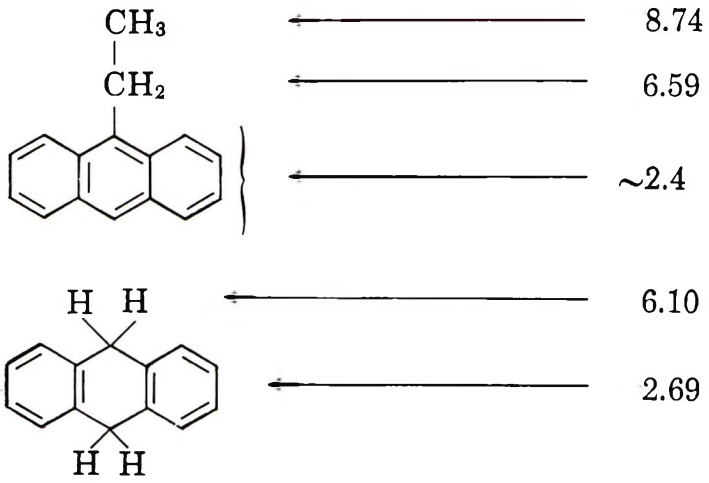


Fig. 5. NMR spectrum of poly-9-vinylanthracene.

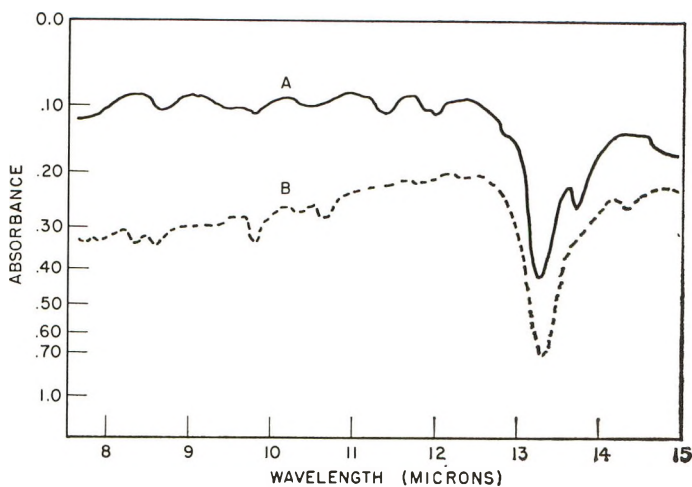


Fig. 6. Infrared spectra of: (A) aromatized poly-9-vinylanthracene; (B) coupling product of 9,10-bis(chloromethyl)anthracene.

ture of the backbone of these cationic polymers it was decided to study them by nuclear magnetic resonance spectroscopy (NMR). Model compounds were prepared in order to determine the location of the hydrogen absorptions which must be considered in deciding the structure of this polymer. Figure 4 shows the chemical shift values ( $\tau$ ) which were found for 9,10-ethano-9,10-dihydroanthracene, for 9,10-dihydroanthracene, and for 9-ethylanthracene in carbon disulfide solution (Varian DP 60 instrument). It should be noted that the dihydro hydrogens absorb at a  $\tau$  value of approximately 6. Ordinary alkyl hydrogen absorbs above 8. Figure 5 is the NMR spectrum of the polymer in a 40–50% carbon disulfide solution. There are four distinct absorptions. The first at 2.80 is obviously due to the aromatic hydrogen. The small peak on its shoulder at 3.94 was identified as olefinic hydrogen.<sup>6</sup> At 6.05 one finds the dihydro hydrogens. The absorption at 7.27 was identified according to the literature as allylic hydrogen. Note that there are no absorptions above 7.5 thus excluding the two structures which would require such absorptions, the Diels-Alder type polymer and the normal vinyl polymer.

The relative areas of these absorptions are indicated in Figure 5. They fit closely the expected ratios. The only exception is the olefinic hydrogen which is on the shoulder of a much stronger absorption band.

### III. Conversion of Poly-9-vinylanthracene to Poly-9,10-dimethyleneanthracene

With the structure established, it was now of interest to determine whether this polymer could be converted via a proton shift to the poly-*p*-xylylene-like poly-9,10-dimethyleneanthracene. When poly-9-vinylanthracene was dissolved in methylene chloride and treated with an excess of



TABLE II  
Effect of Proton Shift in Poly-9-vinylanthracene on Ultraviolet Extinction Coefficients<sup>a</sup>

	$\lambda_{\max}$ $\sim 400 \text{ m}\mu$	$\lambda_{\max}$ $\sim 380 \text{ m}\mu$	$\lambda_{\max}$ $\sim 260 \text{ m}\mu$
Original polymer, $\epsilon^*_{\max}$	570	650	16,300
Rearranged polymer, $\epsilon^*_{\max}$	4,800	5,600	52,000
9,10-Dimethylanthracene, $\epsilon_{\max}^b$	4,500	5,000	170,000

<sup>a</sup> Measured in methylene chloride.

<sup>b</sup> Data of Phillips and Cason.<sup>7</sup>

trifluoroacetic acid, a greenish-yellow precipitate soon formed. In one experiment, a soluble fraction was isolated from the methylene chloride solution. The infrared spectra of the soluble and insoluble products were very much alike. Neither fraction showed the absorption at  $12.8 \mu$  which in the parent polymer is believed to be due to the exocyclic double bond. However, there was no evidence of the addition of trifluoroacetate ion. The remaining strong band at  $13.2 \mu$  was attributed to the 9,10-dialkylanthracene structure. Figure 6 compares the infrared spectrum of this rearrangement product to that of poly-9,10-dimethyleneanthracene prepared according to Golden via the condensation of 9,10-bis(chloromethyl)anthracene by phenyllithium. The spectra are very similar. The rearrangement product has an additional weaker band at  $13.8 \mu$  which is probably due to some 9-alkylanthracene chain irregularity.

The ultraviolet spectrum of the rearranged poly-9-vinylanthracene showed that the extinction coefficients had increased as much as tenfold and that these extinction coefficients were in the same range as those of the model compound 9,10-dimethylanthracene.<sup>7</sup> These data are given in Table II.

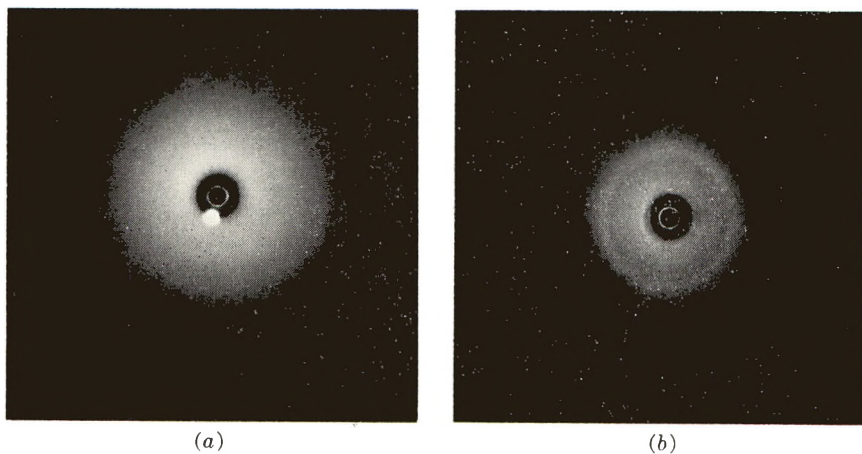


Fig. 7. X-ray diffraction diagrams of: (A) poly-9-vinylanthracene; (B) poly-9,10-dimethyleneanthracene derived from it.

TABLE III  
Conversion of Poly-9-vinylanthracene to Poly-9,10-dimethyleneanthracene

Solvent (CH <sub>2</sub> Cl <sub>2</sub> ), ml.	Reagent (CF <sub>3</sub> - COOH), ml.	Poly-9- vinyl- anthracene, g.	Time, hr.	Temp., °C.	Product
None	10	0.1	2	~70	Fusion point 255–280°C. <sup>a</sup>
5	1	0.2	~18	Room tempera- ture	<sup>2</sup> / <sub>3</sub> Insoluble. Fusion point 290–320°C. Soluble portion pre- cipitated by ethanol.
2.5	0.05	0.05	~18	Room tempera- ture	All insoluble Infusible <360°C.

<sup>a</sup> Poly-9-vinylanthracene generally melted at 210–230°C. with some discoloration. Poly-9,10-dimethyleneanthracene prepared by the condensation of 9,10-bis(chloromethyl)anthracene was infusible <360°C.

X-ray diffraction (Fig. 7) has shown a definite increase in the crystallinity of the polymer on conversion with trifluoroacetic acid. Polymer fusion temperatures (Table III) were substantially raised by the aromatization.

## EXPERIMENTAL

### I. Preparation of 9-Vinylanthracene

The preparation of 9-vinylanthracene by acetylation of anthracene followed by reduction to 1-(9'-anthryl)ethanol and subsequent dehydration of this alcohol has been described in the literature.<sup>8,9</sup> The monomer twice recrystallized from methanol melted at 66.5–67.5°C. (lit.<sup>8</sup> m.p. 64–67°C.). No impurities could be found in this monomer by gas chromatography over either Carbowax 1500 at 230°C. or silicone on brick dust at 200°C. Before use, the monomer was given a final drying at 50°C./1.5 mm. Hg and stored over silica gel.

### II. Cationic Polymerization of 9-Vinylanthracene

**A. Polymerization at –74°C. or above.** The catalyst solutions for the cationic polymerizations were prepared in a nitrogen dry-box. Titanium tetrachloride and triisobutyl aluminum were used as either 0.1*M* or 1*M* solutions in cyclohexane. Details concerning other catalysts are given in Table IV, in which the reaction conditions and results for all the cationic polymerizations are summarized. The solvents had been dried over silica gel. Other purification procedures, wherever used, are shown in Table IV. Except where otherwise indicated, the polymerizations were carried out in a four-necked 100-ml. flask equipped with a stirrer, nitrogen inlet, drying tube, and a rubber serum bottle stopper. The equipment was flame-dried. The solvent and monomer were introduced and cooled to the polymeriza-

TABLE IV  
 Cationic Polymerization of 9-Vinylanthracene

Solvent	Vol. solvent, ml.	Amt. monomer, g.	Catalyst	Amt. catalyst, mmoles	Temp., °C.	Time, hr.	Yield, g.	$\eta_{inh}$	M.W. <sup>a</sup>	Remarks
Heptane	25	0.5 (2.45 mmole)	TiCl <sub>4</sub> Al( <i>i</i> -Bu) <sub>3</sub>	0.2	Room temp.	2	0.4	—	1,700	Polymer precipitated during polymerization in heptane
Toluene	25	0.5	TiCl <sub>4</sub> + Al( <i>i</i> -Bu) <sub>3</sub>	0.2	Room temp.	2	0.35	0.03 <sup>b</sup>	1,324	
Toluene	25	0.5	TiCl <sub>4</sub> + Al( <i>i</i> -Bu) <sub>3</sub>	0.2	-31	2	0.45	0.04 <sup>b</sup>	8,800	
CH <sub>2</sub> Cl <sub>2</sub>	25	0.5	Al( <i>i</i> -Bu) <sub>3</sub>	0.2	Room temp.	2	0.39	0.03 <sup>b</sup>	1,880	
CH <sub>2</sub> Cl <sub>2</sub>	25	0.5		0.2	-74	2	0.48	0.08 <sup>b</sup>	>4,800 <sup>c</sup>	
CH <sub>2</sub> Cl <sub>2</sub>	30	0.5		0.2	-72	2	0.5	0.10	—	
CH <sub>2</sub> Cl <sub>2</sub>	25	0.5	TiCl <sub>4</sub>	0.2	Room temp.	2	0.3	0.03	—	Monomer was not entirely soluble but polymer was
CS <sub>2</sub>	2	0.5	TiCl <sub>4</sub>	0.1	-65	2	0.5	0.14	—	

CH <sub>2</sub> Cl <sub>2</sub>	25	0.5	BF <sub>3</sub>	d	-70	2	0.49	0.10	—
CH <sub>2</sub> Cl <sub>2</sub>	30	0.5	SnCl <sub>4</sub> (0.05M in CH <sub>2</sub> Cl <sub>2</sub> )	0.1	-70	2	0.25	0.08	—
CS <sub>2</sub> <sup>e</sup>	20	5 (24.5 mmoles)	TiCl <sub>4</sub>	0.2	-70	2	1.0	0.14	—
CS <sub>2</sub>	20	5	TiCl <sub>4</sub>	1.0	-70	2	4.5	0.15	—
CS <sub>2</sub>	10	5	TiCl <sub>4</sub>	0.1	-70	2	0.1	0.11	—
CHCl <sub>3</sub> <sup>f</sup>	20	1 (5 mmole)	TiCl <sub>4</sub>	0.5	-130	2	0.94	0.13	—
CHCl <sub>3</sub> F	20	1	TiCl <sub>4</sub>	0.05	-130	2	0.74	0.22	—
CHCl <sub>3</sub> F	20	1	TiCl <sub>4</sub>	0.01	-130	2	0	—	—

<sup>a</sup> Measured ebulliometrically in benzene.

<sup>b</sup> Measured in 0.1% benzene solutions at 30°C.; all others in 0.5% benzene solutions;  $\eta_{inh} = \ln \eta_{rel}/c$  (in g./100 ml.).

<sup>c</sup> Foaming prevented accurate measurement.

<sup>d</sup> Polymerization was brought about by introducing a few bubbles of BF<sub>3</sub> gas.

<sup>e</sup> Redistilled from Type 4A Molecular Sieve.

<sup>f</sup> Passed over Drierite.

tion temperature. The catalyst was injected by means of hypodermic syringe. After the appropriate time, the reaction mixture was added to ethanol containing some hydrochloric acid (100 ml. ethanol, 10 ml. concentrated hydrochloric acid). The polymer was separated by filtration and reprecipitated at least once from a methylene chloride solution before it was dried at room temperature under vacuum. Elevated temperatures (70°C.) during drying would frequently bring about oxidation as indicated by carbonyl absorption at  $5.95 \mu$  in the infrared spectrum.

This band would appear also after the polymer had aged at room temperature for a month or more. Reprecipitation of the polymer did not remove the carbonyl band.

**B. Polymerization below  $-74^{\circ}\text{C}$ .** The same type of flask was used as previously described; however, it was equipped with a magnetic stirrer. The center neck was used for the introduction of solvent. The whole apparatus was flame-dried and then placed in a 2-methylbutane bath which was cooled by liquid nitrogen coils. The flow of nitrogen was controlled by a thermocouple and Solenoid valve. The mixture was not cooled below  $-60^{\circ}\text{C}$ . until all the monomer had dissolved (part of it crystallized out on further cooling). In other respects the procedure was the same as at higher temperatures.

### III. Conversion of Poly-9-vinylanthracene to Poly-9,10-dimethyleneanthracene

The conversion of poly-9-vinylanthracene to poly-9,10-dimethyleneanthracene was brought about by exposing the starting material to trifluoroacetic acid neat or in solution in methylene chloride. A stoppered flask was used. Details of the several runs are given in Table III. The insoluble product was isolated by filtration. The filtrate was added to approximately 50 ml. ethanol which in one experiment resulted in the isolation of a soluble fraction. Both fractions were washed with ethanol before they were dried.

### IV. Preparation of Model Compounds

**A. 9-Ethylanthracene.** 9-Ethylanthracene was prepared by the addition of ethylmagnesium bromide to anthrone according to Sieglitz and Marx.<sup>10</sup> The melting point of the product was  $55\text{--}56^{\circ}\text{C}$ . (lit. m.p.  $59^{\circ}\text{C}$ .).

**B. 9,10-Ethano-9,10-dihydroanthracene.** This compound was prepared by the addition of ethylene to anthracene as described by Thomas.<sup>11</sup> The product was heavily contaminated with anthracene. A 93% pure 9,10-ethano-9,10-dihydroanthracene was obtained from the most toluene-soluble fraction. The purity figure is based on anthracene's absorption at  $356 \text{ m}\mu$ . The melting range was  $136\text{--}142^{\circ}\text{C}$ . (lit. m.p.  $142\text{--}143^{\circ}\text{C}$ .).

### V. Preparation of Poly-9,10-dimethyleneanthracene

9,10-Bis(chloromethyl)anthracene was prepared according to Miller *et al.*<sup>12</sup> It melted at  $256\text{--}258^{\circ}\text{C}$ . (dec.) (lit. m.p.  $258\text{--}260^{\circ}\text{C}$ .). The

condensation of 9,10-bis(chloromethyl)-anthracene was carried out with phenyllithium as described by Golden.<sup>6</sup>

The author wishes to acknowledge the generous help of R. C. Golike and T. J. Dougherty with the NMR work, as well as the loan of equipment from J. J. Sparapany for the polymerizations at  $-130^{\circ}\text{C}$ .

### References

1. Bergmann, E. D., and Katz, D., *J. Chem. Soc.*, **1958**, 3216.
2. Cherkasov, A. S., and K. G. Voldaikina, *Vysokomol. Soedin.*, **3**, 570 (1961).
3. Natta, G., F. Danusso, and D. Sianesi, *Makromol. Chem.*, **28**, 253 (1958).
4. Marvel, C. S., and R. Z. Greenly, Ph.D. Dissertation, University of Illinois, 1961.
5. Golden, J. H., *J. Chem. Soc.*, **1961**, 3746.
6. Jackman, L. M., *Nuclear Magnetic Resonance Spectroscopy*, International Series of Monographs on Organic Chemistry, Vol. 5, Pergamon Press, London, 1957.
7. Phillips, D. D., and J. Cason, *J. Am. Chem. Soc.*, **74**, 2934 (1953).
8. Hawkins, E. G. E., *J. Chem. Soc.*, **1957**, 3859.
9. Sianesi, D., *Gazz. Chim. Ital.*, **89**, 1749 (1959).
10. Sieglitz, A., and R. Marx, *Ber.*, **56**, 1621 (1923).
11. Thomas, C. L., U.S. Pat. 2,406,645 (August 27, 1946).
12. Miller, M. W., R. W. Amidon, and P. O. Towney, *J. Am. Chem. Soc.*, **77**, 2846 (1955).

### Résumé

Le 9-vinylanthracène a été polymérisé avec une grande variété de systèmes cationiques. Dans ces conditions de polymérisation, le groupe vinyle et le cycle central du noyau de l'anthracène agissent comme un système 1,3,5-triène. La structure des produits a été mise en évidence par infra-rouge, analyse ultraviolette et surtout par résonance nucléaire magnétique. En présence d'acide trifluoroacétique le poly-9-vinylanthracène est transformé en poly-9,10-diméthylène-anthracène.

### Zusammenfassung

9-Vinylanthracen wurde mit einer Anzahl kationischer Systeme polymerisiert. Unter diesen Bedingungen verhalten sich die Vinylgruppe und der mittlere Ring des Anthracenkernes wie ein 1,3,5-Triensystem. Die Struktur des gebildeten Produktes wurde durch IR- und UV-Spektroskopie sowie besonders durch magnetische Kernresonanz-Spektroskopie aufgeklärt. In Gegenwart von Trifluoressigsäure wurde Poly-9-vinylanthracen in Poly-9,10-dimethylenanthracen umgewandelt.

Received April 12, 1963

## Thermoelectric Determination of Polymer Molecular Weights\*

MANFRED J. R. CANTOW, ROGER S. PORTER, and JULIAN F. JOHNSON, *California Research Corporation, Richmond, California*

### Synopsis

An apparatus is described for the determination of number-average molecular weights, based on the thermoelectric method as proposed by Hill. With this improved instrument, temperature differences of down to approximately  $5 \times 10^{-5}$ °C. can be recorded. This allows determination of molecular weights up to 40,000 for the case of coiled macromolecules in a poor solvent. The accuracy of measurements, for all molecular weights, has been established by using benzene solutions of polyisobutenes of narrow and defined molecular weight distributions.

### INTRODUCTION

The most sensitive technique for determining polymer number-average molecular weight is the osmotic method. Its disadvantage, however, is the problem of membrane permeability. This determines the magnitude of the lowest molecular weight that still contributes to the measured osmotic pressure. The influence of this effect increases, at any given average molecular weight, with polymer molecular weight inhomogeneity.<sup>1</sup>

Another colligative method, not afflicted with the disadvantage mentioned above, is the indirect determination of vapor pressure lowering of a solution by the thermoelectric method described by Hill.<sup>2</sup> The measured quantity is the steady-state temperature difference established when a drop of solution and one of solvent are exposed to solvent vapor, with heat exchange occurring only through the vapor. This temperature difference is proportional to the difference in vapor pressure of the two drops. The present paper discusses the modification and application of a commercial apparatus of this type to polymers with molecular weights up to 40,000.

### APPARATUS

A Model 301 vapor pressure osmometer (manufacturer: Mechrolab Mountain View, California) was used originally, which operates at 39°C. Calibration plots of dial readings,  $\Delta R$ , after 10 min. as a function of solute molalities,  $m$ , of solutes of known molecular weights (4-methylbenzo-

\* Presented in part at the 144th meeting of the American Chemical Society, Los Angeles, April 1963.

TABLE I  
Calibration Equations for Four Solvents

Solvent	$\Delta R$	Correlation coefficient	% of $E_{\max}$
Acetone	$0.18 + 322 m$	0.9998	93
Benzene	$0.52 + 317 m$	0.9982	80
Chloroform	$1.11 + 604 m$	0.9995	98
Carbon tetra- chloride	$0.88 + 628 m$	0.9996	87

phenone, benzil, methyl stearate, 1-bromooctadecane, dotriacontane, tristearine) were established for acetone, benzene, chloroform, and carbon tetrachloride as solvent. Straight line relationships with small intercepts were obtained in all cases.

The last column in Table I gives the percentage reached from the maximum possible efficiency,  $E_{\max}$ , calculated according to<sup>3</sup>

$$E_{\max} = rRB/Lm_s \quad (1)$$

where  $r$  = resistance of the thermistor,  $R$  = gas constant,  $L$  = molar latent heat of vaporization of the solvent,  $m_s$  = molality of the solvent, and  $B$  is defined by

$$d \ln r/dT = - B/T^2 \quad (2)$$

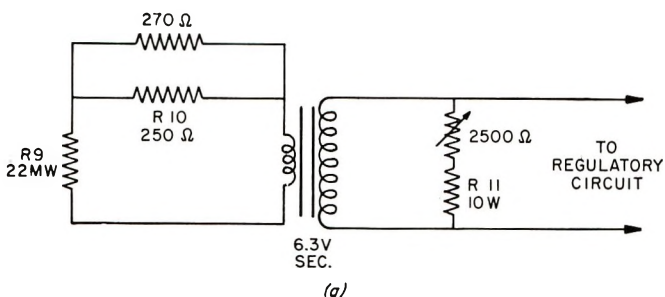
Detailed inspection of the calibration curves seemed to reveal in all four plots an increasing slope at molalities,  $m$ , lower than 0.01. It was attempted to fit the  $\Delta R$  data below this concentration with least square lines going through the origin. The following relations obtained are shown in Table II.

TABLE II  
Calibration Equations for Four Solvents for Molalities below 0.01

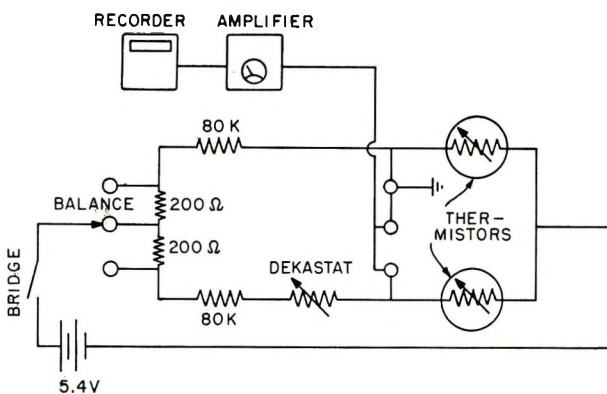
Solvent	$\Delta R$	Correlation coefficient
Acetone	$341 m$	0.9996
Benzene	$768 m$	0.9999
Chloroform	$734 m$	0.9972
Carbon tetrachloride	$748 m$	0.9986

The excellent correlation in Table II seems to justify this procedure. Calibration measurements were carried out down to molalities near 0.003, where  $\Delta R$  readings had a reproducibility within  $\pm 20\%$ . During the course of the investigation, this sensitivity was found to be too low for measuring high molecular weights. Consequently, modifications were made on the commercial instrument. (The manufacturer states improved sensitivity for model 301A.)





(a)



(b)

Fig. 1. Schematic diagrams of (a) modified heater circuit of vapor pressure osmometer; (b) thermistor bridge circuit of vapor pressure osmometer.

Figure 1a shows the additions to the heater circuit. The main heater,  $R_{11}$ , was given a lower output by connecting a 2500-ohm rheostat in series. The small heater,  $R_9$ , was given a higher output by shimming  $R_{10}$  with a 270-ohm resistor. The effect of these alterations was a much shorter non-heating period of about 5 sec., followed by a heating period of approximately the same duration. Thus, the temperature cycle due to the heating period was reduced to about  $1/50$  of the original value.

The thermistor bridge circuit was redesigned, as shown in Figure 1b. Here, the thermistors are supplied with a nearly constant current source, resulting in a voltage output twice as high as before. A Leeds and Northrup 9835-A stabilized dc microvolt amplifier was used, together with a 1-mv. Leeds and Northrup Speedomax G recorder. A new set of thermistors and a thermoregulator set at  $37^\circ\text{C}$ . were employed.

The calibration was carried out with benzene solutions of benzil and dotriacontane. Figure 2 shows as an example a 0.00083 molal solution of dotriacontane. The base line appears very stable; the fluctuations are estimated to be less than  $\pm 5 \cdot 10^{-5}^\circ\text{C}$ . The illumination of the measuring

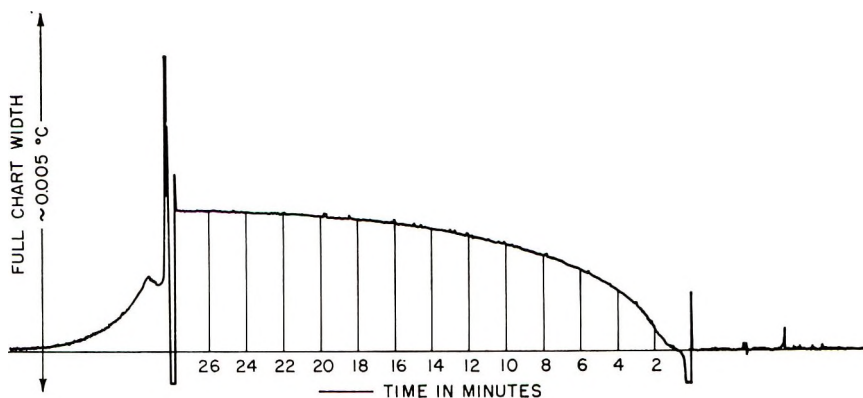
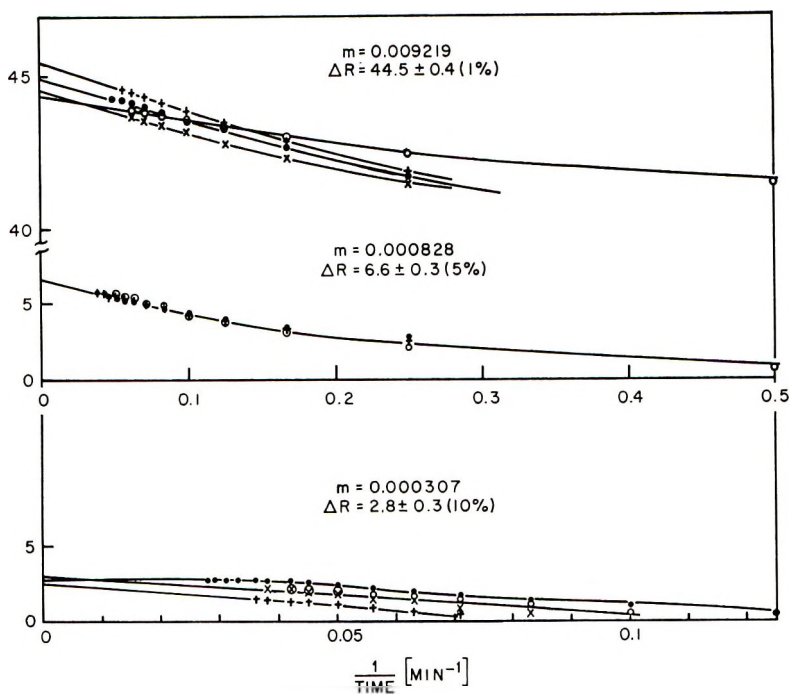


Fig. 2. Sample of recorder chart from vapor pressure osmometer.

Fig. 3. Extrapolation of  $\Delta R$  readings.

chamber is turned on only while applying the drops, because exposure of the thermistor to light is registered immediately on the recorder chart. This is the origin of the first peak in Figure 2. Application of the solution and replenishment of the solute drop cause the strong deflections seen next in time on the diagram. By decreasing the Dekastat setting, the pen is brought back on the chart, if necessary (manual attenuation).

To obtain a measurement, the  $\Delta R$  reading, as in Figure 2, is extrapolated to infinite time by plotting  $\Delta R$  as a function of reciprocal time (in minutes)

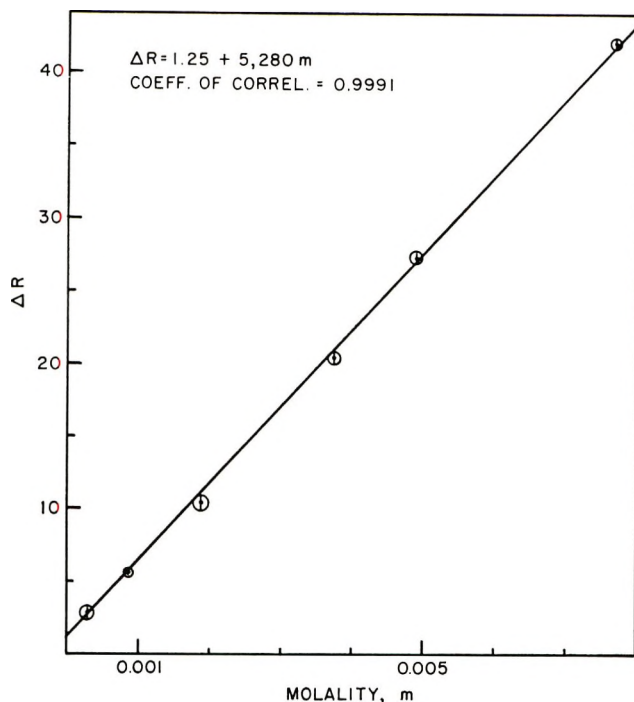


Fig. 4. Calibration curve, benzene, 37.0°C.

as shown in Figure 3. This procedure gives a limiting maximum value. Figure 4 gives the calibration curve for benzene. The limit of error, also shown in Figure 4, was obtained by reproducing the measurements 3 to 6 times. The calibration equation for benzene is

$$\Delta R = 1.25 + 5280m \quad (3)$$

## MEASUREMENTS ON POLYMERS

### 1. Original Apparatus

The measurements were performed on sharp fractions of polyisobutene. The fractionation has been described in detail elsewhere.<sup>4</sup> The first series of molecular weight determinations was carried out in chloroform solutions. Ten fractions, ranging from 3,000 to 80,000 in molecular weight, as determined by intrinsic viscosities in carbon tetrachloride at 30°C.,<sup>5</sup> were measured at 2-9 concentrations,  $c$  (g./1000 g., solvent), between 5 and 30. A plot was made for  $\Delta R/c$  versus  $c$ , according to the formula

$$\Delta R/c = (A/M_n) + Bc + Cc^2 + \dots \quad (4)$$

This is an extended form of the equations in Table II, accounting for a possible concentration dependence of molecular weight. Such plots scattered

badly and could not be evaluated. Graphical representations of  $\Delta R$  as a function of  $c$ , according to eq. (4a), however,

$$\Delta R = (A/M_n) c + Bc^2 \quad (4a)$$

gave good straight lines going through the origin, i.e., no  $B$  coefficient could be detected. The molecular weights thus obtained are plotted versus the intrinsic viscosities,  $[\eta]$ , in deciliters per gram, measured in carbon tetrachloride at 30°C. (see Fig. 5, circles). Figure 5 shows that high molecular weights assume unrealistically low values. This may be due in part to neglecting the zero effect. It is probable, however, that no reliable measurements can be made if polymer molecules in solution overlap considerably, due to high concentration.

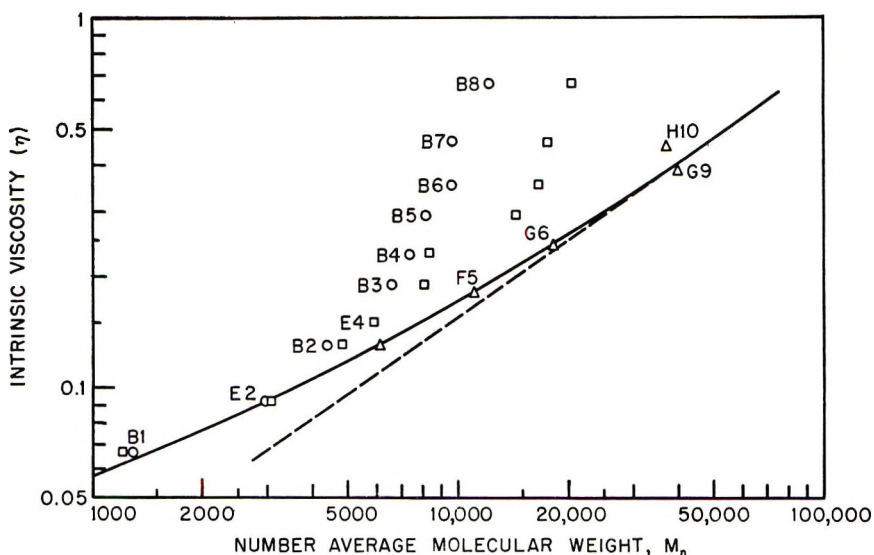


Fig. 5. Intrinsic viscosity  $[\eta]$  in  $\text{CCl}_4$  at 30°C. as a function of molecular weight: (O)  $\text{CHCl}_3$ ; (□) benzene, original instrument; (Δ) benzene, improved instrument.

If a poorer solvent than chloroform could be used, the polyisobutene molecules would occupy a smaller volume. For this reason, the measurements were repeated in benzene solutions ( $\theta = 24^\circ\text{C}.$ ) at 39°C. It should be noted from Table II that the readings in benzene at the same molality amount to only 50% of those in chloroform, i.e., comparing solvent efficiency the latter would be preferable. The measurements in benzene were evaluated in the same way as the ones in chloroform. Again, the data points could be fitted well by straight lines going through the origin in plots of  $\Delta R$  versus  $c$  for each fraction. The molecular weights calculated from the slopes are represented by squares in Figure 5. It can be seen that the upturn occurs at a considerably higher molecular weight (about 15,000 as compared to 6,000 with the better solvent). This seems to substantiate the concept of a limiting concentration mentioned above.

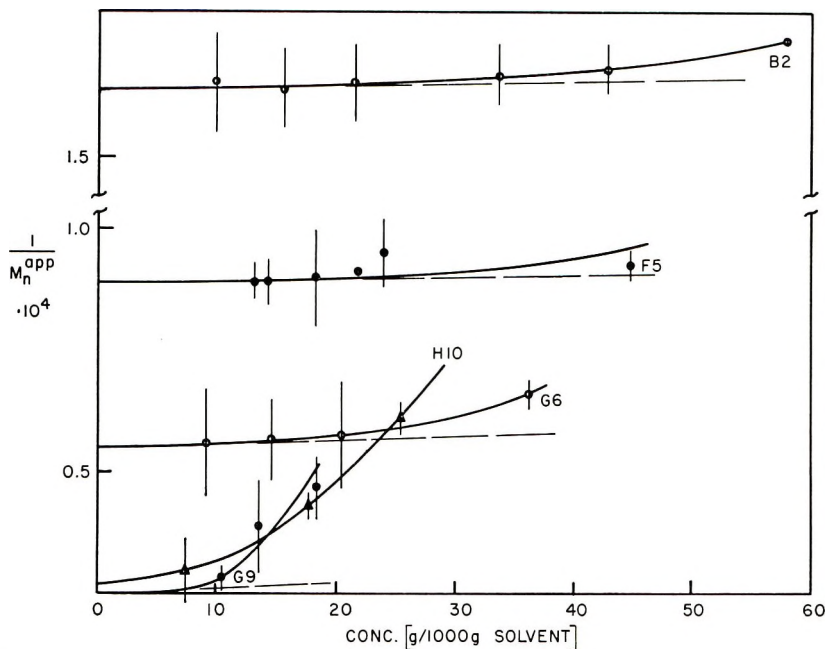


Fig. 6. Extrapolation of reciprocal apparent molecular weights to zero concentration.

## 2. Improved Apparatus

The measurements on five polyisobutene fractions were carried out and evaluated in the same manner as described for the calibration. From the  $\Delta R$  values at infinite time, the apparent molecular weight,  $M_n^{app}$ , was calculated for each concentration, according to eq. (3). In Figure 6 the reciprocals of these values are plotted versus concentrations. The extrapolations to zero concentration on samples G9 and H10 are uncertain. The intercepts have been reconfirmed, however, by plots of the  $1/M_n^{app}$  values versus the square of the concentrations, which give good straight line extrapolations.

The molecular weights obtained from Figure 6 are compiled in Table III and represented on Figure 5 by triangles. The resulting Mark-Houwink relation agrees with the one given by Fox and Flory<sup>5</sup> for polyisobutene fractions in the higher molecular weight region. At lower molecular weights, the curve turns up as previously observed.<sup>5</sup>

TABLE III  
Results of Molecular Weight Determinations

Fraction	$[\eta]_{\text{CCl}_4}^{30^\circ\text{C}}$	$\bar{M}_n$
B2	0.129	6,100
F5	0.181	11,200
G6	0.240	18,200
G9	0.380	40,000

## DISCUSSION

It was shown experimentally that the range of the instrument could be extended from 6,000 to approximately 15,000 by using a poorer solvent, although the measured quantity  $\Delta R$  was smaller in this case. By using a more sensitive instrument, capable of handling more dilute solutions, the molecular weight limit was extended to about 40,000. It seems that measurements with this apparatus have to be performed below a certain limiting concentration, varying with molecular weight and solvent, in order to give reliable results.

The authors are indebted to Mr. R. F. Klaver for his assistance in improving the instrument.

## References

1. Meyerhoff, G., *Z. Elektrochem.*, **61**, 325 (1957).
2. Hill, A. V., *Proc. Roy. Soc. (London)*, **A127**, 9 (1930).
3. Brady, A. P., H. Huff, and J. W. McBain, *J. Phys. Chem.*, **55**, 304 (1951).
4. Cantow, M. J. R., R. S. Porter, and J. F. Johnson, *Nature*, **192**, 752 (1962); *J. Polymer Sci.*, **C1**, 187 (1963).
5. Fox, T. G., Jr., and P. J. Flory, *J. Phys. Chem.*, **53**, 197 (1949).

## Résumé

On décrit un appareil pour déterminer les poids moléculaires moyens en nombre basé sur la méthode thermoélectrique proposée par Hill. Avec cet appareil perfectionné on peut enregistrer des différences de température d'environ  $5.10^{-5}$  °C. Cela permet de déterminer les poids moléculaires jusqu'à 40.000 dans le cas de macromolécules en pelote dans un solvant pauvre. La précision des mesures, pour tous les poids moléculaires, a été établie en utilisant des solutions benzéniques de polyisobutène à distribution étroite et définie du poids moléculaire.

## Zusammenfassung

Es wird ein Apparat zur Bestimmung des Zahlenmittels des Molekulargewichtes auf der Basis der von Hill vorgeschlagenen thermoelektrischen Methode beschrieben. Mit diesem verbesserten Gerät können Temperaturdifferenzen bis etwa  $5.10^{-5}$  °C gemessen werden. Dadurch ist es möglich, im Falle verknäuelter Makromoleküle in einem schlechten Lösungsmittel Molekulargewichte bis hinauf zu 40000 zu bestimmen. Die Messgenauigkeit wurde bei allen Molekulargewichten an Benzollösungen von Polyisobutenen engere und definierter Molekulargewichtsverteilung bestimmt.

Received May 21, 1963

## Preparation and Polymerization of 1,2-Epoxypropyl 2,3,4,6-Tetra-*O*-acetyl- $\beta$ -D-glucopyranoside\*

P. DAS GUPTA and ROY L. WHISTLER, *Department of Biochemistry,  
Purdue University, Lafayette, Indiana*

### Synopsis

Allyl D-glucopyranoside tetraacetate is prepared by reaction of acetobromo-D-glucose with allyl alcohol. The glycoside is not readily polymerized by free radical mechanism but on conversion to the epoxide with peracids, polymerization is easily induced with triethylaluminum. The product with a D.P. of 250 is soluble in organic solvents. On alkaline deacetylation the hydrophilic polymer is water soluble but the aqueous solution possess comparatively low viscosity.

### INTRODUCTION

Polymerization of D-glucose derivatives offers a potential route to the preparation of polymers with new properties, among which could be hydratability and solubility.

In the work undertaken here allyl D-glucopyranoside tetraacetate is used as the starting material. It can easily be prepared by the classical Koenigs-Knorr reaction of acetobromo-D-glucose with allyl alcohol. The glycoside is not readily polymerized by free radical mechanisms but on conversion to the epoxide, polymerization is easily induced. Olefin oxides can be polymerized to high molecular weight polyethers by catalytic reaction with highly electron deficient reagents, such as triethylaluminum.<sup>1</sup> Presumably the organometallic compound opens the epoxide ring to an alkoxide which initiates polymerization.<sup>2</sup>

In most of the polymerization reactions a product is obtained which is partly soluble in benzene (Table I). The soluble portion has a degree of polymerization of 250. It is easily deacetylated by alkaline transesterification in methanol to produce a water-soluble polymer which possesses a comparatively low viscosity.

### EXPERIMENTAL

#### 1,2-Epoxypropyl 2,3,4,6-Tetra-*O*-acetyl- $\beta$ -D-glucopyranoside

Allyl 2,3,4,6-*O*-acetyl- $\beta$ -D-glucopyranoside was prepared from 2,3,4,6-tetra-*O*-acetyl- $\alpha$ -D-glucopyranosyl bromide and allyl alcohol by the

\* Journal Paper No. 2131 of the Purdue University Agricultural Experiment Station.

method of Helferich and Goerdeler.<sup>3</sup> The glycoside was epoxidized by monopero-phthalic acid<sup>4</sup> and by perbenzoic acid.<sup>5</sup> The latter oxidant gave best results.

In this method 20 g. (0.051 mole) of the allyl glycoside acetate in 60 ml. of chloroform was added to 156 ml. of chloroform containing 0.087 moles of perbenzoic acid. During a reaction period of 4 days at 25°C. in the dark, 0.062 moles of oxidant were consumed. The chloroform solution was washed with water containing 1% sodium carbonate then with water and was dried over anhydrous sodium sulfate. After filtration and distillation of the chloroform the 31 g. of crude product was extracted with warm ether and recrystallized twice from benzene; yield, 48%, m.p. 125.5–126.0°C. The oxirane ring<sup>6</sup> content was 97.8%;  $[\alpha]^{25}_{D}$  -23.2° ( $c = 2.1$  in chloroform) and -24.4° ( $c = 2.1$  in acetone).

ANAL. Calcd. for  $C_{17}H_{24}O_{11}$ : OAc, 42.57%; C, 50.48%; H, 5.98%. Found: OAc, 42.45%; C, 50.62%; H, 5.55%.

### Polymerization

Reactions were conducted in sealed tubes. The epoxide in 20 ml. of dry benzene was placed in a Pyrex tube, 22 × 1.5 cm. which was sealed with a rubber cap. After freezing of the solution, the air in the tube was removed through a hypodermic needle, and after thawing the contents of the tube a definite quantity of a 25% solution of triethylaluminum (Texas Alkyl Co.) in *n*-heptane was added through the needle. The solution was frozen and the tube was evacuated and the needle withdrawn. The tube, with others, was placed in an oven at 80 ± 1°C. for a definite period of time. After the polymerization period the contents of the tube were taken up in benzene and washed with a 2% hydrochloric acid solution and then with

TABLE I  
Poly(hydroxypropyl 2,3,4,6-Tetra-*O*-acetyl- $\beta$ -D-glucopyranoside)

Epoxide, g.	Catalyst, mole-%	Time at 80°C., hr.	Yield, % <sup>a</sup>	Limiting viscosity number <sup>a</sup>
3.2	4.36	105	13.1	0.32
3.2	8.46	105	22.5	0.30
3.2	11.04	105	21.3	0.50
3.2	13.32	105	18.7	0.54
			(5.7)	(0.48)
3.2	15.60	105	16.2	0.66
			(8.6)	(0.58)
5.0	8.96	160	18.8	0.32
			(4.6)	(1.16)
5.0	8.96	240	19.9	0.26
			(4.6)	(1.43)
5.0	12.12	160	24.4	0.18
			(7.5)	(1.46)

<sup>a</sup> Numbers in parentheses are values for the benzene insoluble polymer. The first three preparations contained more.



water. The benzene was distilled and fresh benzene added and distilled to remove water. The product was dispersed in benzene and precipitated by addition of a large volume of ether. The suspension was centrifuged and the precipitate shaken with benzene. A portion was insoluble and was removed by centrifugation. On filtration of the supernatant through a coarse sintered funnel the solution was concentrated to a sirup and the polymer precipitated by addition of ether. This material was soluble in many organic solvents but was insoluble in alcohols and in diethyl ether. Its acetyl content was 42.62%,  $[\alpha]_D^{25} - 25.6^\circ$  ( $c = 0.5$  in benzene); melting range 75–95°C. The benzene-insoluble fraction was soluble in dimethylformamide. Its acetyl content was 42.26% (calculated, 42.57%); melting range, 100–125°C.

Solution viscosities of the polymers were measured in dimethylformamide at 25°C. in an Ubbelohde viscometer (Table I).

Number-average molecular weight of the benzene-insoluble component from the last line of Table I was determined in dimethylformamide by the static method to be  $100,900 \pm 1000$ , indicating a degree of polymerization of  $250 \pm 3$ .

### Polymer Deacetylation

Polymers were deacetylated in methanol with sodium methoxide catalyst. The insoluble product was washed with methanol and dried in a vacuum desiccator over calcium chloride. Deacetylated product from the fifth line of Table I had a limiting viscosity number in water of 0.57. The benzene-insoluble material on diacetylation swelled but did not dissolve in water.

The authors gratefully acknowledge a grant from the Corn Industries Research Foundation which helped support this work.

### References

1. Kambara, S., and M. Hatano, *J. Polymer Sci.*, **27**, 584 (1958).
2. Ebert, P. E., and C. C. Price, *J. Polymer Sci.*, **34**, 157 (1959).
3. Helferich, B., and J. Goerdeler, *Ber.*, **73B**, 532 (1940).
4. Böhme, H., *Ber.*, **70B**, 379, 1709 (1937).
5. Tiffeneau, M., *Organic Syntheses*, Col. Vol. I, Wiley, New York, 1932, p. 422.
6. Jungnickel, J. J., E. D. Peters, A. Polgár, and F. T. Weiss, in *Organic Analysis*. J. Mitchell, Jr., I. M. Kolthoff, E. S. Proskauer, and A. Weissberger, Eds., Vol. 1, Interscience, New York, 1953.

### Résumé

Le tétraacétate d'allyle D-glucopyranoside est préparé en faisant réagir l'acéto-bromo-D-glucose avec l'alcool allylique. Le glycoside ne polymérise pas rapidement par un mécanisme radicalaire mais par conversion en époxyde au moyen des peracides, la polymérisation est facilement induite au moyen du triéthyle aluminium. Le produit de DP 250 est soluble dans les solvants organiques. Par dés acétylation alcaline, le polymère hydrophile devient soluble dans l'eau mais la solution aqueuse possède une viscosité relativement faible.

### Zusammenfassung

Durch Reaktion von Acetobrom-D-Glucose mit Allylalkohol wurde Allyl-D-glucopyranosidtetraacetat hergestellt. Die radikalische Polymerisation des Glykosides ist schwierig, doch kann nach der Umwandlung des Monomeren in das Epoxyd mit Hilfe von Persäuren die Polymerisation leicht mit Aluminiumtriäthyl gestartet werden. Das gebildete Polymere mit einem Polymerisationsgrad von 250 ist in organischen Lösungsmitteln löslich. Das durch alkalische Entacetylierung hergestellte hydrophile Polymere ist zwar in Wasser löslich, die wässrige Lösung hat jedoch eine relativ niedrige Viskosität.

Received May 24, 1963

## Polybenzimidazoles. III

L. PLUMMER\* and C. S. MARVEL, *Department of Chemistry, University of Arizona, Tucson, Arizona*

### Synopsis

Polybenzimidazoles have been prepared from 2,3-, 2,7-, and 2,6-naphthalenedicarboxylic acids, 1,1'-ferrocenedicarboxylic acid, maleic acid, fumaric acid, 4,5-imidazole-dicarboxylic acid, perfluoroglutaric acid, perfluorosuberic acid, and 3,3'-diaminobenzidine. A copolymer has been prepared from a mixture of terephthalic acid and 2,2'-diphenic acid. Thermogravimetric curves have been obtained for most of these polymers.

In previous publications<sup>1,2</sup> it was shown that polymers containing the benzimidazole nuclei could be prepared by the melt condensation of suitable tetraamines and the phenyl esters of aromatic dibasic acids. These polymers show remarkable thermal stability and are soluble in various solvents including formic and sulfuric acids.

In continuing this series several new polybenzimidazoles have been prepared. The diphenyl esters of 2,6-, 2,7-, and 2,3-naphthalenedicarboxylic acid were prepared and condensed with 3,3'-diaminobenzidine to yield linear high molecular weight polybenzimidazoles. The 2,7- and 2,3-naphthalene derivatives are soluble in formic and sulfuric acids and partially soluble in dimethylacetamide. The polymer obtained from diphenyl 2,6-naphthalenedicarboxylate was soluble only in sulfuric acid. All these polybenzimidazoles were yellow in color. The polybenzimidazole from diphenyl 2,6-naphthalenedicarboxylate showed good thermal stability, since it lost only 5% of its weight at 500°C., 15% at 600°C., and 30% at 700°C. The 2,7- and 2,3- derivatives, however, were much less stable, losing approximately 25% of their weight at 500°C. and 35-40% at 700°C. (see Fig. 1). Thus the 2,6-naphthalenedicarboxylic acid gives a polybenzimidazole which is essentially equivalent in stability to those derived from a benzenedioic acid. The 2,3-derivative is much more like an aliphatic derivative, and the 2,7-derivative is intermediate in stability between the benzene derivatives and the aliphatic derivatives. These results might be predicted on the basis that the bonds in naphthalene derivatives are more definitely fixed than is the case in benzene derivatives.

The diphenyl esters of 1,1'-ferrocenedicarboxylic acid and 4,5-imidazole-

\* Postdoctoral Research Associate. Supported by Textile Fibers Dept. E. I. du Pont de Nemours and Co., 1961-62.

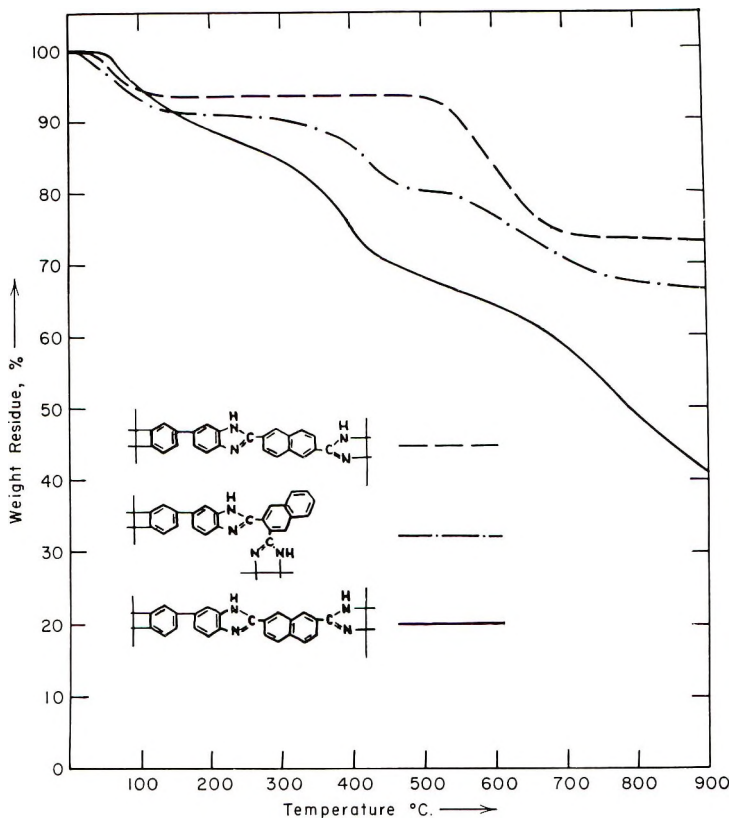


Fig. 1. Thermogravimetric curves for polymers derived from naphthalenedicarboxylic acids.

dicarboxylic acid were each prepared by heating a mixture of the dibasic acid and diphenyl sulfite<sup>3</sup> in pyridine solution. This method afforded good yields of the phenyl esters. The condensation reaction with 3,3'-diaminobenzidine produced polybenzimidazoles having rather low inherent viscosities. Both of these polymers crosslink at temperatures above 350°C., as evidenced by their insolubilities in all solvents. The color of the ferrocene polymer was brown while the polymer from diphenyl 4,5-imidazoledicarboxylate was light yellow in color.

The ferrocene polymer lost 15% of its weight at 300°C., 20% at 400°C., and 25% at 500°C. The thermogravimetric curve shows that this polybenzimidazole is more stable than those with aliphatic links. The polymer derived from 4,5-imidazoledicarboxylic acid has excellent stability and is equivalent to those derived from the phthalic acids (Fig. 2).

When diphenyl fumarate or a mixture of maleic anhydride and phenol were condensed with 3,3'-diaminobenzidine, dark brown to black polymers were obtained. The color depends on the temperature employed in the condensation. The infrared spectra of these polybenzimidazoles from fumaric and maleic acids were identical. It was concluded from a study

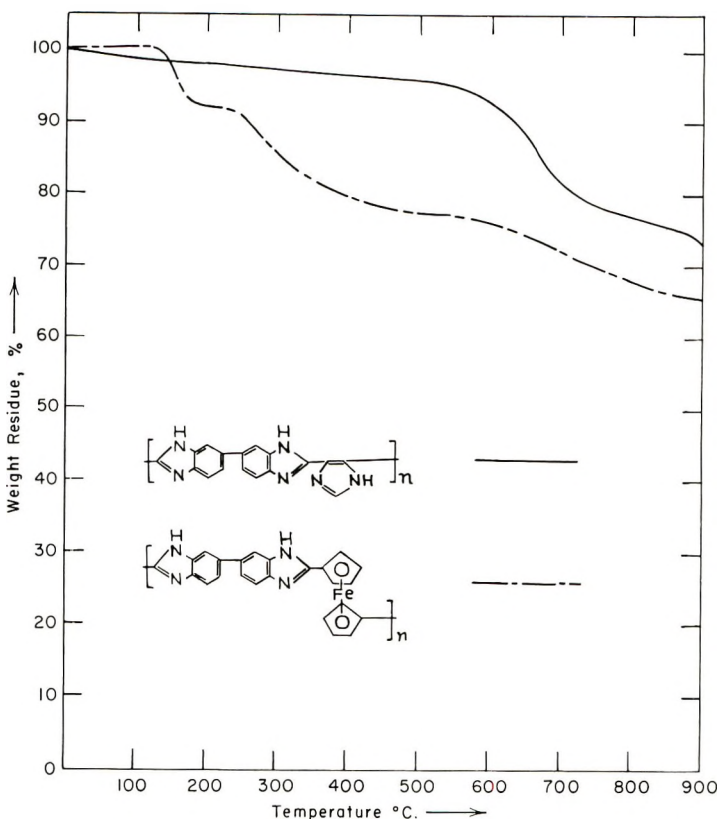


Fig. 2. Thermogravimetric curves for 1,1-ferrocene dicarboxylic acid and 4,5-imidazole-carboxylic acid derivatives.

of these spectra that the polymer contained both *cis* and *trans* double bonds. These polymers are soluble in a wide range of solvents, including sulfuric and formic acids, dimethyl sulfoxide, and dimethylformamide. The inherent viscosity in dimethyl sulfoxide was only 0.07. When heated above 350°C. the products were only partially soluble in sulfuric acid. The thermogravimetric curve (Fig. 3) shows much decomposition of this polymer at 300°C.

The polybenzimidazoles from diphenyl perfluoroglutarate and diphenyl perfluorosuberate showed no particular outstanding heat stability. Both of these polymers began to decompose rapidly at 300°C. It was also observed that the polymers became insoluble in all solvents when heated to 325°C. under high vacuum. In addition, during this heating period their color rapidly turns from brown to black. The thermogravimetric curve (Fig. 4) shows that the suberic acid derivative is more stable than the glutaric acid derivative and approaches the stability of the aromatic polybenzimidazoles.

In an attempt to prepare a polybenzimidazole which would be fusible and possess good thermal stability a copolymer was prepared from 3,3'-

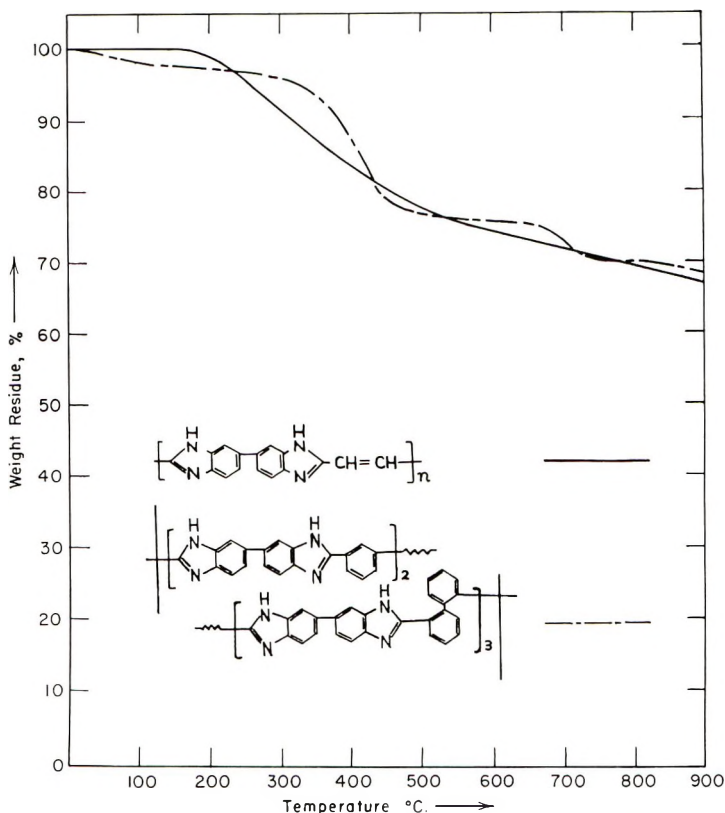


Fig. 3. Thermogravimetric curves for maleic acid derivative and a copolymer derived from isophthalic and 2,2'-diphenic acids.

diaminobenzidine of diphenyl 2,2'-diphenate and diphenyl isophthalate. The melt condensation gave a high molecular weight light yellow polymer. The polymer showed good thermal stability but was infusible at temperatures up to 530°C. The thermogravimetric curve (Fig. 3) showed much weight loss at 400°C. It seems probable that this is due to the use of a rather low molecular weight polymer which had a high percentage of endgroups.

The condensation of 1,8-naphthalic anhydride with 3,3'-diaminobenzidine gave no polybenzimidazole.

The reaction of oxalic acid or diethyl oxalate with *o*-phenylenediamine gives the cyclic amide 2,3-dihydroxyquinoxaline.<sup>4,5</sup> It has also been reported<sup>2</sup> that no polybenzimidazole could be prepared from diphenyl oxalate and 3,3'-diaminobenzidine because of this same cyclic amide formation. However, when this same condensation is carried out in refluxing dimethylacetamide a polymeric material was formed ( $\eta_{inh}$  0.25, 0.2%  $\text{H}_2\text{SO}_4$ ). The infrared spectrum shows maxima characteristic of the benzimidazole nucleus. The presence of a carbonyl function was also noted in the spectrum. The carbon, hydrogen, and nitrogen analyses are

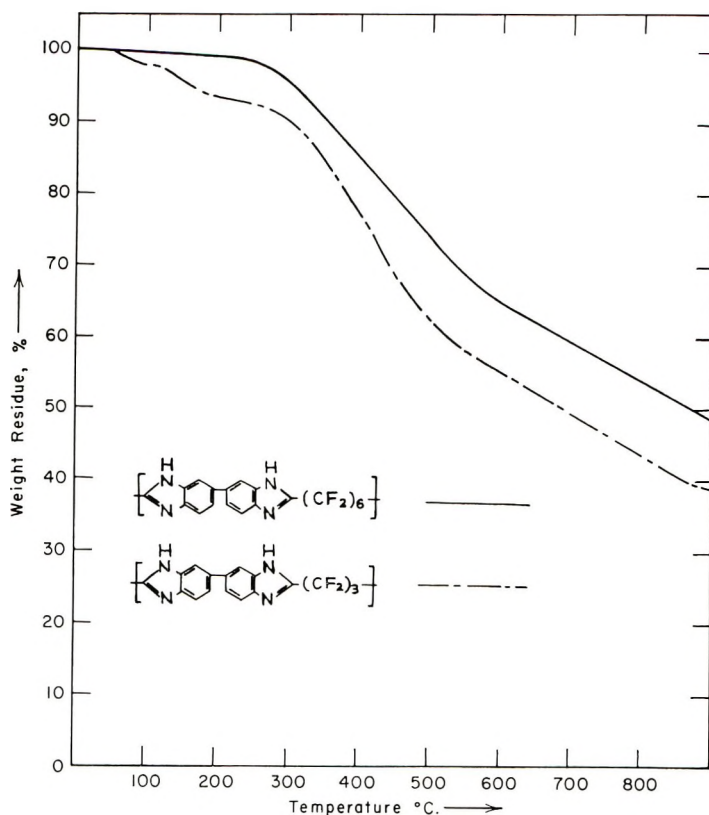


Fig. 4. Thermogravimetric curves for polymers derived from perfluoroglutaric and perfluorosuberic acids.

very close to the values calculated for the polybenzimidazole expected from diphenyl oxalate. From the analytical data and comparison of the infrared spectrum with the spectrum of pure 2,3-dihydroxyquinoxaline it was concluded that the polymer is a polybenzimidazole which has 2,3-dihydroxyquinoxaline endgroups.

## EXPERIMENTAL

### Preparation of Monomers

**Diphenyl 2,6-Naphthalenedicarboxylate.** A mixture of 20 g. (0.093 mole) of 2,6-naphthalenedicarboxylic acid, 40 g. (0.194 mole) of phosphorus pentachloride, and 50 ml. of phosphorus oxychloride was heated to reflux for 16 hr. The phosphorus oxychloride was stripped off to give 23 g. of 2,6-naphthalenedicarboxylic acid chloride. The melting point of the crude acid chloride was 181–185°C.

A 15-g. portion of the acid chloride and 14 g. of phenol were heated together for 30 min. at 300°C. The reaction mixture was recrystallized

from toluene to give 17 g. of diphenyl 2,6-naphthalenedicarboxylate, m.p. 212–213°C.

ANAL. Calcd. for  $C_{24}H_{16}O_4$ : C, 78.25%; H, 4.38%. Found: C, 78.30%; H, 4.55%.

**Diphenyl 2,7-Naphthalenedicarboxylate.** A mixture of 30 g. (0.0134 mole) of 2,7-naphthalenedicarboxylic acid, 62.5 g. (0.030 mole) of phosphorus pentachloride, and 75 ml. of phosphorus oxychloride was heated to reflux for 19 hr. The phosphorus oxychloride was then stripped off and the residue recrystallized from toluene. The yield of 2,7-naphthalenedicarboxylic acid chloride was 16 g.

Then 15 g. of the acid chloride and 14 g. of phenol were heated to 175°C. for 45 min. The reaction product was recrystallized from toluene. The yield of diphenyl ester was 11 g., m.p. 166–167°C. The literature reports m.p. 162°C.<sup>6</sup>

**Diphenyl 2,3-Naphthalenedicarboxylate.** A mixture of 20 g. (0.093 mole) of 2,3-naphthalenedicarboxylic acid, 40 g. (0.194 mole) of phosphorus pentachloride, and 50 ml. of phosphorus oxychloride was heated to reflux for 24 hr. After removal of the phosphorus oxychloride 25 g. of acid chloride was obtained.

A 20-g. portion of the acid chloride and 16 g. of phenol were heated for 1/2 hr. at 175°C. The residue was recrystallized from methanol four times to give 4.2 g., m.p. 113.5–114.5°C., of pure diphenyl 2,3-naphthalenedicarboxylate.

ANAL. Calcd. for  $C_{24}H_{16}O_4$ : C, 78.25%; H, 4.38%. Found: C, 78.62%; H, 4.69%.

**1,1'-Diacetylferrocene.** 1,1'-Diacetylferrocene was prepared in 50% yield by the procedure of Vogel, Rausch, and Rosenberg;<sup>7</sup> m.p. 123–124°C., reported 127.0–127.5°C.

**1,1'-Ferrocenedicarboxylic Acid.** 1,1'-Ferrocenedicarboxylic acid was prepared in 51% yield by sodium hypochlorite oxidation of 1,1'-diacetylferrocene. The free acid was purified by precipitating with dilute hydrochloric acid from a basic solution of the diacid.<sup>8</sup>

**Diphenyl 1,1'-Ferrocenedicarboxylate.** Ferrocenedicarboxylic acid, 5 g. (0.018 mole), 9.9 g. (0.038 mole) of diphenyl sulfite, and 35 ml. of dry pyridine were heated in a flask protected from the light for 18 hr. at 65°C. The reaction mixture was then poured into 300 ml. of 3*N* hydrochloric acid. The black precipitate which formed was subjected to continuous extraction with methanol. On cooling red needles of diphenyl 1,1'-ferrocenedicarboxylate precipitated which were filtered and recrystallized from methanol, m.p. 142.5–143°C. The yield was 3.5 g.

ANAL. Calcd. for  $C_{24}H_{16}O_4Fe$ : C, 67.62%; H, 4.26%. Found: C, 67.48%; H, 4.71%.

**Diphenyl 4,5-Imidazoledicarboxylate.** A mixture of 12.0 g. (0.051 mole) of diphenyl sulfite, 3.9 g. (0.025 mole) of 4,5-imidazoledicarboxylic acid, and 35 ml. of dry pyridine was heated for 2 hr. at 50°C. The tem-



perature was then raised to 105°C. for 4 hr. After filtering the reaction mixture into 200 ml. of 3*N* hydrochloric acid an oil formed which solidified on standing. The solid was recrystallized from methanol three times and ethanol twice, giving 3.4 g. of diphenyl 4,5-imidizoledicarboxylate, m.p. 174–175°C.

ANAL. Calcd. for  $C_{17}H_{12}O_4N$ : C, 66.23%; H, 3.92%; N 9.01%. Found: C, 66.27%; H, 3.99%; N, 9.21%.

**Diphenyl Perfluoroglutarate.** A mixture of 55.4 g. (0.02 mole) of perfluoroglutaryl chloride (Hooker Chemical Corporation) and 38.7 g. (0.4 mole) of phenol was heated for 8 hr. at 100°C. The light red liquid was then subjected to fractional distillation at reduced pressure to give 40 g. of diphenyl perfluoroglutarate, b.p. 126–127°C./0.1 mm. Hg.

ANAL. Calcd. for  $C_{17}H_{10}F_6O_4$ : C, 52.05%; H, 2.54%. Found: C, 52.13%; H, 2.71%.

**Diphenyl Perfluorosuberate.** Dimethyl perfluorosuberate, 159.6 g. (0.39 mole), 50 ml. ethanol, 200 ml. of water, and 5 ml. of concentrated sulfuric acid were refluxed for 3 days. The reaction mixture was cooled and extracted with 700 ml. (seven 100-ml. portions) of diethyl ether. The ether extracts were dried over magnesium sulfate and the ether evaporated. The heavy, colorless oil was fractionated under reduced pressure to give a forerun at 60–70°C./0.2 mm. Hg; the acid distilled at 110–115°C./0.2 mm. Hg.

A mixture of 11.85 g. (0.030 mole) of perfluorosuberic acid and 16 g. (0.079 mole) of freshly distilled phthaloyl chloride were heated at 170°C. for 24 hr. On distillation of the reaction mixture 10 g. of colorless perfluorosuberoyl chloride was obtained, b.p. 168–169°C. The acid chloride was immediately heated with 2.2 g. (0.023 mole) of distilled phenol until the evolution of hydrogen chloride had ceased. After three recrystallizations from pentane at –20°C. 5 g. of diphenyl perfluorosuberate were obtained, m.p. 46.5–48.0°C.

ANAL. Calcd. for  $C_{20}H_{10}F_{12}O_4$ : C, 44.28%; H, 1.86%; F, 42.04%. Found: C 43.87%; H, 2.18%; F, 42.02%.

### Melt Polymerization

The general procedure of Vogel and Marvel<sup>1</sup> was followed in each case.

**Polybenzimidazole from Diphenyl 2,6-Naphthalenedicarboxylate.** A mixture of 2.143 g. (0.010 mole) of 3,3'-diaminobenzidine and 3.684 g. (0.010 mole) of diphenyl 2,6-naphthalenedicarboxylate was heated for 1 hr. at 300°C. in an atmosphere of nitrogen. The polymer was powdered and reheated at 0.01 mm. pressure for an additional 5 hr. at 400°C. to give a product having an inherent viscosity of 1.26 (0.2% sulfuric acid).

ANAL. Calcd. for  $(C_{24}H_{14}N_4)_n$ : C, 80.42%; H, 3.94%; N, 15.63%. Found: C, 79.31%; H, 4.03%; N, 16.48%.

**Polybenzimidazole from Diphenyl 2,7-Naphthalenedicarboxylate.** A mixture of 2.142 g. (0.010 mole) of 3,3'-diaminobenzidine and 3.684 g. (0.010 mole) of diphenyl 2,7-naphthalenedicarboxylate was heated to 220°C. under nitrogen atmosphere for 1/2 hr. Vacuum was applied and the temperature slowly raised to 300°C. over a period of 1 hr. The solid mass was removed and powdered. The polymer was then reheated to 300°C. for 4 hr. and 430°C. for 1 hr. The polymer had an inherent viscosity of 0.61 (0.2% formic acid).

ANAL. Calcd. for  $(C_{24}H_{14}N_4)_n$ : C, 80.42%; H, 3.94%; N, 15.63%. Found: C, 79.36%; H, 4.47%; N, 14.90%.

**Polybenzimidazole from Diphenyl 2,3-Naphthalenedicarboxylate.** A mixture of 2.143 g. (0.010 mole) of 3,3'-diaminobenzidine and 3.694 g. (0.010 mole) of diphenyl 2,3-naphthalenedicarboxylate was heated to 220°C. for 10 min. and then the temperature slowly raised to 280°C. over a period of 1 hr. The solid mass was powdered and reheated to 400°C. under reduced pressure for 4 hr. The polymer had an inherent viscosity of 1.10 (0.2% formic acid).

ANAL. Calcd. for  $(C_{24}H_{14}N_4)_n$ : C, 80.42%; H, 3.94%; N, 15.63%. Found: C, 79.10%; H, 4.30%; N, 14.96%.

**Polybenzimidazole from Diphenyl 4,5-Imidazoledicarboxylate.** A mixture of 3.887 g. (0.013 mole) of diphenyl 4,5-imidazoledicarboxylate and 2.704 g. (0.013 mole) of 3,3'-diaminobenzidine was mixed thoroughly and heated to 210–220°C. After 45 min. the reaction mixture had solidified. The temperature was then raised to 260°C. for 1/2 hr. followed by an additional heating period of 2 hr. under high vacuum (0.01 mm. Hg). After powdering, the polymer was reheated under vacuum for 3 hr. at 300°C. The yellow product, which was not completely soluble in 98% formic acid or sulfuric acid, was subjected to continuous extraction with formic acid. The soluble portion (75%) had an inherent viscosity of 0.16 (0.2% formic acid).

ANAL. Calcd. for  $(C_{17}H_{10}N_6)_n$ : C, 68.42%; H, 3.38%; N, 28.20%. Found: C, 67.03%; H, 3.93%; N, 27.97%.

**Polybenzimidazole from Diphenyl Perfluoroglutarate.** A mixture of 3.983 g. (0.010 mole) of diphenyl perfluoroglutarate and 2.185 g. (0.010 mole) of 3,3'-diaminobenzidine was heated under nitrogen at 180–190°C. for 20 min. The temperature was raised to 220°C. and heating continued for an additional 15 min. Vacuum was applied and the temperature raised to 230–240°C. for an additional 1/2 hr. After purifying, the polymer had an inherent viscosity of 0.20 (0.2% dimethyl sulfoxide).

ANAL. Calcd. for  $(C_{17}H_7F_6N_4)_n$ : C, 53.55%; H, 1.85%; F, 29.90%; N, 14.47%. Found: C, 52.19%; H, 2.08%; F, 28.79%; N, 15.30%.

On heating to 300°C. the polymer turned black and became insoluble.

**Polybenzimidazole from Diphenyl Perfluorosuberate.** A mixture of 3.718 g. (0.0069 mole) of diphenyl perfluorosuberate, 1.479 g. (0.0069

mole) of 3,3'-diaminobenzidine and 5 g. of phenol was heated under nitrogen for 30 min. at 220°C. The pressure was reduced to 0.1 mm. Hg and heating was continued for an additional 1½ hr. while the temperature was raised to 285°C. The brown colored polymer had an inherent viscosity of 0.17 (0.2% sulfuric acid).

ANAL. Calcd. for  $(C_{20}H_8N_4F_{12})_n$ : C, 45.10%; H, 1.51%; N, 10.52%; F, 42.83%. Found: C, 43.94%; H, 2.01%; N, 9.65%; F, 41.95%.

**Polybenzimidazole from Diphenyl 1,1'-Ferrocenedicarboxylate.** A mixture of 2.617 g. (0.0061 mole) of diphenyl 1,1'-ferrocenedicarboxylate and 1.307 g. (0.0061 mole) of 3,3'-diaminobenzidine was heated to 210–215°C., at which point the reaction started. Heating in this manner was continued for 1 hr. and then the temperature was slowly raised to 250°C. and held there for 30 min. After powdering and reheating the polymer at 280–290°C. for 17 hr. a brown product was obtained. Inherent viscosity 0.20 (0.2% formic acid).

ANAL. Calcd. for  $(C_{22}H_{16}N_4Fe)_n$ : C, 69.23%; H, 3.88%; N, 13.46%. Found: C, 67.45%; H, 3.21%; N, 12.85%.

**Polybenzimidazole from Diphenyl Isophthalate, Diphenyl 2,2'-Diphenate, and 3,3'-Diaminobenzidine.** A mixture of 2.185 g. (0.010 mole) of 3,3'-diaminobenzidine, 2.413 g. (0.006 mole) of diphenyl 2,2'-diphenate, and 1.273 g. (0.004 mole) of diphenyl isophthalate were heated under nitrogen to 250°C. The yellow melt which first formed solidified after ½ hr. Vacuum was applied over the period of 1 hr. while the temperature was raised to 300°C. After powdering and reheating to 400°C. under high vacuum (0.01 mm. Hg) a yellow copolymer having an inherent viscosity of 1.85 (0.2% 98% formic acid) was obtained.

The polymer did not soften at temperatures up to 500°C.

**Solution Polymerization of Diphenyl Oxalate and Diaminobenzidine.** A solution of 2.422 g. (0.010 mole) of diphenyl oxalate and 2.143 g. (0.010 mole) of 3,3'-diaminobenzidine in 30 ml. of dimethylacetamide was heated to reflux. After 1 hr. a yellow precipitate formed in the reaction flask. Heating was continued for an additional hour and then the reaction mixture was poured into 600 ml. of distilled water. The precipitate was collected and washed with several portions of water. The yellow solid was powdered and heated to 300°C. under high vacuum to give a polybenzimidazole having an inherent viscosity of 0.24 (0.2% sulfuric acid).

ANAL. Calcd. for  $(C_{14}H_8N_4)_n$ : C, 72.39%; H, 3.47%; N, 24.13%. Found: C, 72.17%; H, 3.47%; N, 23.28%.

**Polybenzimidazole from Diphenyl Fumarate.** Fumaryl chloride was prepared from maleic anhydride and phthaloyl chloride according to a literature procedure.<sup>9</sup> Heating on the water bath of a mixture of the dichloride with two moles of phenol yielded, after three recrystallizations from ethanol (100 ml./g.), 62% of the theoretical amount of diphenyl fumarate (m.p. 161–162°C.).

A mixture of 4.142 g. (0.019 mole) of 3,3'-diaminobenzidine and 6.150 g. (0.019 mole) of diphenyl fumarate was heated to 200°C., at which point the reaction started. Heating was continued at 210–220°C. for about 1 hr. After cooling the brown polymer was powdered and reheated to 245–250°C. under high vacuum. The inherent viscosity at this point was 0.05 (0.5% in DMSO). Further heating to 285–290°C. produced a black polymer having an inherent viscosity of 0.07 (0.5% DMSO). Heating to 360°C. under vacuum produced a black polymer which was only partially soluble in cold sulfuric acid.

ANAL. Calcd. for  $(C_{16}H_{10}N_4)_n$ : C, 74.40%; H, 3.90%; N, 21.70%. Found: C, 73.54%; H, 3.92%; N, 20.93%.

**Polybenzimidazole from Maleic Anhydride.** A mixture of 4.344 g. (0.020 mole) of diaminobenzidine, 1.986 g. (0.020 mole) of maleic anhydride, and 3.81 g. (0.040 mole) of phenol was finely powdered and heated to 165°C. for 1½ hr. The vigorous distillation of water indicated that the reaction was taking place. The temperature was raised to 220°C. over a 3½ hr. period. High vacuum was applied 1 hr. while the temperature was raised from 200°C. to 250°C. The appearance, solubilities, and infrared spectrum of this polymer were identical with those of the polymer from diphenyl fumarate and diaminobenzidine.

We are indebted to Dr. L. Gibbons, Ohio Oil Company, for samples of 2,3-, 2,6-, and 2,7-naphthalenedicarboxylic acids; to Dr. W. E. Gibbs, Materials Laboratory, Wright Air Development Division, for samples of perfluoroglutaryl chloride; and to Dr. J. J. Drysdale, Jackson Laboratory, E. I. du Pont de Nemours and Company, for dimethyl perfluorosuberate. For the thermogravimetric analysis curves, we wish to thank Dr. Ehlers, Wright Air Development Division, Wright-Patterson Air Force Base, Ohio. The analyses were performed by Micro-Tech Laboratories, Skokie, Illinois. Dr. Bernd Reichel prepared the polybenzimidazoles from diphenyl fumarate and maleic anhydride. The financial support of the Textile Fibers Department of E. I. du Pont de Nemours and Company is gratefully acknowledged.

## References

1. Vogel, H., and C. S. Marvel, *J. Polymer Sci.*, **50**, 511 (1961).
2. Vogel, H., and C. S. Marvel, *J. Polymer Sci.*, **A1**, 1531 (1963).
3. Iselin, B., W. Riitel, P. Sieber, and R. Schwyzer, *Helv. Chim. Acta*, **40**, 373 (1957).
4. Phillips, M. A., *J. Chem. Soc.*, **1928**, 2393, 3134.
5. Shriner, R. L., and R. W. Upson, *J. Am. Chem. Soc.*, **63**, 2277 (1941).
6. Purgott, A., *Ann. Scuola Agr. Portici*, [2] **17**, 1 (1922).
7. Vogel, M., M. Rausch, and H. Rosenberg, *J. Org. Chem.*, **22**, 1067 (1957).
8. Knobloch, F. W., and W. H. Rausch, *J. Polymer Sci.*, **54**, 65 (1961).
9. *Organic Syntheses*, Coll. Vol. III, Wiley, New York, 1955, p. 422.

## Résumé

On a préparé des polybenzimidazoles à partir d'acides 2,3-, 2,7- et 2,6-naphtalène-dicarboxyliques, à partir d'acide 1,1'-ferrocènedicarboxylique, acide maléique, acide fumarique, acide 4,5-imidazoledicarboxylique, acide perfluoroglutarique, acide perfluorobutérique et la 3,3'-diaminobenzidine. On a préparé un copolymère à partir d'un mélange d'acide téréphtalique et d'acide 2,2'-diphénique. On a obtenu des courbes thermogravimétriques pour la plupart de ces polymères.

### Zusammenfassung

Aus 2,3-, 2,7- und 2,6-Naphthalindicarbonsäure, 1,1'-Ferrocendicarbonsäure, Maleinsäure, Fumarsäure, 4,5-Imidazoldicarbonsäure, Perfluorglutarsäure, Perfluorkorksäure und 3,3'-Diaminobenzidin wurden Polybenzimidazole hergestellt. Ausserdem wurde aus einem Gemisch von Terephthalsäure und 2,2'-Diphensäure ein Copolymeres dargestellt. Für die meisten dieser Polymeren wurden thermogravimetrische Kurven aufgenommen.

Received May 27, 1963

## $\alpha,\omega$ -Glycols and Dicarboxylic Acids from Butadiene, Isoprene, and Styrene and Some Derived Block Polymers, Esters, and Urethans

KATSUMI HAYASHI\* and C. S. MARVEL, *Department of Chemistry, University of Arizona, Tucson, Arizona*

### Synopsis

The living polymer technique of Szwarc has been employed to synthesize  $\alpha,\omega$ -bifunctional derivatives of polybutadiene, polyisoprene, and polystyrene. The glycols derived from polybutadiene have been hydrogenated to give saturated glycols. The glycols from polyisoprene have been partially hydrogenated. Some block polymer esters and urethans have been characterized.

### INTRODUCTION

Szwarc and co-workers<sup>1-4</sup> have established that the anionic polymerization of styrene and conjugated dienes initiated by alkali metal-naphthalene complex in tetrahydrofuran has proceeded without termination to form so-called "living polymers." The living polymers further react with electrophilic reagents such as ethylene oxide and carbon dioxide to give polymers possessing difunctionality. These macrodifunctional compounds make versatile intermediates for preparation of block polymers. In this way syntheses of polystyrene glycol,<sup>5</sup> polystyrenedicarboxylic acid,<sup>6</sup> and polybutadiene glycol<sup>7,8</sup> have been reported. The present investigation was undertaken to study further the preparations of macrofunctional compounds starting from styrene, butadiene, and isoprene, and to investigate the chain extension reaction of these difunctional intermediates to derive block polymers.

### RESULTS AND DISCUSSION

#### 1. Polybutadiene Glycols and Polyisoprene Glycols

On the basis of the infrared spectrum, the polybutadiene formed by lithium naphthalene-initiated polymerization in tetrahydrofuran contains over 90% of the 1,2-adduct structure. The characteristic bands for 1,2-structure, or for pendant vinyl groups on polyhydrocarbon chains are at

\* Postdoctoral Research Associate. Supported by Textile Fibers Dept., E. I. du Pont de Nemours and Co., 1961-63.

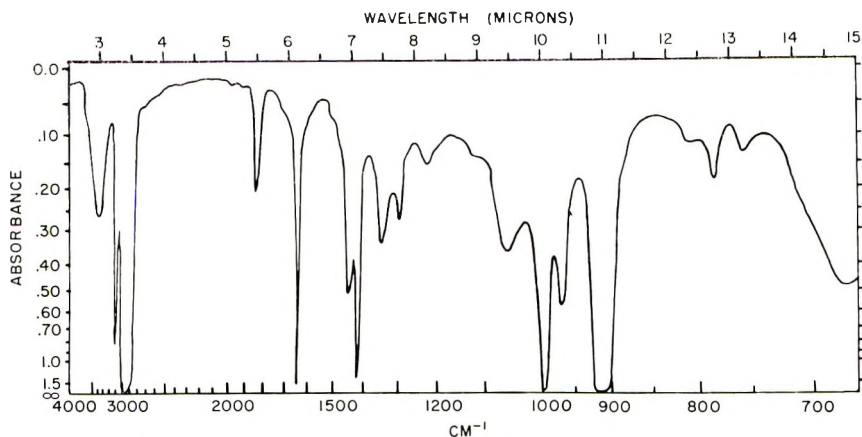


Fig. 1. Infrared spectrum of polybutadiene glycol (PBG-19).

3100 (s), 1850 (m), 1650 (s), 1420 (s), 995 (s), and 915 (vs)  $\text{cm}^{-1}$ . Maxima at 970 (m) and 1360 (m)  $\text{cm}^{-1}$  are characteristic for a 1,4-*trans* structure<sup>9,10</sup> (Fig. 1).

Formation of hydroxyl groups at both ends of polybutadiene has been attempted by the following three methods: (1) termination of  $\alpha,\omega$ -dilithium polybutadiene with ethylene oxide; (2) lithium aluminum hydride reduction of polybutadienedicarboxylic acid dimethyl ester (this macrodiacid ester was made by the carbon dioxide termination of  $\alpha,\omega$ -dilithium polybutadiene followed by esterification with methanol); and (3) termination of  $\alpha,\omega$ -dilithium polybutadiene with formaldehyde.

The results of polybutadiene glycol preparation by method 1 are summarized in Table I.

Polybutadiene glycols having molecular weight ranging from 800 to 4500 were obtained by varying the ratio of catalyst to monomer. It has been reported<sup>3</sup> that the molecular weight of polybutadiene prepared by this method would be given by the simple relationship,  $\bar{M}W = [\text{Monomer}] / \frac{1}{2} [\text{Catalyst}]$ , and this equation has been confirmed for a molecular range of 1,700 to 100,000. This relationship also appeared to be correct in our polymerization system where a higher ratio of catalyst to monomer was used (Fig. 2). However, in reaction conditions where the ratio was much greater than 20, molecular weights were much higher than anticipated. Table I shows this effect for samples PBG-21 and PBG-22.

As pointed out by Szwarc, this type of reaction is very sensitive to contamination by impurities and in order to obtain reproducible results, all reagents must be purged of all compounds which might destroy the carbanion. These include water, oxygen, carbon dioxide, etc. The results pertaining to PBG-2 through 7, PBG-12 and PBG-14 in Table I were obtained at an earlier stage in the work using a less rigorously purified monomer. The molecular weights of these samples are seen to be greater than the theoretical values (cross, dots in Fig. 2). The results of chain extension

TABLE I  
Preparation of Polybutadiene Glycols (PBG) and Polyisoprene Glycols (PIG)

Glycol <sup>a</sup>	Buta- diene, g.	Li, g.-atom	Yield, g.	$\eta_{inh}^b$	OH Equivalent <sup>c</sup>		Degree of Polymer- ization $n^d$	C H Analysis					
					Found			Calcd.		Found		Calcd.	
					Found	Calcd.		C, %	H, %	C, %	H, %	C, %	H, %
PBG-2	120	0.2	—	0.057	1068, 1053	615	37.5	86.62	10.58	87.2	11.2		
PBG-3	130	0.1	109	0.092	1995, 1975	1315	71.7	87.22	10.78	87.9	11.2		
PBG-4	165	0.3	157	0.076	904, 922	565	32.1	87.32	10.76	87.0	11.2		
PBG-5	155	0.15	148	0.065	1220, 1250	1045	44.0	87.92	10.96	87.4	11.2		
PBG-6	175	0.6	165	0.053	602, 651	310	21.5	86.70	11.12	86.4	11.2		
PBG-7	165	0.075	145	0.106	2380, 2360	2215	86.0	88.45	10.91	88.1	11.2		
PBG-8	150	0.15	110	0.067	1147, 1150	1015	40.8	87.64	10.65	87.6	11.2		
PBG-12	70	0.10	58	—	973, 945	715	33.8	—	—	87.1	11.2		
PBG-14	75	0.075	52	—	1310, 1330	1015	46.6	—	—	87.5	11.2		
PBG-15	120	0.15	107	—	769, 762	815	26.6	—	—	86.6	11.2		
PBG-18	120	0.20	112	0.061	721, 723	615	25.0	87.02	10.75	86.4	11.2		
PBG-19	130	0.15	100	0.077	869, 840	880	29.9	—	—	86.8	11.2		
PBG-21	75	0.15	48	0.055	654, 655	515	22.6	85.93	10.76	86.4	11.2		
PBG-22	75	0.20	68	0.055	506, 489	390	16.8	85.19	10.69	85.5	11.2		
PIG-3	75	0.10	69	0.056	934, 947	890	26.3	85.29	12.73	86.4	11.5		
PIG-4	73	0.05	72	0.066	1395, 1430	1500	40.2	—	—	87.2	11.6		
PIG-5	136	0.15	122	0.057	1177, 1177	950	33.2	86.87	11.53	86.9	11.6		

<sup>a</sup> PBG: polybutadiene glycol, PIG: polyisoprene glycol.

<sup>b</sup> Measured at a concentration of 0.500 g./100 ml. toluene and at 30°C.

<sup>c</sup> Determined by acetic anhydride/pyridine method.<sup>11</sup>

<sup>d</sup> Calculated on the basis of hydroxyl equivalent values observed.



employing diisocyanates were unsatisfactory, indicating insufficient difunctionality in the polymer, thereby suggesting prior termination occurring in the polymerization.

The polybutadienedicarboxylic acids were obtained by reacting  $\alpha,\omega$ -dilithium polybutadiene with carbon dioxide, the procedure being essentially the same as for the polybutadiene glycols. The results are listed

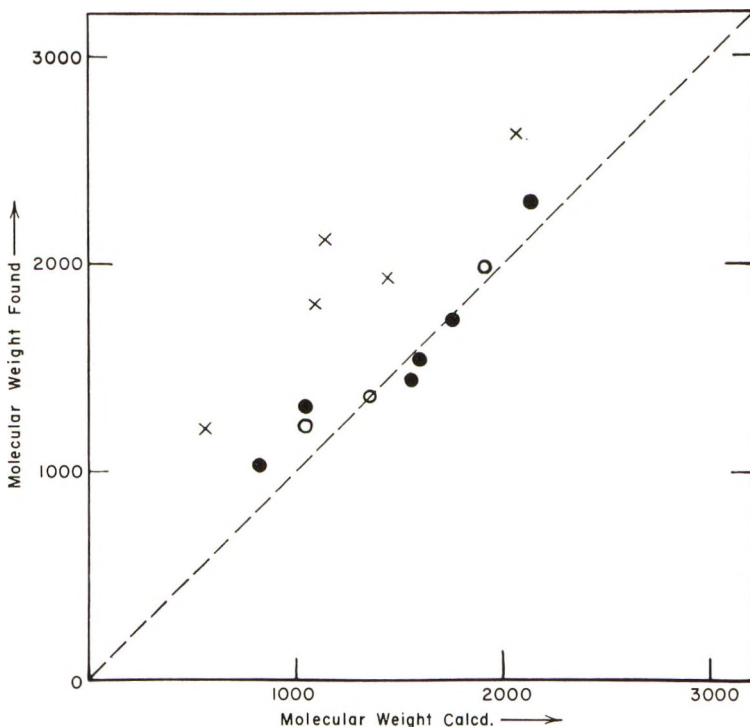


Fig. 2. Relationship between calculated molecular weights and observed molecular weights of polybutadiene glycols and polybutadienedicarboxylic acids: (●) polybutadiene glycols from pure monomer; (×) polybutadiene glycols from insufficiently purified monomer; (○) polybutadienedicarboxylic acids.

in Table II. The molecular weight of the products, determined by a titration of their carboxyl endgroups, obeyed the relationship,  $MW = [\text{Monomer}] / \frac{1}{2} [\text{Catalyst}]$ . The carboxyl groups contained in the products were confirmed from infrared spectra at 2400–3400 (broad and strong), 1725 (s) and 1220 (m)  $\text{cm}^{-1}$ .

These macrodiacids were esterified with an excess of methanol in benzene solution. The  $\text{C}=\text{O}$  stretching band in the infrared spectrum of the product completely shifted from 1725  $\text{cm}^{-1}$  for free acid to 1750  $\text{cm}^{-1}$  for ester carboxyl. The broad absorption band near 3000  $\text{cm}^{-1}$  for the acid also had disappeared after this treatment. The inherent viscosities of esterified products were much lower than those of the corresponding diacids.

TABLE II  
Preparation of Polybutadienedicarboxylic Acids (PBC)

Diacid <sup>a</sup>	Buta- diene, g.	Li, mole	Yield, g.	$\eta_{inh}^b$	CO <sub>2</sub> H Equivalent <sup>c</sup>		Degree of polymer- ization $\eta^d$	CH Analysis			
					Found	Calcd.		Found		Calcd.	
								C, %	H, %	C, %	H, %
PBC-4	95	0.15	80	0.063	683, 680	680	23.7	84.93	10.44	84.8	10.8
PBC-5	95	0.20	74	—	625, 634	520	21.7	—	—	84.6	10.6
PBC-6	135	0.15	124	0.103	905, 1005	960	35.3	86.25	10.55	85.9	10.7

<sup>a</sup> PBC: polybutadiene dicarboxylic acid.

<sup>b</sup> Measured at a concentration of 0.500 g./100 ml. toluene and at 30°C.

<sup>c</sup> Determined by titration with aqueous 0.4N potassium hydroxide in *N,N*-dimethylacetamide solution.

<sup>d</sup> Calculated on the basis of carboxyl equivalent value observed.

TABLE III  
Data on Inherent Viscosities, Functional Endgroup Determination, and Elemental Analyses of Polybutadiene Glycols Derived from  $\text{LiAlH}_4$  Reduction of Polybutadienedicarboxylic Acid Dimethyl Ester and Their Intermediate Compounds

No. of samples	$\eta_{inh}^a$			$\text{CO}_2\text{H}$ Equivalent of PBC <sup>b</sup>	OH Equivalent of PBcG <sup>b,c</sup>
	PBC <sup>b</sup>	Dimethyl ester of PBC <sup>c</sup>	PBcG <sup>b,c</sup>		
4	0.063	0.056	0.062	683, 689	687
6	0.103	0.088	0.100	995, 1005	997; 985

<sup>a</sup> Measured at a concentration of 0.500 g./100 ml. toluene and at 30°C.

<sup>b</sup> PBC: polybutadienedicarboxylic acid; PBcG: polybutadiene glycol prepared by lithium aluminum hydride reduction of polybutadienedicarboxylic acid dimethyl ester.

<sup>c</sup> C and H analyses, Dimethyl ester of PBC-4: found, C 85.84%, H 10.56%; calcd., C 86.6%, H 11.1%. Dimethyl ester of PBC-6: found, C 86.25%; H 10.67%; calcd., C 87.1%, H 10.9%; PBcG-4: found, C 86.58%, H 11.00%; calcd., C 86.6%, H 11.0%; PBcG-6: found, C 87.11%, H 11.00%; calcd., C 87.3%, H 11.2%.

A reduction of the ester group to hydroxyl with lithium aluminum hydride was carried out in tetrahydrofuran solution at ice-water temperature. The infrared spectra showed the products to be completely free from carboxyl groups and were identical, in every respect, with that of polybutadiene glycol prepared by method 1. As shown in Table III, the hydroxyl equivalent values of these glycols gave good agreement with the carboxyl equivalent values of the corresponding macrodiacid.

Two attempts at reaction between dilithium polybutadiene and free formaldehyde did not prove successful. When anhydrous formaldehyde dissolved in tetrahydrofuran was added to the dark red solution of dilithium polybutadiene at  $-77^\circ\text{C}$ ., the formaldehyde was seen to polymerize, forming a transparent film of the aldehyde polymer. The color of the reaction mixture disappeared gradually at room temperature.

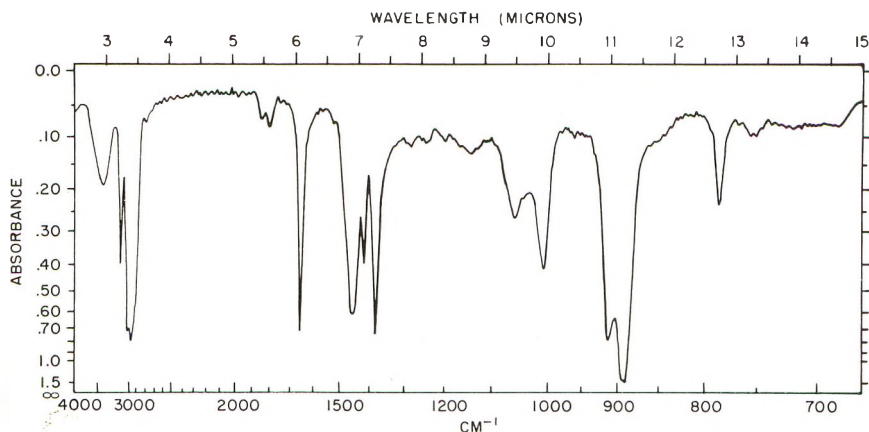


Fig. 3. Infrared spectrum of polyisoprene glycol (PIG-3).

The product here contained a smaller amount of hydroxyl groups than expected and the strong infrared absorption at  $1070\text{ cm.}^{-1}$  is indicative of ether links.

The polyisoprene glycols have been made by much the same way as that used for polybutadiene glycols. The results are shown in Table I. The infrared spectrum of the product (Fig. 3) shows the presence of pendant isopropenyl groups (from 1,2-addition by absorption), at  $1380$  (s) and  $890$  (s)  $\text{cm.}^{-1}$ , and of pendant vinyl groups (from 3,4-addition) at  $1420$  (s),  $1010$  (s) and  $910$  (s)  $\text{cm.}^{-1}$ . There is not sufficient evidence to prove the presence of 1,4-*cis*- and *trans*-structures as far as the infrared spectrum is concerned. However, there is a shoulder at  $860\text{ cm.}^{-1}$  of very weak intensity. This maximum has been assigned to be that of a mixture of 1,4-*cis* and *trans* configurations.<sup>12</sup>

On the basis of calculations involving infrared spectral intensities as described by Richardson and Sacher,<sup>12</sup> the microstructure of this polymer would contain 60–70% 1,2-structure, 20–35% 3,4-structure, and less than 5% 1,4-*cis*- and *trans*-structure.

## 2. Hydrogenation of Polybutadiene Glycols and Polyisoprene Glycols

The hydrogenations were carried out in an ethanol medium over palladium charcoal catalyst at room temperature and under moderate pressure—around  $50\text{ lb./in.}^2$ . The results are listed in Table IV.

The hydrogenation of polybutadiene glycol proceeded smoothly and almost all the hydrogen was absorbed within a period of 30–60 min., but in the final stage external heating by means of an infrared lamp was necessary to complete the hydrogenation. The infrared spectra, shown in Figures 1 and 4, indicate the complete transformation of olefinic linkage to paraffinic and no change of hydroxyl groups by this hydrogenation; i.e., the complete disappearance of absorptions at  $3100$  (s),  $1850$  (m),  $1650$  (s),  $1420$  (s),  $995$  (s),  $970$  (m) and  $915$  (vs)  $\text{cm.}^{-1}$  which are due to C=C double bonds

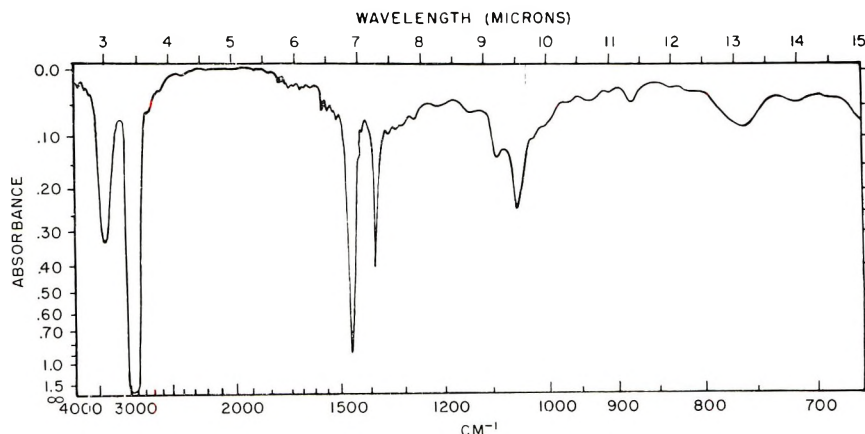


Fig. 4. Infrared spectrum of hydrogenated polybutadiene glycol (PBGH-19).

TABLE IV  
 Hydrogenation of Polybutadiene Glycols and Polyisoprene Glycols

Glycols hydrogenated <sup>a</sup>	Weight of glycols unhydrogenated, g.	Yield, g.	$\eta_{inh}^b$	OH Equivalent <sup>c</sup>	Degree of polymerization	CH Analysis			
						Found		Calcd.	
					$n^d$	C, %	H, %	C, %	H, %
PBGH-2	50	50	0.049	1120, 1113	38.2	84.87	13.61	84.4	14.3
PBGH-3	50	51	0.064	2250, 2210	77.9	—	—	84.9	14.3
PBGH-4	102	102	0.044	974, 985	33.4	85.08	13.21	84.2	14.3
PBGH-5	100	98	0.053	1250, 1280	43.6	85.28	13.36	84.5	14.3
PBGH-6	115	115	0.036	636, 654	21.3	85.02	13.06	83.6	14.2
PBGH-8	75	74	0.053	1218, 1222	42.0	84.74	13.68	84.6	14.3
PBGH-19	17	17	0.059	875, 865	29.5	83.77	13.97	84.1	14.3
PIGH-3	30	29	0.045	938, 936	25.6	84.81	13.44	84.2	14.3
PIGH-5	60	60	0.055	1282, 1292	36.4	85.95	12.59	84.5	14.3

<sup>a</sup> PBGH: polybutadiene glycol hydrogenated, PIGH: polyisoprene glycol hydrogenated.

<sup>b</sup> Measured at a concentration of 0.500 g./100 ml. toluene and at 30°C.

<sup>c</sup> Determined by acetic anhydride/pyridine method.<sup>11</sup>

<sup>d</sup> Calculated on the basis of hydroxyl equivalent values observed.

TABLE V  
Solubilities of Polybutadiene Glycol and Polyisoprene Glycol in Ethanol and DMF

No. of glycols	Molecular weight	Solubility	
		PBG	PBGH
6	1200	Easily soluble in cold	Soluble in hot
4	1800	Soluble in hot	Slightly soluble in hot
5	2500	"	"
3	4000	Slightly soluble in hot	Insoluble

in the polybutadiene glycol, the remarkable increase in intensity at  $1470\text{ cm.}^{-1}$  ( $-\text{CH}_2-$ ), the appearance of new peak at  $1380\text{ cm.}^{-1}$  ( $\text{CH}_3$ ), and no change at  $3400$  (s) and  $1060$  (m)  $\text{cm.}^{-1}$  (OH) confirmed the structure of the product. In the spectrum of the product at the stage where approximately 90% of hydrogen had been absorbed, the maximum at  $970\text{ cm.}^{-1}$  remained almost unchanged. This would indicate that the carbon-carbon double bond of the 1,4-*trans*-structure was reduced with greater difficulty than that of 1,2-structure. The hydroxyl equivalent values and the solution viscosities of hydrogenated glycols were essentially the same as those of corresponding unhydrogenated glycols. A subsequent chain extension reaction indicated that hydrogenation had no effect on the hydroxyl groups. This will be described in the following section.

Both polybutadiene glycols and hydrogenated polybutadiene glycols were soluble in benzene, toluene, pyridine, *n*-hexane, tetrahydrofuran, dimethoxyethane and chloroform and insoluble in methanol and water. As shown in Table V, the unhydrogenated glycols were much more soluble in ethanol and dimethylformamide than unhydrogenated glycols. This solubility behavior illustrates the point that olefinic compounds of small

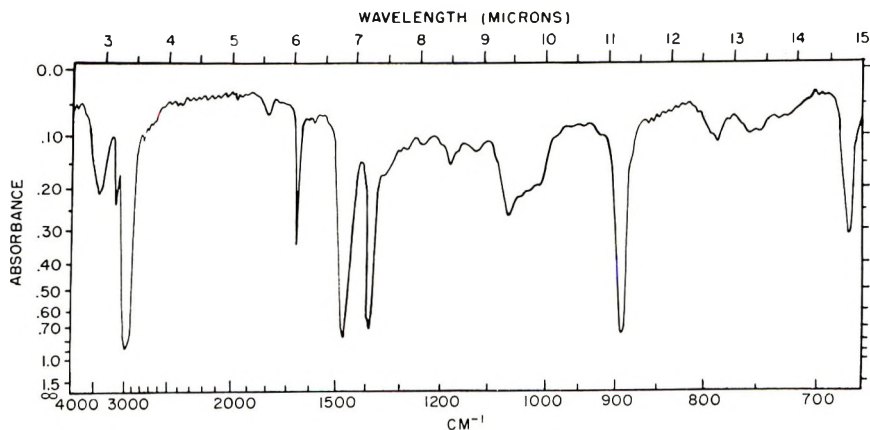


Fig. 5. Infrared spectrum of hydrogenated polyisoprene glycol (PIGH-3.)

molecules have greater affinity for a polar solvent than the corresponding paraffinic compounds.

On the other hand, the polyisoprene glycols could be hydrogenated only partially under all reaction conditions tried, taking up approximately 40% of the amount of hydrogen expected from the number of double bonds.

TABLE VI  
Infrared Analysis of Hydrogenated Polyisoprene Glycol

Observation after hydrogenation	Absorption peaks and intensity, $\text{cm.}^{-1}$	Corresponding structure
Absorption disappearing	1850 (m) 1420 (s) 1010 (s) 910 (vs)	$-\text{CH}=\text{CH}_2$
Absorption decreasing in intensity	1650 (s)	Total $\text{C}=\text{C}$
Absorption decreasing very slightly in intensity	3150 (s) 890 (vs)	$-\text{CH}=\text{CH}_2$ and $-\text{C}(\text{CH}_3)=\text{CH}_2$
Absorption increasing in intensity	1830 (m)	$-\text{C}(\text{CH}_3)=\text{CH}_2$
Absorption remaining unchanged	1460 (s) 1380 (s) 3400 (s) 1060 (s)	$-\text{CH}_2-$ $-\text{CH}_3$ $-\text{OH}$

This was also confirmed from the elemental analysis of the product. The infrared spectra of hydrogenated product showed that pendant vinyl groups formed by 3,4-addition polymerization of isoprene were completely hydrogenated into ethyl groups, but the more sterically hindered isopropenyl groups formed by 1,2-addition remained unchanged. Table VI summarizes the infrared analysis. The infrared spectrum of PIGH-3 is shown in Figure 5. This hydrogenation was tried under more drastic conditions in an autoclave, by using Raney nickel catalyst at 2000 lb./in.<sup>2</sup> and 150°C., but the product here was identical with that mentioned above.

### 3. Chain Extension Reaction of the Macro Glycols with Diisocyanates

The method of chain extension was essentially the same as preparation for well-known urethan elastomers. Two aromatic diisocyanates, 2,4-toluene diisocyanate and diphenylmethane diisocyanate, were used. The macroglycol was treated with 1.3 to 2.0 times excess of diisocyanate to form prepolymer terminated by isocyanate groups at both ends of the chains. This can be done with or without a solvent. The molecular weight of the prepolymer depends on the amount of diisocyanate used. To a solution of this prepolymer was added a chain extender such as water or hydrazine. The chain extension proceeded slowly with water, but rapidly with hydrazine.

TABLE VII  
Chain Extension Reaction of Macroglycol with Diisocyanate

Run No.	Glycol <sup>a</sup>		Diisocyanate <sup>b</sup>		—OH/- —NCO mole ratio	Solvent <sup>c</sup>	Yield g.	η <sub>inh</sub> <sup>d</sup>	Analysis					
	Type	g.	Type	g.					Found			Calcd.		
	Type	g.	Type	g.					C, %	H, %	N, %	C, %	H, %	N, %
1	PBG-18	2.545	TDI	0.386	T/D	20	2.8	0.36	83.09	9.95	2.18	83.1	10.2	2.1
2	PBG-19	1.690	DMD	0.323	T/D	30	1.8	0.36	84.13	9.86	2.20	84.5	10.0	1.8
3	PBG-19	1.588	DMD	0.348	D	10	1.7	0.80	84.31	9.92	2.03	84.3	10.1	1.9
4	PBG-19	3.407	TDI	0.419	T/D	20	3.6	0.72	84.98	10.30	1.93	83.9	10.3	1.9
5	PBeG-5	2.069	TDI	0.265	T/D	20	2.1	0.23	—	—	—	—	—	—
6	PBeG-6	1.408	TDI	0.148	T/D	15	1.1	0.55	—	—	—	—	—	—
7	PBeG-6	2.110	DMD	0.347	T/D	20	2.2	0.55	84.81	10.28	1.83	85.0	10.0	1.6
8	PIG-4	2.409	DMD	0.279	T/D	20	2.5	0.44	85.09	10.82	1.60	85.6	10.8	1.2
9	PIG-5	2.345	DMD	0.324	T/D	20	2.3	0.75	84.85	10.61	1.58	85.1	10.7	1.4
10	PBGH-19	2.052	TDI	0.273	T	20	2.0	0.66	80.60	12.37	2.91	81.3	12.9	1.9
11	PBGH-19	2.429	DMD	0.464	T	20	2.5	0.69	—	—	—	—	—	—
12	PBG-18	8.279	TDI	1.498	D	40	9.3	0.52	82.79	9.86	2.68	82.6	10.0	2.5
13 <sup>e</sup>	PBG-18	12.26	TDI	2.96	D	50	13.9	0.43	80.73	9.67	4.75	80.3	9.8	4.6
14 <sup>e</sup>	PBG-18	15.43	TDI	2.78	D	50	16.2	0.61	82.37	9.82	3.30	81.8	10.0	3.3
15 <sup>e</sup>	PBG-21	12.46	TDI	3.32	D	50	14.8	0.47	80.56	9.82	5.12	79.7	9.6	5.0

<sup>a</sup> PBG: polybutadiene glycol shown in Table I; PBeG: polybutadiene glycol shown in Table III; PIG: polyisoprene glycol shown in Table I; PBGH: hydrogenated polybutadiene glycol shown in Table IV.

<sup>b</sup> TDI: 2,4-toluene diisocyanate; DMD: diphenylmethane diisocyanate.

<sup>c</sup> T/D: Tetrahydrofuran/dimethylacetamide (50/50); D: dimethylacetamide; T: tetrahydrofuran.

<sup>d</sup> Measured at a concentration of 0.500 g./100 ml in tetrahydrofuran/dimethylacetamide (50/50) and at 30°C.

<sup>e</sup> Hydrazine hydrate was used as a chain extender. In the other preparation water was used as extender.



Table VII shows the results. Inherent viscosities of the products ranged from 0.2 to 0.8. The chain extended polymers from polybutadiene glycols or polyisoprene glycols were soluble in dimethylformamide and dimethylacetamide, but insoluble in tetrahydrofuran. On the other hand, the polymers from hydrogenated polybutadiene glycols were soluble in tetrahydrofuran or a mixture of equal volumes of tetrahydrofuran and dimethylacetamide (50/50), and insoluble in dimethylformamide and dimethylacetamide. Solutions of the chain extended polymers gave colorless, transparent elastic films on casting. The products from polyisoprene glycols were less elastic than those from polybutadiene glycols.

#### 4. Polystyrenedicarboxylic Acid

The preparation of polystyrenedicarboxylic acid by lithium naphthalene-initiated styrene polymerization followed by treatment with carbon dioxide has been reported,<sup>6</sup> but the detail of the synthesis has not been described.

The procedure here was the same as that for polybutadienedicarboxylic acid. The results are listed in Table VIII. The presence of carboxylic groups in the product was indicated by the infrared spectra, 1725 (s), 2700–3300 (broad and strong) and 1250 (m)  $\text{cm}^{-1}$ . The quantitative determination of acid groups was achieved by a conventional titration in a dimethylacetamide solution.

An increase in the amount of catalyst used decreased the molecular weight of the product, but the simple relation,  $\overline{MW} = [\text{monomer}] / ^{1/2} [\text{catalyst}]$ , did not appear to be correct for the higher catalyst concentrations tried in these experiments. The deviation increased more and more as the ratio of catalyst to monomer increased. The lowest molecular weight of the diacid was around 3000. This makes a remarkable contrast with the results from polybutadiene glycol preparation where the relationship,  $\overline{MW} = [\text{monomer}] / ^{1/2} [\text{catalyst}]$ , was adaptable to high ratio of catalyst to monomer and the product having a molecular weight around 1,000 could be made. This observation has also been reported by Lyssy<sup>13</sup> and is explained by assuming the competing reaction between electron transfer from catalyst to monomer and propagation. Dilution of both monomer and catalyst, variation in the stirring efficiency, and prolonged addition time of monomer to the catalyst solution were unsuccessful in attempts to reduce further the molecular weight.

In order to determine the bifunctionality, the chain extension reactions of acid with ethylene glycol were carried out. The macrodiacid was treated with an excess of ethylene glycol in tetrahydrofuran solution in the presence of *p*-toluenesulfonic acid to form the di( $\beta$ -hydroxyethyl) ester. This was further heated in high vacuum with a trace amount of lead acetate at a temperature of approximately 200°C. for 12 hr. The polyesterification proceeded evolving ethylene glycol. The inherent viscosities of starting materials ranged from 0.07 to 0.10 and were increased to 0.4–0.6 by this method. The viscosity values of 0.4–0.6 correspond to molecular weights of 80,000–120,000 calculated from the formula  $[\eta] = KM^\alpha$ , taking 0.65

TABLE VIII  
Preparation of Polystyrenedicarboxylic Acids

Diacid <sup>a</sup>	Styrene, g.	Li, mole	THF, ml.	Temp., °C.	Yield, g.	η <sub>inh</sub> <sup>b</sup>	Polymer melt temp., °C.	CO <sub>2</sub> H Equivalent <sup>c</sup>		Degree of polymeriza- tion <i>n</i> <sup>d</sup>	CH Analysis			
								Found	Calcd.		Found		Calcd.	
PSC-2 <sup>e</sup>	52	0.05	600	-50 to -60	45	0.101	108-118	3480, 3420	1080	65.5	91.20	7.81	91.4	7.68
PSC-4 <sup>e</sup>	52	0.10	800	-30 to -40	45	0.107	108-119	3950, 3950	560	75.0	91.85	7.72	91.4	7.68
PSC-5 <sup>e</sup>	26	0.10	800	-30 to -40	24	0.104	108-119	3320, 3330	300	63.0	91.19	7.65	91.4	7.68
PSC-6 <sup>e</sup>	52	0.10	2000	-30 to -40	43	0.121	115-120	4200, 4140	560	78.8	91.72	7.93	91.4	7.68
PSC-7 <sup>e</sup>	52	0.20	2000	-77	45	0.108	112-120	4070, 4080	300	77.5	91.26	7.54	91.4	7.68
PSC-8 <sup>e</sup>	104	0.20	1000	-77	93	0.106	110-120	3760, 3700	560	70.8	91.32	7.75	91.4	7.68
PSC-9 <sup>e</sup>	64	0.20	900 <sup>f</sup>	-77	45	0.073	107-114	2080, 2050	360	38.8	91.00	7.67	90.7	7.62
PSC-12 <sup>g,h</sup>	55	0.20	900	-77	44	0.075	108-114	2060, 2000	320	38.1	90.45	7.61	90.7	7.62
PSC-14 <sup>e</sup>	29	0.10	450	-77	27	0.096	106-114	1980, 1960	330	36.9	90.72	7.43	90.5	7.60
PSC-15 <sup>e</sup>	29	0.50	450	-77	26	0.074	105-112	1200, 1200	150	22.2	88.50	7.51	89.8	7.56
PSC-16 <sup>e</sup>	29	0.025	450	-77	28	0.081	106-114	2230, 2240	1200	41.8	90.85	7.58	91.0	7.65
PSC-17 <sup>e</sup>	29	0.01	450	-77	27	0.234	122-132	9940, 9970	2940	190.3	91.76	7.66	91.9	7.73
PSC-18 <sup>e</sup>	29	0.10	450	-77	26	0.086	108-114	2360, 2310	330	44.0	90.62	7.58	91.0	7.65

<sup>a</sup> PSC: polystyrenedicarboxylic acid.

<sup>b</sup> Measured at a concentration of 0.500 g./100 ml. toluene and at 30°C.

<sup>c</sup> Determined by the titration with aqueous 0.4*N* potassium hydroxide in *N,N*-dimethylacetamide solution.

<sup>d</sup> Calculated on the basis of carboxyl equivalent value observed.

<sup>e</sup> Dry Ice was used as source of carbon dioxide gas which was dried by passing through columns packed with alumina, Drierite, a mixture of Drierite and phosphorus pentoxide, and silica gel, respectively.

<sup>f</sup> Of this 900 ml., 400 ml., solvent was used for the dilution of styrene monomer.

<sup>g</sup> Matheson's carbon dioxide, Coleman grade -99.99 vol.-% of minimum purity, was used without purification.

<sup>h</sup> Efficient mechanical stirring was applied instead of magnetic stirring.

TABLE IX  
Di( $\beta$ -hydroxyethyl) Ester of Polystyrenedicarboxylic Acid and Polyester of Polystyrenedicarboxylic Acid with Ethylene Glycol

PSC <sup>a</sup>	Polymer melt			Di( $\beta$ -hydroxyethyl) ester of PSC				Polymer melt				Polyester of PSC with ethylene glycol			
	$\eta_{inh}^b$	temp., °C.	$\eta_{inh}^b$	Found		Calcd.		temp., °C.	melt	$\eta_{inh}^b$	Found		Calcd.		
				C, %	H, %	C, %	H, %				C, %	H, %	C, %	H, %	
PSC-14	0.096	106-110	0.104	90.16	7.71	90.0	7.56	125-132	0.53	90.23	7.60	91.2	7.66		
PSC-15	0.074	104-110	0.090	90.05	7.85	88.5	7.45	124-132	0.40	90.16	7.24	90.4	7.60		
PSC-16	0.081	103-109	0.087	90.02	7.82	90.3	7.58	124-132	0.32	89.65	7.46	91.2	7.66		
PSC-17	0.234	113-124	0.244	91.18	7.81	91.6	7.70	123-131	0.63	91.50	7.63	92.1	7.73		
PSC-18	0.056	105-110	0.084	91.31	7.88	90.3	7.58	124-132	0.60	90.68	7.84	91.1	7.65		

<sup>a</sup> Polystyrenedicarboxylic acid.

<sup>b</sup> Measured at a concentration of 0.500 g./100 ml. toluene and at 30°C.

TABLE X  
Block Polyesterification between Macrolycol and Polystyrenedicarboxylic Acid

Run No.	Glycol <sup>a</sup>		Diacid <sup>b</sup>		Solvent (toluene), ml.	Yield, g.	Polymer melt temp., °C.	$\eta_{inh}^c$	Molecular weight <sup>d</sup>	Degree of block polymerization $n$	Analysis	
	Type	g.	Type	g.							Found	Calcd.
1	PBG-18	0.5195	PSC-9	1.3374	15	1.55	82-89	0.206	11,200	2.0	—	—
2	PBG-19	0.1178	PSC-17	1.3792	15	1.35	110-120	0.279	17,400	0.8	91.71	8.02
3	PBG-19	0.6107	PSC-14	1.4450	15	2.00	80-85	0.198	10,700	1.9	89.76	8.49
4	PBG-21	0.2431	PSC-14	0.7310	10	0.85	105-112	0.130	6,200	1.2	90.05	8.43
5	PBG-21	0.1030	PSC-17	1.5658	15	1.51	115-125	0.254	15,500	0.7	91.17	7.87
6	PBG-21	0.2399	PSC-18	0.8569	10	0.95	105-114	0.120	5,000	0.6	89.36	8.38
7	PBG-22	0.4068	PSC-14	1.6096	15	1.85	105-112	0.132	6,000	1.2	89.65	8.10
8	PBG-22	0.1885	PSC-17	3.7645	20	3.72	123-128	0.275	17,000	0.8	91.62	7.85
9	PBG-22	0.4312	PSC-18	2.0240	15	2.25	100-108	0.137	6,300	1.1	89.71	8.06
10	PBGH-8	0.8996	PSC-5	2.4481	20	3.15	—	0.348	23,900	2.7	—	—
11	PBGH-8	1.1167	PSC-4	3.3905	20	4.25	—	0.293	18,700	1.8	—	—
12	PBGH-19	0.5804	PSC-14	1.3515	15	1.84	80-88	0.331	21,900	3.8	80.03	9.30
13	PBGH-19	0.3700	PSC-17	4.3292	20	4.65	115-123	0.516	42,700	2.1	91.51	8.40
14	PBGE-19	0.7243	PSC-18	1.9920	15	2.58	80-88	0.342	27,400	4.4	89.45	9.16

<sup>a</sup> PBG: polybutadiene glycol shown in Table I; PBGH: hydrogenated polybutadiene glycol shown in Table IV.

<sup>b</sup> PSC: polystyrenedicarboxylic acid shown in Table VIII.

<sup>c</sup> Measured at a concentration of 0.500 g./100 ml. toluene and at 30°C.

<sup>d</sup> Calculated by applying formula,  $[\eta] = 3 \times 10^{-4} M^{0.7}$ , where the inherent viscosities were used instead of the intrinsic viscosities.

for  $\alpha$  and  $3 \times 10^{-4}$  for  $K$ . This chain extension involved 10–15 units of polystyrenedicarboxylic acid. The results are shown in Table IX.

### 5. Block Copolymer from Polystyrenedicarboxylic Acid and the Macro Glycol

Direct melt polycondensation between polystyrenedicarboxylic acids and either polybutadiene glycols or hydrogenated polybutadiene glycols were unsuccessful because of their incompatible nature. The polycondensation was carried out by refluxing a toluene solution in the presence of *p*-toluenesulfonic acid under an inert atmosphere. Data on the preparation and results are listed in Table X. Formation of block copolymer consisting of polystyrene units and polybutadiene or hydrogenated polybutadiene units is supported by the infrared analyses, viscosity measurements, elemental analyses, and other properties of the products. Infrared spectra show the products to be free or almost free from either carboxyl or hydroxyl groups. The peak at  $1725 \text{ cm.}^{-1}$  for a carbonyl group was displaced to  $1750 \text{ cm.}^{-1}$ , which corresponds to an ester carboxyl. Other spectroscopic features of the product are much the same in every respect to those of a mechanical mixture of the two starting compounds. The product melts to form a clear liquid; it may also be cast into a transparent film from solution. On the other hand, a blend of two starting materials neither gives a clear melt nor a clear film from solution casting.

The molecular weights of the products have been estimated from their inherent viscosities by applying approximate equation  $[\eta] = 3 \times 10^{-4} M^{0.7}$ . They are shown in Table X. The degree of block polymerization, which was calculated by dividing the molecular weight of product by the sum of molecular weights of the corresponding two starting materials, ranged from 0.8 to 2.0 for the polybutadiene glycol series, and from 2.0 to 4.4 for the hydrogenated polybutadiene glycol series.

As expected from a general knowledge concerning conventional polycondensation reactions, the stoichiometric balance between carboxyl and hydroxyl groups is one of the most important factors required to give high molecular weights. Table XI indicates the results of reaction between hydrogenated polybutadiene glycol (OH eq. 850) and polystyrenedicarboxylic acid (CO<sub>2</sub>H eq. 2,340) which were done by varying the mole ratio of diacid to glycol throughout the stoichiometric range. Maximum inherent viscosity was observed at 1.00 ratio of diacid to glycol. The optimum stoichiometric ratio has not been decided, but may be assumed to be between 1.01 and 0.99. Block polymer prepared here were further subjected to melt polycondensation under high vacuum at 200–210°C. This treatment increased the degree of block polymerization of the polymers to approximately 6.0. Results are presented also in Table XI.

Block polymerization of polybutadiene glycols with polystyrenedicarboxylic acids did not exceed a degree of block polymerization of 2.0. Attempts to increase the molecular weight of the products by varying the

TABLE XI  
Data on Reaction between Hydrogenated Polybutadiene Glycol and Polystyrenedicarboxylic Acid. Effect of Variation of Mole Ratio of the Reactants on Molecular Weight of the Products

Run No.	PBGH-19, g. <sup>a</sup>	PSC-18, g. <sup>b</sup>	Ratio of PSC-18 to PBGH-19	Solvent (toluene), ml.	Yield, g.	Polymer melt temp., °C.	Before melt condensation			After melt condensation		
							$\eta_{inh}^c$	Molecular weight <sup>d</sup>	Degree of block polymerization <i>n</i>	$\eta_{inh}^c$	Molecular weight <sup>d</sup>	Degree of block polymerization <i>n</i>
1	0.7243	1.9920	1.00	15	2.58	80-88	0.344	23,500	3.7	0.423	31,700	5.0
2	0.1240	0.3378	0.91	5	0.99	78-88	0.268	16,600	2.6	0.304	19,900	3.2
3	0.1246	0.3361	0.98	5	0.98	77-87	0.238	13,800	2.2	0.264	15,800	2.5
4	0.7568	0.2889	0.95	10	0.96	78-87	0.231	13,500	2.1	0.264	15,800	2.5
5	0.1783	0.4638	0.90	5	0.90	77-87	0.243	14,400	2.3	0.294	18,700	2.9
6	0.7381	0.2658	1.01	10	0.88	77-86	0.258	15,800	2.5	0.351	24,500	3.9
7	0.1967	0.5682	1.05	10	0.67	77-87	0.184	9,800	1.5	0.241	14,100	2.2
8	0.1372	0.7552	2.00	10	0.81	92-100	0.146	6,900	1.1	0.467	36,300	5.7
9	0.6237	0.8596	0.50	10	1.39	65-75	0.172	8,900	1.4			

<sup>a</sup> Hydrogenated polybutadiene glycol in Table IV.

<sup>b</sup> Polystyrenedicarboxylic acid in Table VIII.

<sup>c</sup> Measured at a concentration of 0.500 g./100 ml. toluene and at 30°C.

<sup>d</sup> Calculated by applying formula  $[\eta] = 3 \times 10^{-4} M^{0.7}$ .

ratio of diacid to glycol as well as using higher boiling solvents such as xylene, were unsuccessful. The reaction in xylene showed decolorization of the reaction mixture and resulted in low viscosity polymer. Further melt polycondensation of the product prepared by solution polymerization gave a gelled polymer at temperatures above 130°C.

As would be expected from their high styrene content, the block polymers prepared above have properties very similar to those of polystyrene except for low polymer melt temperatures.

Further study of this block copolymerization method from olefinic monomers promises syntheses of block copolymers having well-defined structure.

## EXPERIMENTAL

### Materials

Tetrahydrofuran previously distilled over calcium hydride was further purified by distilling from the solution of disodium polybutadiene or disodium polyisoprene. To 2 l. of calcium hydride-distilled tetrahydrofuran was added 6.9 g. (0.30 mole) of sodium metal and 40.3 g. ( $0.30 \times 1.05$  mole) of recrystallized naphthalene. The solution was stirred under positive pressure of argon until all of the sodium had disappeared in the formation of sodium naphthalene complex. Into the solution was introduced about 60 g. of butadiene or isoprene, forming  $\alpha,\omega$ -disodium polybutadiene or disodium polyisoprene. The tetrahydrofuran was then distilled from this solution directly into a polymerization flask under positive pressure of argon.

Naphthalene was recrystallized three times from absolute ethanol, dried under high vacuum, and stored over silica gel.

Butadiene, Phillips polymerization grade, was purified by passing through a series of three scrubbers each containing ethylene glycol/sodium ethylene glycolate to remove moisture in the monomer. Anhydrous ethylene glycol (150 ml.) in which sodium (2 g.) had been dissolved was added to each gas scrubber. The system was purged with argon to remove air before use. Butadiene was passed through the scrubbers, then through a Drierite column, and finally condensed in a graduated cylinder immersed in a Dry Ice-acetone bath. About 200 ml. of the monomer was collected over a period of 2-3 hr. In experiments of PBG-2 through 7, PBG 12 and PBG-14 in Table I, butadiene was purified by passage through long columns packed with alumina, a mixture of phosphorus pentoxide and Drierite, and silica gel, but this method did not completely remove water which was retained by the monomer as an azeotropic mixture.

Isoprene, Phillips research grade 99.99 mole-% of minimum purity, was distilled through a 12-in. Vigreux column under positive pressure of argon.

Styrene, Eastman Kodak b.p. 33-35°C./8 mm. Hg, was distilled under diminished pressure before use.

Ethylene oxide, Matheson 99.7% of minimum purity, was distilled through two columns packed with soda lime and condensed into a dropping funnel having a Dry Ice-acetone cooling jacket.

Carbon dioxide, Matheson Coleman grade 99.99 vol.-% of minimum purity, was used without special purification treatment.

### Polybutadiene Glycols and Polyisoprene Glycols

Data on the preparations, inherent viscosities, functional endgroup determinations, and elemental analyses of compounds prepared are given in Tables I-III. Here a typical preparation is shown for each compound.

#### *Polybutadiene Glycol from $\alpha,\omega$ -Dilithium Polybutadiene and Ethylene Oxide (PBG-19 in Table I)*

In a 1000-ml., three-necked flask were placed 1.04 g. (0.15 mole) of lithium metal and 20.2 g. (0.15  $\times$  1.05 mole) of naphthalene. The flask was equipped with a dropping funnel having a Dry Ice-acetone cooling jacket, an adaptor for distillation of solvent, Teflon-coated magnetic stirrer, and a gas inlet tube, the end of which reached just above the surface of reaction mixture. After flaming out the flask under argon, about 900 ml. of tetrahydrofuran was distilled directly into the flask from a tetrahydrofuran solution of disodium polybutadiene. The mixture was stirred for 4 hr. at room temperature. Within this period the lithium disappeared completely. The dark green solution was cooled to  $-77^{\circ}\text{C}.$ , and 130 g. (2.41 mole) of butadiene was introduced into the mixture through the gas inlet tube over 1 $\frac{1}{2}$  hr. at the same temperature. After the addition of butadiene, about 15 ml. of ethylene oxide stored in the dropping funnel was added rapidly into the mixture. The whole solution gelled and decolorized quickly. The flask was allowed to stand in a cooling bath at a temperature below  $-30^{\circ}\text{C}.$  overnight and then for three days at room temperature. All the procedures described above were carried out under argon, and the reactants and reaction mixture were kept from contact with air throughout by the use of stopcocks. The mass was treated with 0.4 g. of du Pont Antioxidant No. 29 (2,6-di-*tert*-butyl-4-methylphenol) and 25 ml. of distilled water. Addition of water produced a nonviscous solution. After pouring into 2000 ml. of water, the separated organic layer was further treated with six successive 1500-ml. portions of hot water, at least 1 hr. being allowed for each wash together with efficient stirring. The glycol was taken up in benzene and dried with anhydrous sodium sulfate. The transparent benzene solution was filtered, evaporated, and finally dried in a rotary high vacuum evaporator at  $80-90^{\circ}\text{C}.$  for 24 hr. During this treatment naphthalene contained in the glycol sublimed away. The product was a colorless viscous liquid, weighing 122 g.;  $\eta_{\text{inh}}$  0.078 ( $c = 0.500$  g./100 ml. toluene at  $30^{\circ}\text{C}.$ ); OH eq. 869, 840.



*Polybutadiene Glycol from Polybutadienedicarboxylic Acid (PBC-6 in Tables II and III)*

**Polybutadienedicarboxylic Acid (PBC-6).** To the  $\alpha,\omega$ -dilithium polybutadiene solution prepared by the same method as that in PBG-19 described above was added rapidly 80 ml. of saturated tetrahydrofuran solution of carbon dioxide at  $-77^{\circ}\text{C}$ . After standing for two days at temperatures below  $-30^{\circ}\text{C}$ ., the mixture was treated with 0.5 g. of anti-oxidant and neutralized with 30 ml. of concentrated hydrochloric acid. It was washed repeatedly with hot water, extracted with benzene, dried over sodium sulfate, and finally dried in a high-vacuum rotary evaporator. The product was a pale yellow viscous liquid, weighing 124 g.;  $\eta_{inh}$  0.103 ( $c = 0.500$  g./100 ml. toluene at  $30^{\circ}\text{C}$ .);  $\text{CO}_2\text{H}$  eq. 995, 1005.

**Dimethyl Ester of Polybutadienedicarboxylic Acid.** A mixture of 90.6 g. of polybutadienedicarboxylic acid (PBG-6), 1000 ml. of benzene, 500 ml. of methanol, and 5.0 g. of *p*-toluenesulfonic acid was refluxed for 24 hr. The mixture was reduced to about 500 ml. by evaporation under diminished pressure and poured into water. The organic layer was separated, repeatedly washed with water, and dried over sodium sulfate. After removal of benzene, the polymer was dried in a high vacuum rotary evaporator at  $80^{\circ}\text{C}$ . for 12 hr. The product was a pale yellow liquid. The yield was 84 g.;  $\eta_{inh}$  0.088 ( $c = 0.500$  g./100 ml. toluene at  $30^{\circ}\text{C}$ .). The compound shows infrared spectra of carboxylic ester at 1750 (s) and 1180 (m)  $\text{cm}^{-1}$ , and no maxima due to the presence of free carboxylic groups was observed.

**Reduction of Polybutadienedicarboxylic Acid Dimethyl Ester with Lithium Aluminum Hydride.** A mixture of 15 g. of pulverized lithium aluminum hydride and 1200 ml. of tetrahydrofuran was stirred at room temperature over night and filtered by suction through a coarse glass filter directly into the reaction flask. To this solution was added dropwise a solution of 80.0 g. of polybutadienedicarboxylic acid dimethyl ester in 200 ml. of tetrahydrofuran under ice water cooling and mechanical stirring over a period of  $1\frac{1}{2}$  hr. After addition of the ester, stirring was continued for  $\frac{1}{2}$  hr. at the same temperature. Excess metal hydride was inactivated by adding wet tetrahydrofuran. Precipitated inorganic hydroxide was filtered off and washed with tetrahydrofuran. After evaporating the filtrate, the residual oil was taken up with benzene, washed with water, dried over sodium sulfate, evaporated, and finally dried in a high vacuum rotary evaporator. The product was a colorless viscous liquid and weighed 63 g.;  $\eta_{inh}$  0.100 ( $c = 0.500$  g./100 ml. toluene at  $30^{\circ}\text{C}$ .); OH eq. 997, 985. The compound shows spectra at 3500 (s), 1070 (s)  $\text{cm}^{-1}$ —OH and no maxima due to the presence of carbonyl groups.

*Polyisoprene Glycol (PIG-5 in Table I)*

This was prepared from 136 g. (2.0 mole) of isoprene under the same reaction conditions and procedure as those for polybutadiene glycol

(PBG-19) described previously. The yield was 122 g. The product was a yellow amorphous semisolid;  $\eta_{inh}$  0.058 ( $c = 0.500$  g./100 ml. toluene at 30°C.).

### Hydrogenation of Polybutadiene Glycols and Polyisoprene Glycols

Data on the hydrogenations, and inherent viscosities, hydroxyl equivalents, and elemental analyses of the products are given in Table IV. The preparation described below is typical.

#### *Hydrogenation of Polybutadiene Glycol (PBGH-19 in Table IV)*

In a 500-ml. centrifuge bottle were placed 17 g. of polybutadiene glycol (PBG-19), 50 ml. of absolute ethanol, and 0.5 g. of 5% palladium in charcoal catalyst. The mixture was shaken under an initial hydrogen pressure of 50 lb./in.<sup>2</sup> at room temperature. The reaction proceeded exothermically and almost all of the hydrogen was absorbed within the first 30 min. The mixture was further treated with hydrogen for another 3 hr. and heated by an infrared lamp. The hydrogenated glycol separated from the solvent on cooling. Benzene was added to dissolve the mixture and the catalyst was removed by filtration. The filtrate was evaporated and dried in a high vacuum rotary evaporator at 90–100°C. for 15 hr. The product was a colorless viscous liquid. The yield was 17 g.;  $\eta_{inh}$  0.078 ( $c = 0.500$  g./100 ml. toluene at 30°C.); OH eq. 875, 865.

#### *Hydrogenation of Polyisoprene Glycol (PIGH-3 in Table IV)*

A mixture of 30 g. of polyisoprene glycol (PIG-30), 100 ml. of absolute ethanol, and 2 g. of 5% palladium charcoal was treated with hydrogen by the same procedure as described above. The product was a colorless amorphous semisolid. The yield was 29 g.;  $\eta_{inh}$  0.056 ( $c = 0.500$  g./100 ml. toluene at 30°C.); OH eq. 938, 936.

### Chain Extension Reaction of the Macroglycols with Diisocyanate

Data on the reactions, inherent viscosities, and elemental analyses of the products are given in Table VII. Two typical reactions are represented here.

#### *Chain Extension of Polybutadiene Glycol by 2,4-Toluene Diisocyanate*

To a solution of 3.407 g. ( $2.0 \times 10^{-3}$  mole) of polybutadiene glycol (PBG-19) in 15 ml. of purified tetrahydrofuran was added 0.419 g. ( $2.0 \times 1.3 \times 10^{-3}$  mole) of 2,4-toluene diisocyanate, a trace amount of iron acetylacetonate, and one drop of triethylamine. The solution was heated at 60°C. under positive pressure of argon for 24 hr. To the solution was added 1.0 ml. of 0.1% wet tetrahydrofuran and the solution was heated at 60°C. for 48 hr. The polymer was precipitated in methanol, washed with methanol, and vacuum-dried. The yield was 3.6 g.;  $\eta_{inh}$  0.72 ( $c = 0.500$  g./100 ml. in 50/50 tetrahydrofuran/dimethylacetamide, at 30°C.).

*Chain Extension of Polybutadiene Glycol by 2,4-Toluene  
Diisocyanate and Hydrazine*

A mixture of 12.26 g. ( $8.52 \times 10^{-3}$  mole) of polybutadiene glycol (PBG-18) and 2.96 g. ( $8.52 \times 2.0 \times 10^{-3}$  mole) of 2,4-toluene diisocyanate was heated at 75°C. for 24 hr. with stirring under positive pressure of argon. The mixture then was dissolved by adding 50 ml. of dimethylacetamide. To this solution was added 0.272 g. of hydrazine as 1% solution in dimethylacetamide at room temperature over a period of 20 min. The mixture was stirred for 5 hr. and poured into methanol. The polymer precipitated was washed with methanol and vacuum-dried. The yield was 13.9 g.;  $\eta_{inh}$  0.43.

### Polystyrenedicarboxylic Acids

Data on the preparation, inherent viscosities, polymer melt temperature, carboxyl equivalents, and elemental analyses are given in Table VIII. A typical preparation is described below.

*Polystyrenedicarboxylic acid (PSC-18 in Table VIII)*

In a 500-ml., three-necked flask were placed 0.69 g. (0.10 mole) of lithium metal and 13.4 g. ( $0.10 \times 1.05$  mole) of naphthalene. The flask was equipped with a stopcock, a Teflon-coated magnetic stirring bar, and two dropping funnels, one for styrene monomer, the other which had a Dry Ice-acetone cooling jacket for distillation of solvent as well as for storage of carbon dioxide solution. After flaming out the flask under argon, about 450 ml. of tetrahydrofuran was distilled into the funnel. The mixture was stirred for 4 hr., during which time the lithium had disappeared completely, forming dark green lithium naphthalene. The mixture was cooled to -77°C., and 29 g. (0.5 mole) of styrene was added dropwise to the solution over 30 min. A saturated solution of carbon dioxide in 80 ml. tetrahydrofuran at -80°C. was added rapidly to the mixture. The solution gelled and decolorized quickly. After standing over night at a temperature below -30°C., the mass was treated with 0.2 g. of antioxidant, neutralized with 15 ml. of concentrated hydrochloric acid and poured into methanol. The polymer precipitated was washed repeatedly with water and methanol, and dried under vacuum at 80°C. The product was a colorless powder. The yield was 26 g.;  $\eta_{inh}$  0.086 ( $c = 0.500$  g./100 ml. toluene at 30°C.); CO<sub>2</sub>H eq. 2360, 2310.

### Polyesters from Polystyrenedicarboxylic Acid and Ethylene Glycol

Data on the polymer melt temperature, inherent viscosities, and elemental analyses of the product are given in Table IX.

*Di( $\beta$ -hydroxyethyl) Ester of Polystyrenedicarboxylic Acid*

A mixture of 3.0 g. of polystyrenedicarboxylic acid (PSC-18), 50 ml. of tetrahydrofuran, 20 ml. of ethylene glycol, and 0.5 g. of *p*-toluenesulfonic

acid was refluxed for 48 hr. The solvent was removed by distillation and the residue was poured into methanol. The precipitate was washed with methanol and dried in vacuo. The product was a colorless powder, weighing 2.7 g.;  $\eta_{inh}$  0.096 ( $c = 0.500$  g./100 ml. toluene at 30°C.). The infrared spectrum of the compound shows absorptions at 3550  $\text{cm.}^{-1}$  (OH) and 1750  $\text{cm.}^{-1}$  (ester carbonyl). No free acid carbonyl at 1725  $\text{cm.}^{-1}$  can be detected.

#### *Melt Polycondensation of the Di( $\beta$ -hydroxyethyl) Ester*

In a tube equipped with a capillary and a sidearm were placed 1.0 g. of the di( $\beta$ -hydroxyethyl) ester obtained above, and a trace amount of lead acetate. The mixture was heated at 200–210°C. for 24 hr. under vacuum, the capillary allowing a slow argon flow through the melt. During the first 10–15 min. heating, vigorous evolution of ethylene glycol was observed. The product was dissolved in benzene and reprecipitated from methanol. The product was a colorless fibrous substance. The yield was 0.8 g.;  $\eta_{inh}$  0.604 ( $c = 0.500$  g./100 ml. toluene at 30°C.). The compound shows infrared absorption at 1750  $\text{cm.}^{-1}$  (ester carbonyl) and no absorption of hydroxyl group.

### **Block Copolymer from Polystyrenedicarboxylic Acids and the Macroglycols**

Data on the preparations, polymer melt temperature, inherent viscosities, molecular weights, degrees of block polymerization, and elemental analyses are given in Tables X and Table XI.

#### *General Procedure. Solution Polycondensation*

The diacid and glycol were weighed accurately according to the ratios, based on their carboxyl and hydroxyl equivalents values, as shown in Table X and XI. The mixtures were subjected to polyesterification in refluxing toluene under argon pressure in the presence of *p*-toluenesulfonic acid for 48 hr. The mixtures were precipitated into methanol using a Waring Blender. The polymers were filtered, washed with methanol, and dried.

#### *Further Melt Polycondensation*

The products obtained above were heated at 200–210°C. in high vacuum for 15 hr. Argon was introduced into the melt through a capillary during heating. The polymer was dissolved in benzene and reprecipitated from methanol.

We are indebted to Dr. John Campbell, Research Division of the Elastomers Department of E. I. du Pont de Nemours and Company, for the suggestion that argon should be used to blanket these reactions. We also wish to thank Dr. R. S. Hammer of the Phillips Petroleum Company for suggesting the use of sodium glyxide in ethylene glycol as a means of purifying butadiene. The financial support of the Textile Fibers Department of E. I. du Pont de Nemours and Company is gratefully acknowledged.

### References

1. Szwarc, M., *Nature*, **178**, 1168 (1956).
2. Szwarc, M., M. Levy, and R. Milkovich, *J. Am. Chem. Soc.*, **78**, 2656 (1956).
3. Brody, H., M. Ladacki, R. Milkovich, and M. Szwarc, *J. Polymer Sci.*, **25**, 221 (1957).
4. Szwarc, M., *Fortschr. Hochpolymer.-Forsch.*, **2**, 275 (1960).
5. Richard, D. H., and M. Szwarc, *Trans. Faraday Soc.*, **55**, 1644 (1959).
6. Sorensen, W. R., and T. W. Campbell, *Preparative Methods of Polymer Chemistry*, Interscience, New York, 1960, p. 134.
7. Nikolov, N., paper presented at the 10th Canadian High Polymer Forum 1960, Ste. Marguerite, Que., Canada.
8. Goldberg, E. J., U. S. Pat. 3,055,952 (Sept. 25, 1962); *Chem. Abstr.*, **58**, 645 (1963).
9. Hampton, R. R., *Anal. Chem.*, **21**, 923 (1949).
10. Binder, J. L., *J. Polymer Sci.*, **A1**, 47 (1963).
11. Ogg, C. L., W. L. Porter, and C. O. Willits, *Ind. Eng. Chem., Anal. Ed.*, **17**, 394 (1945).
12. Richardson, W. S., and A. Sacher, *J. Polymer Sci.*, **10**, 353 (1953).
13. Lyssy, T., *Helv. Chim. Acta*, **42**, 2245 (1959).

### Résumé

On a utilisé la technique du polymère vivant de Szwarc pour synthétiser des dérivés  $\alpha,\omega$ -bifonctionnels du polybutadiène, polyisoprène et polystyrène. Les glycols dérivés du polybutadiène ont été hydrogénés pour donner des glycols saturés. Les glycols du polyisoprène ont été partiellement hydrogénés. On a caractérisé certains polyesters et polyuréthanes séquencés.

### Zusammenfassung

Mit Hilfe der Szwarc'schen "living polymer"-Methode wurden  $\alpha,\omega$ -bifunktionelle Derivate von Polybutadien, Polyisopren und Polystyrol hergestellt. Die von Polybutadien abgeleiteten Glykole wurden zu gesättigten Glykolen hydriert. Die Glykole aus Polyisopren wurden partiell hydriert. Einige Blockpolymerester und -urethane wurden charakterisiert.

Received May 27, 1963

## Ring-Opening Polymerization of a Sugar Episulfide\*

ROY L. WHISTLER and PAUL A. SEIB, *Department of Biochemistry, Purdue University, Lafayette, Indiana*

### Synopsis

Ring-opening polymerization of 5,6-dideoxy-5,6-epithio-1,2-*O*-isopropylidene- $\alpha$ -*D*-idofuranose is catalyzed by boron trifluoride at 60°C. Soluble polymer is produced at monomer: catalyst ratio of 7:1 and monomer concentration 0.077*M* after 1 1-hr. polymerization period. This polymer has a wide molecular weight distribution. A number-average molecular weight of 72,000 is found for the first 40% of the polymer precipitated from a *N,N*-dimethylformamide solution by the addition of water. Polymer is produced in increasing amounts as temperature is raised, catalyst concentration increased, and as water concentration is decreased. Transglycosylation may be the cause of branch formation or crosslinking. Hydrolysis of the soluble polymer removes isopropylidene groups to produce a water soluble reducing polymer which oxidizes with hypiodite to a polymer containing carboxyl groups.

### INTRODUCTION

Ring-opening polymerization of sugar derivatives was initiated in 1918 when Pictet<sup>1</sup> polymerized levoglucosan. Improvements in the polymerization of levoglucosan have been effected by use of chloroacetic acid<sup>2</sup> and boron trifluoride for levoglucosan trimethyl ether.<sup>3,4</sup>

Various other anhydro sugars have been subjected to ring-opening polymerization. These include 1,6-anhydro- $\beta$ -*D*-galactopyranose,<sup>5</sup> 5,6-anhydro-3-*O*-methyl-1,2-*O*-isopropylidene-*D*-glucofuranose,<sup>6</sup> and the copolymerization of levoglucosan with 1,6-anhydro- $\beta$ -*D*-galactopyranose.<sup>7</sup> The synthetic *D*-mannans produced from 1-fluoro- $\alpha$ -*D*-mannose upon treatment with aqueous base are attributed to the ring-opening polymerization of an intermediate anhydro derivative.<sup>8</sup>

In the present work the ring-opening polymerization of 5,6-dideoxy-5,6-epithio-1,2-*O*-isopropylidene- $\alpha$ -*L*-idofuranose (sugar episulfide) is examined. The ease of polymerization of the thiirane ring is well recognized.<sup>9-14</sup> Polymerization has been encountered as a side reaction during chemical transformation of sugar episulfides.<sup>15,16</sup>

\* Journal Paper No. 2138 of Purdue University Agricultural Experiment Station as a collaboration under North Central Regional Project NC60 entitled, "Modification of Starch for Industrial Uses."

## EXPERIMENTAL

5,6 - Dideoxy - 5,6 - epithio - 1,2 - *O* - isopropylidene -  $\alpha$  - L - idofuranose, m.p. 169°C., was prepared according to the method of Hall, Hough, and Pritchard.<sup>15</sup>

Reagent-grade benzene was refluxed and distilled from lithium aluminum hydride and was stored over sodium.

Boron trifluoride etherate (250 ml.) was purified by mixing with 10 ml. of ethyl ether, refluxed with 1 g. of calcium hydride, and distilled under reduced pressure.

Limiting viscosity numbers were determined in *N,N*-dimethylformamide at 25°C. in an Ubbelohde viscometer.

Osmotic molecular weights were determined with the use of the Stabin-Immergut modification<sup>17</sup> of the Zimm-Myerson<sup>18</sup> osmometer with gellophane membranes.

### Polymerization

All polymerizations were conducted in sealed tubes at 60°C. In a typical experiment, 50-mg. portions of sugar episulfide was placed in each of 5 to 10 polymerization tubes (10  $\times$  200 mm.). Each tube was capped with a rubber cap (Aloe Scientific, V 72400), and 2.55 ml. of benzene was injected with a hypodermic syringe. After dissolution of the monomer by warming the mixture, the solution was immediately frozen in a Dry Ice-acetone bath. The air in the tube was removed through a hypodermic needle and while under reduced pressure the tube contents were twice thawed and frozen. With the contents frozen, the tube was filled with anhydrous, oxygen-free nitrogen, and 0.45 ml. of a 1% solution of boron trifluoride etherate in benzene was injected. The tube was evacuated and, after withdrawing the needle, sealed and placed in a constant temperature

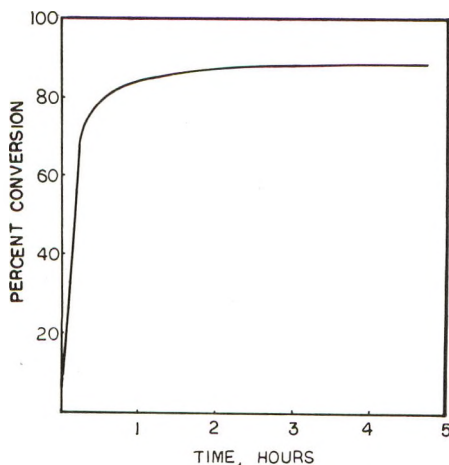


Fig. 1. Rate of conversion of monomer to polymer 1.

bath at 60°C. The tube was shaken vigorously while the contents thawed and was shaken briefly every 5 min. thereafter. Polymerization was evidenced by a gradual precipitation of polymer. At intervals a tube was removed and the entire polymer precipitated in ethyl ether. The polymer was collected by filtering on a tared sintered-glass funnel, and washed well with ether. Conversion to polymer is illustrated in Figure 1.

Solubility of the polymer in *N,N*-dimethylformamide (DMF) was also determined. For a molar ratio of monomer:catalyst of 7:1 and a monomer concentration of 0.077*M*, there was obtained in 1 hr. an 84% conversion to polymer, of which 4–6% was insoluble in DMF (polymer 1, Table I). Two other selected polymers prepared with monomer:catalyst ratios of 14:1 and 22:1 and monomer concentrations of 0.077*M* are shown in Table I. As the time of the conversion period is extended the amount of DMF-insoluble polymer increases. The periods given in the table are those producing maximum conversion to polymer with minimum production of insolubles.

TABLE I  
Polymers Obtained at Different Monomer:Catalyst Ratios

Polymer	Molar ratio monomer/catalyst	Conversion period, hr.	Conversion, %	$[\eta]$ of DMF-soluble polymer
1	7	1	84	0.06
2	14	8	68	0.08
3	22	12	60	0.08

### Polymerization in the Presence of Water

A molar ratio of monomer to catalyst of 7:1 with a monomer concentration of 0.077*M* was maintained in this polymerization. The amount of

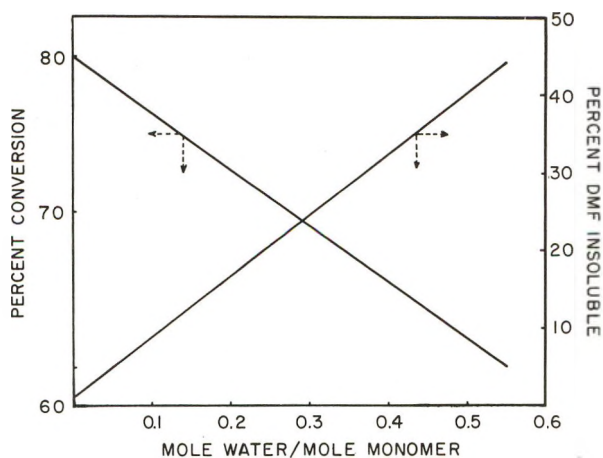


Fig. 2. Effect of water on polymerization.



water present was varied by using appropriate mixtures of benzene and benzene saturated with water. Benzene saturated with water at 25°C. contained  $0.10 \pm 0.01\%$  water as determined by K. Fischer titration. Polymerizations were conducted for 1 hr. The yields of total polymer and polymer insoluble in DMF are shown in Figure 2. The DMF-insoluble polymer was also insoluble in water and DMF-water mixtures.

### Fractionation of Polymer 1

Polymer 1 was fractionated from solution in *N,N*-dimethylformamide at 25°C. by incremental addition of a 0.1*M* aqueous solution of sodium chloride. After centrifugal removal, the successive precipitates were dissolved in acetone and the amounts measured by evaporating the solvent from tared beakers containing Celite. A plot of yields is shown in Figure 3.

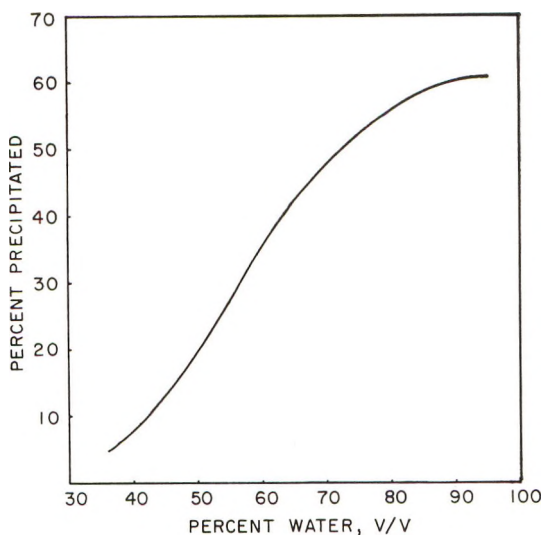


Fig. 3. Fractionation of polymer 1.

Large amounts of polymer 1 were also prepared. For this, crude polymer 1 was dissolved in DMF and filtered through a Celite pad to remove the gel. To the filtrate was added slowly with stirring aqueous 0.1*M* sodium chloride solution until the water content of the solution was 80%. The suspension was centrifuged and the supernatant was discarded. Polymer was dissolved in acetone, dialyzed against distilled water, and lyophilized to obtain a white, fluffy product. Yield from crude polymer was 40%. Its osmotic molecular weight in DMF was 72,000, and its sulfur content was 14.8%. Films were cast on a mercury surface from a 10% acetone solution of polymer. The polymer gave a negative boron flame test, and a negative Benedict's test for reducing groups. An infrared pattern showed no aromatic absorption in the region  $700\text{--}800\text{ cm.}^{-1}$  and no

thiol absorption at 2550–2700  $\text{cm}^{-1}$ . The polymer also gave a negative test for thiol groups with sodium nitroprusside and failed to decolorize iodine solution. Its x-ray diffraction pattern was amorphous. It softened at 110–120°C. and decomposed slowly at 180–250°C.

Polymer 1 was acetylated<sup>19</sup> in pyridine–formamide and acetic anhydride for 9 hr. at 25°C. The product was precipitated in ice–water mixture, washed, and dried. The product was acetylated a second time in pyridine and acetic anhydride; the acetyl content was 16.4%.

### Hydrolysis of Polymer

To 0.5 g. of polymer 1 dissolved in 500 ml. of *p*-dioxane was added 400 ml. of 1*N* hydrochloric acid solution. The mixture was shaken 24 hr., neutralized with base, and dialyzed against distilled water. The product was isolated by freeze-drying; the yield was 100%. The osmotic molecular weight in water with distilled toluene as the manometric liquid was 51,000. No monosaccharide or oligomers were present in the hydrolyzate.

The polymer was oxidized with sodium hypoiodite<sup>20</sup> to a polymer which contained aldonic acid units. This carboxylated polymer precipitated on addition of barium ions.

### Preparation and Polymerization of 3-*O*-Acetyl-5,6-dideoxy-5,6-epithio-1,2-*O*-isopropylidene- $\alpha$ -L-idofuranose

The sugar episulfide was acetylated in a mixture of pyridine and acetic anhydride. Several recrystallizations from *n*-pentane produced needles with a constant melting point, m.p. 90–91°C.

ANAL. Calcd. for  $\text{C}_{11}\text{H}_{61}\text{O}_5\text{S}$ : S, 12.30%. Found: S, 12.04%.

This acetylated sugar episulfide was polymerized under the same conditions which were used in the preparation of polymer 1. Polymerization occurred more slowly than with the nonacetylated monomer, requiring about 7 hr. to reach maximum yield. However, after a polymerization period of 10 hr. the yield of acetylated polymer was only 76%, but the entire product was soluble in DMF.

### Reactions of 1,2:5,6-Di-*O*-isopropylidene-D-glucufuranose

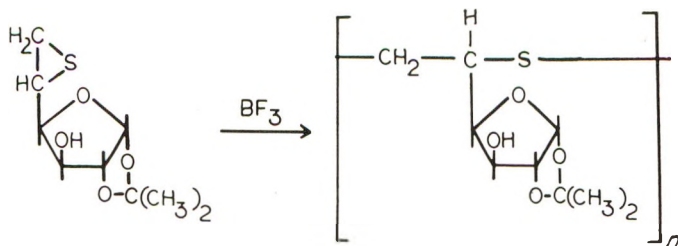
A reaction was undertaken to determine if the hydroxyl at  $\text{C}_3$  participates to produce a branched polymer. In each of three polymerization tubes was sequentially placed 25 mg. of 1,2:5,6-di-*O*-isopropylidene- $\alpha$ -D-glucufuranose in 2.55 ml. of benzene, 25 mg. of the sugar episulfide in 2.55 ml. of benzene, and a mixture of 25 mg. of 1,2:5,6-di-*O*-isopropylidene- $\alpha$ -D-glucufuranose in 2.55 ml. of benzene with 25 mg. of the sugar episulfide. Then to each tube was added in the manner described above 0.45 ml. of a 1% solution of boron trifluoride etherate in benzene. After being subjected to the above described polymerization conditions for 1 hr., the contents were poured onto 5 ml. of 1*N* sulfuric acid solution and heated for 1 hr.

at 90°C. The solutions were cooled, neutralized with barium carbonate, filtered, and paper chromatographed, ethyl acetate:acetic acid:formic acid:water (18:3:1:4) being used as irrigant. None of the hydrolyzates showed thiol activity with formazan spray.<sup>21</sup> Silver nitrate spray<sup>21</sup> of the paper chromatograms disclosed only D-glucose in the hydrolyzate from the tube originally charged with 1,2:5,6-di-*O*-isopropylidene- $\alpha$ -D-glucofuranose. Hydrolyzate from the tube which originally contained the sugar episulfide showed the presence of two components with  $R_{\text{glucose}}$  values of 2.55 and 0.57. These same two components were obtained when sugar episulfide was subjected to hydrolysis conditions. Hydrolyzate from the tube which contained the mixture of 1,2:5,6-di-*O*-isopropylidene- $\alpha$ -D-glucofuranose and the sugar episulfide showed the presence of D-glucose and the components with  $R_x$  values of 2.55 and 0.57. No evidence for oligomers was obtained.

In an attempt to show whether oligosaccharides can be prepared in the reaction, a polymerization tube was charged with 25 mg. of 1,2:5,6-di-*O*-isopropylidene- $\alpha$ -D-glucofuranose in 1.78 ml. of benzene and 0.27 ml. of a 1% solution of boron trifluoride etherate in benzene. After  $\frac{1}{2}$  hr. at 60°C. the contents of the tube were chromatographed by paper chromatography and by thin layer chromatography on glass plates coated with Silica Gel G (Merck). Evidence was obtained for large amounts of unreacted 1,2:5,6-di-*O*-isopropylidene- $\alpha$ -D-glucofuranose, and trace amounts of D-glucose, 1,2-*O*-isopropylidene- $\alpha$ -D-glucofuranose, and a component of  $R_f$  0.61 in acetone which may have been an oligosaccharide. Heavy streaking also indicated the presence of numerous other components. After hydrolysis of the reaction mixture, only D-glucose was observed on paper chromatographic analysis.

## DISCUSSION

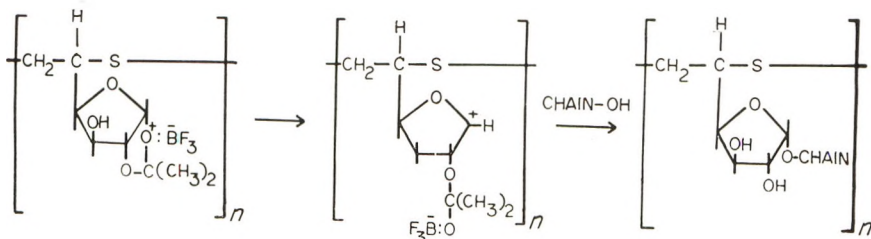
Polymerization of 5,6-dideoxy-5,6-epithio-1,2-*O*-isopropylidene- $\alpha$ -L-ido-furanose should lead to a mainly linear polymer, particularly if the reactivity of the hydroxyl group at C<sub>3</sub> is low and transglycosylation is minimal.



Polymerization of the sugar episulfide is slow even in the presence of boron trifluoride catalyst. To induce a moderate rate of polymerization large amounts of catalyst are required, presumably because much of the catalyst is unproductively bound to oxygens. Reaction rates are increased

at elevated temperatures, but side reactions also become significant at temperatures of 100°C. and above. Consequently, comparison reactions were made at 60°C. where no color development occurred. Reaction rates increase with increasing molar ratios of boron trifluoride to monomer as shown in Table I. The times to reach 60% conversion in the polymerizations used to prepare polymers 1, 2, and 3 are 0.2, 7, and 12 hr., respectively. Increasing the concentration of monomer in solution also increases the reaction rate but leads to an increase in the amount of insoluble polymer formed.

Formation of an insoluble polymer is likely the result of crosslinking through branching due to one or both of two side reactions. One could be participation of the hydroxyl group on carbon atom C<sub>3</sub>. Reaction of this hydroxyl on a midchain unit with an episulfide in a ring-opening chain initiating reaction would lead to branch formation. A second side reaction may lead both to branch formation and crosslinking. This reaction results from catalyzed opening of the 1,2-isopropylidene ring by the elimination of its alkyloxy bridge at carbon C<sub>1</sub> as an anion combined with boron trifluoride, leaving a carbonium ion at C<sub>1</sub>. The carbonium ion can combine with oxygen on other chain monomer units. Such transglycosylation has been observed with methyl  $\alpha$ -D-glucopyranoside in the presence of Lewis acid catalysts.<sup>22</sup>



Branch formation through reaction of the episulfide group with the C<sub>3</sub> hydroxyl of a chain unit does not occur in detectable amounts, since no oligomers are detected when the sugar episulfide and 1,2:5,6-di-*O*-isopropylidene- $\alpha$ -D-glucofuranose are reacted under polymerization conditions and the mixtures subsequently hydrolyzed. Furthermore, secondary hydroxyl groups are not reactive toward ring-opening of episulfides.<sup>23</sup>

Consequently, formation of insoluble polymer seems due, for the most part, to crosslinks arising by the transglycosylation route. Evidence supports this concept. 1,2:5,6-Di-*O*-isopropylidene- $\alpha$ -D-glucofuranose when heated with boron trifluoride produces a number of products among which are oligomers. Hydrolysis of these leads to D-glucose only. Furthermore, formation of insoluble polymer in the polymerization of the acetylated sugar episulfide is negligible. Other observations pointing to transglycosylation crosslinking are the increased formation of insoluble polymer at higher catalyst concentration and upon addition of water to the

polymerization system. In both instances and particularly the latter, removal of isopropylidene groups is facilitated (Fig. 2).

Under conditions where insoluble polymer formation is low, such as those used for the preparation of polymer 1, the polymer produced has a broad molecular weight distribution rather than a Poisson distribution. The broad distribution is evident from a precipitation curve obtained by sequential precipitation of fractions from a *N,N*-dimethylformamide solution by addition of water. The number-average molecular weight for the first 40% of the polymer to precipitate under these conditions is 72,000. Films from the polymer are very brittle. The polymer can be acetylated to introduce one acetyl group per sugar unit. Examination by infrared shows the absence of phenyl and mercapto groups.

On hydrolytic removal of the isopropylidene groups the polymer becomes water soluble and develops a strong reducing power. Hypoiodite converts the aldehyde groups to carboxyls. This polymer with aldonic acid units is precipitated from a water solution by the addition of barium ions.

The authors thank the Corn Industries Research Foundation for grants in partial support of this work.

### References

1. Pictet, A., and J. Sarasin, *Helv. Chim. Acta*, **1**, 87 (1918).
2. Carvalho, J. DaSilva, W. Prins, and C. Schuerch, *J. Am. Chem. Soc.*, **81**, 4054 (1959).
3. Korshak, V. V., O. P. Golova, V. A. Segeev, N. M. Merlis, and R. Ya. Shneer, *Vysokomol. Soedin.*, **3**, 477 (1961).
4. Tu, C. C., and C. Schuerch, *J. Polymer Sci.*, **B1**, 163 (1963).
5. Bhattacharya, A., and C. Schuerch, *J. Org. Chem.*, **26**, 3101 (1961).
6. Nevin, R. S., K. Sarkanen, and C. Schuerch, *J. Am. Chem. Soc.*, **84**, 78 (1962).
7. Goldstein, I. J., and B. Lindberg, *Acta Chem. Scand.*, **16**, 387 (1962).
8. Michael, F., and D. Borrmann, Dissertation, Münster, (1960); *Chem. Ber.*, **93**, 1143 (1960).
9. Delépine, M., *Compt. Rend.*, **171**, 36 (1920); *Bull. Soc. Chim. France*, [4] **27**, 740 (1920).
10. Delépine, M., and S. Eschenbrenner, *Bull. Soc. Chim. France*, [4] **33**, 703 (1923).
11. Culvenor, C. C. J., W. Davies, and N. S. Heath, *J. Chem. Soc.*, **1949**, 282.
12. Gaylord, N. G., *High Polymers*, **13**, Part 3, Interscience Publishers, New York, 1962.
13. Marvel, C. S., and E. D. Weil, *J. Am. Chem. Soc.*, **76**, 61 (1954).
14. Noshay, A., and C. C. Price, *J. Polymer Sci.*, **54**, 533 (1961).
15. Hall, L. D., L. Hough, and R. A. Pritchard, *J. Chem. Soc.*, **1961**, 1537.
16. Christensen, J. E., and L. Goodman, *J. Am. Chem. Soc.*, **83**, 3827 (1961).
17. Stabin, J. V., and E. H. Immergut, *J. Polymer Sci.*, **14**, 209 (1954).
18. Zimm, B. H., and I. Myerson, *J. Am. Chem. Soc.*, **68**, 911 (1946).
19. Carson, J. F., and W. D. Maclay, *J. Am. Chem. Soc.*, **70**, 293 (1948).
20. Martin, A. R., L. Smith, R. L. Whistler, and M. Harris, *J. Res. Natl. Bur. Std.*, **27**, 449 (1941).
21. Trevelyan, W. E., D. P. Procter, and J. S. Harrison, *Nature*, **166**, 444 (1950).
22. Bonner, T. G., E. J. Bourne, and S. McNally, *J. Chem. Soc.*, **1962**, 761.
23. Snyder, H. R., J. M. Stewart, and J. B. Ziegler, *J. Am. Chem. Soc.*, **69**, 2675 (1947).

### Résumé

La polymérisation avec ouverture de cycle du 5,6-didéoxy-5,6-épithio-1,2-*O*-isopropylidène- $\alpha$ -*L*-idofuranose est catalysée par le trifluorure de bore à 60°. Du polymère soluble est produit après 1 heure de polymérisation pour un rapport monomère/catalyseur égal à 7 et pour une concentration en monomère de 0.077 *M*. Ce polymère a une large distribution moléculaire. On trouve un poids moléculaire moyen de 72.000 pour les premiers 40% du polymère précipité d'une solution de *N,N*-diméthylformamide par addition d'eau. Le polymère est produit en quantités croissantes lorsqu'on élève la température, qu'on augmente la concentration en catalyseur et lorsque la concentration en eau est diminuée. La transglycolysation peut être la cause de la ramification et du pontage. L'hydrolyse du polymère soluble enlève les groupes isopropylidènes pour former un polymère réducteur soluble dans l'eau qui est oxydé par l'hypoiodite en un polymère contenant des groupes carboxyles.

### Zusammenfassung

Die unter Ringöffnung verlaufende Polymerisation von 5,6-Didesoxy-5,6-epithio-1,2-*O*-isopropyliden- $\alpha$ -*L*-idofuranose wird bei 60° durch Bortrifluorid katalysiert. Bei einem Verhältnis von Monomerem zu Katalysator von 7 und einer Monomerkonzentration von 0.077 *M* entstand nach einstündiger Polymerisation ein lösliches Polymeres mit breiter Molekulargewichtsverteilung. Das Zahlenmittel des Molekulargewichts des ersten 40% des aus *N,N*-Dimethylformamid-Lösung durch Zugabe von Wasser gefällten Polymeren ist 72000. Die Menge des gebildeten Polymeren nimmt mit steigender Temperatur, steigender Katalysatorkonzentration und abnehmender Wasserkonzentration zu. Durch Transglycosylierung kann Verzweigung oder Vernetzung auftreten. Bei der Hydrolyse des löslichen Polymeren wird unter Abspaltung von Isopropylidengruppen ein wasserlösliches reduzierendes Polymeres gebildet, das durch Hypojodit zu einem Carboxylgruppen enthaltenden Polymeren oxydiert wird.

Received May 29, 1963

## Polyphenylenebenzimidazoles

YOSHIO IWAKURA, KEIKICHI UNO, and YOSHIO IMAI,\*

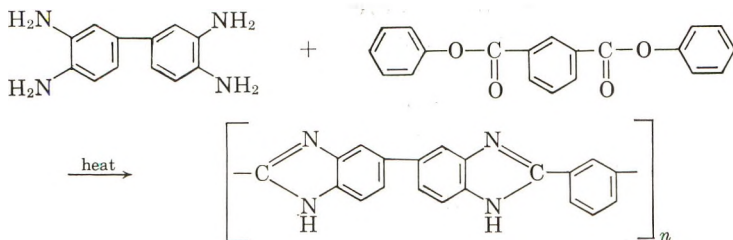
*Department of Synthetic Chemistry, Faculty of Engineering,  
University of Tokyo, Tokyo, Japan*

### Synopsis

The solution polycondensation of 3,3'-diaminobenzidine tetrahydrochloride with aromatic dicarboxylic acid derivatives in polyphosphoric acid was found to give high molecular weight polyphenylenebenzimidazoles easily. Their preparation and physical properties, such as thermal stability, solubility, crystallinity, are described.

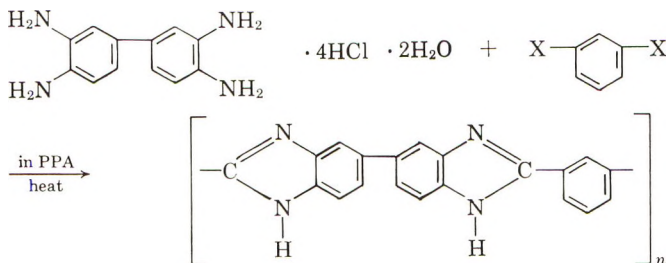
### 1. INTRODUCTION

In recent years, investigations concerning heat resistant polymers have widely been made. Marvel and Vogel<sup>1</sup> prepared polybenzimidazoles and found that these polymers had excellent thermal stability. However, the method of synthesis of these polymers proposed by them required the use of free 3,3'-diaminobenzidine as starting material:



Generally, the aromatic tetraamines are very sensitive to oxidation and the operations should be conducted under an inert gas atmosphere.<sup>1,2</sup> Now, we have prepared the same polymers from more stable 3,3'-diaminobenzidine tetrahydrochloride and aromatic dicarboxylic acid derivatives by solution polycondensation, using polyphosphoric acid both as solvent and as condensing agent.

\* Present address: Teijin Limited, Tokyo, Japan.

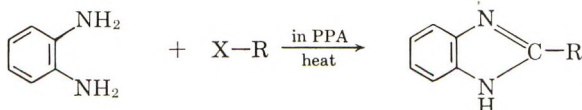


where X is  $-\text{COOH}$ ,  $-\text{COOCH}_3$ ,  $-\text{CONH}_2$ , or  $-\text{CN}$ .

Polyphenylenebenzimidazoles thus obtained were quite the same as those prepared by Marvel and Vogel in physical properties and showed remarkable thermal stability.

## 2. PREPARATION OF POLYPHENYLENEBENZIMIDAZOLES

The utility of polyphosphoric acid (PPA) as a remarkably effective condensing agent has been extensively demonstrated in synthetic organic chemistry in recent years. For example, polyphosphoric acid was employed in the preparation of 2-substituted benzimidazoles from *o*-phenylenediamine and carboxylic acids or their derivatives:<sup>3</sup>



where X is  $-\text{COOH}$ ,  $-\text{COOR}'$ ,  $-\text{CONH}_2$ , or  $-\text{CN}$ .

Nothing has been reported, however, regarding effectiveness of PPA in polycondensation reactions in the field of polymer syntheses. We have succeeded in the preparation of high molecular weight polyphenylenebenzimidazoles by solution polycondensation of 3,3'-diaminobenzidine tetrahydrochloride with isophthalic acid, terephthalic acid, or with their derivatives using polyphosphoric acid both as solvent and as condensing agent.

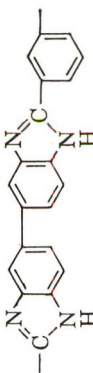
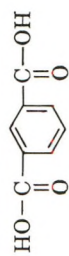
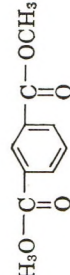
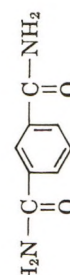
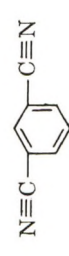
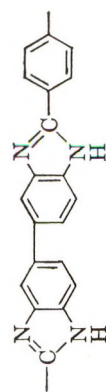
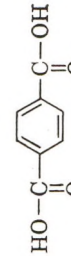
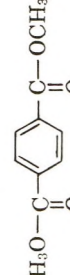
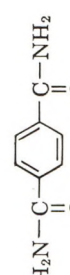
The general procedure of the polycondensation reaction is outlined as follows. 3,3'-Diaminobenzidine tetrahydrochloride is dissolved in polyphosphoric acid at  $140^\circ\text{C}$ . in a flask equipped with a stirrer under a thin stream of nitrogen, and the bubbles of hydrogen chloride gas are eliminated gradually. The aromatic carboxylic acid component is added to this solution and heating is continued with stirring. The reaction mixture develops a blue or violet fluorescence and gradually becomes viscous. After several hours, polyphenylenebenzimidazole is isolated as a yellowish to dark-brown resinous mass by pouring the solution into water. The polymer mass is washed with alkaline water, and afterwards thoroughly with water and methanol, and dried. The yield is almost quantitative.

A list of polyphenylenebenzimidazoles prepared is given in Table I.

As described before, Marvel and Vogel used diphenyl ester as an aromatic carboxylic acid component. We investigated the preparation of poly-*m*-



TABLE I. Preparation of Polyphenylenebenzimidazoles

Polymer	No.	Dicarboxylic acid derivatives, g.	DAB-HCl, g. <sup>a</sup>	116% PPA, g.	Reaction conditions, °C./hr.	$\eta_{sp}/c^b$
	I-1 <sup>†</sup>		2.0	53	170/4.5-200/17	1.38
	I-2		2.0	63	140/7-180/24	0.37
	I-3		2.0	60	200/12	1.68
	I-3'		2.0	56	200/25.5	1.25
	I-4		2.0	51	200/30	0.55
	II-1		2.0	[59]	200/20	0.54
	II-2		2.0	60	200/4.5	2.59
	II-3		2.0	56	200/5.5	1.08
	II-3'		2.0	51	200/7.5	1.20

<sup>a</sup> DAB-HCl is 3,3'-diaminobenzidine tetrahydrochloride.<sup>b</sup> Measured at a concentration of 0.2 g./100 ml. in concentrated sulfuric acid at 30°C.

phenylenebenzimidazole starting from various isophthalic acid derivatives, and found that the use of free acid, dimethyl ester, diamide, and dinitrile gave satisfactory results, while dihydrazide gave inferior results. All attempts to employ diphenyl ester and acid dichloride failed to yield this polymer because of the decomposition of these acid components in polyphosphoric acid.

In the case of poly-*p*-phenylenebenzimidazole, terephthalic acid, the dimethyl ester, and the diamide gave superior results. It was observed that the polycondensation reaction of terephthalic acid derivatives with 3,3'-diaminobenzidine tetrahydrochloride proceeded faster than that in the case of isophthalic acid derivatives.

### 3. PROPERTIES OF POLYPHENYLENEBENZIMIDAZOLES

Various properties of polyphenylenebenzimidazoles, such as viscosities, solubilities, infrared and ultraviolet spectra, crystallinity, and thermal stability, were determined. The viscosity of poly-*p*-phenylenebenzimidazole (II-3) was measured at four points in concentrated sulfuric acid solution; results are shown in Table II and Figure 1. The value in parentheses in Table II shows the result of the one-point measurement listed in Table I.

TABLE II  
Viscosity Measurements on the Polymer (Sample II-3)<sup>a</sup>

$c$ , g./100 ml.	$\eta_{sp}/c$
1.0	1.42
0.67	1.26
0.4	1.16
0.2	1.07 (1.08)

<sup>a</sup> Measured in concentrated sulfuric acid solution at 30°C.

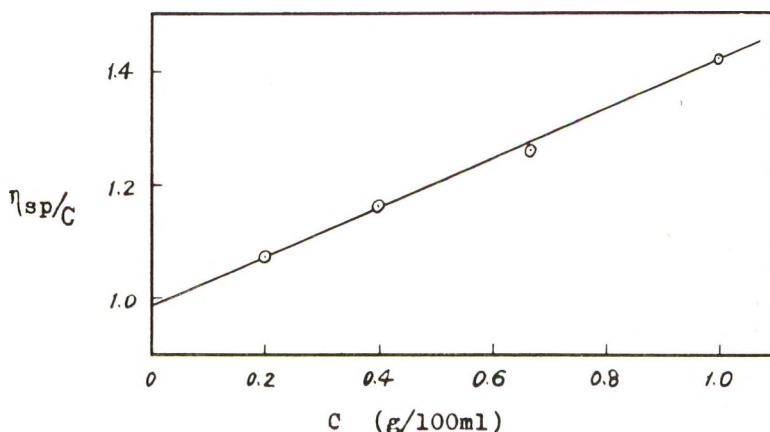


Fig. 1. Viscosity of poly-*p*-phenylenebenzimidazole (II-3).

TABLE III  
Solubilities of Polyphenylenebenzimidazoles

Solvent	Solubility <sup>a</sup>	
	(I-3)	(II-2)
95% Sulfuric acid	+	+
Dimethylsulfoxide (DMSO)	+	+
<i>N,N</i> -Dimethylacetamide (DMAc)	+	+
<i>N</i> -Methylpyrrolidone (NMP)	+	+
<i>N,N</i> -Dimethylformamide (DMF)	+	+
85% Formic acid	+	-
Glacial acetic acid	-	-
<i>m</i> -Cresol	-	-

<sup>a</sup> ++ denotes soluble at room temperature or by heating; + denotes partially soluble or swelling; - denotes insoluble.

It has been reported that solutions of polyphenylenes or polyazophenylenes show an anomalous dependence of  $\eta_{sp}/c$  on  $c$  because of their long conjugated systems, and their compact, rigid, almost linear structures.<sup>4</sup>

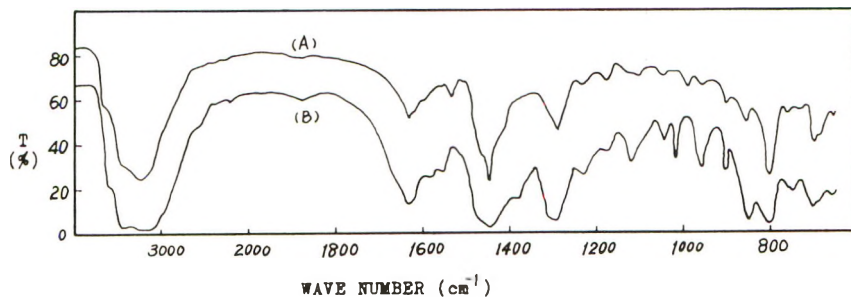


Fig. 2. Infrared spectra of polyphenylenebenzimidazoles: (A) poly-*m*-phenylenebenzimidazole (film); (B) poly-*p*-phenylenebenzimidazole (film).

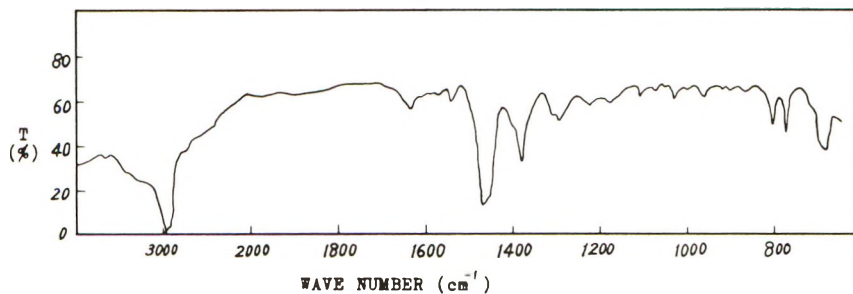


Fig. 3. Infrared spectrum of 2,2'-diphenyl-5,5'-bibenzimidazole (in Nujol).

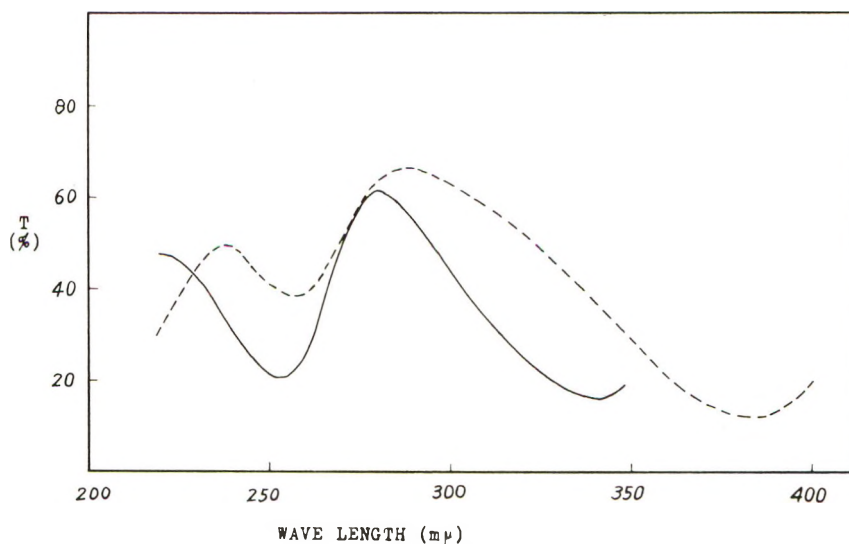


Fig. 4. Ultraviolet spectra of polyphenylenebenzimidazoles: (—) poly-*m*-phenylenebenzimidazole; (---) poly-*p*-phenylenebenzimidazole.

However, the result obtained above indicates that in a concentrated sulfuric acid solution of poly-*p*-phenylenebenzimidazole, the correlation between  $\eta_{sp}/c$  and  $c$  is quite linear. This fact is attributable to a relatively short conjugated system of the polymer as will be described later and to some degree of flexibility.

The reproducibility of the viscosity measurements was good.

Table III shows the qualitative solubilities of polyphenylenebenzimidazoles in various solvents.

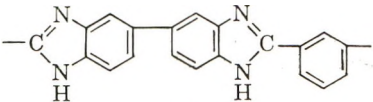
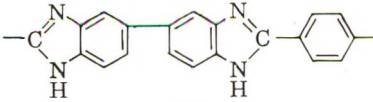
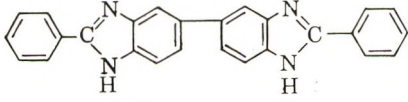
From Table III, it will be seen that poly-*m*-phenylenebenzimidazole is more soluble than the *p*-substituted polymer. The solubilities of polyphenylenebenzimidazoles in DMSO, DMAc, NMP, and DMF were greatly increased by the addition of lithium chloride in these solvents. From these solutions polyphenylenebenzimidazoles could be cast into stiff and tough films.

The infrared absorption spectra of polyphenylenebenzimidazoles, shown in Figure 2, were taken on films prepared as above. For comparison, the spectrum of the model compound, 2,2'-diphenyl-5,5'-bibenzimidazole, is given in Figure 3. The spectra of the polymers agreed well with that of the model compound.

The ultraviolet absorption spectral data of polyphenylenebenzimidazoles and of the model compound in concentrated sulfuric acid solution are shown in Figures 4 and 5 and Table IV.

Ultraviolet absorption curves of these polymers were very similar in shape to that of the model compound, and it was observed that the bathochromic effect based on conjugation of poly-*p*-phenylenebenzimidazole was greater than that of *m*-substituted polymer.

TABLE IV  
Ultraviolet Spectral Data of Polyphenylenebenzimidazoles and the Model Compound

	$\lambda_{\text{max}}$ , m $\mu$	$E_{1\text{cm}}^{1\%}$
 (I-1)	253	1160
	343	1330
 (II-2)	257	690
	385	1670
 (Model compound)	256	980
	333	1160

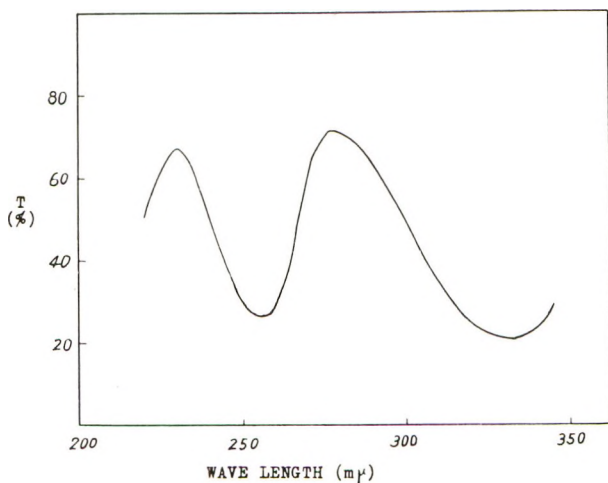


Fig. 5. Ultraviolet spectrum of 2,2'-diphenyl-5,5'-bibenzimidazole.

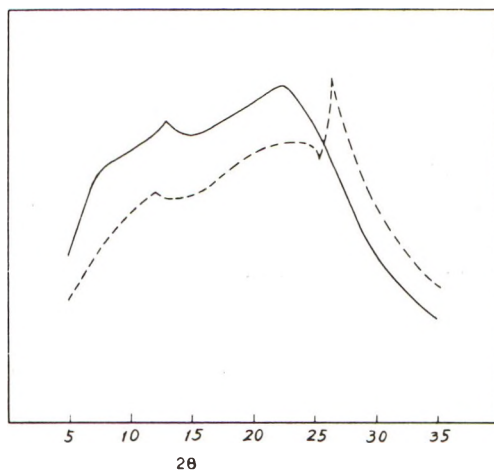


Fig. 6. X-ray diffraction diagrams of polyphenylenebenzimidazoles: (—) poly-*m*-phenylenebenzimidazole; (- -) poly-*p*-phenylenebenzimidazole.

The x-ray diffraction diagrams of polyphenylenebenzimidazoles shown in Figure 6 were obtained by the powder method using nickel-filtered  $\text{CuK}\alpha$  radiation.

These diagrams indicate that poly-*p*-phenylenebenzimidazole has a high degree of crystallinity because of more symmetrical polymer structure, while *m*-substituted polymer is amorphous.

Both *m*- and *p*-substituted polyphenylenebenzimidazoles showed no melting point in a free flame and gradually turned black.

The thermal stability of polyphenylenebenzimidazoles was determined by thermogravimetric analysis. Samples were heated in air, the tempera-

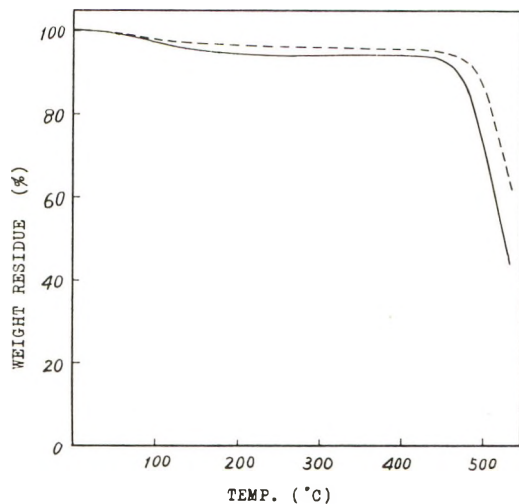


Fig. 7. Thermogravimetric analysis of polyphenylenebenzimidazoles: (—) poly-*m*-phenylenebenzimidazole; (- -) poly-*p*-phenylenebenzimidazole.

ture being increased 3°C./min. The thermogravimetric analysis curves of these polymers are shown in Figure 7.

Only minor weight loss was observed below 450°C. in air both in the case of *m*- and *p*-substituted polyphenylenebenzimidazoles, and then in both cases decomposition occurred, leaving a black residue.

## 4. EXPERIMENTAL

### Monomers and Model Compound

**3,3'-Diaminobenzidine Tetrahydrochloride.** *N,N'*-Di-*p*-toluenesulfonyl benzidine was prepared in 90% yield by the Schotten-Bauman reaction of benzidine with *p*-toluenesulfonyl chloride with sodium bicarbonate as an acid acceptor in acetone and water.

3,3'-Dinitrobenzidine was prepared in 75% yield by the procedure of Bell and Robinson<sup>5</sup> from *N,N'*-di-*p*-toluenesulfonyl benzidine, i.e., nitration with concentrated nitric acid and glacial acetic acid to give 3,3'-dinitro-*N,N'*-di-*p*-toluenesulfonyl benzidine, and then hydrolysis of the latter with concentrated sulfuric acid and water.

3,3'-Diaminobenzidine tetrahydrochloride was prepared in 80% yield by the modification of the method of Le Fèvre, Moir, and Turner<sup>6</sup> from 3,3'-dinitrobenzidine by reduction with hydrosulfite in methanol and water. The product was isolated by pouring the reduction mixture into methanol and concentrated hydrochloric acid, and was recrystallized from water and hydrochloric acid as brown needles. The overall yield based on benzidine was 50%.

ANAL. Calcd. for  $C_{12}H_{13}N_4 \cdot 4HCl \cdot 2H_2O$ : C, 36.38%; H, 5.60%; N, 14.14%. Found: C, 36.14%; H, 5.93%; N, 13.92%.

**Isophthalic and Terephthalic Acid Derivatives.** Isophthalic and terephthalic acid derivatives were obtained as commercial reagents, or synthesized by usual methods, and purified before use.

**2,2'-Diphenyl-5,5'-bibenzimidazole.** A 2-g. portion of 3,3'-diaminobenzidine tetrahydrochloride ( $C_{12}H_{14}N_4 \cdot 4HCl \cdot 2H_2O$ ) was dissolved in 30 ml. of 105% polyphosphoric acid at 140°C., and the bubbles of hydrogen chloride gas were eliminated. Ethyl benzoate (2 ml.) was added to this solution and the mixture was heated at 150°C. for 1.5 hr. The reaction product was isolated by pouring the solution into the water, washed with alkaline water, and recrystallized from methanol and water; it weighed 1.7 g. and melted at 332–333°C.

ANAL. Calcd. for  $C_{26}H_{18}N_4$ : C, 80.83%; H, 4.66%; N, 14.51%. Found: C, 78.72%; H, 4.77%; N, 14.67%.

### Solution Polycondensation

An example of preparation of polyphenylenebenzimidazoles by solution polycondensation will be mentioned.

**Poly-2,2'-(*m*-phenylene)-5,5'-bibenzimidazole (I-3).** A 100-ml. three-necked flask equipped with a stirrer, nitrogen inlet, and calcium chloride drying tube was charged with 60 g. of 116% polyphosphoric acid. Into this flask, 2.0 g. of 3,3'-diaminobenzidine tetrahydrochloride ( $C_{12}H_{14}N_4 \cdot 4HCl \cdot 2H_2O$ ) was added gradually, dissolved at 140°C. under a thin stream of nitrogen, and the bubbles of hydrogen chloride gas were eliminated. To this solution 0.80 g. of isophthalamide was added and heating was continued at 200°C. for 12 hr. The reaction mixture developed a violet fluorescence and gradually became viscous as the polycondensation reaction proceeded. The polymer was isolated by pouring the hot solution into water, washed with water by decantation, and then dipped in dilute sodium bicarbonate solution overnight and washed thoroughly with water and methanol, and dried. The polymer was obtained as a brown resinous mass and weighed 1.5 g. A 0.2 g./100 ml. solution of this polymer in concentrated sulfuric acid at 30°C. showed  $\eta_{sp}/c$  of 1.68.

We are indebted to Prof. Masaki Ohta of Tokyo Institute of Technology for micro-analysis.

### References

1. Vogel, H., and C. S. Marvel, *J. Polymer Sci.*, **50**, 511 (1961).
2. Sorenson, W. R., and T. W. Campbell, *Preparative Methods of Polymer Chemistry*, Interscience, New York, 1961, p. 91.
3. Hein, D. W., R. J. Alheim, and J. J. Leavitt, *J. Am. Chem. Soc.*, **79**, 427 (1957).
4. Berlin, A. A., *J. Polymer Sci.*, **55**, 621 (1961).
5. Bell, F., and P. H. Robinson, *J. Chem. Soc.*, **1927**, 1130.
6. Le Fèvre, R. J. W., D. D. Moir, and E. E. Turner, *J. Chem. Soc.*, **1927**, 2335.

### Résumé

Nous avons trouvé que des polyphénylènes benzimidazols sont facilement préparés par la polycondensation du tétrahydrochlorure de la 3,3'-diamino-benzidine avec les



dérivés d'acides dicarboxyliques aromatiques dans l'acide polyphosphorique. Leur préparation et leurs propriétés physiques tels que la stabilité thermique, la solubilité et la cristallinité sont décrites.

### **Zusammenfassung**

Durch Lösungspolykondensation von 3,3'-Diaminobenzidintetrahydrochlorid mit Derivaten der aromatischen Dicarbonsäuren in Polyphosphorsäure konnten leicht hochmolekulare Polyphenylenbenzimidazole dargestellt werden. Die Darstellung sowie die physikalischen Eigenschaften der Polymeren, wie Wärmebeständigkeit, Löslichkeit und Kristallinität, werden beschrieben.

Received April 30, 1963

Revised June 3, 1963

## Polymerization in Solid Solutions of Acrylamide in Propionamide\*

G. ADLER and W. REAMS, *Brookhaven National Laboratory,  
Upton, L. I., New York*

### Synopsis

It has previously been shown that the polymer formed in solid-state polymerization of acrylamide is amorphous in spite of the fact that the reaction takes place within a crystalline solid. The stage at which it becomes amorphous is not known at present. Work with dilute solid solutions of acrylamide in propionamide suggests that this occurs after the addition of, at most, a very few monomer units.

It has been previously shown that the polymer produced in the solid-state polymerization of acrylamide is amorphous.<sup>1,2</sup> To explain this, it was postulated that the polymer nucleates as a second phase at an early stage of the reaction. Further reaction then takes place at the monomer-polymer interface.<sup>2</sup> Evidence for this was first produced from x-ray diffraction data<sup>3</sup> and then from time-lapse movies of reacting crystals.<sup>4,5</sup> More recently, Sella and Trillat<sup>6</sup> have taken electron micrographs showing polymer nuclei as small as approximately 20 Å.

It seems probable that at least the first monomer unit which adds to the radiation-initiated radical would be the one most favorably oriented in the crystal lattice. This would initiate polymerization in a preferred direction. The available data indicate that the polymer soon becomes amorphous, that is, random in orientation. The problem arises: at which stage does this happen?

Morawetz<sup>7</sup> has pointed out that even the shortest axis of the unit cell is too large for a section of the polymer chain two units long and that, therefore, the growing chain must occasionally add monomer units from other directions. Let us assume that the molecules are oriented in the most favorable manner for propagation consistent with the lattice symmetry and dimensions. Assuming also normal bond lengths and angles in the polymer, and that it grows in a manner consistent with lattice symmetry, it can be shown that there must be a contraction of about 30% of a unit cell length in the direction of the growing chain for every two monomer units added. It is apparent that the growing chain rapidly gets out of phase with the lattice. It must therefore be able to choose among several monomer units at random.

\* Work done under the auspices of the United States Atomic Energy Commission.

Some light can be shed on this problem experimentally. Fadner and Morawetz have shown that acrylamide and propionamide can form solid solutions in all proportions.<sup>8</sup> They measured polymerization in solid solutions containing up to 80% propionamide and showed that the molecular weight decreases when propionamide is added.

Acrylamide and propionamide are essentially isomorphous. The available evidence is that one kind of molecule can randomly be substituted for the other in the crystal lattice.

In an acrylamide crystal, the double bond in a given molecule has roughly 10 double bonds in other molecules within a distance of 5 Å.<sup>9,10</sup> Therefore, in a solid solution containing, say, only 10% acrylamide, a given monomer molecule would have on the average only one other neighboring molecule of the same kind. If the polymerization proceeded in a preferred direction, for example, along the screw axis of the crystal, then a molecule can react with one or, at most, two nearest neighbors if both head-to-tail and tail-to-head polymerization are allowed. Propionamide will not polymerize. Therefore, in a solid solution containing a small amount of acrylamide it can be expected that, under these conditions, only a small fraction of the acrylamide would be polymerized even at large radiation doses. On the other hand, if the propagating molecule can choose among nearest neighbors at random after, at the most, one or two monomer additions, the conversion of acrylamide to polymer can be extensive even in solid solutions containing as little as 10% monomer.

### Experimental

Solid solutions of acrylamide in propionamide were prepared by the method of Fadner and Morawetz.<sup>8</sup> The completeness of solution was checked by x-ray diffraction. Immediately after preparation, samples of these solutions were placed in glass ampules and evacuated to a pressure of  $4 \times 10^{-5}$  mm. Hg. They were then placed in a Co<sup>60</sup> source maintained at a temperature of 25°C. They were given the required dose at the rate of 0.25 Mrad/hr. Dosimetry was done by the ferrous sulfate technique.<sup>11</sup> Immediately after irradiation, the ampules were opened, and the polymer was isolated with methanol. The polymer was then filtered, dried, and weighed. At least duplicate determinations were made at each monomer concentration and dose level. Agreement of results was uniformly good, being within 2 or 3% of each other except at very low monomer conversions.

### Results and Discussion

The data obtained at doses of 6 and 8 Mrad for solid solutions of various composition are shown in Figure 1. The per cent polymer yield is based on the amount of acrylamide originally present. Since the molecular weights of acrylamide and propionamide are nearly the same, the per cent weight composition was plotted rather than the strictly more accurate mole per cent.

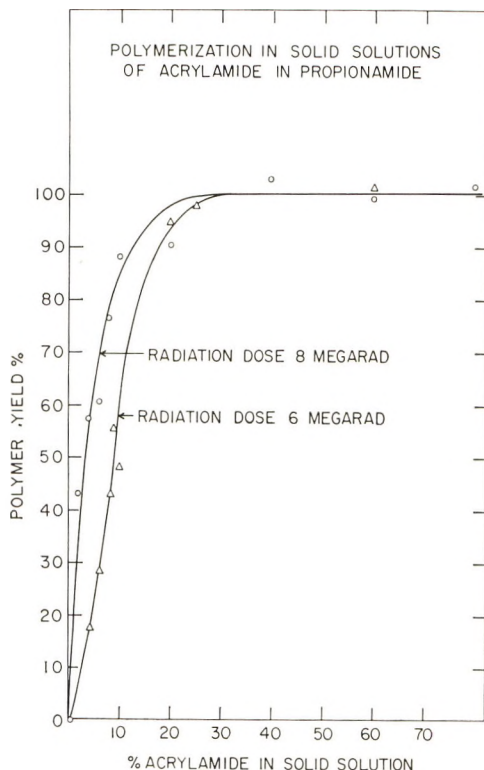


Fig. 1. Polymerization in solid solutions of varying composition.

The results show that even in a solid solution with a monomer concentration as low as 10%, at least 90% of the acrylamide is polymerized at a dose of 8 Mrad. With more massive doses, in the order of 20–25 Mrad, all of the acrylamide can be recovered as polymer if the monomer concentration is 10% or above. If the concentration is much less than 10%, the polymer yield is not complete, even at doses as large as 35 Mrad. This is shown in Figure 2, where the data for a 25% and a 4% solution of acrylamide in propionamide are shown. It can be seen that the polymerization in a 25% solution goes quite rapidly to completion. In the 4% solution, the initial rate is much slower and the yield is never much more than 55% at any radiation dose. However, even in a 2% solid solution an appreciable amount of polymer is formed. In this connection, it should be pointed out that the polymer was isolated with methanol. At present, it is not known what the limiting molecular weight for solubility of the polymer in methanol is. The only relevant data are those of Baysal et al.,<sup>12</sup> who isolated and fractionated polyacrylamide with methanol. The lowest fraction found had a number-average molecular weight of 9000.

The polymer yield pattern can best be understood if it is assumed that the polymer radical can react with neighboring molecules at random

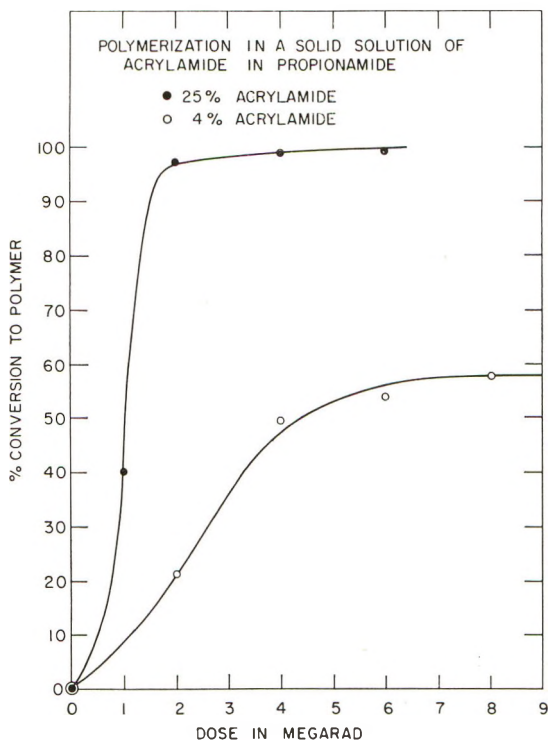


Fig. 2. Polymerization in solid solutions as a function of radiation dose.

after addition of a very few monomer units. Perhaps even the first monomer unit which adds to the originally formed radical can be chosen from among several alternative positions. This should not be too difficult to understand if it is remembered that polymerization tends to nucleate at lattice defects, such as dislocations, where the freedom of motion of the molecules may be somewhat greater than in the normal lattice.

Examination of the polymer by x-ray diffraction shows it to be amorphous under the conditions used. Examination by polarized light shows it to be strained. Polymer nuclei similar to those observed in pure acrylamide have been observed and photographed in solid solutions.<sup>13</sup> These observations are consistent with the proposed mechanism. The observations and proposed mechanism cannot be readily reconciled with the suggestion of Fadner and Morawetz<sup>8</sup> that propionamide acts as a chain transfer agent in limiting the molecular weight of polymer in solid solutions. More work has to be done on this phase.

The relatively high yield of polymer in the 4% solid solution is difficult to explain. It has been shown by electron spin resonance and other techniques<sup>14</sup> that as small a molecule as oxygen will not diffuse through the acrylamide lattice and will diffuse relatively slowly through propionamide. It is hardly likely that a monomer molecule can diffuse through the intact

lattice. The high yield of polymer cannot, therefore, be explained in this fashion.

At present the most likely explanation seems to be that, once the polymer nuclei are formed, propionamide and acrylamide molecules can diffuse along the monomer-polymer interface and possibly along crystal defects. There is probably some recrystallization taking place at the interface. In this connection, it should be remembered that the polymer is denser than the solid solution and its formation produces a net shrinkage and, therefore, lattice strain. Also, at 25°C. the mobility of the molecules at the crystal surfaces is large enough to produce an appreciable amount of sublimation. This again indicates the possibility of diffusion at the interface together with recrystallization. This possibility is at present being checked by other techniques.

### References

1. Mesrobian, R. B., P. Ander, D. S. Ballantine, and G. J. Dienes, *J. Chem. Phys.*, **22**, 565 (1954).
2. Adler, G., *J. Chem. Phys.*, **31**, 848 (1959).
3. Adler, G., and W. Reams, *J. Chem. Phys.*, **32**, 1698 (1960).
4. Adler, G., D. Ballantine, and B. Baysal, *J. Polymer Sci.*, **48**, 195 (1960).
5. Adler, G., and R. F. Smith; quoted by A. Charlesby, *Sci. American*, **201**, 182 (October 1959).
6. Sella, C., and J. J. Trillat, *Compt. Rend.*, **253**, 1511 (1961).
7. Morawetz, H., Proceedings of the Fourth International Symposium on the Reactivity of Solids, Amsterdam, 1960, in *Reactivity of Solids*, J. H. de Boer, et al., Eds., Elsevier, Amsterdam, 1960.
8. Fadner, T. A., and H. Morawetz, *J. Polymer Sci.*, **45**, 475 (1960).
9. Adler, G., unpublished data.
10. Based on private communication by Y. Chatani.
11. A.S.T.M. Method D-1671-59T.
12. Baysal, B., G. Adler, D. Ballantine, and A. Glines, *J. Polymer Sci.*, **B1**, 257 (1963).
13. Adler, G., unpublished data.
14. Adler, G., Proceedings of the International Symposium on Radiation Induced Polymerization and Graft Copolymerization, Battelle Memorial Institute, Columbus, Ohio, (November 1962).

### Résumé

On a montré précédemment que le polymère formé lors de la polymérisation de l'acrylamide en phase solide est amorphe malgré le fait que la réaction se produit dans le solide cristallin. A l'heure actuelle on ne sait pas quand le polymère devient amorphe. Le travail effectué avec des solutions diluées de l'acrylamide dans la propionamide suggère que cela se passe après l'addition tout au plus de quelques unités monomériques.

### Zusammenfassung

Wie schon früher gezeigt wurde, ist das bei der Polymerisation von Acrylamid in festem Zustande gebildete Polymere amorph, obwohl die Reaktion in einem kristallinen Festkörper abläuft. Es ist derzeit noch nicht bekannt, in welchem Reaktionsstadium das Polymere amorph wird, doch weisen Arbeiten mit verdünnten festen Lösungen von Acrylamid in Propionamid darauf hin, dass dies spätestens nach der Addition von sehr wenigen Monomereinheiten der Fall ist.

Received June 3, 1963

## Nuclear Magnetic Absorption in Polystyrene—Styrene Systems\*

F. BORSA,† and G. LANZI, *Istituto di Fisica dell'Università, Pavia, Italy*

### Synopsis

Measurements of line width at different temperatures for samples of styrene partially polymerized are reported. The results obtained point out the importance of segmental motion of polymer chains at low temperatures in relation to the motion of the monomer molecules still present. There is some experimental evidence that under certain conditions the monomer molecules can facilitate the motions of polymer molecules, which seem to pull along in their motion a lot of the monomer molecules.

### Introduction

In the past years nuclear magnetic resonance techniques have been widely used to get useful information about the structure and the molecular motions in polymers.<sup>1</sup>

Recently monomer-polymer systems, at different rates of conversion during the polymerization process, have been investigated by measuring the spin-lattice relaxation time.<sup>2</sup>

In the present work the investigation has been extended by means of line-width measurements on monomer-polymer systems at temperatures down to 100°K. and for the entire composition range, in order to get more information about molecular motion both of monomer and polymer.

In particular we have studied samples of styrene-polystyrene.

### Experimental Apparatus

A self-detecting autodyne was used to observe the proton magnetic resonance line at about 25 Mcycles/sec.

The signal from the autodyne was fed into a lock-in detector after narrow band amplification and the derivative of the resonance line was recorded.

The magnetic field was modulated at 70 cycles/sec. with an amplitude depending on the line-width. The modulator consisted of an AF oscillator followed by a conventional push-pull power stage, permitting a total maximum sweep of 10 gauss peak to peak from a small set of Helmholtz coils located within the air gap. The linear slow magnetic sweep was

\* Supported by a research grant of the Consiglio Nazionale delle Ricerche and NATO.

† Present address: Department of Metallurgy, University of Illinois, Urbana, Illinois, U.S.A.

obtained by injecting the proper variable voltage into the power supply regulating circuit of a Varian V 4012-3B electromagnet.

The sample was placed in a coil made with rigid and self-supporting copper wire in order to avoid spurious signals. The sample and the coil were located in a cryostat, and the temperature was measured with a copper-Constantan thermocouple embedded in the sample.

The lowest temperature reached was that of the coolant (liquid nitrogen), and measurements at temperatures above that of the coolant were performed during the slow return of the sample to room temperature. During the recording of the widest lines an increase of the temperature of about 3°C. took place in the sample from beginning to end of the recording.

The samples were obtained by means of thermal polymerization of styrene (BHD reagent, laboratory) at 90°C. The percentage of polymer in the styrene-polystyrene system was obtained by measuring the refractive index.<sup>3</sup>

### Results and Discussion

The results obtained for samples of 100% monomer and 100% polymer are shown in Figure 1.

The pure monomer at the lowest temperatures displays a line 10 gauss broad which remains practically constant up to the temperature of about 200°K. At higher temperatures the line-width decreases rapidly. When

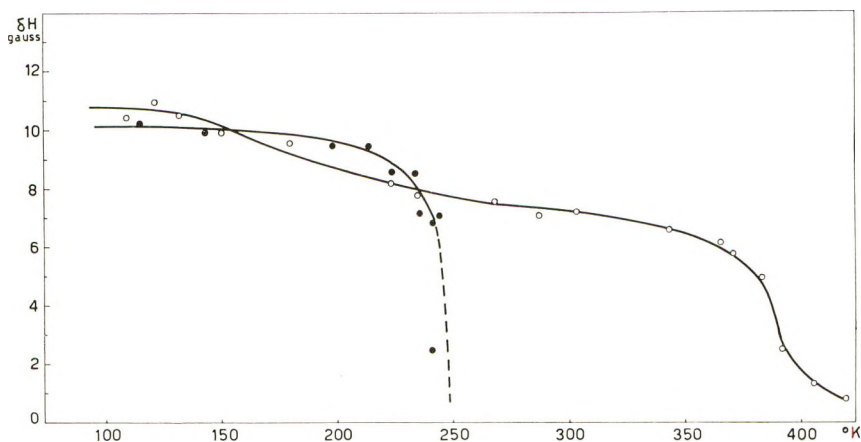


Fig. 1. Line-width  $\delta H$  vs. temperature for (O) completely polymerized polystyrene and (●) pure styrene.

the melting point is reached (234°K.) the narrowing process seems to be complete. The polymer, on the contrary, has an almost constant line width over a shorter range of temperature (up to about 120°K.). Then the width decreases slowly with increasing temperature. There is evidence of a first transition region at about 170°K. and of a second one at about 390°K.



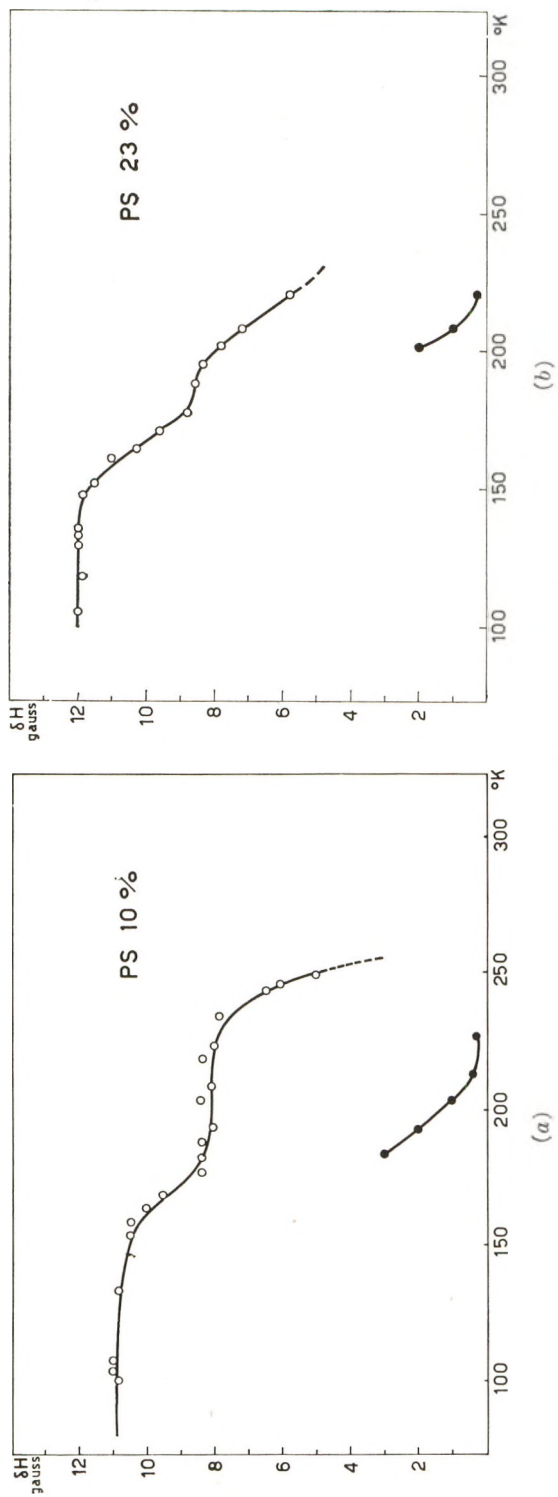


Fig. 2. See caption on page 2627.

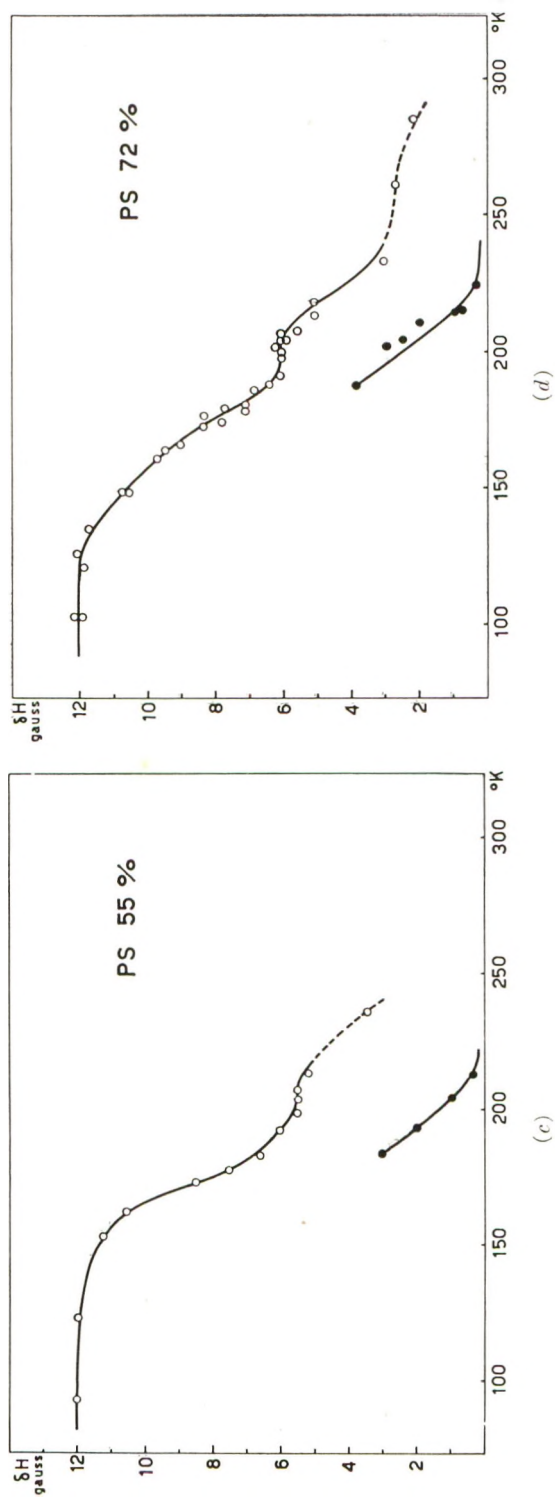


Fig. 2. See caption on page 2627.

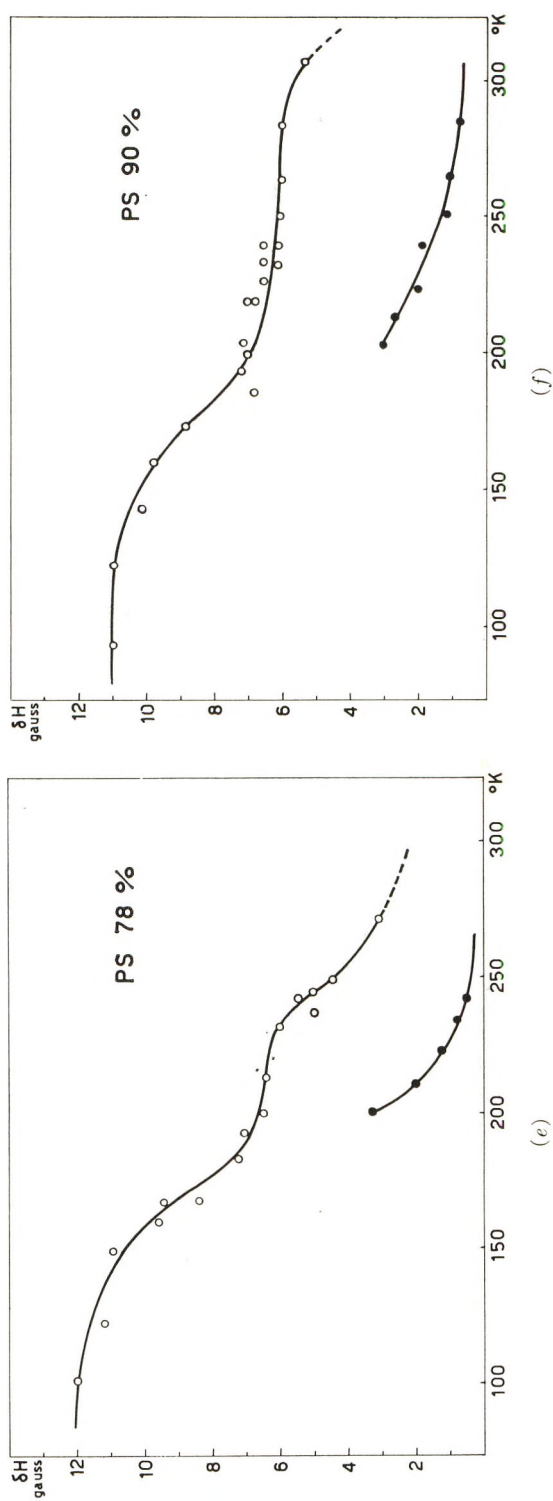


Fig. 2. Line-width  $\delta H$  vs. temperature for some partially polymerized samples containing different amounts of polystyrene: (a) 10 wt.-% polymer; (b) 23 wt.-% polymer; (c) 55 wt.-% polymer; (d) 72 wt.-% polymer; (e) 78 wt.-% polymer; (f) 90 wt.-% polymer. Broad (O) and narrow (●) components are reported.

Our results for temperatures higher than room temperature are in good agreement with previous measurements.<sup>4</sup> In Figure 2, the results for monomer-polymer syrups at different concentrations are shown.

For temperatures less than about 170°K. a single line was found, while for temperatures between 180 and 200°K. the line splits into dual components of different width but of the same resonance frequency.

The broad line has been attributed to the protons in the polymer chains and the narrow one to the protons in the monomer molecules.

The narrowing process proceeds at different rates for the two components. At a higher temperature (depending on the syrup concentration but generally above 250°K.) the two lines are no longer resolvable because both are narrower than the inhomogeneous broadening.

The ratios between the areas limited by the narrow line (attributed to the monomer) and by the broad line (attributed to the polymer) have been estimated. These ratios are far less than those between the quantities actually present in the syrup. This discrepancy can be explained by assuming that the monomer molecules around the polymer chains are less free to move than those further away. It is reasonable to think that the monomer molecules which are nearer to the polymer chains take part in the polymer movements and so contribute to the area of the broader signal.

Furthermore it is interesting to point out that in the monomer-polymer systems a transition of the broad line, which is more pronounced than in the pure polymer, has been found around 170°K. From the comparison with curves in Figure 1, it is evident that this more pronounced transition cannot be accounted for simply by considering the behavior of monomer and polymer separately.

A plausible explanation seems to be the following. In the pure polymer at a temperature around 170°K., segmental motions which contribute to the line narrowing arise while the pure monomer at the same temperature still behaves like a solid with regard to the NMR.

In the monomer-polymer syrup we have polymer chains separated by monomer molecules. This situation prevents the monomer from solidifying and, at the same time, allows the polymer chains more freedom of motion. Therefore the monomer-polymer system, at temperatures of about 170°K., appears to have much more internal mobility. The critical rate of motion at which the narrowing occurs is of the order of 10<sup>4</sup> cycles/sec. in our case. The effect reaches its maximum at a polymer concentration of about 50 wt.-%.

It is well known that from the rate of narrowing of the nuclear magnetic absorption line it is possible to estimate the activation energy of the motion that causes the narrowing. The theory by Bloembergen, Purcell, and Pound,<sup>5</sup> relating line-width and correlation frequency, has been modified by Gutowsky and Pake<sup>6</sup> and by Kubo and Tomita<sup>7</sup> who suggested the following formula:

$$2\pi\nu_c = \alpha\gamma\delta H \left\{ \tan \left[ \pi \left( \frac{\delta H^2 - B^2}{2C^2} \right) \right] \right\}^{-1}$$

Here  $\nu_c$  is the correlation frequency,  $\delta H$  is the line-width as measured in the transition region,  $B$  is the line-width at that temperature (higher than the transition region) which corresponds to complete activation of the motion, and  $C$  is the rigid lattice line-width.

The constant  $\alpha$  is  $(8 \ln 2)^{-1}$  and  $\gamma$  is the gyromagnetic ratio. Assuming

$$\nu_c = \nu_0 \exp\{-E_A/RT\}$$

the activation energy  $E_A$  of the motion can be calculated. However it has to be pointed out that an accurate enough calculation of the activation energy with the previous formulae is practical if in a certain range of temperature only one type of motion is activated. In the case where several motions are activated it is sometimes possible to obtain useful information regarding the total number of such motions and their activation energies.

In the concentration range of the polymer between 10 and 55% two main motions are activated for temperatures ranging from 135 to 200°K.

The corresponding activation energies increase with increasing concentration. The approximate value we obtain for the activation energies are given in Table I.

TABLE I

	Polymer in system		
	10%	23%	55%
$E_{A \text{ max}}$ , kcal./mole	8.70	8.89	9.37
$E_{A \text{ min}}$ , kcal./mole	1.00	2.08	3.39

For samples of concentration between 55 and 100% the behavior seems to be much more complicated because of the presence of many motions that are activated over a larger temperature range.

The authors are grateful to Prof. L. Giulotto for many valuable discussions and also want to acknowledge the assistance of Drs. A. Chierico and G. Del Nero in making many of the measurements.

### References

1. Slichter, W. P., *Fortschr. Hochpolymer.-Forsch.*, **1**, 35 (1958); W. P. Slichter, *Makromol. Chem.*, **34**, 67 (1959); J. G. Powles, *Polymer*, **1**, 219 (1960).
2. Bonera, G., P. De Stefano, and A. Rigamonti, *Nuovo Cimento*, **22**, 847 (1961).
3. Schildknecht, C. E., *Vinyl and Related Polymers*, Wiley, New York, 1959, p. 5.
4. Holroyd, L. V., R. S. Cordington, B. A. Mrowca, and E. Guth, *J. Appl. Phys.*, **22**, 696 (1951); A. Odajima, J. Sohma, and M. Koike, *J. Phys. Soc. Japan*, **12**, 272 (1957).
5. Bloembergen, N., E. M. Purcell, and R. V. Pound, *Phys. Rev.*, **73**, 679 (1948).
6. Gutowsky, H. S., and G. E. Pake, *J. Chem. Phys.*, **18**, 162 (1950).
7. Kubo, R., and K. Tomita, *J. Phys. Soc. Japan*, **9**, 888 (1954).

### Résumé

On donne le résultat des mesures de largeur de raie à différentes températures pour des échantillons de styrène partiellement polymérisés. Les résultats obtenus mettent en évidence l'importance des mouvements des segments de chaînes de polymère à basse

température en relation avec les mouvements des molécules de monomère encore présentes. On a prouvé expérimentalement que, dans certaines conditions, les molécules de monomère peuvent faciliter le mouvement des molécules de polymère, lesquelles semblent entraîner dans leur mouvement une partie des molécules de monomère.

### **Zusammenfassung**

Die Ergebnisse von Linienbreitenmessungen an Proben von teilweise polymerisiertem Styrol bei verschiedenen Temperaturen werden mitgeteilt. Sie zeigen die Bedeutung der Segmentbewegung der Polymerketten bei niedriger Temperatur und ebenso die der Bewegung der anwesenden Monomermoleküle. Die Versuche lassen weiters erkennen, dass unter gewissen Bedingungen die Monomermoleküle die Bewegung der Polymermoleküle erleichtern können, welche letzteren bei ihrer Bewegung einen Teil der Monomermoleküle mitzureissen scheinen.

Received June 5, 1963

## Distribution of Molecular Weight and of Branching in High Molecular Weight Polymers from Bisphenol A and Epichlorohydrin\*

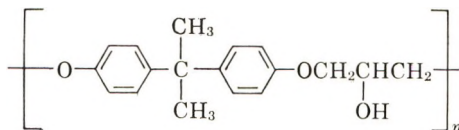
G. E. MYERS† and J. R. DAGON, *Research and Development Department, Union Carbide Plastics Company, Bound Brook, New Jersey*

### Synopsis

The molecular weight distributions and long-chain branching distributions of three samples of Bisphenol A poly(hydroxy ether) have been investigated. The samples were fractionated and the fractions characterized by solution viscosity and light-scattering measurements. A log-log plot of intrinsic viscosity and  $\bar{M}_w$  for fractions of all three resins yields a straight line up to molecular weights of about 70,000 (approximately 80% by weight of each polymer) described by  $[\eta] = 1.48 \times 10^{-4} \bar{M}_w^{0.765}$ . Beyond this molecular weight the viscosities fall increasingly below the straight line whose constants are representative of those expected for linear fractions in a good solvent. It is evident that long-chain branching does not occur appreciably in the lower fractions but does begin abruptly at 70,000 molecular weight and increases continuously above that point. Comparison of both the branching and molecular weight distributions with those predicted from Beasley's random branching mechanism confirms the nonrandom nature of the branching mechanism in these poly(hydroxy ethers). The numbers of branches calculated using the Zimm-Kilb theory reach impossibly high values, while those calculated from the Zimm-Stockmayer theory appear more reasonable. No correlation was found between the Huggins'  $k'$  and molecular weight or branching. The highest molecular weight sample possesses a longer and more highly branched high molecular weight tail, which is reflected in differences in physical properties.

### INTRODUCTION

The reaction of dihydric phenols with epichlorohydrin can be made to yield high molecular weight thermoplastic polymers to which the general name poly(hydroxy ether) has been applied.<sup>1</sup> The use of Bisphenol A as the particular dihydric phenol results in a polymer with the following repeat unit:



\* Paper presented at 144th Meeting of the American Chemical Society, Los Angeles, California, March 31-April 5, 1963.

† Present Address: Lockheed Propulsion Company, Redlands, California.

This Bisphenol A poly(hydroxy ether) is an amorphous, tough, thermally stable thermoplastic with a major glass transition at about 100°C. and a minor transition at about -70°C.<sup>1</sup>

Because of the presence of the secondary aliphatic hydroxyls, the poly(hydroxy ethers) in general possess the capability of modification through subsequent reaction at that group.<sup>2</sup> By the same token, however, they are susceptible to an attack by epichlorohydrin during the polymerization, with the production of long-chain branches having the same repeat unit as exists in the main chain. Questions arise, therefore, regarding the extent of this long-chain branching, the nature of its distribution among the molecular weight species, its effect upon the molecular weight distribution, and the effect of all these upon the properties of the polymer. The present investigation was designed to answer these questions by carrying out fractionations of three selected resins and measuring the intrinsic viscosities and weight average molecular weights of the resultant fractions.

At a given molecular weight, the intrinsic viscosity of a branched molecule is less than that of an analogous linear molecule. This problem was first treated theoretically by Zimm and Stockmayer,<sup>3</sup> who arrived at eq. (1) for the intrinsic viscosities of trifunctionally branched,  $[\eta]_b$ , and of linear,  $[\eta]_l$ , molecules.

$$\left\{ \frac{[\eta]_b}{[\eta]_l} = g^{3/2} = \left[ \left( 1 + \frac{m}{7} \right)^{1/2} + \frac{4m}{9\pi} \right]^{-3/4} \right\}_M \quad (1)$$

Here,  $g$  is the ratio of the mean square radii of the branched and linear molecules and  $m$  is the number of trifunctional branch points. Later, Zimm and Kilb<sup>4</sup> extended the theory and suggested eq. (2) as a more realistic description.

$$\left\{ \frac{[\eta]_b}{[\eta]_l} = g' = g^{1/2} = \left[ \left( 1 + \frac{m}{7} \right)^{1/2} + \frac{4m}{9\pi} \right]^{-1/4} \right\}_M \quad (2)$$

The Zimm-Kilb treatment has in fact found some experimental verification, particularly for rather lightly branched systems.<sup>4-7</sup> Thus, measurements of solution viscosity and molecular weight upon the poly(hydroxy ether) fractions, together with reasonable assumptions as to the viscosity behavior of unbranched fractions should yield at least relative measures of branch content of the fractions. More hopefully, if the fractions tended toward linearity at lower molecular weights—as would be predicted for example by a random branching mechanism—then an exact measure of the viscosity of linear material should be attainable and branch contents calculable within the limits of the above theories.

## EXPERIMENTAL

### Samples

Three samples of poly(hydroxy ether), designated by A, B, and C, were used. They are resins characteristic of preparations differing in reaction



media. These samples are not necessarily characteristic of present-day commercial poly(hydroxy ethers) in average molecular weights or distribution.

### Fractionation

The fractionations were effected with an automated elution column designed to handle approximately 30 g. of polymer with a ratio of sand to

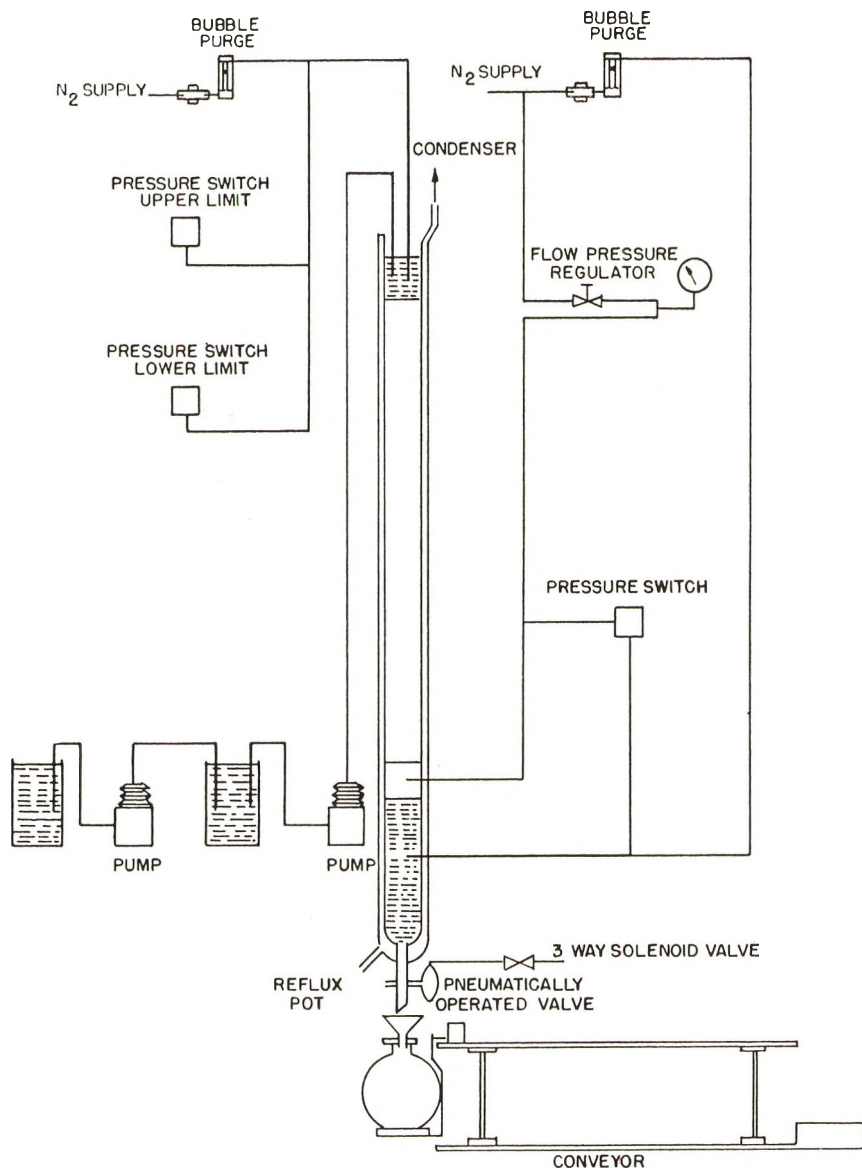


Fig. 1. Automated elution fractionation column.

polymer of about 300:1 by weight. Figure 1 presents a schematic diagram of the column. Briefly, the concentration of the eluting mixture is controlled by the relative pumping speeds of two micro bellows pumps; usually these rates were made equal, thereby producing a logarithmic solvent gradient. The pumps are turned off and on by two differential pressure switches which sense the head of the liquid above the sand column by means of a  $N_2$  bubbler. Similarly, the opening of the bottom valve is controlled by another differential pressure switch which senses the liquid head in the bottom reservoir. The flow rate of eluant through the column is regulated by  $N_2$  pressure applied just below the coarse glass frit. The number of reservoir openings per flask, and thus the movement of the conveyor, is controlled by a stepping switch. Further details of the column may be obtained from the authors. The present fractionations were performed over a minimum of 80 hr. without mechanical failures.

Phase studies at 31°C. indicated that chloroform and hexane constituted a suitable solvent-nonsolvent pair for fractionation since they provided the requisite liquid-liquid separation of polymer at low concentrations. Deposition of the polymer upon the matrix was effected by slow evaporation of solvent from a dilute chloroform solution.

Initial fractionations with the use of Ottawa sand as the matrix resulted in only 80% weight recovery of polymer. Apparently the hydroxyl groups of the polymer were reacting chemically with acidic hydroxyls of the sand. Reaction of the latter with trimethylchlorosilane prior to subsequent depositions resulted in successful fractionations, with weight recoveries between 99 and 100% and viscosity recoveries ( $\Sigma w_i[\eta]_i$ ) between 98 and 100%. Each large-scale run was preceded by a smaller preliminary run ( $\sim 1$  g.) to define the limits and pattern of the extracting eluant composition. Approximately 25 cuts of about 2500 cc. each were obtained during a large-scale fractionation and these were subsequently combined to yield about 15 final fractions per resin.

### Light Scattering

Light-scattering measurements were carried out with a Brice-Phoenix photometer. The instrument was calibrated with standard Cornell polystyrene, a value of  $13.5 \times 10^{-4}$  being used for the turbidity of a 0.5% solution in distilled toluene for green light. The photometer was also calibrated with purified benzene, a value of  $48.7 \times 10^{-6}$  being taken for the absolute turbidity. The polymer solutions were clarified by filtration through an ultrafine (Selas #03) filter at room temperature. A few solutions were also clarified by centrifugation at room temperature for 6-8 hr. at 16,000 rpm.

For most fractions the light-scattering measurements were made at only three concentrations and the resulting straight lines drawn by only visual observation. Therefore, the calculated values of the second virial coefficients can only be considered approximate. Within experimental error no angular dependence was observed for the scattering of all fractions,

By means of a Phoenix differential refractometer the values of  $dn/dc$  for poly(hydroxy ethers) in chloroform and tetrahydrofuran (THF), respectively, were found to be 0.172 and 0.221 in blue light. In addition, no significant variation was found in the  $dn/dc$  values for different fractions of the polymer.

### Viscometry

Determination of the intrinsic viscosities were made using a Ubbelohde dilution type viscometer. When necessary, kinetic energy corrections were applied to the viscosity data. The measurements were taken at three or four concentrations and values for Huggin's  $k'$  were determined by a least squares treatment of the data.

## RESULTS AND DISCUSSION

### Viscosity Distributions

These are shown in Figure 2 for all three samples and the data themselves are given in Tables I, II, and III. There would appear to be little difference between the viscosity distributions of samples A and B, while sample C is differentiated by the presence of much higher viscosity species.

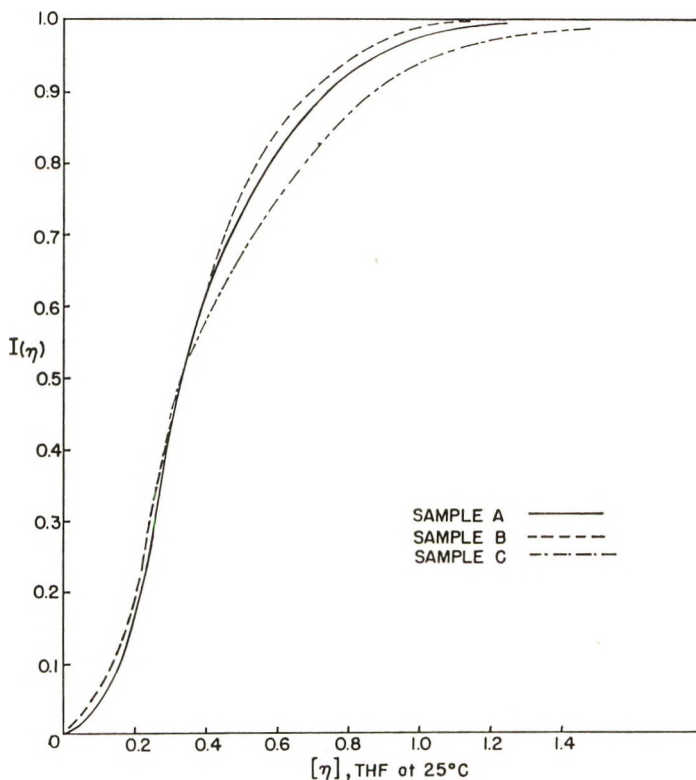


Fig. 2. Viscosity distributions.

TABLE I  
 Fractionation and Viscosity Data for Sample A

$[\eta]$ , THF, 25°C.	$k'$	$\bar{M}_w \times$ $10^{-4}$	$w_i$	$I = 1/2$ $w_i +$ $\sum_0^{i-1} w_j$	$\left\{ \frac{[\eta]_b}{[\eta]_e} \bar{M}_w' \right\}$ THF, 25°C.	$m_{zK}$	$m_{zS}$	$[\eta]$ , $\text{CH}_2\text{Cl}_2$ , 30°C.
0.08	—	—	0.0228	0.0114	1.0	0	0	—
0.16	—	0.86	0.0555	0.0506	1.0	0	0	—
0.19	—	1.2	0.0759	0.1162	1.0	0	0	—
0.22	0.64	—	0.0819	0.1951	1.0	0	0	0.17
0.250	0.52	1.6	0.0535	0.2629	1.0	0	0	0.20
0.254	—	—	0.0603	0.3148	1.0	0	0	—
0.26	—	—	0.0642	0.3712	1.0	0	0	—
0.32	0.40	—	0.0801	0.4420	1.0	0	0	—
0.37	0.43	—	0.0986	0.5335	1.0	0	0	—
0.45	0.49	—	0.1026	0.6341	1.0	0	0	0.34
0.52	0.47	—	0.1085	0.7402	1.0	0	0	—
0.65	0.50	—	0.0986	0.8432	1.0	0	0	—
0.83	0.39	12.0	0.0676	0.9263	0.73	13	3	0.48
1.01	0.48	32.0	0.0297	0.9750	0.44	120	10	0.50
1.04	0.36	40.0	0.0043	0.9919	0.36	210	15	0.51
1.06	—	—	0.0052	0.9967	0.35	220	16	Insol.
1.09	0.53	—	0.0006	0.9995	0.32	270	19	Insol.

It will be seen presently that this same pattern holds true for the molecular weight distributions and the branching distributions.

### Viscosity-Molecular Weight Relation

Weight-average molecular weights have been determined by light scattering for 21 of the total of 48 fractions obtained from the three samples (A, B, and C). The values are included in Tables I, II, and III and are shown in Figure 3 as a conventional plot of  $\log [\eta]$  in THF at 25°C. versus  $\log \bar{M}_w$ . For an homologous series of unbranched polymer samples having the same  $\bar{M}_w/\bar{M}_n$  such a plot should yield a straight line of slope between 0.7 and 0.8 when  $[\eta]$  is determined in a good solvent—such as THF is for Bisphenol A poly(hydroxy ether). Figure 3 exhibits precisely that type of behavior up to a molecular weight of about 70,000, while the fractions above that point deviate increasingly below the straight line of slope 0.765. That straight line was derived from a least squares fit of the lowest 13 points to the Mark-Houwink equation to yield

$$[\eta] = 1.48 \times 10^{-4} \bar{M}_w^{0.765} \quad (3)$$

The values of the two constants are, we repeat, of the proper magnitude for linear fractions in a good solvent.

Intrinsic viscosities were also determined for a number of the fractions in two poorer solvents, i.e., in methylene chloride at 30° and at 25°C. At both temperatures, the data followed the same pattern as those in Figure 3

TABLE II  
 Fractionation and Viscosity Data for Sample B

$[\eta]$ , THF, 25°C.	$k'$	$\bar{M}_w \times$ $10^{-4}$	$w_i$	$I = 1/2$ $w_i +$ $\sum_0^{i-1} w_j$	$\left\{ \begin{array}{l} [\eta]_b \\ [\eta]_l \end{array} \right\} \bar{M}_w'$ THF, 25°C.	$m_{ZK}$	$m_{ZS}$	$[\eta]$ , $\text{CH}_2\text{Cl}_2$ , 30°C.
0.08	—	—	0.0694	0.0347	1	0	0	—
0.10	—	—	0.0542	0.0964	1	0	0	—
0.19	0.10	—	0.0702	0.1586	1	0	0	—
0.21	0.48	—	0.0637	0.2256	1	0	0	—
0.23	—	—	0.0449	0.2799	1	0	0	—
0.25	—	—	0.0555	0.3301	1	0	0	—
0.30	0.43	2.1	0.0679	0.3917	1	0	0	—
0.36	0.46	2.6	0.0904	0.4709	1	0	0	0.28
0.41	0.53	—	0.1375	0.5849	1	0	0	—
0.46	0.70	3.7	0.0946	0.7009	1	0	0	0.34
0.55	—	—	0.0879	0.7919	0.82	6	1	—
0.80	0.52	10.0	0.0926	0.8812	0.63	32	4	0.46
0.92	0.60	29.0	{ 0.0558	0.9564	0.46	110	9	0.50
			{ 0.0122	0.9889				
1.05	0.62	—	0.0210	0.9989	0.36	210	15	0.51

 TABLE III  
 Fractionation and Viscosity Data for Sample C

$[\eta]$ , THF, 25°C.	$k'$	$\bar{M}_w$ $\times$ $10^{-4}$	$w_i$	$I = 1/2$ $w_i +$ $\sum_0^{i-1} w_j$	$\left\{ \begin{array}{l} [\eta]_b \\ [\eta]_l \end{array} \right\} \bar{M}_w'$ THF, 25°C.	$m_{ZK}$	$m_{ZS}$	$[\eta]$ , $\text{CH}_2\text{Cl}_2$ , 30°C.
0.04	—	—	0.0255	0.0128	1	0	0	—
0.06	—	—	0.0098	0.0304	1	0	0	—
0.07	—	—	0.0145	0.0425	1	0	0	—
0.12	—	—	0.0251	0.0890	1	0	0	—
0.14	0.62	—	0.0282	0.1357	1	0	0	—
0.20	0.71	1.4	0.0751	0.2008	1	0	0	—
0.25	0.39	—	0.0451	0.2597	1	0	0	—
0.27	0.45	1.9	0.0728	0.3433	1	0	0	0.22
0.35	0.48	2.6	0.0924	0.4463	1	0	0	0.28
0.42	0.44	3.2	0.1155	0.5668	1	0	0	—
0.50	0.56	4.0	0.1256	0.6628	1	0	0	—
0.64	—	5.6	0.0663	0.7387	1	0	0	—
0.75	0.42	7.5	0.0847	0.8317	0.88	3	1	0.45
0.91	0.48	31.0	0.1013	0.9219	0.44	120	11	0.49
1.14	0.45	52.0	0.0800	0.9725	0.31	280	20	0.52 (partially insol.)
1.21	0.53	60.0	0.0021	0.9831	<0.20 (est.)	>300	>35	Insol.

for tetrahydrofuran up to 70,000 molecular weight. The slopes for the straight lines at 30 and 25°C. were about 0.65 and 0.58, respectively. In each case, however, beyond this 70,000 limit, the fractions became increasingly insoluble, particularly at 25°C. In view of the value for each slope,

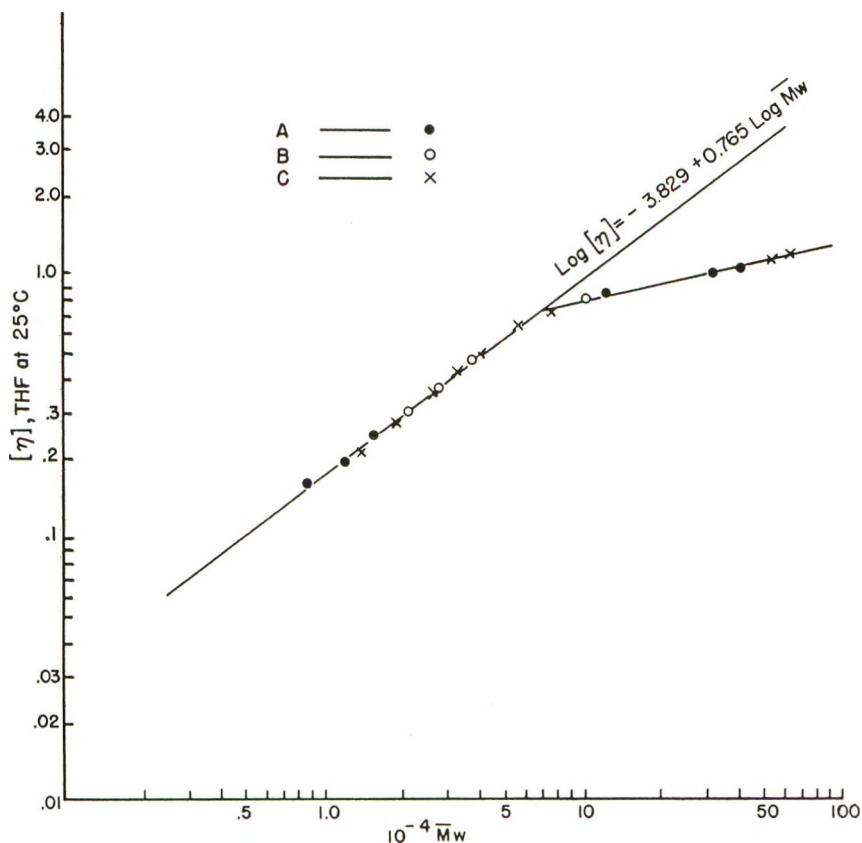


Fig. 3. Viscosity-molecular weight relationship.

neither system can be a theta solvent and hence the insolubility of the higher fractions must be due directly or indirectly to branching.

As indicated previously, the absence of any angular dependence of scattered light precluded direct measurements of molecular size and configuration in solution. Similarly, the relative insolubility of the higher molecular weight fractions in poorer solvents reduced the feasibility of finding a theta solvent and calculating molecular sizes from the Flory-Fox viscosity theory. With the use of Krigbaum's relationship<sup>8</sup> among  $[\eta]$ ,  $[\eta]_\theta$ ,  $A_2$ , and  $\bar{M}_w$ , values of  $[\eta]_\theta$  were calculated but made insufficient sense to warrant their presentation here. We do present in Figure 4, however, a plot of  $\log A_2$  versus  $\log \bar{M}_w$ , and it may be seen that the  $A_2$  values fall off rather sharply above about 70,000 molecular weight. Such behavior is consistent with that reported by Thurmond and Zimm for branched polystyrene.<sup>9</sup>

Tentatively, therefore, we might conclude from these data that fractions from all three resins are unbranched below a molecular weight of about 70,000 and that the fractions above this point are abruptly and increasingly branched to a very high degree (cf. values for  $m$  in Tables I-III). This

conclusion is unexpected and before being accepted requires inquiry into the effects of three factors upon the data.

An increase in breadth of molecular weight distribution, at constant  $\bar{M}_w$ , leads to a reduction in intrinsic viscosity. Is it possible, therefore, that variations in polydispersity among the fractions have appreciably altered the shape of the true  $[\eta]-\bar{M}_w$  curve? To anticipate subsequent discussion, the maximum  $\bar{M}_w/\bar{M}_n$  for the three whole resins is perhaps 5 or 6, and each of these was separated into some 15 to 20 fractions during an 80-hr. elution fractionation. Our previous experience with linear polyethylene resins of much broader distribution than the present poly(hydroxy ethers) indicated that more rapid, and hence less ideal, fractionations produced polyethylene fractions with  $\bar{M}_w/\bar{M}_n$  values of about 1.2. This value is also supported by

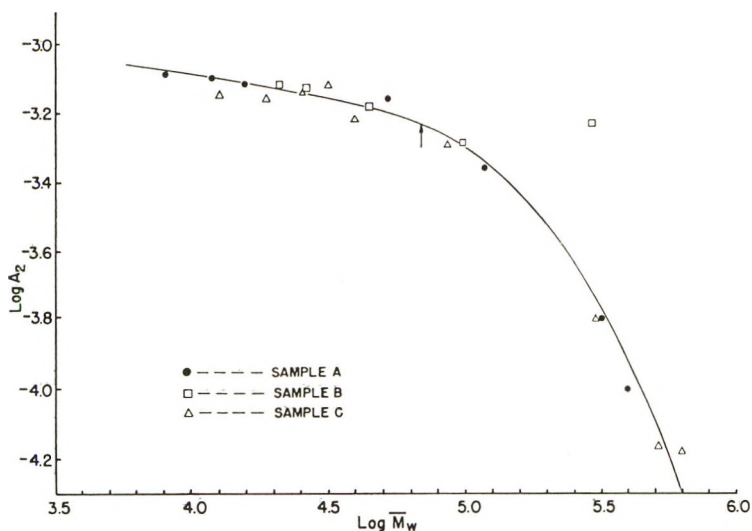


Fig. 4. Second virial coefficient-molecular weight relationship.

published data.<sup>10</sup> The poly(hydroxy ether) fractions, then, might be expected to be at least as narrow as this. It must be admitted, however, that the presence of long-chain branches undoubtedly leads to greater polydispersity in the fractions than would otherwise exist since the fractionation will not always distinguish between molecules solely on the basis of molecular weight. Nevertheless, it hardly seems possible that the  $\bar{M}_w/\bar{M}_n$  ratio of the present fractions would exceed about 1.5. Published calculations show that samples obeying the Schultz-Zimm distribution with an  $\bar{M}_w/\bar{M}_n$  of 1.5 would have their intrinsic viscosities reduced by about 3% below that of a monodisperse samples of the same  $\bar{M}_w$ —and even for an  $\bar{M}_w/\bar{M}_n$  of 2.0, the reduction would only be about 5%.<sup>11</sup> Therefore, since the combined experimental errors in  $[\eta]$  and  $\bar{M}_w$  are of the order of  $\pm 5\%$  and since, further, it is only regularly increasing corrections from fraction to fraction which will effectively change the slope of an  $[\eta]-\bar{M}_w$  plot, we conclude that poly-

dispersity variations among the fractions have a negligible effect upon the data of Figure 3 and upon eq. (3).

Our second question is concerned with the effect upon Figure 3 of variations in branch content among the apparently linear fractions and can be resolved with the aid of eqs. (1) and (2) from the Zimm-Stockmayer<sup>3</sup> and Zimm-Kilb<sup>4</sup> treatments, respectively. It may easily be seen that our experimental error of about  $\pm 5\%$  could conceivably be masking the existence of perhaps 1 or 2 branches per molecule in the species below 70,000 molecular weight. In fact, it is not at all unlikely that branching may be regularly increasing from zero at very low molecular weight to 1 or 2 branches per molecule at 70,000 molecular weight, from whence it begins to increase much more rapidly. It is doubtful, however, that any greater degree of branching occurs in the lower region of molecular weight since this would lead to a lower slope in Figure 3, and we have already emphasized that the observed value of 0.765 is relatively high. (We are, of course, making the very reasonable assumption that the lowest molecular weight fractions would never be more branched than those just below 70,000, i.e., that the greater the number of secondary hydroxyls on a molecule, the greater is its intrinsic susceptibility to branch formation.)

The third factor to be considered arises from the observation that the highest fractions, i.e., those above 70,000 molecular weight, appear to be significantly less soluble than the lower fractions. If carried to an extreme, this might conceivably mean that none of the branched species were eluted during the fractionation until all linear species had been extracted, thereby giving the impression that branching began abruptly, as in Figure 3. However, if this had occurred, the first branched fractions should have contained a significant amount of low molecular weight, branched species and therefore exhibited lower  $[\eta]$  and  $\bar{M}_w$  than possessed by the last linear fraction. That this did not indeed occur is amply illustrated by the data of Tables I-III, the viscosity distributions in Figure 1, and the molecular weight distributions in Figure 6, where in each case the data are presented in the order in which the fractions were extracted from the column.

### Branching Distribution

To reiterate, we conclude that the data of Figure 3 are unequivocal proof of the existence of long-chain branching in the poly(hydroxy ethers). More explicitly, we conclude that for all three resins studied this branching occurs only to a slight extent (maximum of 1-2 branches per molecule), if at all, in species below a molecular weight of about 70,000 and increases sharply above that point.

Assuming eq. (3) to represent the behavior of linear poly(hydroxy ether) fractions over the entire molecular weight range, we are now able to calculate the ratio  $\{[\eta]_b/[\eta]_l\} \bar{M}_w$  for the actual fractions. These ratios may then be combined with the Zimm-Stockmayer and Zimm-Kilb theories [eqs. (1) and (2)] to give us numbers of trifunctional branches in the individual fractions. The resulting values are shown in Tables I-III as  $m_{zs}$  and



$m_{zK}$ . While the  $m_{zS}$  values are at least of reasonable magnitude in all cases, the  $m_{zK}$  values for the highest fractions are so large as to have questionable physical significance. In Table III, for example, 280 branch points for a molecular weight of 520,000 corresponds to only about 6 monomer units per branch point. It is worthy of note that Guillet has recently reported very similar results from measurements upon high pressure polyethylene fractions.<sup>12</sup> It would appear that neither of these theories can be presumed at this time to yield valid numbers for long-chain branch contents of highly branched molecules. That the fault does not lie with our use of a thermodynamically good solvent—instead of the theta solvent for which the theories were derived—is indicated by the fact that the  $[\eta]_b/[\eta]_l$  values were found to be essentially identical in the two solvents for which the molecular weight exponents were 0.77 and 0.65.

Despite this apparent quantitative failure of the branching-viscosity theories, we can make use of them to illuminate the nonrandom nature of the branching reaction in the present polymers. (Here we take random to mean that the probability of branch formation during the polymerization is proportional to the number of aliphatic hydroxyls present and therefore to molecular weight.) Beasley<sup>13</sup> has developed equations for the molecular weight and branching distributions resulting from a free radical polymerization in which random branching occurs and in which the distribution in both the branch lengths themselves and in the chain lengths in the absence of branching are given by Flory's "most probable" distribution. (We have demonstrated, incidentally, by computer calculations that the Beasley distribution is for all practical purposes mathematically identical to that of Flory for trifunctionally branched condensation polymers,<sup>14</sup> except that the former extends to higher molecular weights in the upper 3 to 5 wt.-%.)<sup>15</sup> Beasley's expressions for the weight fraction,  $w(x)$ , of polymer having  $x$  monomer units and for the average number of branches,  $(m)_x$ , for all molecules having  $x$  monomer units are given by eqs. (4) and (5):

$$w(x)dx = \frac{(1 - \beta)(x/x_0)d(x/x_0)}{[1 + \beta x/x_0][1 + (1/\beta)]} \quad (4)$$

$$(m)_x = (x/x_0) - (1/\beta) \ln [1 + \beta x/x_0] \quad (5)$$

Here,  $x_0$  is the average number of monomer units per chain and  $\beta$  is a branching parameter which is zero for no branching and  $1/2$  for incipient gelation.

Combination of eq. (5) for  $(m)_x$  with the Zimm-Stockmayer and Zimm-Kilb treatment permits the calculation of intrinsic viscosities to be expected for monodisperse fractions obtained from a Beasley distribution. Such calculations, shown in Figure 5, have been made for two values of  $\beta$  for both theories, using the experimental value of 0.765 for the molecular weight exponent and a value for  $x_0$  which would permit the lowest point to fall on the experimental curve. It should be noted that for each of the four calcu-

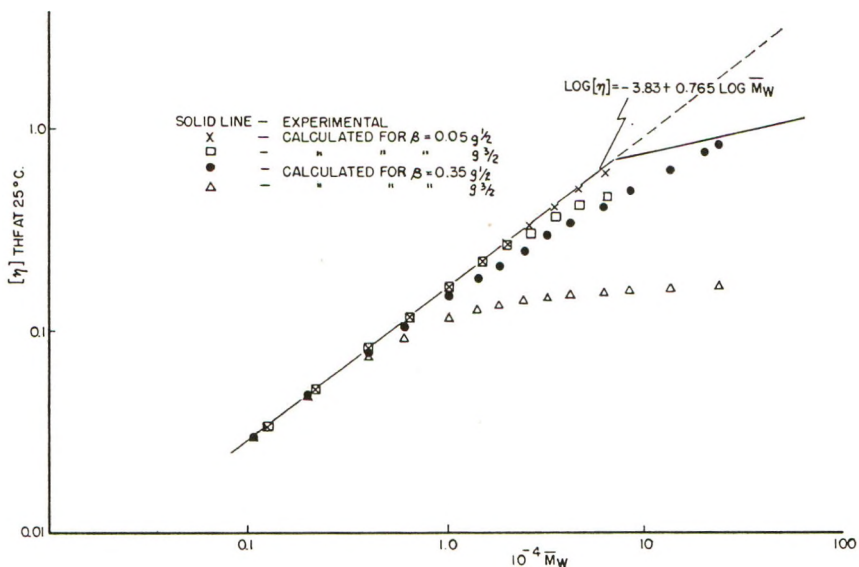


Fig. 5. Comparison of experimental  $[\eta]-\bar{M}_w$  data with random branching calculations.

lated cases in Figure 5 the points extend up to 99.8% by weight of the theoretical distribution. This, together with the smoothly increasing deviations from the experimental line serve to illustrate the nonrandomness of the observed branching.

### Molecular Weight Distributions

Further confirmation of the deviation from an idealized randomly branched material is given by the molecular weight distributions themselves. These are shown in Figure 6, where the curves have been drawn on the basis of smoothed values from Figure 3. As was the case with the viscosity distributions in Figure 1, the molecular weight distributions of samples A and B are very similar, while that of sample C is distinguished by a higher tail which apparently results from increased branching. This distinction is also demonstrated by the calculated whole resin molecular weights in Table IV, the  $\bar{M}_n$  being calculated by assuming monodisperse

TABLE IV  
Intrinsic Viscosities and Calculated Molecular Weights of Poly(hydroxy Ether) Samples

Sample	$[\eta]$ , THF, 25°C.	$\bar{M}_n$ ( $\sum w_i \bar{M}_{wi}$ )	$\bar{M}_n$ ( $\sum \frac{1}{w_i / \bar{M}_{wi}}$ )	$\bar{M}_w / \bar{M}_n$
A	0.41	45,000	18,000	2.5
B	0.44	44,000	17,900	2.5
C	0.53	76,000	17,000	4.5

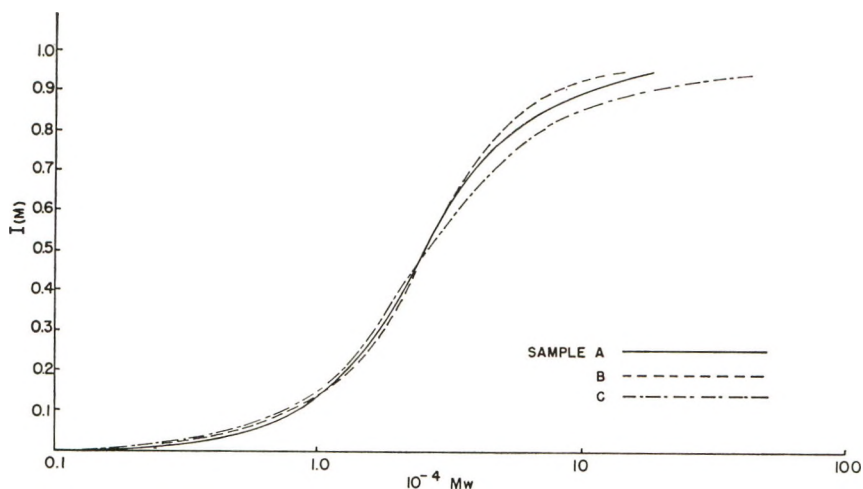


Fig. 6. Integral molecular weight distributions.

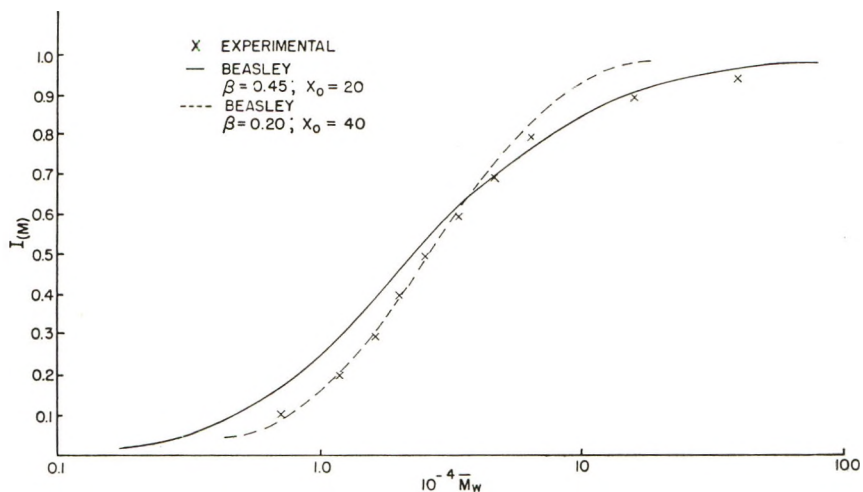


Fig. 7. Comparison of Beasley distribution with experimental distribution for sample C.

fractions. Figure 7 presents a comparison of the measured distribution of sample C with two Beasley distributions, one of which approximates the observed points at the high end and the other at the low end. Obviously, the observed distribution contains too much high molecular weight (and apparently highly branched) material to conform to the Beasley distribution.

#### Effect of Branching and Molecular Weight Upon the Viscosity-Concentration Parameters

The possibility of a correlation between the Huggins'  $k'$  and the degree of branching has been investigated for the fractions. Tables I-III list these

values for several fractions. It is readily evident that no correlation does exist and similarly no correlation exists between  $k'$  and molecular weight.

### Resin Properties

Some pertinent properties of the three samples are given in Table V. The poly(hydroxy ethers) are only mildly non-Newtonian in melt flow behavior but become increasingly so as the distribution broadens and/or as branching increases. Sample C obviously is the preferred material from

TABLE V  
Physical Property Data for Samples A, B, and C

Resin	$[\eta]$ , THF, 25°C.	$\bar{M}_w$	Melt flow MI, dg./min. <sup>a</sup>	Melt flow ratio MFR <sup>b</sup>	$T_g$ , °C. <sup>c</sup>	Elongation (at break), %	Impact strength, ft.-lb./ in. <sup>3d</sup>
A	0.41	45,000	8.8	6.0	90	7-20	60
B	0.44	44,000	3.3		85 <sup>e</sup>	20	50
C	0.53	76,000	0.68	11.8	100-105	60-150	133

<sup>a</sup> At 220°C. and 44 psi.

<sup>b</sup> Ratio of the melt flows measured at 220 and 44 psi.

<sup>c</sup> Glass transition temperature, as determined from stiffness-temperature curve.

<sup>d</sup> As determined from a pendulum impact test.

<sup>e</sup> Sample appeared to be contaminated with residual solvent.

an end-use point of view, having a higher softening temperature and being considerably tougher. Whether this improvement in behavior is due solely to its higher molecular weight or is partially the result of its greater branch content cannot be stated at this time.

The number of those to whom we are indebted for aid in this work approaches infinity and we must perforce limit ourselves to a general expression of our appreciation. Explicit mention must be made, however, of the considerable aid given by C. W. Schultz, R. F. Holler, C. N. Merriam, and A. Barnabeo.

### References

1. Reinking, N. H., A. E. Barnabeo, and W. F. Hale, *J. Appl. Polymer Sci.*, **7**, 2135 (1963).
2. Reinking, N. H., A. E. Barnabeo, W. F. Hale, and J. H. Mason, *J. Appl. Polymer Sci.*, **7**, 2153 (1963).
3. Zimm, B. H., and W. H. Stockmayer, *J. Chem. Phys.*, **17**, 1301 (1949).
4. Zimm, B. H., and R. W. Kilb, *J. Polymer Sci.*, **37**, 19 (1959).
5. Hobbs, L. M., G. C. Berry, and V. C. Long, paper presented at International Symposium on Macromolecular Chemistry, 27 July-1 August 1961.
6. Wenger, F., *J. Polymer Sci.*, **57**, 481 (1962).
7. Cantow, M., G. Meyerhoff, and G. V. Schulz, *Makromol. Chem.*, **49**, 1 (1961).
8. Krigbaum, W. R., *J. Polymer Sci.*, **18**, 315 (1955).
9. Thurmond, C. D., and B. H. Zimm, *J. Polymer Sci.*, **8**, 477 (1952).
10. Henry, P. M., *J. Polymer Sci.*, **36**, 3 (1959).
11. Booth, C., and L. R. Beason, *J. Polymer Sci.*, **42**, 92 (1960).

12. Guillet J. E., paper presented at the 141st National Meeting of the American Chemical Society, Washington, D. C., March 20-29, 1962.
13. Beasley, J. K., *J. Am. Chem. Soc.*, **75**, 6123 (1953).
14. Flory, P. J., *J. Am. Chem. Soc.*, **63**, 3091 (1941).
15. Meyers, G. E., and J. R. Dagon, *J. Polymer Sci.*, in press.

### Résumé

Les distributions de poids moléculaire et les distributions de ramification en longue chaîne de trois échantillons de bisphénol A poly(hydroxyéther) ont été envisagées. Les échantillons ont été fractionnés et les fractions ont été caractérisées par de mesures de viscosités de solution et des mesures de diffusion lumineuse. Un diagramme  $\log - \log$  de la viscosité intrinsèque et de  $\bar{M}_w$  des fractions des trois résines fournit une ligne droite jusqu'à des poids moléculaires de l'ordre de 70.000 (approximativement 80% en poids pour chaque polymère) définie par la relation  $(\eta) = 1.48 \times 10^{-4} \bar{M}_w^{0.765}$ . Au delà de ce poids moléculaire les viscosités tombent de manière croissante au dessous de la ligne droite dont les constantes sont caractéristiques de celles attendues pour des fractions linéaires dans un bon solvant. Il est évident que le partage des longues chaînes ne se présente pas de manière appréciable dans les fractions les plus basses mais commence brusquement à des poids moléculaires de l'ordre de 70.000 et augmente progressivement à partir de ce point. La comparaison des distributions de ramifications et de poids moléculaire avec celles prévues par le mécanisme de ramification statistique de Beasley confirme la nature non-statistique du mécanisme de ramification chez ces poly(hydroxy-éthers). Le nombre de branches calculés au moyen de la théorie de Zimm-Kilb atteint des valeurs improbablement élevées alors que celles calculées à partir de la théorie de Zimm-Stockmayer apparaissent plus raisonnables. On n'a pas trouvé de relation entre le coefficient  $k'$  de Huggins et le poids moléculaire ou la ramification. L'échantillon de poids moléculaire le plus élevé possède un résidu plus important et davantage ramifié de haut poids moléculaire, ce qui se traduit par des différences dans les propriétés physiques.

### Zusammenfassung

Molekulargewichtsverteilung und Verteilung der Langkettenverzweigungen von drei Proben von Bisphenol-A-poly(hydroxyäther) wurden untersucht. Die Proben wurden fraktioniert und die Fraktionen durch Viskositäts- und Lichtstreuungsmessungen charakterisiert. Eine  $\log\text{-}\log$ -Auftragung von Viskositätszahl und  $\bar{M}_w$  ergab bei allen drei Harzen bis hinauf zu Molekulargewichten von etwa 70000 (etwa 80 Gewichtsprozent jeder Probe) eine der Gleichung  $[\eta] = 1.48 \times 10^{-4} \bar{M}_w^{0.765}$  entsprechende Gerade. Bei Molekulargewichten über 70000 lagen die Viskositätswerte in steigendem Masse unterhalb der für lineare Fraktionen in einem guten Lösungsmittel zu erwartenden Geraden. Daraus geht hervor, dass in den niedrigen Fraktionen keine merkliche Langkettenverzweigung auftritt, sondern dass diese erst bei einem Molekulargewicht von 70000 plötzlich einsetzt und oberhalb dieses Wertes kontinuierlich zunimmt. Ein Vergleich der Verzweigungs- und der Molekulargewichtsverteilung mit der auf Grund des Beasley'schen Mechanismus der statistischen Verzweigung vorausgesagten bestätigt die nichtstatistische Natur des Verzweigungsmechanismus in diesen Poly(hydroxyäthern). Die Berechnung der Zahl der Verzweigungen ergibt bei Verwendung der Zimm-Kilb-Theorie viel zu hohe Werte, während die aus der Zimm-Stockmayer-Theorie berechneten Werte plausibel sind. Es wurde keine Beziehung zwischen der Huggins-Konstante  $k'$  und dem Molekulargewicht oder der Verzweigung gefunden. Die Probe mit dem höchsten Molekulargewicht hat einen längeren und stärker verzweigten hochmolekularen Schwanz. Dies kommt in veränderten physikalischen Eigenschaften zum Ausdruck.

Received June 7, 1963

## Radiation-Induced Copolymerization of Acrylonitrile with Methyl Methacrylate

YONEHO TABATA, YOSHIO HASIZUME, and HIROSHI SOBUE,  
*Department of Nuclear Engineering, University of Tokyo, Department of Industrial Chemistry, University of Tokyo, Central Research Laboratory, Dainippon Celloid Company, Tokyo, Japan*

### Synopsis

Radiation-induced copolymerization of acrylonitrile (1) with methyl methacrylate (2) was investigated over a wide range of temperatures. The rate of copolymerization decreased linearly with the molar concentration of acrylonitrile in the liquid-state copolymerization at 15°C. On the contrary, the rate of copolymerization increased linearly with the concentration of acrylonitrile in the solid state at -78°C. The rate of copolymerization was proportional to the square root of the dose rate in an equimolar mixture of the monomers at 15°C. The apparent activation energy of the copolymerization was 4.62 kcal./mole in an equimolar mixture of the monomers. Monomer reactivity ratios  $r_1$  and  $r_2$  were determined from the experiments at various temperatures. From these results, the differences of the activation energies in the propagation steps were obtained as follows:  $E_{11}^\ddagger - E_{12}^\ddagger = 2.76$  kcal./mole;  $E_{22}^\ddagger - E_{21}^\ddagger = 2.58$  kcal./mole.

### INTRODUCTION

Several investigations on the radiation-induced copolymerizations have been reported by various workers.<sup>1-11</sup> In these investigations, the radiation-induced copolymerization of acrylonitrile with methyl methacrylate was briefly reported by Tsuda<sup>12</sup> and Okamura et al.<sup>13</sup>

In our studies, the copolymerization of the same system was investigated more precisely in a wide range of temperatures.

### EXPERIMENTAL

A commercial methyl methacrylate monomer was washed by treatment with saturated aqueous solution NaHSO<sub>3</sub>, 5% aqueous NaOH, 20% aqueous NaCl, and distilled water, was dried by passage through anhydrous CaCl<sub>2</sub>, and finally was purified by distillation at a reduced pressure. The commercial acrylonitrile monomer was dehydrated by passage through anhydrous CaCl<sub>2</sub> and was distilled at a reduced pressure.

An ampule containing solid monomers was evacuated to 10<sup>-3</sup> to 10<sup>-4</sup> mm. Hg. Irradiation was carried out by  $\gamma$ -rays from a Co<sup>60</sup> source in a temperature region of 50 to -78°C. Overall reaction rates were deter-

mined by isolating and weighing the polymer. Polymer composition was determined by infrared analysis.

## RESULTS AND DISCUSSION

### 1. Solubility of Copolymers in Various Solvents

Solubility of the copolymers obtained was examined in various solvents at 20°C. The results are shown in Table I for the product obtained by polymerization at 20°C.

TABLE I  
Solubilities of Copolymers in Various Solvents

Mole fraction of of acrylonitrile in monomers	Solubility <sup>a</sup>				
	Acetone	Toluene	CHCl <sub>3</sub>	CCl <sub>4</sub>	Dimethyl- formamide
1.00	—	—	—	—	+
0.91	+	—	+	—	+
0.83	+	—	+	—	+
0.75	+	—	+	—	+
0.50	+	—	+	—	+
0.25	+	±	+	—	+
0.17	+	+	+	—	+
0.09	+	+	+	—	+
0	+	+	+	+	+

<sup>a</sup> —, insoluble; ±, swelling; +, soluble.

No acrylonitrile or methyl methacrylate homopolymer could be extracted by any solvent extraction techniques. It was concluded that the homopolymerization did not take place in a wide range of monomer ratios.

### 2. Infrared Analysis of Composition of Copolymer

The infrared spectrum of an equimolar mixture of homopolymers and spectra of the copolymers obtained are given in Figure 1. *A* is the spectrum of the equimolar mixture of the homopolymers; *B*, *C*, and *D* are the spectra of various copolymers.

It is apparent from the results that spectrum *B* is very different from that of the homopolymer mixture, in spite of the fact that the amount of monomer units is not so different between the copolymer *B* and the equimolar mixture of homopolymers *A*. This indicates that the copolymerization could take place homogeneously to yield copolymers with a statistical distribution of the monomer units.

The 2230 cm.<sup>-1</sup> band is due to the CN stretching vibration in the acrylonitrile; on the other hand, the 1733 and 2967 cm.<sup>-1</sup> bands are due to the carbonyl and methyl stretching vibrations, respectively, of COCH<sub>3</sub> in the methyl methacrylate. The relative intensities,  $D_{1733}/D_{2230}$  and  $D_{2967}/D_{2230}$ , were plotted for the molar ratios of methyl methacrylate to acrylo-

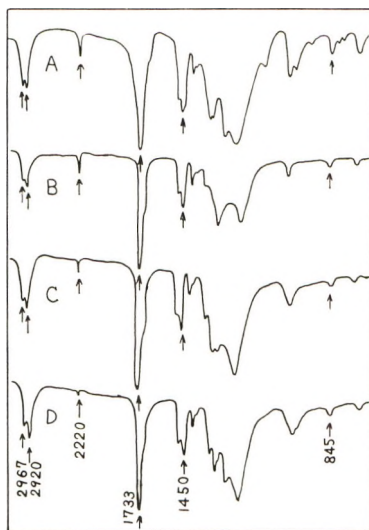


Fig. 1. Infrared spectra of (A) an equimolar mixture of polyacrylonitrile and poly(methyl methacrylate) and (B, C, D) acrylonitrile-methyl methacrylate copolymers.

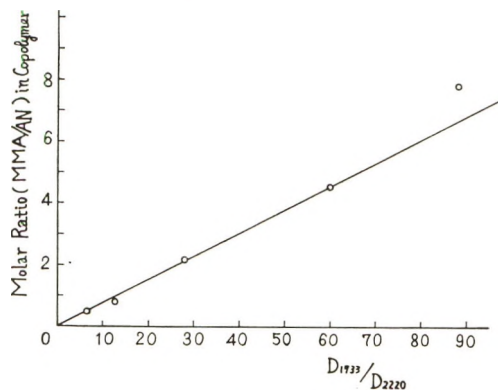


Fig. 2. Infrared calibration.

nitrile in the copolymers, as shown in Figures 2 and 3. A tangential base-line procedure was used for determining absorbances, and the molar concentration of acrylonitrile in the copolymer was determined by elementary analysis.

It is obvious from these results that there exists a linear correlation between the relative absorption intensity and the molar concentration of one component in the copolymer. Therefore, one can easily determine the composition curve of the acrylonitrile-methyl methacrylate on the basis of these calibration curves.

### 3. Copolymerization Rate

The data on conversion versus irradiation time at various dose rates are given in Figure 4. The copolymerization is not preceded by an induction



period. The conversion increases linearly with the irradiation time in the initial stage of the polymerization. An acceleration phenomenon was observed above 10% yield, probably due to a gel effect.

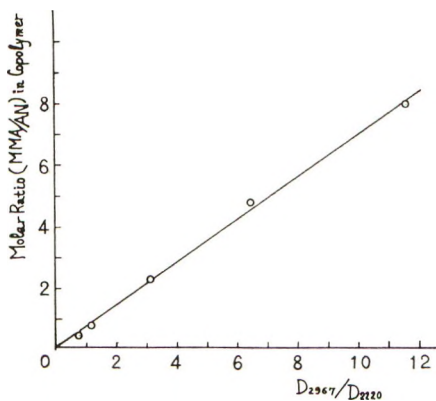


Fig. 3. Infrared calibration.

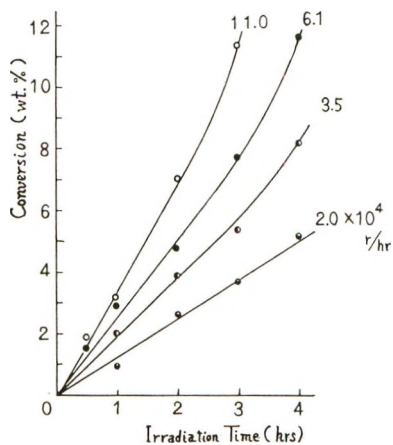


Fig. 4. Relation between the conversion and the irradiation time at 15°C.

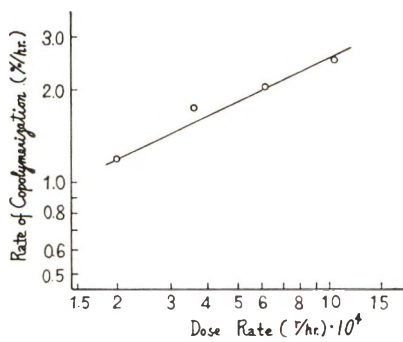


Fig. 5. Dose rate dependence of the rate of copolymerization at 15°C.

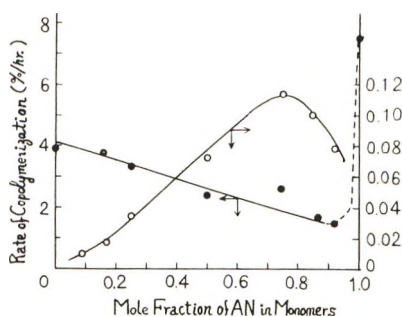


Fig. 6. Relations between the rate of copolymerization and the mole fraction of acrylonitrile in the monomer mixture.

The dose rate dependence of the rate of copolymerization at  $15^{\circ}\text{C}$ . is given in Figure 5.

It is obvious from these results that the rate of copolymerization is proportional to the square root of the dose rate. This indicates that the termination is a bimolecular reaction. It can be readily suggested from these results that the copolymerization proceeds by a radical mechanism in the liquid state of the monomers.

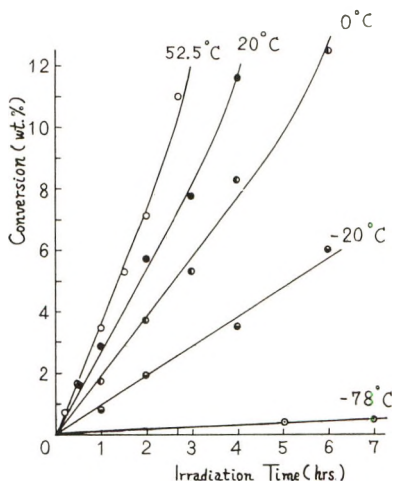


Fig. 7. Effects of temperature on the rate of copolymerization.

The relations between the rate of copolymerization and the mole fraction of acrylonitrile in the monomer mixture are shown in Figure 6.

The rate of copolymerization decreases linearly with the molar concentration of acrylonitrile in the liquid-state copolymerization at  $15^{\circ}\text{C}$ . On the contrary, the rate of copolymerization increases linearly with the molar concentration of acrylonitrile in this solid-state copolymerization at  $-78^{\circ}\text{C}$ .

This suggests that the reactivity of the monomers in the solid state is appreciably different from the reactivity in the liquid state.

#### 4. Temperature Dependence of Rate of Copolymerization

The effects of temperature on the rate of copolymerization are shown in Figure 7. An Arrhenius plot of the results is given in Figure 8. An apparent activation energy of 4.62 kcal./mole was obtained from the results for the copolymerization. Copolymerization was carried out in an equimolar mixture of the monomers at dose rates of  $6.1 \times 10^4$  r/hr.

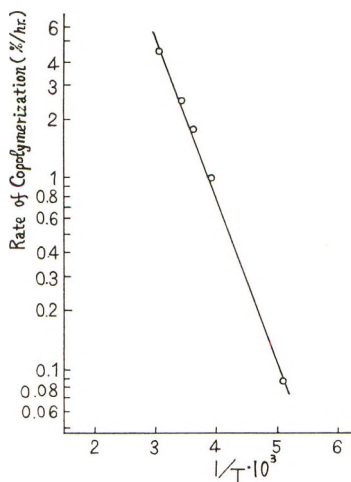


Fig. 8. Arrhenius plot of the rate of copolymerization.

#### 5. Monomer Reactivity Ratio

Composition curves of the acrylonitrile–methyl methacrylate copolymers are shown in Figures 9 and 10.

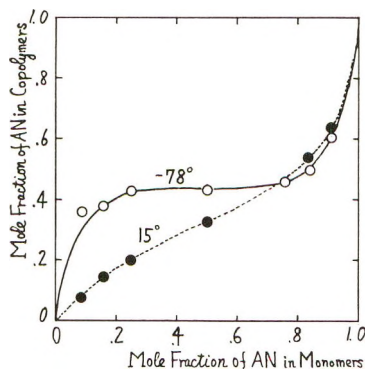


Fig. 9. Composition curve of acrylonitrile–methyl methacrylate copolymers: (●) 15° C.; (○) -78° C.

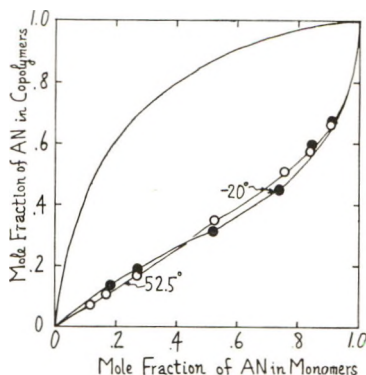


Fig. 10. Composition curve of acrylonitrile-methyl methacrylate copolymers: (O) 52.5° C.; (●) -20° C.; (—) ionic copolymerization.

It is well known that the monomer reactivity ratios are defined as  $r_1 = k_{11}/k_{12}$ ,  $r_2 = k_{22}/k_{21}$ , where  $k$  is the propagation rate constant. And further, the rate constants can be represented as follows;

$$\begin{aligned}k_{11} &= a_{11}e^{-E_{11}^\ddagger/RT} \\k_{12} &= a_{12}e^{-E_{12}^\ddagger/RT} \\k_{22} &= a_{22}e^{-E_{22}^\ddagger/RT} \\k_{21} &= a_{21}e^{-E_{21}^\ddagger/RT}\end{aligned}$$

where  $a_{11}$ ,  $a_{12}$ ,  $\dots$ , are constants and  $E_{11}^\ddagger$ ,  $E_{12}^\ddagger$ ,  $\dots$ , are the activation energies of the propagation. The monomer reactivity ratios are represented as a function of the activation energy of propagation:

$$\begin{aligned}r_1 &= \frac{a_{11}}{a_{12}} e^{-(E_{11}^\ddagger - E_{12}^\ddagger)/RT} \\r_2 &= \frac{a_{22}}{a_{21}} e^{-(E_{22}^\ddagger - E_{21}^\ddagger)/RT}\end{aligned}$$

From the acrylonitrile-methyl methacrylate composition curve, the reactivity ratios can be determined.

The monomer reactivity ratios for the copolymerization over a wide range of temperature are summarized in Table II.

Zutty and Welch<sup>14</sup> carried out copolymerization with various catalysts and they obtained  $r_1 = 7$ ,  $r_2 = 0.40$  for anionic copolymerization and  $r_1 = 0.12$ ,  $r_2 = 1.34$  for a radical copolymerization. These results are also shown in Table II for comparison with our results.

The Arrhenius plots of  $r_1$  and  $r_2$  are shown in Figures 11 and 12.

From these results, the differences in the activation energies in the propagation steps are obtained as,  $E_{11}^\ddagger - E_{12}^\ddagger = 2.76$  kcal./mole;  $E_{22}^\ddagger - E_{21}^\ddagger = 2.58$  kcal./mole. These results indicate that the tendency for copolymerization is much higher than that of homopolymerization. Therefore, one can easily understand that copolymers with a statistical

TABLE II  
Monomer Reactivity Ratios for Acrylonitrile-Methyl Methacrylate Copolymerization

Polymerization conditions	$r_1$	$r_2$
Ionic catalyst <sup>a</sup>	7	0.40
$\gamma$ -Ray initiation		
-78°C.	0.01	0.13
-20°C.	0.10	1.30
0°C.	0.10	1.30
15°C.	0.08	1.10
52°C.	0.15	1.50
Radical catalyst <sup>a</sup>	0.12	1.34

<sup>a</sup> Data of Zutty and Welch.<sup>4</sup>

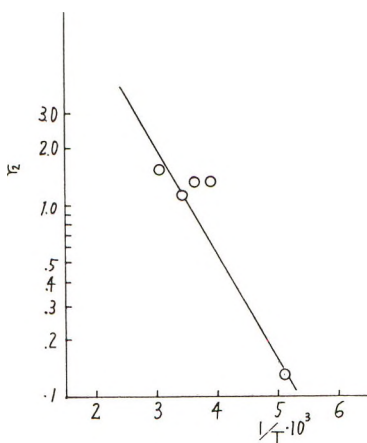


Fig. 11. Arrhenius plot of  $r_1$ .

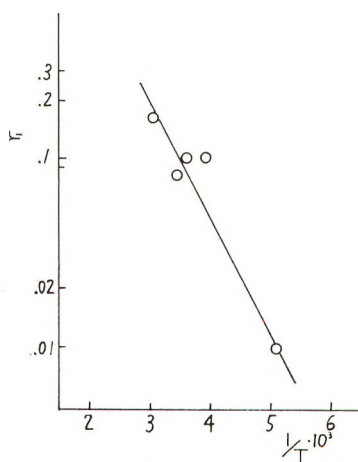


Fig. 12. Arrhenius plot of  $r_2$ .

distribution of monomer units could be obtained from the copolymerization.

The monomer mixture solidifies at  $-78^{\circ}\text{C}$ . and below about 80% molar concentration of acrylonitrile. Even in such a solid state, no homopolymerization of acrylonitrile or methyl methacrylate was observed. This indicates that the monomers can diffuse into each other in the mixed solid system. If the copolymerization can proceed in the solid state where the monomers can not diffuse each other, the molar concentration of one component in the copolymer obtained must be equal to that of the same component in the monomer mixture, that is,  $r_1 = r_2 = 1$ . But in our system, far from this, the monomer reactivity ratios were determined to be  $r_1 = 0.01$ ,  $r_2 = 0.13$  from the experiments.

It can be readily suggested from the above that the copolymerization proceeds homogeneously in the solid state at  $-78^{\circ}\text{C}$ ., as well as in the liquid state, although the reactivity of the monomers is considerably different for liquid and solid state of monomers.

On the other hand, it was observed that the copolymerization was inhibited to an extremely small extent by hydroquinone in the solid state. This is probably due to both the reduction of the mobility of the radical scavengers in the solid system and the change of the polymerization mechanism (from a radical to an ionic one). It is well known that both acrylonitrile and methyl methacrylate can be polymerized by an anionic mechanism under suitable conditions at low temperature by high energy initiation. The authors believe that the copolymerization at  $-78^{\circ}\text{C}$ . in the solid state proceeds by a partial radical (a partial ionic) mechanism.

## References

1. Seizer, W. H., and A. V. Tobolsky, *J. Am. Chem. Soc.*, **77**, 2687 (1955).
2. Schmitz, J. V., and E. J. Lawton, paper presented at 12th I.U.P.A.C. Meeting, New York, 1951.
3. Ballantine, D. S., P. Colombo, A. Glines, and B. Manowitz, *Chem. Eng. Progr.*, **50**, 267 (1954); BNL229(T-35) 1953.
4. Sheinker, A. P., M. K. Yakovleva, E. V. Kristalnyi, and A. D. Abkin, *Dokl. Akad. Nauk SSSR*, **124**, 632 (1959).
5. Burlant, W. J., and H. Green, *J. Polymer Sci.*, **31**, 227 (1958).
6. Krongauz, K. A., and Kh. S. Bagdasaryan, *Zh. Fiz. Khim.*, **32**, 1863 (1958).
7. Chapiro, A., *Radiation Chemistry of Polymeric Systems*, Interscience, New York, 1962, pp. 280, 312.
8. Tabata, Y., H. Shibano, and H. Sobue, *J. Polymer Sci.*, **A2**, 1977 (1964).
9. Tabata, Y., K. Ishigure, and H. Sobue, *J. Polymer Sci.*, **A2**, 2235 (1964).
10. Tabata, Y., K. Ishigure, K. Oshima, and H. Sobue, *J. Polymer Sci.*, **A2**, 2445 (1964).
11. Tabata, Y., K. Ishigure, H. Shibano, K. Oshima, and H. Sobue, Application of Large Radiation Sources in Industry. I.A.E.A. Proceedings May 1963; M. Steinberg and P. Colombo, *ibid*.
12. Tsuda, Y., *J. Polymer Sci.*, **54**, 193 (1961).
13. Okamura, S., et. al., *Ann. Rept. of Radiation Res. Polymers*, **2**, 91 (1960).
14. Zutty, N. L., and F. J. Welch, *J. Polymer Sci.*, **43**, 445 (1960).

### Résumé

On a examiné la copolymérisation initiée par radiation de l'acrylonitrile (1) et du méthacrylate de méthyle (2), dans un large domaine de températures. Dans la copolymérisation en phase liquide à 15°C, la vitesse de copolymérisation diminue linéairement avec la concentration molaire en acrylonitrile. Au contraire en phase solide à -78°C, la vitesse de copolymérisation augmente linéairement avec la concentration en acrylonitrile. En partant d'un mélange équimoléculaire des deux monomères à 15°C, la vitesse de copolymérisation est proportionnelle à la racine carrée de la dose d'irradiation. Dans le cas d'un mélange équimoléculaire des deux monomères, l'énergie d'activation apparente de la copolymérisation est de 4,62 kcal/mole. En effectuant des expériences à des températures différentes, on peut déterminer les rapports des réactivités monomériques  $r_1$  et  $r_2$ . Au moyen de ces résultats, les différences entre les énergies d'activation des étapes de propagation sont obtenues et égales à:  $E_{11}^\ddagger - E_{12}^\ddagger = 2,76$  kcal/mole;  $E_{22}^\ddagger - E_{21}^\ddagger = 2,58$  kcal/mole.

### Zusammenfassung

Die Strahlungscopolymerisation von Acrylnitril (1) mit Methylmethacrylat (2) wurde über einen weiten Temperaturbereich untersucht. Bei der Copolymerisation im flüssigen Zustand bei 15°C nimmt die Copolymerisationsgeschwindigkeit linear mit der molaren Konzentration von Acrylnitril ab. Dagegen nimmt die Copolymerisationsgeschwindigkeit bei der Copolymerisation im festen Zustand bei -78°C linear mit der Konzentration von Acrylnitril zu. Die Copolymerisationsgeschwindigkeit ist bei 15°C in einer äquimolaren Mischung der Monomeren der Quadratwurzel aus der Dosisleistung proportional. Die scheinbare Aktivierungsenergie der Copolymerisation in einer äquimolaren Mischung der Monomeren ist 4,62 kcal/Mol. Die Monomerreaktivitätsverhältnisse  $r_1$  und  $r_2$  wurden aus den bei verschiedenen Temperaturen durchgeführten Versuchen bestimmt. Daraus ergaben sich für die Differenz der Aktivierungsenergien der Wachstumsreaktion folgende Werte:  $E_{11}^\ddagger - E_{12}^\ddagger = 2,76$  kcal/Mol;  $E_{22}^\ddagger - E_{21}^\ddagger = 2,58$  kcal/Mol.

Received June 10, 1963

## Free Radical-Catalyzed Reaction of the Acrylamidomethyl Ether of Cotton

J. L. GARDON, *Rohm and Haas Company, Philadelphia, Pennsylvania*

### Synopsis

A limited number of acrylamidomethyl ether groups can be introduced into cotton. We can assume that the reactive groups form a lattice and that when two or more adjacent sites are occupied, these neighboring vinyl groups will react with each other when a free radical catalyst is applied to them. A monomer group isolated from others by empty neighboring sites will remain unconverted. If each site has  $Z$  neighbors,  $Z$  being the coordination number, the conversion can be calculated as a function of the fractional site occupancy and of  $Z$ . The expression derived from the lattice model is mathematically equivalent to an expression which is based on an excluded volume model. In the latter, it is assumed that each reactive monomer has a reactive shell around it. If another monomer is placed within this shell, the two can react with each other. In terms of this model the parameter  $Z$  is defined as the ratio between the volume of the reactive shell and of the volume occupied by the monomer. The latter model offers some mathematical advantages and allows the calculation of both conversion and degree of polymerization from  $Z$  and the fractional site occupancy. It is shown that the ultimately achievable conversion and the degree of polymerization increases with  $Z$  and with site occupancy. Acrylamidomethylated cotton samples were treated with increasing amounts of ammonium persulfate and the conversion was determined. The data could be extrapolated to infinite initiator concentration and  $Z$  was found to have a value of 3.5-4. Since the reaction between double bonds on neighboring sites of a single cellulose chain would have a coordination number equal to 2, the fact that  $Z > 2$  indicates that reaction between double bonds attached to different cellulose chains must occur. The fraction of links which are intermolecular is  $(Z-2)/Z$ , being 43-50%. This result is an excellent agreement with previous data showing that only 42% of the crosslinks contribute to the increased resilience of cotton. It is likely that the termination of the polymerization reaction involves the combination of two radicals. Consequently, each polymeric or oligomeric chain contains two sulfate groups when ammonium persulfate is used as initiator. The molecular weight of these chains can be calculated from the mole ratio between the converted monomers and sulfur. The molecular weights determined this way agreed reasonably well with the molecular weight values calculated from the theory with  $Z = 4$ .

In the two-step crosslinking of cotton with *N*-methylol acrylamide, the acrylamidomethyl ether of cellulose,



is formed first. The pendant double bonds can subsequently be homopolymerized with free radical catalysts. The conversion of the attached monomers increases with the acrylamidomethyl content of the cotton for a given reaction time, temperature, and catalyst concentration because



with increasing acrylamidomethyl content the probability that there is a double bond near enough to any given double bond to be able to react with it also increases.<sup>1</sup>

In conventional solution polymerization the conversion at a given reaction time, temperature, and catalyst concentration is independent of the monomer concentration because the steady-state reaction is first-order with respect to the monomer. The main difference between solution polymerization and the present system is that in the former a given monomer can potentially react with any other monomer, while in the latter the position of the monomers is fixed in space so that only neighboring monomers can react.

It would be of interest to form a quantitative estimate of how this geometric restriction affects the reaction efficiency and the degree of polymerization obtainable. Such a theoretical treatment would be applicable not only to the vinyl polymerization of acrylamidomethyl cellulose, but also to the free radical-catalyzed crosslinking of polyesters, polyamides, or polyepoxides which contain polymerizable unsaturated groups.

The purpose of this treatment is to obtain correlations between initial double bond content and conversion, to predict how many double bonds can react with each other to form a single chain, i.e., to predict the degree of polymerization of the secondary acrylic polymer, and to predict the ratio of intermolecular and intramolecular links between the primary polymer, i.e., cellulose molecules. This latter information would be especially interesting because in the previous paper<sup>1</sup> the total number of links between cellulose molecules was determined and correlated with mechanical properties. It was also found that the type of links which improved the resilience of cotton could be easily hydrolyzed, while the links which were ineffective were relatively stable. As will be seen, the present theory supports the hypothesis that the effective links are intermolecular and the ineffective links are intramolecular.

### LATTICE TREATMENT

In the previous work it was shown that it is possible to graft only a limited number of acrylamidomethyl groups onto cotton. This number was found to be about 1.6 mmole/g. and corresponds to the number of accessible anhydroglucose units. There is some circumstantial evidence indicating that only the primary hydroxyl on the accessible units can be acrylamidomethylated.

The model for the theoretical treatment is shown in Figure 1. It is assumed that the reactive sites on cotton, which are presumably the accessible primary hydroxyls, form a lattice. Acrylamidomethyl groups are grafted to a fraction of these sites. Furthermore, it is assumed that if two or more neighboring sites are occupied, the double bonds on them will form a single secondary polymer, oligomer, or dimer when the sample is treated with the free radical catalyst. The condition for a monomer to remain

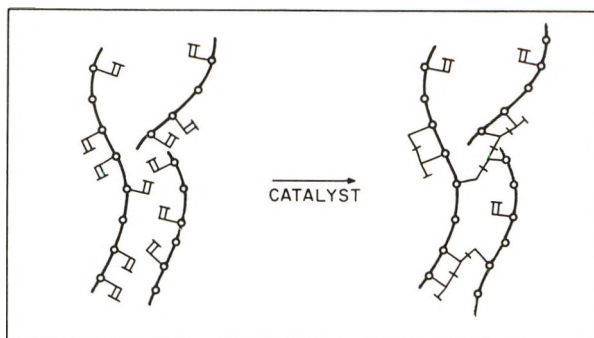


Fig. 1. Model used in the present theory. The heavy lines represent the backbone polymer (cellulose) which does not take part in the reaction. The circles are reactive spots to which monomers (*N*-methylol acrylamide) can be grafted so that their double bonds remain intact. The number of such spots is proportional either to the number of lattice sites or to the total available volume. The unconverted monomers are represented by the flaglike symbol. When a catalyst is applied to the system, the monomers which are close enough to each other become converted to a polymer or oligomer which is covalently attached to the backbone polymer at each repeating unit. This polymer is drawn with thin line on the right-hand side.

unconverted is that it should be isolated from other monomers by empty sites. If each site has  $Z$  neighbors,  $Z$  being the coordination number, all  $Z$  sites around an occupied site have to be empty so that the monomer on this occupied site should remain unconverted after the reaction is completed.

The probability that a given site is occupied is  $x$ . The probability that a given site is occupied and all  $Z$  sites around it are empty is  $x(1-x)^Z$ , this value being the probability that a given site is occupied by an unconverted monomer after the reaction is complete. The probability that a given site is occupied by a converted monomer is  $[x - x(1-x)^Z]$ . This value divided by the probability that the site is occupied,  $x$ , gives the conversion  $C^*$ , where  $1 > C^* > 0$ .

$$C^* = 1 - (1 - x)^Z \quad (1)$$

The main disadvantage of this treatment is that it does not define the situation with  $Z < 1$ . In terms of the model,  $Z < 1$  would mean that some sites have a coordination number of one and some have a coordination number of zero. The monomers on the sites with zero coordination number cannot be converted even if  $x = 1$ , although eq. (1) predicts complete conversion at  $x = 1$  for any finite positive value of  $Z$ . This inconsistency indicates that the lattice treatment is not satisfactory.

As will be shown below, an excluded volume model leads to expressions which give results numerically similar to those of eq. (1) but with the parameter  $Z$  defined for any finite positive value. This treatment can also take into account the difference between the reaction of two monomers (initiation) and the reaction between a monomer and a growing chain

(propagation). Furthermore it allows the calculation of the degree of polymerization of the secondary chains in a simple fashion.

## EXCLUDED VOLUME TREATMENT

### Basic Assumptions

It is assumed that any monomer which has a monomer near enough to be able to react with it becomes converted, i.e., conversion is limited only by the geometry of the system. This situation could occur if the rate of polymerization is faster than the rate of initiation and if there is a steady but slow supply of free radicals reacting sooner or later with all convertible monomers in the system. It is also assumed that if a free radical reaches a cluster of neighboring monomers these neighboring monomers will become part of a single polymeric chain. At present the method of termination, be it disproportionation or chain transfer with the backbone polymer or combination of radicals, is not defined. It is assumed that the double bonds on isolated monomers remain intact at the end of the reaction. Furthermore, if a polymer chain stops growing, the end unit is counted as a converted monomer whether or not it contains a double bond.

It is assumed that there is a limited volume  $W$  available in the system into which monomers can be placed. This volume does not include the polymeric backbone to which the monomers are attached and is proportional to the total number of sites to which monomers can be grafted. The monomers can react with neighboring monomers on the same polymeric backbone in an intramolecular reaction or with monomers on a different polymeric backbone to form intermolecular crosslinks. No distinction is made between these two reactions.

Each isolated monomer is assumed to have a hypothetical shell around it, which has a volume equal to  $S_1$ . If  $V$  is the volume occupied by the monomer, the value of  $Z$  is defined as

$$Z = S_1/V \quad (2)$$

The parameter  $Z$  can be considered to be a generalized coordination number. If the monomer is absolutely immobile,  $V$  would be its molar volume. If it has a limited mobility,  $V$  would be the volume within which it can move but from which other monomers are excluded.

Reaction occurs if there is a monomer either within a shell of another monomer or within the shell of a reactive endgroup of a growing polymer. The shell around such an endgroup would be smaller than that around an unreacted monomer because the connection to the polymeric chain occupies a portion of the shell around the monomer. We define the parameter  $f$ ,  $1 > f > 0$ , with the aid of the value of  $S_e$ , the shell around an end monomer, and  $S_1$  as follows:

$$f = S_e/S_1 \quad (3a)$$

$$S_e = fZV \quad (3b)$$

The value of  $f$  can be considered as the reactivity of a polymeric free radical with a monomer divided by the reactivity of a monomeric free radical with a monomer, i.e.,  $f$  is some type of reactivity ratio. As will be shown later,  $f$  can be a function of  $Z$ .

If there are more than two monomers within the shell of a given unreacted monomer, it can react only with two of these monomers. The additional monomers within the shell could stay unreacted. Similarly, if there is more than one monomer within the shell of an end monomer, it can react only with one of these monomers, not with the additional ones. No correction is made for this inefficient overlapping of shells. Thus, the possibility of polymeric chains enveloping an unreacted monomer in a way that this monomer cannot find reactive neighbors is disregarded.

### Definitions

The values of  $Z$ ,  $f$ ,  $V$ ,  $S_e$ , and  $S_1$  are defined above. Some additional definitions are made below.  $W$  is the total available volume. The total number of monomers in this volume is  $n$  and the total number of converted monomers is  $m$ . The converted monomers can be either end monomers,  $m_e$ , or monomers within the chain,  $m_t$ . It follows that

$$m = m_e + m_t \quad (4)$$

The degree of polymerization of the converted monomers is  $P$ . In calculating  $P$  we disregard the unconverted monomers. It follows that

$$P = 2m/m_e \quad (5a)$$

$$m_e = 2m/P \quad (5b)$$

$$m_t = m(1 - 2/P) \quad (5c)$$

The volume fraction of all monomers is  $x$  and of converted monomers is  $y$ , so that we can write

$$x = nV/W \quad (6a)$$

$$y = mV/W \quad (6b)$$

The conversion  $C$  is defined as follows:

$$C = m/n = y/x \quad (7)$$

### Variation of Conversion with Monomer Content

Two situations will be compared, one when the space contains  $n$  monomers and  $m$  converted monomers, the other when it contains  $(n + dn)$  monomers and  $(m + dm)$  converted monomers. The problem will be treated as if  $dn$  monomers were added to  $n$  monomers to obtain  $dm$  additional converted monomers. It must be realized that this does not conform to the true situation where all the monomers are present in the system before the reactions leading to their conversion start (cf. Fig. 1).

The free space in the system containing  $n$  monomers is  $(W - nV)$ . The total volume of the shells around isolated monomers is  $(n - m)VZ$ . If a monomer is placed into the shell of an isolated monomer, two end monomers are obtained. It follows that

$$dm_e/dn = 2(n - m)VZ/(W - nV) \quad (8)$$

The total volume of shells around end monomers is  $m_eVfZ$ . Since the polymers can grow only in one direction, only half of this volume provides favorable space for conversion of additional monomers. The reaction of a single monomer with a growing chain increases the number of internal monomers but has no effect on the number of end monomers. Thus we can write

$$dm_i/dn = m_eVfZ/2(W - nV) = mVfZ/P(W - nV) \quad (9)$$

Combining Eqs. (8) and (9) one obtains

$$dm/dn = d(m_i + m_e)/dn = [2(n - m) + mf/P]VZ/(W - nV) \quad (10)$$

To eliminate  $W$  and  $V$  from this equation it is convenient to express the monomer contents in volume fractions by substituting from eqs. (6a) and (6b).

$$dy/dx = [2(x - y) + yf/P]Z/(1 - x) \quad (11)$$

### Variation of the Degree of Polymerization with Monomer Content

To obtain an accurate solution for eq. (11) the variation of  $P$  with  $x$  and  $y$  has to be defined. By differentiating eq. (5a) and substituting from eq. (5b) we obtain

$$\begin{aligned} dP/dm &= 2/m_e - (2m/m_e^2)(dm_e/dm) \\ &= P/m - (P^2/2m)(dm_e/dm) \end{aligned} \quad (12)$$

The value of  $dm_e/dm$  is defined by eqs. (8) and (10).

$$dP/dm = P/m - (P^2/2m)2(n - m)/[2(n - m) + mf/P] \quad (13)$$

Converting the number of monomers into volume fraction gives the final form of this relationship.

$$dP/dy = P/y - (P^2/y)(x - y)/(2x - 2y + yf/P) \quad (14)$$

Simultaneous solution of eqs. (11) and (14) for the boundary conditions

$$x = 0, y = 0, P = 2$$

defines the system. The boundary condition involving  $P$  follows from the fact that  $P$  cannot be lower than 2. If we would extrapolate the function describing the dependence of  $P$  on  $y$  to  $y = 0$ , the extrapolated value of  $P$  would be equal to 2.

### Effect of Parameters $Z$ and $f$

By using a Bendix G-15D computer, eqs. (11) and (14) were solved numerically. Figure 2 shows that the conversion ( $C = y/x$ ) increases

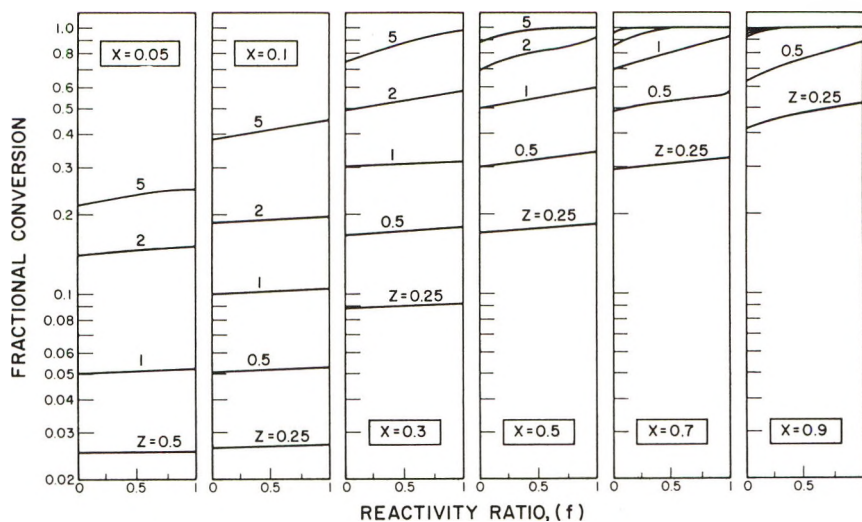


Fig. 2. The effect of the reactivity ratio  $f$  on conversion at various volume fractions  $x$  and generalized coordination numbers  $Z$ .

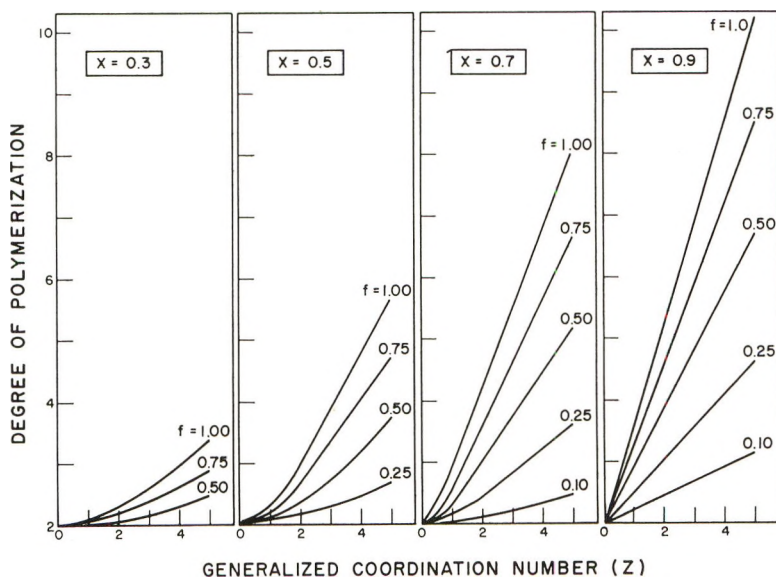


Fig. 3. Variation of the degree of polymerization with the generalized coordination number  $Z$ , reactivity ratio  $f$ , and volume fraction  $x$ .

with the coordination number  $Z$  and with the volume fraction  $x$  but is relatively insensitive to the reactivity ratio  $f$ . However, the degree of polymerization  $P$  is very sensitive to both parameters  $Z$  and  $f$  and to the variable  $x$ . As can be seen in Figure 3,  $P$  increases rapidly with  $Z$ ,  $f$ , and  $x$ .

**Limiting Case with  $f = 0$ .** If  $yf/P$  is negligibly small, eq. (11) reduces to

$$dy/dx = 2Z(x - y)/(1 - x) \quad (15)$$

It may be of interest that this equation can also be derived for a lattice model. The lattice coordination number is  $Z$ , the probability of site occupancy by any monomer is  $x$  and the probability of site occupancy by converted monomers is  $y$ . If we disregard conversion on growing chains,  $dy/dx$  will be equal to the ratio between twice the fraction of sites around isolated monomers,  $2(x - y)Z$ , and the fraction of unoccupied sites,  $(1 - x)$ .

Solution of eq. (15) for the boundary condition  $y = 0$  when  $x = 0$  is given below:

$$y = x + [(1 - x)^{2Z} - (1 - x)]/(2Z - 1) \quad (16)$$

$$C = y/x = 1 - [(1 - x) - (1 - x)^{2Z}]/(2Z - 1)x \quad (17)$$

Since both eqs. (17) and (1b) can be derived from the lattice model, they should be equivalent. Expansion in series of both equations reveals that in these series higher than the first powers of  $x$  have slightly different coefficients.

$$C = Zx - (2/3)Z(Z - 1)x^2 + (1/6)Z(Z - 1)(2Z - 3)x^3 \\ - (1/15)Z(Z - 1)(Z - 2)(2Z - 3)x^4 + \dots$$

$$C^* = Zx - (1/2)Z(Z - 1)x^2 + (1/6)Z(Z - 1)(Z - 2)x^3 \\ - (1/24)Z(Z - 1)(Z - 2)(2Z - 3)x^4 + \dots$$

It is evident that the equations are identical either for low values of  $x$  or for any value of  $x$  if  $Z$  is not too different from unity. The conversion values according to these two equations are shown in Figure 4. As can be seen,  $C^*$  is higher than  $C$  for  $Z > 1$ . The reason for this is that in calculating  $C^*$  initiation and propagation rates were assumed to be identical, while in calculating  $C$  from eq. (17) it was assumed that the reaction is limited to dimerization. It follows that eq. (1) should be more meaningfully compared to the numerical solution of eqs. (11) and (14) with  $f = 1$ . In such comparison  $C^* < C$ , again the difference being the larger the more  $Z$  exceeds unity. This discrepancy is probably due to the difference between the lattice and excluded volume models. For the present purpose it is sufficient to state that the conversion result of eq. (1) is intermediate between that of combined eqs. (11) and (14) with  $f = 0$  and  $f = 1$ .

Since the conversion is relatively independent of  $f$ , in future discussions eq. (17) will be used for establishing the interdependence of  $C$ ,  $x$ , and  $Z$ .

**Dependence of  $f$  on  $Z$ .** Up to this point it was not necessary to assign any shape to the molecules. However, if we desire to describe the system in terms of the single parameter  $Z$ , we have to derive a relationship between  $Z$  and  $f$ . The simplest assumption would be to picture the monomers as spheres with a spherical shell around them, disregarding the links that connect them to the cellulose. The growing polymer chain can be pictured

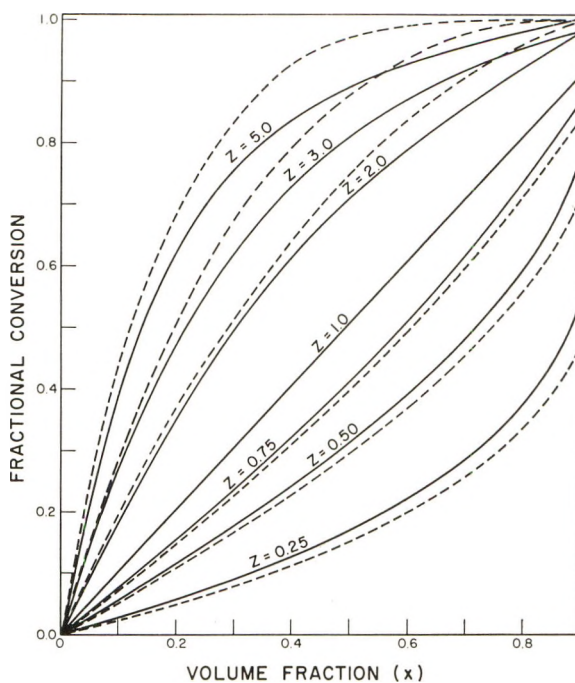


Fig. 4. Variation of conversion with site occupancy or volume fraction  $x$ : (---)  $C^*$  according to eq. (1); (—)  $C$  according to eq. (17).

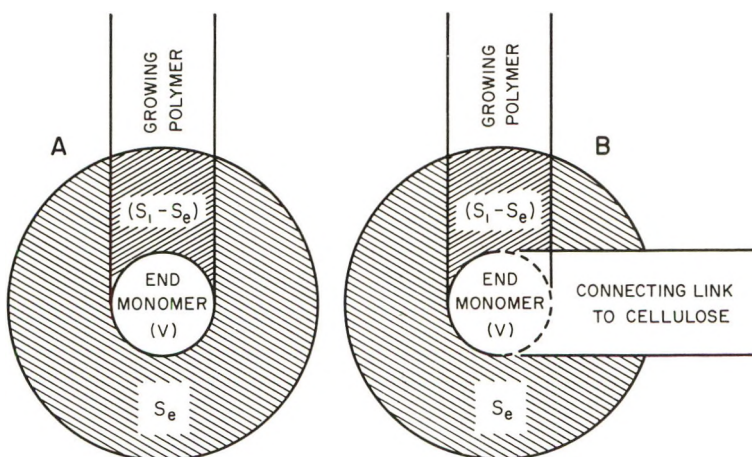


Fig. 5. Cross sections of models for calculating  $f_A$  or  $f_B$  from the relationship  $f = S_e/S_1$ . The sphere of volume  $V$  is occupied by the monomer. The total shaded area represents  $S_1$ , the volume of the reactive shell around an isolated monomer. The area shaded with the from left to right descending lines represents  $S_e$ , the volume of the reactive shell around an end monomer.



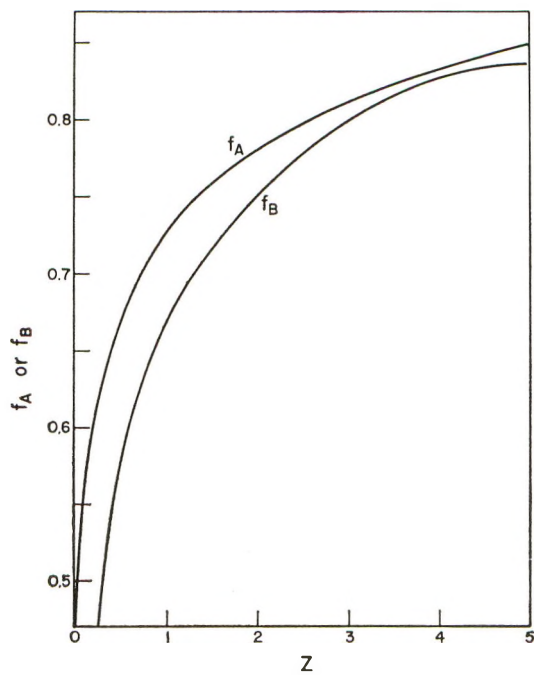


Fig. 6. Dependence of  $f_A$  and  $f_B$  upon  $Z$ .

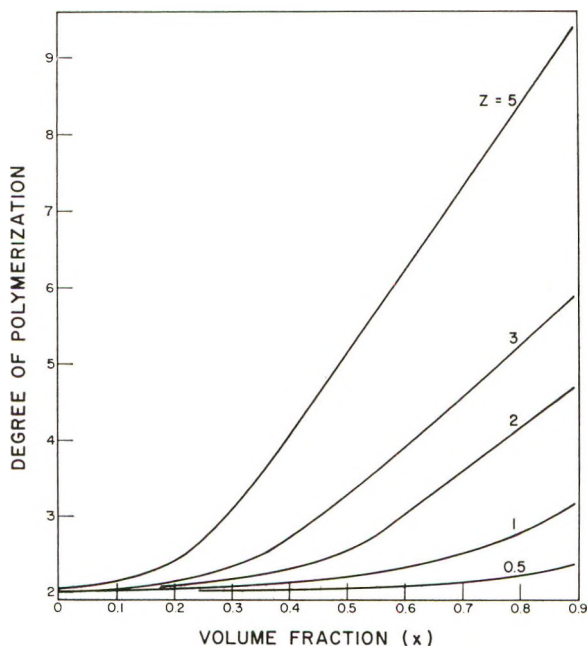


Fig. 7. Variation of the degree of polymerization with the volume fraction  $x$  at different generalized coordination numbers  $Z$  when the reactivity ratio is equal to  $f_B$ .

as a cylinder with a radius identical to that of the monomer sphere. As shown in model A of Figure 5, this cylinder cuts out a volume element from the reactive shell, and this volume element is the difference between  $S_1$  and  $S_e$ . It follows from this model and eqs. (2) and (3) that

$$f_A = 1/2 + [(1 + Z)^{2/3} - 1]^{3/2}/2Z \quad (18)$$

A refinement over these assumptions is model B of Figure 5. Model B differs from model A in that the connecting link between the isolated monomer and the cellulose is also considered and is assumed to be a cylinder of the same cross section as the cylinder representing the growing polymer. For calculating the  $f$  value based on this model it is convenient to define the parameter  $r$  which is the ratio of the radius of outer and inner spheres, then calculate  $r$  from  $Z$  and  $f_B$  from  $r$ .

$$Z = 0.5(r^3 - 1) + 0.5(r^2 - 1)^{3/2} \quad (19a)$$

$$f_B = 2(r^2 - 1)^{3/2}/[(r^3 - 1) + (r^2 - 1)^{3/2}] \quad (19b)$$

The values of  $f_A$  and  $f_B$  are shown in Figure 6. The dependence of  $P$  on  $Z$  and  $x$  when  $f = f_B$  is shown in Figure 7. It may be noted that, since  $f_A$  and  $f_B$  are not too different, the use of  $f_A$  instead of  $f_B$  for calculating  $P$  would not cause a significant change in the  $P$  values. When the theory is to be applied to experimental data,  $P$  values based on Figure 7 will be used.

## EXPERIMENTAL RESULTS AND DISCUSSION

### General Considerations

Previous results<sup>1</sup> indicated that when NMAAm is applied to cotton with a mild acid catalyst, only one acrylamidomethyl group reacts with each accessible anhydroglucose unit. It is probable that only the C<sub>6</sub> hydroxyl takes part in this reaction.

In the single-ended reaction one cannot introduce more than 1.6 mmole/g. of acrylamidomethyl ether groups into cotton.<sup>1</sup> Thus it may be convenient to use 1.6 as a measure of the total number of lattice points or the total available volume and to calculate  $x$ , the fractional site occupancy or volume fraction by dividing the actual acrylamidomethyl group content with 1.6.

When acrylamidomethyl cotton is treated with ammonium persulfate, a fraction of the double bonds becomes saturated. When such a sample is hydrolyzed, the double bonds that survived the ammonium persulfate treatment are removed at the same rate as the unconverted monomers.<sup>1</sup> This indicates that double bonds are present only on unconverted monomers, so that the termination of the polymerization cannot be by disproportionation. It is likely that the predominant method of termination is combination of two radicals because the chain transfer properties of cellulose are poor. The hydrolysis experiments also indicate<sup>1</sup> that all mono-

meric acrylamidomethyl groups contain double bonds. It is possible that there is a reversible reaction between an initiator free radical and an isolated monomer which cannot react further with another monomer because of geometric restrictions. Thus if reaction between the sulfate ion radical and the monomer involves a monomer which is part of a cluster of closely packed monomers, polymerization is initiated. If the monomer involved is an isolated one, the addition product of the sulfate ion radical and monomer decomposes to the unsaturated monomer and to the sulfate ion radical.

### Estimation of the Fraction of Links that are Intermolecular from the Coordination Number

The previously presented conversion data<sup>1</sup> are unsuited for interpretation in terms of the present theory because the ammonium persulfate treatment of acrylamidomethylated cotton was carried out under mild conditions and not all of the potentially polymerizable monomers were converted. In the present work cotton was acrylamidomethylated at three levels and after-treated at a given reaction time and temperature with increasing amounts of ammonium persulfate. Details of these experiments are as follows.

**Single-Ended Reaction.** Pad 80<sup>2</sup> cotton print cloth with a solution containing 2% of the hydrochloride of 2-amino-2-methylpropanol catalyst and 16, 25, or 32% NMAAm, to obtain about 90% wet pickup. Cure for 3.5 min. at 150°C. Rinse in hot 1% NaNO<sub>2</sub> solution and subsequently in cold water; dry.

**After-Treatment.** Pad small portions of the acrylamidomethylated cotton samples with 0.1–2.5% ammonium persulfate (APS) to obtain about 90% wet pickup. Cure for 3.5 min. at 150°C.; rinse as above; dry.

**Analysis.** Determine sulfur by the micro-Schroedinger method. For determining double bonds, treat samples with an excess of alkaline mer-

TABLE I  
Analytical Data of Cotton Samples Which were Single-Endedly Acrylamidomethylated and Subsequently Treated with Ammonium Persulfate

	Analyses, mmole/g. based on cellulose					
	Double bond	Sulfur	Double bond	Sulfur	Double bond	Sulfur
After single-ended reaction	0.67	—	1.12	—	1.36	—
After APS after-treatment						
0.1% APS	0.66	~0	0.90	~0	1.08	~0
0.2% APS	0.63	~0	0.85	~0	0.78	~0
0.5% APS	0.48	0.046	0.59	0.015	0.53	0.018
1.0% APS	0.37	0.072	0.39	0.018	0.25	0.035
1.5% APS	0.32	0.110	0.30	0.040	0.27	0.018
2.0% APS	0.28	0.130	—	—	0.19	0.052
2.5% APS	0.27	0.190	0.24	0.066	—	—

TABLE II  
Calculated Parameters for Acrylamidomethylated and Subsequently Ammonium  
Persulfate Treated Cotton Samples

APS concn. in after treatment, %	$D_0 = 0.67,$ $x = 0.42,$ $P_t = 3.5$			$D_0 = 1.12,$ $x = 0.70,$ $P_t = 6.0$			$D_0 = 1.36,$ $x = 0.84,$ $P_t = 7.0$		
	$C$	$Z_{app}$	$P_e$	$C$	$Z_{app}$	$P_e$	$C$	$Z_{app}$	$P_e$
0.1	0.018	0.04	—	0.198	0.13	—	0.205	0.08	—
0.2	0.075	0.15	—	0.240	0.20	—	0.320	0.15	—
0.5	0.290	0.62	8.3	0.474	0.50	71	0.613	0.45	93
1.0	0.455	1.17	8.3	0.652	0.76	81	0.816	0.92	63
1.5	0.518	1.44	6.3	0.734	1.15	91	0.800	0.87	77
2.0	0.564	1.70	6.0	—	—	—	0.863	1.30	45
2.5	0.598	1.80	4.2	0.790	1.60	26	—	—	—

captomethanol solution and back-titrate with iodine. Details of these methods were given previously. Results of analysis are given in Table I.

As can be seen in Table II, the conversion increases with the initiator concentration. Since any pair of  $x$  and  $C$  values defines a coordination number by eq. (17), an apparent coordination number can be calculated for each pair of  $x$  and  $C$  data. The true coordination number of the system would be obtained when the initiator concentration is infinite so that all polymerizable monomers are converted. The data can be conveniently extrapolated by plotting the log of the apparent coordination number against the inverse square root of the initiator concentration, as shown in Figure 8. If this empirical extrapolation is correct, the true coordination number of our system is 3.5–4. It may be noted that the choice of square root function for the initiator concentration is based on the fact that in kinetic descriptions of the free radical-catalyzed polymerization, the initiator concentration comes in under the square root sign when the termination is by the combination of two radicals.

In the theoretical treatment it was shown that the coordination number derived from conversion data is equally valid for the lattice and for the excluded volume model. Since it would be difficult to assign a structural significance to the coordination number in terms of the latter model, we will discuss it in terms of the former. It is fair to assume that  $Z$  is equal to 2 for intramolecular reaction when double bonds attached to neighboring anhydroglucose units of the same cellulose chain react with each other. If  $Z > 2$ , reaction takes place between double bonds of different cellulose chains and/or between double bonds attached to nonneighboring anhydroglucose units of the same chain. If we disregard the latter possibility, the difference ( $Z - 2$ ) is a measure for the probability for intermolecular reaction. In fact,  $(Z - 2)/Z$  should be the fraction of total bonds which are intermolecular. The present experiments suggest that this fraction is 43–50%. This is in excellent agreement with previous hydrolysis data,<sup>1</sup> obtained with a cotton sample that contained 0.97 mmole/g. acrylamido-

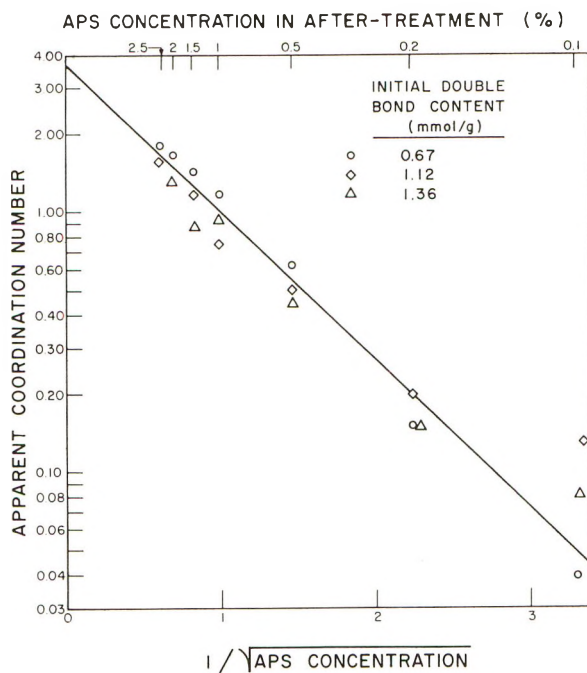


Fig. 8. Dependence of the apparent coordination number upon ammonium persulfate concentration based on the data of Table II.

methyl ether groups and which was after-treated with 0.5% ammonium persulfate at the same reaction conditions as presently employed. According to these data only 42% of the crosslinks were effective in improving the resilience of cotton.

### Degree of Polymerization

If the main method of termination is combination of free radicals, each polymer or oligomer chain has a sulfate group on each end. Thus the experimental degree of polymerization  $P_e$  should be equal to twice the mole ratio or converted monomers to sulfur. Based on the analytical data of Table I,  $P_e$  values were calculated in Table II. Calculations were made on the basis of the equations:

$$C = (D_0 - D)/D_0$$

$$P_e = 2(D_0 - D)/s$$

where  $C$  is fractional conversion;  $D_0$  and  $D$  are the double bond contents (in mmole/g.) after single-ended reaction and APS treatment, respectively;  $S$  is the sulfur content after APS treatment. The theoretical degree of polymerization  $P_t$  was obtained by interpolating the data of Figure 7 to  $Z = 4$  and its values are also presented in Table II. In Table II,  $x = D_0/1.6$  is the volume fraction or fraction of sites occupied, and  $Z_{app}$ , the

apparent coordination number, is the coordination number corresponding to the observed conversion at the given  $x$  calculated from eq. (17).

The  $P_e$  values are rather erratic because some of them have to be based on very low sulfur contents which cannot be determined with high accuracy. Nevertheless, the data show a clear trend in that  $P_e$  decreases with increasing catalyst concentration and is larger than  $P_t$ . The reason for this is that when the catalyst concentration is low, the probability that monomer clusters containing many monomers become initiated is much larger than the probability of initiating clusters containing few monomers or the probability of initiating two neighboring monomers which are isolated from the others. Thus at low conversion  $P_e$  must be higher than  $P_t$  but it should approach  $P_t$  as the conversion is increased. Unfortunately, the present  $P_e$  data are not suited for extrapolation to infinitely large catalyst content. Nevertheless, the  $P_e$  data obtained at low degree of acrylamidomethylation, where the molecular weight distribution of the oligomers can be expected to be narrow, are in excellent agreement with the theory. At higher degree of acrylamidomethylation the discrepancy between  $P_t$  and  $P_e$  is relatively large but here the molecular weight distribution should be broad and the dimers formed when the last of the convertible monomers would react, would in all probability reduce the  $P_e$  levels to that of  $P_t$ .

Dr. S. Gusman suggested the application of the lattice model to this problem. The calculations on the computer were carried out by Mr. L. DeFonso. The samples were prepared and tested by Miss R. E. Hopkins. Drs. R. Steele, A. Weiss, and H. Greenwald were helpful in numerous discussions.

### Reference

1. Gardon, J. L., *J. Appl. Polymer Sci.*, **5**, 734 (1960).

### Résumé

On peut introduire dans le coton un nombre limité de groupements éther méthyl-acrylamide. On suppose que les groupements réactionnels forment un réseau et que, dans le cas où deux ou plusieurs emplacements adjacents sont occupés, ces groupes vinyliques voisins réagiront mutuellement quand un catalyseur produisant des radicaux libres est utilisé. Un groupe monomérique qui est séparé des autres groupes par des emplacements inoccupés ne réagira pas. Admettant que chaque place a  $Z$  voisins,  $Z$  étant donc le nombre de coordination, on peut calculer la conversion en fonction de la fraction d'emplacements occupés et de  $Z$ . L'expression déduite du modèle de réseau est mathématiquement équivalente à l'expression basée sur le modèle du volume exclu. Dans le dernier cas on suppose que chaque monomère réactionnel possède autour de lui une couche réactionnelle. Quand un autre monomère est placé dans cette couche, les deux peuvent réagir mutuellement. A partir de ce modèle, le paramètre  $Z$  est défini comme étant le rapport entre le volume de la couche réactionnelle et le volume occupé par le monomère. Le dernier modèle offre quelques avantages mathématiques et permet de calculer, en partant de  $Z$  et de la fraction d'emplacements occupés, la conversion et à la fois le degré de polymérisation. On montre que la conversion limite et le degré de polymérisation augmentent avec  $Z$  et avec le nombre d'emplacements occupés. On traite des échantillons de coton acrylamidométhylé avec des quantités croissantes de persulfate d'ammonium et on détermine les conversions. Les données peuvent être extrapolées à une concentration infinie de l'initiateur, et une valeur de 3.5 à 4 est trouvée

pour  $Z$ . Le fait que  $Z$  est plus grand que 2 indique que la réaction s'effectue entre des liaisons doubles attachées à des chaînes différentes, puisque la réaction entre deux liaisons doubles se trouvant sur la même chaîne cellulosique aurait un nombre de coordination égal à 2. La fraction de liaisons intermoléculaires représentée par  $(Z-2)/Z$  est de 43 à 50%. Ce résultat est en accord parfait avec les données précédentes, qui montraient que seulement 42% des pontages contribuent à l'augmentation de l'élasticité du coton. Il est probable que la terminaison de la polymérisation implique la combinaison de deux radicaux. Par conséquent, dans le cas où le persulfate d'ammonium est employé comme initiateur, chaque chaîne polymérique ou oligomérique contient deux groupements sulfates. Le poids moléculaire de ces chaînes peut être calculé à partir du rapport molaire entre les monomères convertis et le soufre. Les poids moléculaires déterminés de cette façon s'accordent suffisamment bien avec les valeurs calculées théoriquement en admettant que  $Z$  est égal à 4.

### Zusammenfassung

In Baumwolle kann eine beschränkte Anzahl von Acrylamidomethyläthergruppen eingeführt werden. Man kann annehmen, dass die reaktionsfähigen Gruppen ein Gitter bilden und dass falls zwei oder mehrere benachbarte Gitterplätze besetzt sind, diese benachbarten Vinylgruppen in Gegenwart eines radikalischen Katalysators miteinander reagieren. Ist dagegen eine Monomergruppe durch leere benachbarte Gitterplätze von den anderen getrennt, so reagiert sie nicht. Wenn jeder Gitterplatz  $Z$  benachbarte Gitterplätze hat, wobei  $Z$  die Koordinationszahl ist, kann man den Umsatz als Funktion des Bruchteiles an besetzten Gitterplätzen und von  $Z$  berechnen. Die aus dem Gittermodell abgeleitete Beziehung ist einer auf dem Modell des ausgeschlossenen Volumens beruhenden Beziehung mathematisch äquivalent. Im letzteren Fall wird angenommen, dass jedes reaktionsfähige Monomere von einer reaktionsfähigen Schale umgeben ist. Wenn sich ein anderes Monomeres innerhalb dieser Schale befindet, können die beiden miteinander reagieren. In diesem Modell ist der Parameter  $Z$  als das Verhältnis zwischen dem Volumen der reaktionsfähigen Schale und dem vom Monomeren beanspruchten Volumen definiert. Letzteres Modell bietet gewisse mathematische Vorteile und ermöglicht die Berechnung sowohl des Umsatzes als auch des Polymerisationsgrades aus  $Z$  und dem Bruchteil an besetzten Gitterplätzen. Der erreichbare Endumsatz und der Polymerisationsgrad nehmen mit  $Z$  und der Gitterbesetzung zu. Acrylamidomethylierte Baumwollproben wurden mit steigenden Mengen von Ammoniumpersulfat behandelt und der Umsatz bestimmt. Die Messdaten wurden auf unendliche Starterkonzentration extrapoliert und der Wert von  $Z$  zu 3,5 bis 4 bestimmt. Der Reaktion zwischen Doppelbindungen auf benachbarten Stellen einer einzelnen Cellulosekette entspricht die Koordinationszahl 2. Daher folgt aus dem Befund  $Z > 2$ , dass an verschiedenen Celluloseketten hängende Doppelbindungen miteinander reagieren müssen. Der Bruchteil der intermolekularen Bindungen ist  $(Z-2)/Z$ , also 43 bis 50%. Dieses Ergebnis stimmt mit früher ermittelten Daten ausgezeichnet überein, wonach nur 42% der Vernetzungen zur erhöhten Resilienz der Baumwolle beitragen. Der Abbruch der Polymerisation erfolgt wahrscheinlich durch Rekombination zweier Radikale. Daher enthält bei Verwendung von Ammoniumpersulfat als Starter jede polymere oder oligomere Kette zwei Sulfatgruppen. Das Molekulargewicht dieser Ketten kann aus dem Molverhältnis von umgesetztem Monomeren zu Schwefel berechnet werden. Die auf diesem Wege bestimmten Molekulargewichte stimmen gut mit den aus der Theorie für  $Z = 4$  berechneten Molekulargewichtswerten überein.

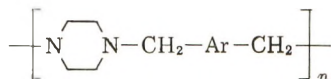
Received June 10, 1963

## Poly(xylylenylpiperazine), A Novel Polyamine

J. F. KLEBE, *General Electric Research Laboratory, Schenectady, New York*

### Synopsis

The condensation polymerization of  $\alpha,\alpha$ -dichloroxylylene and similar reactive halides with difunctional silylamines leads to novel high molecular weight polyamines of the type



The halogen is eliminated in the form of halosilane which is inert in this reaction system and acts as a solvent for the polymer. The polymers can be cast from solution or pressed to strong films. They exhibit typical amine properties; they are soluble in inorganic and organic acids and form polyelectrolyte solutions, from which stable polyelectrolyte films can be cast. Reactions with alkyl iodides lead to polyquaternary compounds. Ammonium salts and a cyclic sulfone were found to enhance catalytically the rate of reaction of benzylchloride with silylamines.

Polyamines with nitrogen in the backbone structure have been prepared mainly by acid-catalyzed ring opening reactions of strained rings. The addition polymerization of ethyleneimine is well known and has been studied in detail.<sup>1,2</sup> Larger rings like pyrrolidine, piperidine, and hexamethyleneimine are reported to give low polymers.<sup>3</sup> Several bicyclic systems containing nitrogen have been polymerized;<sup>4-6</sup> the most recent of these is the ring-opening polymerization of 1,4-diazabicyclo[2.2.2]octane and of 3-azabicyclo[3.2.2]nonane, reported by Hall,<sup>7</sup> which lead to ring-containing polyamines.

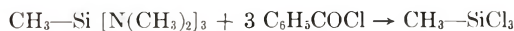
The preparation of polybenzimidazoles from tetraamino aryl compounds and aromatic difunctional phenylesters by Vogel and Marvel<sup>8</sup> is an example of a condensation polymerization leading to polyamine structures. Benzimidazole is a weak base; these polymers are highly aromatic in character and do not show typical amine properties.

Condensation polymerizations of diamines with reactive difunctional halides of the benzylchloride type appear to be an obvious route to polyamines. However, no reaction of this type leading to a product of high molecular weight has been reported. This straightforward approach becomes complicated by the formation of hydrogen halide during the process of the reaction; salt formation with the starting material or the product is bound to upset the stoichiometry and leads to inhomogeneous reaction mixtures; addition of acid acceptors of higher base strength than the diamine favors side reactions with the halide.



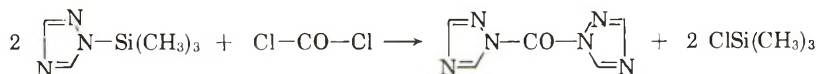
It appeared possible to avoid these difficulties by devising a reaction in which the halogen is eliminated in the form of a neutral inert species. The reaction of silylamines with acid halides in which chlorosilanes are formed indicated such a possibility.

Anderson reported the first example of this kind:<sup>9</sup>



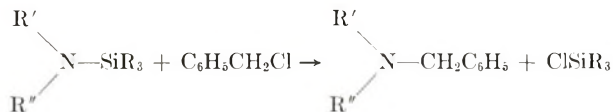
The other product, presumably  $\text{C}_6\text{H}_5\text{CON}(\text{CH}_3)_2$ , was not isolated.

Birkofer, Richter, and Ritter<sup>10</sup> utilized this reaction for the preparation of *N*-acyl-substituted heterocyclics, e.g.,



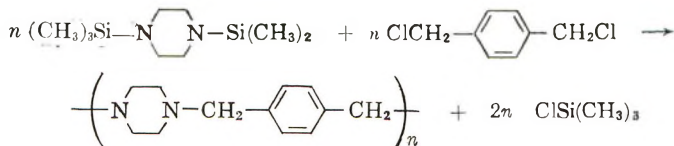
Other reactive halides like sulfurdichloride and chloroacetic ester were also employed by these authors.

We have now found in our studies with silylamines that: (1) halides of much lower reactivity than those previously used, e.g. benzyl chloride, will also cleave the Si-N bond with formation of halosilanes and amines; (2) There is no interaction between the (tertiary) amines and the chlorosilane formed. The reaction



proceeds quantitatively, and the products can be separated by distillation. This result made the reaction applicable for polyamine synthesis, using difunctional starting materials.

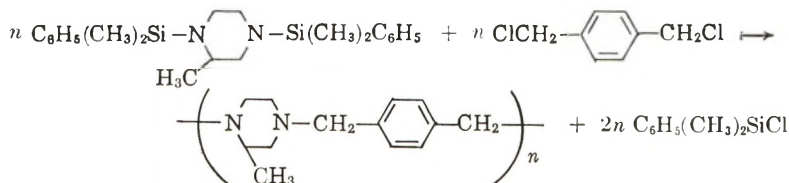
When stoichiometric amounts of bis-*N,N'*-(trimethylsilyl)piperazine and  $\alpha,\alpha'$ -dichloro-*p*-xylene were mixed and heated to about 120°C. in an anhydrous atmosphere, a sudden vigorous reaction set in, trimethylchlorosilane distilled over, and a light yellow solid was formed according to the equation



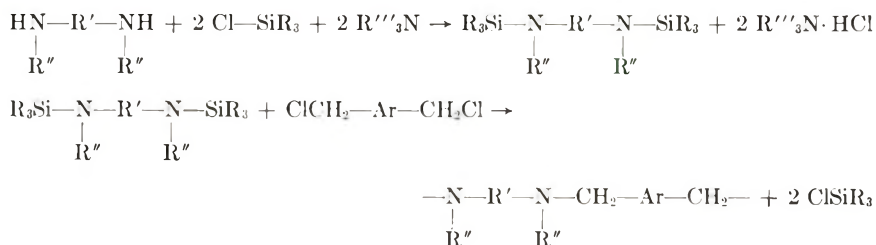
The product was insoluble in organic solvents but easily soluble in organic and inorganic acids. With this system, only materials of low molecular weight could be prepared, due to the fact that the required reaction temperature is much higher than the boiling point of the trimethylchlorosilane formed, which thus escapes from the reaction mixture and leaves a solid product before complete conversion can occur.

In order to make use of the solubilizing effect of the chlorosilane produced by the polycondensation, silylamines with heavier silyl substituents were

employed; one or two alkyl substituents on the piperazine ring improved the solubility of the polymer. Thus, a mixture of *N,N'*-bis(phenyldimethyl)-2-methylpiperazine and  $\alpha,\alpha'$ -dichloro-*p*-xylene, heated to 150–200°C. under a protective atmosphere, formed a melt whose viscosity increased gradually as the polycondensation proceeded:



After several hours a light yellow, extremely viscous solution of the polymer in phenyldimethylchlorosilane was obtained. Removal of the chlorosilane *in vacuo* gave the solid polymer, which could be dissolved in chloroform or *sym*-tetrachloroethane and purified by precipitation with ethanol. The chlorosilane can be collected and recycled so that the complete reaction may be written in this general form:



The difunctional silylamines employed in this reaction are shown in Table I. Other dihalides successfully used for the condensation polymerizations included *m*-dichloroxylylene, *p*- and *m*-dibromoxylylene, bis-(chloromethyl)biphenyl, and bis(chloromethyl)diphenylether.

X-ray measurements showed partial crystallinity of the alcohol-precipitated polyxylylenylpiperazines. Molecular weights of the polyamines prepared in this way range from 20,000 to 40,000. The polymers have melting ranges between 240 and 300°C. and films can be pressed from these materials or cast from their solutions. Chloroform and tetrachloroethane are strongly adsorbed by these polyamines; a film of 12 mil thickness cast from chloroform contained 18% chlorine after pumping for 24 hr. at room temperature and 0.1 mm. pressure which corresponds approximately to one  $\text{HCCl}_3$  for two piperazine units. After 60 hr. of pumping at 150°C. and 0.1 mm. pressure the Cl content decreased to 0.7%.

Among the studies done on these novel polyamines were reactions with alkyl iodides which lead to quaternary products. Methyl iodide and poly(xylyleul-2-methylpiperazine) yielded a quaternary polyamine which is soluble in polar solvents like dimethylformamide and, when quaternized to a sufficiently high degree, can also be dissolved in water. Reaction with

TABLE I  
Silylamines

Structure	Boiling pt., °C./mm. Hg	Refractive index, $n_D^{20}$	Nominal/Found, %			
			C	H	N	Si
$  \begin{array}{c}  \text{CH}_3 \\    \\  (\text{CH}_3)_3\text{Si}-\text{N} \begin{array}{c} \diagup \quad \diagdown \\ \text{---} \quad \text{---} \\ \diagdown \quad \diagup \end{array} \text{N}-\text{Si}(\text{CH}_3)_3  \end{array}  $	106/11	1.4516	54.0 54.5	11.5 11.8	11.5 11.0	23.0 22.7
$  \begin{array}{c}  \text{CH}_3 \\    \\  (\text{CH}_3)_3\text{Si}-\text{N} \begin{array}{c} \diagup \quad \diagdown \\ \text{---} \quad \text{---} \\ \diagdown \quad \diagup \end{array} \text{N}-\text{Si}(\text{CH}_3)_3 \\  \text{(cis)}  \end{array}  $	112/11	1.4563	—	—	—	—
$  \begin{array}{c}  \text{CH}_3 \\    \\  (\text{CH}_3)_3\text{Si}-\text{N} \begin{array}{c} \diagup \quad \diagdown \\ \text{---} \quad \text{---} \\ \diagdown \quad \diagup \end{array} \text{N}-\text{Si}(\text{CH}_3)_3 \\  \text{(trans)}  \end{array}  $	112/11	1.4522	—	—	—	—
$  \begin{array}{c}  \text{CH}_3 \\    \\  (\text{CH}_3)_2\text{C}_6\text{H}_5\text{Si}-\text{N} \begin{array}{c} \diagup \quad \diagdown \\ \text{---} \quad \text{---} \\ \diagdown \quad \diagup \end{array} \text{N}-\text{Si}(\text{CH}_3)_2\text{C}_6\text{H}_5 \\  \text{(trans)}  \end{array}  $	197-8/2.5	1.5448	67.7 67.2	8.5 8.6	—	—
$  \begin{array}{c}  \text{CH}_3 \\    \\  (\text{CH}_3)_2\text{C}_6\text{H}_5\text{Si}-\text{N} \begin{array}{c} \diagup \quad \diagdown \\ \text{---} \quad \text{---} \\ \diagdown \quad \diagup \end{array} \text{N}-\text{Si}(\text{CH}_3)_2\text{C}_6\text{H}_5  \end{array}  $	198/2.8	1.5417	68.4 68.3	8.7 8.8	7.6 7.9	15.3 15.1

$  \begin{array}{c}  \text{CH}_3 \\    \\  (\text{CH}_3)_2\text{C}_6\text{H}_4\text{Si}-\text{N}-\text{N}-\text{Si}(\text{CH}_3)_2\text{C}_6\text{H}_5 \\    \quad   \\  \text{CH}_2 \quad \text{CH}_2 \\  \text{(cis)}  \end{array}  $	206/2.8	1.5425	$  \begin{array}{c}  69.0 \\  \hline  68.9  \end{array}  $	$  \begin{array}{c}  9.0 \\  8.9  \end{array}  $	—	—
$  \begin{array}{c}  \text{CH}_3 \\    \\  (\text{CH}_3)_2\text{C}_6\text{H}_4\text{Si}-\text{N}-\text{N}-\text{Si}(\text{CH}_3)_2\text{C}_6\text{H}_5 \\    \quad   \\  \text{CH}_2 \quad \text{CH}_2 \\  \text{(trans)}  \end{array}  $	206/2.5	1.5401	$  \begin{array}{c}  69.0 \\  \hline  68.8  \end{array}  $	$  \begin{array}{c}  9.0 \\  8.9  \end{array}  $	—	—
$  \begin{array}{c}  (\text{CH}_3)_2\text{Si}-\text{N}-\text{CH}_2-\text{CH}_2-\text{N}-\text{Si}(\text{CH}_3)_3 \\    \quad   \\  \text{CH}_3 \quad \text{CH}_3  \end{array}  $	213/1 atm.	1.4360	$  \begin{array}{c}  51.7 \\  \hline  51.9  \end{array}  $	$  \begin{array}{c}  12.1 \\  \hline  12.3  \end{array}  $	—	—
$  \begin{array}{c}  (\text{CH}_3)_2\text{C}_6\text{H}_4\text{Si}-\text{N}-\text{CH}_2-\text{CH}_2-\text{N}-\text{Si}(\text{CH}_3)_2\text{C}_6\text{H}_5 \\    \quad   \\  \text{CH}_3 \quad \text{CH}_3  \end{array}  $	184-5/2.6	1.5294	$  \begin{array}{c}  67.4 \\  \hline  67.8  \end{array}  $	$  \begin{array}{c}  9.0 \\  9.1  \end{array}  $	—	—

TABLE II  
 Polyxylylenylpiperazines

No.	Structure	[ $\eta$ ] (HCCl <sub>3</sub> )	Mol. wt. <sup>a</sup>	Elonga- tion (break), %	Tensile strength, psi	Nominal/Found, %				
						C	H	N	Cl	
1		0.77	15,600	—	—	77.8 77.1	9.3 8.9	12.9 12.7	0 0.8	
2		1.97	40,600	95	9880	77.2 76.7	9.0 8.8	13.8 13.8	0 0.5	
3	 1/2 HCCl <sub>3</sub>	1.97	40,600	263	1850	—	—	—	—	18.0 <sup>b</sup>

4 <sup>c</sup>		—	—	52	8900	—	—	0.68
5 <sup>d</sup>		—	—	147	6250	61.2 63.0	8.5 8.3	10.8 10.5
6 <sup>e</sup>		—	—	45	3880			% I = 18.0

<sup>a</sup> By osmotic measurements.

<sup>b</sup> One HCl<sub>3</sub> for every other piperazine unit corresponds to 20.3% Cl.

<sup>c</sup> Obtained by pumping film No. 3, 60 hr. at 150°C./0.1 mm. Hg.

<sup>d</sup> Film cast from 50% HCOOH.

<sup>e</sup> 0.36 CH<sub>3</sub>I/piperazine unit.

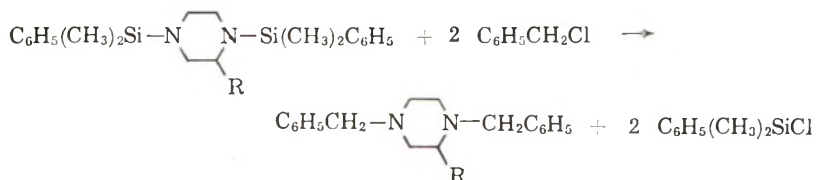
diiodopropane results in a water-insoluble membrane in which the chains of the quaternary polyamine are crosslinked by propylene groups.

Aqueous or concentrated inorganic or organic acids dissolve these polyamines with formation of polyelectrolyte solutions. A film cast from poly(xylylenyl-2-methylpiperazine) in 50% formic acid retains approximately one molecule of formic acid and one molecule of water per piperazine unit after pumping at room temperature and 0.1 mm. pressure for two days. Such a film is stable in air and shows considerable strength (see Table II); it is nonhygroscopic but can easily be redissolved in water.

Some physical data of these polyamines and their derivatives are shown in Table II.

The initial step of the reaction between benzylic halides and silylamines is likely to be a nucleophilic attack by the halide on the silicon atom. The reaction is similar in this respect to the silylamine-amine exchange reaction, in which an amine is the attacking nucleophilic species. Fessenden and Crowe found this latter reaction to be catalyzed by amine salts and ammonium salts.<sup>11</sup>

Experiments were undertaken to determine whether such compounds would exhibit any catalytic activity in the halide-silylamine system. The reaction of bis(phenyldimethylsilyl)piperazine and bis(phenyldimethylsilyl)-2-methylpiperazine with benzyl chloride:

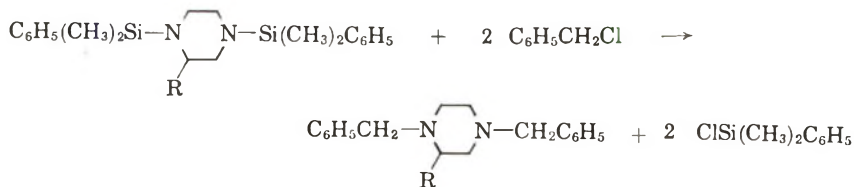


where R = H, CH<sub>3</sub>, was studied with and without addition of small amounts of ammonium chloride, ammonium sulfate, dimethylsulfoxide, or tetramethylene sulfone at several temperatures. At certain times, samples of the reaction mixtures were taken and analyzed by vapor phase chromatography.

The conversion was calculated based on the peak areas of starting materials and products. The semiquantitative data obtained from the vapor phase chromatograms are shown in Table III; they indicate that addition of ammonium chloride or sulfate increases the reaction rate by factors of 5-10 at the temperatures studied. Tetramethylenesulfone enhances the reaction rate somewhat less; dimethylsulfoxide (not shown in the table) changes the course of the reaction and leads to the formation of side products.

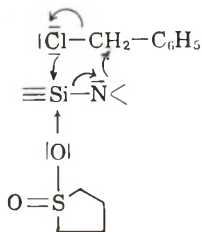
The role of the catalyst is not known with certainty. The activity of ammonium salts may be explained as the result of proton transfer to silylamine nitrogen, which results in enhanced polarity of the Si-N bond. On the other hand, the fact that tetramethylenesulfone exhibits the same kind of catalytic activity suggests that nucleophilic attack on silicon by the

TABLE III



R	Catalyst	Temp., °C.	Reaction time, min.	Conversion, %
CH <sub>3</sub>	None	180	16	16
			60	88
			120	100
CH <sub>3</sub>	(NH <sub>4</sub> ) <sub>2</sub> SO <sub>4</sub> , 5 mole-%	180	2	76
			5	98
			16	100
CH <sub>3</sub>	None	100	10	<1
			60	5
			1200	97
CH <sub>3</sub>	(NH <sub>4</sub> ) <sub>2</sub> SO <sub>4</sub> , 5 mole-%	100	10	15
			60	35
			180	90
H	None	150	15	28
			60	78
			180	>95
H	NH <sub>4</sub> Cl, 10 mole-%	150	5	54
			15	91
			60	100
H	Tetramethylenesulfone, 10 mole-%	150	5	10
			15	63
			60	100

catalyst is the first step. The  $d\pi-p\pi$  bonding between the lone electron pair on nitrogen and the vacant  $3d$  orbitals of the silicon<sup>11</sup> should be weakened by the approach of the nucleophilic oxygen or halogen of the catalyst. Chloride ion released upon bond formation between nitrogen and the  $\alpha$ -carbon may subsequently replace the catalyst at the silicon. This process, of course, may be concerted with no free ions formed at any time:



Fessenden and Crowe reported<sup>11</sup> that chlorosilanes also showed catalytic activity in silylamine-amine exchange reactions, although to a somewhat



smaller degree than ammonium salts. Chlorosilane is one of the products formed from silylamines and benzylchloride; the reaction might thus be self-catalyzed. Addition of small amounts of a more active catalyst like ammonium chloride then has only a moderately accelerating effect on the reaction rate.

By adding ammonium chloride to the mixture of  $\alpha, \alpha'$ -dichloro-*p*-xylene and bis(phenyldimethylsilyl)-2-methylpiperazine it was possible to run the reaction at lower temperatures and obtain a product of about twice the molecular weight (40,000) compared with "uncatalyzed" runs.

## EXPERIMENTAL

### 1. Bis-*N,N'*-trimethylsilyl-2-methylpiperazine

The preparation of all trimethylsilyl- and phenyldimethyl-silylpiperazines and their methyl derivatives was done in analogous manner. The following preparation is given as an example.

To 1 mole of 2-methylpiperazine dissolved in about three liters of dry ether (or one liter of benzene or toluene) was added with stirring, 2 moles of trimethylchlorosilane. The mixture warmed up spontaneously and a white precipitate was formed. When the reaction had subsided, 2.5 moles of triethylamine was added and the stirring continued for 12–15 hr. The precipitate of triethylaminehydrochloride was filtered off and the filtrate distilled. A second distillation on a spinning band column was usually necessary to obtain a pure, colorless product in about 40% yield. (The phenyldimethylpiperazines were generally obtained in about 70% yield.) Physical data of the products are shown in Table I.

### 2 *N,N'*-Bistrimethylsilyl-*N,N'*-dimethylethylenediamine

This material was prepared by dissolving 30 g. of *N,N'*-dimethylethylenediamine (redistilled commercial material, 80% pure according to VPC analysis) in 50 cc. of dry benzene and adding to the ice-cooled solutions 74 g. of freshly distilled trimethylchlorosilane in 150 cc. of dry benzene. After the addition was complete, 70 g. of triethylamine was added to the white slurry and the mixture stirred overnight. The precipitate of triethylaminehydrochloride was then filtered off in an atmosphere of dry nitrogen and the filtrate was distilled on a spinning band column. The product was obtained in 53% yield.

### 3. Poly(1,4-xylylenyl)-2-methylpiperazine

Bis-*N,N'*-(phenyldimethylsilyl)-2-methylpiperazine, 36.87 g., was mixed in a dry atmosphere with 17.50 g of  $\alpha, \alpha'$ -dichloro-*p*-xylene (regular Eastman grade, recrystallized from ethanol) and 0.2 g of ammonium chloride.

The distillation flask containing the mixture was placed in an oil bath and heated at 150°C. for 4–6 hr. The mixture was kept under a cover of dry nitrogen during this time. The viscosity of the mixture started in-

creasing after about one hour reaction time; at the end of the heating period a highly viscous yellow mass was obtained. Vacuum was applied and the phenyldimethylchlorosilane formed during the reaction was distilled off. Heating at 150°C. and 0.1 mm. pressure for 10 hr. completed the removal of volatile materials. The crude polymer was obtained in the form of a tough yellow foam. It was dissolved in chloroform and filtered through a coarse sintered glass filter funnel lined with glass wool in order to remove gel particles. The filtrate was concentrated to a fairly viscous solution and poured into vibromixed ethanol. The polymer precipitated in form of nearly white fiber. In an average run of this kind, 10–15 g. of polymer was obtained, corresponding to 50–75% yield. The balance was 2–5 g. crosslinked material and 2–5 g. low molecular weight product.

#### 4. Quaternization of Poly(1,4-xylylenyl)-2-methylpiperazine

A 2-g. portion the polyamine (molecular weight of the repeating unit = 202) was dissolved in 25 cc. of chloroform and to this solution was added 0.7 g. (0.005 moles) of methyl iodide in 25 cc. of ethanol. The mixture was allowed to stand at room temperature for 48 hr. (higher temperature shortened the reaction time but led to partially crosslinked material). The viscous oil that had separated after about 24 hr. was dissolved in dimethylformamide and the product obtained in solid form by precipitation with ethanol.

#### 5. Reactions of Benzyl Chloride with Disilylpiperazines

Reaction flasks containing mixtures of 10 mmoles (1.27 g.) of freshly distilled benzyl chloride and 5 mmoles of bis-*N,N'*-(phenyldimethylsilyl)-piperazine or -2-methylpiperazine (1.77 or 1.84 g.), with or without addition of the catalysts shown in Table II, were sealed off with rubber caps under dry N<sub>2</sub> and placed in oil baths heated at the temperatures shown in Table II. Samples were drawn by means of a hypodermic syringe, diluted with dry benzene 1:10, and analyzed by a F & M gas chromatograph, Model 720, with 2 ft. SE-30 silicone rubber columns using temperature programming from 50 to 275°C. with a helium flow of 60 cc./min. The four compounds involved in this reaction, C<sub>6</sub>H<sub>5</sub>CH<sub>2</sub>Cl, disilylpiperazine, dibenzylpiperazine, and phenyldimethyl-chlorosilane, gave clearly resolved sharp peaks under these conditions with the following retention times: 6.8, 37.2, 34.6, and 9.4 min., respectively.

The author is indebted to D. F. Flewellin for technical assistance. Helpful discussions with Dr. E. M. Boldebuck and Dr. J. G. Murray are gratefully acknowledged. The determination of physical properties of the polymers were done by Miss W. Balz, Mrs. G. Crandall, and Mrs. M. DeSieno.

#### References

1. Jones, G. D., A. Langsjoen, M. M. C. Neumann, and J. Zomlefer, *J. Org. Chem.*, **9**, 125 (1944).
2. Barb, W. G., *J. Chem. Soc.*, **1955**, 2564, 2577.
3. Friedrich, H., German Pat. 1,037,126 (1958).

4. Cope, A. C., and T. Y. Shen, U.S. Pat. 2,932,650 (1960).
5. Lavagnino, E. R., R. R. Chauvette, W. N. Cannon, and E. C. Kornfeld, *J. Am. Chem. Soc.* **82**, 2609 (1960).
6. Toy, M. S., and C. C. Price, *J. Am. Chem. Soc.*, **82**, 2613 (1960).
7. Hall, H. K., Jr., *J. Org. Chem.*, **28**, 223 (1963).
8. Vogel, H., and C. S. Marvel, *J. Polymer Sci.*, **50**, 511 (1961).
9. Anderson, H. H., *J. Am. Chem. Soc.*, **74**, 1421 (1952).
10. Birkofer, L., P. Richter, and A. Ritter, *Chem. Ber.*, **93**, 2804 (1960).
11. Fessenden, R., and D. F. Crowe, *J. Org. Chem.*, **26**, 4638 (1954).
12. Eaborn, C., *Organosilicon Compounds*, Butterworths, London, 1960, pp. 94-113.

### Résumé

La polycondensation du  $\alpha,\alpha$ -dichloroxyène ou des halogénures de réactivité analogue avec des silylamines bifonctionnelles conduit à des nouvelles polyamines de poids moléculaires élevés (v. le résumé anglais). L'halogène est éliminé sous forme de halosilane; ces halosilanes sont inertes dans ce système de réaction et servent comme solvant pour le polymère. Les polymères peuvent être coulés d'une solution, ou pressés sous forme de films solides. Ils présentent les propriétés typiques des amines, ils sont solubles dans les acides organiques et inorganiques, et ils forment des solutions de polyélectrolytes, d'où l'on peut couler des films stables de polyélectrolytes. On constate que les sels d'ammonium ainsi qu'une sulfone cyclique augmentent catalytiquement la vitesse de la réaction entre le chlorure de benzoyl et les silylamines.

### Zusammenfassung

Die Kondensationspolymerisation von  $\alpha,\alpha$ -Dichlorxylyl und ähnlichen reaktionsfähigen Halogeniden mit bifunktionellen Silylaminen führt zur Bildung neuer hochmolekularer Polyamine (siehe englische Zusammenfassung). Das Halogen wird in Form eines Halogensilans abgespalten, das im vorliegenden Reaktionssystem inert ist und als Lösungsmittel für das Polymere wirkt. Die Polymeren können aus Lösung gegossen oder zu festen Filmen gepresst werden. Sie weisen ein für Amine typisches Verhalten auf. Sie sind in anorganischen und organischen Säuren löslich und bilden Polyelektrolytlösungen, aus denen stabile Filme gegossen werden können. Die Reaktion mit Alkyljodiden führt zu polyquaternären Verbindungen. Die Reaktion von Benzylchlorid mit Silylaminen wird durch Ammoniumsalze und ein zyklisches Sulfon katalytisch beschleunigt.

Received June 11, 1963

## Copolymerizations in Electron-Donor Solvents with Organolithium Catalysts

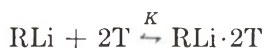
LEO REICH, *Polymer Research Section, Picatinny Arsenal, Dover, New Jersey*, and SALVATORE S. STIVALA, *Department of Chemistry and Chemical Engineering, Stevens Institute of Technology, Hoboken, New Jersey*

### Synopsis

A general scheme is postulated for copolymerizations in electron-donor solvents with organolithium catalysts. The general mathematical expression obtained is simplified by utilizing two extreme conditions. The simplified equations are shown to be consistent with experimental evidence. While it is difficult to decide in favor of either solvation theory or O'Driscoll's concepts, the latter is favored based upon simplicity, plausibility and experimental evidence.

### Introduction

Several workers<sup>1,2</sup> have carried out studies on the anionic homopolymerization of styrene in electron-donor solvents, e.g., tetrahydrofuran (T). They indicated that two moles of T formed a complex with one mole of organolithium catalyst (RLi), as follows:



Welch<sup>2</sup> calculated values of  $K$  for different concentrations of RLi and T and obtained values ranging from  $1.3 \times 10^6$  to  $4.6 \times 10^6$ . However, Bywater and Worsfold<sup>3</sup> found that, in the anionic homopolymerization of styrene in the presence of T, the kinetic order in respect to RLi (R = *n*-butyl) changed from one-half to first order as the concentration of T was increased. This necessitated the postulation of the formation of a monoetherate, RLi·T, as well as that of a dietherate. Also, dimeric lithium polystyryl anions were assumed to exist and it was shown that even at low concentrations of T, the initiation step was complete in a matter of seconds. Because of this, the concentration of polymerizing chain ends could always be taken to be the same as the initial concentration of RLi.

Several workers<sup>4-9</sup> have also carried out studies on the anionic copolymerization of mixtures of styrene and various dienes in the presence of RLi and either in the presence or absence of T and other electron-donor solvents (EDS). In the absence of T or EDS, it was observed that the copolymerization behavior of diene-containing systems, e.g., butadiene

and styrene, was markedly different from that to be expected based on homopolymerization studies of these monomers. Thus, although the ratio of the homopolymerization propagation rate constants for butadiene/styrene was calculated as 0.15, the observed reactivity ratio was 7.0. This inferred a reversal in the reactivity of these monomers when they were copolymerized. One explanation offered for such behavior was the suggestion that the anionic chain ends show selective solvation of one of the monomers, thus effectively raising the concentration of that monomer in the vicinity of the chain ends.<sup>4</sup> Korotkov and Chesnokova<sup>5</sup> attributed this behavior to the participation of unsaturated groups in the polydiene in a complex with the active chain ends. Kuntz<sup>7</sup> postulated solvation or complex formation between monomer and the C—Li bond of the growing chain. However, later on, Kuntz and O'Driscoll<sup>9</sup> were able to apply straightforward copolymerization kinetics to the styrene-butadiene system and found that with the aid of steady-state conditions they could explain experimental data involving copolymerization rates without resorting to solvation effects. Morton and Eills<sup>10</sup> ascribed the apparently unusual copolymerization behavior, not to solvation effects, but to a large difference in cross-propagation rates.

In the presence of T or EDS, it was found<sup>4,6,7</sup> that the copolymerization of butadiene and styrene proceeds at a higher rate and that there is a more uniform uptake of the monomers and that the polymerization rates of the monomers converge.

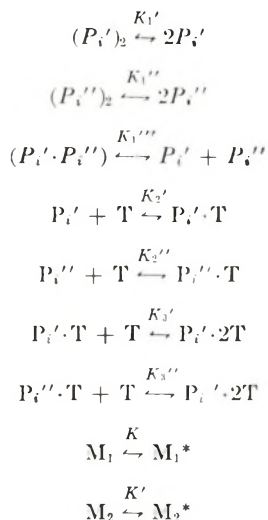
It is the purpose of this paper to present a general mathematical treatment of the anionic copolymerization of olefins and/or dienes in electron-donor solvents in the presence of RLi catalysts. In order to maintain the generality of the treatment, solvation or monomer complexation which involves a solvation monomer concentration (arbitrarily based on the total volume of the solution and denoted by an asterisk, e.g.,  $M^*$ ) will be assumed along with a bulk phase monomer concentration. The general expression obtained will be simplified and it will be shown that the simplified equations obtained can be further reduced by assuming that solvation effects are negligible or do not occur.

### Kinetic Scheme

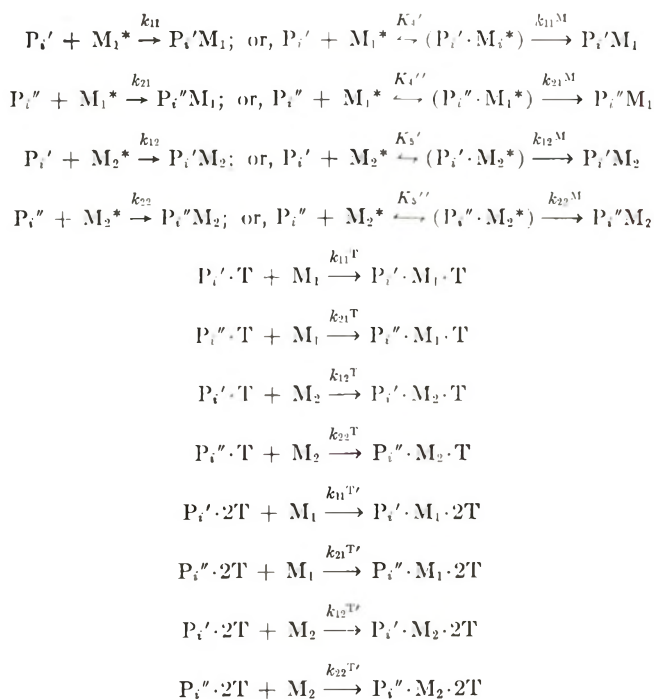
The following general kinetic scheme will be employed. The initiation step was assumed to be very rapid and dimeric organolithium species were assumed to apply.<sup>3</sup> The polar solvent, T, will be used arbitrarily and it will be postulated that a monoether and diether complex can form.<sup>1-3</sup> Monomer may add directly to the active chain end or may form a complex, prior to adding to the chain. Although both types of monomer addition are portrayed in the scheme, the latter will be utilized in the mathematical treatment. The starred monomers denote monomer molecules at the site of the free active chain end (however, their concentrations are arbitrarily based on the total volume) while the nonstarred monomers represent monomer molecules in the bulk phase. A growing polymer chain may be

represented as  $P_i'$ , where  $i$  denotes the number of units and the single prime denotes that the terminal chain group consists of monomer 1,  $M_1$ , whereas a double prime denotes that the terminal chain group consists of monomer 2,  $M_2$ . The  $i$ -values of the various species are not necessarily equal.

**Equilibrium Reactions.** Equilibrium reactions are as follows.



**Propagation Reactions.** These are as follows.



From the above, we may write for the rate of disappearance of monomer,  $M_1$ ,

$$(1 + K) \frac{(-)d \ln[M_1]}{dt} = k_{11}^M K_4' [P_i'] \frac{[M_1^*]}{[M_1]} + k_{21}^M K_4'' [P_i''] \frac{[M_1^*]}{[M_1]} \\ + k_{11}^T [P_i' \cdot T] + k_{21}^T [P_i'' \cdot T] + k_{11}^{T'} [P_i' \cdot 2T] + k_{21}^{T'} [P_i'' \cdot 2T] \quad (1)$$

The following material balances may also be written (where  $[C]_0$  = original concentration of initiator):

$$2([P_i']_2) + [P_i'']_2 + [(P_i' \cdot P_i'')] + [P_i'] + [P_i''] \\ + [(P_i' \cdot M_1^*)] + [(P_i'' \cdot M_1^*)] + [(P_i' \cdot M_2^*)] + [(P_i'' \cdot M_2^*)] \\ + [P_i' \cdot T] + [P_i'' \cdot T] + [P_i' \cdot 2T] + [P_i'' \cdot 2T] = [C]_0 \quad (2)$$

and

$$2([P_i' \cdot 2T] + [P_i'' \cdot 2T]) + [P_i' \cdot T] + [P_i'' \cdot T] = (T_0 - T) = \Delta T \quad (3)$$

Utilizing the various equilibrium reactions, eqs. (2) and (3) can be expressed in terms of  $[P_i' \cdot T]$  and  $[P_i'' \cdot T]$ . Thus, eq. (3) may be written as

$$[P_i' \cdot T] = (\Delta T - \beta [P_i'' \cdot T]) / \alpha \quad (4)$$

where

$$\alpha = (1 + 2K_3'[T])$$

and

$$\beta = (1 + 2K_3''[T])$$

Equation (2) may also be rewritten as follows,

$$\frac{[P_i' \cdot T]^2}{M} + \frac{[P_i'' \cdot T]^2}{N} + \gamma [P_i' \cdot T] + \sigma [P_i'' \cdot T] + \frac{[P_i' \cdot T][P_i'' \cdot T]}{\psi} = [C]_0 \quad (5)$$

where

$$2M = K_1'(K_2')^2[T]^2$$

$$2N = K_1''(K_2'')^2[T]^2$$

$$2\psi = K_1'''K_2'K_2''[T]^2$$

$$\gamma = \left\{ 1 + \frac{1}{K_2'[T]} (1 + K_4'[M_1^*] + K_5'[M_2^*]) + K_3'[T] \right\}$$

$$\sigma = \left\{ 1 + \frac{1}{K_2''[T]} (1 + K_4''[M_1^*] + K_5''[M_2^*]) + K_3''[T] \right\}$$

Substituting eq. (4) into eq. (5) and collecting terms, we obtain

$$[P_i'' \cdot T] = \frac{-J \pm (J^2 - 4HL)^{1/2}}{2H} \quad (6)$$

where

$$H = \left( \frac{\beta^2}{M\alpha^2} + \frac{1}{N} - \frac{\beta}{\alpha\psi} \right)$$

$$J = \left( \sigma - \frac{\beta\gamma}{\alpha} - \frac{2\beta \cdot \Delta T}{M\alpha^2} + \frac{\Delta T}{\alpha\psi} \right)$$

$$L = \left\{ \frac{(\Delta T)^2}{M\alpha^2} + \frac{\gamma \cdot \Delta T}{\alpha} - [C]_0 \right\}$$

Equation (1) can also be expressed in terms of  $[P_i' \cdot T]$  and  $[P_i'' \cdot T]$ , and when eq. (4) is then substituted into the resulting expression, the following equation results for the disappearance of  $M_1$ ,

$$(1 + K) \frac{(-)d \ln[M_1]}{dt} = \frac{A\Delta T}{\alpha} + \left( B - \frac{A\beta}{\alpha} \right) [P_i'' \cdot T] \quad (7)$$

where

$$A = k_{11}^T + k_{11}^{T'} K_3' [T] + \frac{k_{11}^M K_4' [M_1^*]}{K_2' [T] [M_1]}$$

and

$$B = k_{21}^T + k_{21}^{T'} K_3'' [T] + \frac{k_{21}^M K_4'' [M_1^*]}{K_2'' [T] [M_1]}$$

In a similar manner, we may obtain an expression for rate of disappearance of monomer,  $M_2$ ,

$$(1 + K') \frac{(-)d \ln[M_2]}{dt} = \frac{C\Delta T}{\alpha} + \left( D - \frac{C\beta}{\alpha} \right) [P_i'' \cdot T] \quad (8)$$

where

$$C = k_{12}^T + k_{12}^{T'} K_3' [T] + \frac{k_{12}^M K_5' [M_2^*]}{K_2' [T] [M_2]}$$

and

$$D = k_{22}^T + k_{22}^{T'} K_3'' [T] + \frac{k_{22}^M K_5'' [M_2^*]}{K_2'' [T] [M_2]}$$

Dividing eq. (7) by eq. (8) leads to

$$\frac{(1 + K) d \ln[M_1]}{(1 + K') d \ln[M_2]} \equiv R$$

$$= \frac{A\Delta T + \alpha \left( B - \frac{A\beta}{\alpha} \right) \left[ \frac{-J \pm \sqrt{J^2 - 4(H)(L)}}{2H} \right]}{C\Delta T + \alpha \left( D - \frac{C\beta}{\alpha} \right) \left[ \frac{-J \pm \sqrt{J^2 - 4(H)(L)}}{2H} \right]} \quad (9)$$



### Discussion

Equation (9) represents an exact expression, for the scheme presented, which has been derived without recourse to any steady-state assumptions. However, it is too cumbersome to work with but may be simplified by using two extreme cases as in the following. Although the simplified equations agree with experimental findings, such concordance does not prove eq. (9).

**Case 1: When  $[T]_0/[C]_0$  is Relatively Large.** In this case, the principal species are now  $(P_i' \cdot 2T)$  and  $(P_i'' \cdot 2T)$ , and we may assume that  $[P_i'' \cdot T] \approx 0$ .<sup>2,3</sup> (Or,  $\Delta T/2 \approx [C]_0$  and consequently,  $L \approx 0$ .) Equation (9) may now be written,

$$R \approx A/C = k_{11}{}^{T'} k_{12}{}^{T'} \quad (10)$$

or

$$\frac{d \ln[M_1]}{d \ln[M_2]} = \frac{(1 + K')k_{11}{}^{T'}}{(1 + K)k_{12}{}^{T'}} \quad (10a)$$

When no solvation effects are assumed, eq. (10a) becomes

$$\frac{d \ln[M_1]}{d \ln[M_2]} = \frac{k_{11}{}^{T'}}{k_{12}{}^{T'}} \quad (10b)$$

**Case 2: When  $[T]_0/[C]_0$  Is Relatively Small.** In this case, the principal species consist of  $(P_i' \cdot P_i'')$ ,  $(P_i')_2$  and  $(P_i'')_2$ , and we may again assume that  $[P_i'' \cdot T] \approx 0$ .<sup>2,3</sup> Equation (9) now becomes

$$R \approx \frac{k_{11}{}^M K_4' \frac{[M_1^*]}{[M_1]}}{k_{12}{}^M K_5' \frac{[M_2^*]}{[M_2]}} = \frac{k_{11}{}^M K_4' K}{k_{12}{}^M K_5' K'} \quad (11)$$

or

$$\frac{d \ln[M_1]}{d \ln[M_2]} = \frac{(1 + K')K k_{11}{}^M K_4'}{(1 + K)K' k_{12}{}^M K_5'} \quad (11a)$$

A form of expression similar to eqs. (10) and (10b) has been found to apply to the system, styrene-butadiene-RLi, in the presence of  $T^7$  and diethyl ether.<sup>6</sup> Thus, for the latter solvent, as the concentration of the ether was increased (maintaining the initial concentrations of the monomers and catalyst constant), the styrene found initially in the copolymer increased and then leveled off to about 32 mole-%. Similarly, as the concentration of T was increased, the initial content of styrene in the copolymer leveled off to about 30-34 mole-%.

A form of expression similar to eq. (11a) was also found to apply when the value of T was relatively small.<sup>7</sup> Thus, for the system, styrene-butadiene-RLi, when the value of T was varied from 0 to  $2.6 \times 10^{-4}M$ ,

the content of styrene in the copolymer varied from 10 to 11 mole-%. Furthermore, Kuntz<sup>7</sup> found that an expression similar to eq. (11a) was valid for the copolymerization of butadiene and styrene in *n*-heptane with *n*-butyllithium. He estimated the value of  $[K(1 + K')/K'(1 + K)]$  (which he denoted as  $a_B/a_S$ ) to be 85. O'Driscoll<sup>9</sup> suggested that such a high value would require an enormous extent of preferential solvation in order to explain the experimental data. He therefore considered solvation factors not to be of prime importance and proposed instead that the utilization of the expressions,  $k_{11} = xk_{21}$  and  $k_{12} = xk_{22}$ , could account for the high copolymerization reactivity of butadiene as compared with styrene and would also explain the observation that the product of the reactivity ratios is close to or equal to unity. Assuming that solvation effects, as indicated in the scheme, can be neglected, then eq. (11a) becomes

$$d \ln[M_1]/d \ln[M_2] = k_{11}^M K_4'/k_{12}^M K_5' = k_{11}/k_{12} \quad (11b)$$

In the light of what has been discussed above, eq. (11b) is now consistent with the experimental evidence, and solvation factors need not be considered in this respect. Thus, based on the above, it is very difficult to decide in favor of either solvation theory or O'Driscoll's concepts.<sup>9</sup> However, we favor the latter in view of the simplicity, plausibility, and experimental evidence<sup>10</sup> that has accumulated.

We would like to express our gratitude to Dr. D. W. Levi for aid in preparing the manuscript.

## References

1. O'Driscoll, K. F., and A. V. Tobolsky, *J. Polymer Sci.*, **35**, 259 (1959).
2. Welch, F. J., *J. Am. Chem. Soc.*, **82**, 6002 (1960).
3. Bywater, S., and D. J. Worsfold, *Can. J. Chem.*, **40**, 1564 (1962).
4. Kelley, D. J., and A. V. Tobolsky, *J. Am. Chem. Soc.*, **81**, 1597 (1959).
5. Korotkov, A. A., and N. N. Chesnokova, *Vysokomol. Soedin.*, **2**, 365 (1960).
6. Korotkov, A. A., S. P. Mitsengendler, and K. M. Aleyev, *Vysokomol. Soedin.*, **2**, 1811 (1960).
7. Kuntz, I., *J. Polymer Sci.*, **54**, 569 (1961).
8. O'Driscoll, K. F., *J. Polymer Sci.*, **57**, 721 (1962).
9. O'Driscoll, K. F., and I. Kuntz, *J. Polymer Sci.*, **61**, 19 (1962).
10. Morton, M., and F. R. Ells, *J. Polymer Sci.*, **61**, 25 (1962).

## Résumé

On propose un schéma général pour les copolymérisations effectuées au moyen de catalyseurs organolithiens au sein de solvants électro-donneurs. On simplifie l'expression mathématique obtenue en se plaçant dans deux conditions extrêmes. On montre que ces équations simplifiées s'accordent avec les résultats expérimentaux. Bien qu'il soit difficile de se prononcer en faveur soit de la théorie de la solvation, soit de celle d'O'Driscoll, cette dernière paraît préférable parce qu'elle est simple, plausible et en bon accord avec l'expérience.

### Zusammenfassung

Ein allgemeines Schema für die Copolymerisation in Elektronendonator-Lösungsmitteln mit Organolithiumkatalysatoren wird aufgestellt. Der erhaltene allgemeine mathematische Ausdruck wird durch die Verwendung von zwei Extremalbedingungen vereinfacht. Die vereinfachten Gleichungen stehen mit den experimentellen Befunden in Einklang. Es ist zwar schwierig zwischen der Solvatationstheorie und dem Konzept von O'Driscoll zu entscheiden, doch wird letzteres wegen seiner Einfachheit, Plausibilität und der experimentellen Unterlagen vorgezogen.

Received May 2, 1963

Revised June 25, 1963

## Preparation of Polyamides, Polyurethanes, Polysulfonamides, and Polyesters by Low Temperature Solution Polycondensation

STEPHANIE L. KWOLEK and PAUL W. MORGAN, *Pioneering Research Division, Textile Fibers Department, E.I. du Pont de Nemours & Company, Inc., Wilmington, Delaware*

### Synopsis

Solution polycondensation was used to prepare four classes of polymers. Polymers in each class were obtained with molecular weights high enough for formation into flexible, tough structures. In all instances the molecular weights were not as high as could be obtained from the same reactants by the interfacial polycondensation process. Many of the polyamides from aliphatic diamines were highly branched through diacylation of the amino groups. On the other hand, polysulfonamides were linear. Despite some limitations, as indicated above, the solution polycondensation process provides another route to forming condensation polymers and should be of special advantage in use with hydrolytically unstable intermediates, with water-insoluble diamines and diols, and for forming uniform or block copolymers.

### INTRODUCTION

Preceding papers<sup>1,2</sup> have presented in some detail the preparation of polyamides from piperazines by a low temperature solution process and a discussion of some of the variables affecting the polymerization method. The literature review<sup>1</sup> indicated that solution polycondensation had been used in many instances; yet these reports, more often than not, described products with low molecular weights.

This paper describes the application of low temperature solution polycondensation to the preparation of several classes of polymers.

### EXPERIMENTAL

Three typical preparations are given, each of which is representative of the majority of experiments outlined in the corresponding three tables of preparations and results.

Inherent viscosities ( $\eta_{inh} = [\ln \eta_{rel}]/c$ ) were determined in the solvents given with the data. The temperature was 30°C. and the concentration  $c$  was 0.5 g./100 ml. of solution.

### Poly(hexamethylene Sebacamide)

In a dry blender jar was placed a solution of 5.81 g. (0.05 mole) of hexamethylenediamine and 15.3 ml. (0.11 mole) of triethylamine in 100 ml. of alcohol-free chloroform. By means of a powder funnel inserted through the cap a solution of 10.70 ml. (0.05 mole) of sebacyl chloride in 41 ml. of chloroform was added in about 5 sec. with rapid stirring and the stirring was continued 5 min. A precipitate of polymer formed immediately. The initial temperature of the mixture was about 25°C. and the temperature was allowed to rise spontaneously from the heat of reaction and stirring.

At the end of the reaction period the mixture was cooled and filtered. The precipitate was stirred and washed in succession with chloroform, petroleum ether, 3% aqueous hydrochloric acid, water, and 50% acetone. The yield was 71% and the inherent viscosity 1.51 (*m*-cresol). The original filtrate was concentrated and mixed with petroleum ether. Additional polymer (8%) was obtained with an inherent viscosity of 0.08.

### Polyurethane from Piperazine and Ethylene Bischloroformate

Piperazine (10.35 g.; 0.12 mole) was dissolved in 75 ml. of alcohol-free chloroform in a blender jar at room temperature. To this was added with rapid stirring 7.64 ml. (0.06 mole) of ethylene bischloroformate in 25 ml. of chloroform. The addition was done by means of a dropping funnel over a period of 3 min. because of the heat and fuming produced by the reaction. Stirring was continued for 7 min., the jar was cooled, and the mixture filtered. The precipitate, which was completely soluble in water, was piperazine salt. The filtrate was evaporated to one-half volume and the polymer was isolated by precipitation with petroleum ether. After thorough washing with water and one wash with 50% aqueous acetone, the polymer was obtained as a tough, white, granular material; yield 70%; inherent viscosity 1.01 (*m*-cresol).

The reagents used in this and other preparations given in Table II were capable of producing this polyurethane by the interfacial polycondensation method with inherent viscosities from 2.0 to 2.6.

### Poly(hexamethylene-1,3-benzenesulfonamide)

In a round-bottomed flask equipped with stirrer, condenser, and dropping funnel was placed 11.62 g. (0.10 mole) of hexamethylenediamine, 18.5 g. (0.25 mole) of powdered calcium hydroxide, and 65 ml. of a 90:10 (by volume) mixture of tetramethylene sulfone and alcohol-free chloroform.

A solution of 27.51 g. (0.10 mole) of *m*-benzenedisulfonyl chloride in 35 ml. of the same solvent mixture was added over a period of 2 min. with stirring and without cooling to control the appreciable heat of reaction. The mixture was immediately heated with a water bath at 100°C. and stirring was continued.

Samples of polymer were isolated at several points. After 6.5 min. of heating, the inherent viscosity of the polymer was 1.18 (H<sub>2</sub>SO<sub>4</sub>); at 15 min., 1.25; thereafter there was no change. The total yield was 89%.

The polymer was isolated by slowly pouring the viscous solution into water stirred rapidly in a blender. The polymer was then washed in the blender twice with 5% aqueous acetic acid, three times with hot water and finally rinsed several times on the funnel.

When this preparation was carried out with cooling to 30°C. during the acid chloride addition, the inherent viscosity of the product was 0.95.

A control preparation with the same reactants carried out by the interfacial polycondensation process gave a 63% yield of polymer with inherent viscosities of 2.2 (H<sub>2</sub>SO<sub>4</sub>) and 1.48 (dimethylformamide).

## DISCUSSION

Low temperature solution polycondensation is a fast, easy route to a variety of polymers having molecular weights acceptable for practical uses. In comparison with the interfacial polycondensation method, it has a number of advantages and disadvantages.

Most of the advantages reside in an avoidance of acid chloride hydrolysis and the possibility of carrying out the reaction in a homogeneous system. The homogeneity may lead to a more nearly statistical molecular weight distribution. Copolymers may have a more random distribution of components or in some cases they may be purposely and more controllably ordered. None of the reactants need be soluble in water or aqueous alkali and, when the polymer remains dissolved or highly swollen, rather slow reactions can be employed.

Some disadvantages, or at least negative considerations, are the findings that the molecular weights attained are frequently lower than those obtained in an interfacial polycondensation reaction; purer reactants are needed for a given degree of polymerization; side reactions other than hydrolysis are encountered, such as diamine-solvent interactions; many polymers are not soluble in suitable solvents and so the gains possible from homogeneity cannot be realized; and finally, for scale-up operations organic amines as acceptors are expensive. Even with the number of shortcomings listed, solution polycondensation is a useful adjunct to other polymer-making techniques.

Specific comments on the preparation of the several groups of polymers follow.

### Polyamides

Although soluble polyamides were made from primary aliphatic diamines and aliphatic diacid chlorides (Table I), many other preparations yielded products which were insoluble or only partially soluble in *m*-cresol. This undesirable result is believed to be due to branching and network formation which arises from diacylation of the primary amine groups with the formation of imide structures. We have reported the occurrence of this side reaction in interfacial polycondensation.<sup>3</sup> It was particularly pronounced in the latter case when the acid chloride concentration was high.

TABLE I. Polyamides

Poly- amide code <sup>a</sup>	Mole ratio diamine: acid chloride	Acid acceptor, moles/mole of diacid chloride	Wt. of polymer, g./100 ml. solvent <sup>b</sup>	Reaction time and temperature <sup>b</sup>		Polymer precipitate			Polymer in solution		
				Addition, sec.	Contin- uation, min.	Yield, %	$\eta_{inh}$		Yield, %	$\eta_{inh}$	
							<i>m</i> -Cresol	H <sub>2</sub> SO <sub>4</sub>		<i>m</i> -Cresol	H <sub>2</sub> SO <sub>4</sub>
2-10	3	2 Diamine	8	30 <sup>c</sup>	5	86	0.14		5	0.04	
	2	1 Diamine	5.4	15 <sup>c</sup>	4	74	0.15				
4-10	1	2.2 (C <sub>2</sub> H <sub>5</sub> ) <sub>2</sub> N	3.3	5	5	66	0.82	0.62			
	3	2 Diamine	3.2	10	5	78	0.14				
	1	2.2 (C <sub>2</sub> H <sub>5</sub> ) <sub>2</sub> N	3.2	10	5	52	1.50	0.80	14	0.06	
6-6	1	2 (C <sub>2</sub> H <sub>5</sub> ) <sub>2</sub> N	4	10	4	42	0.30				
	1	2 (C <sub>2</sub> H <sub>5</sub> ) <sub>2</sub> N	9.8	60	3	60	0.33				
6-10	3	2 Diamine	5.6	30 <sup>c</sup>	5	80	0.23				
	2	1 Diamine	1.5	10 <sup>c</sup>	3	60	0.19	0.14	5	0.90	0.04
	1	2 (C <sub>4</sub> H <sub>9</sub> ) <sub>2</sub> N	3.3	10	5	68	0.67	0.45	28	0.08	
	1	2 (C <sub>3</sub> H <sub>7</sub> ) <sub>2</sub> N	3.3	10	5	55	1.01	0.49	13	0.08	0.06
6-T	1	2.2 (C <sub>2</sub> H <sub>5</sub> ) <sub>2</sub> N	2.1	5	5	42	0.89	0.64			
	1	2 (C <sub>2</sub> H <sub>5</sub> ) <sub>2</sub> N	3.2	10	3	63	0.81	0.45			
	1	2.2 (C <sub>2</sub> H <sub>5</sub> ) <sub>2</sub> N	10	5	5	71	1.51	0.74	8	0.14	0.08
	1	2 (C <sub>2</sub> H <sub>5</sub> ) <sub>2</sub> N	10	10	3	84	Insoluble	0.66			
	1	2 <i>N</i> -Ethylmorpholine	3.2	5	5	52	0.89				
	1	2 <i>N</i> -Methylmorpholine	3.1	10	5	36	0.52				
	1	10 <i>N</i> -Methylmorpholine	3.1	10	5	51	0.28				
	1	2 <i>N,N</i> -Diethyl- toluidine	3.2	10	7	33	0.62				
	1	2.2 (C <sub>2</sub> H <sub>5</sub> ) <sub>2</sub> N	4.4	10	5	88	d	1.00	2.5	—	0.08
	1	2 (C <sub>2</sub> H <sub>5</sub> ) <sub>2</sub> N	3.3	10 <sup>c</sup>	5	90	1.06	0.90			
PACM-10	1	2 (C <sub>2</sub> H <sub>5</sub> ) <sub>2</sub> N	6.4 <sup>e</sup>	5	3	96	0.76	0.68			
PACM-T	1	2.2 (C <sub>2</sub> H <sub>5</sub> ) <sub>2</sub> N	3	10	7	96	0.97		2	0.15	

<sup>a</sup> Diamines are designated first by 2, 4, and 6 for the number of methylene groups, 7F for 9,8-bis(aminopropyl)fluorene, and PACM for bis(4-aminocyclohexyl)methane (70% *trans-trans* isomer). Acid chlorides are 6, 10, and T for adipic, sebacic, and terephthaloyl.

<sup>b</sup> All the polymerizations were carried out in chloroform as described in the experimental section unless otherwise indicated in the notes.

<sup>c</sup> Diamine solution added to acid chloride.

<sup>d</sup> Normally insoluble in *m*-cresol.

<sup>e</sup> In 1,1,2-trichloroethane.

The presence of the imide structure in the aliphatic polyamides is shown by the large difference in the inherent viscosities in *m*-cresol and concentrated sulfuric acid. For a linear polyamide of this type the two viscosity numbers are usually close together. When imide groups are present, they are cleaved by the acid easily and randomly back to amide groups and there is a consequent drop in viscosity. If the inherent viscosity of the acid-treated polymer is taken in *m*-cresol, it will correspond closely with this lowered value. The linear polyamides which can be obtained from the branched structures have molecular weights of useful magnitude.

The conditions which are believed to promote imide formation during the solution polycondensation process are slow stirring and reactant addition, a concentrated system, and polymer precipitation. All of these conditions favor the poor distribution of intermediates and the reaction of acid chloride with NH groups in polyamide chain. The introduction of steric effects and lowering of reactivity, as in the use of terephthaloyl chloride, bis(4-aminocyclohexyl)methane, and ethylenediamine, reduced or prevented imide formation.

The best acid acceptors for use with aliphatic and cycloaliphatic primary diamines were strongly basic tertiary amines. Low yields or polymer with lower inherent viscosities were obtained when weak tertiary amines were used. Excess aliphatic diamine was completely unsuitable as an acid acceptor.

The yields of polymer were highest in the most concentrated systems although concentration favored imide formation. All of the chloroform systems examined contained a considerable amount (5–28%) of low polymer dissolved in the liquors. The separation of cyclic oligomers was not attempted. Even with this added material, the yields were sometimes low. In one case the liquors contained a dispersed 6–10 polyamide which had a high inherent viscosity in *m*-cresol. This was cleaved to very low molecular weight in sulfuric acid and so must have had the character of a microgel.

The polyamides derived from bis(4-aminocyclohexyl)methane and 9,9-bis(aminopropyl)fluorene represent preparations from water-insoluble diamines.

### Polyurethanes

Polyurethanes can be prepared by solution polycondensation through two reactions: (1) the combination of a diisocyanate with a diol<sup>4</sup> and (2) from bischloroformates and diamines.<sup>5</sup> The latter route was used in this study (Table II).

The solution polycondensation method with a tertiary amine as the acid acceptor is difficult to apply to reactions with bischloroformates because of the rapid rate of reaction between acid chloride and acceptor (Table II, Nos. 1 and 8). This interference can sometimes be reduced by use of an acceptor with lower base strength (Table II, Nos. 12 to 14). Such a reduction in acceptor base strength is of greatest value when the diamine is



TABLE II. Polyurethanes Prepared by the Solution Polycondensation Method

No.	Diamine	Bischloroformate	Mole ratio diamine: acid chloride	Acid acceptor, moles/mole of diacid chloride	Wt. of polymer, g./100 ml. solvent	Reaction time and temperature <sup>a</sup>			Yield, %	$\eta_{inh}$ <i>m</i> -Cresol
						Addition, min.	Continuation, min.	Temperature, °C.		
1	1,4-Tetramethylene-	Ethylene	1	2 Triethylamine	3	0.17	7	55 <sup>b</sup>	0.46	
2	Piperazine	Ethylene	3	2 Diamine	5.5	0.25	10	48	0.15	
3	Piperazine	Ethylene	2	1 Diamine	5.5	0.25	7	69	0.54	
4	Piperazine	Ethylene	2	1 Diamine	12	3	7	70	1.01	
5	Piperazine	Ethylene	2	1 Diamine	12	5 at 10°C.	40/10°C. <sup>c</sup> 15/25°C.	65	0.60	
6	Piperazine	Ethylene	2	1 Diamine	12	5 at 10°C.	5/10°C. <sup>e</sup> 120/60°C.	67	0.81	
7	Piperazine	Ethylene	2	1 Diamine	12	10	30/60°C. <sup>e</sup>	65	1.61 <sup>d</sup>	
8	Piperazine	Ethylene	1	2 Triethylamine	13	3	7	72	0.63	
9	Piperazine	2,2-Dimethyl-trimethylene	2	1 Diamine	12	10	30/60°C. <sup>e</sup>	96	1.26	
10	<i>trans</i> -2,5-Dimethyl-piperazine	Ethylene	2	1 Diamine	12	10	45/60°C. <sup>e</sup>	70	0.70	
11	<i>trans</i> -2,5-Dimethyl-piperazine	2,2-Dimethyl-trimethylene	2	1 Diamine	13	10	30 <sup>c</sup>	99	0.72	
12	4,6-Dimethyl-1,3-phenylene-	Ethylene	1	2 Triethylamine	12	5	45/60°C. <sup>e</sup>	90	0.10	
13	4,6-Dimethyl-1,3-phenylene-	Ethylene	1	2 <i>N</i> -methyl-morpholine	12	0.2	45/60°C. <sup>e</sup>	94	0.23	
14	4,6-Dimethyl-1,3-phenylene	Ethylene	1	2 Diethylamine	12	5	45/60°C. <sup>e</sup>	91	0.57	

<sup>a</sup> The preparations were carried out in chloroform in a blender except those marked for note c. Unless otherwise noted the temperature was initially 25°C. and was allowed to rise and fall spontaneously.

<sup>b</sup> Yield of polymer ( $\eta_{inh}$  0.06) recovered from liquors of 6%.

<sup>c</sup> Performed in a round-bottomed flask as in the method for polysulfonamides.

<sup>d</sup> Yield of polymer ( $\eta_{inh}$  0.04) recovered from liquors of 8%.

TABLE III. Polysulfonamides

Diamine	Disulfonyl chloride	Mole ratio diamine:acid chloride	Acid acceptor, moles/mole of diacid chloride	Solvent	Wt. of polymer, g./100 ml. solvent	Reaction times and temperature <sup>a</sup>			$\eta_{inh}$ (H <sub>2</sub> SO <sub>4</sub> )
						Addition, min.	Continuation, min.	Yield, %	
1,6-Hexamethyl-ene	1,3-Benzene-	3	2 Diamine	TMS <sup>b</sup>	12	7 <sup>c</sup>	45	90	0.48
		2	1 Diamine	TMS	12	7 <sup>c</sup>	45	87	0.45
	2	1 Diamine	TMS	31	2 <sup>d</sup>	45	90	0.72	
	1	2 (C <sub>2</sub> H <sub>5</sub> ) <sub>2</sub> N	TMS-CHCl <sub>3</sub>	15	0.13 <sup>e</sup>	20	15	0.24	
	1	2 (C <sub>2</sub> H <sub>5</sub> ) <sub>2</sub> N	90:10 by vol. TMS-CHCl <sub>3</sub>	15	10 <sup>f</sup>	10	62	0.21	
	1	2 (C <sub>2</sub> H <sub>5</sub> ) <sub>2</sub> N <sup>g</sup>	90:10 by vol. TMS	34	5 <sup>h</sup>	60	76	0.26	
	1	2.8 Ca(OH) <sub>2</sub>	TMS	34	2	60/30°C.	67	1.46	
	1	2.5 Ca(OH) <sub>2</sub>	TMS-CHCl <sub>3</sub>	34	2	15/100°C.	89	1.25	
	1	2.5 Na <sub>2</sub> CO <sub>3</sub>	90:10 by vol. TMS-CHCl <sub>3</sub>	34	0.25	15/60°C. 90/100°C.	86	0.41	
	1	2 KOAc	90:10 by vol. TMS-CHCl <sub>3</sub>	12	0.25	60	40	0.19	
Piperazine	1,3-Benzene-	2	1 Diamine	TMS-dioxane	30	5/30°C.	15/60°C.	98	0.12
1,6-Hexamethyl-ene-	1,6-Hexane-	1	2.5 Ca(OH) <sub>2</sub>	TMS	32	5/30°C.	45/60°C.	63	0.28
						65:35 by vol.	60/100°C.	45/60°C.	60/100°C.

<sup>a</sup> See experimental section for general method. Normally the acid chloride solution in one-third of the solvent was added to the diamine and acid acceptor mixture. The temperature was allowed to rise spontaneously and subsided during the continued reaction at room temperature.

<sup>b</sup> Tetramethylene sulfone.

<sup>c</sup> Diamine solution added to acid chloride.

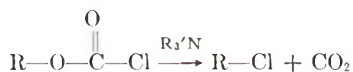
<sup>d</sup> Addition of diamine solution to acid chloride gave an 89% yield with  $\eta_{inh}$  0.60. Concentration of reaction mixture was 24 g./100 ml. of solvent.

<sup>e</sup> Stirred in high-speed blender.

<sup>f</sup> Triethylamine is not soluble in TMS alone and was entered as a two-phase mixture.

also low in base strength and the polymer and diamine remain dissolved in the reaction medium.<sup>2</sup>

Several reports<sup>6-11</sup> show that in most cases chloroformates react very rapidly with tertiary amines to form alkyl halides and carbon dioxide.



This reaction takes place at low temperature and may even be violent. Some chloroformates with trialkylamines have yielded alkyl chloride and a dialkyl urethane.<sup>10</sup> Since the reaction of chloroformates with primary or secondary amines is slower than acylation with many carboxylic acid chlorides, greater interference from the side reaction is to be expected during the preparation of polyurethanes than in polyamide preparation from the same diamines.

Polyurethanes from piperazines were prepared in high molecular weight by use of excess diamine as the acceptor. In contrast to aliphatic polyamide preparations, these preparations gave the best results when the reaction mixture was concentrated. When the reaction mixtures were cooled to 10°C., even during the early part of the polycondensation, the resulting polymers were appreciably lower in molecular weight than those prepared at 60°C. A reaction time of 10-30 min. was needed to form a polymer with high molecular weight.

### Polysulfonamides

Schlack<sup>12</sup> has described in patents the preparation of wholly aliphatic polysulfonamides with excess diamine as the acceptor. Sulfones were suggested as suitable media. No quantitative indication of molecular weights was reported.

In our hands the preparation of poly(hexamethylene-1,6-hexanesulfonamide) proceeded poorly, but poly(hexamethylene-1,3-benzenesulfonamide) was prepared successfully by solution polycondensation both with excess diamine and with calcium hydroxide as acceptors (Table III).

The formation of high polymer in the presence of excess diamine is surprising, for this is the first instance in which an aliphatic diamine has performed well as an acceptor in a single phase polycondensation system. Even at the ratio of three moles of diamine to one of disulfonyl chloride an 89% yield of polymer with an inherent viscosity of 0.48 was obtained. No doubt this good performance results from the combined effects of good polymer solubility, precipitation of diamine as salts having low solubility, relatively rapid local polymerization, and slow mixing or distribution of the intermediates.<sup>1</sup>

Polymers with the highest inherent viscosities were obtained by use of stoichiometric amounts of intermediates and an excess of powdered calcium hydroxide as the acceptor. Presumably the diamine is the primary acid acceptor, but in a medium such as tetramethylene sulfone the diamine salts are sufficiently soluble to permit a slow regeneration of diamine by the

inorganic base and the gradual incorporation of the diamine into the polymer.

Triethylamine was a poor acid acceptor. The work of Jones and Whalen<sup>13</sup> shows that tertiary amines react easily with sulfonyl chlorides to form a sulfonamide and an alkyl halide. Such a reaction would lead to chain termination in a polycondensation.

The reaction of disulfonyl chlorides with diamines is slow compared to corresponding reactions of many carboxylic acid chlorides. Hence, polysulfonamides with higher inherent viscosities were obtained by increases in time, temperature and concentration. Piperazines, which react more slowly than aliphatic diamines, did not yield polysulfonamides with high molecular weight.

The polysulfonamides made by solution polycondensation gave no evidence for the presence of sulfonimide groups analogous to the imide structures found in the aliphatic polyamides. Branching through sulfonimide groups has been encountered under some conditions in the preparation of polysulfonamides by the interfacial polycondensation process.<sup>14</sup> The test in this case is cleavage of the sulfonimide group to a sulfonamide group by concentrated sulfuric acid or aqueous alkali. Poly(hexamethylene-1,3-benzenedisulfonamide) in linear form has a much lower inherent viscosity in dimethylformamide than in sulfuric acid. Insolubility in dimethylformamide or an abnormally high viscosity in this solvent indicates branching and network formation.

### Aromatic Polyesters

The preparation of polyesters by low temperature solution methods is outlined in the work of Schnell<sup>15</sup> on polycarbonates and Conix<sup>16</sup> on aromatic polyesters. Specific examples are to be found in a number of recent patents, in the book by Christopher and Fox,<sup>17</sup> and the study of Shirokova

TABLE IV  
Preparation of the Polyester from 2,2-Bis(4-hydroxyphenyl)propane  
and Terephthaloyl Chloride<sup>a</sup>

Reaction time, min.	$\eta_{inh}^b$
3	0.26
5	0.46
38	0.56
155	0.60
230	0.64

<sup>a</sup> Reaction in chloroform at 0.05M with slow stirring; triethylamine acceptor; yield 90%.

<sup>b</sup> In *sym*-tetrachloroethane-phenol (40:60 by wt.).

and co-workers.<sup>18</sup> The commonly used reaction media are anhydrous pyridine or pyridine together with a chlorinated aliphatic hydrocarbon such as dichloromethane.

The base strength of pyridine is so low that an excess of the base over the stoichiometric amount is needed for the formation of a polyester with high molecular weight.<sup>18</sup> The results presented here show that a strong tertiary amine can be used in stoichiometric quantity in a diluent to yield a high polymer (Table IV).

The rate of formation of an aromatic polyester in the presence of a tertiary amine is much slower than that for the polymers derived from many diamines. The rate of polymerization is indicated by the data in Table IV. The reaction mixture was rather dilute (0.05M) and the stirring rate was low. These conditions, of course, affect the rate for the system as a whole. However, there are some restrictions on the range of reaction conditions imposed by the solubility limits of the bisphenoxides and the polymers. In this case the bisphenol had very low solubility in chloroform. The phenoxide was easily soluble at the above concentration. The polymer remained dissolved during the reaction but after isolation, it was insoluble in chloroform. A similar metastable condition has been observed in the preparation of polyamides from piperazines by solution polycondensation<sup>1</sup> and by interfacial polycondensation.<sup>19</sup>

### References

1. Morgan, P. W., and S. L. Kwolek, *J. Polymer Sci.*, **A2**, 181 (1964).
2. Morgan, P. W., and S. L. Kwolek, *J. Polymer Sci.*, **A2**, 209 (1964).
3. Morgan, P. W., and S. L. Kwolek, *J. Polymer Sci.*, **A1**, 1147 (1963).
4. Lyman, D. J., *J. Polymer Sci.*, **45**, 49 (1960).
5. Wittbecker, E. L., and M. Katz, *J. Polymer Sci.*, **40**, 367 (1959).
6. Hopkins, T., *J. Chem. Soc.*, **117**, 278 (1920).
7. Choppin, A. R., and J. W. Rogers, *J. Am. Chem. Soc.*, **70**, 2967 (1948).
8. Delaby, R., R. Damiens, and G. D'Huyteza, *Compt. Rend.*, **236**, 2076 (1953).
9. Gerrard, W., and F. Schild, *Chem. Ind. (London)*, **73**, 1232 (1954).
10. Campbell, J. A., *J. Org. Chem.*, **22**, 1259 (1957).
11. Wright, W. B., and H. J. Brabander, *J. Org. Chem.*, **26**, 4057 (1961).
12. Schlack, P., German Pat. 916,226 (8/5/54) and French Patent 903,983 (10/23/45), assigned to I. G. Farbenindustrie A.-G.
13. Jones, L. W., and H. F. Whalen, *J. Am. Chem. Soc.*, **47**, 1343 (1925).
14. Sundet, S. A., W. A. Murphey, and S. B. Speck, *J. Polymer Sci.*, **40**, 389 (1959).
15. Schnell, H., *Ind. Eng. Chem.*, **51**, 157 (1959).
16. Conix, A., *Ind. Eng. Chem.*, **51**, 147 (1959).
17. Christopher, W. F., and D. W. Fox, *Polycarbonates*, Reinhold, New York, 1962.
18. Shirokova, N. I., E. F. Russkova, A. B. Alishoeva, R. M. Gitina, I. I. Levkoev, and P. V. Kozlov, *Vysokomol. Soedin.*, **3**, 642 (1961).
19. Morgan, P. W., and S. L. Kwolek, *J. Polymer Sci.*, **62**, 33 (1962).

### Résumé

On a employé la polycondensation en solution afin de préparer quatre classes de polymères. Dans chaque classe on obtient des polymères dont le poids moléculaire est assez élevé pour former des structures flexibles et tenaces. Dans tous les cas les poids moléculaires étaient moins élevés que ceux obtenus en appliquant le processus de la polycondensation interfaciale. Une grande partie des polyamides des diamines aliphatiques étaient hautement ramifiée par diacylation des groupements amines. D'autre part les polysulfonamides étaient linéaires. Malgré quelques limitations, comme indiquées ci-

dessus, le processus de polycondensation en solution nous donne une autre méthode pour la formation de polymères de condensation et il présente un avantage spécial en l'employant avec des diols insolubles dans l'eau, et pour la formation de copolymères uniformes ou séquencés.

### Zusammenfassung

Die Lösungspolykondensation wurde zur Darstellung von vier Klassen von Polymeren herangezogen. In jeder Klasse wurden Polymere mit genügend hohem Molekulargewicht zur Bildung biegsamer, zäher Strukturen erhalten. In allen Fällen waren die Molekulargewichte nicht so hoch, wie sie aus den gleichen Komponenten durch Grenzflächenpolykondensation erhalten werden konnten. Viele der Polyamide aus aliphatischen Diaminen waren durch Diacylierung der Aminogruppen hochgradig verzweigt. Andererseits waren die Polysulfonamide völlig linear. Trotz der oben angeführten Beschränkungen bildet die Lösungspolykondensation einen weiteren Weg zur Bildung von Kondensationspolymeren und sollte bei hydrolytisch instabilen Zwischenprodukten, bei wasserunlöslichen Diaminen und Diolen und zur Bildung einheitlicher oder Block-Copolymerer spezielle Vorteile bieten.

Received June 24, 1963

Revised June 27, 1963

## Amylose V Complexes. II. Lower Molecular Weight Ketones\*

FELIX J. GERMINO, R. J. MOSHY, and ROBERT M. VALLETTA,†  
*Research and Development Division, American Machine & Foundry Company,  
Springdale, Connecticut*

### Synopsis

The acetone- and methyl ethyl ketone-amylose V complexes have been prepared and their unit cell dimensions calculated from their x-ray powder patterns. This work demonstrates the size-determining effect of these two ketones on the amylose V complex. The small unit cell, with a helix diameter of 13.0 Å, observed with the wet methanol and ethanol complexes, is not found with the acetone and methyl ethyl ketone complexes. The wet ketone-amylose V complexes and the thoroughly dried ketone complexes have the larger helix diameter of 13.7 Å. This is the first report of an anhydrous amylose V complex with the expanded helix diameter. Thorough extraction of the methyl ethyl ketone-amylose complex with methyl alcohol did not change the 13.7 Å helix diameter, although methyl alcohol-extracted acetone-amylose complex resulted in a mixture of the 13.0 Å and 13.7 Å helix diameter types. This work demonstrates the size effect of the lower molecular weight ketones on the amylose crystalline structure.

### INTRODUCTION

The small unit cell previously associated only with anhydrous "V" amylose complex<sup>1</sup> has also been observed in the wet methanol-amylose and the wet ethanol-amylose complexes.<sup>2</sup> In the latter work, the small unit cell, with a helix diameter of 13.0 Å, was observed for the wet methanol and ethanol-amylose complexes. The wet propanol complex had a larger helix diameter of 13.7 Å. Thus, it was shown that the ratio of one mole of water per mole of glucose in the amylose V complex does not necessarily dictate a larger helix diameter. Nor could a sample of amylose V complex, having a helix diameter of 13.0 Å, be classified arbitrarily as an anhydrous V complex. Further, there was no smooth variation in helix diameter in the transition from 13.0 to 13.7 Å; rather, there was an abrupt increase of 0.7 Å in the helix diameter.

More recently, Pulley<sup>3</sup> has reported the existence of amylose V complexes with helix diameters larger than 13.7 Å, and corresponding to seven glucose residues per helical turn. Zaslow<sup>4</sup> has reported, from x-ray

\* This paper was presented at the 145th meeting of the American Chemical Society, September, 1962.

† Present address: I.B.M. Components Division, Poughkeepsie, New York.

diffraction data, a pseudo-hexagonal unit cell for the partially dried amylose-*tert*-butyl alcohol V complex having lattice constants  $a = b = 14.94$  A. and  $c = 7.93$  A. This, then, corresponds to a helical diameter of about 15 A. These two reports are further evidence of the effect of the organic complexing molecule, in the amylose V complex, on the helix diameter. Until the reports by Pulley<sup>3</sup> and Zaslav,<sup>4</sup> and work from this laboratory,<sup>2</sup> there were two defined states of the amylose V complexes. These were: (1) the hydrated V amylose complex, containing one mole of water per mole of glucose and having a helix diameter of 13.7 A., as characterized by the *n*-butanol complex reported by Rundle,<sup>1</sup> and (2) the amylose V complex which was essentially free of solvent and water having a helix diameter of 13.0 A., as reported by a number of workers.<sup>1,5-8</sup> Generally these studies indicated that the determinant factor affecting the helix diameter of the amylose V complexes, was the presence or absence of water.

Bear<sup>9</sup> made amylose V complex preparations with *n*-propanol, *n*-butanol, and acetone. He found that the x-ray patterns of these three complexes were indistinguishable, as examined with 3-em. photographs, from the amylose V complexes formed with ethanol.

This paper reports our work with the acetone- and methyl ethyl ketone-amylose V complexes.

## EXPERIMENTAL

### Preparation of Amylose-Acetone and Amylose-Methyl Ethyl Ketone V Complexes

The amylose V complexes of acetone and methyl ethyl ketone were prepared as follows. A 130-g. portion of potato amylose (Superlose, Stein Hall & Co.) was solubilized in two liters of water by heating the mixture at 160°C. for 1 min. in a Parr reaction apparatus. The resulting solution was cooled to approximately 90°C., and the amylose complex was precipitated by the rapid addition of two liters of either acetone or methyl ethyl ketone. After waiting 5 min. for the crystals to form, the precipitate was filtered through a Buchner funnel, washed by dispersing the filter cake in the ketone for one minute in a Waring Blendor, and then filtered. The precipitate was washed two times more and the final precipitate was taken as the corresponding wet V complex. The wet V complexes were dried to constant weight at 113°C. over P<sub>2</sub>O<sub>5</sub> at less than 1 mm Hg. for 24 hr. These were taken as the corresponding dry V complexes.

### Procedure for Methanol Exchange

The methanol-exchanged samples were prepared in the following way. The wet acetone, or methyl ethyl ketone V complexes were dispersed in sufficient methanol to make approximately a 5% slurry of the complex in the methanol. The slurry was mixed for 1 min. in a Waring Blendor and then filtered. The step, with fresh methanol, was repeated twice, and the



final precipitate was taken as the corresponding wet V complex. Earlier study had shown that this washing did not remove all the water, and consequently this is the reason for taking this precipitate as the wet complex.

### Carbonyl Analysis

The analysis of the residual acetone or methyl ethyl ketone in the amylose complexes was determined by the hydroxylamine-triethanolamine carbonyl analysis of Klimova and Zabrodina.<sup>10</sup>

### Water Analysis

The water content of the amylose V complexes was determined by using the Karl Fisher reagent. An appropriately sized sample was weighed into a clean dried titration flask, and 50 ml. of anhydrous methanol was added. The slurry was stirred for 15 min. and titrated with a Beckman Aquameter. The Karl Fisher reagent was standardized daily with a known water-in-methanol solution.

### Determination of X-Ray Patterns

The patterns of the V complexes were obtained with a Norelco x-ray diffraction unit using Cu  $K\alpha$  radiation, and a 114.6 mm. powder camera. Exposure times were approximately 9 hr. at 45 k.v. and 18 ma. The samples were prepared by packing the complexes into 0.3 mm. i.d. Pyrex capillaries which were then sealed. All x-ray samples were run within 2 hr. from the time they were prepared and, in most cases, in duplicate.

## RESULTS

The patterns of the acetone and methyl ethyl ketone complexes had only a few broad lines which showed little change on drying, except there was a decrease in the number of lines, and an increase in their width. The patterns could be indexed with the orthorhombic cell, derived from the hexagonal lattice constants previously reported for the butanol and fatty acid complexes, that is,  $a = 13.7$  A.,  $b = 23.8$  A.,  $c = 8.05$  A. Although the number of lines of the ketone complexes was small, the similarity of these cells to the wet butanol cell<sup>5</sup> makes this indexing reasonable. The agreement between the observed and the calculated  $\sin^2\theta$  is shown in Table I for the wet methyl ethyl ketone complex. The acetone complex is identical, with the exception that it had a small number of broader lines.

In order to obtain a measure of the effect of the residual water in the amylose ketone complex as it could possibly affect the helix diameter, the ketone complexes were prepared using from one to nine washes of the complex by the corresponding ketone in the complex. For example, the acetone complex was washed one, two, three, six, and nine times, and the amount of water in each of the samples determined as well as the x-ray diffraction pattern being examined for the size of the helix diameter. Table II contains a summary of the data obtained with multiple-washed acetone

TABLE I  
Powder Diffraction Data of Wet Methyl Ethyl Ketone Complex

Intensity	Orthorhombic	$\sin^2 \theta$	
		Observed	Calculated
m <sup>+</sup>	(100)	0.0038	0.0032
w	(110)	0.0049	0.0042
	(020)		0.0042
w	(120)	0.0077	0.0074
sb	(101)	0.0117	0.0124
	(130)		0.0126
w	(140)	0.0199	0.0199
s	(050)	0.0253	0.0262
	(041)		0.0260
	(221)		0.0261
w <sup>-</sup> b	(310)	0.0302	0.0295
	(231)		0.0313
	(141)		0.0291
w <sup>-</sup>	(061)	0.0473	0.0470
	(251)		0.0481
	(331)		0.0471
w	(450)	0.0767	0.0768
	(162)		0.0775
	(081)		0.0763
	(441)		0.0766
w	(033)	0.0919	0.0919
	(172)		0.0912
	(352)		0.0913
	(422)		0.0914

and methyl ethyl ketone (MEK) complexes. It can be seen from this table that the water levels in the complexes, from as high as 12 moles of water per mole of glucose down to 0.5 mole of water to a mole of glucose, do not have a direct affect upon the size of the helix diameter, since in all cases the helix diameter was the expanded diameter of 13.7 Å. It will be observed from these data in Table II that the water in the acetone-amylose complex is apparently more tenaciously held than in the case of the methyl ethyl ketone-amylose complex.

TABLE II  
Relationship of the Number of Acetone or MEK Washes to the Water Content of the V Complex as it Affects the Helix Diameter

Number of acetone washes	H <sub>2</sub> O/glucose mole ratio	Helix diameter, Å.
1	12/1	13.7
2	3/1	13.7
3	2/1	13.7
6	0.6/1	13.7
9	0.65/1	13.7
3 Washes with MEK	0.55/1	13.7

The residual water in the solvent-washed amylose complexes is not too surprising, since in previous work<sup>2</sup> it was shown that for methanol- and propanol-V amylose complexes, which had been washed three times with the corresponding alcohol, that as much as one mole of water to one mole of glucose remained in each case.

The acetone- and methyl ethyl ketone-amylose V complexes were examined in a series of experiments in which the complexes were extracted three times each with methyl alcohol. Table III summarizes the data obtained from the methanol extracted ketone complexes. Acetone- and methyl ethyl ketone-amylose V complexes, which had been washed three to six times each with the corresponding ketone, were extracted three times each with methyl alcohol. Although the patterns of the ketone complexes prior to methanol extraction were quite diffuse, very clear, sharply defined patterns were obtained with both of these complexes after the methanol exchange. In the case of the acetone-amylose V complex, the methanol extraction effected a rather complete removal of the acetone from the complex as witnessed by the mole ratio of the residual carbonyl to glucose of 1/36. The complex had a water to glucose mole ratio of 1/1. Very interesting was the resulting mixture of two helical diameters, 13.0 A. and 13.7 A. Since the patterns obtained were very sharp, the presence of the two diameter species is unequivocal. In the case of the acetone complex, which was washed six times with acetone prior to methanol extraction, a relatively poor pattern was obtained since this was an old sample; however, a mixture of the two diameter species was observed.

The extraction with methanol of the methyl ethyl ketone complex with methanol gave results which were somewhat different than those obtained with the acetone complex. The residual carbonyl, after three methanol washes of the methyl ethyl ketone complex, was 1 mole of carbonyl per 12 moles of glucose. In the two examples of methyl ethyl ketone complexes shown in Table III, in both cases a helix diameter of 13.7 A. was observed. The x-ray patterns were very sharp, and there was no evidence of the 13.0 A. species as was observed in the acetone complex washed with methanol.

Thorough drying of the wet acetone and methyl ethyl ketone complexes at 113°C. *in vacuo* over P<sub>2</sub>O<sub>5</sub> for 24 hr. gave V complexes whose x-ray diffraction patterns showed helix diameters in both cases of 13.7 A. The

TABLE III  
Methanol-Exchanged Ketone-Amylose V Complexes

	Methanol washes	Carbonyl/ glucose mole ratio	Water/ glucose mole ratio	Helix diameter, A.
3 Acetone washes	3 Washes	1/36	1/1	13.0 and 13.7
3 Acetone washes	"	—	1.4/1	13.0 and 13.7
6 Acetone washes	"	—	1.3/1	13.0 and 13.7
3 MEK washes	"	1/12	1.4/1	13.7
6 MEK washes	"	—	0.8/1	13.7

dried acetone amylose complex had a residual carbonyl content corresponding to 1 mole of acetone per 17 moles of glucose and a residual water content of 1 mole of water per 6.7 moles of glucose. The dried methyl ethyl ketone complex, on the other hand, was virtually devoid of residual methyl ethyl ketone, with a carbonyl content corresponding to 1 mole of methyl ethyl ketone per 80 moles of glucose. The water content of the dried methyl ethyl ketone complex was 1 mole of water per 5 moles of glucose.

The effect upon the helix diameter due to methanol extraction of a wet *n*-propyl alcohol-amylose V complex which had a helix diameter of 13.7 Å. was determined. The wet propanol complex<sup>11</sup> was extracted three times with methyl alcohol in exactly the same manner as the ketones. The wet propanol-amylose complex had a water/glucose ratio of 1/0.9, and there was an excess of propanol in the complex. The propanol amylose complex after extraction with methanol had a helix diameter of 13.0 Å. and a water/glucose ratio of 1/0.8. The residual propanol, as determined by C<sup>14</sup> analysis, was 0.29%, which is roughly equivalent to a propanol/glucose ratio of 1/60. Therefore, 13.7 Å. helix diameters associated with the wet propanol-, wet acetone-, and wet methyl ethyl ketone-amylose complexes, upon extraction with methyl alcohol, were converted to 13.0 Å. helix diameters for the propanol complex, a mixture of 13.0 Å. and 13.7 Å. helix diameters for the acetone complex, and 13.7 Å. helix diameter for the methyl ethyl ketone complex.

## DISCUSSION

The results obtained with the acetone- and methyl ethyl ketone-amylose V complexes demonstrate the determinant role played by the organic complexing agent in affecting the size and symmetry of the amylose V complex unit cell. The effect of water on the size and symmetry of the unit cell is complemented by the effect of the organic complexing agent.

It is clear from the work of Mikus et al.<sup>7</sup> that in the case of some of the higher fatty acids; namely, lauric, oleic, and palmitic, that the presence or absence of water has a definite affect on the diameter of the helix. These workers showed that the hydrated higher fatty acid-amylose V complexes have helix diameters of 13.7 Å. They also showed that the thoroughly dried fatty acid complexes had helix diameters of 13.0 Å. Data on the helical diameters of the higher fatty acid complexes with intermediate amounts of water, would be very interesting in light of the data on the ketone complexes presented in this paper.

It is clear that under all condition of hydration, right through to the thoroughly dried methyl ethyl ketone complex, that the methyl ethyl ketone-amylose complex retains a helix diameter of 13.7 Å. throughout. Further, extraction of the methyl ethyl ketone complex with methyl alcohol is not effective in reducing the helical diameter.

It appears in the case of methyl ethyl ketone complex that the ketone has permanently affected the structure of the crystalline complex, so that

even in the substantial absence of complexing agent, such as in the dried form in which there is 1 mole of residual ketone per 80 moles of glucose, the helix diameter remains at 13.7 Å. In the case of the fairly dried (1 mole of water to 6.7 moles of glucose) acetone-amylose V complex, the expanded helix diameter of 13.7 Å. persists.

This is the first report of a substantially anhydrous amylose V complex which has a helix diameter of 13.7 Å. Coupled with previous work<sup>2</sup> on the lower alcohol complexes in which the amylose V complexes of methanol and ethanol, with a residual water content of 1½ moles of water per mole of glucose, had helix diameters of 13.0 Å., this work demonstrates the size and determinant effect of the complexing agent.

The methyl alcohol extraction of the V complex: (1) changed the propanol complex from a helix diameter of 13.7 Å. to a 13.0 Å., and (2) changed an acetone-amylose complex from 13.7 Å. to a mixture of 13.0 Å and 13.7 Å. species, and (3) was ineffective in reducing the 13.7 Å. helix diameter of the methyl ethyl ketone complex. Thus, the variation of helix diameter is directly correlatable with the residual nonmethanol content. It is interesting that the degree of retention of the organic complexing agent varies. The degree of retention of the organic complexing agent, and the permanent distorting effect, as observed in the enlarged helix diameter of 13.7 Å. of the dried ketone complexes, is probably a function of the size and the dipole properties of the organic complexing agent.

The authors wish to thank Miss Patricia Beckman for her assistance in packing the x-ray samples and reading the powder patterns reported in this paper.

The carbonyl analyses were done by Schwarzkopf Microanalytical Laboratory, Woodside, N. Y.

### References

1. Rundle, R. E., *J. Am. Chem. Soc.*, **69**, 1769 (1947).
2. Valletta, R. M., F. J. Germino, R. E. Lang, and R. J. Moshy, *J. Polymer Sci.*, **A2**, 1085 (1964).
3. Pulley, A. O., Ph.D. Thesis, Iowa State University, 1962.
4. Zaslow, B., *Biopolymers*, **1**, 165 (1963).
5. Rundle, R. E., and F. C. Edwards, *J. Am. Chem. Soc.*, **65**, 2200 (1943).
6. Rundle, R. E., and D. French, *J. Am. Chem. Soc.*, **65**, 1707 (1943).
7. Mikus, F. F., R. M. Hixon, and R. E. Rundle, *J. Am. Chem. Soc.*, **68**, 1115 (1946).
8. Zaslow, B., and R. L. Miller, *J. Am. Chem. Soc.*, **83**, 4378 (1961).
9. Bear, R. S., *J. Am. Chem. Soc.*, **64**, 1388 (1942).
10. Klimova, V. A., and K. S. Zabrodina, *Zhur. Anal. Khim.*, **15**, 726 (1960); *Anal. Abstracts*, **9**, 726 (1962).
11. Germino, F. J., R. M. Valletta, and R. J. Moshy, paper presented at 142nd Meeting, American Chemical Society, Atlantic City, N. J., September 1962.

### Résumé

On a préparé les complexes 'V' acétone- et méthyl-éthyl-cétone-amylose et calculé leurs dimensions cellulaires unitaires à partir des diagrammes de rayons-X (poudres). Ce travail démontre l'influence déterminante des dimensions de ces deux cétones sur le complexe 'V' de l'amylose. La petite cellule unitaire avec un diamètre d'hélice de 13.0 Å, qui a été observée pour les complexes avec le méthanol et l'éthanol humides, n'est

pas trouvée dans le cas des complexes avec l'acétone et la méthyl-éthyl-cétone. Les complexes 'V' cétone-amylose humides et les complexes cétoniques complètement secs, possèdent un diamètre de l'hélice plus grand, 13.7 Å. Ceci constitue le premier exemple décrit d'un complexe anhydre d'amylose ayant un diamètre d'hélice accru. L'extraction intensive pratiquée sur le complexe méthyléthyle-cétone-amylose au moyen d'alcool méthylique ne change pas de diamètre de 13.7 Å bien que dans le cas du complexe acétone amylose l'extraction à l'alcool méthylique provoque l'apparition de deux types de diamètres d'hélices à savoir 13.0 Å et 13.7 Å. Ce travail montre l'effet de la dimension des cétones de bas poids moléculaire sur la structure cristalline de l'amylose.

### Zusammenfassung

Die Aceton- und Methyläthylketon-Amylose-"V"-Komplexe wurden dargestellt und ihre Elementarzeldimensionen aus den Röntgenpulverdiagrammen berechnet. Der grösse-bestimmende Einfluss dieser beiden Ketone auf den Amylose-"V"-Komplex wird gezeigt. Die kleine, an feuchten Methanol- und Äthanolkomplexen beobachtete Elementarzelle mit einem Helixdurchmesser von 13,0 Å wird bei den Aceton- und Methyläthylketonkomplexen nicht gefunden. Die feuchten Keton-Amylose-"V"-Komplexe und die vollständig getrockneten Ketonkomplexe besitzen den grösseren Helixdurchmesser von 13,7 Å. Dies ist der erste Nachweis eines wasserfreien Amylose-"V"-Komplexes mit einem expandierten Helixdurchmesser. Vollständige Extraktion des Methyläthylketon-Amylosekomplexes mit Methylalkohol veränderte den Helixdurchmesser von 13,7 Å nicht, wohl aber führte die Methanolextraktion des Aceton-Amylosekomplexes zu einem Gemisch des Helixtypes vom Durchmesser 13,0 Å und 13,7 Å. In der vorliegenden Arbeit wird der Grösseneinfluss der niedrigerenmolekularen Ketone auf die Kristallstruktur der Amylose gezeigt.

Received June 26, 1963

## Redox Polymerization of Unsaturated Polyester Resins. I. Effect of Metal Species on Polymerization Rates in the Presence of a Variety of Peroxides and Hydroperoxides

GLENN R. SVOBODA, *Freeman Chemical Corporation, Port Washington, Wisconsin*

### Synopsis

A study of a series of metal compounds as promoters of acyl peroxide and hydroperoxide dissociation in an unsaturated polyester-styrene resin solution has shown vanadic and vanadyl chelates to be the most active. All of the results were compared to a standard cobalt-methyl ethyl ketone peroxide promoter-catalyst system. It was found that the reactivity of 2 mg. of vanadium or vanadyl ion as vanadic or vanadyl acetyl acetonate with respect to 1% cumene hydroperoxide was greater than 24 mg. of cobalt as cobalt naphthenate with respect to 1% methyl ethyl ketone peroxide. This is significant, in that considerably less metallic promoter can be used at ambient temperatures for the fabrication of finished articles with considerably less associated color. Of the vanadium compounds studied, vanadic and vanadyl chelates were about equally reactive. Vanadyl acetyl acetonate was considered the promoter of choice, since vanadic acetyl acetonate solutions appeared to be air-oxidized readily. Study has shown that benzene solutions of vanadic acetyl acetonate lost some activity after a week, whereas chloroform solutions of vanadyl acetyl acetonate remained stable for a period of six to nine months. The utility of vanadium promoters for ambient temperature redox polymerization would be enhanced if they could be incorporated into unsaturated polyester resins at the time of preparation. However, results obtained indicated that both vanadic and vanadyl chelates limit the stability of such prepromoted resins, normally leading to gelation in about 17 days. A further indication of the utility of vanadium chelates as redox promoters was the observation that these materials are reactive towards diacyl peroxides as well as hydroperoxides. Vanadium chelates were the only materials studied which showed this wide spectrum of reactivity.

### INTRODUCTION

Cobalt naphthenate or octoate is commonly used to promote the ambient temperature dissociation of methyl ethyl ketone peroxide into free radicals. It was the intent of this investigation to compare the effect of cobalt naphthenate (6% cobalt) with that of a series of other metals. The results indicated that the polymerization rates were dependent upon the type of peroxide used. A redox promoter effective with hydroperoxides may be utterly useless with diacyl peroxides. The peroxides utilized in this study included examples of similar chemical types with different thermal dissociation characteristics.

It was found that both vanadic and vanadyl chelates were much more active toward hydroperoxides than was cobalt naphthenate at an equivalent metal concentration. Of the metallic compounds studied, only vanadium chelates were particularly active in promoting diacyl peroxide dissociation.

## EXPERIMENTAL METHODS

### Materials

The metal chelates of acetyl acetonate were supplied by the McKenzie Chemical Works. The metallic naphthenates were obtained from the Nuodex Products Division of Heyden Newport Corporation.

The unsaturated polyester used in this investigation was a general-purpose *o*-phthalic acid (56.5 mole-%)/maleic (43.5 mole-%)/propylene glycol (78.6 mole-%)/diethylene glycol (21.6 mole-%). The polyester was prepared by a modified fusion process. Initially the ingredients were heated to 93°C. At this point a mild exotherm was noted. When this subsided, the reaction mass temperature was raised rapidly to 210°C, the vapor temperature being controlled at a maximum of 110°C. When the reaction mass temperature reached 210°C, the packed column was removed from the reflux train. At this time, 2% xylene was added to assist in removing the water of condensation. When the reaction mass reached an acid value of 32 and a Gardner-Holt viscosity of R, both measured at 70% solids in methyl cellosolve, the xylene was removed *in vacuo*. The reaction mass was then diluted to 31% styrene content. In addition to 30 ppm hydroquinone initially added to the reactants, sufficient hydroquinone was added to give a system containing 160 ppm hydroquinone. The styrene solution of resin had a 1600 cpoise viscosity and an acid value of 32. When properly cured this resin exhibited a Barcol hardness reading of 40-45.

### Procedure

Determination of ambient temperature redox gel times was made in the following manner. To 100 g. of unsaturated polyester resin solution was added 1 g. of peroxide. After thorough mixing, the appropriate amount of promoter solution was added. The gel time as recorded in this paper is defined as the time from which the promoter was added to that point at which the resin solution would no longer flow together as it was stirred. The temperature was controlled at  $24 \pm 2^\circ\text{C}$ . It is this temperature range which is defined as ambient temperature.

## RESULTS AND DISCUSSION

### Evaluation of Metals as Possible Promoters

The activity of a series of metals with both diacyl peroxides and hydroperoxides is compared with the results obtained with methyl ethyl ketone



peroxide in Table I. Examples of similar chemical types of peroxides with higher and lower thermal dissociation characteristics are included.

Of the series of metals studied, both vanadic and vanadyl acetyl acetonate exhibited exceptional activity. The spectrum of activity of these promoters extended to acyl peroxides as well as hydroperoxides. Only the vanadium compounds were more reactive toward methyl ethyl ketone peroxide than was cobalt naphthenate.

### Study of Vanadium Chelates

The high activity of both vanadic and vanadyl chelates with all of the peroxides studied indicated that dilution studies were desirable. For this study, vanadic acetyl acetonate was prepared as a 2% metal solution, whereas vanadyl acetyl acetonate was prepared as a 2% vanadyl ion solution, both in chloroform. Table II is a summary of the results obtained.

### Study of other Vanadium Compounds

During the course of this study, publications describing the use of vanadium compounds as ambient temperature free-radical promoters were published. The first of these<sup>1</sup> described the use of vanadium pentoxide as a solution in di-*n*-butyl phosphate. An attempt to prepare a 1% metal solution showed that vanadium pentoxide was only sparingly soluble in the cited solvent. This was further indicated by the comparison data for gel times with vanadium pentoxide vs. vanadic and vanadyl acetyl acetonates with 1% cumene hydroperoxide (Table III).

Due to the plasticizing effect exhibited by the use of more than 5 ml. of saturated vanadium pentoxide solution per 100 g. of resin, further investigation was discontinued.

Other references<sup>2,3</sup> described the use of vanadium compounds in the valence range of +2 to +5, used in conjunction with benzene phosphinic acid. The results of the present study are comparable to the results cited<sup>2,3</sup> at an equivalent metal concentration, but do not require the auxiliary phosphinic acid.

Ammonium vanadyl tartrate was also investigated as a promoter. The insolubility of this compound in various solvents prevented thorough evaluation, although some activity was noted.

### Investigation of Vanadyl Acetyl Acetonates Promoted Resins

The results in Table II showed that approximately the same gel times would be obtained at the same metal concentration regardless of the valence state of the vanadium chelate, although the vanadic chelate tended to give slightly shorter gel times. Due to stability considerations, it was decided to use vanadyl acetyl acetonate. Solutions of vanadyl acetyl acetonate declined in activity after about a week. The gel times noted were based on the addition of 1% cumene hydroperoxide to periodically withdrawn samples of a larger batch of unsaturated polyester prepared

TABLE I  
Ambient Temperature Gel Times of an Unsaturated Polyester Obtained with a Series of Different Metals (0.024 g.) and Peroxides (1.0 g.)

Metal	Form of metal	Gel time					
		<i>tert</i> -Butyl hydroperoxide	Cumene hydroperoxide	Acetyl peroxide	Benzoyl peroxide	Methyl ethyl ketone peroxide	
Co	Naphthenate <sup>a</sup>	42 hr.	89 hr.	105 hr.	128 hr.	34.3 min.	
Co <sup>+3</sup>	Acetyl acetone <sup>b</sup>	94 hr.	41 hr.	105 hr.	> 128 hr.	7.5 hr.	
Cr <sup>+3</sup>	Acetyl acetone <sup>b</sup>	>116 hr.	>164 hr.	129 hr.	>128 hr.	13.0 hr.	
Cu <sup>+2</sup>	Acetyl acetone <sup>a</sup>	18 hr.	96 hr.	16 hr.	>128 hr.	130.0 hr.	
Mn <sup>+2</sup>	Acetyl acetone <sup>d</sup>	93 hr.	57 hr.	>117 hr.	>117 hr.	19.0 hr.	
Mn <sup>+3</sup>	Acetyl acetone <sup>b</sup>	71 hr.	8.5 hr.	105 hr.	>128 hr.	13.0 hr.	
V <sup>+3</sup>	Acetyl acetone <sup>b</sup>	30 sec.	20 sec.	5 min.	32.3 min.	5.7 sec.	
Vo <sup>+2</sup>	Acetyl acetone <sup>e</sup>	30 sec.	20 sec.	7 hr.	29 hr.	105 sec.	
Fe <sup>+3</sup>	Acetyl acetone <sup>b</sup>	16 hr.	164 hr.	11.5 min.	75 hr.	16.0 hr.	
Ti <sup>+3</sup> -Ti <sup>+6</sup>	Acetyl acetone <sup>o,l</sup>	>117 hr.	106 hr.	>117 hr.	>117 hr.	2.3 hr.	
Al <sup>+3</sup>	Acetyl acetone <sup>g</sup>	>53 hr.	>46 hr.	46 hr.	>50 hr.	24.0 hr.	
Th <sup>+4</sup>	Acetyl acetone <sup>g</sup>	>53 hr.	>46 hr.	>120 hr.	>50 hr.	70.0 hr.	
Be <sup>+2</sup>	Acetyl acetone <sup>h</sup>	>53 hr.	>46 hr.	8.5 hr.	>50 hr.	10.3 hr.	
Ni <sup>+3</sup>	Acetyl acetone <sup>i</sup>	>53 hr.	>46 hr.	>120 hr.	>50 hr.	70.0 hr.	
Pb <sup>+2</sup>	Naphthenate <sup>j</sup>	>116 hr.	>164 hr.	>115 hr.	>128 hr.	94.0 hr.	
Zn <sup>+2</sup>	Naphthenate <sup>k</sup>	>116 hr.	>164 hr.	>115 hr.	>128 hr.	68.0 hr.	
Ca <sup>+2</sup>	Naphthenate <sup>l</sup>	>116 hr.	>164 hr.	>115 hr.	>128 hr.	80.0 hr.	

Ce <sup>+4</sup>	Naphthenate <sup>m</sup>	>116 hr.	>164 hr.	>115 hr.	>128 hr.	62.0 hr.
La and Ce	Naphthenate <sup>n</sup>	>116 hr.	>164 hr.	>115 hr.	>128 hr.	75.0 hr.
Zr	unidentified complex <sup>o</sup>	>116 hr.	>164 hr.	>115 hr.	>128 hr.	88.0 hr.
Ba <sup>+2</sup>	Acetyl acetone <sup>o</sup>	>53 hr.	>46 hr.	>120 hr.	>50 hr.	22.0 hr.
Hg <sup>+2</sup>	Phenyl-mercury oleate <sup>p</sup>	>53 hr.	>46 hr.	>120 hr.	>50 hr.	70.0 hr.
Sn <sup>+2</sup>	Octoate <sup>q</sup>	>53 hr.	>46 hr.	>120 hr.	>50 hr.	70.0 hr.

<sup>m</sup> 6% Co.

<sup>n</sup> Prepared as 2% metal in benzene.

<sup>o</sup> Prepared as 2% metal in chloroform.

<sup>p</sup> Prepared as a saturated solution. (<2%) in deoxygenated chloroform; the Mn<sup>+2</sup> acetyl acetone was not readily soluble in chloroform until the solution had darkened to the Mn<sup>+3</sup> solution color.

<sup>q</sup> Prepared as 2% VO<sup>+2</sup> in chloroform.

<sup>r</sup> Hexachloride complex.

<sup>s</sup> Prepared as 1% metal in chloroform.

<sup>t</sup> Prepared as 0.5% metal in chloroform.

<sup>u</sup> Prepared as a saturated (<2%) solution in chloroform.

<sup>v</sup> 24% Pb.

<sup>w</sup> 8% Zn.

<sup>x</sup> 4% Ca.

<sup>y</sup> 6% Ce.

<sup>z</sup> 4% metal.

<sup>aa</sup> 6% Zr.

<sup>ab</sup> 11% Hg.

<sup>ac</sup> 28% Sn.

TABLE II  
Ambient Temperature Gel Times and Times to Maximum Barcol Development (Complete Polymerization) of a Series of Dilutions of Vanadium Chelates<sup>a</sup>

Vol. 2% solution, ml.	Cumene hydroperoxide		<i>tert</i> -Butyl hydroperoxide		Methyl ethyl ketone peroxide		Benzoyl peroxide		Acetyl peroxide	
	Gel time	Time to Barcol 40	Gel time	Time to Barcol 40	Gel time	Time to Barcol 40	Gel time	Time to Barcol 40	Gel time	Time to Barcol 40
1.20 V <sup>+3</sup>	20 sec.	Instant	30 sec.	Instant	13.3 min.	35 min.	12 min. <sup>b</sup>	2 days	4 hr.	19 hr.
0.60 V <sup>+3</sup>	35 sec.	Instant	45 sec.	15 min.	33.3 min	1.5 hr.	53.5 min. <sup>c</sup>	5 days	5 hr.	25 hr.
0.30 V <sup>+3</sup>	60 sec.	7 min.	105 sec.	43 min.	42 min.	3 days	—	—	6 hr.	35 hr.
0.10 V <sup>+3</sup>	24 min.	29 hr.	22.5 min.	24.5 hr.	54 min.	4 days	—	—	27 hr.	3 days
0.05 V <sup>+3</sup>	84 min.	53 hr.	1.5 hr.	58 hr.	—	—	—	—	—	—
0.01 V <sup>+3</sup>	13 hr.	6 days	4 hr.	3 days	—	—	—	—	—	—
1.20 VO <sup>+2</sup>	20 sec.	Instant	27 sec.	Instant	3 min.	30 min.	16.5 hr. <sup>b</sup>	5.5 days	4.5 hr. <sup>b</sup>	30 hr.
0.60 VO <sup>+2</sup>	20 sec.	Instant	36 sec.	Instant	13 min.	40 min.	1.5 days <sup>b</sup>	7 days	5.5 hr. <sup>c</sup>	40 hr.
0.30 VO <sup>+2</sup>	100 sec.	10.5 min.	9.5 min.	8 hr.	35 min.	5.5 hr.	—	—	—	—
0.10 VO <sup>+2</sup>	28 min.	15 hr.	50 hr.	35 hr.	44 min.	2.5 days	—	—	—	—
0.05 VO <sup>+2</sup>	101 min.	2 days	4 hr.	3 days	—	—	—	—	—	—
0.01 VO <sup>+2</sup>	17.5 hr.	8 days	7.5 hr.	7 days	—	—	—	—	—	—

<sup>a</sup> The dilution study was discontinued when complete polymerization was not obtained within several days.

<sup>b</sup> 3.6 cc.

<sup>c</sup> 2.4 cc.

TABLE III

Solution and volume, ml.	Gel time, min.
2% V <sup>+3</sup> , 0.10	24
2% VO <sup>+2</sup> , 0.10	28
Sat'd V <sub>2</sub> O <sub>5</sub> , 5.0	89

to contain 2 mg. of vanadyl ion as vanadyl acetyl acetate per 100 g. of resin. Such a resin is known commercially as a prepromoted resin. The high activity of vanadium chelates as gelation promoters even without any added peroxide was evidenced by the fact that a maximum of 15 days prepromoted resin stability was obtained.

### References

1. Allen, L. H., *Plastics (London)*, **25**, 250 (1960).
2. Brit. Patent 840,021 (November 10, 1958), to Allied Chemical Co.
3. Marazewski, C. A., and J. O. Koontz, U. S. Patent (October 10, 1961), to Allied Chemical Co.

### Résumé

L'étude d'une série de composés métalliques, promoteurs de la dissociation de peroxyde d'acyle et d'hydroperoxydes, dans une solution d'une résine polyester insaturé/polystyrène, a montré que les chélates vanadiques et de vanadyle sont les plus actifs. Tous les résultats ont été comparés avec le système standard catalyseur/promoteur (système cobalt/péroxyde de la méthyléthylcétone). Il a été trouvé que la réactivité de 2 mg d'ion vanadium ou vanadyle sous forme d'acétylacétate vanadique ou de vanadyle par rapport à un pourcent d'hydroperoxyde de cumène est plus grande que 24 mg de cobalt sous forme de naphthénate par rapport à un pourcent de peroxyde de méthyléthylcétone. Ceci montre qu'on peut utiliser considérablement moins de promoteur métallique à température ambiante pour la fabrication d'articles finis avec une coloration concomitante considérablement aminodiée. Des composés de vanadium étudiés, les chélates vanadiques et de vanadyle sont à peu près équivalents. Il s'est avéré que l'acétylacétate de vanadyle était le promoteur de choix, la solution d'acétylacétate vanadique s'oxydant rapidement à l'air. Les études ont montré que des solutions benzéniques d'acétylacétate vanadique ont perdu une partie de leur réactivité après une semaine alors que des solutions chloroformiques d'acétylacétate de vanadyle restent stables pour une période de six à neuf mois. L'utilité de promoteurs au vanadium pour les polymérisations redox à température ambiante serait considérablement augmentée s'ils pouvaient être incorporés dans des résines de polyesters insaturés au moment de la préparation. Néanmoins, les résultats obtenus indiquent que et les chélates de vanadyles et les chélates vanadiques limitent la stabilité des résines ainsi pré-initiées conduisant à une gélification endéans les seize jours environ. Une indication supplémentaire de l'utilité des chélates de vanadium en tant que promoteurs redox est le fait que ces substances réagissent aussi bien avec les peroxydes de diacyle que les hydroperoxydes. Les chélates de vanadium sont les seuls parmi les substances étudiées qui montrent un aussi large spectre de réactivité.

### Zusammenfassung

Bei der Untersuchung einer Reihe von Metallverbindungen als Promotoren der Acylperoxyd- und Hydroperoxyddissoziation in der Lösung eines ungesättigten Polyester-Styrol-Harzes zeigten Vanadium(V)- und Vanadylchelate die höchste Aktivität. Alle Ergebnisse wurden mit einem aus Cobalt und Methyläthylketonperoxyd bestehenden

Promotor-Katalysator-System als Standard verglichen. Die Reaktionsfähigkeit von 2 mg Vanadium oder Vanadylion als Vanadium(V)- oder Vanadyl-acetylacetonat für 1% Cumolhydroperoxyd ist grösser als diejenige von 24 mg Cobalt oder Cobaltnaphthenat für 1% Methyläthylketonperoxyd. Dies ist insofern von Bedeutung, als merklich weniger metallischer Promotor bei Raumtemperatur zur Herstellung bedeutend schwächer gefärbter Fertigprodukte verwendet werden kann. Von den untersuchten Vanadiumverbindungen waren Vanadium(V)- und Vanadylchelate etwa gleich reaktionsfähig. Vanadyl-acetylacetonat ist der beste Promotor, da Vanadium(V)-acetylacetonat-Lösungen anscheinend leicht von der Luft oxydiert werden. Während die Aktivität benzolischer Lösungen von Vanadium(V)-acetylacetonat innerhalb einer Woche etwas abnimmt, sind Chloroformlösungen von Vanadyl-acetylacetonat sechs bis neun Monate lang stabil. Die Brauchbarkeit von Vanadiumpromotoren zur Redoxpolymerisation bei Raumtemperatur würde erhöht, wenn diese zum Zeitpunkt der Herstellung in ungesättigte Polyesterharze eingeführt werden könnten. Wie jedoch die experimentellen Befunde ergaben, beschränken sowohl Vanadium(V)- als auch Vanadylchelate die Stabilität solcher vorher mit einem Promotor versetzten Harze, indem sie normalerweise zur Gelbildung nach etwa siebzehn Tagen führen. Die Brauchbarkeit von Vanadiumchelaten als Redoxpromotoren geht ausserdem aus der Beobachtung hervor, dass diese Stoffe gegen Diacylperoxyde ebenso wie gegen Hydroperoxyde reaktionsfähig sind. Die Vanadiumchelate haben als einzige von den untersuchten Stoffen ein so weites Reaktivitätsspektrum.

Received April 18, 1963

Revised July 5, 1963

## Redox Polymerization of Unsaturated Polyester Resins. II. Effect of Copromoter Metals on the Redox Polymerization Activity of Vanadium Chelates

GLENN R. SVOBODA, *Freeman Chemical Corporation, Port Washington, Wisconsin*

### Synopsis

Of a series of copromoter metal species investigated, it was found that several of these were strongly effective in synergizing the redox polymerization activity of vanadyl acetyl acetonate. Notable among these were  $\text{Cu}^{+2}$ ,  $\text{Fe}^{+3}$ ,  $\text{Ti}^{+3}$ - $\text{Ti}^{+6}$ ,  $\text{Be}^{+2}$ ,  $\text{Al}^{+3}$ , and  $\text{Th}^{+4}$ . Particularly notable was the effect of  $\text{Ti}^{+3}$ - $\text{Ti}^{+6}$ , which strongly synergized the rate at which complete polymerization was obtained, eg., within 15 min. as compared to 20 hr. when vanadyl acetyl acetonate was used alone. Synergism with copromoter metal species was noted with as low as 2 mg. titanium used in conjunction with 2 mg. of vanadyl ion as the chelate. A minimal concentration for synergistic effect was noted for those metal species thus studied. This was found to range from 0.18 to 0.41 mmole of copromoter metal species per 100 g. of resin system. Advantage was taken of the peculiar effect of manganic acetyl acetonate to prolong gel times without affecting the rate at which complete polymerization was obtained. By using manganic acetyl acetonate in conjunction with vanadyl acetyl acetonate, it was possible to prolong the shelf-life of a prepromoted resin from 17 to at least 110 days.

### INTRODUCTION

A study of the possible synergistic effects of a series of metals with vanadium chelates as redox copromoters in the presence of acyl peroxides and hydroperoxides is presented. The effect of these systems upon the polymerization rates of a general purpose unsaturated polyester indicated also that some of the metals studied inhibit the strongly promoting effect of vanadium chelates. The inhibiting effect was studied as a possible route to producing a stable resin system prepromoted with vanadium chelates.

### EXPERIMENTAL AND RESULTS

#### Effect of a Series of Metals Species as Copromoters of Vanadium Chelates

A study of the possible synergistic effects of a series of metals was carried out in the following manner. To 100 g. of a general-purpose polyester<sup>1</sup> was added 2 mg. of vanadyl ion (as 7.94% vanadyl acetyl acetonate in chloroform) and 24 mg. of the copromoter metal. Each of

TABLE I  
Effect of Various Metal Species (24 mg. Metal) Upon the Redox Polymerization Rates of an Unsaturated Polyester Resin System Containing Vanadyl Acetyl Acetonate and 1% of the Designated Peroxide Component

Copolymer metal	Gel time				
	Cumene hydroperoxide	<i>tert</i> -Butyl hydroperoxide	Methyl ethyl ketone peroxide	Benzoyl peroxide <sup>a</sup>	Acetyl peroxide <sup>b</sup>
2 mg. VO <sup>+2</sup> blank	18.3 min.	40.8 min.	1.5 hr.	17.0 hr.	7.5 hr.
24 mg. Co octoate blank	—	—	31.3 min.	—	—
Co <sup>+2</sup>	4.3 hr.	5.6 hr.	26.0 min.	72.0 hr.	10.5 hr.
Cr <sup>+3</sup>	11.8 min.	32.3 min.	1.5 hr.	26.0 hr.	10.0 hr.
Cr <sup>+6</sup>	10.5 min.	31.3 min.	2.5 hr.	26.5 hr.	10.0 hr.
Cu <sup>+2</sup>	5.2 min.	13.3 min.	48.8 min.	26.0 hr.	3.5 hr.
Mn <sup>+2</sup>	83.3 min.	95.5 min.	2.4 hr.	15.5 hr.	9.0 hr.
Fe <sup>+2</sup>	4.3 min.	10.0 min.	3.3 hr.	2.0 hr.	2.2 hr.
La + Ce <sup>d</sup>	2.5 hr.	9.8 hr.	13.5 hr.	18.0 hr.	9.2 hr.
Pb <sup>+2</sup>	13.0 min.	52.5 min.	72.0 hr.	17.5 hr.	10.5 hr.
Zn <sup>+2</sup>	9.0 min.	25.8 min.	12.5 hr.	72.0 hr.	7.0 hr.
Ca <sup>+2</sup>	49.7 min.	35.3 min.	14.5 hr.	72.0 hr.	9.0 hr.
Ce <sup>d</sup>	2.8 hr.	8.3 hr.	38.5 hr.	72.0 hr.	10.0 hr.
Zr <sup>e</sup>	24.3 min.	30.5 min.	21.0 hr.	17.0 hr.	9.6 hr.
Ti <sup>+3</sup> -Ti <sup>+6</sup>	4.5 min.	5.6 min.	2.0 hr.	4.0 hr.	6.6 hr.
Be <sup>+2</sup>	4.3 min.	11.7 min.	93.5 min.	18.0 hr.	4.0 hr.
Al <sup>+3</sup>	4.3 min.	8.3 min.	2.5 hr.	18.0 hr.	2.0 hr.
Ni <sup>+2</sup>	19.0 min.	24.0 min.	2.5 hr.	>49 hr.	11.0 hr.
Th <sup>+4</sup>	9.2 min.	26.2 min.	>48.0 hr.	40.0 hr.	31.0 hr.
Ba octoate	73.0 min.	3.0 hr.	>48.0 hr.	>49.0 hr.	32.0 hr.
Phenylmercury octoate	14.0 min.	18.4 min.	2.5 hr.	45.0 hr.	36.0 hr.
Sn <sup>+2</sup> octoate	24.4 min.	30.7 min.	2.5 hr.	>49.0 hr.	16.0 hr.

<sup>a</sup> 36 mg. VO<sup>+2</sup>. <sup>b</sup> 24 mg. VO<sup>+2</sup>. <sup>c</sup> As the acetyl acetonate; 24 mg. metal. <sup>d</sup> As the naphthenate; 24 mg. metal. <sup>e</sup> As an undefined complex 24 mg. metal.



TABLE II  
Relationship of Gel Time to Rate of Attainment of Maximum Ambient Temperature Redox Cure for a Series of Metals Synergistic with Vanadyl Acetyl Acetate with Respect to at Least One of the Peroxides Studied

Copolymer metal	Cumene hydroperoxide		<i>tert</i> -Butyl hydroperoxide		Methyl ethyl ketone peroxide		Benzoyl peroxide		Acetyl peroxide	
	Gel time	Time to Barcol 40	Gel time	Time to Barcol 40	Gel time	Time to Barcol 40	Gel time	Time to Barcol 40	Gel time	Time to Barcol 40
2 mg. VO <sup>+2</sup> blank	20.3 min.	20.0 hr.	30.0 min.	22.0 hr.	86.0 min.	66.0 hr.	17.0 hr.	>3 days	7.5 hr. <sup>a</sup> 32.0 hr. <sup>b</sup>	4.0 days 5.0 days
24 mg. Co octoate, blank	—	—	—	—	31.3 min.	41.0 hr.	—	—	—	—
Co octoate	—	—	—	—	26.0 min.	42.0 hr.	—	—	—	—
Co <sup>+3</sup>	11.8 min.	20.0 hr.	32.2 min.	11.5 hr.	90.0 min.	19.0 hr.	—	—	—	—
Cr <sup>+3</sup>	10.5 min.	20.0 hr.	—	—	2.5 hr.	25.0 hr.	—	—	—	—
Cu <sup>+2</sup>	5.2 min.	4.0 hr.	13.3 min.	7.0 hr.	48.9 min.	1.5 hr.	—	—	3.5 hr. <sup>a</sup>	3.0 days
Mn <sup>+3</sup>	83.3 min.	26.0 hr.	95.5 min.	33.5 hr.	2.3 hr.	30.0 hr.	15.5 hr. <sup>c</sup>	>3 days	8.5 hr. <sup>a</sup>	3.0 days
Fe <sup>+3</sup>	4.3 min.	2.0 hr.	10.0 min.	6.5 hr.	3.3 hr.	12.7 hr.	2.0 hr. <sup>c</sup>	42.5 hr.	2.2 hr. <sup>a</sup>	2.5 days
Pb <sup>+2</sup>	13.0 min.	37.0 hr.	—	—	—	—	—	—	—	—
Zn <sup>+2</sup>	9.0 min.	36.0 hr.	25.8 min.	15.5 hr.	—	—	—	—	7.0 hr. <sup>a</sup>	4.0 days
Zr	—	—	—	—	—	—	—	—	9.6 hr. <sup>a</sup>	3.0 days
Ti <sup>+3</sup> -Ti <sup>+6</sup>	4.5 min.	15.0 min.	5.6 min.	24.0 min.	—	—	—	—	6.6 hr. <sup>a</sup>	3.0 days
Be <sup>+2</sup>	4.3 min.	4.1 hr.	11.7 min.	16.0 hr.	93.3 min.	11.0 hr.	—	—	4.0 hr. <sup>b</sup>	4.0 days
Al <sup>+3</sup>	4.3 min.	1.0 hr.	8.3 min.	17.0 hr.	2.5 hr.	30.0 hr.	—	—	2.1 hr. <sup>b</sup>	4.0 days
Ni <sup>+3</sup>	19.0 min.	16.8 hr.	24.0 min.	17.0 hr.	2.5 hr.	28.0 hr.	—	—	—	—
Th <sup>+4</sup>	9.2 min.	24.0 hr.	26.2 min.	50.0 hr.	—	—	—	—	—	—

<sup>a</sup> 24 mg. VO<sup>+2</sup>.<sup>b</sup> 20 mg. VO<sup>+2</sup>.<sup>c</sup> 36 mg. VO<sup>+2</sup>.

these systems was catalyzed with 1% of a series of peroxides and hydroperoxides as noted in Table I. All of the results were compared to the ambient temperature ( $24^{\circ} \pm 2^{\circ}\text{C}$ .) gel times obtained with 2 mg. of vanadyl ion (as the chelate solution) along with 1% of the peroxide.

The identity of the metallic species has been described previously.<sup>1</sup> The gel time was considered to be the time from which the vanadium chelate was added to the resin, containing the peroxide component and the copromoter metal to the time at which the resin would no longer flow together when stirred.

Of particular interest was the relationship of the gel time to the time of development of complete polymerization (time to a 40 Barcol reading) for synergistic metal systems. The results are noted in Table II.

As can be noted in Table I, some of the metal species combinations were antagonistic in effect as measured by the polymerization rates. Only those results which indicate a synergistic effect of the copromoter metal species as compared to the results obtained with  $\text{VO}^{+2}$  alone are presented in Table II.

Synergism of several types was noted. One type was typified by a decrease in gel time and an increase in the rate of cure. Excellent examples of this type are the systems  $\text{VO}^{+2}/\text{Cu}^{+2}$ ,  $\text{VO}^{+2}/\text{Fe}^{+3}$ ,  $\text{VO}^{+2}/\text{Ti}^{+3}-\text{Ti}^{+6}$  (very dramatic),  $\text{VO}^{+2}/\text{Be}^{+2}$ ,  $\text{VO}^{+2}/\text{Al}^{+3}$ , all with hydroperoxides. Another type of synergism was typified by a decrease in gel time without effect upon the rate of cure. Examples of this type are the systems  $\text{VO}^{+2}/\text{Th}^{+4}$  with cumene hydroperoxide,  $\text{VO}^{+2}/\text{Ni}^{+3}$  with *tert*-butyl hydroperoxide, and  $\text{VO}^{+2}/\text{Be}^{+2}$  and  $\text{VO}^{+2}/\text{Al}^{+3}$ , both with acetyl peroxide. A third type of synergism was that in which the gel time was basically unaffected but in which the rate of cure was increased. Examples of this type include the systems  $\text{VO}^{+2}/\text{Ni}^{+3}$  with cumene hydroperoxide,  $\text{VO}^{+2}/\text{Co}^{+3}$ ,  $\text{VO}^{+2}/\text{Zr}^{+2}$ , and  $\text{VO}^{+2}/\text{Ni}^{+3}$  with *tert*-butyl peroxide,  $\text{VO}^{+2}/\text{Be}^{+2}$  with methyl ethyl ketone peroxide, and  $\text{VO}^{+2}/\text{Mn}^{+3}$ ,  $\text{VO}^{+2}/\text{Zr}$ ,  $\text{VO}^{+2}/\text{Ti}^{+3}-\text{Ti}^{+6}$ , all with acetyl peroxide. One interesting observation of copromoter species was the effect of lengthening the gel time without significantly affecting the rate of polymerization. Such an example is  $\text{VO}^{+2}/\text{Mn}^{+3}$  with cumene hydroperoxide. Other effects of copromotion were noted in other individual examples.

The effect of metal copromotion was most readily noted with hydroperoxides and methyl ethyl ketone peroxide, (a mixture of peroxides which include hydroperoxide types). Only  $\text{VO}^{+2}/\text{Fe}^{+3}$ ,  $\text{VO}^{+4}/\text{Cu}^{+2}$ , and  $\text{VO}^{+2}/\text{Al}^{+3}$ , gave significant effects with one or both of the diacyl peroxide examples studied.

#### Determination of the Optimum Concentration of Copromoter Metal Species for Use with Vanadyl Chelate

A study of the effect of several active copromoter metal species concentration upon the gel time and rate of polymerization was next investigated. The results of this study are presented in Table III.

TABLE III  
Effect of Concentration Upon the Polymerization of the System 100 g. Unsaturated Polyester Resin, 1% Hydroperoxide, Vanadyl Chelate (2 mg. as VO<sup>+2</sup>) and Copromoter Concentration As Noted

Copromoter metal	Amt. copromoter, mg. metal	Cumene hydroperoxide		<i>tert</i> -Butyl hydroperoxide	
		Gel time	Time to Barcol 40	Gel time	Time to Barcol 40
VO <sup>+2</sup>	2	20.3 min.	20.0 hr.	30.0 min.	22.0 hr.
Fe <sup>+3</sup>	24	4.3 min.	2.0 hr.	29.0 min.	18.0 hr.
	16	3.3 min.	15.0 hr.	10.8 min.	17.0 hr.
	8	3.25 min.	16.0 hr.	13.3 min.	17.5 hr.
	2	6.0 min.	>17.0 hr.	—	—
Ti <sup>+3</sup> -Ti <sup>+6</sup>	24	4.5 min.	15.0 min.	5.1 min.	24.0 min.
	16	4.5 min.	16.0 min.	5.0 min.	1.0 hr.
	8	3.4 min.	17.0 min.	4.6 min.	16.7 hr.
	2	5.3 min.	18.0 hr.	6.8 min.	17.0 hr.
Cu <sup>+2</sup>	28	5.2 min.	4.0 hr.	9.8 min.	7.0 hr.
	24	4.0 min.	4.75 hr.	8.8 min.	6.0 hr.
	18	4.0 min.	4.6 hr.	9.6 min.	8.0 hr.
	12	5.5 min.	6.0 hr.	—	—
Zn <sup>+2</sup>	24	9.0 min.	36.0 hr.	27.8 min.	45.0 hr.
	12	9.1 min.	30.0 hr.	20.0 min.	44.0 hr.
	6	—	—	22.0 min.	45.0 hr.

The effect of copromoter metal concentration upon the polymerization of vanadyl chelate-promoted, hydroperoxide-catalyzed, unsaturated polyester systems was most dramatic in the case of titanium. Below 8 mg./100 g. resin with respect to cumene and 16 mg./100 g. resin with respect to *tert*-butyl hydroperoxide, the rate of polymerization falls drastically. In all other examples studied, it appeared that a concentration of 0.18 to 0.41 mmole copromoter metal gave the optimum relationship between gel time and time to complete cure.

#### Attempt to Prepare a Stable Prepromoted Resin via a Copromoted Route

Previous attempts<sup>1</sup> to prepare a stable, prepromoted, unsaturated polyester resin system with vanadyl acetyl acetonate resulted in polymerization of the system within 17 days. The unusual effect of lengthening gel time without affecting complete polymerization time, as noted with the VO<sup>+2</sup>/Mn<sup>+3</sup> system with cumene hydroperoxide, indicated that such a system might be utilized to prepare a stable prepromoted system.

Since the effect of copromotion of VO<sup>+2</sup> with Mn<sup>+3</sup> was a lengthening of gel time, it was decided to use more VO<sup>+2</sup> to give a desired 15–20 min. gel time. The following system was prepared. To 5 gal. of unsaturated polyester resin<sup>1</sup> was added 40 mg. VO<sup>+2</sup>, 80 mg. Mn<sup>+3</sup> (both as acetyl acetonate solutions in chloroform) per each 100 g. of resin. Periodically 100-g. aliquots were withdrawn and catalyzed with 1 g. cumene hydroperoxide. The gel times obtained are recorded in Table IV.

TABLE IV  
Gel Times Noted For the System, 100 g. Resin, 40 mg. VO<sup>+2</sup>, 80 mg. Mn<sup>+3</sup> and 1 g. Cumene Hydroperoxide At Cited Time Interval After Preparation

Interval after preparation, days	Average gel time, min.
6	12.33
8	15.00
13	17.38
19	15.04
26	16.38
42	20.88
68	25.53
81	19.25
92	16.25
110	14.25
125	Gelled

The results of Table IV indicate that manganic acetyl acetonate can be utilized to stabilize a resin prepromoted with vanadyl acetyl acetonate for a period of almost four months as compared to a shelf-life of only a half month with the vanadyl chelate alone. Such a procedure made possible the practical application of vanadium prepromoted resins, enabling one to overcome the objection of multicomponent systems.

### Reference

1. Svoboda, G. R., *J. Polymer Sci.*, **A2**, 2715 (1964).

### Résumé

Sur une série d'espèces métalliques cocatalysatrices étudiées on en a trouvé plusieurs qui sont fort efficaces pour augmenter l'activité de polymérisation rédox de l'acétate de vanadyle. Parmi ceux-ci il y a Cu<sup>+2</sup>, Fe<sup>+3</sup>, Ti<sup>+3</sup>-Ti<sup>+6</sup>, Be<sup>+2</sup>, Al<sup>+3</sup> et Th<sup>+4</sup>. Particulièrement appréciable est l'effet de Ti<sup>+6</sup>-Ti<sup>+6</sup> qui accélère fortement la vitesse à laquelle une polymérisation totale est obtenue: elle se ramène à 15 min. alors quelle est de 20 heures lorsque seul l'acétylacétonate est utilisé. On observe une accélération avec ces espèces métalliques cocatalysatrices même pour des quantités aussi faibles que 2 mg de titane en conjonction avec 2 mg d'ion vanadyle comme chélate. Pour ces espèces métalliques on a noté une concentration minimale pour observer l'effet d'activation. Elle s'étend de 0.18 à 0.41 mM d'espèce métallique cocatalysatrice par 100 g de résine. On a pris avantage de l'effet particulier de l'acétylacétonate de manganèse qui prolonge la durée de l'état gel sans affecter la vitesse à laquelle on obtient la polymérisation complète. En utilisant de l'acétylacétonate de manganèse en conjonction avec de l'acétylacétonate de vanadyle, il est possible de prolonger de 17 jusqu'au 110 jours la durée de vie d'une résine préactivée.

### Zusammenfassung

Es wurde eine Reihe von Metallverbindungen hinsichtlich ihrer Eignung als Copromotoren untersucht und gefunden, dass einige von ihnen die Aktivität von Vanadylacetylacetonat bei der Redoxpolymerisation stark erhöhen. Erwähnenswert sind davon Cu<sup>+2</sup>, Fe<sup>+3</sup>, Ti<sup>+3</sup>-Ti<sup>+6</sup>, Be<sup>+2</sup>, Al<sup>+3</sup> und Th<sup>+4</sup>. Besonders bemerkenswert ist die starke synergetische Wirkung von Ti<sup>+3</sup>-Ti<sup>+6</sup>, bei dessen Verwendung die Polymerisationsdauer

bis zum vollständigen Umsatz stark herabgesetzt wird, z.B. auf 15 Min. im Vergleich zu 20 Std. bei Verwendung von Vanadylacetylacetonat allein. Die synergetische Wirkung von Copromotor-Metallverbindungen wurde noch bei Verwendung so geringer Mengen wie 2 mg Titan in Verbindung mit 2 mg Vanadylion als Chelat festgestellt. Die zur synergetischen Wirkung dieser Metallverbindungen nötige minimale Konzentration liegt im Bereich von 0,18 bis 0,41 *mM* Copromotor-Metallverbindung auf 100 g des Harzsystems. Die besondere Wirkung von Mangan(III)-acetylacetonat, die Zeit bis zur Gelbildung, ohne Beeinflussung der zur Erreichung vollständiger Polymerisation nötigen Zeit, zu verlängern, wurde ausgenutzt. Unter Verwendung von Mangan(III)-acetylacetonat in Verbindung mit Vanadylacetylacetonat war es möglich, die Lagerfähigkeit eines vorher mit Promotor versetzten Harzes von 17 auf mindestens 110 Tage zu erhöhen.

Received April 18, 1963

Revised July 5, 1963

**Redox Polymerization of Unsaturated Polyester Resins. III. Catalytic Properties of Tertiary Amine *N*-Oxides. Redox Polymerization with the System, Dimethylaniline *N*-Oxide with Vanadyl Acetyl Acetate**

GLENN R. SVOBODA, *Freeman Chemical Corporation, Port Washington, Wisconsin*

**Synopsis**

Catalytic activity has been shown for both trialkyl and aryl dialkyl amine *N*-oxides. Of the series, unsaturated polyester resins catalyzed with dimethylaniline *N*-oxide exhibited complete polymerization in a practical length of time (24 hr.), when promoted with vanadyl acetyl acetate. Such a resin system may also be heat cured without the addition of any promoter. A unique property of dimethylaniline *N*-oxide-catalyzed resins is the extraordinary stability exhibited by these resin systems. Up to two years precatalyzed resin and catalyst stability has been noted with resins stored at normal ambient temperatures. Lower storage temperatures are recommended.

**INTRODUCTION**

Past work<sup>1,2</sup> with the redox polymerization catalyst system, benzoyl peroxide-dimethylaniline, has led to postulates regarding the identity of the active intermediate responsible for the polymerization. None of these appeared to have taken into account the possibility of an *N*-oxide as an active intermediate. Since tertiary *N*-oxides are the reaction products of a tertiary amine with a peroxide, e.g., hydrogen peroxide, or peracetic acid, investigation of tertiary amine *N*-oxides was indicated. Furthermore, a system which appeared to produce *in situ* a tertiary amine *N*-oxide was shown to catalyze effectively the polymerization of acrylic monomers.<sup>3</sup>

**EXPERIMENTAL AND RESULTS**

**Survey of Tertiary Amine *N*-Oxides for Catalytic and Promoter Activity**

A series of amine *N*-oxide compounds was investigated for ambient temperature ( $24 \pm 2^\circ\text{C}$ .) catalytic activity in the following manner. To 100 g. of a general purpose unsaturated polyester resin<sup>4</sup> was added 500 mg. of the *N*-oxide compound. No evidence of polymerization could be noted after 56 hr. The effect of these *N*-oxide compounds as promoters was also investigated. To 100 g. of unsaturated polyester resin was added 1 g. of

benzoyl peroxide (or 1 g. of cumene hydroperoxide) and 500 mg. of the specific *N*-oxide compound. No evidence of polymerization was observed with either catalyst after 5 days. For comparison, a system consisting of 100 g. unsaturated polyester resin, 1 g. of benzoyl peroxide, and 0.5 g. of dimethylaniline gave a gel time of 42 min. The present tertiary amines were ineffectual in promoting a cure of unsaturated polyester system containing the specific *N*-oxide compounds investigated.

Another series of resins was prepared as follows. To 100 g. of unsaturated polyester resin was added 1 g. of the specific *N*-oxide compound and 1 ml. of a chloroform solution of vanadyl acetyl acetonate (3.97%) prepared to contain 1% vanadyl ion. The results are shown in Table I. Gel times have been previously defined.<sup>4</sup>

TABLE I  
Redox Polymerization Rates of an Unsaturated Polyester Resin With a Series of Tertiary Amine *N*-Oxides (500 mg.) and Vanadyl Acetyl Acetonate (1 ml. of 1% VO<sup>+2</sup> Solution)

Tertiary amine <i>N</i> -oxide	Gel time	Time to Barcol 40
2-Picoline <i>N</i> -oxide	7 days	—
3-Picoline <i>N</i> -oxide	7 days	—
4-Picoline <i>N</i> -oxide	7 days	—
2,6-Lutidine <i>N</i> -oxide	7 days	—
4-Azopyridine <i>N</i> -oxide	7 days	—
Tributylamine <i>N</i> -oxide	20 hr.	48 hr. <sup>a</sup>
Triethylamine <i>N</i> -oxide	82 min.	48 hr.
Dimethylaniline <i>N</i> -oxide	24 min.	23 hr.
Diethylaniline <i>N</i> -oxide	60 min.	ca. 36 hr.

<sup>a</sup> This system showed only surface gelation after several days.

The trialkyl, and the aryl dialkyl amine *N*-oxides showed considerable catalytic activity.

### Effect of Concentration on the Catalytic Activity of Trialkyl and Aryl Dialkyl Amine *N*-Oxides

Since the *N*-oxide compounds of interest were hygroscopic, low melting solids, they were prepared as 25% active solutions in chloroform. The effect of concentration of both the *N*-oxides and vanadyl promoter is cited in Table II.

The optimum concentration appeared to be 0.5–1.0% of dimethylaniline *N*-oxide with 10 mg. of vanadyl chelate as VO<sup>+2</sup> used as the sole promoter. Although dimethylaniline was ineffective in promoting decomposition of the *N*-oxide, it was effective in promoting polymerization when used in conjunction with vanadyl acetyl acetonate.

### Stability of Unsaturated Polyester Resins Catalyzed With Dimethylaniline *N*-Oxide

Since only vanadium chelates appeared to be effective in promoting the decomposition of dimethylaniline *N*-oxide, there exists the possibility of

TABLE II  
Effect of Concentration of *N*-Oxide and Promoter Upon the Polymerization of an Unsaturated Polyester Resin System

<i>N</i> -Oxide	<i>N</i> -Oxide concn., %	Promoter	Amt. promoter, mg.	Gel time	Time to Barcol 40
Et <sub>3</sub> N→O	1.0	VO <sup>+2</sup>	10	33.5 min.	48 hr.
"	1.0	"	20	12.3 min.	>48 hr.
Bu <sub>3</sub> N→O	1.0	"	10	20 hr.	> 7 days
C <sub>6</sub> H <sub>5</sub> N(CH <sub>3</sub> ) <sub>2</sub> O	1.0	"	10	10.5 min.	23 hr.
"	0.5	"	10	7.0 min.	30 hr.
"	0.2	"	10	7.2 min.	>48 hr.
"	0.2	"	2	58.5 min.	>48 hr.
"	0.2	"	5	12.5 min.	>48 hr.
"	0.1	"	2	38.8 min.	>48 hr.
"	1.0	C <sub>6</sub> H <sub>5</sub> N(CH <sub>3</sub> ) <sub>2</sub>	300	> 114 hr.	—
"	1.0	{ VO <sup>+2</sup> + C <sub>6</sub> H <sub>5</sub> N(CH <sub>3</sub> ) <sub>2</sub>	{ 10 300	{ 4 min.	{ 30 hr.
"	0.5	{ VO <sup>+2</sup> + C <sub>6</sub> H <sub>5</sub> N(CH <sub>3</sub> ) <sub>2</sub>	{ 5 100	{ 2.2 min.	{ 15 min.
"	0.5	{ VO <sup>+2</sup> + C <sub>6</sub> H <sub>5</sub> N(CH <sub>3</sub> ) <sub>2</sub>	{ 10 100	{ 3.1 min.	{ 15 min.

producing stable precatalyzed resins. A study of the stability of such systems was conducted as follows. To 100 g. of an unsaturated polyester resin solution was added 1 g. of dimethylaniline *N*-oxide. Samples of these precatalyzed resins were stored at various temperatures. The results are shown in Table III.

The series of resins catalyzed with dimethylaniline *N*-oxide and stored at 23.5°C. exhibited excellent resin stability for periods ranging from 18 to 24 months, as indicated in Table III. Catalyst stability was excellent over the same time period. When 100-g. samples of catalyzed resin were promoted with 10 mg. of vanadyl ion as vanadyl acetyl acetate after 18 and 24 months, full Barcol development was evidenced in 24 hr.

Obviously, resins precatalyzed with dimethylaniline *N*-oxide should be stored at lower temperature.

TABLE III  
Stability of Unsaturated Polyester Resins Precatalyzed with 1% Dimethylaniline *N*-Oxide

System	Temperature, °C.	Stability
Control	70	180 hr.
1% C <sub>6</sub> H <sub>5</sub> N(CH <sub>3</sub> ) <sub>2</sub> O	70	15 hr.
Control	50	10-12 days
1% C <sub>6</sub> H <sub>5</sub> N(CH <sub>3</sub> ) <sub>2</sub> O	50	4 days
Control	23.5	24-36 months
1% C <sub>6</sub> H <sub>5</sub> N(CH <sub>3</sub> ) <sub>2</sub> O	23.5	18-24 months



### Synthesis of Dimethylaniline *N*-Oxide

To 1.00 mole of dimethylaniline was added 1.05 mole of peracetic acid at 50°C. over a 2.5-hr. period. The reaction temperature was then maintained at 50–60°C. for 5.5 hr. At the end of this time the reaction was cooled to room temperature, activated charcoal was added, and the reaction mass was digested for 16 hr. at 40°C. to decompose any residual peracetic acid. The product was then filtered, made alkaline with 10*N* sodium hydroxide, and extracted with chloroform. The extract was dried and evaporated *in vacuo*. Repeated syntheses gave yields of 16–24% of a light yellow solid. This product was immediately diluted to a 25% solution in chloroform.

Dimethylaniline *N*-oxide prepared in this manner gave equivalent catalytic activity to the commercial material used to give the results cited in this investigation.

### DISCUSSION

As indicated by the gel times cited in Tables I and II, dimethylaniline *N*-oxide is variable in catalytic activity. Examination of different lots of this material from a common source showed that the material varied from a viscous deep yellow liquid to a low melting light yellow solid. Attempts to synthesize dimethylaniline *N*-oxide in this laboratory via the reaction of dimethylaniline with either hydrogen peroxide or peracetic acid resulted in low (16–24%) yields of a light yellow solid which readily liquefied after being exposed to air. For this reason, the material was immediately dissolved and used in chloroform.

The hygroscopic nature of dimethylaniline *N*-oxide may account for a degree of the catalyzed stability of unsaturated polyester resins containing this material. Work in this laboratory has confirmed the inhibitory effect of water upon the polymerization of unsaturated polyester systems.

### References

1. Horner, L., and E. Schlenk, *Angew Chem.*, **61**, 411 (1949).
2. Tobolsky, A. V., and R. B. Mesrobian, *Organic Peroxides*, Interscience, New York, 1954.
3. Yehara, R., *Bull. Chem. Soc. Japan*, **32**, 1079 (1959).
4. Svoboda, G. R., *J. Polymer Sci.*, **A2**, 2723 (1964).

### Résumé

On a démontré les activités catalytiques des triacétyl et amyloxyamine-*N*-oxydes. Les résines polyester de ces séries, catalysés avec le *N*-oxyde de diméthylaniline, polymérisent complètement dans un délai de temps de longueur pratique (24 H.) quand il y a une activation par l'acétylacétonate de vanadyle. Un tel système de résines peut être vulcanisé en chauffant sans addition d'un agent activant. Une propriété unique des résines catalysés par le *N*-oxyde de diméthylaniline est une stabilité extraordinaire. Pendant deux ans, la stabilité des résines précatalysées et du catalyseur a été notée pour des résines stockées à température normale. Des températures plus basses de stockage sont à recommander.

### Zusammenfassung

Die katalytische Wirksamkeit sowohl von Trialkyl- als auch von Aryldealkyl-*N*-Oxyden wurde nachgewiesen. Mit Dimethylanilin-*N*-oxyd als Katalysator versetzte ungesättigte Polyesterharze polymerisierten mit Vanadylacetylacetonat als Promotor innerhalb einer brauchbaren Zeit (24 Std.) vollständig. Ein derartiges Harzsystem kann auch ohne Zusatz eines Promotors hitzegehärtet werden. Eine besondere Eigenschaft der mit Dimethylanilin-*N*-oxyd als Katalysator versetzten Harze ist die aussergewöhnliche Stabilität dieser Harzsysteme. Das vorher mit dem Katalysator versetzte Harz sowie der Katalysator waren bei Lagerung des Harzes bei Raumtemperatur bis zu zwei Jahren stabil. Niedrigere Lagerungstemperaturen werden empfohlen.

Received April 18, 1963

Revised July 5, 1963

## General Relationships among Monomers in Copolymerization

GEORGE E. HAM, *Research Center, Spencer Chemical Company,  
Merriam, Kansas*

### Synopsis

Although there is general recognition of the value of the Alfrey-Price relationship, controversy has not abated concerning the theoretical basis for the equations and the accuracy of the monomer reactivity ratios predicted. A heretofore unrecognized possibility for approaching the problem of general monomer reactivity relationships appears to lie in the consideration of terpolymers. The relationship between monomer and terpolymer compositions is given by the equations

$$\frac{a}{b} = \frac{P_{ba}P_{ca} + P_{bc}P_{ca} + P_{cb}P_{ba}}{P_{ab}P_{cb} + P_{ac}P_{cb} + P_{ca}P_{ab}} \quad (1)$$

$$\frac{a}{c} = \frac{P_{ba}P_{ca} + P_{bc}P_{ca} + P_{cb}P_{ba}}{P_{ac}P_{bc} + P_{ba}P_{ac} + P_{ab}P_{bc}} \quad (2)$$

A more general and yet simplified relationship underlying terpolymers which has not been previously recognized is derived. This relationship is shown to hold for a wide range of monomer types and concentrations. The overall probability of initiating a, c, and b sequences immediately preceded by b, a, and c, respectively, and of undefined terminating units is equal to the probability of terminating a, c, and b sequences with b, a, and c units, respectively, but of undefined initiating units. This relationship of product probabilities is as follows:

$$P_{ba}P_{ac}P_{cb} + P_{ab}P_{ca}P_{bc} \quad (3)$$

and is shown to hold for numerous terpolymer and related copolymer systems. It follows that

$$\frac{a}{b} = \frac{P_{ba}}{P_{ab}} = \frac{P_{ba}P_{ca} + P_{bc}P_{ca} + P_{cb}P_{ba}}{P_{ab}P_{cb} + P_{ca}P_{ab} + P_{ac}P_{cb}} \quad (4)$$

$$\frac{a}{c} = \frac{P_{ca}}{P_{ac}} = \frac{P_{ba}P_{ca} + P_{bc}P_{ca} + P_{cb}P_{ba}}{P_{ac}P_{bc} + P_{ba}P_{ac} + P_{ab}P_{bc}} \quad (5)$$

Methods are presented for predicting the behavior of monomers A and C in copolymerization when the behaviors of A-B and B-C are known. Furthermore, it is shown that the value of eq. (3) is frequently in the range of 0.02-0.06. This result is probably related to the fact that terpolymerization of monomers of equal reactivity in equimolar concentrations will yield product probabilities equal to 0.037. Variations in individual probabilities require compensating changes in the other related probabilities. Application of this relationship allows the calculation of  $r_{13}$  and  $r_{31}$  where  $r_{23}$ ,  $r_{32}$ ,  $r_{12}$ , and  $r_{21}$  are known.

Today it is broadly recognized that a general order of reactivity exists among monomers in copolymerization. It was observed in the early forties that monomers could be arranged with respect to their relative reactivities with specific radicals by comparing reciprocals of the reactivity ratios found in a series of copolymerizations.<sup>1</sup> However, comparisons of reactivity of a given monomer with a variety of radicals required knowledge of the actual propagation rate constants. The Alfrey-Price relationship<sup>2</sup> offered for the first time a means of predicting monomer reactivity in copolymerization from two fundamental parameters:  $Q$ , a measure of the resonance stability of a monomer in copolymerization, and  $e$ , a polar factor. Thus,

$$r_1 = K^{11}/K^{12} = (Q_1/Q_2) \exp \{ -e_1(e_1 - e_2) \} \quad (1)$$

$$r_2 = K^{22}/K^{21} = (Q_2/Q_1) \exp \{ -e_2(e_2 - e_1) \} \quad (2)$$

for relationships between monomers 1 and 2.

Although there is general recognition of the value of this relationship, controversy has not abated concerning the theoretical basis for the equations and the accuracy of the monomer reactivity ratios predicted.

A logical approach to the problem of general monomer reactivity must lie in a consideration of terpolymerization. The relationship between monomer and terpolymer compositions is given by the equations<sup>3</sup>

$$\frac{a}{b} = \frac{A[(A/r_{31}r_{21}) + (B/r_{21}r_{32}) + (C/r_{31}r_{23})][A + (B/r_{12}) + (C/r_{13})]}{B[(A/r_{12}r_{31}) + (B/r_{12}r_{32}) + (C/r_{32}r_{13})][B + (A/r_{21}) + (C/r_{23})]} \quad (3)$$

$$\frac{a}{c} = \frac{A[(A/r_{31}r_{21}) + (B/r_{21}r_{32}) + (C/r_{31}r_{23})][A + (B/r_{12}) + (C/r_{13})]}{C[(A/r_{13}r_{21}) + (B/r_{23}r_{12}) + (C/r_{13}r_{23})][C + (A/r_{31}) + (B/r_{32})]} \quad (4)$$

This relationship may be expressed more simply as

$$\frac{a}{b} = \frac{P_{ba}P_{ca} + P_{cb}P_{ba} + P_{bc}P_{ca}}{P_{ac}P_{cb} + P_{ca}P_{ab} + P_{ac}P_{cb}} \quad (5)$$

$$\frac{a}{c} = \frac{P_{ba}P_{ca} + P_{cb}P_{ba} + P_{bc}P_{ca}}{P_{ac}P_{bc} + P_{ba}P_{ac} + P_{ab}P_{bc}} \quad (6)$$

It is interesting to note that the numerators of both equations are the same and contain the elements of the cumulative probabilities of producing (or finding) a sequences preceded by b or c. Corresponding significances may be attached to the denominators concerning b and c sequences.

The probability  $P_{b-a-c}$  of finding a sequence of the series bc, bac, baac, baaac, . . . , is

$$N_n = P_{ba}P_{aa}^{n-1}P_{ac} \quad (7)$$

except

$$N_o = P_{bc}$$

where  $n = 1, 2, 3, \dots$ , and corresponds to the number of a's in a given sequence.  $N_n$  is also the proportion of all b-a-c sequences containing  $n$  a units. The sum of all of the separate ways (probabilities) of producing such sequences is, of course, equal to 1, i.e.,

$$P_{bc} + P_{ba}P_{ac} \sum_{n=1}^{\infty} P_{aa}^{n-1} = 1 \quad (8)$$

Now it seems reasonable that the probability of finding an individual member of a certain sequence, say, baa . . . c, in a terpolymer chain produced from equimolar concentrations of monomers might be, under certain circumstances, equal to the probability of finding an individual member of the reversed sequence, caa . . . b. Possibly, but not necessarily, there may exist for every sequence of this type a reversed sequence of equal length (in the same chain, for instance). Once formed such sequences would be chemically indistinguishable. In the absence of this equality there will be sequence distributions and number-average sequence lengths characteristic of each type. If equality exists, then this relationship follows

$$N_n = P_{ba}P_{aa}^{n-1}P_{ac} = P_{ca}P_{aa}^{n-1}P_{ab} \quad (9)$$

$$P_{ba}P_{ac} = P_{ca}P_{ab} \quad (10)$$

Other relationships which may hold are

$$P_{ab}P_{bc} = P_{cb}P_{ba} \quad (11)$$

$$P_{ac}P_{cb} = P_{bc}P_{ca} \quad (12)$$

One of these three relationships will nearly always hold approximately for terpolymers derived from equimolar monomer concentrations as shown in Table I (based on reported reactivity ratios). A second equality will be often approached and this would lead to

$$P_{ba} = P_{ca}P_{ab}/P_{ac} \quad (13)$$

$$P_{ba} = P_{ab}P_{bc}/P_{cb} \quad (14)$$

yielding

$$P_{ca}/P_{ac} = P_{bc}P_{cb} \quad (15)$$

As will be shown later, this condition is tantamount to

$$a/c = c/b \quad (16)$$

A third equality cannot exist since it leads to

$$\frac{b}{a} = \frac{a}{c} \quad (16a)$$

which means equimolar concentrations in the terpolymer composition. With the further premise of equal initial monomer concentrations, then all reactivity ratios would have to equal 1 for this special condition to result.

TABLE I

A	B	C	$P_{ab}P_{bc}$	$P_{cb}P_{ba}$	$P_{ba}P_{ac}$	$P_{ac}P_{ab}$	$P_{ac}P_{cb}$	$P_{cb}P_{ca}$	$P_{ba}P_{ca}$	$P_{ca}P_{bc}$	$P_{bc}P_{ca}$	$P_{ca}P_{cb}$
SM	MMA	VCl <sub>2</sub>	0.06 <sup>a</sup>	0.148 <sup>a</sup>	0.093 <sup>a</sup>	0.385	0.038 <sup>a</sup>	0.077 <sup>a</sup>	0.335	0.0268	0.335 <sup>a</sup>	0.11 <sup>a</sup>
SM	MeAc	VCl					0.00516 <sup>a</sup>	0.00878 <sup>a</sup>				0.11
SM	MMA	AN	0.067 <sup>a</sup>	0.093 <sup>a</sup>	0.256 <sup>a</sup>	0.28 <sup>a</sup>	0.081 <sup>a</sup>	0.1495 <sup>a</sup>			0.199 <sup>a</sup>	0.365 <sup>a</sup>
VCl	MeAc	VAc	0.079	0.060			0.03 <sup>a</sup>	0.024 <sup>a</sup>	0.0887 <sup>a</sup>	0.030 <sup>a</sup>		
MMA	AN	VCl <sub>2</sub>			0.136 <sup>a</sup>	0.185 <sup>a</sup>	0.064 <sup>a</sup>	0.075 <sup>a</sup>				0.099 <sup>a</sup>
SM	MMA	2-VP	0.178 <sup>a</sup>	0.1465 <sup>a</sup>	0.1465 <sup>a</sup>	0.116 <sup>a</sup>	0.148 <sup>a</sup>	0.127 <sup>a</sup>	0.154 <sup>a</sup>	0.170 <sup>a</sup>	0.154 <sup>a</sup>	0.110 <sup>a</sup>
SM	MMA	MeAc	0.054 <sup>a</sup>	0.146 <sup>a</sup>	0.187 <sup>a</sup>	0.283 <sup>a</sup>	0.0765 <sup>a</sup>	0.0775 <sup>a</sup>	0.27 <sup>a</sup>	0.20 <sup>a</sup>	0.27 <sup>a</sup>	0.170 <sup>a</sup>

<sup>a</sup> These numbers are sufficiently similar to those numbers representing reversed sequences to be regarded as equal for calculating reactivity ratios.

TABLE II

A	B	C	A:B:C	$P_{ab}P_{bc}P_{ca}$	$P_{ca}P_{cb}P_{ba}$	Ratio
SM	MMA	AN ( $r_{31} = 0.04$ )	Equimolar	0.053	0.0454	
SM	MeAc	VCl	"	0.00504	0.00435	
SM	MeAc	VAc	"	0.0084	0.00058 ( $r_{12}, r_{31}?$ )	
SM	MMA	VCl <sub>2</sub>	"	0.042	0.023	
MMA	AN	VCl <sub>2</sub>	"	0.0202	0.0467	
SM	MMA	2-VP	"	0.051	0.0562	
SM	MMA	MeAc	"	0.0348	0.046	
SM	MMA	AN ( $r_{31} = 0.04$ )	"	0.053	0.0454	1.17
SM	MMA	AN	0.359:0.360:0.28	0.0493	0.0405	1.22
SM	MMA	AN	0.2776:0.5206:0.2018	0.0513	0.0425	1.21
SM	MMA	AN	0.532:0.2651:0.2026	0.0275	0.0225	1.22

The more general relationship underlying terpolymerization which has not been previously recognized but will be dealt with here is as follows. This relationship will be shown to hold for a wide range of monomer types and concentrations. The overall probability of initiating a, c, and b sequences immediately preceded by b, a, and c, respectively, and of undefined terminating units is equal to the probability of terminating a, c, and b sequences with b, a, and c units, respectively, but of undefined initiating units. This relationship of product probabilities is as follows:

$$P_{ba}P_{ac}P_{cb} = P_{bc}P_{ca}P_{ab} \quad (17)$$

and is shown to hold for numerous ternary and related binary systems in Table II.

The equality

$$P_{ba}P_{ab}(P_{cb} + P_{ca}) = P_{ab}P_{ba}(P_{ca} + P_{cb})$$

is added to both sides of eq. (17). It follows that

$$\frac{P_{ba}}{P_{ab}} = \frac{P_{ba}P_{ca} + P_{bc}P_{ca} + P_{cb}P_{ba}}{P_{ab}P_{cb} + P_{ca}P_{ab} + P_{ac}P_{cb}} \quad (18)$$

From eq. (5) the terpolymer composition equation is

$$\frac{a}{b} = \frac{P_{ba}}{P_{ab}} = \frac{P_{ba}P_{ca} + P_{cb}P_{ba} + P_{bc}P_{ca}}{P_{ab}P_{cb} + P_{ca}P_{ab} + P_{ac}P_{cb}} \quad (19)$$

Similarly, adding  $P_{ca}P_{ac}(P_{bc} + P_{ba})$  to both sides of eq (17) yields

$$\frac{a}{c} = \frac{P_{ca}}{P_{ac}} = \frac{P_{ba}P_{ca} + P_{bc}P_{ca} + P_{cb}P_{ba}}{P_{ac}P_{bc} + P_{ab}P_{bc} + P_{ba}P_{ac}} \quad (20)$$

The advantages of the simple relationships

$$a/b = P_{ba}/P_{ab} \quad (21)$$

$$a/c = P_{ca}/P_{ac} \quad (22)$$

for expressing terpolymer compositions from monomer ratios are self-evident.

The analogy to the simple binary copolymer relationship

$$a/b = P_{ba}/P_{ab} \quad (23)$$

is obvious, but eqs. (21) and (22) contain probabilities which represent the possibilities of additions of A, B, and C to radicals, whereas eq. (23) only includes additions of A and B.

Since the individual probabilities in ternary systems may be calculated from binary reactivity ratios, as

$$P_{ab} = \frac{K^{ab}[A\cdot][B]}{K^{ab}[A\cdot][B] + K^{aa}[A\cdot][A] + K^{ac}[A\cdot][C]} = \frac{(B/r_{12})}{(B/r_{12}) + A + (C/r_{13})} \quad (24)$$

the relations expressed in Tables I and II may be tested. The apparent equality of individual pairs of relationships in Table I and similarity of other pairs will be shown to be of value in checking questionable reactivity ratios.

The value of the above findings in ternary systems (Table II) may be seen in their applications to data reported by Walling and Briggs<sup>4</sup> on the terpolymer system styrene-methyl methacrylate-acrylonitrile. Excellent agreement between reported and calculated copolymer composition ratios using the simplified equation, eq. (21), was obtained (Table III). The fact that eq. (22) did not give the expected  $a/c$  ratios in this system suggested that adjustments in the questionable value of  $r_{31}$  might be necessary. Terpolymer compositions are much more sensitive to sequence distribution and reactivity ratios than binary systems, so offer an unusual chance to check on questionable reactivity ratios. Values in Table III were obtained by using the values:  $r_{13} = 0.41$ ;  $r_{12} = 0.52$ ;  $r_{23} = 1.35$ ;  $r_{31} = 0.04$ ;  $r_{21} = 0.46$ ;  $r_{32} = 0.18$ . It appears that the reported value for the reactivity

TABLE III

Monomer composition			Polymer composition (A/B ratio)		
SM, mole-%	MMA, mole-%	AN, mole-%	Found	Calculated from simplified equation	Calculated from Alfrey- Goldfinger equation
35.92	36.03	28.05	1.70	1.44	1.49
53.23	26.51	20.26	2.60	2.26	2.27
28.32	28.24	43.44	1.67	1.76	1.82
27.76	52.06	20.18	0.898	0.84	0.84

ratio  $r_{31} = K^{\text{AN-AN}}/K^{\text{AN-S}}$  is too low for the range of AN-S compositions studied and may only hold at very high AN/S ratios. A value of 0.114 calculated by eq. (22) from the observed  $a/c$  ratio in experiment 7<sup>4</sup> predicts an  $a/c$  ratio of 1.50 from eq. (22), in good agreement with the value of 1.53 found in experiment 4.<sup>4</sup> Of course, knowledge of  $a/b$  and  $a/c$  determines precisely terpolymer composition. The conventional Alfrey-Goldfinger terpolymer equation tends to obscure the effects of  $r_{31}$  in determining terpolymer composition.

These calculations suggest that the new relationships presented may constitute a highly precise means of evaluating questionable reactivity ratios, especially those which are very small or very large. Stated otherwise, the composition of terpolymers is greatly influenced by sequence distributions resulting from very small changes in relative reactivity ratios. Furthermore, because of these factors penultimate effects in copolymerization can be determined more precisely from composition studies in terpolymerization experiments than in binary polymerizations. Specifically, it may be concluded that for the binary system styrene-acrylonitrile



$$r_2 = K^{bbb}/K^{bba} = 0.04 \text{ (reported)} \quad (25)$$

$$r_2' = K^{abb}/K^{aba} = 0.114 \quad (26)$$

In effect, growing chains rich in acrylonitrile tend to exclude acrylonitrile monomer in competition with styrene monomer, whereas a growing acrylonitrile radical preceded by a styrene unit accepts acrylonitrile more readily.

Revised calculations using the simplified equation for the system styrene-methyl methacrylate-acrylonitrile based on  $r_{31} = 0.114$  with other reactivity ratios remaining the same are shown in Table IV.

It is interesting to note that agreement between predicted and obtained values of  $a/c$  is excellent with  $r_{31} = 0.114$  except in expt. 5. At this ratio of styrene to acrylonitrile  $r_{31}$  would be expected to have less effect on composition. It is to be strongly suspected that the higher styrene/acrylonitrile ratio in expt. 5 does not allow  $r_{13}$  to be simply equated to 0.41. It has been previously established<sup>5</sup> that in the binary system styrene-acrylonitrile the reactivity of styrene relative to acrylonitrile with a growing styrene radical is considerably influenced by whether the penultimate unit in the growing radical is acrylonitrile or styrene. If it is styrene,  $r_{13} = 0.30$ , but if it is acrylonitrile  $r_{13} = 0.45$ . In the above calculations the widely used literature value of  $r_{13} = 0.41$  has been used because it is a reasonable average value in the intermediate composition ranges usually studied. However, in expt. 5 a simple calculation shows that the  $a/c$  ratio obtained in the copolymer could arise from an average  $r_{13} = 0.33$  in this monomer composition range. Because of the many factors involved, including the possibility of experimental error, it is only possible to conclude that a value of  $r_{13}$  less than 0.41 is probable in the composition range of expt. 5.

TABLE IV

Expt.	Monomer composition		Polymer composition					
			A/B			A/C		
			Found	Simp. eq. A-G eq. ( $r_{31} = 0.114$ )   ( $r_{31} = 0.04$ )		Found	Simp. eq. A-G eq. ( $r_{31} = 0.114$ )   ( $r_{31} = 0.04$ )	
No.	Mole-%	Monomer						
4	35.92	SM	1.70	1.44	1.49	1.53	1.50	1.60
	36.03	MMA						
	28.05	AN						
5	53.23	SM	2.60	2.26	2.27	1.93	2.28	2.21
	26.51	MMA						
	20.26	AN						
6	28.32	SM	1.67	1.76	1.82	0.995	1.01	1.16
	28.24	MMA						
	43.44	AN						
7	27.76	SM	0.898	0.84	0.84	1.58	1.58	1.89
	52.06	MMA						
	20.18	AN						

TABLE V

SM	MMA	AN	$P_{ab}P_{bc}P_{ca}$	$P_{ac}P_{cb}P_{ba}$	Ratio
0.333	0.333	0.333	0.0375	0.094	2.51
0.359	0.360	0.28	0.0365	0.082	2.25
0.532	0.2651	0.2026	0.0228	0.055	2.42
0.2832	0.2824	0.4344	0.042	0.099	2.35
0.2776	0.5206	0.2018	0.0295	0.0696	2.35

A remaining problem to be dealt with is that the calculated equality (as distinguished from the necessary theoretical equality)

$$P_{ab}P_{bc}P_{ca} = P_{ac}P_{cb}P_{ba}$$

is disturbed when the value  $r_{31} = 0.114$  is substituted for 0.04 in the system styrene-methyl methacrylate-acrylonitrile (Table V).

There appear to be several good reasons for using the simplified equations in spite of this problem.

(1) The probability of the various sequences being initiated must equal the probability of their being terminated—a fact which is a statement of eq. (17) and amounts to a steady-state condition. This fact suggests that errors in other experimental reactivity ratios may exist accounting for the inequality.

(2) A highly consistent relationship between monomer and terpolymer composition is possible through use of the simplified equations. New compositions can be predicted, and logical conclusions about general monomer reactivity and interrelationships are made possible.

(3) A consistent ratio between  $P_{ac}P_{cb}P_{ba}$  and  $P_{ab}P_{bc}P_{ca}$  is maintained in spite of changes in both  $P_{cb}$  and  $P_{ca}$  arising from the adjustment of  $r_{31}$ .

(4) The addition of  $P_{ac}P_{cb}P_{ba}$  and  $P_{ab}P_{bc}P_{ca}$  to the equalities in the derivation of eq. (19) and (20) serve to contribute changes which are self-compensating in their effects.

(5) Finally, Table II shows remarkably close agreement between the product probabilities in question despite wide variations in monomer types.

It is now possible to deal directly with the matter of predicting monomer reactivity in novel combinations not previously tried. Thus, if the reactivity of monomer A with monomer B and of monomer B with monomer C are known, then the reactivity of monomer A with C is now fixed precisely and can be predicted from the considerations discussed above. Our earlier conclusions dealt almost entirely with terpolymerizations, but it will be apparent that all were bound together by the behavior of binary systems.

Since  $P_{ab}P_{bc}P_{ca} = P_{ac}P_{cb}P_{ba}$  it is possible to write for equimolar monomer concentrations:

$$\begin{aligned} & \left( \frac{r_{13}}{r_{13} + r_{12}r_{13} + r_{12}} \right) \left( \frac{r_{21}}{r_{21} + r_{23}r_{21} + r_{23}} \right) \left( \frac{r_{32}}{r_{32} + r_{32}r_{31} + r_{31}} \right) \\ & = \left( \frac{r_{12}}{r_{12} + r_{13}r_{12} + r_{13}} \right) \left( \frac{r_{31}}{r_{31} + r_{31}r_{32} + r_{32}} \right) \left( \frac{r_{23}}{r_{23} + r_{23}r_{21} + r_{21}} \right) \quad (27) \end{aligned}$$

This equation readily reduces to:

$$r_{13}r_{21}r'_{32} = r_{12}r'_{31}r'_{23} \quad (28)$$

Now if reactivity ratios are known for two binary systems with a common monomer and it is desired to learn the reactivity ratios for the hypothetical combination of the two monomers yet to be reacted then eq. (28) becomes

$$r_{13}/r_{31} = r_{12}r'_{23}/r_{21}r'_{32} \quad (29)$$

Now if  $P_{bc} = P_{cb}$  (similar treatment for  $P_{ab} = P_{ba}$  or  $P_{ac} = P_{ca}$ ) which would follow if  $P_{ca}P_{ab} = P_{ba}P_{ac}$  (Table I):

$$\frac{r_{21}}{r_{31}} = \frac{r_{21} + r_{23}r'_{21} + r_{23}}{r_{31} + r_{32}r'_{31} + r_{32}} \quad (30)$$

In the case of styrene-methyl methacrylate-acrylonitrile solution of these simultaneous equations yields

$$r_{13} = 0.370 \text{ (calc.)}; r_{13} = 0.41 \text{ (reported)}$$

$$r_{31} = 0.0435 \text{ (calc.)}; r_{31} = 0.04 \text{ (reported)}$$

This is of course remarkable agreement and requires close examination. First, the calculated ratio  $r_{13}/r_{31} = 8.5$  agrees well with the reported ratio, and is an unequivocal answer. However, in determining precise values of  $r_{13}$  and  $r_{31}$  the choice of  $P_{bc} = P_{cb}$  was quite fortuitous. Choice of  $P_{ab} = P_{ba}$  or  $P_{ac} = P_{ca}$  would have led to erroneous results. At best there was one chance in three of getting a reasonably correct answer. More experience with such systems may develop some guides. Perhaps the monomer pair to be chosen for "probability reversibility" might be the pair with most similar polarity as, for instance, acrylonitrile and methyl methacrylate. However, insufficient data are available for such generalizations at present.

Furthermore, it is apparent that such a general treatment cannot pick up subtle penultimate effects as readily as the terpolymer treatment given above.

There is some basis for suspecting that if a growing radical displays a penultimate effect in competition between its own and another monomer, that the opposite radical may also display a penultimate effect and in a related manner. Thus, a growing radical ending in two acrylonitrile units may repel acrylonitrile in preference to styrene and a growing radical ending in -AN-SM· may repel acrylonitrile in preference to styrene.

Substituting in eq. (28) appropriate ratios for the addition to "purest" growing chains yields:

$$\begin{aligned} r_{13}r'_{21}r'_{32} &= r_{12}r'_{31}r'_{23} \\ (0.30)(0.46)(0.18) &= (0.52)(0.04)(1.35) \\ 0.0249 &= 0.0259 \end{aligned}$$

TABLE VI

Monomers			Selected equality	$r_{12}/r_{31}$ ratio		$r_{13}$		$r_{31}$	
A	B	C		Calcd.	Reported	Calcd.	Reported	Calcd.	Reported
MMA	AN	VCl <sub>2</sub>	$P_{eb} = P_{bc}$	18.4	10.6	1.22	2.53	0.066	0.24
SM	MMA	VCl <sub>2</sub>	$P_{ab} = P_{ba}$	11.95	21.8	5.28	1.85	0.441	0.085
SM	MMA	2-VP	$P_{ab} = P_{ba}$	0.52	0.483	0.48	0.55	0.92	1.14
SM	MMA	MeAcr	$P_{bc} = P_{cb}$	14.4	4.17	0.995	0.75	0.069	0.18

and substitution for addition to growing chains with penultimate units differing from terminal units yields:

$$\begin{aligned} r_{13}r_{21}r_{32} &= r_{12}r_{31}r_{23} \\ (0.45)(0.46)(0.18) &= (0.52)(0.11)(1.35) \\ 0.0352 &= 0.077 \end{aligned}$$

It is apparent that this equation applies most satisfactorily to normal rather than to penultimate phenomena, but that where penultimate effects exist, the trend is exhibited. It must be recalled that in the two "model" copolymerizations styrene-methyl methacrylate and methyl methacrylate-acrylonitrile there are no penultimate effects observed, so it is not surprising that the parameters obtained for styrene-acrylonitrile by these calculations are more representative of "normal" additions.

Applications of the technique to other systems are also illustrative.

A recent investigation<sup>6</sup> of the copolymerization of methyl acrylate and methyl methacrylate by a deuterium tracer method has yielded  $r_1 = 0.47 \pm 0.09$  and  $r_2 = 2.3 \pm 0.5$ . Application of eq. (28) to the known systems styrene-methyl methacrylate and styrene-methyl acrylate predicts an  $r_1/r_2$  ratio of 0.272 for methyl acrylate-methyl methacrylate compared with an actual  $r_1/r_2$  ratio of 0.204. *Q-e* treatment predicted  $r_1 = 0.504$  and  $r_2 = 1.91$  and an  $r_1/r_2$  ratio of 0.265. Using the new methyl acrylate-methyl methacrylate ratios and the known values of styrene-methyl methacrylate, Table VI shows the resulting values for styrene-methyl acrylate compared with the reported values, assuming  $P_{bc} = P_{cb}$ . Moderate agreement results.

Thus, it is seen that the application of eq. (29) to the prediction of binary copolymerization behavior is only good for systems where reversible probability for the three monomer system exists in at least a single case, i.e.,  $P_{cb} = P_{bc}$ ,  $P_{ab} = P_{ba}$ , or  $P_{ac} = P_{ca}$ . Fortunately, this situation is approximated in a sufficiently large number of cases for the method to be of value. The treatment, of course, requires no recourse to a table of independent and, to a degree, arbitrary parameters such as *Q* and *e*. In addition, the ratios  $r_{13}/r_{31}$ ,  $r_{12}/r_{21}$ , and  $r_{23}/r_{32}$  are often of value and can be obtained from eq. (29) alone.

Table II shows that the broad range of ternary combinations of binary copolymerizations fits into general categories with respect to specific values of  $P_{ab}P_{bc}P_{ca}$  and  $P_{ac}P_{cb}P_{ba}$ , especially where due allowance is made for experimental inaccuracies. It is possible that individual monomers might be assigned "general reactivity parameters" which might be multiplied together to yield values equal to  $P_{ab}P_{bc}P_{ca}$  of use in calculating unknown reactivity ratios.

Table II shows that a remarkable number of product probabilities lies in the range of 0.02-0.06. This fact may be related to the fact that given equal concentrations of monomers equally reactive with the various radicals the product probability would be  $(1/3)(1/3)(1/3) = 0.037$ . (Stated other-

wise, if any individual probabilities exceed 1/3, others must be modified to compensate for it.) Employing the relationship  $P_{ab}P_{bc}P_{ca} = P_{ac}P_{cb}P_{ba} = 0.037$  predictability of relative reactivity ratios for a wide variety of monomers will result. The principle may be demonstrated with the system styrene-methyl methacrylate-vinylidene chloride. Solution of two simultaneous equations based on  $P_{ab}P_{bc}P_{ca} = 0.037$ ,  $P_{ac}P_{cb}P_{ba} = 0.037$ , with values for all reactivity ratios except  $r_{13}$  and  $r_{31}$  substituted and with equimolar concentrations of monomers yielded  $r_{13} = 1.83$ ,  $r_{31} = 0.154$ ; experimental values were  $r_{13} = 1.85 \pm 0.05$  and  $r_{31} = 0.085 \pm 0.01$ , respectively. This treatment should have wide applicability because of its simplicity.

It is, of course, quite remarkable that relations such as

$$P_{ba}P_{aa}^{n-1}P_{ac} = P_{ca}P_{aa}^{n-1}P_{ab}$$

hold approximately and that the relationship

$$P_{ab}P_{bc}P_{ca} = P_{ac}P_{cb}P_{ba}$$

holds more precisely. These imply that a sequential process of a very special sort is occurring. From the mathematical standpoint stochastic processes do not require at all the equivalence of any region of a process with that of a reverse process. Indeed, the specific mathematics have not even been developed to cover such natural occurrences. This equivalence undoubtedly arises from polar and steric factors unifying any three monomers and their radicals in all possible combinations. Fortunately for the procedures outlined above it is not necessary to isolate and identify each of these factors to make use of the methods. On the other hand, there can be no doubt that the extension of these calculations will shed much additional light on steric and polar factors in copolymerization.

### References

1. Mayo, F. R., and C. Walling, *Chem. Revs.*, **46**, 191 (1950).
2. Alfrey, T., Jr., and C. C. Price, *J. Polymer Sci.*, **2**, 101 (1947).
3. Alfrey, T., Jr., and G. Goldfinger, *J. Chem. Phys.*, **12**, 322 (1944).
4. Walling, C., and E. R. Briggs, *J. Am. Chem. Soc.*, **67**, 1774 (1945).
5. Ham, G. E., *J. Polymer Sci.*, **14**, 87 (1954).
6. Shima, M., and A. Kotera, *J. Polymer Sci.*, **A1**, 1115 (1963).

### Résumé

Malgré la valeur généralement admise de la relation d'Alfrey-Price, on n'a pas pu résoudre la controverse concernant le fondement théorique des équations et l'exactitude des rapports prévus pour la réactivité des monomères. Une possibilité nonreconnue jusqu'à présent pour résoudre le problème des relations générales sur la réactivité des monomères semble être reliée à la considération de terpolymères. La relation entre les compositions en monomères et en terpolymère est donnée par les équations

$$\frac{a}{b} = \frac{P_{ba}P_{ca} + P_{bc}P_{ca} + P_{cb}P_{ba}}{P_{ab}P_{cb} + P_{ac}P_{cb} + P_{ca}P_{ab}} \quad (1)$$

$$\frac{a}{c} = \frac{P_{ba}P_{ca} + P_{bc}P_{ca} + P_{cb}P_{ba}}{P_{ac}P_{bc} + P_{ba}P_{ac} + P_{ab}P_{bc}} \quad (2)$$

On en dérive une relation encore plus générale et plus simplifiée concernant les terpolymères; cette relation n'a pas été admise antérieurement. Cette relation s'applique à un large domaine de monomères et de concentrations. La probabilité d'initier des séquences a, c et b immédiatement précédées de b, a et c respectivement, et la probabilité de terminaison par des unités non-définies est égal à la probabilité de terminaison des séquences a, c et b avec des unités b, a et c respectivement, mais avec une initiation par des unités non-définies. La relation concernant ces probabilités est la suivante:

$$P_{ba}P_{ac}P_{cb} + P_{ab}P_{ca}P_{bc} \quad (3)$$

et peut être employée pour de nombreux terpolymères et systèmes de copolymères dérivés. Il s'ensuit que

$$\frac{a}{b} = \frac{P_{ba}}{P_{ab}} = \frac{P_{ba}P_{ca} + P_{bc}P_{ca} + P_{cb}P_{ba}}{P_{ab}P_{cb} + P_{ca}P_{ab} + P_{ac}P_{cb}} \quad (4)$$

$$\frac{a}{c} = \frac{P_{ca}}{P_{ac}} = \frac{P_{ba}P_{ca} + P_{bc}P_{ca} + P_{cb}P_{ba}}{P_{ac}P_{bc} + P_{ba}P_{ac} + P_{ab}P_{bc}} \quad (5)$$

On présente des méthodes pour prévoir le comportement des monomères A et C lors de leur copolymérisation lorsqu'on connaît les comportements de A-B et B-C. De plus on montre que la valeur de (3) se situe fréquemment dans le domaine de 0.02-0.06. Ce résultat est probablement relié au fait que la terpolymérisation de monomères de réactivités égales en concentration équimolaire donnera un produit de probabilités égal à 0.037. Des changements dans les probabilités individuelles exigent des changements dans les autres probabilités. L'application de cette relation permet de calculer  $r_{13}$  et  $r_{31}$  lorsque  $r_{33}$ ,  $r_{32}$ ,  $r_{12}$  et  $r_{21}$  sont connus.

### Zusammenfassung

Der Wert der Alfrey-Price-Beziehung wird zwar allgemein anerkannt, doch bestehen immer noch gegensätzliche Meinungen über die theoretische Fundierung der Gleichungen sowie über die Genauigkeit der erhaltenen Reaktivitätsverhältnisse. Eine bis jetzt unbeachtete Möglichkeit zur Behandlung der Problems allgemeiner Beziehungen für die Monomer-Reaktivitätsverhältnisse scheint in der Betrachtung von Terpolymeren zu liegen. Die Beziehung zwischen der Zusammensetzung der Monomermischung und des Polymeren ist durch die Gleichungen

$$\frac{a}{b} = \frac{P_{ba}P_{ca} + P_{bc}P_{ca} + P_{cb}P_{ba}}{P_{ab}P_{cb} + P_{ac}P_{cb} + P_{ca}P_{ab}} \quad (1)$$

$$\frac{a}{c} = \frac{P_{ba}P_{ca} + P_{bc}P_{ca} + P_{cb}P_{ba}}{P_{ac}P_{bc} + P_{ba}P_{ac} + P_{ab}P_{bc}} \quad (2)$$

gegeben. Eine allgemeinere und noch vereinfachte, bisher unbekannt Beziehung für Terpolymere wird abgeleitet. Diese Beziehung gilt für einen weiten Bereich von Monomertypen und Konzentrationen. Die Bruttowahrscheinlichkeit a-, c- und b-Sequenzen zu starten, deren unmittelbare Vorgänger b bzw. a bzw. c und deren Endeinheiten unbestimmt sind, ist der Wahrscheinlichkeit gleich bei unbestimmter Starteinheit a, c und b-Sequenzen durch b- bzw. a- bzw. c-Einheiten zu beenden. Diese Beziehung für die Wahrscheinlichkeitsprodukte lautet folgendermassen:

$$P_{ba}P_{ac}P_{cb} + P_{ab}P_{ca}P_{bc} \quad (3)$$

und gilt für zahlreiche Terpolymer- und verwandte Copolymersysteme. Es folgt, dass

$$\frac{a}{b} = \frac{P_{ba}}{P_{ab}} = \frac{P_{ba}P_{ca} + P_{bc}P_{ca} + P_{cb}P_{ba}}{P_{ab}P_{cb} + P_{ca}P_{ab} + P_{ac}P_{cb}} \quad (4)$$

$$\frac{a}{c} = \frac{P_{ca}}{P_{ac}} = \frac{P_{ba}P_{ca} + P_{bc}P_{ca} + P_{cb}P_{ba}}{P_{ac}P_{bc} + P_{ba}P_{ac} + P_{ab}P_{bc}} \quad (5)$$

ist. Es werden Methoden zur Bestimmung des Verhaltens der Monomeren A und C bei der Copolymerisation aus dem bekannten Verhalten von A-B und B-C angegeben. Weiters wird gezeigt, dass der Wert von (3) häufig im Bereich von 0,02 bis 0,06 liegt. Dieses Ergebnis steht wahrscheinlich zu dem Umstand in Beziehung, dass die Terpolymerisation von Monomeren gleicher Reaktivität in äquimolarer Konzentration ein Wahrscheinlichkeitsprodukt von 0,037 liefert. Änderungen von individuellen Wahrscheinlichkeiten erfordern kompensierende Änderungen bei den anderen, dazu in Beziehung stehenden Wahrscheinlichkeiten. Eine Anwendung dieser Beziehung erlaubt die Berechnung von  $r_{13}$  und  $r_{31}$  bei bekanntem  $r_{23}$ ,  $r_{32}$ ,  $r_{12}$  und  $r_{21}$ .

Received June 13, 1963

Revised June 27, 1963



## Rubber Elasticity in Highly Crosslinked Systems: Crosslinked Styrene, Methyl Methacrylate, Ethyl Acrylate, and Octyl Acrylate

A. V. TOBOLSKY, D. KATZ,\* M. TAKAHASHI, and  
R. SCHAFFHAUSER, *Frick Chemical Laboratory,  
Princeton University, Princeton, New Jersey*

### Synopsis

Styrene, methyl methacrylate, ethyl acrylate, and octyl acrylate were each copolymerized with tetraethylene glycol dimethacrylate (TEGDM) over the complete range of copolymer compositions. Modulus-temperature curves of these polymers were constructed and compared. The equation of state for rubber elasticity was applied to the rubbery plateau regions of these polymers.

### Introduction

As reported previously<sup>1,2,3</sup> some highly crosslinked systems have modulus-temperature curves with well-defined glassy, transition, and rubbery plateau regions. Four vinyl-divinyl systems were studied and shear modulus-temperature measurements were made on samples with different compositions. The divinyl monomer in the presently reported work was TEGDM, and the vinyl monomers were: styrene, methyl methacrylate, ethyl acrylate and octyl acrylate. The reasons for choosing these monomers were: (1) their technological importance; (2) they form a group of homopolymers which have over a very wide range of temperatures different viscoelastic properties as their  $T_g$  changes from close to  $-80^\circ\text{C}$ . for poly(octyl acrylate) to  $+105^\circ\text{C}$ . for poly(methyl methacrylate); (3) having different molecular structures and a different viscoelastic behavior in the same temperature range, they offer a good opportunity for the study of the correlation between their structure and viscoelastic properties.

### Experimental

Series of polymer sheets were prepared from monomeric mixtures of TEGDM and each of the vinyl monomers by using a technique similar to the one described in a previous paper.<sup>4</sup> The composition of the samples varied between mole fraction of zero to unity for both monomers used in all the systems. The shear modulus-temperature measurements were made

\* On leave from the Scientific Department, Israel Ministry of Defence.

TABLE I. Styrene(S)-Tetraethylene Glycol Dimethacrylate (TEGDM)

No.	TEGDM, mole-%	$c_{TEGDM}$ , mole/cm. <sup>3</sup>	$\rho$ , g./cm. <sup>3</sup>	$G$ , dynes/cm. <sup>2</sup>	$\epsilon$			$\Phi\epsilon$	$\Phi$
					crosslink efficiency	$\epsilon'$ , mole/cm. <sup>3</sup>	$z\Phi\epsilon$		
1	0.53	0.00053	1.0549	$6.75 \times 10^6$			3.59	1.80	
2	0.97	0.00097	1.0595	$7.40 \times 10^6$			2.15	1.08	
3	2.05	0.00200	1.0627	$1.30 \times 10^7$			1.83	0.92	
4	5.33	0.00495	1.0788	$2.93 \times 10^7$	0.48	0.000238			3.47
5	10.37	0.00892	1.0971	$6.00 \times 10^7$	0.53	0.000473			3.58
6	15.05	0.01212	1.1117	$8.51 \times 10^7$	0.57	0.000691			3.48
7	22.58	0.01649	1.1324	$1.44 \times 10^8$	0.61	0.001006			4.04
8	25.65	0.01810	1.1426	$1.87 \times 10^8$	0.67	0.001213			4.35
9	51.15	0.03769	1.1885	$4.50 \times 10^8$	0.70	0.001938			6.55
10	78.44	0.063400	1.2191	$7.00 \times 10^8$	0.73	0.002482			7.96
11	100.00	0.063748	1.2367	$1.07 \times 10^9$	0.72	0.002699			11.19

TABLE II. Methyl Methacrylate (MM)-Tetraethylene Glycol Dimethacrylate (TEGDM)

No.	TEGDM, mole-%	$c_{TEGDM}$ , mole/cm. <sup>3</sup>	$\rho$ , g./cm. <sup>3</sup>	$G$ , dynes/cm. <sup>2</sup>	$\epsilon$			$\Phi\epsilon$	$\Phi$
					crosslink efficiency	$\epsilon'$ , mole/cm. <sup>3</sup>	$z\Phi\epsilon$		
1	0.50	0.00059	1.1874	$1.45 \times 10^7$			6.94	3.47	
2	1.01	0.00117	1.1875	$1.50 \times 10^7$			3.62	1.81	
3	1.51	0.00173	1.1910	$2.00 \times 10^7$			3.26	1.63	
4	2.02	0.00230	1.1945	$2.01 \times 10^7$			2.47	1.24	
5	5.54	0.00588	1.1984	$4.17 \times 10^7$	0.67	0.000394			2.99
6	10.02	0.00979	1.2026	$6.67 \times 10^7$	0.66	0.000646			2.91
7	15.38	0.01371	1.2033	$1.04 \times 10^8$	0.66	0.000905			3.24
8	19.97	0.01654	1.2085	$1.72 \times 10^8$	0.68	0.001125			4.32
9	25.04	0.01929	1.2143	$2.40 \times 10^8$	0.69	0.001331			5.09
10	49.98	0.02851	1.2262	$5.80 \times 10^8$	0.71	0.002024			8.09
11	74.79	0.03391	1.2335	$1.05 \times 10^9$	0.73	0.002475			11.97

TABLE III  
 Octyl Acrylate (OcAc)-Tetraethylene Glycol Dimethacrylate (TEGDM)

No.	TEGDM, mole-%	TEGDM, mole/cm. <sup>3</sup>	$\rho$ , g./cm. <sup>3</sup>	$G$ , dynes/cm. <sup>2</sup>	$\epsilon$ crosslink efficiency	$c'_{\text{TEGDM}}$ mole/cm. <sup>3</sup>	$z\Phi\epsilon$	$z\Phi$	$\Phi\epsilon$	$\Phi$
1 <sup>a</sup>		0.00026 <sup>a</sup>							0.17 <sup>a</sup>	
2 <sup>a</sup>		0.00035 <sup>a</sup>							0.20 <sup>a</sup>	
3 <sup>a</sup>		0.00052 <sup>a</sup>							0.17 <sup>a</sup>	
4	1.27	0.00067	0.9827	$1.48 \times 10^6$			0.62		0.31	
5 <sup>a</sup>		0.00067 <sup>a</sup>							0.17 <sup>a</sup>	
6 <sup>a</sup>		0.00170 <sup>a</sup>							0.22 <sup>a</sup>	
7	3.47	0.00181	0.9873	$3.20 \times 10^6$			0.50		0.25	
8	5.85	0.00304	0.9989	$5.33 \times 10^6$	0.69	0.000210		0.72		0.36
9	11.32	0.00575	1.0187	$1.28 \times 10^7$	0.75	0.000431		0.84		0.42
10	16.67	0.00829	1.0359	$2.71 \times 10^7$	0.78	0.000645		1.19		
11	25.13	0.01212	1.0643	$5.63 \times 10^7$	0.82	0.000994		1.60		
12	27.97	0.01336	1.0738	$5.73 \times 10^7$	0.84	0.001122		1.44		
13	50.78	0.002239	1.1383	$1.92 \times 10^8$	0.82	0.001836		2.95		
14	75.27	0.003051	1.1913	$6.85 \times 10^8$	0.76	0.002319		8.34		

<sup>a</sup> Data of Tobolsky et al.<sup>4</sup>

TABLE IV  
Ethyl Acrylate (EtAc)-Tetraethylene Glycol Dimethacrylate (TEGDM)

No.	TEGDM, mole-%	$c'_{\text{TEGDM}}$ , mole/cm. <sup>3</sup>	$\rho$ , g./cm. <sup>3</sup>	$G$ , dynes/cm. <sup>2</sup>	$\epsilon$ crosslink efficiency	$c'$ , mole/cm. <sup>3</sup>	$z\Phi\epsilon$	$\Phi\epsilon$	$\Phi$
1 <sup>a</sup>		0.000037 <sup>a</sup>						1.09 <sup>a</sup>	
2	1.41	0.000154	1.1309	$6.88 \times 10^6$			1.26	0.63	
3	3.42	0.000362	1.1406	$1.37 \times 10^7$			1.07	0.54	
4	5.46	0.000557	1.1472	$2.16 \times 10^7$	0.71	0.000395			0.77
5	7.10	0.000702	1.1505	$3.90 \times 10^7$	0.70	0.000491			1.12
6	10.17	0.000956	1.1593	$5.74 \times 10^7$	0.72	0.000688			1.18
7	13.39	0.001191	1.1650	$6.60 \times 10^7$	0.74	0.000881			1.06
8	15.10	0.001253	1.1691	$7.80 \times 10^7$	0.75	0.000940			1.17
9	18.13	0.001507	1.1781	$8.99 \times 10^7$	0.81	0.001221			1.04
10	22.29	0.001747	1.1856	$1.35 \times 10^8$	0.85	0.001485			
11	30.41	0.002140	1.1961	$1.96 \times 10^8$	0.81	0.001733			3.19
12	35.18	0.002339	1.2026	$2.29 \times 10^8$	0.80	0.001871			3.45
13	41.57	0.002564	1.2066	$2.65 \times 10^8$	0.78	0.002000			3.74
14	67.60	0.003244	1.2252	$6.30 \times 10^8$	0.76	0.002465			7.22

<sup>a</sup> Data of Tobolsky et al.<sup>4</sup>

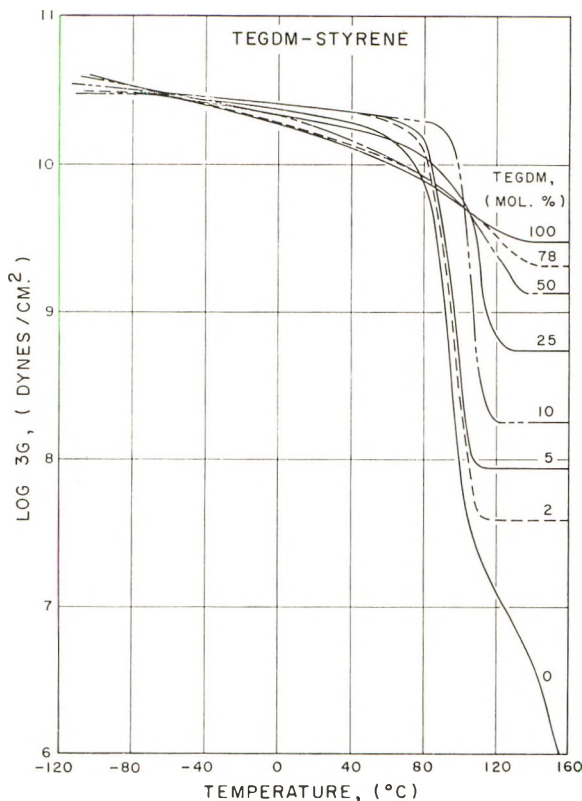


Fig. 1. Plot of  $\log 3G$  vs. temperature for tetraethylene glycol dimethacrylate-styrene copolymers.

on the samples with the use of a modified Gehman apparatus.<sup>5</sup> For samples with high torsion moduli values (above  $5 \times 10^9$  dynes/cm.<sup>2</sup>), especially in the low temperature region, the modulus was calculated also from data obtained by use of the Clash-Berg torsion apparatus.<sup>6</sup> The agreement between the results obtained using both instruments was good. The densities of all the samples were measured by displacement at 25°C. The results of the experiments are given in Tables I-IV, and the modulus-temperature curves are shown in Figures 1-4.

### Efficiency of Crosslinking

As mentioned in an earlier publication,<sup>2</sup> it is well known from previous work 7-9 that the crosslinking in dimethacrylate systems is not complete. In our work we took into consideration the crosslinking efficiencies calculated from the volume contraction of the monomer mixtures after polymerization by determination of the densities before and after the polymerization as done previously by Fox and Loshaek.<sup>7</sup> The measured molar volume contraction for methyl methacrylate was 22.5 cm.<sup>3</sup>, and we assumed that the same molar contraction is associated with each vinyl group in

TEGDM. For styrene the measured molar contraction was  $16.64 \text{ cm}^3$ . In the case of ethyl acrylate the measured contraction after polymerization was  $20.5 \text{ cm}^3/\text{mole}$ . Inasmuch as the value of  $21 \text{ cm}^3/\text{mole}$  was cited previously<sup>7</sup> and we measured for polybutyl acrylate a volume contraction of  $20.75 \text{ cm}^3/\text{mole}$ , we assumed an average shrinkage of  $20.75 \text{ cm}^3/\text{mole}$  for ethyl and octyl acrylate. For mixtures with less than 5 mole-% of TEGDM the determination of crosslinking efficiency is not too reliable by

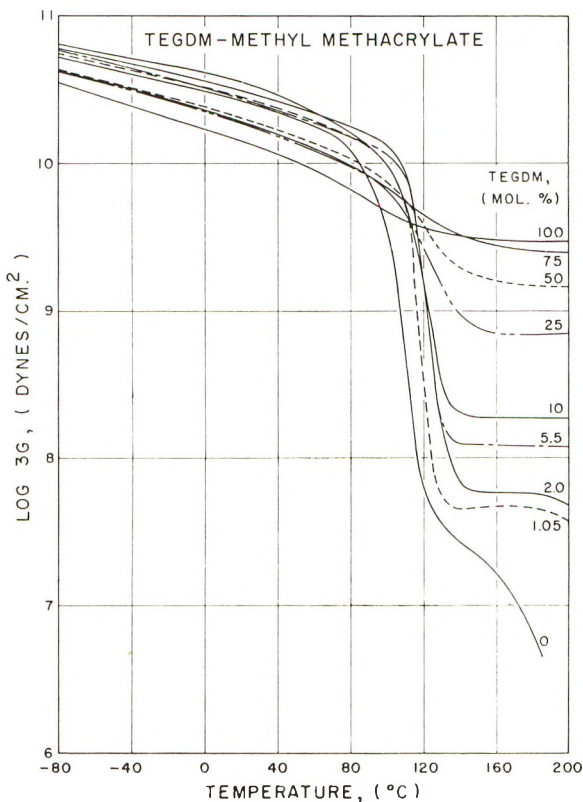


Fig. 2. Plot of  $3G$  vs. temperature for tetraethylene glycol dimethacrylate-methyl methacrylate copolymers.

the density method. It is possible that the efficiencies approach an asymptotic value not much different than the one measured at 5 mole-%. There is, of course, the second possibility, proposed by Loshack and Fox, that for very low mole percentages of TEGDM the efficiencies of crosslinking should continuously increase to 100%.

The efficiencies  $\epsilon$  are presented in Tables I-IV. Once more, as in reference 2, we do not indicate in the tables any numerical values for crosslink efficiency of polymers with less than 5 mole-% of dimethacrylate. The stoichiometric concentration of TEGDM in the polymer expressed in moles per cubic centimeter has been denoted as  $c$  and is tabulated. The concen-

tration of crosslinks  $c'$  expressed in moles per cubic centimeter is obtained by multiplying  $c$  by the efficiency  $\epsilon$ .

$$c' = \epsilon c \quad (1)$$

### Results

As already observed in the case of the ethyl acrylate-TEGDM system,<sup>1</sup> all the compositions have a glassy region, a transition region, and a plateau region. The modulus of the plateau and the temperature at which this

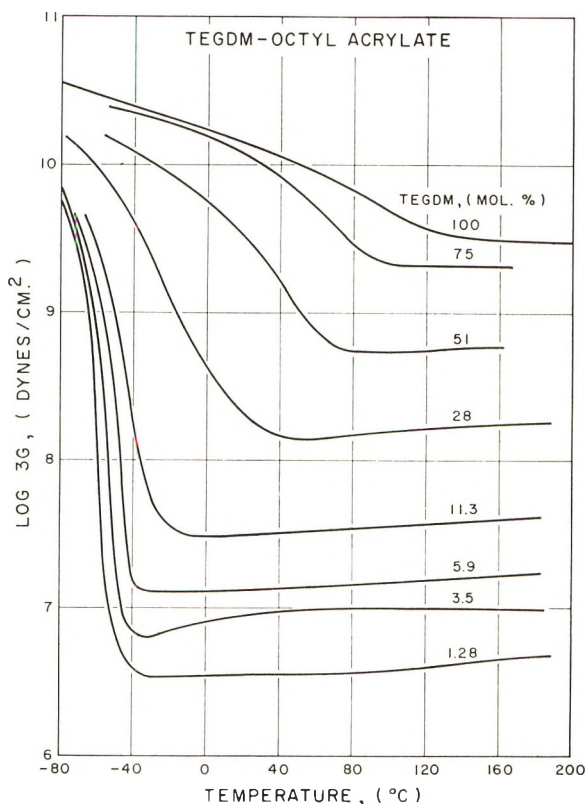


Fig. 3. Plot of  $3G$  vs. temperature for tetraethylene glycol dimethacrylate-octyl acrylate copolymers.

plateau is reached increase with the increase of the amount of the divinyl compound in the polymer. If the results are compared for similar mole percentages of TEGDM in all four systems, it can be seen that the values for the plateau modulus and for the temperature at which the plateau is reached increase in the following order of vinyl compound used: octyl acrylate, ethyl acrylate, styrene, methyl methacrylate.

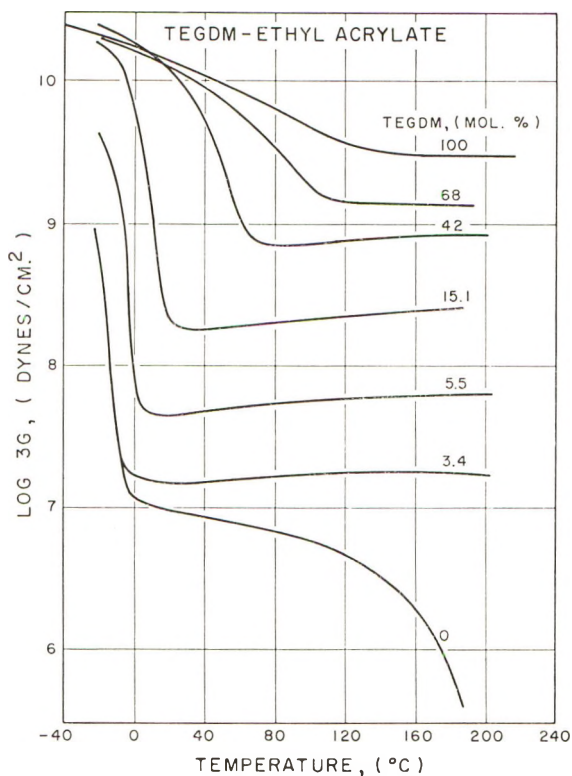


Fig. 4. Plot of  $\log 3G$  vs. temperature for tetraethylene glycol dimethacrylate-ethyl acrylate copolymers.

### Discussion

The equation for the rubbery shear modulus

$$G = \Phi nRT \quad (2)$$

was applied to the experimental data in an attempt to calculate the front factor<sup>4</sup>  $\Phi$  at various crosslink densities. In eq. (2)  $n$  is the concentration of network chains in moles per cubic centimeter,  $R$  is the gas constant, and  $T$  the absolute temperature at which the measurement  $G$  in the rubbery plateau region was made. To make possible the comparison between the four systems, the calculations were made for 153°C., a temperature at which all the investigated polymers have their plateau regions. The amount of network chains per cc. is given by eq. (3):

$$n = c'z \quad (3)$$

when  $c'$  is the actual crosslink density (after taking into consideration the efficiency of crosslinking) and  $z$  a quantity defined by eq. (3). For a tetra-functional crosslink the  $z$  value is two because each network chain is shared by two crosslinks.



By substituting eqs. (1) and (3) into eq. (2) one obtains:

$$G = \Phi z \epsilon c R T \quad (4)$$

In eq. (4) the quantities  $G$ ,  $c$ ,  $\epsilon$ ,  $R$ , and  $T$  are experimental quantities or constants. Hence we were able to compute and tabulate  $\Phi z$  for all samples with higher amounts of dimethacrylate than 5 mole-% and  $\epsilon \Phi z$  for polymers with lower mole percentages of the crosslinking agent at 153°C.

We do not therefore mean to imply that eq. (4) is valid or significant for the very high crosslink densities. We leave this point as a completely open question. The evaluation of  $z$  at high crosslink densities is also an unresolved question.

In a previous paper<sup>2</sup> we established that eq. (4) was valid for ethyl acrylate copolymerized with EGDM, TrEGDM, and TEGDM up to values of dimethacrylate of at least 12 mole-% or crosslink densities up to  $1 \times 10^{-3}$  mole/cm.<sup>3</sup> Also in this range of crosslink density the  $z$  values were shown to be the same for all these three dimethacrylates and therefore it had to be equal to 2.0, since EGDM must be regarded as a tetrafunctional "point" crosslink. The intramolecular chain in EGDM is too short to act as a network chain.

We therefore assume that in this same range of crosslink density, the  $z$  values for TEGDM with styrene, methyl methacrylate, and octyl acrylate are also equal to 2.0. This enables us to compute  $\Phi$  and  $\epsilon \Phi$  (for low amounts of dimethacrylate) in these systems for the entire range of crosslink densities up to  $1 \times 10^{-3}$  mole/cc.

The results that we obtain in this manner are shown in the tables.

Table III includes data previously obtained<sup>4</sup> for the  $\Phi \epsilon$  values for the octyl acrylate system at low crosslink densities. In the previous work we assumed  $\epsilon$  to be unity at these low crosslink densities, but we now prefer to leave this question open. These former  $\Phi \epsilon$  values are somewhat lower than the values obtained in this experimental study. Nevertheless the qualitative agreement is gratifying, inasmuch as the earlier elastic measurements were made in tension and at high values of the extension, whereas the elastic measurements reported in this paper were carried out in shear at very low extensions. For this reason we do not wish to weigh the values of  $\Phi \epsilon$  from the earlier work as heavily as the work reported here.

Two interesting observations can be made by comparison of the results in the tables. The first one is that the  $\Phi$  values up to  $1 \times 10^3$  mole/cm.<sup>3</sup> of dimethacrylate, in the range where the value of  $\epsilon$  can be established, is reasonably constant for each system, and is characteristic for the vinyl compound used in the system. The values are: styrene,  $\sim 1.75$ ; methyl methacrylate,  $\sim 1.55$ ; octyl acrylate,  $\sim 0.38$ ; ethyl acrylate,  $\sim 1.0$ .

A second observation can be made: for polymers of ethyl and octyl acrylate the value of  $\Phi$  remains approximately constant (or possibly decreases) at very low crosslink densities but in polymers of methyl methacrylate, at very low crosslink densities the value for  $\Phi$  increases considerably. These conclusions are drawn by considering the possible range of efficiency

values. (It should be noted that the point at 0.5 mole-% crosslink for methyl methacrylate was checked three times.) The increase in the value of  $\Phi$  for methyl methacrylate copolymerized with low percentages of dimethacrylate can perhaps be attributed to the existence of trapped entanglements in the copolymer as discussed by Hwa.<sup>9</sup> Perhaps this tendency for forming trapped entanglements is related to chain conformation. It is interesting to recall that in an earlier work<sup>1</sup> it was shown that methacrylate polymers tended to favor folded configurations.

The partial support of the Office of Naval Research is gratefully acknowledged.

### References

1. Tobolsky, A. V., D. Katz, R. Thach, and R. Schaffhauser, *J. Polymer Sci.*, **62**, S176 (1962).
2. Katz, D., and A. V. Tobolsky, *J. Polymer Sci.*, **A2**, 1587, 1595 (1964). M.S. Thesis, Cornell University, 1963; P. Sullivan, and B. Wunderlich, *S.P.E. Trans.*
3. Katz, D., and A. V. Tobolsky, *Polymer*, in press.
4. Tobolsky, A. V., D. Carlson, and N. Indictor, *J. Polymer Sci.*, **54**, 175 (1961).
5. A.S.T.M. Standards, Designation D 1053-58 (1958).
6. A.S.T.M. Standards, Designation D 1043-51 (1951).
7. Loshaek, S., and T. G. Fox, *J. Am. Chem. Soc.*, **75**, 3544 (1953).
8. Shultz, A. R., *J. Am. Chem. Soc.*, **80**, 1854 (1958).
9. Hwa, J. C. H., *J. Polymer Sci.*, **58**, 715 (1962).

### Résumé

On a effectué la copolymérisation du styrène, du méthacrylate de méthyle, de l'acrylate d'éthyle et de l'acrylate d'octyle avec le diméthacrylate de tétraéthylène (TEGDM) dans une gamme complète de composition en copolymère. Les courbes du module de température de ces polymères sont construites et comparées. L'équation d'état pour l'élasticité du caoutchouc est appliquée aux régions du plateau caoutchouteux de ces polymères.

### Zusammenfassung

Styrol, Methylmethacrylat, Äthylacrylat und Octylacrylat wurden mit Tetraäthylenglycol-dimethacrylat (TEGDM) über den gesamten Bereich der Copolymerzusammensetzung copolymerisiert. Die Modul-Temperatur-Kurven dieser Polymeren wurden ermittelt und verglichen. Die Zustandsgleichung für die Kautschukelastizität wurde auf die Kautschukplateaubereiche dieser Polymeren angewandt.

Received May 10, 1963

Revised June 13, 1963

## Crystallization of Polyethylene from *o*-Xylene

BERNHARD WUNDERLICH,\* EDWARD A. JAMES, and TSAO-WEN SHU, *Department of Chemistry, Cornell University, Ithaca, New York*

### Synopsis

The upper limit of platelike growth of polyethylene from a 0.1% solution by weight in *o*-xylene can be represented by the equation  $T' = M \times 10^3 / (2.747M + 170.6)$ . This equation was derived on kinetic and thermodynamic arguments. Dendritic growth occurs 8–10°C. below  $T'$ . Higher molecular weights give more irregular and more branched dendrites. The ratio of heterogeneously nucleated hedgehog dendrites is constant for any one preparation crystallized at different temperature. Polymethylene can crystallize in a different morphology above  $T'$ . Interference microscopy was used as a main tool in this research.

### INTRODUCTION

Cooling a polyethylene solution results in either single crystal growth<sup>1</sup> or dendrite formation.<sup>2,3</sup> In this paper the region of single crystal and dendritic growth on isothermal crystallization of polyethylene of different molecular weight will be analyzed.

### EXPERIMENTAL

#### Materials

A series of fractions of linear polyethylene was obtained from the laboratories of the Polychemicals Department of the duPont de Nemours Company. Other samples included polymethylene with an estimated molecular weight of  $10^6$  or larger and two *n*-hydrocarbons,  $C_{36}H_{74}$  and  $C_{94}H_{190}$  (PSU-221). Table I contains the designation of the samples, their molecular weight, the number of carbons per chain and the melting point for a large crystal formed of fully extended chains as calculated by the extrapolation formula given by Broadhurst.<sup>4</sup> The weights of the fractions available were about 5 mg.

#### Crystallization

The samples were weighed into a test tube ( $\sim 5$  mg.) and the calculated amount of *o*-xylene was added to make a 0.1% solution by weight. The *o*-xylene was fractionally distilled (b.p. 141–142°C.) and filtered through

\* Present Address: Department of Chemistry Rensselaer Polytechnic Institute, Troy, New York.

TABLE I  
 Samples Used for Crystallization

Sample	Molecular weight (avg.)	No. of carbons per molecule	Calculated melting point, °K.	$\chi$	$\Delta$ , °K.
00	507	36	348.6	—	—
0	1,321	94	387.1	—	(46)
1	<1,000	—	—	—	—
2	2,275	160	398.0	0.27	42
3	2,500	180	399.7	0.27	42
4	6,400	455	408.4	0.19	48
5	9,000	640	410.1	0.21	49
6	10,000	715	410.6	0.23	49
7	11,000	785	410.9	0.23	49
8	32,500	2,300	413.1	0.24	50
9	34,000	2,400	413.2	0.24	50
10	60,200	4,300	413.7	0.24	50
11	99,000	7,075	413.9	0.26	50
12	212,000	15,100	414.1	0.26	50
13	430,000	30,700	414.2	0.25	50
14	740,000	52,900	414.2	0.25	50
15	>1,000,000	>70,000	414.3	0.25	50

sintered glass. Dissolution was accomplished by dipping the test tube into a 110–120°C. oil bath. To avoid decomposition, the solutions were saturated with N<sub>2</sub> during heating and closed by a ground glass stopper after attaining 110°C.

Crystallization was achieved by quickly plunging the test tube into an isothermal crystallization bath. It took about 2 min. for the solution to reach equilibrium temperature. The temperature of the bath was recorded to  $\pm 0.1^\circ\text{C}$ . Samples of the crystals were removed from the crystallization bath at the crystallization temperature by immersion of a preheated microscope slide. Most of the solution ran off the slide depositing the crystals on the glass. In case of incomplete crystallization at the time of withdrawal of the sample for microscopy, a minor amount of secondary crystallization was found on cooling the wet slide. Under the microscope this secondary growth could easily be distinguished from the dendrites and lamellae grown isothermally.

After removing the microscope slide, the solutions were cooled and prepared for the next crystallization temperature. About ten different temperatures were examined for each fraction.

### Analysis

Analysis of the samples was done by interference microscopy.<sup>5</sup> Visual observations included a description of the morphology, percentage count of different types of crystals, thickness determination, and measurement of the angle between the growth faces of the crystals. The magnification used for visual observation was  $400\times$  ( $40\times$  shearing-type interference objective).

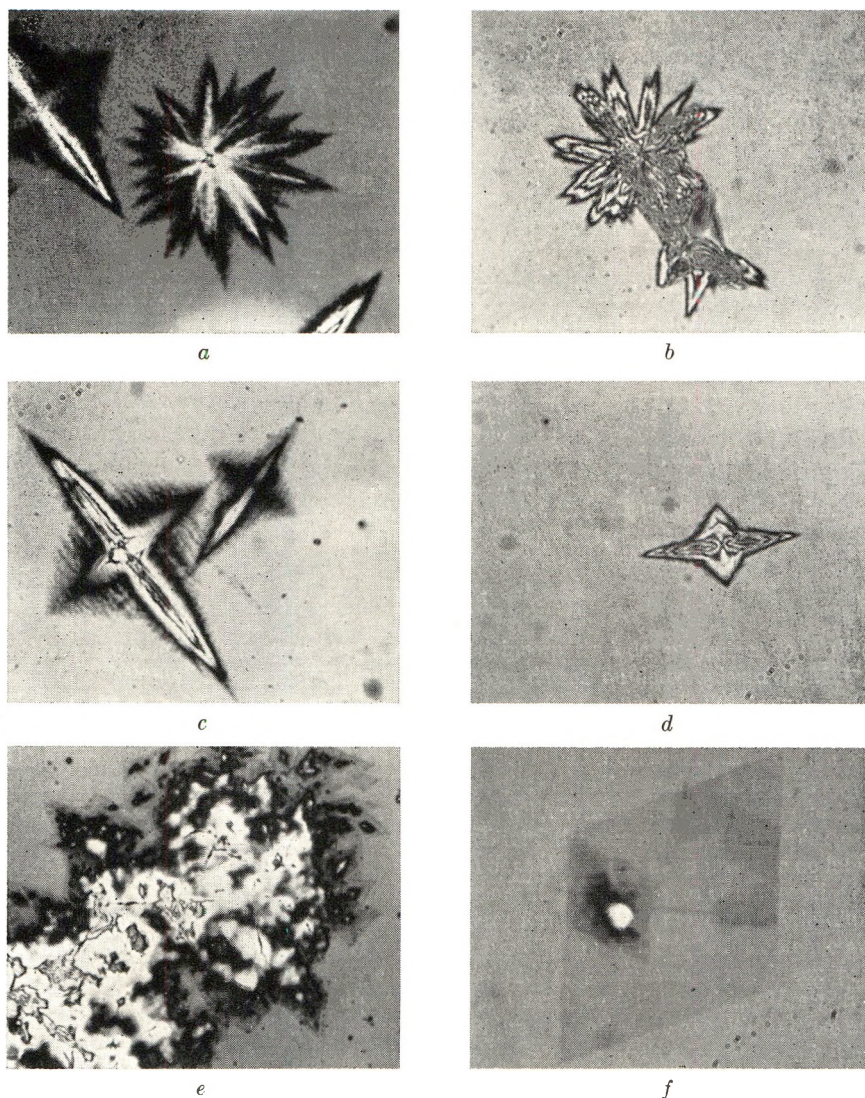


Fig. 1. Types of crystal growth of fractions of polyethylene from *o*-xylene: (a), (b) hedgehog dendrites of different degree of featheriness; (c), (d) Regular dendrites of different degree of featheriness; (e) single crystals with growth spirals clustered together; (f) large separate single crystal lamella. The diameter of all structures is about 0.1 mm.

For thickness determination of single lamellae samples 9, 11, and 14 were crystallized after dilution to 0.04% by immersion of the hot solution into an 87°C. bath and subsequent slow cooling to 85°C. This procedure proved to yield the most uniform large lamellae necessary for thickness determination.

Figure 1 summarizes the structures encountered. Dendrites always were a mixture of hedgehog and right-angle dendrites<sup>3</sup> of different degree of

featheriness (Figs. 1*a*, *b*, *c*, and *d*). Single crystals formed (110) growth faces only and were frequently covered with growth spirals. Figure 1*f* shows the type of crystal grown by the special procedure for thickness determination, while Figure 1*e* shows a typical example of single crystals crystallized from fractions.

## RESULTS AND DISCUSSION

### Lamellar Single Crystal Growth

To establish the region of single crystal growth Figure 2 shows the temperatures where no crystallization could be obtained within 8 hr. (filled circles). The open circles represent the lower limit of perfect single crystal growth on isothermal crystallization. This temperature was found by extrapolation of the angle intersecting (110) and (1 $\bar{1}$ 0) faces to the theoretical angle of 67.5° as a function of temperature. Figure 3 shows a sample extrapolation of fraction 8.

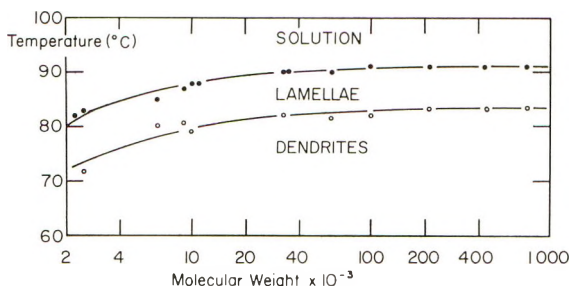


Fig. 2. Molecular weight dependence of the morphology of polyethylene crystallized from *o*-xylene at the temperature given at the ordinate: (●) upper limit of crystallization for times shorter than 8 hr.; (○) lower limit of single crystal growth with perfect growth angles (see Fig. 3). The curve drawn through the filled circles represents eq. (6).

From Figure 2 it can be concluded that for the molecular weight range  $2 \times 10^3$  to  $1 \times 10^6$  the region of perfect lamellar single crystal growth is only 8–10°C. wide. There is a molecular weight dependence of the upper and lower temperatures which is, however, less than that given by Holland and Lindenmeyer<sup>6</sup> for four fractions in the range 10,000–120,000. In fact, the molecular weight dependence is less than that of the bulk melting points extrapolated for extended chain paraffin crystals.<sup>4</sup> The last column in Table I shows that the difference,  $\Delta$ , between the melting point and the maximum crystal growth temperature from solution decreases with decreasing molecular weight.

To gain a thermodynamic description of the temperatures where no plateletlike growth occurred within 8 hr., it is necessary to analyze the kinetic theory of lamellar type growth.<sup>7,8</sup> An upper limit of lamellar type growth is predicted by Frank and Tosi.<sup>8</sup> At this upper limit,  $T'$ , the thick-

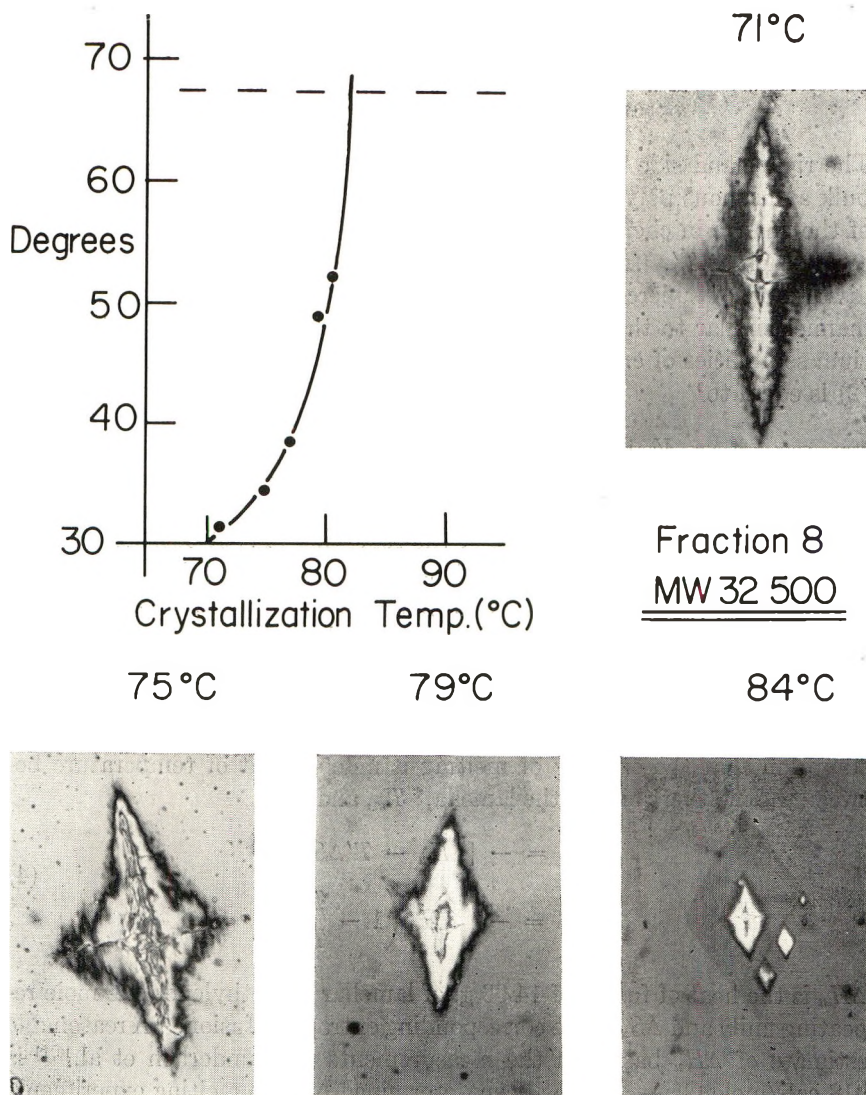


Fig. 3. Extrapolation procedure for fraction 8 to obtain dendrite-single crystal boundary line. Plot shows the average angle of 10–20 crystals between (110) and ( $\bar{1}\bar{1}0$ ) growth faces as a function of crystallization temperature. The photographs show selected crystals grown at the temperatures given. The long dimension of the crystals is approximately 0.1 mm.

ness of the final lamella is  $l_0$ , which is the thickness of a large lamella whose chemical potential is equal to that of the solution.

$$\mu_{\text{solution}} = \mu_{\text{lamella}} \text{ at } T' \quad (1)$$

Subtracting the chemical potential of the bulk amorphous polymer at  $T'$  on

both sides of eq. (1) leads to an expression amenable to comparison with the experiment:

$$\mu_{\text{solution}} - \mu_{\text{amorphous}} = \mu_{\text{lamella}} - \mu_{\text{amorphous}} \quad (2)$$

The right-hand side represents the difference in chemical potential of the bulk amorphous polymer and the lamellae or in other words, the negative of the change in chemical potential on melting of a lamellae into a supercooled melt at  $T'$ . The left-hand side represents the chemical potential of dissolution of supercooled melt at  $T'$ . Equation (2) can be solved in a manner similar to the method used by Huggins<sup>9</sup> for calculation of equilibrium solubilities of crystalline chain polymers. The left-hand side of eq. (2) is equal to<sup>9</sup>

$$\text{LHS} = \frac{V_u}{V_1} \left[ \frac{\ln v_2}{x} - \left( 1 - \frac{1}{x} \right) (1 - v_2) + \chi (1 - v_2)^2 \right] RT'$$

$V_u$  and  $V_1$  are the molar volume of the repeating unit of polymer and the solvent, respectively; for polyethylene-xylene,  $V_u/V_1 = 0.137$ .  $v_2$  is the volume fraction of polymer; for a 0.1% by weight solution  $v_2 = 0.0013$ .  $x$  represents the ratio of the molar volume of the whole polymer molecule to that of the solvent molecule; in the present case  $x = 0.137 \times$  (number of carbon atoms).  $\chi$  is the interaction coefficient,<sup>9</sup> which is assumed to be constant. The right-hand side of eq. (2) can be calculated under the assumption that the entropy of melting is independent of temperature between the melting point of the lamella,\*  $T_m$ , and  $T'$ .

$$\begin{aligned} \text{RHS} &= - [\Delta H_u - T' \Delta S_u] \\ \text{RHS} &= - \left[ \Delta H_u \left( 1 - \frac{T'}{T_m} \right) \right] \end{aligned} \quad (4)$$

$\Delta H_u$  is the heat of fusion of 14.03 g. of lamellar polyethylene (one mole repeating unit) and  $\Delta S_u$  is the corresponding entropy of fusion. A reasonable estimate of  $\Delta H_u$  based on the measurements of Wunderlich et al.<sup>10,11</sup> is 918 cal./mole  $\text{CH}_2$ .  $T_m$  has been determined by fast melting experiments on lamellae  $149 \pm 17$  A. thick which were grown at  $90^\circ\text{C}$ . from xylene.<sup>11</sup>  $T_m$  was found<sup>11</sup> to be  $396.0^\circ\text{K}$ . Samples 9, 11, and 14 in this research were crystallized analogously at about  $86^\circ\text{C}$ . and gave thicknesses of  $140 \pm 17$  A.,  $140 \pm 6$  A., and  $146 \pm 6$  A., respectively. For practical purposes all these values can be assumed constant and grown at the upper limit ( $\sim 91^\circ\text{C}$ . for these high molecular weights). These thicknesses were determined by interference microscopy and compare well with the data of Holland and Lindenmeyer<sup>6</sup> (140 A. at  $90^\circ\text{C}$ .) which were measured from shadow length of electron micrographs.

Combining eqs. (3) and (4) and inserting all data mentioned above, yields

\* For a discussion of the nonequilibrium melting of lamellar crystals and the applicability of eq. (4), see Wunderlich.<sup>14</sup>



for the maximum temperature of lamellar growth of polyethylene from 0.1 wt.-% *o*-xylene solution, the following relation:

$$2.525 - 0.296\chi + \frac{0.296M + 170.6}{\bar{M}} = \frac{1}{T'} \times 10^3 \quad (5)$$

where  $M$  is molecular weight. The  $\chi$  values in Table I have been calculated by use of this equation.  $\chi$  is reasonably constant and averages 0.25. This constant average can be substituted in eq. (5) to obtain:

$$T' = \frac{M \times 10^3}{2.747M + 170.6} \quad (6)$$

Equation (6) has been plotted in Figure 2 as the curve running through the solid circles.

Comparison of the  $\chi$  value with literature values<sup>12,13</sup> shows the right order of magnitude. Values for *p*-xylene run from 0.15 to 0.40 for different molecular weights.<sup>13</sup> Such a strong molecular weight dependence of  $\chi$  is not apparent from the data presented here. It must, however, be kept in mind that the theoretical description presented here is based on the assumption that the surface free energy does not change on lowering the molecular weight and that there is no influence on  $T_m$  by the increasing number of ends of chains. Both are only first-order approximations on which the present experimental data cannot improve. In particular it is felt that the lower molecular weight fractions may easily be fractionated further on crystallization near  $T'$ , making an analysis beyond eq. (6) uncertain.

It is of interest to note, that the dendrite-single crystal boundary remains approximately parallel to eq. (6). There is no continuation of the dendrite-lamella boundary to the nonfolded *n*-paraffins. Even quenching in ice water produced lath-shaped (110)-twin lamellae of C<sub>94</sub>H<sub>190</sub> with little changed angles. The dendritic habit is thus characteristic of the non-uniform molecular weight crystals. The upper crystallization temperature of C<sub>94</sub>H<sub>190</sub> (68–69°C.) and C<sub>36</sub>H<sub>74</sub> (<20°C.) are also not represented by eq. (6).

### Dendritic Growth

A cross section of polyethylenes of different molecular weights crystallized isothermally to dendritic structures at a temperature about 10 degrees below the dendrite-lamella boundary is shown in Figure 4. Also shown is a similarly grown structure from a broad molecular weight distribution polymer (Marlex 50). The following generalizations can be made: (1) the higher the molecular weight the more branched are the dendrites; (2) for molecular weights above 100,000 the dendrites become more irregular; (3) the broad molecular weight distribution gives the most perfect large dendrites.

Low molecular weights grow to relatively thick compact shapes resembling the single crystal platelets with somewhat sharpened angles. Occasion-

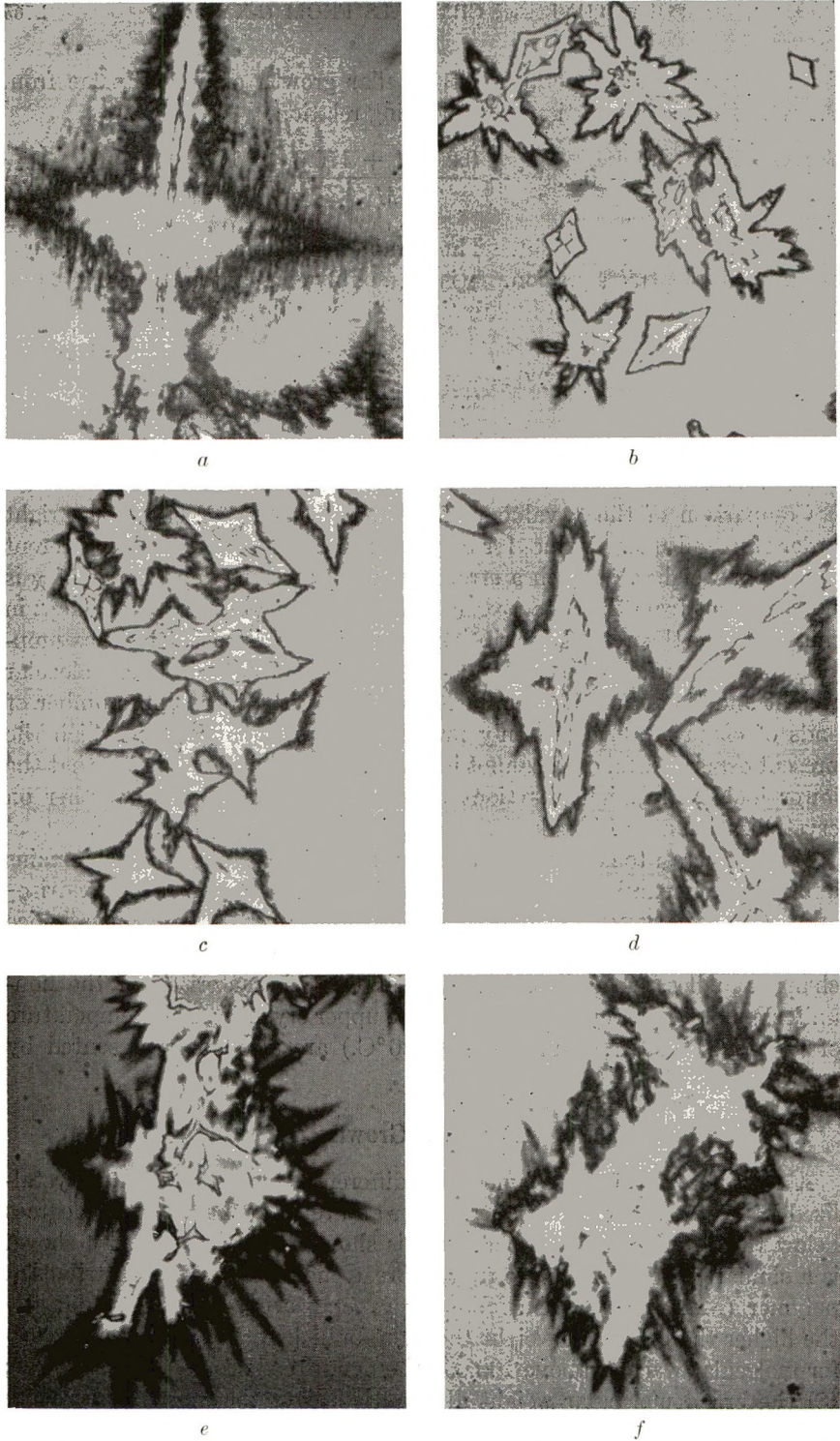


Fig. 4. Molecular weight dependence of the shape of dendrites grown at approximately constant supercooling: (a) broad molecular weight distribution (Marlex 50) crystallized at 72°C.; (b) sample 2 (MW 2,275) crystallized at 62°C. ( $\Delta = 18^\circ\text{C}.$ ); (c) sample 9 (MW 34,000) crystallized at 68°C. ( $\Delta = 21^\circ\text{C}.$ ); (d) sample 11 (MW 99,000) crystallized at 74°C. ( $\Delta = 17^\circ\text{C}.$ ); (e) sample 13 (MW 430,000) crystallized at 74°C. ( $\Delta = 17^\circ\text{C}.$ ); (f) sample 15 (MW  $> 10^6$ ) crystallized at 74°C. ( $\Delta = 17^\circ\text{C}.$ ).

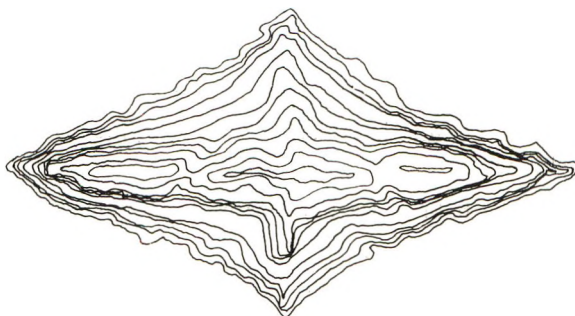


Fig. 5. Composite drawing of a thick polyethylene crystal grown from *o*-xylene. Difference in thickness between two successive lines is 1300 Å. The long dimension of the crystal is 0.08 mm.

ally branches of dendritic material grow from the sides of these compact shapes. Figure 5 gives a contour map of such a compact structure similar to those shown in Figures 4*b* and 4*c*. The outermost line indicates the boundary. Every successive line marks an increase in height of 1300 Å, so that the total height is about 15,000 Å. The contour map was constructed by superimposing eight interference photographs<sup>5</sup> at different analyzer setting (22.5° apart) and tracing the sharp interference fringes of all photographs.

All fractions showed regular and hedgehog dendrites<sup>3</sup> (see Fig. 1). The percentage of hedgehog dendrites varied between 5 and 40% for the different fractions. For different temperatures of crystallizations of the same fraction this percentage stayed constant or increased slowly for later experiments on the same solution. This is in accord with the original assumption<sup>3</sup> that hedgehog dendrites are nucleated heterogeneously and depend on the amount of contamination of the solution.

### Polymethylene

The polymethylene sample with a molecular weight far above  $10^6$  formed relatively irregular dendrites, as can be seen in Figure 4. Its single crystals also were hard to observe for the low resolution interference micrograph. The upper limit of crystal growth within 8 hr. was 91°C. and lies on the extension of the upper lamellar growth curve in Figure 3.

At temperatures a few degrees above 91°C. very slow growth of large isolated stringlike structures, originally described in reference 15 was observed. Microscopically this material was made up of a finely divided irregularly structured strongly birefringent material of considerable thickness which was beyond the capability of the interference microscope. The growth of the few original nuclei per batch continued for weeks without new nucleation.

The only other sample for which occasionally similar growth was obtained was the unfractionated sample, so that one might conclude that this material consists of very high molecular weight polyethylene growing on a

heterogeneous nucleus in a nonplateletlike habit as predicted by Frank and Tosi<sup>8</sup> above  $T'$ .

Financial support from the Advanced Research Projects Agency (E.A.J.), the National Science Foundation (T.W.S.) and the Office of Naval Research is gratefully acknowledged.

The authors would like to thank Dr. F. Billmeyer, Jr. for supplying the polyethylene fractions used in this research.

PSU-221, courtesy of Prof. J. A. Dixon, Director, Whitmore Laboratory, College of Chemistry and Physics, Am. Petrol. Res. Inst. Res. Proj. 42, Penn. State University.

### References

1. See for example, A. Keller, *Makromol. Chem.*, **34**, 1 (1959).
2. Geil, P. H., and D. H. Reneker, *J. Polymer Sci.*, **51**, 569 (1961).
3. Wunderlich, B., and P. Sullivan, *J. Polymer Sci.*, **61**, 195 (1962).
4. Broadhurst, M. G., *J. Chem. Phys.*, **36**, 2578 (1962).
5. Wunderlich, B., and P. Sullivan, *J. Polymer Sci.*, **56**, 19 (1962); P. Sullivan, M.S. Thesis, Cornell University; 1963; P. Sullivan, and B. Wunderlich, *S.P.E. Trans.* (1964).
6. Holland, V. F., and P. H. Lindenmeyer, *J. Polymer Sci.*, **57**, 589 (1962).
7. Lauritzen, J. I., Jr., and J. D. Hoffman, *J. Res. Natl. Bur. Std.*, **64A**, 73 (1960); *ibid.*, **65A**, 297 (1961); F. P. Price, *J. Polymer Sci.*, **42**, 49 (1960); F. P. Price, *J. Chem. Phys.*, **35**, 1884 (1961).
8. Frank, F. C., and M. Tosi, *Proc. Roy. Soc. (London)*, **A263**, 323 (1961).
9. Huggins, M. L., *J. Am. Chem. Soc.*, **64**, 1712 (1942); *Ann. N. Y. Acad. Sci.*, **44**, 431 (1943); M. L. Huggins, *Physical Chemistry of High Polymers*, Wiley, New York, 1958, p. 73.
10. Wunderlich, B., and M. Dole, *J. Polymer Sci.*, **24**, 201 (1957).
11. Wunderlich, B., P. Sullivan, T. Arakawa, A. B. DiCyan, and J. F. Flood, *J. Polymer Sci.*, **A1**, 3581 (1963).
12. Harris, I., *J. Polymer Sci.*, **8**, 353 (1952).
13. Trementozzi, Q. A., *J. Polymer Sci.*, **23**, 887 (1957).
14. Wunderlich, B., *Polymer*, in press; preprinted in *Am. Chem. Soc., Div. Polymer Chemistry Preprints Volume 3, No. 2*, pg. 63-73 (1962).
15. Wunderlich, B., *J. Polymer Sci.*, **A1**, 1245 (1963).

### Résumé

La limite supérieure de la croissance en plaques du polyéthylène à partir d'une solution de 0.1% en poids dans l'*o*-xylène peut être représentée par l'équation  $T' = M \times 10^3 / (2.747 M + 170.6)$ . L'équation est dérivée d'arguments cinétiques et thermodynamiques. La croissance dendritique a lieu vers 8-10°C au-dessous de  $T'$ . Des poids moléculaires plus élevés donnent des dendrites plus irréguliers et plus ramifiés. Le rapport des dendrites maclés, formés par nucléation hétérogène, est constant pour n'importe quelle préparation cristalline à différentes températures. Le polyméthylène peut être cristallisé dans une morphologie différente au-dessus de  $T'$ . La microscopie interférentielle est l'instrument principal utilisé au cours de ces travaux.

### Zusammenfassung

Die obere Temperaturgrenze für das plättchenartige Wachstum von Polyäthylen aus einer Lösung von 0,1 Gewichtsprozent in *o*-Nylol kann durch die Gleichung  $T' = M \times 10^3 / (2,747 M + 170,6)$  dargestellt werden. Diese Gleichung wurde aus kinetischen und thermodynamischen Überlegungen hergeleitet. 8-10°C unterhalb von  $T'$

tritt Dendritenwachstum auf. Bei höheren Molekulargewichten entstehen unregelmässige und stärker verzweigte Dendrite. Der Anteil der durch heterogene Keimbildung entstandenen Igeldendrite ist für jedes einzelne der bei verschiedenen Temperaturen hergestellten Kristallisate konstant. Polymethylen kann oberhalb von  $T'$  morphologisch andersartig kristallisieren. Bei diesen Untersuchungen bediente man sich hauptsächlich der Interferenzmikroskopie.

Received June 17, 1963

## Association of Organic Quaternary Ammonium Cations with Polyacrylates. Conductivity and Viscosity Measurements

A. PACKTER,\* *School of Pharmacy, Chelsea College of Science and Technology, London, England*

### Synopsis

The association of series of alkyl and aryl quaternary ammonium cations with polyacrylate and acrylate copolymers (with acrylamide, butyl acrylate, and styrene) was studied by combined conductivity and viscosity measurements on the organic ammonium polysalts. The degree of counterion binding in the low molecular weight alkyl trimethylammonium polysalts is basically determined—as with small organic counterions—by the distance between the carboxylate groups on the polyion backbone, i.e., electrostatic effects predominate with these cations. However, the counterion-polyion interaction decreases significantly with increase in counterion size and steric effects from tetramethyl- to hexyltrimethylammonium cation. In the octyl- and decyltrimethylammonium polysalts, van der Waals' effects become more effective and the degree of association then increases with increase in counterion size. Phenyl- and naphthyltrimethylammonium cations behave similarly to the lower alkyl homologs. Pyridine- and quinolinemethonium cations interact more markedly with polyacrylates, especially with the butyl acrylate and styrene copolyacrylates. Van der Waals' interaction between the organic sections of counterion and polyion backbone is indicated with these cations; the estimated free energy due to this effect (with these cations) is 0.2–0.5  $RT$  cal./g. mole.

### INTRODUCTION

The interaction of organic counterions with polyelectrolytes is a phenomenon of great theoretical interest, since the association is caused by both electrostatic coulombic interaction<sup>1-4</sup> between charged polyion and counterion and by van der Waals' interaction<sup>5-8</sup> between the organic section of the counterion and polyion backbone. Steric effects<sup>4,9</sup> may also be important. However, although the highly specific interactions of organic anions with certain proteins have been studied extensively,<sup>7,8</sup> only a few experimental investigations with simple polyelectrolytes have been reported.<sup>3,5,6</sup>

This paper presents a systematic study of the association of alkyl and aryl quaternary ammonium cations with polyacrylate and acrylate copolymers, by combined conductivity and viscosity measurements<sup>3</sup> on the organic ammonium polysalts.

\* Present address: Chemistry Department, West Ham College of Technology, London, England.

The counterion-polyion interaction has been studied as a function of polysalt concentration, and of the chemical and physical properties of the counterion and polyelectrolyte structure.

## EXPERIMENTAL

### A. Materials

#### *Polyacrylic Acid*

Polyacrylic acid was prepared by two methods: redox polymerization in aqueous solution<sup>10</sup> and benzoyl peroxide polymerization in benzene.<sup>11</sup>

**Redox Polymerization in Aqueous Solution.** Acrylic acid (20 g.) was dissolved in distilled water (300 ml.) containing 0.2 mole-% catalyst mixture (equimolecular amounts of potassium metabisulfite and persulfate) and previously deoxygenated by 60 min. nitrogen stirring.

Polymerization was allowed to proceed to 25°C. for 6 hr.

The polyacrylic acid was precipitated from the viscous solution with acetone and further purified by dissolving the precipitate in water and reprecipitating with acetone.

This precipitate was dried at 105°C. and ground to a fine powder.

The molecular weight, as determined viscometrically,<sup>12</sup> was 300,000.

**Benzoyl Peroxide Polymerization in Benzene.** Acrylic acid (20 g.) and benzene (100 ml.) containing benzoyl peroxide catalyst (0.0030 g.) were reacted for 4 hr. at 75°C. in a 500 ml. flask under continuous nitrogen stirring (after 30 min. preliminary deoxygenation).

The suspended white powder was washed free of unreacted acrylic acid with benzene, then with petroleum ether, filtered, and dried at 40°C.

The molecular weight as determined viscometrically, was 500,000.

#### *Copolymers of Acrylic Acid*

**50/50 Polyacrylic Acid-Acrylamide and 20/80 Polyacrylic Acid-Acrylamide.** Acrylic acid was copolymerized with acrylamide in aqueous solution by redox polymerization at the same catalyst/total monomer ratio as for polymerization of acrylic acid.

**50/50 Polyacrylic Acid-Butyl Acrylate.** Acrylic acid was copolymerized with butyl acrylate in benzene solution by the benzoyl peroxide method,<sup>10</sup> at the same catalyst/total monomer ratio as for polymerization of acrylic acid.

**50/50 Polyacrylic Acid-Styrene.** Acrylic acid was copolymerized with styrene in benzene solution by the benzoyl peroxide method at the same catalyst/total monomer ratio as for polymerization of acrylic acid.

Acrylic acid contents were determined by potentiometric titration in 1*N* KCl against standard sodium hydroxide solution.

### *Preparation of Solutions*

Stock solutions of the polyacids were standardized by potentiometric titration and all concentrations expressed as gram-equivalents monomer acid per liter.

The water for the preparation of solutions and conductivity measurements was prepared by passing fresh glass-distilled water (specific conductivity of  $3\text{--}5 \times 10^{-6}$  ohms. $^{-1}$ ) through a bed of mixed ion-exchange resins (in an Elgostat) and used immediately. Its specific conductivity, at 25°C., varied between  $0.8$  and  $1.2 \times 10^{-6}$  ohms. $^{-1}$ .

### *Quaternary Salts*

**Alkyl Trimethylammonium Bromides.** These were prepared by Tartar's method<sup>13</sup> by interacting the alkyl bromide (of 98–100% purity as supplied by Kodak Laboratories Ltd.) with excess alcoholic trimethylamine solution. The salts were dried over silica gel and recrystallized from acetone.

Tetramethylammonium bromide was supplied by British Drug Houses Ltd. and recrystallized from alcohol.

**Aryl Trimethylammonium Iodides.** These were prepared by interacting the tertiary amine (of 98–100% purity, as supplied by British Drug Houses Ltd.) with slight excess of methyl iodide<sup>14</sup> and recrystallized from alcohol solution.

These salts were analyzed for halide by potentiometric titration with standard silver nitrate. The halide contents were found to be 99.5–99.9% of the theoretical values.

**Quaternary Ammonium Hydroxide Solutions.** These hydroxide solutions were then prepared by treating the corresponding halide salt solution (0.1*N*) with slight excess silver oxide.

The solution was then centrifuged, filtered free of silver halide, and standardized by potentiometric titration with standard hydrochloric acid.

**Organic Ammonium Polysalts.** Polyacid solutions (0.05*N*) were titrated potentiometrically with the appropriate organic base to pH 8.5 and the neutralized solution diluted when required with conductivity water.

## **B. Conductivity Measurements**

A titration cell with platinized platinum electrodes was used, similar to that described by previous workers.<sup>3,14</sup> The cell constant at 25°C. was determined with standard potassium chloride solutions. Solutions were stirred with nitrogen, saturated with water vapor at 25°C.

Conductivity measurements were made with a Pye conductance bridge (Model 11700) operating at 300 cycles/sec. and fitted with a cathode-ray oscillographic detector; cell capacitance effects were balanced out by means of a condenser in parallel with the variable resistance. The bridge operated with an accuracy of 0.1%. Measurements were made at  $25.0 \pm 0.1^\circ\text{C}$ .

Measured volumes of the organic ammonium polysalt solution were run into conductivity water, the solution allowed to come to equilibrium at



25°C., the stirring stopped and the conductivity measured. In all, 10–12 measurements were taken with each salt to study the concentration range 0.0003–0.003*N*.

### C. Viscosity Measurements

Viscosities were measured at 25.0°C. with a suspended level dilution viscometer (Ubbelohde type, A.S.T.M. Specification D445–46T).

The effluent time for distilled water was 250 sec. at 25.0°C. and kinetic energy corrections were negligible.

### D. Determination of Degree of Counterion–Polyion Association

#### Conductivity Results

Some typical  $\Lambda-\sqrt{c}$  graphs are presented in Figure 1; they are similar to those obtained with inorganic polysalts.

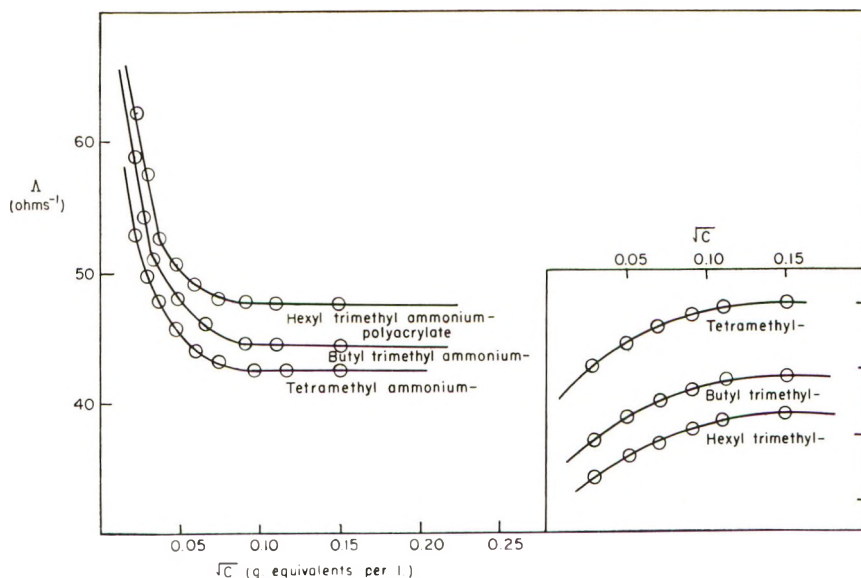


Fig. 1. Variation of equivalent conductivity (and degree of association) of organic ammonium polyacrylates with concentration, at 25°C.

The equivalent conductivity ( $\Lambda$ ) decreases rapidly from  $\Lambda_0$  (at  $C = 0$ ) to values in the range 0.4–0.7  $\Lambda_0$  at  $c = 0.0001N$ ; then, with further increase in polysalt concentration,  $\Lambda$  decreases gradually to a minimum value.

#### Viscosity Results

Typical  $\eta_{sp}/c-c$  graphs are presented in Figure 2.  $\eta_{sp}/c$  decreases continuously with increasing polysalt concentration  $c$ , i.e., with increasing

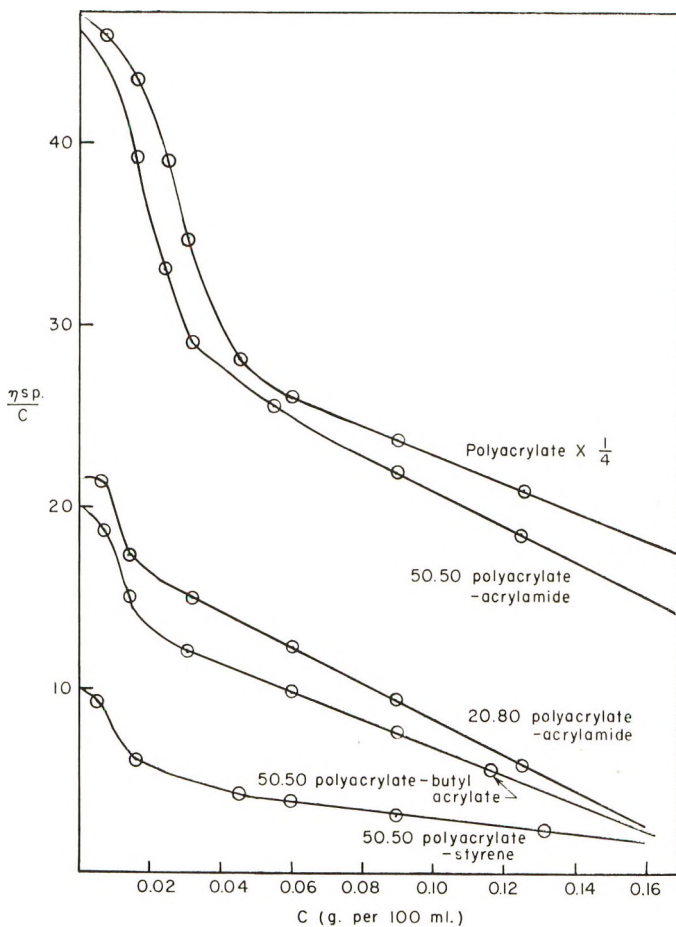


Fig. 2. Variation of specific viscosity of tetramethyl ammonium polyacrylates with concentration, at 25°C.

ionic strength of the system. These  $\eta_{sp}/c$  and  $\Lambda$  values, in turn, were used to determine the polyanion mobility and degree of association at various polysalt concentrations.

#### Polyanion Mobility

$\lambda_{p-(0)}$  Values. The mobility,  $\lambda_{p-(0)}$ , of the extended polyanion in very dilute solution and free from associated counterions was first determined.

Previous workers<sup>3,16</sup> have indicated that in dilute polycarboxylic acid solutions, neutralized up to about 20% with sodium hydroxide, the degree of polysalt dissociation corresponds exactly to the fraction ( $x$ ) of polysalt formed.

There is very limited ionization of the free carboxylic acid groups in the presence of the common anion and practically no counterion association in

these systems. The equivalent conductivity of such polysalt solutions is then

$$\Lambda_{(0)} = x(\lambda_{0\text{Na}^+} + \lambda_{p-(0)}) \quad (1)$$

The equivalent conductivity of polysalt solutions, prepared by partial neutralization of polyacid with exactly one tenth an equivalent of sodium hydroxide, was therefore measured at a series of dilutions.  $\Lambda_{(0)}$  at  $c = 0.0001N$  was then determined by extrapolation and  $\lambda_{p-(0)}$  calculated from the eq. (1). The  $\lambda_{p-(0)}$  values, determined by the above method are given in Table I.

TABLE I

Polyacrylate	$\lambda_{p-(0)}$ , ohms <sup>-1</sup>
Polyacrylate	40.0
50/50 Polyacrylate-acrylamide	45.0
20/80 Polyacrylate-acrylamide	70.0
50/50 Polyacrylate-butyl acrylate	55.0
50/50 Polyacrylate-styrene	57.5

**$\lambda_p$ -Values at Other Concentrations.** The viscosity results (Fig. 2) indicate that in dilute solutions ( $c < 0.01N$ ), the polyanions studied exist as extended rod-shaped coils, but at higher concentrations, certain of the copolyacrylates may become less extended and more oblate-spheroidal in form.

For extended coil or rod-shaped polyanions,  $\lambda_p$ -values are practically independent of concentration and length.<sup>17</sup> As a first approximation, therefore, it was assumed that  $\lambda_{p-} = \lambda_{p-(0)}$  at all concentrations up to  $c = 0.01N$ .

However, the effective polyanion mobility at any concentration varies with the degree of counterion binding, i.e., on the degree of dissociation ( $\alpha$ ) of polysalt, according to the relation,<sup>16,17</sup>

$$\lambda_{p-eff} = \alpha\lambda_{p-} \quad (2)$$

#### *Degree of Association*

The degree of polysalt dissociation ( $\alpha$ ) was then determined from the equation:<sup>3,16</sup>

$$\begin{aligned} \Lambda &= \alpha(\lambda_{R^+} + \lambda_{p-eff}) \\ &= \alpha(\lambda_{R^+} + \alpha\lambda_{p-}) \end{aligned} \quad (3)$$

where  $\lambda_{R^+}$  is the ionic conductivity of the organic ammonium cation, and  $\lambda_{R^+}$  values were taken from earlier work.<sup>13</sup>

The degree of polysalt association<sup>2</sup> is then\*

$$z = (1 - \alpha) \quad (4)$$

## RESULTS AND DISCUSSION

### Variation of Degree of Association with Polysalt Concentration

Degree of association–(concentration)<sup>1/2</sup> graphs were plotted: some typical results are presented in Figure 1 (inset).

The  $z-\sqrt{c}$  curves are similar to those reported for inorganic polysalts.<sup>3,15</sup>

In all the systems studied,  $z$  values increase rapidly from  $z = 0$  at  $c = 0$  to  $> 0.2$  at  $c = 0.003N$ , then increase only gradually with further increase in concentration to  $c > 0.003N$ .

### Variation of Degree of Association with Type of Counterion and Polyion

Both electrostatic and van der Waals' type interactions between polyions and organic counterions are determined essentially by the counterion size.<sup>3,4,8</sup> The mode of interaction is best investigated by presenting the experimental results as a function of this property.

$z$  values at various polysalt concentrations were therefore plotted against organic counterion length  $l$ .

$l$  values were measured from Courtauld models as the lengths of the organic section of the quaternary ammonium cations.<sup>18–19</sup>

The results for the 0.01*N* systems are presented in Figures 3 and 4.

They are typical of all the systems studied.

The results for the polyacrylates prepared from the two different polyacrylic acids did not differ significantly.

The results for polysalts of the small (practically unhydrated)  $\text{K}^+$  cation are included for comparison.

#### *Alkyl Trimethylammonium Counterions*

The degree of counterion association, as measured by  $z$ , for lower ammonium polysalts with the same cation, increases in the order, 20/80 copolyacrylates < 50/50 copolyacrylates < polyacrylates. Association is basically determined by the distance apart of the carboxylate groups on the polyion backbone: this phenomenon is also observed with small inorganic cations.<sup>1,2,4</sup>

\* The dependence of mobility on polyanion concentration and dimensions is far more complex with oblate-spheroidal polyanion coils.<sup>17</sup>

Gregor<sup>3</sup> has suggested that for spherical coils,  $\lambda_{p-}$  varies approximately as  $(1/\eta_{sp})^{1/3}$ . Hence in the more concentrated copolysalt systems studied, we might expect that  $\lambda_{p-}$  would vary approximately as  $(1/\eta_{sp})^n$ , where  $n < 0.3$ ; i.e.,  $\lambda_{p-}$  values would increase from  $\lambda_{p-(0)}$  at  $c = 0.001N$  to  $> 1.3\lambda_{p-(0)}$  at  $c > 0.01N$ .

The  $z$  values calculated for these copolysalts would then be up to 0.01 too low at  $c = 0.001N$  and up to 0.05 too low at  $c = 0.01N$  (see Figs. 3A,B). However, the overall variation of  $z$  with counterion size would not be affected.

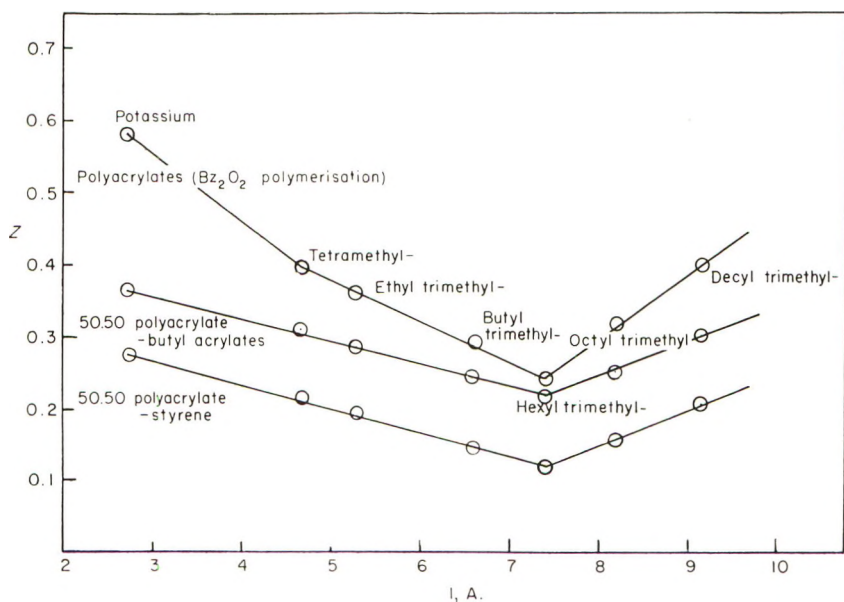
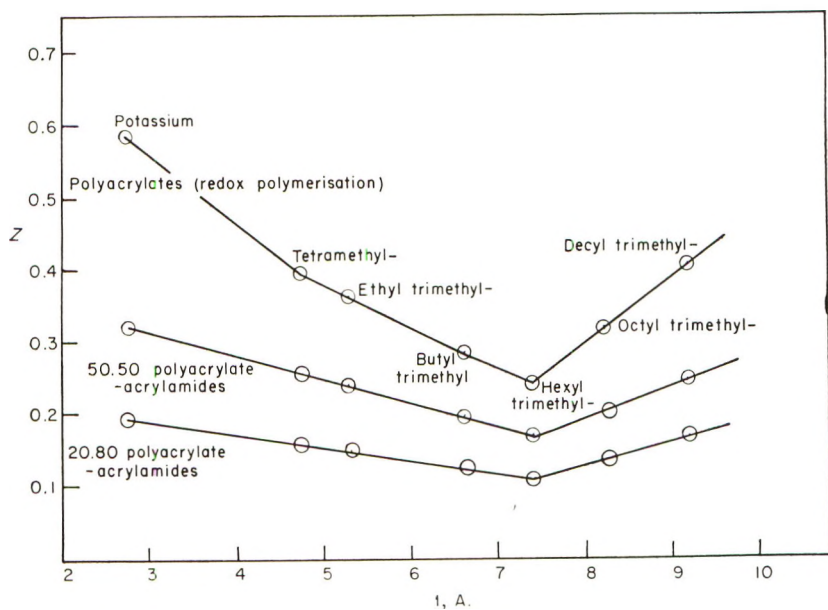


Fig. 3. Variation of degree of association of alkyl quaternary ammonium polyacrylates (0.01  $N$ ) with counterion length, at 25°C.

Electrostatic effects thus predominate with these lower ammonium poly-salts.

The counterion-polyion association for any series of polysalts, however, decreases significantly with increase in size and steric hindrance of the bulky organic counterion; the increase in length of the organic counterion

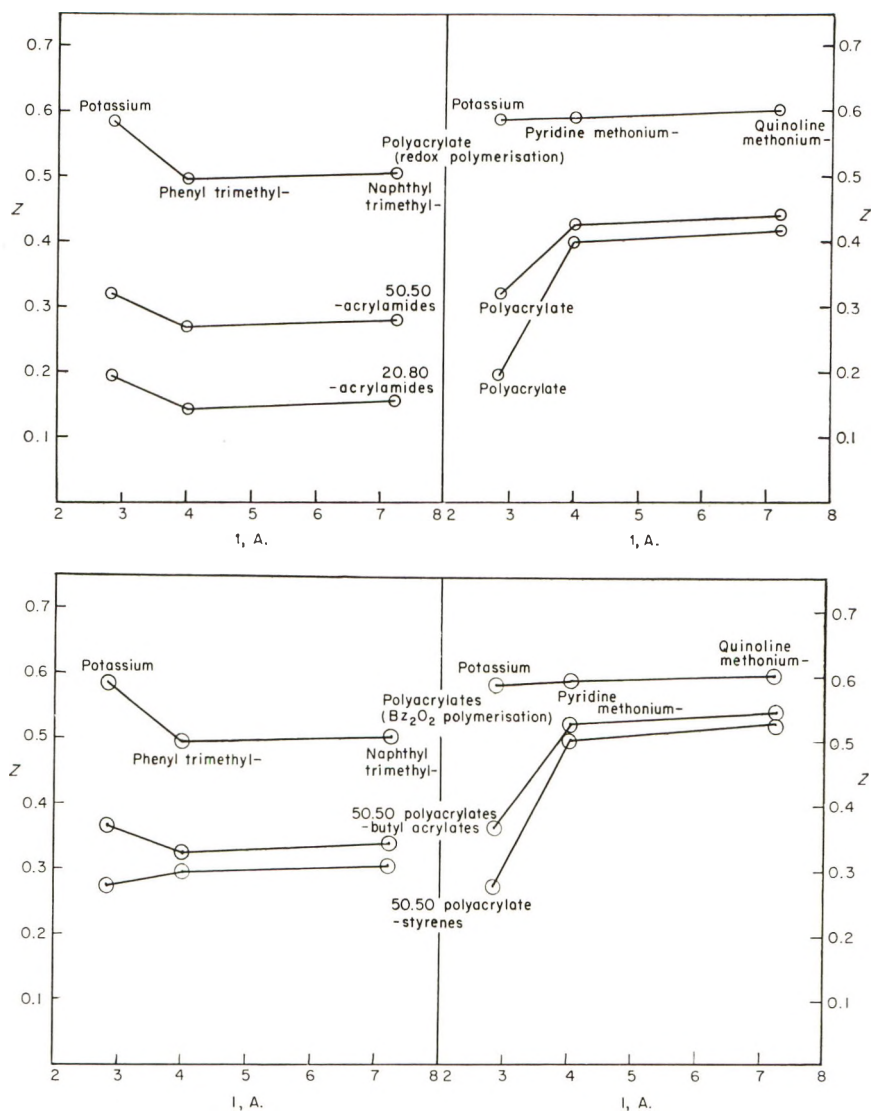


Fig. 4. Variation of degree of association of aryl quaternary ammonium polyacrylates (0.01N) with counterion length, at 25°C.

modifies the closest radius of approach. This effect is most marked ( $z$  decreases from ca. 0.43 to 0.28) with the polyacrylates in which the distance apart of the carboxylate groups is greatest.

In the octyl- and decyltrimethylammonium salts, the van der Waals' interaction between the organic sections of counterion and polyion backbone becomes more effective, and the degree of association then increases with increase in counterion size.

The decrease in  $z$  values with increasing counterion size may be explained semiquantitatively by Lifson's<sup>20</sup> and Oosawa's<sup>21</sup> model for counterion asso-

ciation, if the mathematical analysis is modified<sup>9</sup> to take finite counterion size and radius of closest approach into consideration.

#### *Aryl Quaternary Ammonium Counterions*

The degree of counterion-polyion association with phenyl- and naphthyl-trimethylammonium cations is similar to that of the alkyl quaternary, ammonium cation of the same length.

The less bulky pyridine- and quinolinemethonium cations, on the other hand, interact more markedly with polyacrylates, especially with the 50/50 acrylate-butyl acrylate and acrylate-styrene copolymer salts.

Van der Waals' attraction between the organic sections of the counterion and the pendant groups on the polyion backbone is indicated with these cations.<sup>1,19</sup>

However, the quinoline- and naphthalene-derived cations are only slightly more strongly bound than the corresponding pyridine- and benzene-derived cations. Presumably, increased steric hindrance of the organic section and decrease in radius of closest approach balances out the slightly enhanced van der Waals' attraction that results from increased length of aromatic ammonium cation.

#### *Van der Waals' Free Energy*

In systems showing appreciable van der Waals' interactions between counterion and polyion, the total free energy change,  $(-\Delta G)$ , may be considered as an additive function of electrostatic and van der Waals' free energies:<sup>8,22</sup>

$$(-\Delta G) = (-\Delta G)_{\text{el.}} + (-\Delta G)_{\text{v. der W.}} \quad (5)$$

It has been noted<sup>3,9</sup> for organic ammonium polysalt systems, in which little or no van der Waals' and/or steric effects are likely, that the total free energy,  $(-\Delta G)$ , was approximately equal to the total free energy,  $(-\Delta G)_{\text{KP}}$ , of the corresponding potassium polysalt. For these systems,

$$(-\Delta G) = (-\Delta G)_{\text{el.}} \simeq (-\Delta G)_{\text{KP}} \quad (6)$$

It was then assumed that eq. (6) was also valid for systems showing van der Waals' effects, but no appreciable steric effects. For these systems,

$$(-\Delta G) \simeq (-\Delta G)_{\text{KP}} + (-\Delta G)_{\text{v. der W.}} \quad (7)$$

or

$$(-\Delta G)_{\text{v. der W.}} \simeq (-\Delta G) - (-\Delta G)_{\text{KP}} \quad (8)$$

Generally, for organic cation association,

$$(-\Delta G) = -2.303RT \log K \quad (9)$$

where  $K$  is the mass-action constant for association.<sup>7</sup>

Neglecting activity coefficients, we have.

$$K = (1 - \alpha)/\alpha^2c = z/[(1 - z)^2c] \quad (10)$$

Then

$$(-\Delta G) = -2.303RT \log \{z/[(1-z)^2c]\} \quad (11)$$

and

$$(-\Delta G)_{KP} = -2.303RT' \log \{z_{K^+}/[(1-z_{K^+})^2c]\} \quad (12)$$

Approximate van der Waals' free energies were then determined from degree of association values for the aryl ammonium polysalt systems studied by using equations (8), (11) and (12).

$(-\Delta G)_{v. der w.}$  values for the 0.01*N* systems are presented in Table II.

TABLE II  
van der Waals' Free Energies for 0.01*N*  
Aryl Ammonium-Polysalt Systems (25.0°C)

	$(-\Delta G)$ van der Waals/ $RT$ , cal./g.-mole				
		50/50 Poly- acrylate- acryla- mide	20/80 Poly- acrylate- acryla- mide	50/50 Poly- acrylate- butyl acrylate	50/50 Poly- acrylate -styrene
Phenyltrimethyl ammonium		Steric effects predominate			0.07
Naphthyltrimethyl- ammonium		Steric effects predominate			0.10
Pyridine methonium	0.05	0.28	0.32	0.45	0.52
Quinoline-methonium	0.09	0.31	0.37	0.43	0.55

van der Waals' effects are appreciable with the pyridine- and quinoline-methonium copolyacrylates.

### References

- Harris, F. E., and S. A. Rice, *J. Phys. Chem.*, **61**, 1360 (1957).
- Wall, F. T., *J. Am. Chem. Soc.*, **79**, 15506 (1957); *J. Chem. Phys.*, **26**, 114 (1957).
- Gregor, H. P., D. H. Gold, and M. Frederick, *J. Polymer Sci.*, **23**, 467 (1957).
- Schellman, J. A., *J. Phys. Chem.*, **57**, 472 (1953).
- Higuchi, T., L. Kennon, and T. Higuchi, *J. Am. Pharm. Soc.*, **46**, 21 (1956).
- Cavallito, J., *J. Am. Pharm. Soc.*, **47**, 165 (1957).
- Klotz, I. M., F. M. Walker, and R. B. Pivan, *J. Am. Chem. Soc.*, **68**, 1486 (1946).
- Fredericq, E., *Bull. Soc. Chim. Belges* **63**, 158 (1954).
- Packter, A., in preparation.
- Bourdais, J., *Bull. Soc. Chim. France*, **1955**, 485.
- Trementozzi, Q., *J. Am. Chem. Soc.*, **76**, 5273 (1954).
- Ito, H., *Kogyo Kagaku Zasshi*, **59**, 930 (1956).
- Tartar, H. V., *J. Am. Chem. Soc.*, **65**, 692 (1943).
- Vogel, A. J., *Practical Organic Chemistry*, Longmans, London, 1957, p. 660.
- Bourdais, J., *J. Chim. Phys.*, **56**, 194 (1959).
- Oth, A., and P. Doty, *J. Phys. Chem.*, **56**, 43 (1952).
- Hermans, J. J., *J. Polymer Sci.*, **18**, 527 (1955).
- Edwards, J. T., *Sci. Proc. Roy. Dublin Soc.*, **27**, 273 (1956).



19. Packter, A., and M. Donbrow, *Proc. Chem. Soc.*, **1962**, 220.
20. Lifson, S., *J. Polymer Sci.*, **13**, 43 (1954).
21. Oosawa, F., *J. Polymer Sci.*, **23**, 421 (1957).
22. Kagawa, I., and M. Nagasawa, *J. Polymer Sci.*, **16**, 299 (1955).

### Résumé

On a étudié, par des mesures combinées de conductivité et de viscosité des polysels organiques d'ammonium, l'association d'une série de cations d'ammonium quaternaire alcoyle ou aryle avec les copolymères d'acrylate et polyacrylate (avec l'acrylamide, l'acrylate de butyle et avec le styrène). Pour les polysels d'alcoyltriméthylammonium de poids moléculaire faible, comme pour les petits contréions organiques, le degré de liaison du contre-ion est déterminé principalement par la distance entre les groupes carboxylates sur la chaîne principale du polyion; cela veut dire que l'effet électrostatique est prédominant pour ces cations. Cependant l'interaction entre le contre-ion et le poly-ion diminue fort lorsqu' on augmente la dimension du contre-ion et les effect stériques du cation du tétraméthyl à l'hexyl-triméthyl ammonium. Pour les polysels d'actyle et de décyl-triméthyl-ammonium les effets de Van der Waals deviennent plus efficaces et le degré d'association augmente alors lorsqu'on augmente la dimension du contre-ion. Les cations de phényl et de naphthyl-triméthylammonium se comportent comme les homologues alcoyles inférieurs. L'interaction du cation méthonium de la quinoline et de la pyridine est plus marquée avec les polyacrylates spécialement avec les acrylates de butyle et les copolyacrylates de styrène. L'interaction de van der Waals entre les sections organiques du contre-ion et la chaîne principale du poly-ion est indiquée par trois cations. L'énergie libre estimée pour cet effet (avec ces cations) est de 0.2-0.7 *RT* calories par q. mole.

### Zusammenfassung

Die Assoziation einer Reihe quaternärer Alkyl- und Aryl-Ammoniumkationen mit Polyacrylaten und Acrylatecopolymeren (mit Acrylamid, Butylacrylat und Styrol) wurde durch Leitfähigkeits- und Viskositätsmessungen an den organischen Ammoniumpolysalzen untersucht. Das Ausmass der Gegenionen-Bindung in den niedrigmolekularen Alkyltrimethylammonium-Polysalzen wird grundsätzlich—wie im Falle kleiner organischer Gegenionen—durch den Abstand der Carboxylatgruppen von der Polyion-Hauptkette bestimmt, d.h. im Falle dieser Kationen herrschen elektrostatische Effekte vor. Die Gegenion-Polyion-Wechselwirkung nimmt jedoch mit zunehmender Grösse des Gegenions und mit zunehmenden sterischen Effekten vom Tetramethyl- zum Hexyl-trimethylammoniumkation deutlich ab. Im Falle der Octyl- und Decyltrimethylammonium-Polysalze werden die van der Waals'schen Kräfte stärker wirksam und der Assoziationsgrad nimmt mit steigender Grösse des Gegenions zu. Phenyl- und Naphthyltrimethylammonium-Kationen verhalten sich ähnlich wie die niedrigeren Äthylhomologen. Die Wechselwirkung von Pyridin- und Chinolmethonium-kationen mit Polyacrylaten, insbesondere mit Butylacrylat und mit Styrol-Copolyacrylaten ist stärker ausgeprägt. Bei diesen Kationen tritt van der Waals-Wechselwirkung zwischen dem organischen Teil des Gegenions und der Polyion-Hauptkette auf. Die diesem Effekt bei diesen Kationen entsprechende freie Energie wurde zu 0,2-0,5 *RT* Kalorien pro Mol bestimmt.

Received October 31, 1962

Revised June 21, 1963

## Preparation of Polyconjugated Systems by New Reaction of Dihydrohalogen Polymerization

I. M. PAUSHKIN and S. A. NIZOVA, *I. M. Gubkin Institute of Petroleum and Gas Chemistry, Moscow, U.S.S.R.*

### Synopsis

The reaction of dihydrohalogen polymerization was suggested by the authors as a method for the preparation of polymers with conjugated double bonds on the basis of  $\alpha,\beta$ -dihalogen derivatives, oxides, and hydroxides. The reaction was carried out in an autoclave at 200°C.; the reaction time was 6 hr. Polymers, obtained from  $\alpha,\beta$ -dibromopropylnitrile,  $\alpha,\beta$ -dibromopropyl alcohol, and  $\alpha,\beta$ -dibromoethylbutyl ether, are black and brown powders soluble in concentrated acids. The polymers show a sharp peak in EPR-spectra characteristic of polyconjugated systems with concentration of paramagnetic particles of  $10^{17}$ – $10^{19}$ /g. The infrared spectra have characteristic absorption bands peculiar to polyconjugated systems.

In the past several years several reports have appeared on the preparation of polymers with conjugated double bonds which are of interest in connection with such specific properties such as semiconductor properties, paramagnetism, and high thermal resistance. Polyvinylenes were prepared by polymerization of acetylene hydrocarbons. Polymerization can be thermal, radiation-induced under pressure, or with a catalyst of the Ziegler type.<sup>1-4</sup>

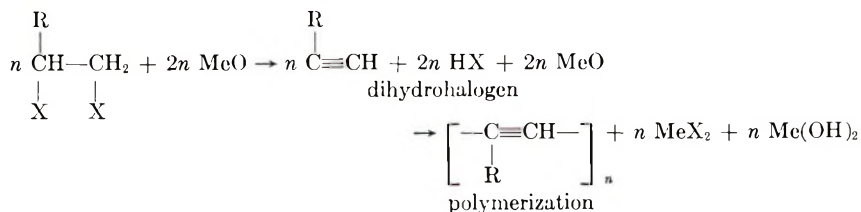
Some methods of the preparation of polyvinylenes involve intermolecular abstraction of small molecules from the saturated macromolecules.

It is possible to use polyvinyl alcohol and the esters of polyvinyl alcohol which on heating, photolysis, or irradiation cause removal of water or alcohol without breaking of the carbon chain.<sup>5</sup>

Winslow and his co-workers<sup>6</sup> on heat treatment of polyvinylene chloride and oxidized polyvinylbenzene have obtained products with semiconductor properties.

Kargin and Kabanov<sup>7</sup> have found a new method of preparation of polyvinylene hydrocarbons from aldehydes and ketones in the presence of zinc chloride as a dehydrating catalyst of polymerization.

The dihydrohalogen polymerization reaction was suggested by the authors as a method for preparation of polymers with conjugated double bonds from  $\alpha,\beta$ -dihalogen derivatives, oxides, and hydroxides.



where R is an alkyl or aryl radical.

From the reaction of dihydrohalogen polymerization there have been obtained polyconjugated systems starting from the monomers listed in Table I.

TABLE I

Monomers	Polymers
$\text{CH}_2\text{Br}-\text{CHBr}-\text{C}\equiv\text{N}$	$\left[ \begin{array}{c} -\text{C}=\text{CH}- \\   \\ \text{C}\equiv\text{N} \end{array} \right]_n$
$\text{CH}_2\text{Br}-\text{CHBr}-\text{C}_6\text{H}_5$	$\left[ \begin{array}{c} -\text{C}=\text{CH}- \\   \\ \text{C}_6\text{H}_5 \end{array} \right]_n$
$\text{CH}_2\text{Cl}-\text{CHCl}-\text{C}_6\text{H}_5$	
$\text{CH}_2\text{Br}-\text{CHBr}-\text{O}-\text{R}$	$\left[ \begin{array}{c} -\text{C}=\text{CH}- \\   \\ \text{OR} \end{array} \right]_n$
$\text{CH}_2\text{Br}-\text{CHBr}-\text{CH}_2\text{OH}$	$\left[ \begin{array}{c} -\text{C}=\text{CH}- \\   \\ \text{CH}_2\text{OH} \end{array} \right]_n$
$\text{CH}_2\text{Br}-\text{CHBrCN} + \text{CH}_2\text{Br}-\text{CH}_2\text{Br}-\text{C}_6\text{H}_5$	$\left[ \begin{array}{c} -\text{C}=\text{CH}-\text{C}=\text{CH}- \\   \quad   \\ \text{C}\equiv\text{N} \quad \text{C}_6\text{H}_5 \end{array} \right]_n$

The dihydrohalogen polymerization was carried out in an autoclave of 50 ml. capacity at 200°C. and at a  $\alpha,\beta$  dibromo derivative:calcium oxide molar ratio of 1:2. The reaction time was 6 hr.

The starting monomer was thoroughly mixed with calcium oxide and placed in the autoclave from which the air was evacuated.

The obtained product was washed several times in hot water to remove  $\text{CaBr}_2$  and dried at 60°C. in vacuum; then it was dissolved in benzene (in the case of a soluble polymer).

The residue insoluble in benzene was treated with 10% hydrochloric acid in order to turn calcium hydroxide, which is almost insoluble in water into easily soluble calcium chloride and to permit the presence of the organic component in the residue insoluble in benzene to be determined.

From the benzene filtrate there was precipitated with methanol a polymer which was filtered, washed in benzene-methanol mixed solvent, and then dried at 40-60°C. in vacuum.

The precipitation of the polymer was repeated several times.

Polyphenylacetylene prepared from  $\alpha,\beta$ -dibromo or  $\alpha,\beta$ -dichloroethylbenzene is a polymer soluble in benzene and acetone, having a mean molec-

ular weight of 1000–1100, and similar to the polymer obtained by polymerization of phenylacetylene.

The polymers prepared from  $\alpha,\beta$ -dibromopropylnitrile,  $\alpha,\beta$ -dibromopropyl alcohol, and  $\alpha,\beta$ -dibromoethylbutyl ether are black and brown powders insoluble in simple organic solvents but easily soluble in organic concentrated acids.

The polymers show sharp peaks in EPR-spectra characteristic of polyconjugated systems with concentration of paramagnetic particles of  $10^{17}$ – $10^{19}$ /g.

The infrared spectra have characteristic absorption bands peculiar to polyconjugated systems.

The melting points for the soluble polymers are within the range 240–260°C. The polymers insoluble in the organic solvents are thermoresistant, i.e., they do not melt up to 400°C.

The dihydrohalogen polymerization makes it possible to prepare polyconjugated systems from various  $\alpha,\beta$ -dihalogen derivatives by varying dihydrohalogen reagents and temperatures of the reaction.

At present we are carrying out further research on the preparation of new polyconjugated systems and a close study of their properties.

### References

1. Barkanov, I. M., A. A. Berlin, V. K. Goldansky, and B. T. Dzantiev, *Vysokomol. Soedin.*, **2**, 231, 1960.
2. Berlin, A. A., *Khim. Tekhnol. Polimerov*, **1960**, No. 7–8, 000.
3. Korshak, V. V., A. M. Polyakova, and M. D. Suchkova, *Vysokomol. Soedin.*, **2**, 208 (1960).
4. Natta, G., *Angew. Chem.*, **69**, 21 (1957).
5. Grassie, N., *Chemistry of High Polymer Degradation Processes*, Butterworths, London, 1956.
6. Winslow, F. H., and W. O. Baker, *J. Am. Chem. Soc.*, **77**, 7751 (1955).
7. Kargin, V. A., V. A. Kabanov, and V. P. Zubov, *Dokl. Akad. Nauk SSSR*, **140**, 1 (1961).

### Résumé

Les auteurs ont suggéré que la réaction de polymérisation par déhydrohalogénéation est une méthode de préparation des polymères à doubles liaisons conjuguées au départ de dérivés  $\alpha\beta$  dihalogénés, d'oxydes et d'hydroxydes. La réaction a été effectuée en autoclave à 200°C; le temps de réaction a été de 6 heures. Les polymères obtenus au départ d' $\alpha\beta$ -dibromopropylnitrile, d'alcool  $\alpha\beta$ -dibromopropylique, d'ester  $\alpha\beta$ -dibromoéthylbutyrique sont des poudres brunes et blanches solubles dans des acides concentrés. Les polymères présentent un signal aigu dans le spectre EPR, caractéristique de systèmes polyconjugués, les concentrations en particules paramagnétiques étant de  $10^{17}$  à  $10^{18}$  unités par gramme. Les spectres infrarouges révèlent également des bandes d'absorption caractéristique de systèmes polyconjugués.

### Zusammenfassung

Die Dehydrohalogenierungspolymerisation wurde von den Autoren als Methode zur Darstellung von Polymeren mit konjugierten Doppelbindungen auf der Basis von  $\alpha,\beta$ -Dihalogenderivaten, Oxyden und Hydroxyden vorgeschlagen. Die Reaktion wurde in

einem Autoklaven bei 200°C durchgeführt und dauerte 6 Stunden. Die aus  $\alpha,\beta$ -Dibrompropylnitril,  $\alpha,\beta$ -Dibrompropylalkohol und  $\alpha,\beta$ -Dibromäthylbutylester erhaltenen Polymeren sind braune und schwarze, in konzentrierten Säuren lösliche Pulver. Die Polymeren zeigen eine scharfe Spitze in dem für polykonjugierte Systeme charakteristischen EPR-Spektrum mit einer Konzentration an paramagnetischen Teilchen von  $10^{17}$ – $10^{19}$  in einem gr. der Verbindung. Die infrarotspektren besitzen für polykonjugierte Systeme charakteristische Absorptionsbanden.

## Carriers and Unpaired Spins in Some Organic Semiconductors

HERBERT A. POHL, *Polytechnic Institute of Brooklyn, Brooklyn, New York*, and RICHARD P. CHARTOFF, *School of Engineering, Princeton University, Princeton, New Jersey*

### Synopsis

Semiconduction and electron spin resonance studies on a number of conjugated polymers representative of the polyacetylenes, the polybenzimidazoles, and the polyacene quinone radical polymers were made. Observed resistivities ranged from 270 to  $10^{16}$  ohm-cm. at room temperature. These and the spin concentrations, the relaxation times, and the energies of activation of conductance and spin concentration were found to be functions of the molecular structure. It was considered impressive evidence that impurity effects on the electronic properties of molecular solids are far less than those commonly observed with the covalently bonded semiconductors such as Ge and Si, for example. A detailed analysis was made of the carrier and free radical formation and lifetimes in these ekaconjugated molecular solids using a simple model.

Because of the possible meaning for biological as well as solid state science, one seeks interpretive insight into the electronic behavior of organic solids. In this paper we discuss some observations made using semiconduction and electron spin resonance on several classes of organic molecular solids which are polymeric. Semiconducting polymers are of especial interest as a class because they contain examples of stable new semiconducting materials which may have widely adjusted electronic properties. They can exhibit, for example, the highest known piezoconductive coefficients.

The term semiconduction as applied here implies conduction only by electronic transport, in accord with usual definitions.<sup>1,2</sup> We exclude from our discussion materials which conduct substantially by ionic (electrolytic) means, or those which conduct because they are mixtures of a nonconductor and a conductive filler. Semiconductors, whether organic or inorganic, are those substances exhibiting conduction intermediate between that of metals and insulators ( $10^3$ – $10^{-10}$  mho/cm.); which supply their own carriers, and exhibit various junction phenomena. Additional criteria may include a positive temperature–conductivity coefficient, a high sensitivity to impurity or morphology, photoconduction, photovoltaism, and possibly high Seebeck or Hall coefficients.

In this study we have examined several classes of conjugated polymers, namely, the polyacetylenes, the polybenzimidazoles, and the polyacene-

quinone radical polymers (called the PAQR polymers). As we shall see, these cover a wide range in electronic characteristics. By comparing their electronic characteristics with their molecular structure we shall endeavor to gain an insight as to the mechanisms of enhanced electronic behavior in organic molecular solids.

The synthesis and study of stable semiconducting macromolecules is a new and fascinating aspect of chemistry.<sup>3-9</sup> Conjugated macromolecules may be subdivided into (1) those having acyclic (linear) systems of conjugated bonds and (2) those containing aromatic, heterocyclic, or metallocyclic structures in their main chains.

The orbitals of the  $\pi$  electrons in a conjugated molecule can be considered as overlapping with the resultant mixing of wave functions to form delocalized molecular orbitals encompassing all nuclei of the conjugated system.<sup>10</sup> This, in principle, permits easing the transmission of an electrical disturbance along the molecule (polarizability). The orbital delocalization also causes a decrease in the internal energy of the system resulting in a molecular structure of greater thermodynamic stability. Many highly conjugated polymers have been found, for example, to possess thermal stability at temperatures in excess of 400°C.<sup>11-13</sup> Orbital delocalization, besides increasing the polarizability and the thermodynamic stability, also brings about a decrease in the excitation energy required to promote  $\pi$  electrons to triplet and other excited states. Of particular import is the increased ease of "mixing in" the ionic states, necessary for carrier formation in the semiconductors. This decrease in the promotional energies is reflected in the observed enhanced semiconducting, magnetic, optical, and chemical properties of these materials.<sup>11,14-16</sup> If the degree of conjugation is sufficient, and if certain geometric properties governed by symmetry are met, then excited electronic states can exist in appreciable degree at room temperature, and the molecule is said to be ekaconjugated.<sup>3</sup> Prior work in this field has been reviewed by Berlin,<sup>11</sup> by Pohl,<sup>2</sup> and by Semenov.<sup>17</sup>

As experimental data have accumulated it has become apparent that ekaconjugation in macromolecules containing double bonds depends upon such parameters as (a) the extent of geometrical symmetry, (b) the length of the sequence of neighboring  $\pi$ -orbitals, (c) the presence of heteroatoms, and (d) the physical state of the polymer. It will be the purpose of this paper to present data and considerations which might be useful in the clarification of just how structural factors might enhance electronic properties of macromolecules.

## EXPERIMENTAL

### Materials

Various alkyl and aryl acetylenes may be polymerized at room temperature or slightly higher (20-70°C.) in the presence of Ziegler-type catalysts. Samples of polypropyne, polybutyne-1, polypentyne-1, and polyphenyl-

acetylene were prepared and carefully purified for this study by the Polymer Corporation Limited of Canada, at Sarnia. These materials were prepared under dry  $N_2$ , then vacuum-dried at 0.1 mm. Hg pressure for 72 hr., sealed off, and sent to us. Our further examination was made under dry  $N_2$  atmosphere.

The polypropyne sample was an orange-colored, brittle solid; the polybutyne-1 and polypentyne-1 were deep blue-black in color, and soft and rubbery; the polyphenylacetylene was a deep orange-colored powder. X-ray spectra showed that these materials were at most only slightly crystalline, but that they possessed a preferred periodicity. Infrared and ultraviolet spectra indicated a high degree of conjugated unsaturation, together with some unconjugated unsaturation. Intrinsic viscosity and solubility data for these polymers are shown in Table I.

TABLE I  
Intrinsic Viscosity and the Solubility of Polyalkynes in Toluene at 30.1°C.

Polymer	$[\eta]$ , dl./g.	Solubility, %
Polypropyne	0.07	100
Polybutyne-1	0.16	99
Polypentyne-1	0.21	93
Polyphenylacetylene	0.16	96

Polybenzimidazoles<sup>12</sup> can be prepared by the melt polycondensation of aromatic tetraamines and diphenyl esters or aromatic dicarboxylic acids. The evidence so far available<sup>12</sup> shows these materials to be completely conjugated and wholly aromatic polymers of great stability and of high molecular weight. These polymers are quite resistant to treatment with hydrolytic media and can withstand long exposure at high temperature. They are soluble and stable in concentrated  $H_2SO_4$  or  $HOOCH$ . Many are also soluble in dimethyl sulfoxide. Eleven well-characterized polymers were furnished by Professor C. S. Marvel for this study. Their structures are shown in Table II.

Polyacene quinone radical polymers were prepared<sup>5,8,13</sup> by the melt condensation polymerization of various aromatic hydrocarbons or their derivatives, with acids or acid anhydrides. A detailed infrared study by the KBr pellet technique on one polymer prepared from phenol and phthalic anhydride showed it to contain much of the phthalide structure, and to be consistent over all with a polyphenolphthalein structure linked directly between the phenolic benzene rings.<sup>13</sup> The compositions newly made here are given in Table III.

### Measurements

Conductivity and its temperature coefficient were determined on molded specimens at moderate pressure (1850 atm.) as described earlier.<sup>7,8,13</sup> Measurements of the electron spin resonance characteristics were made with the generous assistance of Dr. Robert Pressley on apparatus at the



TABLE II. Polybenzimidazole Structure

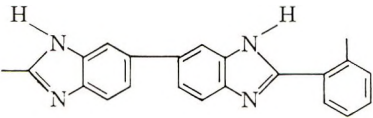
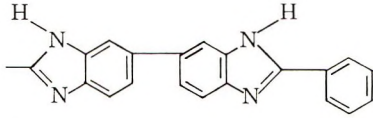
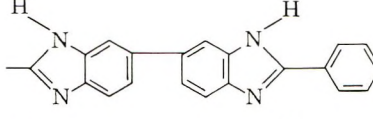
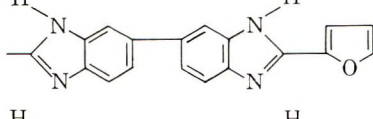
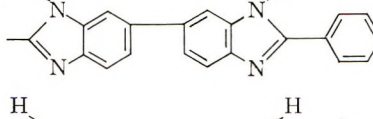
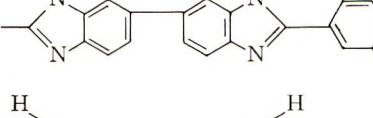
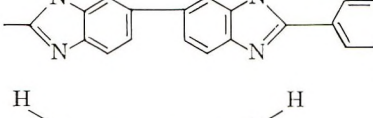
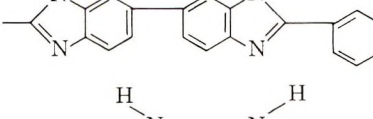
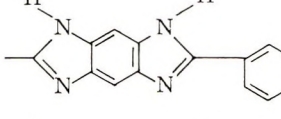
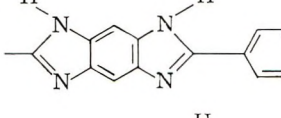
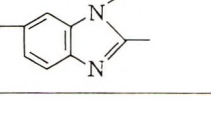
Polymer number	Repeating unit
1	
2	
3	
5	
6	
7	
8	
9	
10	
11	
12	

TABLE III  
 PAQR Polymers Used in This Investigation

Sample No.	Reactants	Mole ratio reactants (catalyst $ZnCl_2$ )	Reaction temp., °C.	Specific resistivity $\rho$ at 25°C., ohm-cm
3A	Anthraquinone, pyromellitic anhydride	3:1:2	306	$2.0 \times 10^4$
19	Phenanthrene, benzoic acid	1:1:1	256	$2.4 \times 10^5$
7A	$\alpha$ -Naphthol-phthalein, phthalic anhydride	2:1:1	256	$6.5 \times 10^6$
26	Anthracene, phthalic anhydride	2:1:2	256	$9.5 \times 10^7$
6A	Phenol, phthalic anhydride	4:3:2	256	$1.1 \times 10^8$
21	Terephthaloyl chloride, naphthalene	1:1:1	256	$6.0 \times 10^{11}$
9A	Phenolphthalein	1:1	256	$4.7 \times 10^8$
22	Anthracene, terephthaloyl chloride	1:1:1	256	$1.3 \times 10^8$
5	Phenolphthalein, phthalic anhydride	2:1:2	256	$8.8 \times 10^7$
13	Phenanthrene, acetic anhydride	2:1:1	256	$4.1 \times 10^8$

Palmer Physical Laboratory Princeton University, and by Mr. Emil Bretz, on apparatus at the Department of Chemistry, Rutgers University. Measurements of the relative spin signals, compared to recrystallized and dried DPPH at temperatures ranging from  $-100$  to  $+100^\circ\text{C}$  were made on the latter apparatus. The data on spin resonance are summarized in Table IV. Data on electronic properties of the polyalkynes are given in Table V, and those for the polybenzimidazoles are in Table VI.

## RESULTS AND DISCUSSION

It will be recalled that it is common to observe that the conductivity in molecular solids obeys the semiempirical equation:<sup>2,11,19</sup>

$$\sigma = \sigma_0 \exp\{-\Delta E/2kT\} = \sigma_0 \exp\{-E_a/kT\} \quad (1)$$

where  $\sigma$  is the specific conductivity in mho/cm.,  $\sigma_0$  is a constant, and  $\Delta E = 2E_a$  is the energy interval and is somewhat analogous to the forbidden gap,  $E_g$ ,  $E_a$  is the Arrhenius activation energy.

In all the specimens examined here plots of  $\log \sigma$  versus  $1/T$  were quite linear over the entire temperature range examined so the behavior is usual in that respect. If desired, one may interpret such data in terms of a mobility guided by hopping<sup>20</sup> processes,<sup>2,6,19</sup> and a carrier birth rate governed by an energy gap,<sup>6</sup> i.e.:

$$\sigma = en\mu \text{ (by definition)} \quad (2)$$

$$\sigma = |e|^{1/2} n_0 \frac{Ld}{3h} \exp\left\{\frac{\Delta S_0^\ddagger T - \Delta H_0^\ddagger - E_0}{kT}\right\} \exp\left\{\frac{P^{1/2}}{kT} (b''T + b_0)\right\} \quad (3)$$

TABLE IV. Electronic Characteristics of Some PAQR Polymers

Sample No.	Hydrocarbon derivative	Reaction temp., °C.	Acid <sup>a</sup>	Reactant ratio <sup>b</sup>	$\rho_{25}$ , ohm-cm.	$2E_a = \Delta E$ , e.v.	log $\rho_0$	No. fused rings in HC	$s_k$ , spins/g.	ESR	
										$E_0$ , e.v.	Peak width, gauss
55JTK	Pyrene	306	<i>o</i> -Chlorobenzoic acid	1:1:1	$7.3 \times 10^2$			4	32		2
57JTK	Pyrene	306	Syringic acid	1:1:1	$2.2 \times 10^7$			4	5		5
58JTK	Pyrene	306	Galic acid	1:1:1	$1.3 \times 10^7$			4	4		5.5
59JTK	Pyrene	306	<i>m</i> -Chlorobenzoic acid	1:1:1	$1.3 \times 10^2$			4	34		3
64JTK	Pyrene	306	<i>o</i> -Iodobenzoic acid	1:1:1	$2.7 \times 10^2$			4	7		5
70JTK	Pyrene	306	1,12-Benzoperylene Dicarboxylic anhydride	1:1:1	$2.8 \times 10^4$			4	17		3.5
28JTK	Pyromellitic dianhydride	306	Chloroacetic acid	1:1:1	$4.0 \times 10^2$	0.30	0.06	5			3.7
60JTK	Pyrene	306	<i>m</i> -Amino benzoic acid	1:1:1	$4.7 \times 10^{12}$			4	0.06		8
63JTK	Pyrene	306	<i>p</i> -Fluorobenzoic acid		$7.8 \times 10^4$			4	25		3.5
62JTK	Pyrene	306	<i>p</i> -Nitrobenzoic acid	1:1:1	$2.7 \times 10^3$			4	5		8.8
68JTK	Pyrene	306	Chloroacetic acid	1:1:1	$5.9 \times 10^2$			4	8		5.5
72JTK	Pyrene	306	Nanthene-10-carboxylic acid	1:1:1	$1.5 \times 10^7$			4	8		4
36EHE	Anthracene	253	PMA	1:2:4	$7.9 \times 10^2$	0.82	-1.0	3	6	0.011	5
51EHE	Terphenyl	306	PMA	1:1:2	$1.4 \times 10^7$	0.82	0.22	1	9	0.010	4.5
52EHE	Naphthalene	306	PMA	1:1:2	$1.4 \times 10^6$	1.05	-3.29	2	9	0.008	3.8
53EHE	Anthracene	306	PMA	1:1:2	$3.2 \times 10^5$	0.53	1.03	3	9	0.009	
54EHE	Phenanthrene	306	PMA	1:1:2	$9.2 \times 10^4$	0.55	0.30	3	7	0.010	4.3
55EHE	Pyrene	306	PMA	1:1:2	$7.6 \times 10^3$	0.31	1.26	4	16	0.024	
56EHE	Chrysene	306	PMA	1:1:2	$2.1 \times 10^4$	0.39	-1.02	4	17	0.020	3
58EHE	Triphenylchloro-methane	306	PMA	1:1:2	$3.7 \times 10^9$			1	1	0.005	
59EHE	Fluoranthrene	306	PMA	1:1:2	$3.5 \times 10^6$			3+	18	0.016	
67EHE	Triphenylmethane	306	PMA	1:1:2	$3.1 \times 10^9$			1	3	0.007	
71EHE	Pyrene	256 (6 hr.)	PMA	1:1:1	$2.6 \times 10^4$	0.45	0.61	4	9	0.019	4

85EHE	Perylene	306	PMA	1:1:2	$1.3 \times 10^6$	0.32	2.40	5	9	0.019	3.5
86EHE	Dibenzopyrene	306	PMA	1:1:2	$9.5 \times 10^2$	0.26	0.78	6	13		2.8
87EHE	Picene	306	PMA	1:1:2	$1.6 \times 10^3$	0.22	2.34	5	9	0.018	4
106EHE	1,4-Naphthoquinone	306	TODI		$1.2 \times 10^{11}$	2.00	-6.18	2	0.3		4.8
	(18 hr.)										
66EHE	Triphenylmethane	253	PMA	1:1:2	$5.8 \times 10^{11}$	0.84	4.58	1	0.05		8
33EHE	Naphthalene	253	PMA	1:1:2	$9.7 \times 10^6$	0.64	1.58	2	0.15		5.8
37EHE	Phenanthrene	253	PMA	1:1:2	$1.0 \times 10^6$	0.41	1.53	3	1.5		5.0
39EHE	Pyrene	253	PMA	1:1:2	$1.6 \times 10^3$	0.40	0.82	4	19	0.016	3.5
26EHE	Phenanthrene	306	PMA	1:1:2	$6.6 \times 10^3$	0.40	1.14	3	6.5		4.3
5RPC	Phenolphthalein	256	PA	2:1:2	$8.8 \times 10^7$			1			6.3
3A-RPC	Anthraquinone	306	PMA	3:1:2	$2.0 \times 10^3$	0.38	1.09	3	2.4		3.5
19RPC	Phenanthrene	256	Benzoic acid	1:1:1	$2.4 \times 10^6$	0.41	1.66	3	4.0		3.4
7A-RPC	$\alpha$ -Naphtholphthalein	256	PA	2:1:1	$6.5 \times 10^6$	0.54	2.25	2	1.3		7.7
26RPC	Anthracene	256	PA	2:1:2	$9.5 \times 10^7$	0.70	2.06	3	1.7		5.0
6A-RPC	Phenol	256	PA	4:3:2	$1.1 \times 10^8$	0.64	2.64	1	1.8		6.7
21RPC	Naphthalene	256	Terephthaloyl chloride	1:1:1	$6.0 \times 10^{11}$	0.96	3.66	2	0.96		8.3
10RPC	$\alpha$ -Naphtholphthalein	256	None	1:0:1	$7.5 \times 10^8$	—	—	2	1.5		5.5
107DAO	1-Hydroxyanthraquinone	306	1,8-NA	2:1:2	$5.0 \times 10^6$	0.50	1.48	3	0.7		6
109DAO	1,8-Dihydroxyanthraquinone	306	1,8-NA	2:1:2	$2.2 \times 10^7$	0.77	0.83	3	0.56		
110DAO	1-Bromo-2-naphthol	256	PA	2:1:2	$1.5 \times 10^7$	0.62	1.95	2	0.61		
132DAO	Phenolphthalein	256	1,8-NA	2:1:2	$9.0 \times 10^6$	0.45	3.15	1	0.50		
134DAO	1,8-Dihydroxyanthraquinone	256	1,8-NA	2:1:2	$2.9 \times 10^6$	0.52	1.06	3	1.7		
135DAO	1,5-Dihydroxyanthraquinone	256	1,8-NA	2:1:2	$3.5 \times 10^6$	0.63	0.24	3	1.4		
F-DAO	1,4-Dihydroxynaphthalene	256	PMA	2:1:2	$5.6 \times 10^{11}$	1.00	3.30	2	0.27		
G-DAO	1,4-Dihydroxynaphthalene	306	PMA	2:1:2	$1.4 \times 10^9$	0.67	3.49	2	0.45		

<sup>a</sup> Acids: PA = phthalic anhydride; NA = naphthalic anhydride; TODI = toluene diisocyanate; PMA = pyromellitic dianhydride.

<sup>b</sup> Indicates mole ratio of hydrocarbon (HC), acid, and ZnCl<sub>2</sub> at synthesis outset.

TABLE V  
Summary of Observed Electronic Properties for Polyalkynes

Sample	Resistivity at 25°C. $\rho_{25}$ , ohm-cm.	$\Delta E$ , e.v.
Polyptyne-1	$3 \times 10^9$ (10–15°C.)	—
Polypropyne	$1.5 \times 10^{11}$	0.645
Polyphenylacetylene	$4.8 \times 10^{10}$	0.432

TABLE VI  
Summary of Observed Electronic Properties for Polybenzimidazoles

Sample	Resistivity at 25°C. $\rho_{25}$ , ohm-cm.	$\Delta E$ , e.v.	$\rho_0$
9	$4.1 \times 10^{10}$	1.12	13.5
6	$1.3 \times 10^{13}$	1.39	23
10	$5.7 \times 10^{13}$	1.56	3.6
3	$1.8 \times 10^{12}$	1.57	$9.5 \times 10^{-2}$
6	$3.2 \times 10^{15}$	1.66	29
8	$1.0 \times 10^{14}$	1.78	$9.1 \times 10^{-2}$
7	$7.5 \times 10^{14}$	1.91	$5.4 \times 10^{-2}$
2	$9.0 \times 10^{11}$	2.15	$5.6 \times 10^{-7}$
5	$1.4 \times 10^{13}$	2.15	$8.7 \times 10^{-6}$
1	$5.0 \times 10^{12}$	2.23	$7.2 \times 10^{-7}$
12	$1.0 \times 10^{16}$	2.90	$3.2 \times 10^{-9}$

where  $|e|$  is the electronic charge,  $n_0$  is the ultimate available carrier concentration,  $L$  is the length of the intramolecular path (i.e., a molecular length),  $d$  is the intramolecular barrier distance through which the carrier must tunnel,  $h$  is Planck's constant,  $S_0^\ddagger$  and  $H_0^\ddagger$  are the entropy and enthalpy of the activated state, respectively,  $E_0$  is the energy required to form a carrier pair from two neutral precursor molecules,  $k$  is Boltzmann's constant,  $T$  is the absolute temperature,  $P$  is the externally applied pressure, and  $b''$  and  $b_0$  are deformability constants describing the intermolecular barrier to tunneling.

Equation (3) has been derived using the absolute reaction rate formalism, and contains a description also as to how one expects the conductivity to vary with pressure. To date, the available data appear to be describable by eq. (3).

An estimate of the extent of ekaconjugation may be made from the energy of activation of the semiconducting organic solid. Using the "particle-in-a-box" model, one may estimate the minimal energy (in electron volts) for excitation of a system of ekaconjugated bonds as<sup>8,19,21</sup>

$${}^3E = 19.2(Z + 1)/Z^2 \quad \text{for a linear system} \quad (4)$$

$${}^3E = 38.4/Z \quad \text{for an annular system}$$

where  $Z$  is the number of successive  $\pi$ -electron orbitals in the system. For example, considering fused ring systems as having  $Z = 4 \text{ FR} + 2$ ,

where FR is the number of contiguous fused rings in the compound, one calculates for the 11 ring hydrocarbon, quaterrylene,  ${}^3E = 0.83$  e.v.; the literature value<sup>22</sup> is 0.6 e.v. In the PAQR series of polymers having differing numbers of fused rings, one sees from examination of Table III that  $E = 1.5/\text{FR}$  describes the results, and can be taken to indicate that the average hydrocarbon monomeric unit is coupled at least  $38.4/(1.5 \times 4) = 6$ -fold in the semiconducting polymer.

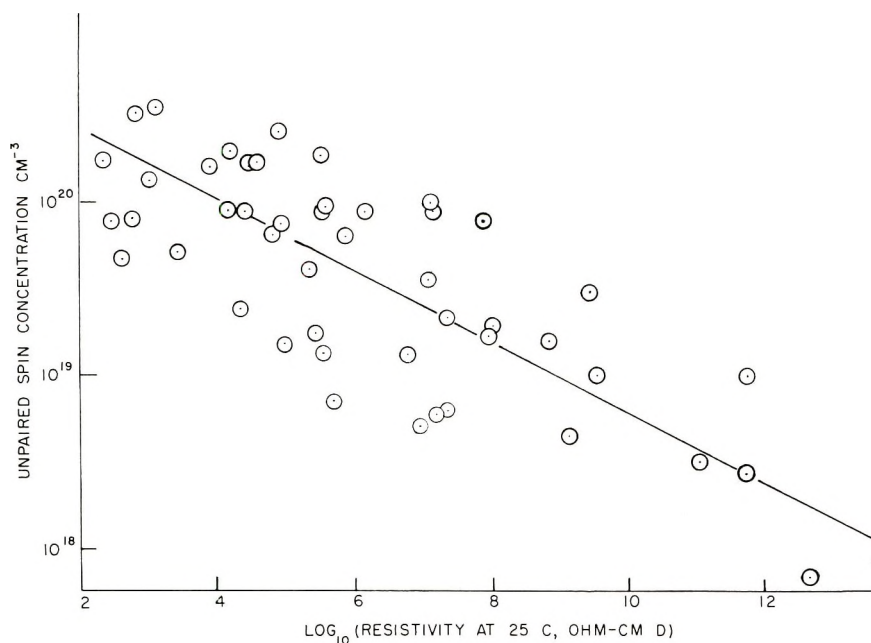


Fig. 1. A comparison of the spin concentration and resistivities of various PAQR semiconducting polymers.

Comparison of the various PAQR polymer shows (Fig. 1) that the higher the conductivity, the higher the concentration of unpaired spins observable. The empirical relation  $s = 7 \times 10^{20} \sigma^{1/6}$  fits the results rather well, where  $s$  is the number of spins per cubic centimeter, and  $\sigma$  is, again, the conductivity. The interrelation is not surprising in view of the fact that both carriers and unpaired spins are manifestations of excited states.

The observed paramagnetic susceptibility of the PAQR polymers appeared to vary with temperature in a manner interpretable most simply as that obeying a Boltzmann distribution both as to birth of unpaired spins, and as to their alignment with the field, i.e.,

$$s = s_0 \exp \{ -E_e/kT \} \quad (5)$$

where the susceptibility  $x_0$  is

$$x_0 = (g^2 B^2 s_0 / 4kT) \exp \{ -E_e/kT \} \quad (6)$$

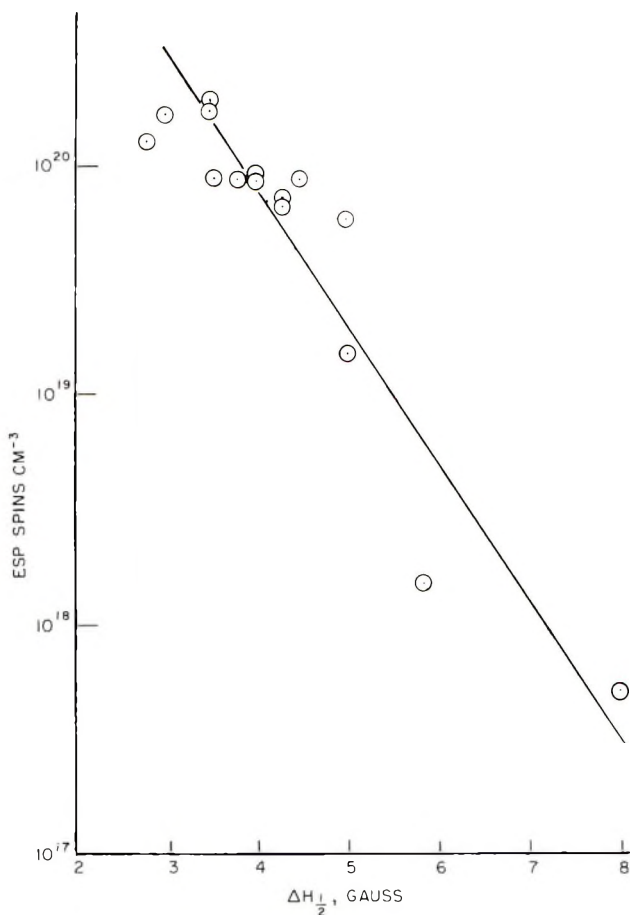


Fig. 2. Concentration of unpaired spins vs. electron spin resonance peak width at maximum slope.

where  $g$  is the gyromagnetic ratio for free electrons and  $B$  is the Bohr magneton. The values of the spin source activation energy  $E_s$  appears to be quite small, about 0.01–0.025 e.v. for the polymers examined. The values of the resonance peak width at maximum slope,  $\Delta H_{1/2}$ , as determined from the differential curves, varies from polymer to polymer, and is narrower for those polymers with higher spin concentrations (Fig. 2).

### Ekaconjugation

It might be expected from preliminary considerations that molecules which consist of long series of alternating double and single bonds, and are thus "conjugated" in the sense long used by the organic chemist, would exhibit enhanced electronic behavior.<sup>23–25</sup> However, the PAQR polymers and the polyacetylenes exhibited measurable ESR signals, but the polybenzimidazoles did not, despite their having both high molecular weights

(up to 50,000) and long chains of alternate single double bonds. Clearly it is not enough to possess both the latter attributes so as to exhibit enhanced electronic behavior. A further factor such as exalted correlation of the  $\pi$ -electron orbitals is required. This is describable in terms of what may be called ekaconjugation. The extent of potential ekaconjugation is proportional to the number of successive  $\pi$ -electron orbitals in the structure; the degree of it is proportional to the coupling between successive  $\pi$ -electron orbitals. In a practical sense, the definition states that those molecular systems exhibiting appreciable amounts of excited electronic states at room temperature are defined as being ekaconjugated. As shown earlier,<sup>2,7</sup> the concept of ekaconjugation permits a rather successful interpretation and prediction of the properties of exhilarated electrons in organic molecular solids. This includes the observation of (1) unpaired spins, (2) semiconduction dependence upon molecular structure, (3) major dependence of semiconduction upon ekaconjugated as compared to other impurities, (4) pressure effects upon mobility and upon activation energy of conduction, (5) Hall and Seebeck effects, (6) field dependence of conduction, and (7) frequency dependence of conduction. Major problems still remain, however, in the deeper understanding of mobility in such systems.

Let us compare the three classes of polymers still further, (Table VII).

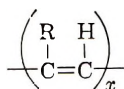
TABLE VII  
Summary of the Enhanced Electronic Properties of Some Conjugated Polymers

Polymer	Conductivity, mho/cm.	Energy interval, $\Delta E$ , e.v.	Unpaired spin concentration, no./cm <sup>3</sup>	Spin concentration activation energy $E_a$ , e.v.
Polybenzimidazoles	$10^{-10}$ – $10^{-16}$	1.1–2.9	$<10^{17}$	—
Polyacetylenes	$10^{-9}$ – $10^{-11}$	0.4–0.7	$10^{17}$ – $10^{18}$	—
PAQR polymers	$10^{-2}$ – $10^{-12}$	0.1–0.9	$10^{18}$ – $10^{20}$	0.01–0.025

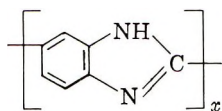
On examining the proposed structures of the three classes of polymers studied, it is evident that one can trace out long series of alternate single and double bonds in all three. The polybenzimidazoles and polyacetylenes possess a possible degree of rotational freedom about the single bonds. This could bring about interruptions in the sequence of  $\pi$ -electron orbital alignments, reducing the symmetry and extent of orbital delocalization, especially if the crystal symmetry were limited in extent. The PAQR polymers, in contrast to the others, display especially high  $\sigma_0$  values,<sup>18</sup> indicating a high electron "mobility" and probable possession of long-range order. Earlier studies of these substances<sup>7,8,26,27</sup> showed the conductivity to depend strongly upon the chemical structure expressed in terms of the number of fused rings in the starting monomer. This strong structural dependence and the relative insensitivity to valence impurity (but sen-



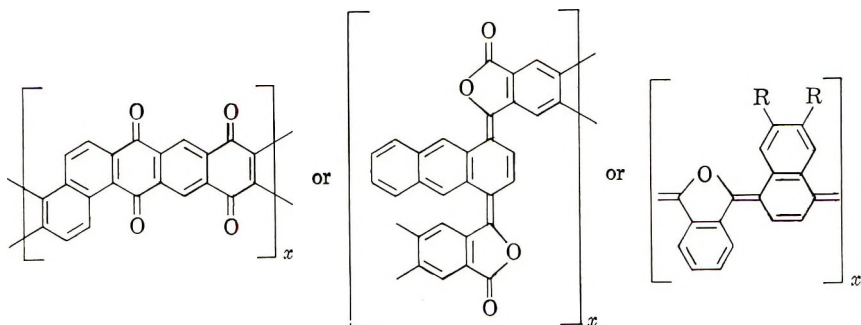
sitivity to ekaconjugated impurity remains) confirmed the hypothesis that ekaconjugation is a major factor in the electronic behavior.



Polyacetylenes



Typical polybenzimidazole



Proposed ekaconjugated structure types (unproven) for typical PAQR polymers

Another piece of evidence for the importance of ekaconjugation in the electronic properties of organic solids may be drawn from the known behaviors of polyphenylene and of pyropolymers. The polyphenylenes, constructed of benzene rings coupled serially by single bonds, have a possible flexibility in their structure which the large planar nets of the pyropolymers do not. In terms of ekaconjugation we say that the extent will be much lower in the polyphenylenes than in the pyropolymers. The electronic conductivity bears this out, for the conductivity of the polyphenylenes<sup>2</sup> is about  $10^{-8}$ – $10^{-10}$ , while that of the pyropolymers<sup>28–32</sup> is as high as  $10^{-3}$  to  $10^{+3}$ .

### Radical and Carrier Formation in Ekaconjugated Solids

The ekaconjugated molecules can presumably exist in various excited states. The simplest way in which ionized pairs acting as carriers can arise is by the direct reaction:

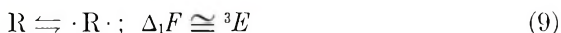


for which the equilibrium expression can be written as

$$\frac{[\text{R}_0^+][\text{R}_0^-]}{[\text{R}]^2} = K_3 = e^{-\Delta F_3/kT} \cong e^{-E_0/kT} \quad (8)$$

Here we have written  $R_0^+$  and  $R_0^-$  to signify the positively and negatively charged moieties bearing unpaired electrons which function as carriers. We immediately reject this simple system as an adequate description of events because we note that the temperature dependence of the carrier population varies, as judged from conductivity measurements according to  $E_g \cong 0.1-1$  e.v. whereas the spin population varies as  $E_e \cong 0.01-0.025$  e.v. An intermediate step is indicated.

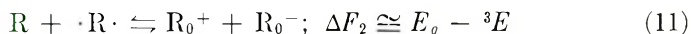
The required intermediate step can be pictured as shown in eq. (9), where  $\cdot R \cdot$  represents a biradical or internal exciton:



for which the equilibrium reaction may be written as:

$$[\cdot R \cdot]/[R] = K_1 = e^{-\Delta F_1/kT} = k_{1f}/k_{1b} = e^{-2E/kT} \quad (10)$$

The succeeding reaction (or reactions) to form carriers can be considered to arise either from lone or paired exciton reactions. For the lone exciton case:



and

$$\frac{[R_0^+][R_0^-]}{[R][\cdot R \cdot]} = K_2 = e^{-\Delta F_2/kT} = \frac{k_{2f}}{k_{2b}} \quad (12)$$

where  $k_{1f}$ ,  $k_{1b}$ ,  $k_{2f}$ , and  $k_{2b}$  are the specific reaction rate constants.

Ignoring for the moment the specific action of traps on the carriers, we set

$$[R_0^+] = [R_0^-] \quad (13)$$

and obtain from eqs. (10), (12), and (13)

$$[R_0^-][\cdot R \cdot] (K_2/K_1)^{1/2} \quad (14)$$

for the lone exciton process.

For the exciton pair process:



and

$$\frac{[R_0^+][R_0^-]}{[\cdot R \cdot]^2} = K_2' = \frac{k_{2f}'}{k_{2b}'} = e^{\Delta F_2'} \quad (16)$$

and eq. (14) again applies.

We now attempt to evaluate the various quantities of interest for a representative semiconducting polymer. We note that the unpaired spins can arise in either an ionized [eqs. (11) or (15)] or an unionized [eq. (9)] form. The measured paramagnetic susceptibility signal can arise from either or both contributions and will depend upon the concentrations and lifetimes of the several species. We recall from the data given earlier that the charged species of unpaired spin states apparently do not con-

tribute strongly, as judged from the temperature dependence. Accordingly we provisionally set

$$s_{\text{total}} = s_{\text{neut}} + s_{\text{ionic}} \cong s \neq s_{\text{neut}} \cong s \quad s \cong 2[\cdot R \cdot] \quad (17)$$

and from eq. (14) obtain

$$[R_0^-] = (s/2) (K_2/K_1)^{1/2} \quad (18)$$

Recalling eqs. (1) and (2) which for a hopping-type mobility becomes

$$\sigma = |e|^2 n_0 \exp \{E_g/2kT\} \mu_0 \exp \{-E_s/kT\} \quad (19)$$

whence

$$E_a = E_g/2 + E_s \quad (20)$$

where  $E_s$  is the saddle height energy of the hopping process.

Let us consider a typical PAQR polymer, prepared from pyrene and pyromellitic dianhydride, No. 39 (cf. Pohl and Engelhardt,<sup>8</sup> Table 1) for which  $\sigma_{25} = 0.6 \times 10^{-4}$  mho/cm.,  $E_a = 0.20$  e.v.,  $s = 10^{20}$  cm.<sup>-3</sup>,  $^3E \cong 0.02$  e.v. Ignoring  $E_s$ , which is presently unknown but judged to be less than 0.1 e.v., we obtain from eq. (18)

$$n = 2[R_0^-] = s(K_2/K_1)^{1/2} \quad (21)$$

$$n = 10^{20} \exp \{ (0.2 - 2 \times 0.02) / (1/40) \} = 7 \times 10^{16} \text{ cm.}^{-3} \text{ carriers}$$

This result may be compared with the value one calculates from simple band theory<sup>8</sup> on this substance:

$$n = 2.2 \times 10^{16} \text{ cm.}^{-3}$$

Let us now estimate the various rate constants which we can do using the carrier "lifetime" estimated from photocurrent measurements,<sup>8</sup> and from the peak widths of the ESR measurements.

### Photocurrent and Carrier Lifetime

While illuminated at one electrode the steady-state increment in<sup>33</sup> carrier concentration  $\Delta n$  is

$$\Delta n = f \cdot \tau_c \quad (22)$$

$$\Delta \sigma = \Delta n |e| \mu = f \tau_c |e| \mu \quad (23)$$

$$\Delta j = \epsilon_0 \Delta \sigma' = \epsilon_0 f \tau_c |e| \mu \quad (24)$$

$$j_0 = \epsilon_0 \sigma_0 = \epsilon_0 n_0 |e| \mu \quad (24)$$

whence

$$\tau_c = (\Delta j_0 / j_0) (n_0 / f) \quad (25)$$

where  $f$  is the concentration of free carriers liberated by photons in one second in the thin layer near the illuminated electrode, i.e., strong absorption;  $\tau_c$  is the mean free time (lifetime) of the a.c. carrier (seconds) in that

thin layer;  $\sigma$  is conductivity (in mho/centimeter),  $|e|$  is electronic charge,  $\mu$  is mobility (in square centimeters/volt second),  $j$  is specific current (in coulombs/square centimeter second), and  $\epsilon$  is electric field strength (in volts/centimeter). For example, in the cast of PAQR polymer No. 39,<sup>8</sup>

$$\begin{aligned}\Delta j/j &= 0.6 \\ n_0 &= 10^{16} \text{ cm.}^{-3} \\ f &\cong 3 \times 10^{17} \text{ photons/cm.}^2 \text{ sec.} \times 1/10^{-4.5} \\ &= 3 \times 10^{21.22} \text{ cm.}^{-3} \text{ sec.}^{-1}\end{aligned}$$

where the absorption depth,  $d$ , is assumed to be  $10^{-4}$ – $10^{-5}$  cm. Hence

$$\tau_c = 10^{-6}$$
– $10^{-7}$  sec.

We may now identify  $k_{2b}$ , the specific back reaction rate constant, i.e., the rate at which a particular carrier is removed by recombination, with  $1/\tau_{2b}$

$$k_{2b} = 1/\tau_{2b} \cong 1/\tau_c \approx 10^7 \text{ sec.}^{-1} \quad (26)$$

For the single exciton process

$$k_{2f} = k_{2b}K_2$$

where

$$\begin{aligned}K_2 &= e^{-E_2/kT} \cong e^{- (E_2 - 2E_1)/kT} = e^{\frac{-(0.4-0.02)}{1/40}} \\ &= 3 \times 10^{-7}\end{aligned}$$

and  $k_{2f} = 10^7 \times 3 \times 10^{-7} \approx 3 \text{ sec.}^{-1}$

$$\tau_{2f} \approx 0.3 \text{ sec.}$$

For the exciton pair process, very similar results for  $k_{2f}'$  and  $\tau_{2f}'$  are obtained, as would be expected.

The relaxation time,  $\tau_{\text{mean}}$  obtained from ESR measurements of the peak width at half peak power,  $\Delta\omega$ , is a measure of the mean lifetime during which a particular configuration exists.<sup>34</sup> Taking the relation as for a Lorentzian distribution<sup>35</sup> we have

$$T_2 = 0.577/\Delta\omega \cong \tau_{\text{mean}} \quad (27)$$

$$\Delta\omega = 1.8 \times 10^7 (\Delta H) \text{ sec.}^{-1} \text{ (if } \Delta H \text{ in gauss)}$$

$$\tau_{\text{mean}} = 3.1 \times 10^{-8} (\Delta H)^{-1}; \text{ sec. (if } \Delta H \text{ in gauss)}$$

For example, for the range of  $\Delta H$  values observed here of 2–8 gauss,

$$\tau_{\text{mean}} = 0.4$$
– $1.6 \times 10^{-8}$  sec.  $\sim 10^{-8}$  sec.

Although the period  $T_2 \sim \tau_{\text{mean}}$  may approximately express the mean lifetime during which a particular configuration exists, certainly the specific

duration of the radical state is no shorter than this. For example  $\tau_{1b} \geq T_2$ ; saying that the relaxation time of the paramagnetic susceptibility may be shortened by processes other than the death of the radical. The tendency to identify  $\tau_{1b} \geq T_2 \cong 10^{-8}$  sec. with the mean carrier lifetime,  $\tau_c \sim 10^{-7}$  sec. previously calculated must be resisted for the reason that we gave earlier. That is, the ESR data is based on observing a population obeying  $E_s \sim 0.02$  e.v., while the conduction processes are based on carriers obeying  $E_g \sim 0.4$  e.v., and the  $T_2$  and  $\tau_c$ , although similar in magnitude, must really therefore be descriptive of separate processes.

For the moment let us regard  $T_2$  as a minimum value for  $\tau_{1b}$ , the radical lifetime. Then

$$k_{1b} = \frac{1}{\tau_{1b}} = \frac{1}{\tau_{\text{radical}}} \leq \frac{1}{T_2} \leq 10^8 \text{ sec.}^{-1}$$

and

$$k_{1f} = K_1 k_{1b} \cong 1/2 \times 10^{-8} \text{ sec.}^{-1}$$

as

$$K_1 \cong e^{-2E/kT} \cong e^{\frac{-0.02}{0.0257}} \approx 1/2$$

Let us quickly summarize the above remarks. We concluded that conduction and ESR measurements measured separate species which however were interrelated by a family lineage. For a selected semiconductor, a pyrene-pyromellitic dianhydride polymer, No. 39EHE, we arrived at results as summarized in Table VIII. The ekaconjugated precursor molecules frequently form unpaired spin states and, much less frequently, form

TABLE VIII  
Kinetic and Equilibrium Data for a Semiconducting Polymer (No. 39)

	Symbol	Value
Specific conductivity	$\sigma$	$0.6 \times 10^{-4}$ mho/cm.
Thermal activation energy of conduction	$E_a$	0.20 e.v.
Estimated carrier birth energy	$E_g$	0.40 e.v.
Estimated saddle height energy	$E_s$	0-0.1 e.v.
Unpaired spin concentration	$s$	$10^{20}$ cm. <sup>-3</sup>
Spin birth energy	$E_e$	0.02 e.v.
Carrier lifetime	$\tau_{2b} = \tau_c$	$10^{-6}$ - $10^{-7}$ sec.
Spin configuration mean lifetime	$T_2 \cong \tau_{\text{mean}}$	$\sim 10^{-7}$ sec.
Biradical lifetime	$\tau_{1b} = \tau_{\text{mean}}$	$\geq 10^{-8}$ sec.
Carrier concentration	$[R_0^-] = [R_0^+] = n_i$	$7 \times 10^{16}$ cm. <sup>-3</sup>
Carrier concentration (by band theory)	$n_i(B - T)$	$2.2 \times 10^{16}$ cm. <sup>-3</sup>
Biradical equilibrium constant	$K_1$	$\sim 1/2$
Carrier equilibrium constant	$K_2$	$\sim 3 \times 10^{-7}$
Specific rate of biradical birth	$k_{1f}$	$\sim 1/2 \times 10^8 \text{ sec.}^{-1}$
Specific rate of biradical death	$k_{1b}$	$\sim 10^8 \text{ sec.}^{-1}$
Specific rate of carrier birth	$k_{2f}$	$\sim 3 \text{ sec.}^{-1}$
Specific rate of carrier death	$k_{2b}$	$\sim 10^7 \text{ sec.}^{-1}$

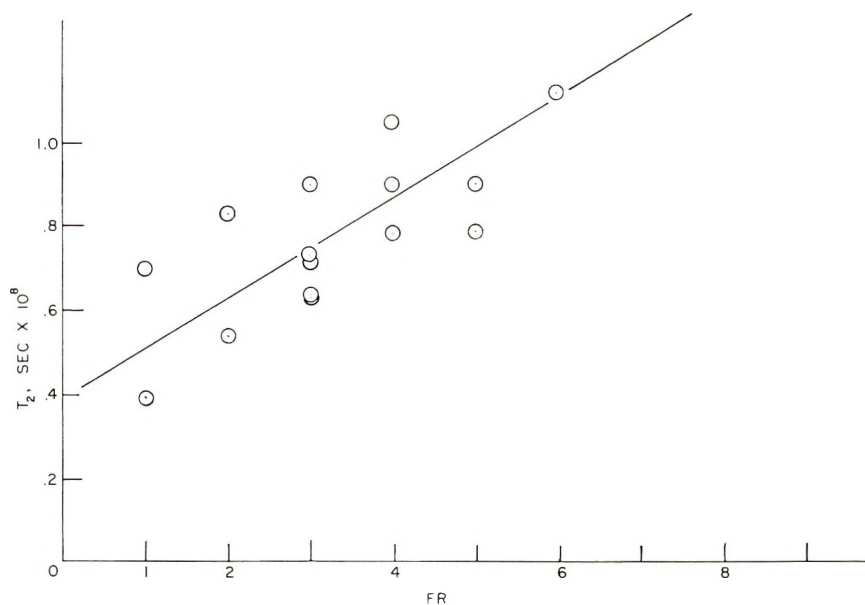


Fig. 3.  $T_2$  from ESR signals vs. number of fused rings FR in PAQR hydrocarbon portion.

ionized carrier states. The carrier concentration inferred from the spin concentration is of the same order of magnitude as that obtained using simple band theory.

A clue as to the behavior of the unpaired spins lies in the observation that the ESR peak width is greater for those semiconducting polymers with lower spin concentrations. This is expectable if we use the assumption of eq. (27) relating

$$T_2 = \tau_{1b} = k_{1b}^{-1} \propto (\Delta H)^{-1}$$

or  $k_{1b}$  is proportional to  $\Delta H$ . Since we expect the more stable free radical to have a smaller specific rate of return to the ground state, the observed trend may thus be understood. Indeed, a plot of  $T_2$  versus FR, the number of fused rings in the hydrocarbon portion of PAQR polymers made with pyromellitic dianhydride shows a linear relationship as might be expected (Fig. 3).

This same trend of the peak width decreasing with observed spin concentration can have other explanations, however. It could be due to exchange narrowing or to delocalization narrowing in connection with nuclear spin interaction. During exchange narrowing the electron dwells on a large number of molecules in a time roughly equivalent to the reciprocal of the hyperfine angular frequency because the overlap of the unpaired electron wave functions promotes electron exchange between molecules. The electron then sees many possible nuclear spin orientations in this time, the net effect of which is averaged to near zero, and the line is sharpened as

exchange (or mobility) increases. During delocalization narrowing, a similar averaging out of nuclear spin effects occurs as the electron wave function is extended intramolecularly in larger delocalizing molecular orbitals. For the moment we conclude that any one or even several of the mechanisms, i.e., radical lifetime, exchange narrowing, or delocalization narrowing, might be operative in causing the observed decrease in  $T_2$  in the semiconducting polymers with higher spin populations.

The usual interpretation on seeing unpaired spins and carriers in organic molecular solids is that they represent excited states of individual molecules in the solid. An interesting new concept by Semenov is that spin states can here be regarded as existing as part of a collectivized ground state wave function of the solid as a whole. One way of deciding between the two interpretations is to examine the resonance peak sharpness. If spins arise in states separate from the ground state, as for example on molecules bearing extra electrons, then factors increasing the mobility, i.e., the charge transfer among molecules, will operate to increase exchange narrowing. Analogously, factors operating to increase biradical lifetime or orbital delocalization such as increased ekaconjugation, will decrease line width.

If spins arise as part of a collectivized ground state of molecules, on the other hand, then according to the views of Semenov and Talroze, the resonance should broaden as the polymeric material is more conductive.

The data of this study, contrary to the expectations of Semenov, exhibit resonance which is narrower the higher the conductance of the PAQR polymer. Furthermore, the apparent existence of an observable thermal activation energy confirms the interpretation of spin states as separate excited states lying above (about 0.02 e.v.) the ground states in these substances. The ground state triplet of lone molecules as in  $O_2$  or methylene compounds<sup>36</sup> is well known, but not an issue here.

The authors express their sincere appreciation to Dr. Robert Pressley, Palmer Physical Laboratory, Princeton University, and to Mr. Emil Bretz, Dept. of Chemistry, Rutgers University for assistance in making ESR determinations. One of us (R. P. C.) received Fellowship support during this work for which he expresses his appreciation to the Celanese Corporation of America. A portion of the work reported here was supported jointly by the Army, Navy, and Air Force under Signal Corps Contract DA-036-039 ac 78105; DA Project 3-99-15-105; WADD Project 7371 at the Plastics Laboratory, Princeton University, and a portion was supported by an Administrative Grant, Polytechnic Institute of Brooklyn.

## References

1. Smith, R. A., *Semiconductors*, Cambridge University Press, 1959, p. 4.
2. Pohl, H. A., in *Modern Aspects of the Vitreous State*, Vol. II, J. D. Mackenzie, Ed., Butterworths, London, 1962, Chap. 2.
3. Merrifield, R. E., and W. D. Phillips, *J. Am. Chem. Soc.*, **80**, 2278 (1958).
4. Pohl, H. A., *Chem. Eng.*, **68**, 104 (1961).
5. Pohl, H. A., J. A. Bornmann, and W. Ito, *Organic Semiconductors*, J. J. Brophy and J. W. Buttrey, Eds., Macmillan, New York, 1962, p. 142.
6. Pohl, H. A., A. Rembaum, and A. W. Henry, *J. Am. Chem. Soc.*, **84**, 2699 (1962).

7. Pohl, H. A., and D. A. Opp, *J. Phys. Chem.*, **66**, 2121 (1962).
8. Pohl, H. A., and E. H. Engelhardt, *J. Phys. Chem.*, **66**, 2085 (1962).
9. Pohl, H. A., and M. L. Iuggins, in *Unsolved Problems in Polymer Science*, F. R. Mayo, Ed., ASD Tech. Rept. 62-283, Stanford Research Institute, Menlo Park, Calif., Feb. 1963.
10. Eyring, H., J. Walter, and G. Kimball, *Quantum Chemistry*, Wiley, New York, 1944, p. 254.
11. Berlin, A. A., *J. Polymer Sci.*, **55**, 621 (1961).
12. Vogel, H., and C. S. Marvel, *J. Polymer Sci.*, **50**, 511 (1961).
13. Berlin, A. A., V. I. Liogonkii, and V. P. Parini, *J. Polymer Sci.*, **55**, 675 (1961); *ibid.*, **55**, 621 (1961).
14. Mette, H., and C. Loscoe, *Organic Crystal Symposium Abstracts*, National Research Council, Ottawa, Canada, Oct. 1962, p. 139.
15. Heilmeier, G. H., G. Warfield, S. Harrison, and J. Assour, *Organic Crystal Symposium Abstracts*, National Research Council, Ottawa, Canada, Oct. 1962, p. 133.
16. Delocoot, G., and M. Schott, *Organic Crystal Symposium Abstracts*, National Research Council, Ottawa, Canada, Oct. 1962, p. 143.
17. Semenov, N. N., *J. Polymer Sci.*, **55**, 563 (1961).
18. Chartoff, R. P., M. S. Thesis, Princeton Univ., Princeton, N. J., 1962.
19. Eley, D. D., *Horizons in Biochemistry*, Eds., B. Pullman and M. Kasha, Academic Press, New York, 1962.
20. Schultz, R. D., Space and Information Systems Div. Report. #SID-61-269 Aug. 10, 1961, North American Aviation, Inc.
21. Platt, J. R., *J. Chem. Phys.*, **17**, 484 (1949).
22. Inokuchi, H., *Organic Crystal Symposium Abstracts*, National Research Council, Ottawa, Canada, Oct. 1962, p. 129.
23. Akamatu, H., *Kagaku to Kogyo (Tokyo)*, **11**, 607 (1958).
24. Mark, H. F., *Proc. Symp. Role Solid State Phenomena Elec. Circuits*, Microwave Research Inst., Polytechnic Inst. of Brooklyn Symp. Series, Vol. 7, Interscience, New York, 1957, p. 125.
25. Pople, J. A., and S. H. Walmsley, *Trans. Faraday Soc.*, **58**, 441 (1962).
26. Pohl, H. A., C. Cappas, and G. Gogos, *J. Polymer Sci.*, **A1**, 2207 (1963).
27. Pohl, H. A., in *Progress in Chemistry of the Solid State*, H. Reiss, Ed., Pergamon Press, New York-London, 1963, Chap. 8.
28. Pohl, H. A., in *Proceedings of the Fourth Conference on Carbon*, S. Mrozowski, Ed., Pergamon Press, New York-London, 1960, pp. 241-58.
29. Pohl, H. A., and J. P. Laherrere, in *Proceedings of the Fourth Conference on Carbon*, S. Mrozowski, Ed., Pergamon Press, New York-London, 1960, pp. 259-65.
30. Laherrere, J. P., and H. A. Pohl, *Semiconduction in Molecular Solids* (Proc. of Princeton U. Conf.), H. A. Pohl, Ed., Ivy-Curtis Press, Phila., Pa., 1960, p. 93-121.
31. Mrozowski, S., *Phys. Rev.*, **85**, 609 (1952); *ibid.*, **86**, 1056 (1952) (erratum).
32. Pohl, H. A., and S. A. Rosen, *Proceedings of the Fifty Conference on Carbon*, Vol. II, S. Mrozowski, Ed., Pergamon Press, New York-London, 1963.
33. Cusack, N., *The Electrical and Magnetic Properties of Solids*, Longmans, Green, London, 1958.
34. Ward, R. L., and S. I. Weissman, *J. Am. Chem. Soc.*, **76**, 3612 (1954).
35. Ingram, D. J. E., *Free Radicals*, Academic Press, New York, 1958, p. 122.
36. Hutchison, C. A., Jr., *Organic Crystal Symposium Abstracts*, National Research Council, Ottawa, Canada, Oct. 1962, p. 160.

### Résumé

Dés études de semi-conductivité et de résonance de spin électronique ont été effectuées sur un certain nombre de polymères conjugués représentatifs de polyacéthylènes, de polybenzimidazoles et de radicaux polymériques polyacènequinones. Les résistivités observées se situaient de 270 à  $10^{16}$  ohm/cm à température de chambre. Celles-ci ainsi



que les concentrations en spin, les temps de relaxation, les énergies d'activation de conductance et de concentration en spin, se sont avérés être des fonctions de la structure moléculaire. Ceci peut être considéré comme une preuve parlante de ce que les effets des impuretés sur les propriétés électroniques des solides moléculaires sont beaucoup moindres que ceux communément observés avec les semi-conducteurs liés par covalence tels que le Ge et le Si par exemple. En utilisant un modèle simple, on a opéré une analyse détaillée de la formation du porteur et de celle du radical libre ainsi que des temps de vie dans ces solides conjugués.

### Zusammenfassung

Die Halbleitereigenschaften und die Elektronenspinresonanz einer Anzahl konjugierter Polymerer vom Polyacetylen-, Polyimidazol- und Polyacenchinonradikaltyp wurden untersucht. Der beobachtete spezifische Widerstand lag im Bereich von 270 bis  $10^{16}$  Ohm cm bei Raumtemperatur. Dieser sowie die Spinkonzentration, die Relaxationszeit und die Aktivierungsenergie der Leitfähigkeit und Spinkonzentration erwiesen sich als Funktionen der Molekülstruktur. Das wurde als eindrucksvoller Beweis dafür betrachtet, dass bei den Molekül-Festkörpern viel geringere Einflüsse der Verunreinigungen auf die elektronischen Eigenschaften bestehen als sie gewöhnlich bei Halbleitern mit kovalenter Bindung wie z.B. Ge und Si beobachtet werden. Unter Benützung eines einfachen Modells wurde eine detaillierte Analyse der Bildung und Lebensdauer von Trägern und freien Radikalen in diesen eka-konjugierten Molekülfestkörpern durchgeführt.

Received April 1, 1963

Revised July 1, 1963

## Incorporation of Hydroxyl Endgroups in Vinyl Polymer. Part I. Initiation by Hydrogen Peroxide Systems

PREMAMOY GHOSH, ASISH RANJAN MUKHERJEE, and SANTI R. PALIT, *Indian Association for the Cultivation of Science, Jadavpur, Calcutta, India*

### Synopsis

Hydroxyl endgroups were incorporated in polymers of methyl methacrylate obtained by initiation with hydrogen peroxide with the monomer in bulk and in aqueous solution. Hydroxyl endgroups in the respective polymer samples were estimated by means of the dye interaction technique. Aqueous photoinitiation with hydrogen peroxide was found to incorporate an average of about 1-1.5 hydroxyl endgroups per polymer chain, depending on the concentration of the initiator used. Aqueous thermal (60°C.) polymerization leads to an average of nearly 1 hydroxyl endgroup per chain. Polymerization in the dark at room temperature was carried out by activation with  $\text{Fe}^{2+}$  and  $\text{Fe}^{3+}$  ions, and an average of nearly 1 hydroxyl endgroup per chain was obtained in both cases. Bulk polymerization (photo- and thermal) produces polymer having nearly 1.3-1.7 hydroxyl endgroups per chain.

The present paper reports the results of endgroup determination by means of the dye interaction technique<sup>1,2</sup> recently developed in our laboratory in polymethyl methacrylate obtained by initiation with hydrogen peroxide with the monomer in bulk and in aqueous solution.

### EXPERIMENTAL

#### Materials

Methyl methacrylate monomer was purified by washing with 2% sodium hydroxide solution until free from stabilizers, then rendered free from alkali by washing with distilled water, and dried over fused calcium chloride. It was finally purified by fractional vacuum distillation and preserved in a refrigerator at 5°C.

Water used for polymerization experiments was obtained by redistilling ordinary distilled water with alkaline permanganate in an all-glass distillation unit.

E. Merck 30% (w/v) hydrogen peroxide was used. All other reagents were either E. Merck or equivalent B.D.H. analytical grade products.

### Preparation of Polymers

Aqueous polymerization of methyl methacrylate was carried out in clean well-stoppered 150-ml. conical flasks in an atmosphere of nitrogen. Redistilled water taken in a clean conical flask was flushed profusely with purified nitrogen, a known amount of the monomer was then added with thorough shaking, and finally the mouth of the flask was closed with an airtight stopper after the addition of a known amount of hydrogen peroxide. The polymerization was allowed to continue at room temperature ( $\approx 30^\circ\text{C}$ .) in presence of ultraviolet light or in the dark in a thermostated bath.

Polymerizations involving hydrogen peroxide and activators such as ferrous ammonium sulfate and ferric chloride was carried out at room temperature and in the dark. Solutions of activators of known concentration were flushed profusely with purified nitrogen, and on subsequent addition of monomer and the peroxide the polymerization was allowed to continue under completely air-tight conditions.

Bulk polymerization of methyl methacrylate with the use of hydrogen peroxide as initiator was also carried out by following the method of Nandi and Palit.<sup>3</sup> The bulk polymerization was carried out both thermally at 60 and 90°C., and photochemically at room temperature with the use of ultraviolet light.

### Purification of Polymers

Polymers obtained by aqueous initiation with hydrogen peroxide were filtered, washed thoroughly with distilled water to remove all soluble impurities, and then dried in an air oven at 45–50°C. The dried aqueous polymers and also the polymers obtained in bulk were finally purified by the usual method of repeated precipitation,<sup>4</sup> benzene being used as the solvent and a mixture of alcohol and petroleum ether as the precipitant.

### Transformation of Hydroxyl Endgroups to Carboxyl Endgroups

It was found that hydroxyl endgroups presumably incorporated in the polymers obtained by initiation with hydrogen peroxide systems<sup>5–7</sup> are not responsive to the dye test for endgroup analysis. They were however, transformed into dye-responsive, ionizable endgroups such as carboxyl ( $\text{COO}^-$ ) by the phthalic anhydride–pyridine technique developed for the purpose.<sup>8</sup> A 0.1–0.2 g. portion of polymer was dissolved in 10 ml. of pyridine containing 0.5 g. phthalic anhydride in a standard joint refluxing unit, and the whole mixture was refluxed on a water bath for a period of 6 hr. The polymer was then precipitated from the pyridine solution with petroleum ether, dissolved in benzene solution, again precipitated with petroleum ether, and the process was repeated until the polymer was free of pyridine. The benzene solution was then filtered to free it from unreacted insoluble phthalic anhydride and purified by the usual method of repeated precipitation with an alcohol–petroleum ether mixture.<sup>4,8</sup> After proper purification,<sup>8</sup> the phthalated polymers were examined for OH endgroups (transformed to COOH) by the application of the dye interaction technique.<sup>2</sup>

### Determination of Endgroups

In the dye interaction test for endgroups, the reagent used was the orange-yellow benzene extract of rhodamine 6Gx (from its aqueous solution of pH 10).<sup>4</sup> Known amounts of the polymers were dissolved in benzene, and equal volumes of this polymer solution and the rhodamine reagent were mixed together. The phthalated polymers changed the color of the rhodamine reagent to pink but the same polymers before phthalation did not produce any change in the dye reagent. This clearly indicated the presence of hydroxyl endgroups (in the form of carboxyls) in the polymers.<sup>5</sup> Uncatalyzed thermal polymers of methyl methacrylate, however, do not give any response to the dye interaction test even after phthalation. Estimation of hydroxyl endgroups (transformed to COOH) was carried out by measurements of the color changes of the rhodamine dye reagent in a Hilger spectrophotometer at 515  $m\mu$  with the use of 1-cm. cells. The details of the method for endgroup estimation has been described elsewhere.<sup>4</sup>

The carboxyl endgroup content of the phthalated polymers was determined by comparison with a calibration curve for formic acid, obtained by a similar procedure. The suitability of this method has been checked by quantitative estimation of carboxyl groups in a large number of copolymers in which one of the reactant monomers is a carboxylic monomer.<sup>4</sup>

### Determination of Molecular Weight

The number-average molecular weights  $\bar{M}_n$  of the poly(methyl methacrylate) samples were calculated from the respective intrinsic viscosity  $[\eta]$  values obtained by the usual method of extrapolation. Viscosity measurements were carried out in an Ostwald-type viscometer at  $35 \pm 0.1^\circ\text{C}$ . with benzene solutions of the polymers.  $\bar{M}_n$  values were obtained with the help of the equation<sup>9</sup>

$$\bar{M}_n = 2.81 \times 10^5 \times [\eta]^{1.32}$$

## RESULTS AND DISCUSSION

Hydrogen peroxide has been found incapable of initiating aqueous polymerization of methyl methacrylate at room temperature ( $\approx 30^\circ\text{C}$ .) when kept in the dark. Polymerization in the dark, however, takes place at higher temperature (ca.  $60^\circ\text{C}$ .), though associated with a fairly long induction period, e.g., about 2–3 hr. with 0.2*M*  $\text{H}_2\text{O}_2$ , as against only a few minutes in aqueous photopolymerization. Bulk polymerization of MMA initiated by  $\text{H}_2\text{O}_2$  shows more or less similar features.<sup>3</sup> Aqueous polymerization in the dark with  $\text{H}_2\text{O}_2$  activated by  $\text{Fe}^{2+}$  and  $\text{Fe}^{3+}$  ions in solution, however, starts quite readily with a negligible induction period.

### Aqueous Photopolymerization of MMA

The results of endgroup analysis are given in Table I. Hydroxyl endgroups have been detected in all the methyl methacrylate polymers ob-

TABLE I  
 Determination of Hydroxyl Endgroups in Poly(methyl Methacrylate) Obtained by Hydrogen Peroxide Initiation in Aqueous Medium:  $[MMA] = 0.094$  mole/l.;  $N_2$  Atmosphere

$H_2O_2$ concn., mole/l.	Condition of polymerization	$[\eta]$	% Polymer solution (phthalated)	Dye interaction test for OH endgroup estimation		Average number of OH endgroups per poly- mer chain
				using rhodamine reagent <sup>a</sup>	O.D. at 515 $m\mu$	
0.004	UV light, 30°C.	1.75	0.05	0.45	0.88	
0.008	" "	1.50	0.05	0.462	1.0	
0.01	" "	1.30	0.05	0.474	1.08	
0.02	" "	1.07	0.05	0.495	1.07	
0.05	" "	0.81	0.05	0.53	1.07	
0.08	" "	0.70	0.05	0.565	1.10	
0.10	" "	0.61	0.05	0.60	1.12	
0.20	" "	0.37	0.05	0.925	1.52	
0.40	" "	0.23	0.025	0.86	1.45	
0.50	" "	0.20	0.025	1.015	1.54	
0.60	" "	0.18	0.025	1.12	1.57	
0.05	Dark, 60°C.	0.88	0.05	0.50	1.00	
0.20	" "	0.33	0.05	0.77	0.96	

<sup>a</sup> O.D. of original polymer solution corresponds to 0.40.

tained by aqueous initiation with hydrogen peroxide. This is in agreement with the observation of Dainton, who qualitatively detected OH endgroups by infrared spectroscopy in such polymers. In aqueous photoinitiation with  $H_2O_2$ , the average content of the hydroxyl endgroup varies within certain limits. At concentration of  $H_2O_2$  below about  $0.1M$ , an average of 1 hydroxyl endgroup per polymer chain has been obtained, but at higher initiator concentrations this value tends to increase rapidly to an average of 1.5 hydroxyl endgroups per polymer chain. The yield curve (Fig. 1), representing a plot of per cent yield of polymer versus initiator concentration, passes through a maximum at about the same concentration, viz.  $0.1M$ , from which point the endgroup content has been found to change rapidly from 1 to 1.5 per polymer chain. The plot of  $1/[\eta]$  against  $\sqrt{C}$  (Fig. 2), where  $c$  is the initiator concentration, undergoes a fairly sharp change of slope at about this concentration. So the transition in the average endgroup content is also reflected in the average molecular weights of the polymers. This fall in the percentage yield of polymer at relatively high  $H_2O_2$  concentration ( $\geq 0.1M$ ) as shown in Figure 1 may be attributed to the increased photooxidation of monomer molecules to nonpolymerizable oxidation products. A change in the hydroxyl endgroup content from 1 to 1.5 per polymer chain (from  $c \geq 0.1M$ ) as determined by the dye interaction method indicates that probably the termination mechanism is also changed

from about this point onwards. At low initiator concentration range ( $c < 0.1M$ ), termination takes place presumably by disproportionation leading to 1 endgroup per chain. At higher values of  $c$  ( $c \geq 0.1M$ ), termination by primary hydroxyl radicals and/or by chain transfer probably becomes more and more important, leading to the increased value of

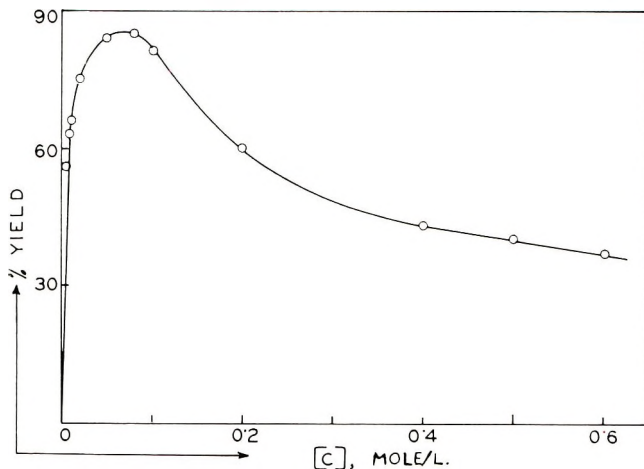


Fig. 1. Plot of yield of poly(methyl methacrylate) vs. initiator ( $H_2O_2$ ) concentration  $C$ .

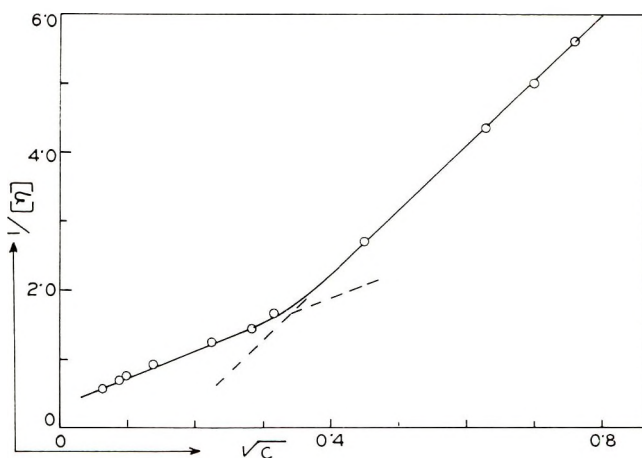
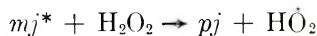
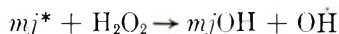


Fig. 2. Plot of  $1/[\eta]$  vs.  $\sqrt{c}$  of poly(methyl methacrylate).

average hydroxyl endgroup content. In aqueous photopolymerization of acrylamide initiated by  $H_2O_2$ , Dainton<sup>10</sup> reported a decrease in the initiator exponent below 0.5 above certain concentration of  $H_2O_2$  without subsequent increase in intensity exponent and explained it in terms of degradative chain transfer with  $H_2O_2$ :



but this explanation cannot account for the increase in endgroup content as observed here. Termination by primary hydroxyl radicals and/or by chain transfer with undissociated  $\text{H}_2\text{O}_2$ :



at least in part, appears more probable at higher concentration of  $\text{H}_2\text{O}_2$ .

### Aqueous Thermal Polymerization of MMA

Aqueous thermal initiation of MMA polymerization by hydrogen peroxide even at  $60^\circ\text{C}$ . is very sluggish, and the yield of polymer is very low (20–40%). Two experiments were carried out at 0.05*M* and 0.2*M* concentration of  $\text{H}_2\text{O}_2$ , and the polymers obtained were found to contain approximately an average of one hydroxyl endgroup per polymer chain (Table I).

### Bulk Polymerization of MMA

In thermal (60 and  $90^\circ\text{C}$ .) and photo ultraviolet-induced bulk polymerization of methyl methacrylate initiated by  $\text{H}_2\text{O}_2$ , hydroxyl endgroups have also been detected in the polymers. Thermal initiation is associated in general with a longer induction period, and the average number of hydroxyl endgroups per polymer chain is found to be in the range of 1.3–1.6. Photoinitiation, however, is more efficient, the induction period being relatively short, and the average number of hydroxyl endgroup per polymer chain has been found to be about 1.4–1.7. The results are shown in Table II. It appears that at least a part of the termination is caused by primary hydroxyl radicals and/or by chain transfer with undissociated  $\text{H}_2\text{O}_2$ .

TABLE II  
Determination of Hydroxyl Endgroups in Poly(methyl Methacrylate) Obtained by Initiation with Hydrogen Peroxide in Bulk ( $\text{H}_2\text{O}_2$  Extracted by MMA Monomer and Dried Over Anhydrous  $\text{Na}_2\text{SO}_4$ ;  $\text{N}_2$  Atmosphere)

$\text{H}_2\text{O}_2$ concn., mole/l.	Condition of polymerization	$[\eta]$	Dye interaction test with rhodamine reagent	
			O.D. of 0.1% polymer solution (phthalated) <sup>a</sup>	Average number of OH endgroups per polymer chain
0.15	UV light, $30^\circ\text{C}$ .	0.50	1.06	1.41
0.1	" "	0.54	1.10	1.65
0.075	" "	0.60	0.98	1.57
0.15	" $60^\circ\text{C}$ .	1.61	0.55	1.45
0.1	" "	1.75	0.53	1.48
0.075	" "	1.9	0.50	1.32
0.15	" $90^\circ\text{C}$ .	0.9	0.66	1.30
0.1	" "	1.2	0.60	1.41
0.075	" "	1.45	0.58	1.61

<sup>a</sup> O.D. of original polymer solution at  $515 \text{ m}\mu$  corresponds to 0.40.

Effect of  $\text{Fe}^{++}$  and  $\text{Fe}^{+++}$  Ions

Fenton's reagent ( $\text{Fe}^{2+}-\text{H}_2\text{O}_2$ ) is a prolific source of hydroxyl radicals and has long been widely used to initiate aqueous vinyl polymerization.<sup>11-17</sup> The decomposition of hydrogen peroxide is also known to be highly catalyzed by traces of  $\text{Fe}^{3+}$  ion,<sup>18,19</sup> and the generation of hydroxyl radical intermediates has been proposed by Marvel et al.,<sup>20</sup> Cahill and Taube,<sup>7</sup> and by Kremer.<sup>21</sup> Polymerization of methyl methacrylate has been carried out in aqueous media with the use of  $\text{Fe}^{2+}-\text{H}_2\text{O}_2$  and  $\text{Fe}^{3+}-\text{H}_2\text{O}_2$  initiating systems. The concentration of  $\text{H}_2\text{O}_2$  varied from 0.005 to 0.05*M*. By the application of the dye interaction technique all the polymers have been found to contain hydroxyl endgroups, Table III. The results provide

TABLE III  
Determination of Hydroxyl Endgroups in Poly(methyl Methacrylate) Obtained by Initiation with Hydrogen Peroxide Activated by  $\text{Fe}^{2+}$  and  $\text{Fe}^{3+}$  Ion in Aqueous Medium  
[MMA] = 0.094 mole/l.; Temp  $\approx$  30°C.;  $\text{N}_2$  Atmosphere

$\text{H}_2\text{O}_2$ concn., mole/l.	Activator	Activator concn. $\times 10^3$ , mole/l.	$[\eta]$	Dye interaction test with rhodamine reagent	
				O.D. of 0.05% polymer solution (phthalated) <sup>a</sup>	Average number of OH end- groups per polymer chain
0.01	$\text{Fe}(\text{NH}_4)_2(\text{SO}_4)_2 \cdot 6\text{H}_2\text{O}$	1	1.05	0.50	1.10
0.01		5	0.64	0.615	1.27
0.01		10	0.38	0.78	1.15
0.01		20	0.18	1.24	0.98
0.001		20	0.29	0.82	0.84
0.02		1	0.85	0.535	1.20
0.02	$\text{FeCl}_3 \cdot 6\text{H}_2\text{O}$	2.5	0.73	0.575	1.24
0.04		1	0.76	0.56	1.17
0.005		3	0.42	0.87	1.60
0.01		3	0.25	1.06	1.15
0.05		3	0.12	0.89 <sup>b</sup>	1.60
0.02		0.4	0.60	0.63	1.20
0.02		2	0.30	0.90	1.08

<sup>a</sup> O.D. of original polymer solution at 515  $\mu$  corresponds to 0.40.

<sup>b</sup> This O.D. value was obtained for 0.01% solution of the respective polymer (phthalated).

strong evidence for the existence of transient hydroxyl radicals in the initiating media. An average of 1 hydroxyl endgroup per polymer chain has been obtained with  $\text{Fe}^{2+}-\text{H}_2\text{O}_2$  initiation (Table III). Using the same initiator for styrene polymerization, Evans<sup>6</sup> showed that the molecular weights obtained by osmotic pressure measurements and from endgroup analysis showed good agreement if mutual chain termination (2 endgroups



per chain) was considered. So it appears that in MMA polymerization, termination takes place mainly by disproportionation, at least in the concentration range of the initiator components used herein.

$\text{Fe}^{3+}$ - $\text{H}_2\text{O}_2$  initiator also conforms more or less to the same pattern, and an average of approximately 1 hydroxyl endgroup per polymer chain has been obtained. In a dozen experimental runs with varying proportions of  $\text{Fe}^{3+}$  and  $\text{H}_2\text{O}_2$ , three polymer samples have been found to contain higher amount of hydroxyl endgroups, viz., 1.6 per polymer chain. Five representative experiments with  $\text{FeCl}_3$ - $\text{H}_2\text{O}_2$  initiation are presented in Table III. It appears that there is a tendency to produce polymers with higher hydroxyl content in  $\text{Fe}^{3+}$  medium than in  $\text{Fe}^{2+}$  medium.

Thanks are due the Council of Scientific & Industrial Research (India) for financial assistance in the form of a fellowship to one of the authors (A. R. M.).

### References

1. Palit, S. R., *Chem. Ind. (London)*, **1960**, 1531.
2. Palit, S. R., and P. Ghosh, *Microchem. Tech.*, **2**, Proc. Internatl. Symp. Microchem. Tech. Pennsylvania State Univ., August 14-18, (1961), p. 663.
3. Nandi, U. S., and S. R. Palit, *J. Polymer Sci.*, **17**, 65 (1955).
4. Palit, S. R., and P. Ghosh, *J. Polymer Sci.*, **58**, 1225 (1962).
5. Dainton, F. S., *J. Phys. Colloid Chem.*, **52**, 490 (1948).
6. Evans, M. G., *J. Chem. Soc.*, **1947**, 266.
7. Cahill, A. E., and H. Taube, *J. Am. Chem. Soc.*, **74**, 2312 (1952).
8. Palit, S. R., and A. R. Mukherjee, *J. Polymer Sci.*, **58**, 1243 (1962).
9. Baxendale, J. H., S. Bywater, and M. G. Evans, *J. Polymer Sci.*, **1**, 237 (1946).
10. Dainton, F. S., and M. Tordoff, *Trans. Faraday Soc.*, **53**, 499 (1957).
11. Baxendale, J. H., M. G. Evans, and G. S. Park, *Trans. Faraday Soc.*, **42**, 156 (1946).
12. Baxendale, J. H., M. G. Evans, and J. K. Killham, *Trans. Faraday Soc.*, **42**, 668 (1946), *J. Polymer Sci.*, **1**, 466 (1946).
13. Baxendale, J. H., S. Bywater, and M. G. Evans, *Trans. Faraday Soc.*, **42**, 675 (1946).
14. Schulz, R. C., H. Cherdron, and W. Kern, *Makromol. Chem.*, **24**, 141 (1957).
15. Bond, J., and T. I. Jones, *J. Polymer Sci.*, **42**, 67, 75 (1960).
16. Dainton, F. S., and P. H. Seaman, *J. Polymer Sci.*, **39**, 279 (1959).
17. Dainton, F. S., P. H. Seaman, D. G. L. James, and R. S. Eaton, *J. Polymer Sci.*, **34**, 209 (1959).
18. Barb, W. G., J. H. Baxendale, P. George, and K. R. Hargrave, *Trans. Faraday Soc.*, **47**, 462 (1951).
19. Parts, A. G., *J. Polymer Sci.*, **37**, 131 (1959).
20. Marvel, C. S., R. Deanin, C. J. Clans, and M. B. Wild, *J. Polymer Sci.*, **3**, 350 (1948).
21. Kremer, M. L., *Trans. Faraday Soc.*, **58**, 702 (1962).

### Résumé

On a incorporé des groupements hydroxyles terminaux à des polymères de méthacrylate de méthyle qui ont été initiés au moyen de peroxyde d'hydrogène en bloc et en solution aqueuse. Les groupements hydroxyles terminaux dans les différents échantillons des polymères ont été dosés par la technique d'interaction avec un colorant. La photoinitiation en solution aqueuse au moyen de peroxyde d'hydrogène provoque une incorporation moyenne en groupements hydroxyles terminaux de 1 à 1.5 par chaîne de

polymère suivant la concentration en initiateur dont on s'est servi. Une polymérisation thermique (à 60°C) effectuée en milieu aqueux provoque une incorporation d'environ 1 groupement hydroxyle terminal par chaîne. Une polymérisation à l'obscurité et à température de chambre a été réalisée par activation au moyen d'ions ferreux et ferriques et une moyenne d'environ un groupement terminal par chaîne a été obtenue dans les deux cas. La polymérisation en bloc (sous l'action de la lumière et de la chaleur) produit un polymère contenant de 1.3 à 1.7 groupements hydroxyles par chaîne.

### Zusammenfassung

Aus Methylmethacrylat wurde nach Polymerisation in Substanz und in wässriger Lösung mit Wasserstoffperoxyd als Starter Polymeres mit Hydroxylendgruppen erhalten. Die Hydroxylendgruppen in den entsprechenden Polymerproben wurden mittels einer Anfärbemethode bestimmt. Bei der photoinitierten Polymerisation mit Wasserstoffperoxyd in wässriger Lösung werden je nach der verwendeten Starterkonzentration im Mittel etwa 1–1.5 Hydroxylendgruppen pro Polymerkette eingebaut. Die thermische Polymerisation (60°C) in wässriger Lösung führt zu durchschnittlich etwa einer Hydroxylendgruppe pro Kette. Bei der im Dunkeln bei Raumtemperatur durch Aktivierung mit  $\text{Fe}^{2+}$ - und  $\text{Fe}^{3+}$ -Ionen ausgeführten Polymerisation wurde in beiden Fällen im Durchschnitt etwa eine Hydroxylendgruppe pro Kette eingebaut. Die thermische und die Photopolymerisation in Substanz ergibt Polymere mit etwa 1,3–1,7 Hydroxylendgruppen pro Kette.

Received February 6, 1963

Revised July 8, 1963

## **Incorporation of Hydroxyl Endgroups in Vinyl Polymer. Part II. Aqueous Polymerization of Methyl Methacrylate Initiated by Salts or Complexes of Some Metals in Their Higher Oxidation States**

PREMAMOY GHOSH, ASISH R. MUKHERJEE, and SANTI R. PALIT, *Indian Association for the Cultivation of Science, Jadavpur, Calcutta, India*

### **Synopsis**

Hydroxyl endgroups have been incorporated in polymers of methyl methacrylate obtained by initiation with salts or complexes of  $Mn^{4+}$ ,  $Ce^{4+}$ ,  $Co^{3+}$ , and  $Ag^{3+}$  with the monomer in aqueous solution. Hydroxyl and carboxyl endgroups in the respective polymer samples have been estimated with the help of the dye interaction technique. Initiation with  $Mn^{4+}$  and  $Ce^{4+}$  ions in dilute  $H_2SO_4$  medium in the dark at room temperature has been found to incorporate an average of about 2 hydroxyl endgroups per polymer chain. Initiation with potassium trioxalato cobaltate (III) complex has been carried out both in the dark and in the presence of ultraviolet light at room temperature, and both carboxyl and hydroxyl endgroups have been characterized in the polymers formed. An average total of 1 endgroup (both  $COOH$  and  $OH$  combined) per polymer chain has been obtained in case of photoinitiation, and about 2 per polymer chain in the case of thermal initiation in dark. Polymerization in the dark at room temperature has been carried out in neutral medium with ethylene dibiguanidinium nitrate complex of tripositive silver as the initiator, and an average of 2 hydroxyl endgroups per polymer chain has been found to be incorporated in the process.

### **INTRODUCTION**

Certain metals in their simple or complexed higher valence states can replace peroxy compounds in redox catalysts.<sup>1-3</sup> The high reactivity of cobaltic ( $Co^{3+}$ ) and ceric ( $Ce^{4+}$ ) salts in aqueous media is well known,<sup>4-6</sup> and they have been found to be potent initiators of aqueous vinyl polymerization.<sup>2,3</sup> Little direct evidence has so far been adduced regarding the endgroups in the resulting polymers with respect to the initiating radical. Systematic investigations on endgroups in vinyl polymers obtained by aqueous initiation with salts or complexes of  $Mn^{4+}$ ,  $Ce^{4+}$ ,  $Co^{3+}$ , and  $Ag^{3+}$  have therefore been carried out with the help of the sensitive dye interaction technique,<sup>7</sup> and the results are reported in the present paper.

## EXPERIMENTAL

### Materials

Methyl methacrylate monomer was purified by the same method as described in Part I.<sup>8</sup> A.R. grade potassium permanganate was obtained from B.D.H.; ceric sulfate (L.R. grade) was also obtained from B.D.H. and used without further purification. Potassium trioxalato cobaltate (III) complex,  $K_3[Co(C_2O_4)_3] \cdot 3H_2O$  and ethylene dibiguanidinium nitrate complex of tripositive silver were prepared in our laboratory according to the methods of Sorensen,<sup>9</sup> and Ray and Chakravarty,<sup>10</sup> respectively.

### Preparation and Purification of Poly(methyl Methacrylate)

The aqueous polymerization of methyl methacrylate was carried out in clean, well-stoppered conical flasks in an atmosphere of nitrogen. Polymerization initiated by potassium permanganate and ceric sulfate was carried out in acid aqueous solution, sulfuric acid being used in both cases. A minimal amount of acid was used so as to dissolve the colloidal manganese dioxide formed in permanganate initiation and to check hydrolysis of the initiator to its hydroxide in ceric sulfate initiation. The minimum possible time was allowed for polymerization in acidic medium so that carboxyl groups generated by extensive hydrolysis of ester units of methyl methacrylate might not mask the response due to endgroups incorporated in the process. Polymerization with trivalent cobalt and silver complexes as initiators was carried out in neutral solutions. The trioxalato cobaltate (III) complex was selected as an initiator for its static stability in water and light absorption peak in the blue and the polymerization was, therefore, carried out both in presence of ultraviolet light and in the dark. The polymerization with all other initiators were, however, carried out in the dark. All the polymerization experiments were carried out at room temperature ( $\sim 30^\circ C.$ ).

The polymers obtained were filtered, washed scrupulously with distilled water to remove all soluble impurities and the unreacted monomer, and dried in an air oven at  $45^\circ C.$  They were then finally purified by a method of repeated precipitation<sup>11</sup> as described in Part I. The purified polymers were then subjected to the dye interaction test<sup>7,11</sup> for endgroup characterization and determination.

### Transformation of Hydroxyl Endgroups to Carboxyl Endgroups

Since the hydroxyl endgroups in polymers were found not to respond to the dye interaction test for endgroup characterization, their analysis was carried out by transforming them to dye-responsive carboxyl (COOH) groups by the phthalic anhydride/pyridine technique developed for the purpose. The process is known as phthalation and has been described elsewhere.<sup>12</sup> After phthalation the polymers were properly purified before being examined for endgroups.

### Dye Interaction Test for Endgroup Determination

Orange yellow benzene extract of rhodamine 6Gx (from its aqueous solution of pH 10) is the dye reagent for the purpose.<sup>11</sup> The method of detection and estimation of carboxyl and hydroxyl (transformed to carboxyl) endgroups in the purified polymers is the same as described in Part I.<sup>8</sup>

### Determination of Molecular Weight

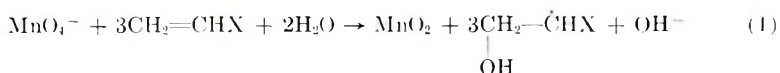
Number-average molecular weights  $\bar{M}_n$  for poly(methyl methacrylate) samples were obtained viscometrically with the help of the equation:<sup>13</sup>  $\bar{M}_n = 2.81 \times 10^5 [\eta]^{1.32}$  (in benzene solution at  $35 \pm 0.1^\circ\text{C}$ ).

## RESULTS AND DISCUSSION

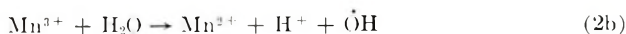
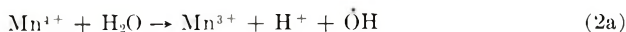
### Initiation by Permanganate ( $\text{MnO}_4^-$ )

$\text{KMnO}_4$  in neutral medium cannot initiate polymerization in aqueous medium except in case of acrylonitrile, where a slight polymerization is observed. This inability is attributed to the inhibiting action of colloidal  $\text{MnO}_2$  which is formed by the reaction of  $\text{MnO}_4^-$  with the monomer. But, if sufficient acid is present in the system and if the polymerization is allowed to follow its course undisturbed, the colloidal  $\text{MnO}_2$  visible in the initial stages gradually dissolves and disappears and the polymerization proceeds at a fairly rapid rate in the coagulated phase. The inhibition period is only a few minutes (5–10 min.), and when the polymerization is over, a perfectly white polymer in a colorless clear supernatant aqueous medium is obtained. The initiating capacity of this system as judged by the degree of polymerization of the polymer produced has been found to be almost independent of sulfuric acid concentration over a wide range. (Table 1A).

Tompkins et al.<sup>14–16</sup> suggested two principal mechanisms by which organic compounds are oxidized by acid permanganate, viz., (a) direct oxidation by  $\text{MnO}_4^-$  and (b) prior formation of  $\text{Mn}^{4+}$  and subsequent oxidation by OH radicals produced by the reaction between this ion and water. The overall reaction of mechanism (a) is probably as follows



Formation of hydroxylated radical of this type has also been suggested by Baxendale and Wells<sup>3</sup> during initiation of vinyl polymerization by  $\text{Co}^{3+}$  ion in aqueous solution.  $\text{MnO}_2$  formed according to eq. (1) may gradually dissolve in acid solution to give  $\text{Mn}^{4+}$  ion in solution, and this may again generate .OH radicals according to Tompkin's mechanism (b):



Hydroxyl radicals are therefore expected to be responsible for aqueous polymerization of methyl methacrylate in acid permanganate initiation. Ex-

TABLE I  
Endgroups in Poly(methyl Methacrylate) Initiated by  $\text{MnO}_4^-$  and  $\text{Ce}^{4+}$  Ions in Acid Aqueous Medium ( $[\text{MMA}] = 0.094$  mole/l.; Temperature  $\sim 30^\circ\text{C}$ .;  $\text{N}_2$  atmosphere)

Initiator	Initiator concn. $\times 10^4$ , mole/l.	$\text{H}_2\text{SO}_4$ concn. $\times 10^2$ , mole/l.	$[\eta]$	Dye interaction test with rhodamine reagent for endgroup estimation			
				O. D. of 0.05% polymer soln.		Endgroups/chain	
				(Original) <sup>a</sup>	Phthalated	OH	COOH <sup>a</sup>
A. $\text{KMnO}_4$							
	1	7.5	2.00	0.65	0.73	2.10	6.85
	2	7.5	1.70	0.66	0.75	2.00	5.60
	5	7.5	1.40	0.69	0.82	2.20	4.84
	10	7.5	0.95	0.655	0.87	2.16	2.60
	10	2.5	1.00	0.50	0.70	2.13	1.00
	10	5.0	0.95	0.50	0.695	2.03	0.95
	10	10.0	0.90	0.635	0.855	2.16	2.34
B. $\text{Ce}(\text{SO}_4)_2$ in dilute $\text{H}_2\text{SO}_4$							
	0.6	—	2.8	0.56	0.615	2.2	—
	1.2	—	2.6	0.56	0.62	2.2	—
	2.4	—	2.4	0.57	0.63	2.1	—
	12.0	—	1.5	0.65	0.77	2.16	—
	30.0	—	1.2	0.79	0.95	2.15	—
	75.0	—	0.7	0.73	1.03	2.01	—

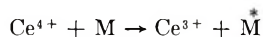
<sup>a</sup> Original response to rhodamine is due to carboxyl groups formed by hydrolysis of the polymer in acidic medium.

perimental confirmation of hydroxyl endgroups by dye interaction technique in all the polymers formed (Table IA) provides evidence at least for the existence of hydroxyl radicals in the polymerization medium, but it cannot distinguish between Tompkin's mechanisms (a) and (b). All the polymers were found to contain about 2 hydroxyl endgroups per chain and some carboxyl groups formed by hydrolysis of the polymer in acidic medium (Table I). So hydroxyl radicals not only initiate polymerization but also terminate the same under these experimental conditions.

#### Initiation by Ceric Salt ( $\text{Ce}^{4+}$ )

Ceric sulfate in dilute  $\text{H}_2\text{SO}_4$  medium initiates aqueous polymerization of methyl methacrylate in the dark at room temperature with some induction period (10–30 min). The percentage yield gradually decreases with increase in initiator concentration, probably due to oxidation of monomer. An average of about 2 hydroxyl endgroups and some carboxyl groups (formed by hydrolysis of the polymer in acidic medium) per polymer chain has been obtained by the application of dye interaction technique, (Table IB). This provides experimental support to the idea that hydroxyl radicals act as the initiating as well as the terminating radical.

Photoinitiation of vinyl polymerization by  $\text{Ce}^{4+}$  ion was reported by Weiss.<sup>17</sup> Saldick<sup>2</sup> first noticed that  $\text{Ce}^{4+}$  ion can initiate vinyl polymerization even in the dark at room temperature, and he expected the process to proceed through a normal free radical mechanism. Venkatakrisnan and Santappa<sup>18</sup> proposed on the basis of their kinetic studies that the initiation was due to the generation of free radicals according to the reaction between  $\text{Ce}^{4+}$  ion and monomer:



However, oxidation of acetone by ceric sulfate in the presence of dilute  $\text{H}_2\text{SO}_4$  has been shown by Shorter and Hinshelwood<sup>5</sup> to proceed through the intermediacy of hydroxylated products. Mino and Kaizerman<sup>19</sup> also suggested that oxidation of alcohol by  $\text{Ce}^{4+}$  ion is a free radical process whereby a hydroxylated radical is generated from the alcohol with the expulsion of a proton. It appears therefore certain from endgroup analysis by dye technique that initiation of polymerization by  $\text{Ce}^{4+}$  ion is due to OH radicals formed by the reaction



and a mechanism as proposed by Venkatakrisnan and Santappa does not appear to be tenable.

The initiating capacity of this system as judged by the degree of polymerization of the polymers formed appears to be less than that of the  $\text{KMnO}_4\text{--H}_2\text{SO}_4$  system (Table I).

#### Initiation by Trivalent Cobalt ( $\text{Co}^{3+}$ ) Complex

The reactivity of potassium trioxalato cobaltate (III) complex,  $\text{K}_3[\text{Co}(\text{C}_2\text{O}_4)_3] \cdot 3\text{H}_2\text{O}$ , to initiate aqueous vinyl polymerization<sup>20</sup> is rather interest-

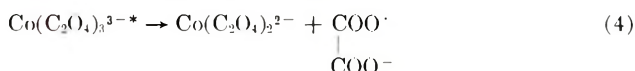
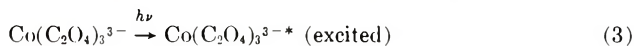
TABLE II  
 Endgroups in Poly(methyl Methacrylate) Initiated by Complex Salts of  $\text{Co}^{3+}$  and  $\text{Ag}^{3+}$  Ions in Aqueous Medium:  
 $[\text{MMA}] = 0.094$  mole/l.;  $\text{N}_2$  Atmosphere

Initiator	Initiator concn., mmole/l.	Condition of polymerization	$[\eta]$	Dye interaction test with rhodamine reagent							
				Polymer soln. concn., %	O.D. at 515 m $\mu$ for polymer samples		Average number of end-groups per polymer chain				
					Original	Phthalated	COOH	OH	Total		
<b>A. <math>\text{K}_3[\text{Co}(\text{C}_2\text{O}_4)_3] \cdot 3\text{H}_2\text{O}</math></b>											
	0.048	30°C., ultraviolet	2.16	0.2	0.46	0.55	0.47	0.71	1.18		
	0.094	" "	1.9	0.2	0.50	0.57	0.65	0.46	1.11		
	0.16	" "	1.8	0.2	0.53	0.57	0.75	0.25	1.00		
	0.22	" "	1.7	0.2	0.56	0.59	0.85	0.21	1.06		
	0.40	" "	1.56	0.2	0.59	0.63	0.88	0.24	1.12		
	0.80	35°C., dark	2.20	0.2	0.48	0.69	0.60	1.40	2.00		
	1.60	" "	1.80	0.2	0.52	0.72	0.67	1.20	1.87		
<b>B. <math>[\text{Ag}^{III}\text{En}(\text{BigH}^+)_2](\text{NO}_3)_4</math></b>											
	0.04	30°C., dark	2.85	0.1	0.40	0.495	0.0	1.96	—		
	0.10	" "	2.70	0.1	0.398	0.50	0.0	1.92	—		
	0.80	" "	2.50	0.1	0.401	0.52	0.0	2.02	—		



ing. At a relatively higher concentration ( $c > 0.001M$ ), this compound can bring about initiation of aqueous polymerization of MMA in the dark at room temperature after a relatively long induction period. However, the complex is highly photosensitive, and photoinitiation of MMA polymerization takes place with an induction period of only about 5–10 min. even at an initiator concentration as low as  $2 \times 10^{-5}M$ .

Aqueous photopolymerization of MMA has been carried out with the use of this initiator, and the polymers have been examined for endgroups (Table IIA). Carboxyl endgroups are found in the polymers to an extent of 0.5–0.9 per polymer chain. The polymers also give a positive test for the OH endgroup, the content of which varies from about 0.2 to 0.7 per polymer chain. An average total of 1 endgroup (both COOH and OH combined) per polymer chain has been obtained. At relatively high concentration of the initiator, carboxyl endgroups are found to be predominant, while at lower initiator concentration hydroxyl endgroups tend to be more predominant. The generation of carboxyl and hydroxyl radicals in solution probably takes place according to the mechanism given in eqs. (3)–(6).



Initiation by the oxalate ( $\dot{\text{C}}_2\text{O}_4^-$ ) radical generated by electron transfer within the ion pair complex according to reaction (4) or by its decomposition product carboxyl ( $\dot{\text{C}}\text{OO}^-$ ) radical generated according to reaction (5) gives rise to carboxyl endgroups and that by  $\dot{\text{O}}\text{H}$  radicals probably generated by reaction between oxalate/carboxyl radicals and water molecules [reaction (6)] gives rise to OH endgroups.

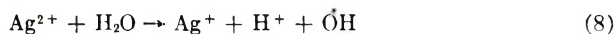
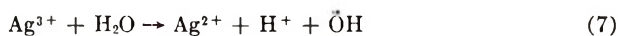
Aqueous thermal initiation by the same complex at relatively high concentrations of the initiator probably takes place by a similar mechanism, but the polymers obtained are of much higher molecular weight. Both carboxyl and hydroxyl endgroups are found in the polymers to an average total of about 2 per polymer chain, (Table IIA).

It may be mentioned in this connection that poly(methyl methacrylate) obtained by aqueous initiation with oxalic acid systems such as photoinitiation with oxalic acid and redox initiation with permanganate and oxalic acid<sup>21</sup> has been subjected to the dye interaction test in this laboratory and has been found to contain both carboxyl and hydroxyl endgroups in varied proportions.

#### Initiation by Trivalent Silver Complex ( $\text{Ag}^{3+}$ )

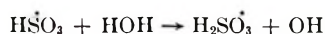
Ethylenedibiguanidinium nitrate complex of tripositive silver,  $[\text{Ag}^{(\text{III})} \text{En}(\text{BigH})_2^+](\text{NO}_3)_3$ , where  $\text{En}(\text{BigH})_2$  is  $\text{C}_6\text{N}_{10}\text{H}_{16}$ , is unstable in aqueous

solution and gradually decomposes to univalent silver salt. The complex can initiate aqueous polymerization of methyl methacrylate in dark at room temperature.<sup>12</sup> The polymers obtained are of high molecular weight, and hydroxyl endgroups have been found in them to an extent of about 2 per polymer chain, (Table IIB).  $\text{Ag}^{3+}$  ion reacts with water and generates hydroxyl radicals according to the scheme:



Hydroxyl radicals thus generated in the medium initiate polymerization and appear as endgroups. Interestingly, wide variation in the concentration of the initiator does not bring about appreciable change in the molecular weight of the polymers obtained, but the effect of increase in initiator concentration is adequately reflected in the decrease in the induction period: e.g., at an initiator concentration of  $0.04 \times 10^{-3}M$ , the induction period was found to be nearly 10 hr., while at an initiator concentration of  $0.8 \times 10^{-3}M$ , an induction period of less than 1 hr. was observed.

It may be concluded that initiation with any initiator in aqueous media almost invariably leads to the incorporation of certain amount of hydroxyl endgroups in the polymer chain. The simple explanation seems to be that the free radicals generated by the initiating reaction have the immense opportunity of abstracting hydrogen from surrounding water molecules prior to initiation of polymerization. Once hydroxyl radicals are generated by this process, they can survive long in water by the process of regeneration by transfer and can easily initiate polymerization. Moreover, the hydroxyl radicals may have greater initiating power than most of the other free radicals. The only exception to this general finding has been noticed in case of aqueous initiation with bisulfite,<sup>22</sup> when little or no hydroxyl endgroups could be detected in the polymers produced. This may be due to the fact that the hydrogen abstraction reaction in this case, viz.,



is not favored, probably owing to the fact that the product is rather unstable. In fact, the transfer reaction to produce unstable product has been already surmised to be a less favored reaction path.<sup>23</sup>

Thanks are due the Council of Scientific and Industrial Research for financial assistance in the form of a fellowship to one of the authors (A. R. M.).

### References

1. Evans, M. G., and N. Uri, *Nature*, **164**, 404 (1949).
2. Saldick, J., *J. Polymer Sci.*, **19**, 73 (1956).
3. Baxendale, J. H., and C. F. Wells, *Trans. Faraday Soc.*, **53**, 800 (1957).
4. Bawn, C. E. H., and A. G. White, *J. Chem. Soc.*, **1951**, 331, 339, 343.
5. Shorter, J., and C. Hinshelwood, *J. Chem. Soc.*, **1950**, 3276.

6. Hardwick, T. J., and E. Robertson, *Can. J. Chem.*, **29**, 828 (1951).
7. Palit, S. R., and P. Ghosh, *Microchem. Tech.*, **2**, Proc. Internatl. Symp. Microchem. Tech, Pennsylvania State Univ., August 14-18, 1961, p. 663.
8. Ghosh, P., A. R. Mukherjee, and S. R. Palit, *J. Polymer Sci.*, **A2**, 2807 (1964).
9. Booth, H. S., *Inorganic Synthesis*, Vol. I, McGraw-Hill, New York, 1939, p. 37.
10. Ray, P., and K. Chakravarty, *J. Ind. Chem. Soc.*, **21**, 47 (1944).
11. Palit, S. R., and P. Ghosh, *J. Polymer Sci.*, **58**, 1225 (1962).
12. Palit, S. R., and A. R. Mukherjee, *J. Polymer Sci.*, **58**, 1243 (1962).
13. Baxendale, J. H., S. Bywater, and M. G. Evans, *J. Polymer Sci.*, **1**, 237 (1946).
14. Ladbury, J. W., and C. F. Cullis, *Chem. Revs.*, **58**, 403 (1958).
15. Mann, D. R., and F. C. Tompkins, *Trans. Faraday Soc.*, **37**, 201 (1941).
16. Alexander, E. A., and F. C. Tompkins, *J. S. African Chem. Inst.*, **23**, No. 2, 1 (1940).
17. Weiss, J., *Nature*, **139**, 1019 (1937).
18. Venkatakrisnan, S., and M. Santappa, *Makromol. Chem.*, **27**, 51 (1958).
19. Mino, G., and S. Kaizerman, *J. Polymer Sci.*, **31**, 242 (1958).
20. Copestake, T. B., and N. Uri, *Proc. Roy. Soc. (London)*, **A228**, 252 (1955).
21. Palit, S. R., and R. S. Konar, *J. Polymer Sci.*, **57**, 609 (1962).
22. Mukherjee, A. R., P. Ghosh, S. C. Chadha, and S. R. Palit, unpublished results.
23. Das, S., and S. R. Palit, *Proc. Roy. Soc. (London)*, **A226**, 82 (1954).

### Résumé

Des groupements hydroxyles terminaux ont été incorporés à des polymères de méthacrylate de méthyle obtenu par initiation au moyen de sels ou de complexes de  $Mn^{4+}$ ,  $Ce^{4+}$ ,  $Co^{3+}$  et  $Ag^{3+}$  en présence du monomère en solution aqueuse. Les groupements hydroxyles et carboxyliques terminaux dans les échantillons respectifs de polymère ont été estimés au moyen d'une technique d'interaction avec un colorant. L'initiation au moyen d'ions  $Mn^{4+}$  et  $Ce^{4+}$  dans un milieu  $H_2SO_4$  dilué dans l'obscurité à la température de chambre provoque l'incorporation en moyenne d'environ deux groupements hydroxyles terminaux par chaîne de polymère. L'initiation au moyen du complexe cobalte(III)-trioxalate de potassium a été effectuée dans l'obscurité et en présence de lumière UV à température de chambre, et les groupements hydroxyliques et carboxyliques terminaux ont été caractérisés dans les polymères formés. Une moyenne totale d'un groupement terminal (COOH et OH combinés) par chaîne polymérique fut obtenue au moyen de l'initiation photochimique, et environ deux groupements terminaux par chaîne polymérique dans le cas d'une initiation thermique à l'obscurité. Une polymérisation à l'obscurité et à température de chambre a été effectuée en milieu neutre au moyen du complexe éthylène dibiguanidinium-nitrate d'argent trivalent comme initiateur et il fut trouvé qu'une moyenne de deux groupements hydroxyles terminaux par chaîne polymérique était incorporée par ce procédé.

### Zusammenfassung

In Methylmethacrylat-Polymeren wurden bei der Polymerisation der Monomeren mit Salzen oder Komplexen von  $Mn^{4+}$ ,  $Ce^{4+}$ ,  $Co^{3+}$  und  $Ag^{3+}$  als Starter in wässriger Lösung Hydroxylendgruppen eingeführt. Die Hydroxyl- und Carboxylendgruppen in den entsprechenden Polymeren wurden mittels einer Anfärbemethode bestimmt. Bei der Polymerisation im Dunkeln bei Raumtemperatur mit  $Mn^{4+}$   $Ce^{4+}$ -Ionen in verdünnter  $H_2SO_4$  als Starter wurden im Mittel etwa zwei Hydroxylendgruppen pro Polymerkette eingebaut. Der Start mit dem Kaliumtrioxalatkobaltat(III)-Komplex wurde sowohl im Dunkeln als auch in Gegenwart von UV-Licht bei Raumtemperatur durchgeführt und sowohl die Carboxyl- als auch die Hydroxylendgruppen im gebildeten Polymeren bestimmt. Im Falle der Photoinitiation wurde durchschnittlich insgesamt eine Endgruppe (COOH und OH zusammen) pro Polymerkette eingebaut, im Falle

des thermischen Startes im Dunkeln etwa zwei pro Polymerkette. Die Polymerisation im Dunkeln bei Raumtemperatur mit dem Äthylendibiguanidiniumnitrat-Komplex von dreifach positivem Silber als Starter wurde in neutralem Medium ausgeführt und ein Einbau von durchschnittlich zwei Hydroxylendgruppen pro Polymerkette festgestellt.

Received February 6, 1963

Revised July 8, 1963

## Polymerization of Isoprene with Normal-, Iso-, Secondary and Tertiary Butyllithium\*

IRVING KUNTZ, *Chemicals Research Division, Esso Research and Engineering Company, Linden, New Jersey*

### Synopsis

When isoprene (3.3*M*) in *n*-heptane is polymerized at 23.1°C. by the different butyllithiums (0.004*M*), the times to reach 50% conversion to polymer are 3.5, 2.3, 2.0, and 2.2 hr. for the normal, iso, secondary, and tertiary butyllithiums, respectively. When the same experiment is carried out at an initiator concentration of 0.02*M*, the  $t_{0.5}$  for the same sequence of isomers is 3.1, 2.6, 1.4, and 1.3 hr., respectively. In these and other experiments, the inherent viscosity of the polymers prepared with *tert*-butyllithium appears to be lower than those obtained with *n*-butyllithium. The stereochemistry of the polyisoprene polymers obtained with the different initiators is identical. The results with *n*- and isobutyllithium at 0.02*M* concentration seem to show the greatest deviation from first-order kinetics. Using data from experiments at different initiator concentrations and constant isoprene concentrations, the kinetic order in *tert*-butyllithium has been found to be  $0.54 \pm 0.17$ . These observations reflect differences in initiation rate for the varied butyllithiums. The kinetic order in initiator indicates that the growing isoprenyllithium chains are involved in dimer formation whose dissociation is the slow step in the propagation reaction.

### Introduction

We have studied the polymerization of isoprene with normal, iso-, secondary, and tertiary- butyllithium. The rate of the reaction and the geometrical configuration and inherent viscosity of the polyisoprene polymers produced have been examined. Some studies of the effect of variation in the nature of the hydrocarbon moiety in organolithium initiated polymerizations have been reported. Tobolsky and Rogers found that the polyisoprenes produced by butyllithium or phenyllithium in ethers had similar structures.<sup>1</sup> Kuntz and Gerber found that the polybutadienes produced by *n*- and isobutyllithium in *n*-heptane were structurally indistinguishable.<sup>2</sup> It has been reported that branched lithium alkyls, as contrasted with the straight-chain isomers, did not give stereoregular polystyrene in low temperature polymerizations.<sup>3</sup> In relatively concentrated solutions of organolithium (RLi) in tetrahydrofuran, the degree of polymerization (DP) of the polystyrenes produced at 20°C. indicated the following decreasing reactivities as the R group was varied: butyl  $\gg$  benzyl  $\sim$

\* Presented in part before the 140th Meeting of the American Chemical Society, Chicago, Illinois, September 1961.

allyl > vinyl  $\sim$  phenyl.<sup>4</sup> Very recently it has been reported that ethyllithium and *n*-butyllithium showed similar kinetics in styrene and isoprene polymerizations.<sup>5</sup>

### Results

Figure 1 shows the results obtained from dilatometric experiments in which isoprene (3.3*M*) was polymerized in *n*-heptane at 23.1°C. by the different butyllithiums in a solution 0.004*M* in initiator. The figure shows that there are differences in the rate of polymerization, with *n*-butyllithium being slower than the other butyllithiums. A convenient measure of the difference in rate is to compare the time required to reach the same level of conversion to polymer in the various experiments. The time required to reach 50% conversion,  $t_{0.5}$ , for the various butyllithiums is given in Table I. Table I also shows the inherent viscosity of the polyisoprene polymers isolated from the dilatometric experiments at essentially complete conversion of monomer. In these experiments, the inherent viscosity of the polymer increases in the sequence *tert*-, *sec*-, *iso*-, *n*-butyllithium.

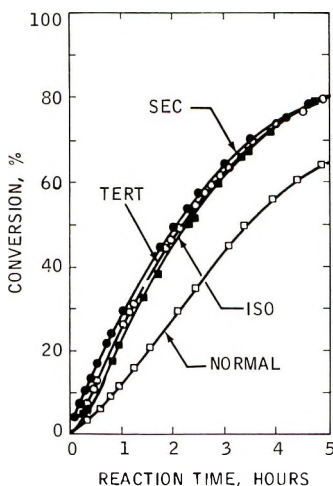


Fig. 1. Polymerization of isoprene (3.3*M*) with 0.004*M* butyllithium, *n*-heptane, 23.1°C.

Figure 2 shows the results of similar experiments in which the initiator concentration was 0.02*M*. Here, the results obtained show a greater difference in rate for the various butyllithiums, being fastest for *tert*- and *sec*-, followed by *iso*-, and with *n*-butyllithium being slowest. The inherent viscosity for the products of these experiments (Table I) is closer and increases in the sequence *tert*-, *sec*-, *iso*-, and *n*-butyllithium. Figure 3 shows the inherent viscosity of other experiments with *n*- and *tert*-butyllithium. While there is appreciable scatter in the data, it appears that the experiments with *tert*-butyllithium give polymers with lower inherent viscosities than do the *n*-butyllithium experiments. These differences seem to be

Table I  
Butyllithium Polymerizations of Isoprene

Alkyl	[BuLi], moles/l.	$t_{0.5}$ , hr.	Inherent viscosity	Time to $k_1$ , hr.	Polymer microstructure	
					<i>cis</i> -1,4, %	3,4, %
Normal	0.0047	3.5	0.92	2.2	91	9
Iso	0.0046	2.3	0.68	2.4	91	9
Secondary	0.0043	2.0	0.56	0.7	94	6
Tertiary	0.0044	2.2	0.37	1.1	90	10
Normal	0.023	3.1	0.22	7.4	92	8
Iso	0.023	2.6	0.22	4.0	92	8
Secondary	0.023	1.4	0.20	1.2	92	8
Tertiary	0.023	1.3	0.15	0.9	91	9

more consistent at high concentrations of initiator where the [isoprene]/[butyllithium] ratios are lower.

We have examined the infrared spectra of the polyisoprene polymers produced by the different butyllithiums. In simplifying these calculations, we have used the procedure of Binder and Ransaw<sup>6</sup> and, on the basis of the results of other workers, have considered that in heptane only *cis*-1,4- and 3,4- polyisoprene structures are formed.<sup>1</sup> Table I shows the results of these analyses and indicates that the stereochemistry of the polyisoprenes produced by *n*-, iso-, *sec*- and *tert*-butyllithium are the same within the precision of the infrared analysis.

Figure 4 shows a first-order plot of the experiment at 0.02*M* concentration of the different butyllithiums. It is seen that not all the curves show a good fit to a first-order kinetic relationship. The curves for *n*- and iso-

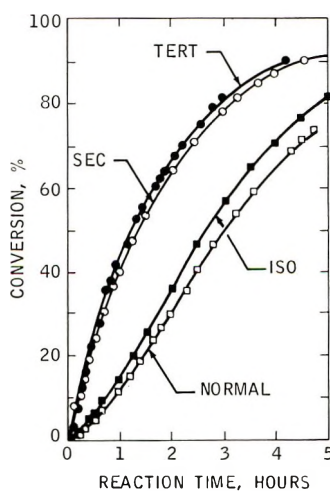


Fig. 2. Polymerization of isoprene (3.3*M*) with 0.02*M* butyllithium, *n*-heptane, 23.1°C.

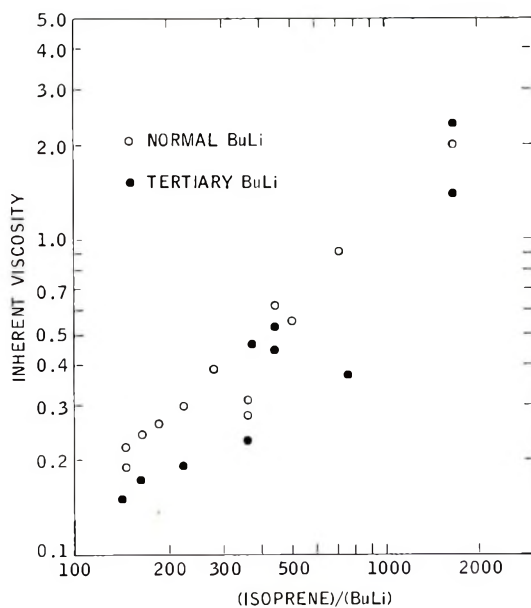


Fig. 3. Inherent viscosity of polyisoprenes.

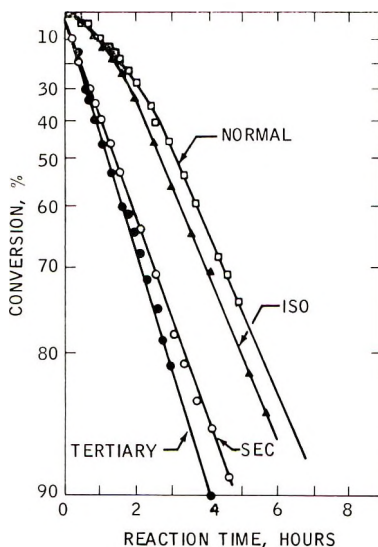


Fig. 4. First-order kinetic plot for data of Fig. 2.

butyllithium show an initial region of increasing downward slope followed by a lengthy region of more constant slope. The curves are similar to those reported by Welch for the butyllithium-initiated polymerization of styrene in benzene.<sup>7</sup> By considering the tangent to first-order plots at different times, we can estimate when a constant slope is attained, indicating that the polymerization is then in agreement with a first-order relationship.



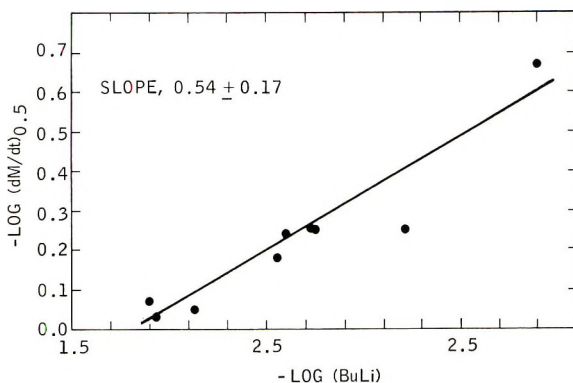


Fig. 5. Kinetic order in *tert*-butyllithium.

(It must be remembered that this first-order fit does not necessarily indicate complete consumption of initiator.) Table I contains these times for the different experiments under the heading time to  $k_1$ . It is seen that for these experiments, the time varies from about 1 hr. for *sec*, and *tert*-butyllithium to 4 hr. for the iso-isomer and 7 hours for *n*-butyllithium. It will be noted from the table that the times to reach the first-order region are shorter for the iso- and *n*-butyllithiums at the 0.004*M* initiator concentration than at the 0.02*M* concentration.

Since the experiments with *tert*-butyllithium seem to give a good fit to the first-order relationship, we have used the data obtained from experiments with concentrations of this initiator from 0.002–0.024*M*, at constant isoprene concentrations to determine the kinetic order of the reaction with respect to *tert*-butyllithium. From the generalized rate expression (1),

$$-dM/dt = K[M]^m[\text{BuLi}]^n \quad (1)$$

$$-\log dM/dt = n \log [\text{BuLi}] + \log c \quad (2)$$

where [M] and [BuLi] represent the concentrations of monomer and initiator, respectively, the relationship (2) can be obtained for constant concentrations of monomer. Figure 5 shows the plot based on eq. (2) for the experiments with *tert*-butyllithium. To try to eliminate any initial deviation from first-order kinetics, we have plotted the relationship for the reaction at 50% conversion, using the pseudo-first-order rate constant to describe monomer disappearance. The slope of the least squares line of Figure 5 is  $0.54 \pm 0.17$  (95% confidence limits) which is the order of the reaction in *tert*-butyllithium, the value of  $n$  in the generalized rate expression (1).

### Discussion

Organolithium-initiated polymerizations involve the successive addition of monomer units at the terminal C-Li bond of a macromolecular lithium compound. A number of mechanistic and kinetic studies have indicated the reaction sequence shown below.<sup>8</sup>

Initiation:



Propagation:



It would seem most probable that the differences in the rate of isoprene polymerization observed with the various butyllithiums in this research arise primarily from the sensitivity of the initiation process to organolithium structure.

The association of the initiator molecule shown in eq. (3) would be sensitive to both steric and electronic factors. Organolithium association may be a reflection of dipole-dipole interactions of the highly polar C-Li bond. Variations in the extent of polar character may affect the extent of association. The  $\sigma$  substituent constants for the different butyl groups have been determined. They indicate the effectiveness of electron release to decrease in the sequence, tertiary, normal, secondary, *iso*.<sup>9</sup> The steric requirements of the alkylithium would be expected to be important in determining the size of the  $(\text{RLi})_x$  aggregate. The addition of the first monomer unit should also be sensitive to electronic and steric factors. The steric factors may be very important and operate in a direction opposite to the electronic effects.

The observed results with the various butyllithiums obtained in this research would suggest that the initiation process is slowest for *n*-, faster with *iso*-, and still faster with *sec*- and *tert*-butyllithium. The faster the initiation step, the sooner active centers are produced which can consume monomer. This is the origin of the differences in polymerization rate we observe for the different butyllithiums. The kinetic results in the literature indicate that the initiation process is slower than the propagation reaction.<sup>8</sup> At suitable monomer/RLi ratios, unreacted initiator can even remain when all monomer has been consumed.<sup>4</sup>

Waak and Doran observed that the polystyrene produced in their experiments had higher DP's as less initiator was consumed in the polymerization.<sup>4</sup> Our observed higher inherent viscosities for the polyisoprenes obtained with *n*-butyllithium (compared to the tertiary isomer) must also reflect differences of this type in the initiation process in our system. With the slow initiation process of the organolithium system, Morton and co-workers have shown that the molecular weight distribution can be broadened unless certain experimental precautions are taken.<sup>10</sup> With a slower initiation with *n*-butyllithium the final polymer would be expected to contain some higher molecular weight species than the product obtained with *tert*-butyllithium. The inherent viscosity measurement is one in which high molecular weight species play an exaggerated role.

We found the kinetic order in *tert*-butyllithium to be  $0.54 \pm 0.17$ . Bywater and Worsfold observed that in the styrene-butyllithium system the order with respect to butyllithium in the propagation step was 0.5.<sup>8</sup> These observations concur with Morton's suggestions that the polyisoprenyllithium chains are dimeric;<sup>8</sup> that is,  $m$  in eq. (5) is 2. It suggests that in the propagation reaction the dissociation of the dimer is the rate controlling step.

### Experimental

Dilatometric experiments were carried out in 10 cc. dilatometers filled in a glove box under a nitrogen atmosphere. *n*-, iso-, and *sec*-butyllithium were prepared from lithium wire in heptane according to the procedure of Gilman.<sup>11</sup> *n*- and *tert*-butyllithium were obtained from the Lithium Corporation of America. Initiator concentration was determined by acid titration.<sup>12</sup> Polymer inherent viscosity was determined in toluene at 23°C. at concentrations which gave relative viscosities of about 1.1. Solvents were purified and procedures carried out as previously described.<sup>13</sup>

### References

1. Tobolsky, A. V., and C. E. Rogers, *J. Polymer Sci.*, **40**, 73 (1959).
2. Kuntz, I., and A. Gerber, *J. Polymer Sci.*, **42**, 299 (1960).
3. Braun, D., W. Betz, and W. Kern, *Makromol. Chem.*, **42**, 89 (1960).
4. Waack, R., and M. A. Doran, *Polymer*, **2**, 365 (1961).
5. East, G. C., P. F. Lynch, and D. Margerison, *Polymer*, **4**, 139 (1963).
6. Binder, J. L., and H. C. Ransaw, *Anal. Chem.*, **29**, 503 (1957).
7. Welch, F. J., *J. Am. Chem. Soc.*, **81**, 1345 (1959).
8. Worsfold, D. J., and S. Bywater, *Can. J. Chem.*, **38**, 1891 (1960); C. Lindborg and H. Sinn, *Makromol. Chem.*, **41**, 242 (1960); M. Morton, E. E. Bostick, R. A. Livigni, and L. J. Fetters, *J. Polymer Sci.*, **A1**, 1735 (1963); R. C. P. Cubbon and D. Margerison, *Proc. Roy. Soc. (London)*, **A268**, 260 (1962).
9. Jaffe, H. H., *Chem. Revs.*, **53**, 191 (1953).
10. Morton, M., E. E. Bostick, and R. G. Clarke, *J. Polymer Sci.*, **A1**, 475 (1963).
11. Gilman, H., W. Langham, and F. W. Moore, *J. Am. Chem. Soc.*, **62**, 2333 (1940).
12. Kamienski, C. W., and D. L. Esmay, *J. Org. Chem.*, **25**, 115 (1960).
13. Kuntz, I., *J. Polymer Sci.*, **54**, 569 (1961).

### Résumé

Quand on polymérise de l'isoprène (3.3 molaire) dans l'heptane normal à 23°1 par les différents butyl-lithiums (0.004 M), les temps nécessaires à atteindre 50% de conversion en polymère sont de 3 heures 1/2 dans le cas du butyle normal, de 2 heures 31 avec l'isobutyle, de 2 heures avec le butyle secondaire et de 2 heures 20 avec le butyle tertiaire. Quand on effectue la même expérience à une concentration en initiateur de 0.02 molaire, les  $t_{1/2}$  pour la même séquence d'isomères sont 3.1 H. 2.6 H. 1.4 H. et 1.3 H. Dans les expériences ci-dessus ainsi que dans d'autres la viscosité inhérente des polymères préparés avec le butyl-lithium tertiaire est inférieure à celle obtenue avec le butyl-lithium normal. La stéréochimie des polymères de polyisoprène obtenus avec les différents initiateurs est identique. Les résultats obtenus avec les butyl-lithiums normal et iso à une concentration 0.02 M semblent présenter l'écart le plus important par rapport à une cinétique du premier ordre. En utilisant les résultats des expériences effectuées à

différentes concentrations en initiateur et à concentration constante en isoprène, on trouve un ordre par rapport à la concentration en butyl-lithium tertiaire de  $0.54 \pm 0.17$ . Ces observations reflètent les différences existant entre les vitesses d'initiation des différents butyl-lithiums. L'ordre par rapport à l'initiateur indique que les chaînes isoprényl-lithium en croissance sont engagées dans la formation de dimère dont la dissociation constitue l'étape lente de la réaction de propagation.

### Zusammenfassung

Bei der Polymerisation von Isopren (3.3 molar) in *n*-Heptan bei 23,1° durch die verschiedenen Lithiumbutyle (0.004 *M*) beträgt die Dauer für 50% Polymerisationsumsatz für die normal-Verbindung 3,5 Stunden, für iso 2,3 Stunden, für sekundär 2,0 Stunden und für tertiär 2,2 Stunden. Beim gleichen Versuch mit einer Starterkonzentration 0,02 molar beträgt  $t_{0.5}$  in der gleichen Reihenfolge 3,1, 2,6, 1,4 und 1,3 Stunden. Bei diesen und anderen Versuchen scheint die Viskositätszahl der mit *tert.*-Butyllithium hergestellten Polymeren niedriger zu sein als diejenige der mit *n*-Butyllithium erhaltenen. Stereochemisch sind die mit den verschiedenen Startern erhaltenen Isopren-Polymeren identisch. Die Ergebnisse mit *n*- und *i*-Butyllithium bei einer Konzentration von 0,02 *M* scheinen am stärksten von einer Kinetik erster Ordnung abzuweichen. Aus Versuchen bei variiertem Starterkonzentration und konstanter Isoprenkonzentration wurde die Reaktionsordnung in bezug auf *tert.*-Butyllithium zu  $0,54 \pm 0.17$  bestimmt. Die Beobachtungen sprachen für Unterschiede in der Startgeschwindigkeit bei den verschiedenen Lithiumbutylen. Die Reaktionsordnung in bezug auf den Starter zeigt, dass die wachsenden Isoprenyllithiumketten Dimere bilden, deren Dissoziation den langsamen Schritt bei der Wachstumsreaktion bilden.

Received June 20, 1963

## Radiation Crosslinking of Polyethylene— Polyfunctional Monomer Mixtures

GEORGE ODIAN\* and BRUCE S. BERNSTEIN,  
*Radiation Applications Inc., Long Island City, New York*

### Synopsis

Polyfunctional monomers such as allyl methacrylate, allyl acrylate, and diallyl maleate have been found to greatly enhance the radiation crosslinking of polyethylene. The radiation dose for incipient gelation is decreased by a factor of approximately 25 by the presence of small amounts of these monomers. The ultimate scission/crosslinking ratio is unchanged by the presence of these monomers and the swelling behavior of the gels follows the Flory-Rehner equation. The monomer-crosslinking process is compared to the monomer-free process as regards the physical properties (tensile strength, elongation, modulus) of the crosslinked materials. A mechanism is presented for the enhancement of polyethylene crosslinking by polyfunctional monomers.

### INTRODUCTION

Radiation crosslinking in the presence of polyfunctional monomers (i.e., monomers containing more than one double bond per molecule) has been studied with poly(vinyl chloride),<sup>1,2</sup> cellulose acetate,<sup>3</sup> poly(methyl methacrylate),<sup>4</sup> and several other polymers.<sup>5</sup> This reaction is of interest since it allows crosslinking to be brought about at reduced doses compared to those normally required. It further allows for the crosslinking of polymers not normally crosslinked by radiation. Work has progressed at this laboratory employing this technique with polyethylene, polypropylene, polyisobutylene, cellulose acetate, and other polymers in conjunction with a variety of polyfunctional monomers.<sup>6</sup>

The effect of radiation on polyethylene has been studied in detail.<sup>7,8</sup> It is a polymer that predominantly crosslinks and has a scission/crosslinking ratio of 0.2-0.3. Lyons has reported a "slight enhancement" in the radiation crosslinking of polyethylene by triallyl cyanurate.<sup>5</sup> We have observed substantial enhancement of polyethylene crosslinking via the use of polyfunctional monomers. It is the purpose of this paper to present the results of a detailed study on the radiation crosslinking of polyethylene in the presence of allyl methacrylate, allyl acrylate, and diallyl maleate.

\* Present address: Department of Chemical Engineering, Columbia University, New York, N. Y.

## EXPERIMENTAL

### Materials

du Pont Alathon 15 low density polyethylene ( $\bar{M}_n = 15,000$ – $20,000$ ;  $\bar{M}_w = 500,000$ ; density =  $0.915$  g./cc.) was used as 50 mil extruded tape. The monomers (allyl methacrylate, allyl acrylate, and diallyl maleate) were commercial products which were washed with sodium hydroxide or sodium bicarbonate to remove inhibitor.

### Swelling of Polymer by Monomer

Polyethylene was equilibrium swollen with monomer at  $25^\circ\text{C}$ . The time necessary for equilibrium to be reached was approximately 2 days. The amount of monomer picked up at equilibrium by the polymer was determined by weighing the equilibrium swollen polymer sample and the per cent pickup calculated from the equation

$$\% \text{ monomer swollen} = [(W_s - W_I)/W_I] \times 100 \quad (1)$$

where  $W_I$  and  $W_s$  are the initial and monomer swollen polymer weights, respectively. The equilibrium swelling at  $25^\circ\text{C}$ . of polyethylene by allyl methacrylate, allyl acrylate, and diallyl maleate is 4.5, 3.0, and 0.3%, respectively.

Some experiments were performed under nonequilibrium swelling conditions. These involved swelling at  $25^\circ\text{C}$ . and other temperatures for various time intervals.

### Irradiation of Polymer-Monomer Mixtures

Irradiations of polymer-monomer samples were performed using both gamma radiation from a  $\text{Co}^{60}$  source and electrons from a 1.5 M.e.v. Van de Graaff accelerator; the former for irradiations to 12 Mrad and the latter for irradiations above 12 Mrad. The gamma irradiations were performed in a nitrogen atmosphere. Monomer-free specimens were irradiated similarly.

Electron irradiations were performed on samples which were first irradiated via  $\text{Co}^{60}$  to doses of 0.5–1.0 Mrad to insure monomer incorporation. The monomer-containing test specimens were placed on Dry Ice in trays which in turn were sitting on a moving belt that passed back and forth under the electron beam. A 2-Mrad dose was imparted to the surface of the polyethylene with each pass under the beam. The samples were turned over after one-half of the total surface dose had been imparted in order to compensate for secondary ionization and obtain a uniform dose throughout the polymer sample. Monomer-free controls were irradiated simultaneously but were not subjected to the prior  $\text{Co}^{60}$  irradiation.

After the completion of the irradiation, the samples were vacuum-

dried at 60–90°C. for 1–3 days, weighed, and the amount of monomer incorporated into the polymer calculated from the equation

$$\% \text{ monomer incorporated} = [(W_R - W_I)/W_I] \times 100 \quad (2)$$

where  $W_R$  is the weight of the polymer sample after irradiation and drying.

### Gel Content Determination

The irradiated samples were extracted by a modification of the method of Charlesby and Pinner.<sup>9</sup> Samples were placed in individual stainless steel cages and then extracted with xylene (containing 0.1% phenyl- $\beta$ -naphthylamine as an antioxidant) at 115–120°C. for 4 days. The samples were then vacuum-dried at 90°C. for 24 hr., weighed, and the per cent gel present in the irradiated specimens calculated from the equation

$$\% \text{ gel} = (W_G/W_R) \times 100 \quad (3)$$

where  $W_G$  is the weight of the nonextractable (i.e., gel) fraction. All gel determinations were performed at least in duplicate.

### Swelling Ratio

The weight swelling ratios ( $q_m$ ) were determined from the equation

$$q_m = W_{WG}/W_G \quad (4)$$

where  $W_{WG}$  is the weight of the wet (swollen) polymer gel at 115°C. The  $q_m$  is, thus, the ratio of the weights of the swollen gel to dry gel. No attempt was made to convert the values obtained to volume swelling ratios.

### Tensile Strength Measurements

Tensile strength and elongation measurements at 25°C. were performed according to ASTM D-1708-59T. Specimens were stamped from a die having a gage length of  $7/8$  in. and an overall length of 2.9 in. A table model Instron tensile tester was used at a crosshead speed of 5 in./min. (Speed D).

Tensile strengths of crosslinked polyethylenes at 115°C. (above the normal  $T_m$  of the original uncrosslinked polyethylene) were determined by using a constant temperature Missimers, Inc. heating cabinet in conjunction with the Instron tester. Except for temperature, the same conditions as for the 25°C. tests were employed here.

The stress-strain data were employed to determine the modulus of elasticity of the polyethylene and polyethylene-allyl methacrylate systems. The stress-strain curves did not contain initial straight-line portions; instead, continuous sweeping curves were obtained. This was probably due to the fact that the data were obtained at a faster rate of strain than that recommended for elastic (Young's) modulus determination. (This was the case because the data were determined primarily for tensile strength determinations.) Thus, tangent or Young's moduli could not be obtained; instead, secant moduli were calculated. For the 25°C. measurements, we

employed the slope of the line joining the points of zero stress and the yield stress; for the 115°C. measurements, the slope of the line joining the points of zero stress and the ultimate tensile stress.

## RESULTS AND DISCUSSION

### Gel Dose Studies

Upon irradiation, polyethylene undergoes crosslinking and an increase in gel content with dose. The presence of polyfunctional monomers such as allyl methacrylate, allyl acrylate, and diallyl maleate has been found to greatly increase the efficiency of polyethylene crosslinking (Fig. 1). (Allyl acrylate data were virtually indistinguishable from those for allyl methacrylate and are therefore not shown.) Thus, the incipient gelation dose (obtained by extrapolation of the log gel-log dose curves to zero dose) is reduced from approximately 0.5 to 0.02 Mrad (a factor of 25) by the presence of allyl methacrylate.

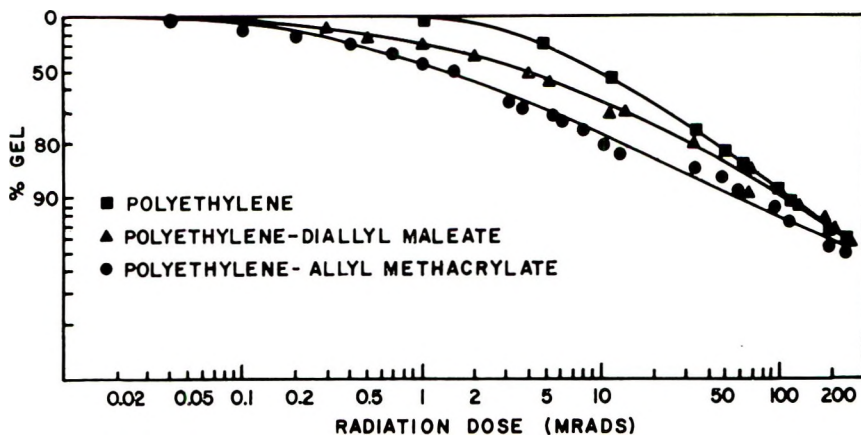


Fig. 1. Effect of radiation dose on the crosslinking of polyethylene and polyethylene-monomer systems.

The  $G(\text{crosslink})$  value for polyethylene has been calculated by Charlesby<sup>8</sup> from the equation

$$G = 4.8 \times 10^5 / r_{\text{gel}} \bar{M}_w \quad (5)$$

where  $r_{\text{gel}}$  is the dose for incipient gelation and  $\bar{M}_w$  is the weight-average molecular weight of the initial polymer. From eq. (5), the  $G(\text{crosslink})$  values of our monomer-free and allyl methacrylate-containing polyethylene systems were calculated as 1.9 and 48, respectively. The  $G$  value of 1.9 for monomer-free polyethylene is in good agreement with the literature value of  $2.0 \pm 0.4$ .<sup>7</sup>

The accelerating effect of the polyfunctional monomers is seen to cause a very rapid initial increase in gel content with dose. After approximately



2 Mrad, the effect begins to level off. For both the monomer-free and monomer-containing systems, an almost linear log-log relationship occurs above a specific dose (ca. 1 and 5 Mrad, respectively). Below this dose, the relationship is also almost linear, but the slope is greater. The insoluble fraction in the monomer-containing system always remains greater than that of the monomer-free system, although the two curves converge as the dose increases.

The data would seem to indicate that diallyl maleate is not as efficient as allyl methacrylate in accelerating the crosslinking process. It is important to note, however, that whereas there is 0.031 mole-% allyl methacrylate monomer present, the diallyl maleate level is only  $1/20$  of that. Thus, equilibrium swollen polyethylene-diallyl maleate gives smaller overall gel fractions than equilibrium swollen polyethylene-allyl methacrylate; however, the former is much more efficient from a monomer concentration standpoint.

### Dose Rate of Radiation

The crosslinking of monomer-free polyethylene has been shown by many workers to be totally dose-dependent with a first-order dependence on radiation dose rate.<sup>7,10</sup> The effect of radiation intensity on the crosslinking of the polyethylene-allyl methacrylate system was studied and is shown in Figure 2. It is seen that the monomer-crosslinking reaction is also total dose-dependent with a first-order dependence on dose rate.

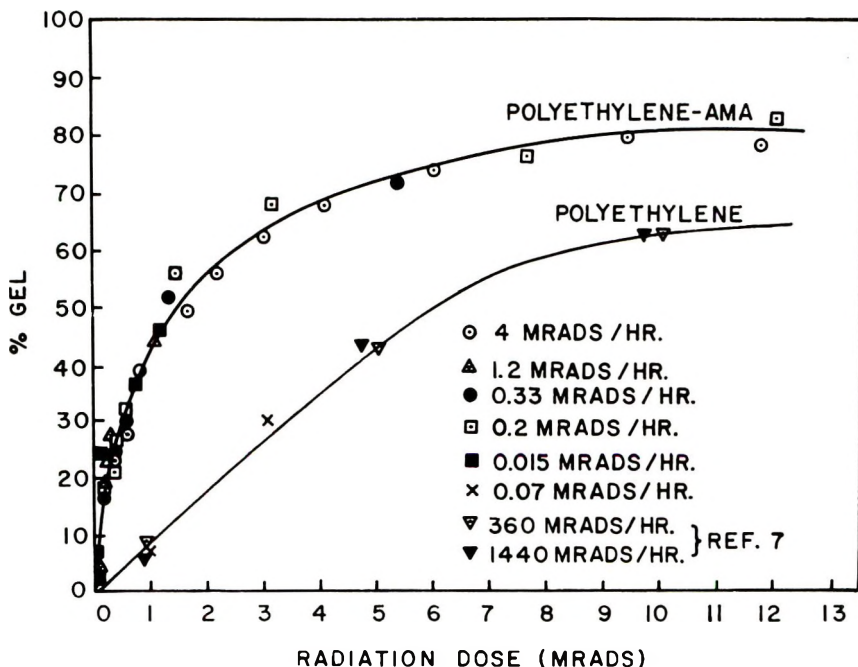


Fig. 2. Effect of dose rate on the crosslinking of polyethylene and polyethylene-allyl methacrylate.

### Monomer Incorporation

Our results showed that monomer desorption from the polymer-monomer specimens was negligible ( $<2-3\%$ ) during the irradiation step. In addition, it was found that almost all of the monomer is reacted immediately. After a dose of only 0.1 Mrad, over 90% of the allyl methacrylate and allyl acrylate is polymerized. In the case of diallyl maleate, the extremely small amount (0.3%) of monomer present renders difficult any judgements based on weight changes; however, the results appear to be similar in that the monomer polymerizes very rapidly.

### Monomer Concentration

It was seen from the results discussed above that the accelerating effects of the polyfunctional monomers were brought about by small amounts of

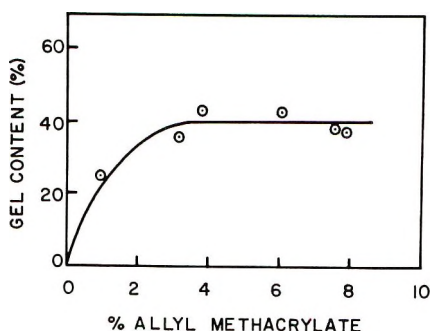


Fig. 3. Effect of monomer concentration on crosslinking of polyethylene.

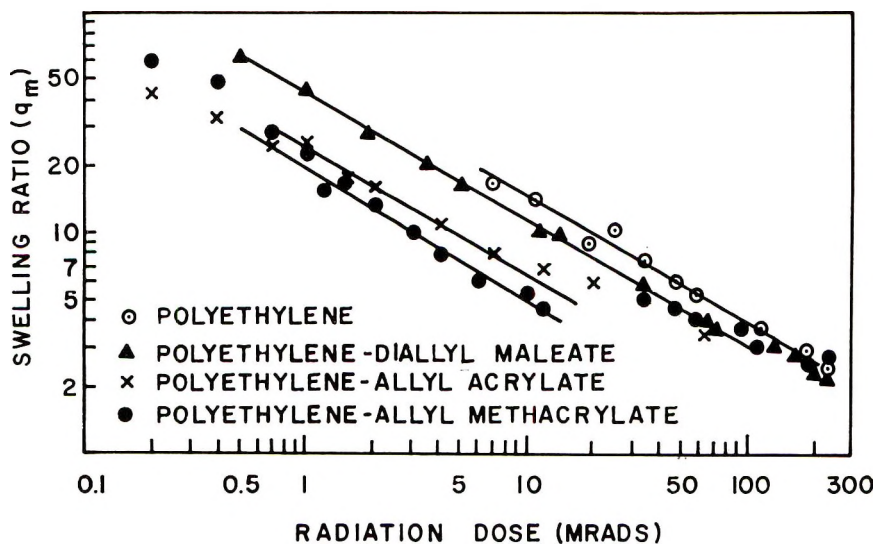


Fig. 4. Effect of radiation dose on the swelling ratio of crosslinked polyethylene and polyethylene-monomer.

the monomers. It was of interest to determine the exact effect of monomer concentration on the monomer-crosslinking process. This was studied for the allyl methacrylate-polyethylene system at monomer levels of 0–8%. The experimental procedure involved both equilibrium and nonequilibrium swelling at various temperatures followed by irradiation to a constant dose of 1 Mrad. It is seen (Fig. 3) that crosslinking is directly dependent on monomer concentration, with the effect leveling off rapidly at approximately 3% monomer.

### Swelling Ratios

Another indication of increased crosslinking efficiency in the monomer-containing systems as compared to monomer-free polyethylene is found in the swelling ratios observed for the two systems (Fig. 4). It is seen that at the same dose the monomer-containing systems yield gels with lower swelling ratios than monomer-free polyethylene. Furthermore, in order to obtain a gel of a specific swelling ratio, lower radiation doses are required in the monomer-polyethylene systems. Thus, for example, to obtain a polyethylene gel having a swelling ratio of 5, monomer-free polyethylene requires 60 Mrad while the presence of allyl methacrylate lowers this dosage to 10 Mrad. It is seen that diallyl maleate and allyl acrylate are not as efficient as allyl methacrylate in this respect.

Flory has derived a theoretical relationship for the swelling of crosslinked polymers which indicates the volume swelling ratio  $V$  to be inversely proportional to the  $3/5$  power of the crosslink density  $q$ .<sup>11</sup> For radiation crosslinking,  $q$  is proportional to the radiation dose  $r$ , and thus one derives<sup>8</sup> eq. (6):

$$V \propto r^{-0.6} \quad (6)$$

This relationship has been experimentally verified for crosslinked polyethylene.<sup>8</sup> The  $\log q_m$ -log dose plots for both our monomer-free and monomer-containing polyethylene systems (Fig. 4) yield straight-line portions possessing the theoretical slope of  $-0.6$ . The deviations observed at high and low swelling ratios are expected because of the assumptions inherent in the derivation of eq. (6).<sup>8,11</sup>

### Ultimate $\beta/\alpha$ Ratio

As was seen above, the accelerating effect of the monomer decreased after 2–3 Mrad, and the curves for both systems (Fig. 1) converged with increasing radiation dose. The failure of the monomer to play a role in the later stages of the crosslinking reaction is further indicated by limiting solubility data. Solubility data from gel extractions can be used to calculate the frequency with which crosslinking and main chain scission occur. For a predominantly crosslinking polymer like polyethylene, the limiting value of the sol fraction (% sol at infinite dose) represents this value and can be obtained by plotting the sol fraction ( $S + S^{1/2}$ ) versus the reciprocal dose

( $1/R$ ) and extrapolating to infinite dose. The intercept of this line represents the scission/crosslinking ( $\beta/\alpha$ ) ratio.<sup>8</sup>

Figure 5 represents a plot of  $S + S^{1/2}$  versus  $1/R$  for monomer-free polyethylene and allyl methacrylate-containing polyethylene. The data indicate an intercept of 0.20 for both systems upon extrapolation to infinite dose. Allyl acrylate and diallyl maleate-containing polyethylene also yielded a  $\beta/\alpha$  ratio of 0.20. This value is in good agreement with the literature<sup>9,12</sup> values of 0.3 and 0.2. Thus, the presence of (0.3–4.5%) polyfunctional monomer, while markedly affecting the course of the crosslinking reaction at low doses (<2–3 Mrad), does not alter the ultimate effect of radiation.

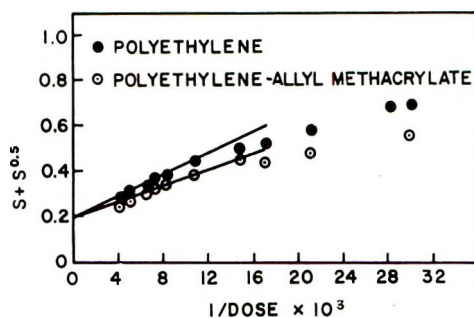


Fig. 5. Determination of  $\beta/\alpha$  for polyethylene and polyethylene-allyl methacrylate.

### Physical Properties

The tensile strengths (at break) of the monomer-free and allyl methacrylate-polyethylene crosslinked systems were studied at 25°C. and 115°C. as a function of radiation dose. The data are shown in Figure 6. It is seen that the tensile strength of the monomer-crosslinked system is greater than the monomer-free system over the entire dose range. The tensile strengths are smaller when the temperature of testing (115°C.) is above the crystalline melting point,  $T_m$ , of the polymer. The monomer-crosslinked system is superior to monomer-free polyethylene in tensile strength at both the ambient and elevated temperatures.

A further indication of the superiority of the monomer-crosslinked system is seen from heat-aging tests. To compare the various crosslinked materials, samples were heat-aged in an air oven for ca. 5 hr. at 185°C. The results are shown in Figure 7. Sample 1 is unirradiated, and not heat-aged, and sample 2 is unirradiated but heat-aged. All other samples were subjected to various radiation-crosslinking procedures with and without monomer and then heat-aged. As Figure 7 clearly shows, the 1.2 Mrad polyethylene which contained approximately 4% allyl methacrylate is superior to the 1.2 and 10 Mrad "straight" radiation-crosslinked polyethylenes and is, in fact, about equal to the 30 Mrad "straight" radiation-crosslinked polyethylene in high temperature form stability.

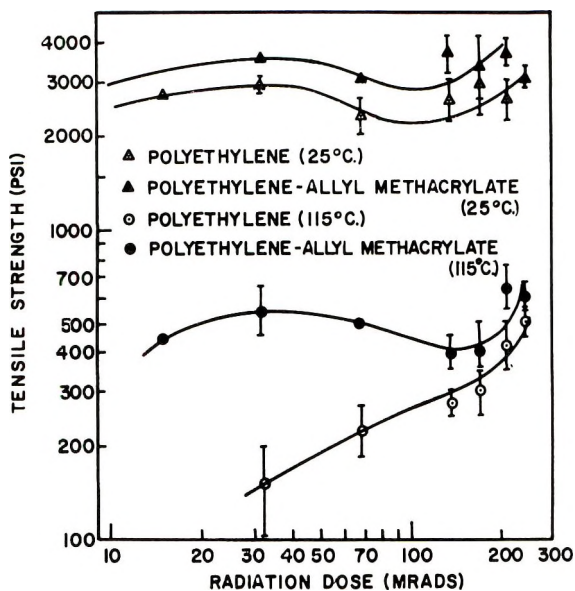


Fig. 6. Tensile strengths of crosslinked polyethylene and polyethylene-allyl methacrylate.

The effect of radiation on the elongation at break of the monomer-free and monomer-containing systems is shown in Figure 8. It is seen that the elongation drops sharply with increasing dose for both systems at both 25°C. and 115°C. The polyethylene-allyl methacrylate system has decreased elongation at any dose compared to the monomer-free polyethylene. This is to be expected, since at any specific dose, the monomer-containing system is more highly crosslinked.

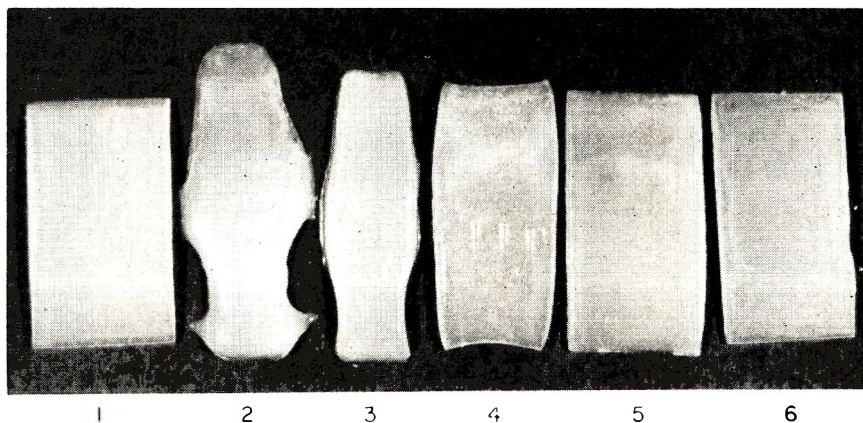


Fig. 7. Heat stability of crosslinked polyethylene in air: (1) unirradiated; (2) unirradiated, heat-aged; (3) 1.2 Mrad, heat-aged; (4) 10 Mrad, heat-aged; (5) 1.2 Mrad, 4% allyl methacrylate, heat-aged; (6) 30 Mrad, heat-aged. Heat aging carried out at 185°C. for 5 hr.

It has been previously found that the room temperature (20°C.) modulus of polyethylene is unchanged with increasing radiation dose up to over 200 Mrad while the high temperature (above  $T_m$ ) modulus increases with in-

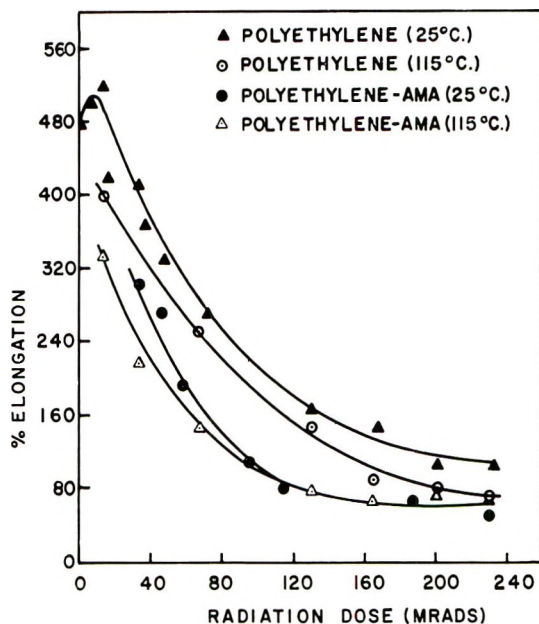


Fig. 8. Effect of radiation dose on elongation of polyethylene and polyethylene-allyl methacrylate.

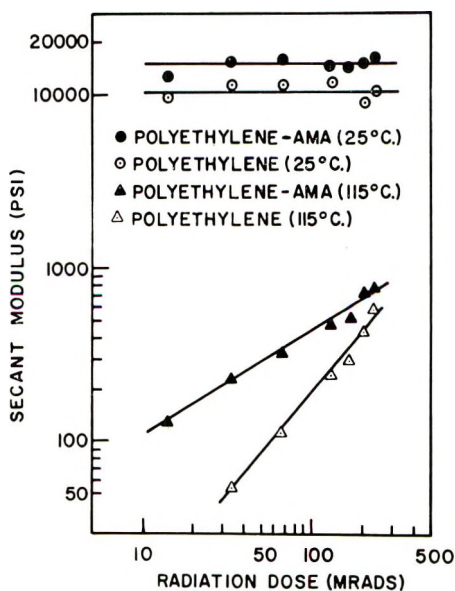


Fig. 9. Effect of radiation dose on secant modulus of polyethylene and polyethylene-allyl methacrylate.

creasing dose.<sup>13</sup> Our data (Fig. 9) show similar effects of dose on the secant moduli above (115°C.) and below (25°C.) the polyethylene  $T_m$ . It should be pointed out that the monomer-free and monomer-containing systems show analogous behavior, the latter having higher moduli under similar conditions. The 25°C. modulus is dependent largely on the polymer crystallinity. Since crystallinity is little affected until high doses (>200 Mrad), the 25°C. modulus is relatively unaffected by radiation dose. Above the  $T_m$ , crystallinity does not exist, and the modulus is dependent on the crosslink density. Thus, the 115°C. modulus increases with increasing radiation dose. The greater moduli of the allyl methacrylate-polyethylene relative to the monomer-free system is due to the fact that at any specific radiation dose the former has a higher crosslink density.

### Mechanism of Crosslinking

The question naturally arises as to the mechanism of crosslinking in the polyethylene-polyfunctional monomer systems. Although the experimental evidence is not conclusive, we should like to suggest that the reaction be depicted as a two-step process: step (1) The rapid initial polymerization of the polyfunctional monomer, e.g., allyl methacrylate; step (2) reaction of the polymerized allyl methacrylate with polyethylene chains which "ties" the latter into the former to form a crosslinked polyethylene-poly(allyl methacrylate) network.

The first step is in agreement with our data showing that over 90% of the polyfunctional monomer is polymerized after a radiation dose of only 0.1 Mrad. The polymerized monomer is probably a mixture of homo- and graft polymer, since most polymer-monomer systems yield both reactions upon radiolysis.<sup>14</sup> The chain length of the polymerized allyl methacrylate is low due to degradative chain transfer through the allyl groups.<sup>15</sup> The poly(allyl methacrylate) should also contain a high concentration of unpolymerized allyl groups in view of various data available on the homopolymerization of allyl methacrylate. Thus, it has been found that the vinyl group in allyl methacrylate has a much greater reactivity than the allyl group in the ultraviolet,<sup>16</sup> thermal,<sup>17</sup> and radiation<sup>18</sup> polymerization.

Thus, the polymerized monomer may be pictured as a relatively low molecular weight graft and homopolymer containing pendant allyl groups. This structure is responsible for the enhanced reaction in the initial stages of the crosslinking of the polyethylene-monomer systems. There are many favorable paths available for the attachment of this structure to the polyethylene chains: (1) The pendant allyl double bonds may react with free radicals on adjacent polyethylene chains resulting in crosslinking. (2) A high proportion of the pendant allyl groups would be expected under radiolysis to be converted to allyl radicals. These would further enhance crosslinking via coupling with polyethylene radicals. (3) Alternately, these allyl radicals could abstract hydrogen atoms from

polyethylene chains to effectively increase the  $G$  value for polyethylene radical production and subsequently the  $G(\text{crosslink})$ .

Various experiments with additives other than the polyfunctional monomers described above yielded insight into the mechanism of enhanced crosslinking in the polyethylene-monomer systems. These included experiments with allyl acetate, chloroform, and carbon tetrachloride, which resemble the polyfunctional monomers in that they are chain transfer agents and also possess high  $G$  values for radical production. No enhancement of polyethylene crosslinking was observed for the three additives. Additionally, monofunctional monomers such as styrene, methyl methacrylate, and vinyl acetate were observed to have no effect on polyethylene crosslinking under conditions in which enhanced crosslinking occurred with the polyfunctional monomers. Thus, the data indicate that a monomer, in order to enhance crosslinking, must be polyfunctional and that the enhancement is due to a combination of reactions (1-3) above and not to a single one. Furthermore, results with a variety of polyfunctional monomers, including divinylbenzene, indicate that the presence of at least one allyl group as opposed to vinyls is highly desirable.

Our finding regarding the absence of a dose rate effect in the crosslinking of the polyethylene-polyfunctional monomer systems is compatible with the proposed mechanism although allyl methacrylate homopolymerization shows a dependence on radiation intensity by an exponent of 0.5-0.8.<sup>17,18</sup> The proposed mechanism (1-3 above) does not require such a dose rate effect except in the very initial stages of reaction (i.e., up to approximately 0.1-0.2 Mrad); in this region, the experimental procedures were incapable of detecting a dose rate effect.

It is generally accepted that liquids are absorbed only in the amorphous regions of polymers and not in the crystalline regions.<sup>19,20</sup> Thus, the monomer-crosslinking reaction would be expected to occur only in the amorphous regions of the polymer since the monomer would be present only in those regions. This picture explains the observation (Fig. 1) that the overall crosslinking efficiency of the monomer-crosslinking reaction decreases rapidly with radiation dose and at approximately 40-50% gel is similar to that of the monomer-free crosslinking reaction. Since the polyethylene employed in this study contains 50-55% of crystalline material,<sup>21</sup> this corresponds to essentially 100% gelation of the amorphous regions, and the crosslinking of the crystalline regions proceeds in a manner exactly analogous to the crosslinking of the monomer-free polyethylene. The results of the studies on the effect of monomer concentration on crosslinking (Fig. 3) are also consistent with this mechanism. The gel fraction reaches 40-45% with 3-4% monomer. This corresponds to approximately complete gelation of the amorphous regions, and thus higher concentrations of monomer are ineffective in increasing the gel fraction.

The authors wish to acknowledge the assistance of Messrs. James J. Kelly, Sidney Binder, and Robert Connolly with the experimental work. We wish also to acknowledge the generous support of this work by the Division of Isotopes Development, U. S. Atomic Energy Commission, under Contracts AT(30-1)-2554 and AT(30-1)-2816.



## References

1. Miller, A. A., *Ind. Eng. Chem.*, **51**, 1271 (1959); A. A. Miller, *J. Appl. Polymer Sci.*, **5**, 388 (1961).
2. Pinner, S. H., *Nature*, **183**, 1108 (1959).
3. Pinner, S. H., T. T. Greenwood, and D. G. Lloyd, *Nature*, **184**, 1303 (1959).
4. Pinner, S. H., and V. Wycherly, *J. Appl. Polymer Sci.*, **3**, 388 (1960).
5. Lyons, B. J., *Nature*, **185**, 604 (1960).
6. Odian, G., and B. S. Bernstein, *Nucleonics*, **21**, 80 (1963); G. Odian and B. S. Bernstein, paper presented at 142nd Natl. Meeting, American Chemical Society, Atlantic City, N. J., September 1962.
7. Chapiro, A., *Radiation Chemistry of Polymeric Systems*, Wiley, New York, 1962, Chap. IX.
8. Charlesby, A., *Atomic Radiation and Polymers*, Pergamon Press, London, 1960, Chap. 13.
9. Charlesby, A., and S. H. Pinner, *Proc. Roy. Soc. (London)*, **A249**, 367 (1959).
10. Atchison, G. J., *J. Polymer Sci.*, **35**, 557 (1959).
11. Flory, P. J., and J. Rehner, *J. Chem. Phys.*, **11**, 521 (1943).
12. Baskett, A. C., and C. W. Miller, *Nature*, **174**, 364 (1954).
13. Woodward, A. E., C. W. Deeley, D. E. Kline, and J. A. Sauer, *J. Polymer Sci.*, **26**, 383 (1957).
14. Chapiro, A., *Radiation Chemistry of Polymeric Systems*, Wiley, New York, 1962, Chap. XII.
15. Bartlett, P. D., and R. Altschul, *J. Am. Chem. Soc.*, **67**, 812, 816 (1945).
16. Cohen, S. G., and D. B. Sparrow, *J. Polymer Sci.*, **3**, 693 (1948).
17. Bristow, G. M., *Trans. Faraday Soc.*, **54**, 1239 (1958).
18. Pinner, S. H., and V. Wycherly, International Symposium on Macromolecular Chemistry, Section IIIB, Paper 9, Wiesbaden, Germany, October 1959.
19. Richards, R. B., *Trans. Faraday Soc.*, **42**, 11 (1946).
20. McCall, D. W., *J. Polymer Sci.*, **26**, 151 (1957).
21. Film Department, E. I. du Pont de Nemours and Co., Inc., private communication.

## Résumé

On a trouvé que les monomères polyfonctionnels tels que le méthacrylate d'allyle, l'acrylate d'allyle et le maléate de diallyle augmentent grandement le pouvoir de pontage par irradiation du polyéthylène. La dose de radiation pour le début de la gélation décroît d'un facteur d'environ 25 en présence de faibles quantités de ces monomères. Le bilan scission/pontage demeure inchangé en présence de ces monomères et la faculté de gonflement des gels suit l'équation de Flory-Rehner. On a comparé le processus de pontage du monomère au processus en absence de monomère en ce qui concerne les propriétés physiques (force de tension, élongation, module) des matériaux pontés. Un mécanisme de l'augmentation du pontage du polyéthylène par des monomères polyfonctionnels est présenté.

## Zusammenfassung

Polyfunktionelle Monomere, wie Allylmethacrylat, Allylacrylat und Diallylmaléat bewirken eine starke Erhöhung der Strahlungsvernetzung von Polyäthylen. Durch Anwesenheit kleiner Mengen dieser Monomeren wird die für den Eintritt der Gelbildung nötige Strahlungs-dosis auf etwa 1/15 herabgesetzt. Das Endverhältnis Spaltung zu Vernetzung wird durch die Gegenwart dieser Monomeren nicht verändert; das Quellungsverhalten der Gele gehorcht der Gleichung von Flory und Rehner. Der Vernetzungsprozess in Gegenwart von Monomerem wird in bezug auf die physikalischen

Eigenschaften (Zugfestigkeit, Dehnung, Modul) der vernetzten Stoffe mit dem monomerfreien Prozess verglichen. Ein Mechanismus für die gesteigerte Vernetzung von Polyäthylen durch polyfunktionelle Monomere wird aufgestellt.

Received June 20, 1963

Revised June 28, 1963

# Synthesis of New Monomers and Polymers.

## IV. Synthesis and Properties of Polydiphenyldiacetylenes

PH. TEYSSIE and A. C. KORN-GIRARD, *Laboratoire de Chimie Macromoléculaire, Institut Français du Pétrole, Rueil-Malmaison (S.-et-O.), France*

### Synopsis

Polymerization of diphenyldiacetylene was effected in the presence of Ziegler type catalysts. The polymers, studied as obtained from the polymerization or after further reaction, are soluble products of relatively low molecular weight with interesting properties: very high thermal resistance, continuous absorption in ultraviolet and near visible regions, broad visible fluorescence spectra, semiconducting and catalytic properties.

### I. INTRODUCTION

A rapidly growing interest in polymers with semiconducting properties led to the investigation of different acetylenic monomers; a literature survey<sup>1</sup> suggested the study of diacetylenic derivatives, which could give rise to different isomeric polymers and allow subsequent reactions on the polymers obtained. In order to prepare soluble highly conjugated products, and by comparison with the properties of substituted monoacetylenic polymers, the first monomer chosen for this study was diphenyldiacetylene, which was readily synthesized from commercially available phenylacetylene.

### II. EXPERIMENTAL\*

Diphenyldiacetylene was prepared according to the procedure of Hay<sup>2</sup> by oxidative dimerization of phenylacetylene in homogeneous solution, in the presence of oxygen, a cuprous salt, and a tertiary amine. A 90% yield of a relatively pure product is obtained, which was recrystallized from methanol (m.p. 87-88°C.). A synthesis based on the method of Strauss<sup>3</sup> involving the use of copper phenylacetylides gave a lower yield of a much less pure product.

Polydiphenyldiacetylene was obtained by using conventional Ziegler-type catalysts (triisobutylaluminum and titanium tetrachloride). A vacuum line was used, carrying polymerization tubes with Suba-seals self-

\* With the collaboration of G. Ravidat.

seal, through which the reagents were transferred (from similarly scaled containers) by using a hypodermic syringe. The apparatus was carefully degassed and the products introduced in the following order: a benzene solution of the monomer, a heptane solution of the triisobutylaluminum, and a similar solution of titanium tetrachloride (a benzene-heptane ratio of 7 was used throughout all experiments). Mixing was effected at liquid nitrogen temperature, and the tubes sealed under vacuum. Under warming, the mixture turns dark-brown, and the tubes are transferred to a constant temperature bath.

After completion of the reaction, the content of each tube was poured into acidified methanol with vigorous stirring, after several washings, the brown powdery polymer obtained was extracted with hot methanol to eliminate the lower oligomers produced; these latter products were isolated by evaporation of the methanol.

ANAL. Calcd. for the polymer: C, 95.02%; H, 4.98%; Found: C, 92.45%; H, 5.34%; O, 2.19%; M.W. 1270. Found for the oligomer: C, 87.82%; H, 5.48%; O, 3.49%; M.W. 819 (no chloride was found in the polymer).

The polymers obtained were converted to new products by two different procedures: either they were treated thermally for 6 hr. under an argon atmosphere in a furnace held at  $400 \pm 5$  °C., or they were submitted to a Friedel-Crafts reaction. Therefore 500 mg. of polymer was dissolved in 5 ml. of cyclohexane together with 250 mg. of antimony pentachloride and kept at 20°C. for 5 hr. The polymer was precipitated in acidified methanol, filtered, and purified by successive dissolution and precipitation in dioxane and methanol.

Cryometric molecular weight determinations were effected on 2% benzene solutions; results were found to be independent of the solute concentration.

Absorption spectra were recorded on a Perkin-Elmer Model 221 infrared spectrophotometer and on a Beckman DK 2 S spectrophotometer; fluorescence spectra were also obtained with this latter instrument.

The thermal stability of the products was investigated thermogravimetrically with a recording D.A.M. thermobalance.

### III. RESULTS

#### A. Polymerization

The results obtained under various polymerization conditions are summarized in Table I; a monomer concentration of 1 mole/l. was used in these experiments.

The catalyst was chosen following the indications of Watson<sup>4</sup> who describes a mixture of triisobutylaluminum and titanium tetrachloride, with an Al/Ti ratio of 2.7, as the most interesting catalyst for the polymerization of acetylenic monomers; this is in agreement with the data obtained with diphenyldiacetylene and presented in Table I and Figure 1a.

TABLE I  
 Polymerization of Diphenyldiacetylene

Reaction temp., °C.	Ratio Al/Ti	TiCl <sub>4</sub> concn., mole/l. × 10 <sup>2</sup>	Al( <i>i</i> -Bu) <sub>3</sub> concn., mole/l. × 10 <sup>2</sup>	Molar ratio, % Ti/monomer	Reaction time, hr.	Polymer yield, %	Softening point, °C.	$\bar{M}_n$ (cryoscopic)
0	2.7	2.5	6.75	2.5	6	6	255-260	1270
25	1	2.5	2.5	2.5	24	—	—	—
25	1.8	2.5	4.5	2.5	24	—	—	—
25	2.7	2.5	6.75	2.5	24	17	255-260	1270
25	4	2.5	10	2.5	24	6	255-260	—
25	2.7	3.3	8.91	3.3	24	18	255-260	—
25	2.7	4	10.8	4	24	26.4	237-240	1145
25	2.7	5	13.5	5	24	32.3	215	1078
25	2.7	2.5	6.75	2.5	3	11.4	255-260	—
25	2.7	2.5	6.75	2.5	6	14.2	255-260	—
25	2.7	2.5	6.75	2.5	15	17	255-260	—
25	2.7	2.5	6.75	2.5	48	17	255-260	—
25	2.7	2.5	6.75	2.5	80	17	255-260	—
50	2.7	2.5	6.75	2.5	24	20.4	255-260	1253
70	2.7	2.5	6.75	2.5	24	25.7	255-260	1253
50	2.7	<sup>a</sup>	0.2	2.5	24	9	235-240	—

<sup>a</sup> Suspension of TiCl<sub>3</sub> used instead of TiCl<sub>4</sub>; 16.2 g./l.

As indicated also in Table I, increasing the catalyst concentration increases the yield of polymer, but reduces its softening temperature; below a minimum Ti/monomer molar ratio of 0.02, no polymerization occurs.

Temperature also influences the yield of the polymer (Table I and Fig. 1b); more polymer is formed at higher temperatures, and this yield increase does not affect appreciably the molecular weight.

Finally, it is shown in Fig. 2 how the polymerization stops at low degrees of conversion, although the catalyst does not seem to be deactivated (persistence of the dark-brown color of the solution), a time of 15 hr. seems to be the limit of the growing process.

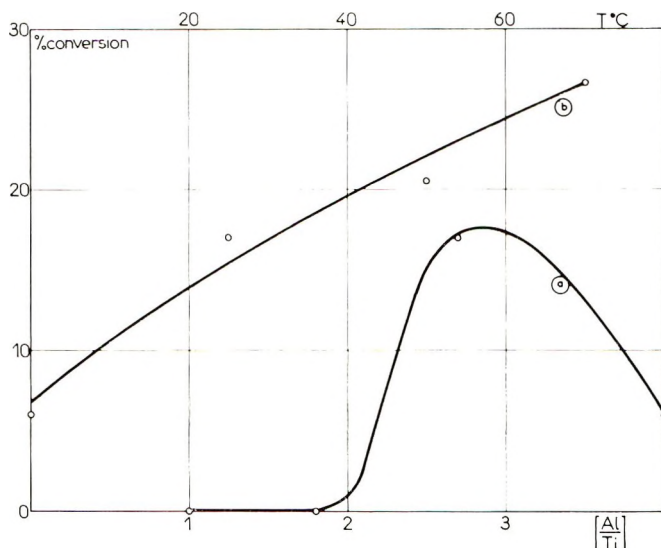


Fig. 1. Influence of (a) the Al/Ti ratio and of (b) the reaction temperature on the polymerization of diphenyldiacetylene.

It has to be noticed that these data are based on the yields measured after extraction of the products with boiling methanol; the residual product was called polymer and the one obtained by evaporation of the methanolic solution oligomer, not on the basis of their molecular weights (which differ only by a factor of 1.5), but of their ultraviolet absorption spectra: the polymers exhibited continuous absorption spectra toward  $330\text{ m}\mu$ , similar to the spectra of simple acetylenic polymers, in contrast to the spectra of the oligomers, which are very similar to that of the monomer.

This will be further discussed in section B below. Some experiments were also performed with the type of catalysts described by Luttinger<sup>5,6</sup> and Green.<sup>7,8</sup> A mixture of 0.3 mole/l. of sodium borohydride and 0.0015 mole/l. of cobalt nitrate trihydrate was used to polymerize a 1.5 *M* methanolic solution of the monomer (1.5 hr. at reflux conditions). A brown product was obtained with a softening point around  $190^\circ\text{C}$ . and a spectrum very similar to that of the polymer obtained with Ziegler-type catalysts.

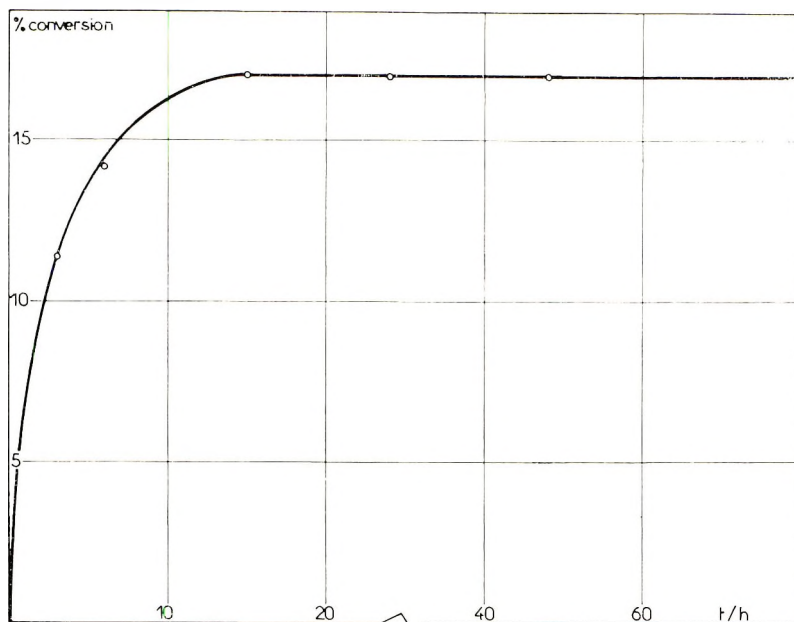


Fig. 2. Polymerization of diphenyldiacetylene at 25°C. (Al/Ti = 2.7).

### B. Properties of the Products

The products obtained at the end of the polymerization have physico-chemical properties which appear as less interesting than those of the polymers transformed by thermal or chemical treatment. The properties of both types of polymers will be presented here; a discussion of their probable structure will be given in the Discussion.

All the products obtained are easily soluble in the usual organic solvents such as chloroform, benzene, carbon disulfide, dioxane, giving brown or deep red solutions.

Their softening points are related to their molecular weight (determined by cryoscopy and hence representing a minimal value), as shown in Table II.

TABLE II  
Dependence of the Softening Point of the Polymers on their Molecular Weight

Softening point, °C.	Molecular weight
185-190	819 (oligomer)
210-215	1078
220-230	1145
250-260	1250

The absorption spectra of the different compounds studied are given in Figure 3: it is interesting to notice that the spectrum of the initial polymer is very similar to that of polymonosubstituted acetylenes,<sup>10,11</sup> while

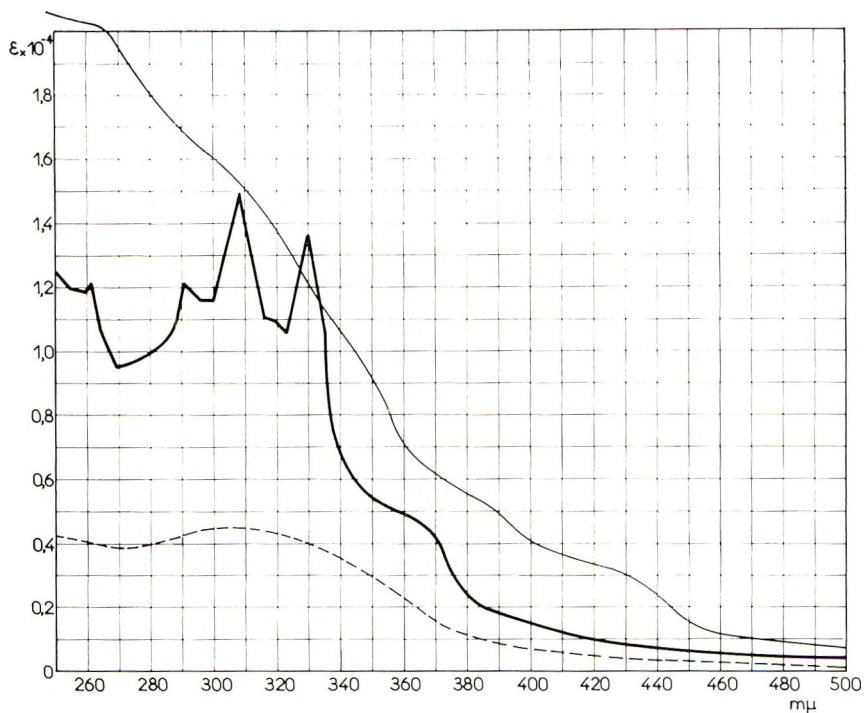


Fig. 3. Absorption spectra in chloroform: (—) oligomer,  $4.7 \times 10^{-5}$  mole/l.; (- - -) polymer,  $2.7 \times 10^{-4}$  mole/l.; (- · -) cyclized polymer,  $3.4 \times 10^{-5}$  mole/l.

after thermal or chemical treatment the shape of the spectrum has changed and the absorptivity increased (this absorption being very significant far in the visible region). The oligomer has a spectrum very similar to that of the monomer, but a weak band around  $365 \text{ m}\mu$ . Another interesting feature is the green fluorescence of these polymer solutions, compared to the blue fluorescence of the oligomers, and to the virtual lack of fluorescence of the monomer solutions. The corresponding spectra are recorded in Figure 4.

The polymers exhibit a very good heat resistance. The initial polymers lose only 3% of their weight after 6 hr. at  $250^\circ\text{C}$ . under an argon atmosphere; the treated polymers have a softening point around  $480^\circ\text{C}$ ., and decompose around  $510^\circ\text{C}$ ., becoming insoluble. They enjoy a remarkable thermostability as shown in Fig. 5 (the product was kept at least 2 hr., and in any case till complete equilibrium was reached, at each temperature mentioned).

These products exhibit also a narrow electron spin resonance signal; the initial polymers contain  $5 \times 10^{18}$  spins/g. (with a  $\Delta H$  value of 3.6 gauss and a  $g$  value of 2.0021 very similar to that of a free electron) while the thermally treated polymers contain  $4 \times 10^{19}$  spins/g. ( $\Delta H = 5.3$ ).

They have a low conductivity (around  $10^{-14}$  mho/cm.) which obeys an exponential dependence on the temperature ( $\sigma = \sigma_0 e^{-E/kT}$ ) the activation energy of the process amounts to 0.7 e.v. for the parent polymer and to



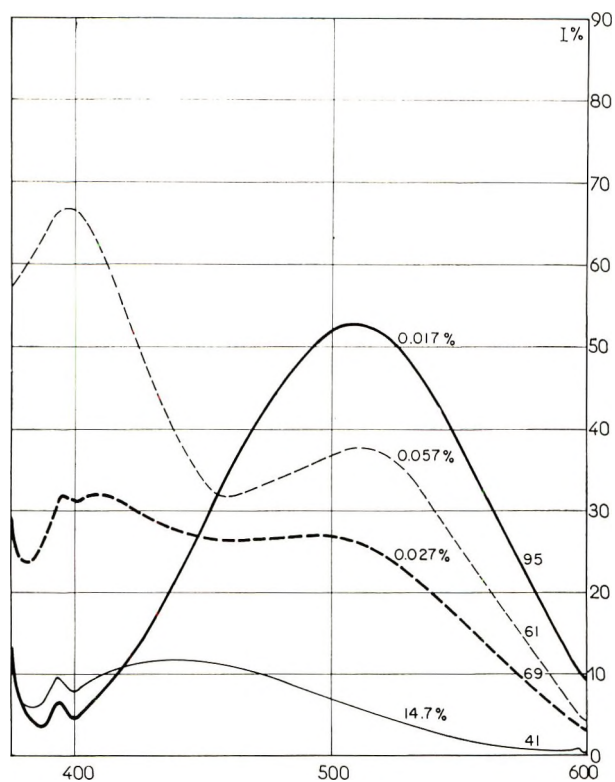


Fig. 4. Fluorescence spectra of (—) monomer, (---) oligomer, (- · -) polymer, and (— —) cyclized polymer of diphenyldiacetylene. (Concentrations of the solute in chloroform expressed in wt.-%.)

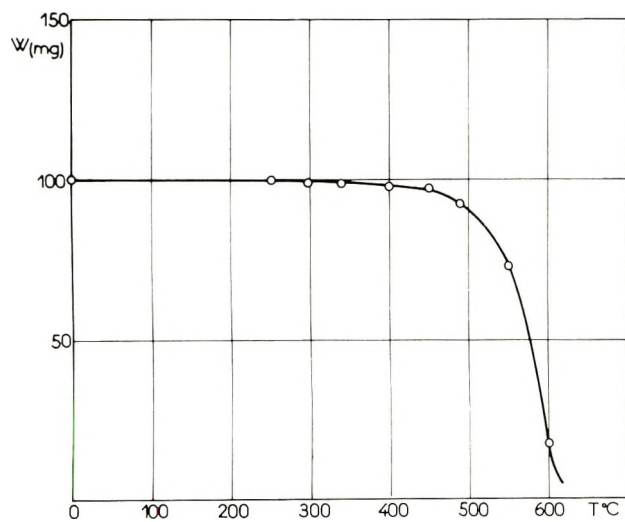


Fig. 5. Thermostability under vacuum of polydiphenyldiacetylene treated at 400°C.

0.4 e.v. for the treated product. They also gave indications of photoconductivity.

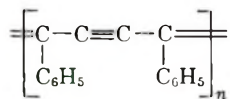
These properties are paralleled by a definite catalytic activity toward the decomposition of  $N_2O$ , characteristic of many organic polymers containing paramagnetic centers.<sup>9</sup>

All these properties will be the subject of further investigations.

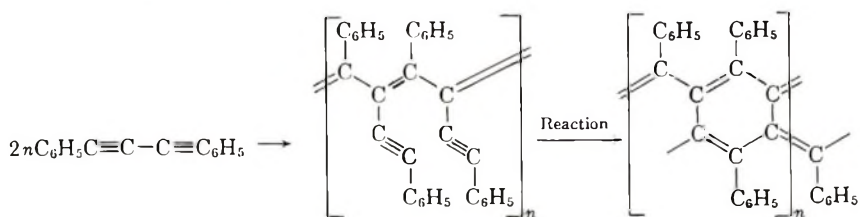
#### IV. DISCUSSION

Ziegler-type catalysts only are active enough to ensure the polymerization of the monomer studied, and experiments with radical type catalysts (AIBN) or anionic ones (biphenylsodium) failed to give any polymer; this could lead to a certain amount of stereospecificity in the synthesized products.

Two types of polymers might be obtained from this monomer, depending on the way of addition takes place at the triple bonds. Either this addition takes place at the 1,4 position and leads to a linear polymer of the following structure:



or the addition takes place at the 1,2 position and yields a linear conjugated chain with acetylenic side groups:



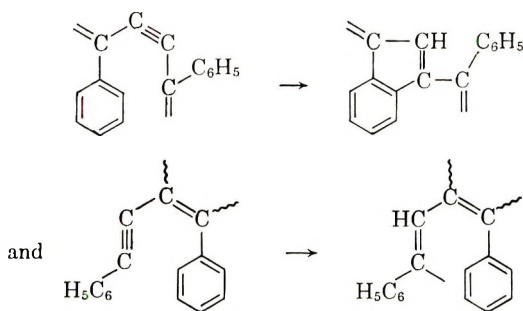
Both structures appear to be plausible on the basis of study of the molecular models; however, the 1,2 type addition yields a polymer more sterically hindered than the 1,4 type.

Besides its highly conjugated character, the 1,2 polymer would be also very interesting for its potential for undergoing a cyclization reaction, analogous to that postulated in the thermal treatment of polyacrylonitrile.

This type of reaction probably accounts for an important fraction of the product obtained, as it seems substantiated by several experimental results. Both heat and Friedel-Crafts catalysts convert the initial polymer to the same product, which exhibits different properties characteristic of condensed aromatic systems: the ultraviolet absorption is much more intense than for the initial polymer and also unlike the initial polymer has a maximum at the lower wavelengths; there is significant absorption in the

visible region. The cyclized product has an intense fluorescence spectrum with a maximum at  $510 \text{ m}\mu$ . It has also a much lower activation energy for the electronic conductivity process. Finally, it has a much higher thermal resistance, and is very stable in vacuum up to  $450^\circ\text{C}$ ., which corresponds to the stability of many polynuclear aromatic compounds.

The presence of a broader absorption band at  $755 \text{ cm.}^{-1}$  in the infrared spectra of the cyclized polymers could support the existence of some *ortho* disubstituted aromatic rings, formed by intramolecular cyclization on the phenyl groups, for polymers obtained both by 1,4 or 1,2 addition:



The formation of unsaturated macrocyclic compounds<sup>12</sup> which could be suggested by the low values of the molecular weights, is invalidated by the different physicochemical properties of these products, namely their absorption spectra and stability.

The structure of the oligomer, however, was not elucidated. From the absorption and fluorescence spectra (and also some other properties) its structure appears to be essentially different from that of the so-called polymer. Although it is well known<sup>13-15</sup> that the Ziegler-Natta catalysts may promote the formation of cyclic trimers (yielding in this case a hexa-substituted benzene ring), the spectrophotometric and cryometric determinations do not support this hypothesis.

## V. CONCLUSION

Although of low molecular weight, the polydisubstituted diacetylenes described in this paper have interesting electronic properties: continuous absorption in ultraviolet and visible regions, fluorescence not exhibited by the monomer, high stability, semiconducting and catalytic properties. The authors feel that this class of polymers deserves special interest, since besides their promising properties, they might be obtained from many synthetic or naturally occurring monomers already known.<sup>1</sup> Further investigations will be devoted to the polymerization of other monomers of this type as well as to attempts to increase the molecular weight of the products obtained.

The authors are indebted to Mrs. J. Gallard for the determination of the catalytic activity, to Miss Le Goff for the spectrophotometric determinations, and to Mr. de Charentenay for the conductivity measurements.

### References

1. Korn-Girard, A. C., and Ph. Teyssié, *Rev. Inst. Franc. Pétrole*, **17**, 1214 (1962).
2. Hay, A. S., C. Fr. Thomson-Houston, Fr. Pat. 1,290,401 (March 1962).
3. Strauss, F., and L. Kollek, *Ber.*, **56**, 1680 (1926).
4. Watson, N., J. K. Warren, W. C. McMordie, Jr., and L. G. Lands, *J. Polymer Sci.*, **55**, 137 (1961).
5. Luttinger, L. B., *Chem. Ind.*, **1960**, 1135.
6. Luttinger, L. B., and E. C. Colthup, *J. Org. Chem.*, **27**, 1591, 3752 (1962).
7. Green, M. L. H., M. Nehme, and G. Wilkinson, *Chem. Ind.*, **1960**, 1136.
8. American Cyanamid Co., Brit. Pat. 897,099 (May 23, 1962).
9. Dawans, F., J. Gallard, Ph. Teyssié, and Ph. Traynard; *J. Polymer Sci.*, in press.
10. Sadron, C., J. Parrod, and J. P. Roth, *Compt. Rend.*, **250**, 2206 (1960).
11. Stille, J. K., *J. Am. Chem. Soc.*, **83**, 1697 (1961).
12. Sondheimer, F., R. Wolovsky, and Y. Gaoni, *J. Am. Chem. Soc.*, **82**, 755 (1960).
13. Franzus, B., P. J. Canterino, and R. A. Wickliffe, *J. Am. Chem. Soc.*, **81**, 1514 (1959).
14. Lutz, F., *J. Am. Chem. Soc.*, **83**, 2551 (1961).
15. Forlani Donda, A., E. Cervone, and M. A. Biancifiori, *Rec. Trav. Chim.*, **81**, 581 (1962).

### Résumé

La polymérisation du diphenyldiacétylène a été étudiée en présence de catalyseurs du type Ziegler. Les polymères, tant au sortir de la polymérisation qu'après réaction ultérieure, sont des produits solubles de faible masse moléculaire, doués de propriétés intéressantes: très haute résistance thermique, absorption continue dans l'ultra-violet et le visible, large spectre de fluorescence dans le visible, propriétés de semiconduction et de catalyse.

### Zusammenfassung

Die Polymerisation von Diphenyldiacetylen in Gegenwart von Ziegler-Katalysatoren wurde untersucht. Die Polymeren, die als unmittelbare Polymerisationsprodukte oder nach weiterer Reaktion untersucht wurden, erwiesen sich als lösliche, relativ niedermolekulare Produkte mit interessanten Eigenschaften: sehr hohe thermische Beständigkeit, kontinuierliche Absorption im ultravioletten und sichtbaren Bereich, breite Fluoreszenzspektren im Sichtbaren sowie Halbleiter und Katalysatoreigenschaften.

Received June 24, 1963

## Mechanisms of Thermal Degradation of Phenolic Condensation Polymers. I. Studies on the Thermal Stability of Polycarbonate\*

LIENG-HUANG LEE, *Polymer and Chemicals Research Laboratory,  
The Dow Chemical Company, Midland, Michigan*

### Synopsis

Bisphenol-A polycarbonate gradually degrades at temperatures above 310°C. as detected by differential thermal analysis. The first stage of degradation of the dry and purified resin is induced by oxygen. In connection with oxidation, zinc stearate causes a notable degradation. This compound may act partly as an oxidation catalyst. The initial site attacked by oxygen is presumably the isopropylidene linkage of the polymer. The second stage of degradation shows a characteristic endothermic peak between 340 and 380°C. This stage is chiefly associated with depolymerization since only a small amount of volatiles is detectable. Depolymerization can be caused by hydroperoxide cleavage, hydrolysis, alcoholysis and bisphenol cleavage. Bisphenol-A can decompose in the presence of acid into phenol and isopropenylphenol. The latter compound is a color-forming material. As temperature increases above 400°C., volatilization rate gradually increases. The last stage of degradation becomes uncontrollable above 500°C. At this stage, decarboxylation, dehydration, hydrolysis, hydrogen abstraction, ether cleavage, crosslinking as well as chain scission interact to yield aromatic hydrocarbons, phenolic compounds, and tar. The quantity of aromatic hydrocarbons is determined by the intensity of the thermal degradation.

### INTRODUCTION

Since bisphenol-A polycarbonate was separately discovered by Farben-fabrieken Bayer Company in Germany and General Electric Company in this country, this resin has been known to be outstanding with respect to stability against heat, light, and numerous chemicals. It seems rather unnecessary to discuss the problem of stabilization regarding this polymer. However, there are difficulties encountered during fabrication, if proper precautions are not taken. For instance, without drying prior to molding, the resin degrades and causes fabrication problems such as streaking and bubbling. It was found by Fiedler, Christopher, and Calkins<sup>1</sup> that over-heating causes the resin to darken. Since polycarbonate has a high softening temperature and becomes reactive with chemicals such as phenols and amines at high temperatures, it is not easy to stabilize this polymer with conventional stabilizers. It seems that a different concept of stabilization

\* Paper presented at the 142nd National American Chemical Society Meeting, Atlantic City, New Jersey, September 1962.

is needed. A new stabilization approach should be based on a full understanding of the degradation mechanisms of polycarbonate.

Unfortunately this basic knowledge is not available in the literature. Korshak and Vinogradova<sup>2</sup> made an extensive review on polyarylates in April 1961 and did not find any basic study regarding the thermal stability of polycarbonate. Thompson and Goldblum<sup>3</sup> first briefly described the effects of moisture and the residual sodium salt on the thermal stability of polycarbonate. In this paper, we present some preliminary studies made in an attempt to elucidate the mechanisms of thermal degradation of polycarbonate.

## EXPERIMENTAL

### Raw Materials

Lexan polycarbonate (Lot 125) and Makralon polycarbonate (Lots 574, 130) were used for references. Several experimental polymers prepared in the laboratory with Dow polycarbonate-grade bisphenol-A were used for various studies.

### Determination of Melt Viscosity

Melt viscosity was determined in a capillary melt viscometer designed by Karam and co-workers.<sup>4</sup> The apparent viscosity was taken at 700,000 dynes/cm.<sup>2</sup> shear stress. The thermal stability of polycarbonates was determined by taking several melt viscosity readings at 310° or 320°C. as a function of time. The plot of the apparent viscosity against time at a constant temperature should be a straight line parallel to the time axis if the sample is thermally stable at that temperature.

### Differential Thermal Analysis (DTA)

Differential thermal analysis equipment has been described by Cobler and Miller.<sup>5</sup> When a phase change or a reaction occurs involving absorption or evolution of heat, the temperature difference between the sample and the reference material increases. In general, phase transformations and depolymerization are endothermic, whereas, oxidation and polymerization are exothermic.

### Thermogravimetric Analysis (TGA)

A simple thermogravimetric balance was used.<sup>6</sup> The sample holder was attached to the arm of the torsion balance by a fine quartz fiber. The holder was centered in a furnace, the temperature of which was measured with a thermocouple situated directly beneath the sample holder. The weight of the remaining sample was recorded at definite time intervals.

### Vapor-Phase Chromatography

The pyrolysis was conducted directly in the injector inlet of the chromatography unit (HY-FI Model 600 manufactured by Wilkens Instrument

and Research Inc.). The material was pyrolyzed on a hot platinum filament. A mannitol column<sup>7</sup> was recommended for the separation of phenolic compounds. Limitations were found especially for the polyphenols.

### Mass Spectroscopy

Both bisphenol-A and the polymers were pyrolyzed in a Pyrex flask under vacuum and in the presence of air. The pyrolyzed products were analyzed with a mass spectrometer and an infrared spectrophotometer.

### Spot Test for Chloroformoxy Group ( $-\text{OCOCl}$ )

A new spot test for detecting the chloroformoxy group was developed during the course of this study. The test was originally used to detect the vapor of  $\text{HCl}$ . The test solution was prepared by dissolving 5 g. each of *p*-dimethylaminobenzaldehyde and diphenylamine in 50 ml.  $\text{CCl}_4$ . A small piece of polymer or several drops of the polymer solution were placed in a white spot-test plate. A drop of the reagent was placed on top of the polymer and mixed. After a few seconds, the mixture turned yellow or orange color indicating the presence of the chloroformoxy groups. The intensity of color was closely related to the number of the chloroformoxy groups.

## RESULTS AND DISCUSSION

Melt viscosity<sup>3</sup> was first used to describe the thermal stability of polycarbonate at  $300^\circ\text{C}$ . In our laboratory, we used  $310^\circ$  and  $320^\circ\text{C}$ . for the determination of thermal stability. Figure 1 shows results of determinations on three samples of polycarbonate at  $310^\circ\text{C}$ . It is noted that the melt viscosity tends to decrease with time. When the fourth sample was measured at  $320^\circ\text{C}$ ., a more rapid decrease was noted. This indicates that above  $300^\circ\text{C}$ . polycarbonates start to degrade.

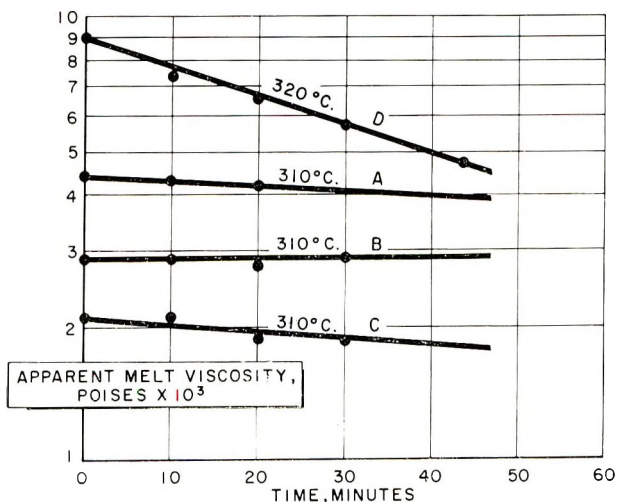


Fig. 1. Thermal stability of polycarbonate.

### Oxidative Degradation

In Figure 2, a typical differential thermogram for polycarbonate is shown. Cobler and Miller<sup>5</sup> discussed the implications of these peaks. Our study was concerned with a correlation of the various reactions with these peaks. There is one exothermic peak at 310–320°C., and there are three endothermic peaks at 360, 460, and 565°C. Our findings have shown that the first endothermic peak is the most characteristic, the second and the third endothermic peaks vary with the size and the methods of preparation of the sample.

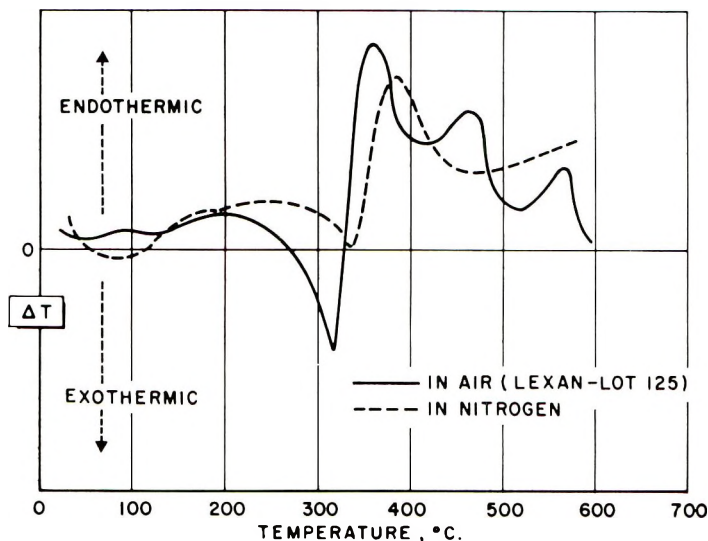


Fig. 2. Effect of oxygen upon thermal stability (differential thermogram).

It was thought that the first exothermic peak was caused by the oxidation of polycarbonate. Differential thermal analysis was carried out in the presence of nitrogen and the exothermic peak diminished. This made us believe that this peak was truly associated with oxidation. Furthermore, in nitrogen, the first endothermic peak shifted from 360° to 380°C., and the other endothermic peaks disappeared. This indicates that nitrogen can retard the oxidation as well as later degradations.

In connection with the problem of oxidation, it was found that a small amount of zinc stearate caused a notable degradation of polycarbonate. This compound should not be used as the mold-releasing agent for polycarbonate. The function of zinc stearate in the decomposition is not clearly known. However, the DTA results indicate that zinc stearate may function at least as an oxidation catalyst (Fig. 3). It is noted that both the exothermic and the endothermic peaks are about 20°C. lower than those in the blank. The shifts clearly indicate that polycarbonate is oxidized more readily in the presence of zinc stearate. The function of transition



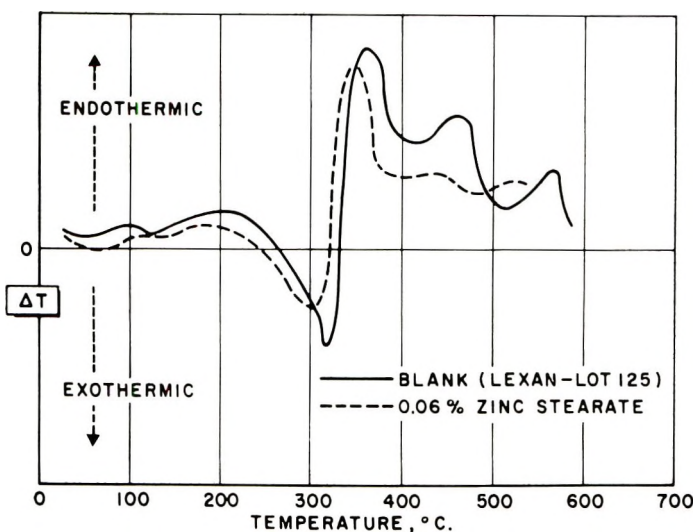


Fig. 3. Effect of zinc stearate upon thermal stability (differential thermogram).

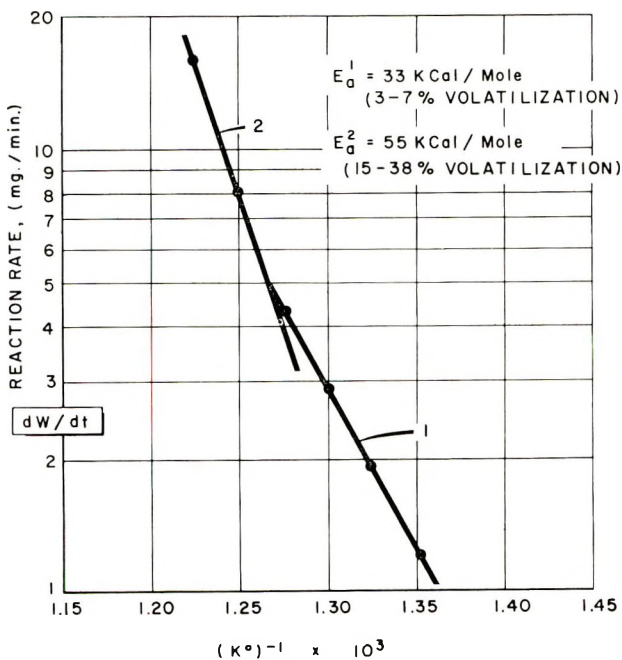


Fig. 4. Temperature-dependency plot of polycarbonate (Lexan lot 125).

metals as oxidation catalysts has been recently confirmed. It is also known that copper stearate<sup>3</sup> catalyzed the oxidation of cellulose ester. Therefore, the above finding, that zinc stearate functions similarly is not surprising.

Thermogravimetric analysis (TGA) was then used to determine the activation energy of the degradation. If the degradation is induced by oxida-

tion, the initial activation energy is generally between 15 and 35 kcal./mole. Wilson<sup>9</sup> reported an activation energy for the oxidation of polyethylene to be in the range 25–30 kcal. Heron<sup>10</sup> found the initial activation energy for the degradation of phenolformaldehyde resin to be 15 kcal.

The modified nonisothermal method of Freeman and Carroll<sup>11</sup> was employed to investigate the kinetics of degradation under a vacuum of 4 mm. Hg with the hope that an excessive oxidation could be prevented. The activation energies were calculated from the temperature dependency plot in Figure 4. The temperature-dependency plot was obtained from the plot of the first derivative of a continuous weight-loss curve. The initial 7% reaction gave an activation energy of 33 kcal./mole which is within the range considered for the oxidative degradation. The second stage of reaction with the high activation energy will be discussed later.

The initial site attacked by oxygen is not clearly known but is likely to be the isopropylidene linkage. Presumably, after a hydrogen of the methyl group is abstracted, an unstable radical,  $(-\text{OC}_6\text{H}_4)_2\text{C}(\text{CH}_3)\text{CH}_2\cdot$ , is formed. It would immediately rearrange into a stable radical,  $-\text{OC}_6\text{H}_4-\dot{\text{C}}(\text{CH}_3)-\text{CH}_2-\text{C}_6\text{H}_4\text{O}-$ . This radical is then readily attacked by oxygen to form a hydroperoxide. At temperatures above 300°C., besides initiating a chain reaction, the hydroperoxide may cleave homolytically to give a reactive hydroxy radical ( $\cdot\text{OH}$ ) and an alkoxy radical ( $\text{RO}\cdot$ ). Through hydrogen abstraction, the hydroxy radical would produce a molecule of water, and the alkoxy radical would form a compound with a hydroxy group. Both water and hydroxy compounds can induce further degradation. It should be pointed out that a hydroperoxide was also found to cleave heterolytically under the pyrolysis conditions described in the later sections.

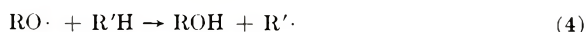
Cleavage:



Formation of water:



Formation of hydroxy compound:



Since oxidation has been shown to be the prelude of the later thermal degradation, the most effective approach to stabilizing polycarbonate seems to be the inhibition of the initial oxidation. Unfortunately, most phenolic antioxidants are undesirable, due to their role in the alcoholysis of the carbonic ester. Most amine-containing antioxidants are even worse, due to their reactivities with carbonic ester. It is now known that better antioxidants have been used in commercial polycarbonates made in recent years.

### Depolymerization

In the differential thermogram of polycarbonate (Fig. 2), the first endothermic peak at 340–380°C. is the most characteristic. Since thermo-

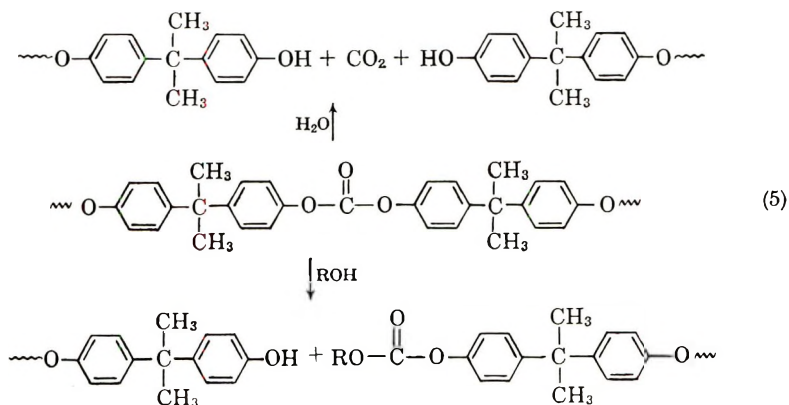
TABLE I  
 Effect of Moisture upon Viscosities

Expt. No. (PI-50)	K value <sup>a</sup> before deter- mination	Molded sample (without drying)		Molded sample (with drying)	
		K value after deter- mination	$\eta_r$ , <sup>b</sup> poise (310°C.)	K value after deter- mination	$\eta_r$ , poise (310°C.)
24	53	40	1,170	46	2,080
27	45	35	301	42	747
28	53	37	732	47	2,880
31	54	39	934	45	3,350

<sup>a</sup>  $\log \eta_r = [75 k^2 / (1 + 1.5 kc) + k]C$ , where  $k = 1000$ ,  $k$  = relative viscosity,  $c$  = concentration (g./ml.).

<sup>b</sup>  $\eta_r$ , the melt viscosity, was determined under 700,000 dynes/sq. cm. shear stress.

gravimetric results (Fig. 5) showed that the rate of volatilization was slow between 400 and 500°C. and became very fast after the temperature was raised above 500°C., it may be assumed that the main transformation involving heat at this stage is depolymerization. Even for a dry and pure sample, after the initial oxidation, water and hydroxy compounds resulting from the decomposition of hydroperoxide are sufficient to induce depolymerization through hydrolysis or alcoholysis of the carbonic ester. Depolymerization is enhanced by the presence of acidic or basic impurities or the surface moisture of the resin.



The result of hydrolysis in lowering the molecular weight is shown in Table I. For the resins not oven-dried, both solution and melt viscosities were significantly lower than those of the oven-dried resins measured under the same conditions in the capillary melt viscometer. The products of hydrolysis are carbon dioxide and bisphenol-A if the carbonate linkage is close to the chain end. Otherwise, two shorter chains of polymer are obtained instead of bisphenol-A.

A chemical method of preventing polycarbonate from being hydrolyzed is not known. The best preventive measure is to dry the resin prior to

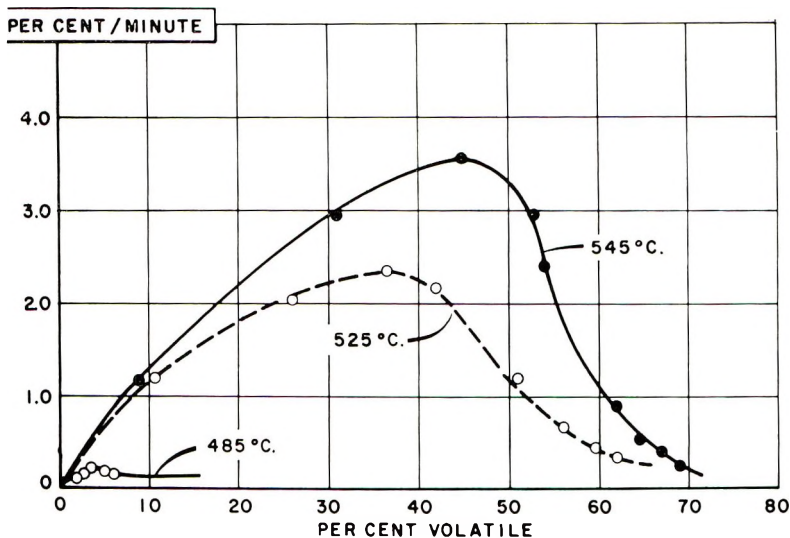
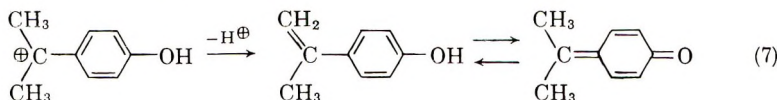
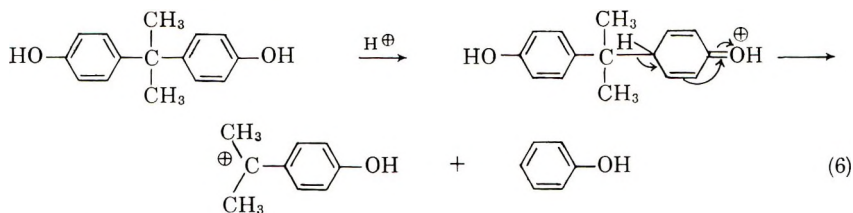


Fig. 5. Rate of volatilization (Lexan lot 125).

fabrication. Certainly, inhibition of the initial oxidation is also very important, based on the fact that oxidation can result in the formation of water.

One of the hydrolyzed products, bisphenol-A, is known to be unstable at elevated temperatures especially in the presence of a trace amount of acid catalyst. There is less than 0.1% of free bisphenol-A detected in the commercial polycarbonates. As a result of hydrolysis, some additional bisphenol-A is formed. Upon decomposition by acid, a highly conjugated material results. Both phenol and *p*-isopropenylphenol were identified in the decomposition products; the tautomer of *p*-isopropenylphenol could be one of the color-forming materials. The reaction is similar to a reverse Friedel-Crafts reaction [eqs. (6) and (7)]; therefore the proton is regenerated to start successive reactions. The same type of cleavage may also take place at the isopropylidene linkage of the polymer chain.



The stabilization measure against the acidic cleavage of bisphenol-A is to remove any acidic impurity or to prevent the formation of acid.

We found that the residual chloroformoxy group ( $-\text{OCOC}\text{I}$ ) was very detrimental due to its ease of producing  $\text{HCl}$  at elevated temperatures. We have used various chain terminators to reduce the number of the chloroformoxy groups. Terminators such as silanes<sup>12</sup> and fluoro alcohols<sup>13</sup> are very effective. In order to determine a trace amount of a chloroformoxy group, we developed a new spot-test as described in the experimental part, which can be applied directly to the polymer.

In addition to the introduction of coloring material, bisphenol-A cleavage results in the formation of monohydric phenols which would cause the lowering of molecular weight through alcoholysis. Alcoholysis is one form of ester exchange; however, in this case, the polymer chain breaks in the middle to give a shorter chain carbonate. Alcoholysis, therefore, also causes depolymerization without volatilization. Presumably, another ill effect of phenolic compounds is their function as acidic catalysts. At extremely high temperatures, they induce further cleavages of bisphenol-A and polycarbonate.

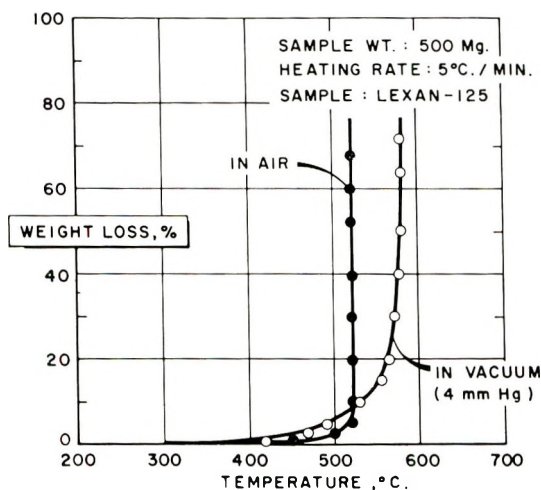


Fig. 6. Thermogravimetric curves for the degradation of polycarbonate.

### Thermal Degradation

The previous two stages of degradation involve only a small weight loss. As the temperature increases, the thermal energy begins to surpass the bond energies of various bonds in the polymer. At this stage, random chain scission takes place and the rate of degradation increases rapidly as shown in Figure 6. In the presence of air, the thermal degradation occurred 60°C. sooner than that in vacuum. This confirms the previous discussion on the role of oxygen related to the later stages of degradation.

Undoubtedly this last phase of degradation is complicated. It was hoped that a study of the degradation mechanism at this uncontrollable stage may throw some light on the stabilization problem as a whole. Vapor-

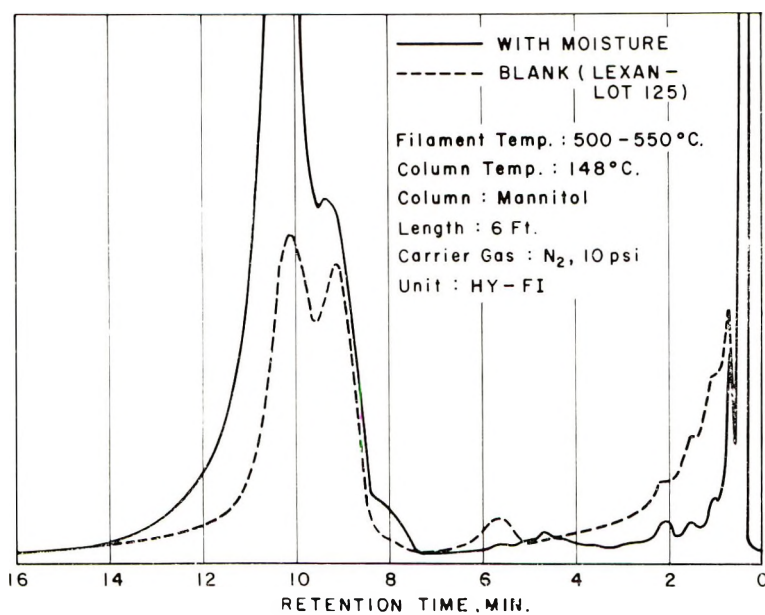


Fig. 7. Pyrogram of polycarbonate.

 TABLE II  
 Thermal Degradation of Bisphenol-A and Polycarbonate at 475°C.<sup>a</sup>

Mass (M.W.)	Compounds	Polycarbonate <sup>b</sup>		Bisphenol-A (Recrys- tallized) in air <sup>c</sup>
		In vacuum	In air	
18	Water	L	L	L
44	Carbon dioxide	L	L	
58	Acetone		L	Trace
78	Benzene		L	S
92	Toluene		L	S
106	Ethylbenzene		S	Trace
94	Phenol	L	L	L
108	Cresol	L	L	Trace
122	Ethylphenol	L	L	Trace
134	Isopropenylphenol	S	S	L
136	Isopropylphenol	L	L	S
214	Diphenyl carbonate	*S		
228	Bisphenol-A	Major	Major	

<sup>a</sup> Both Lexan-125 and Makralon-130 were analyzed. Only a trace amount of mass 214 was found in Lexan-125. (\*) Both polymers gave a trace amount of chloroform.

<sup>b</sup> The unidentified degraded polycarbonate fractions are: 120, 210, 212, 226, and 238.

<sup>c</sup> The unidentified degraded Bisphenol-A fractions are: 110, 168, 186, 210, 212, 226, 238, 242, 253, and 268.

<sup>d</sup> L = large; S = small.

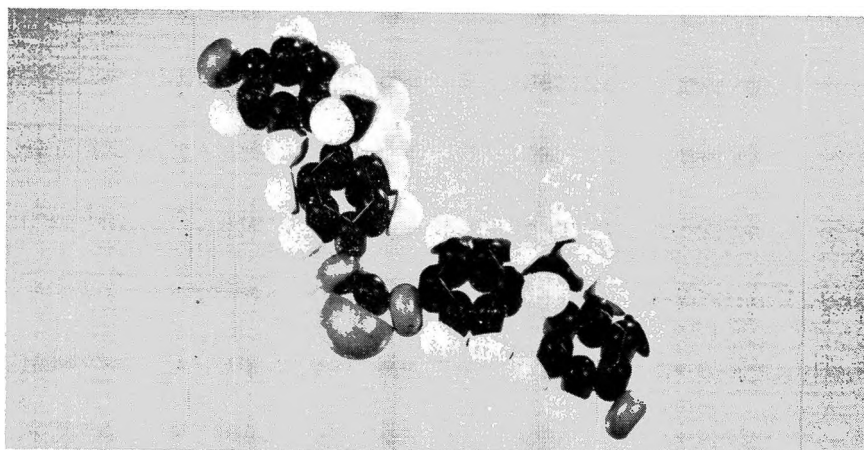


Fig. 8. Molecular model of bisphenol-A polycarbonate.

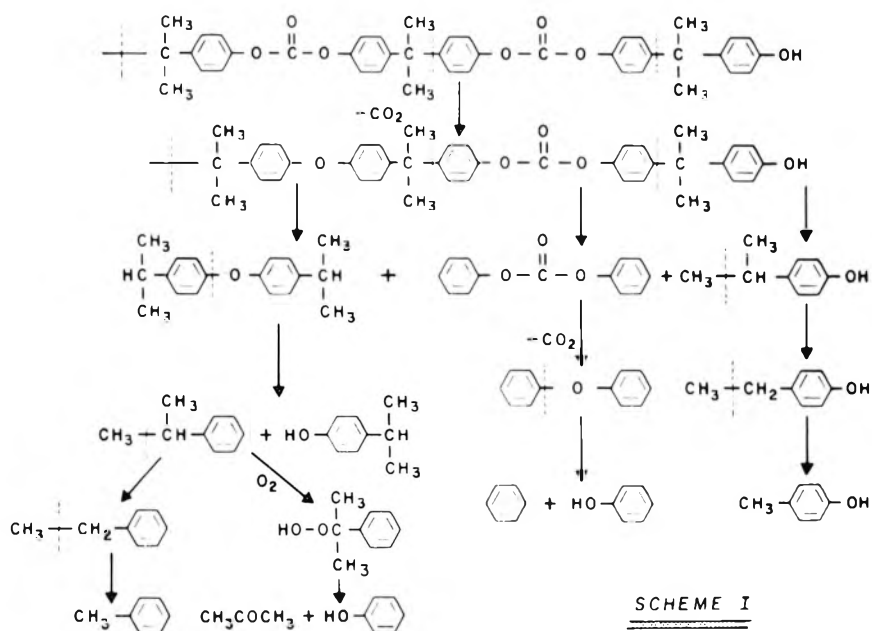


Fig. 9. Scheme I for the thermal decomposition of polycarbonate.

phase chromatography, mass spectroscopy, and infrared analysis were then used to identify the pyrolyzates. In Figure 7, a pyrogram of polycarbonate is shown. The pyrolysis was carried out both in the presence and in the absence of moisture. It was found that more phenolic compounds were obtained in the presence of moisture. In each case, there were at least eight compounds present.

In order to confirm each of these fractions, the conventional pyrolysis technique was used, and the soluble products were analyzed by mass spec-

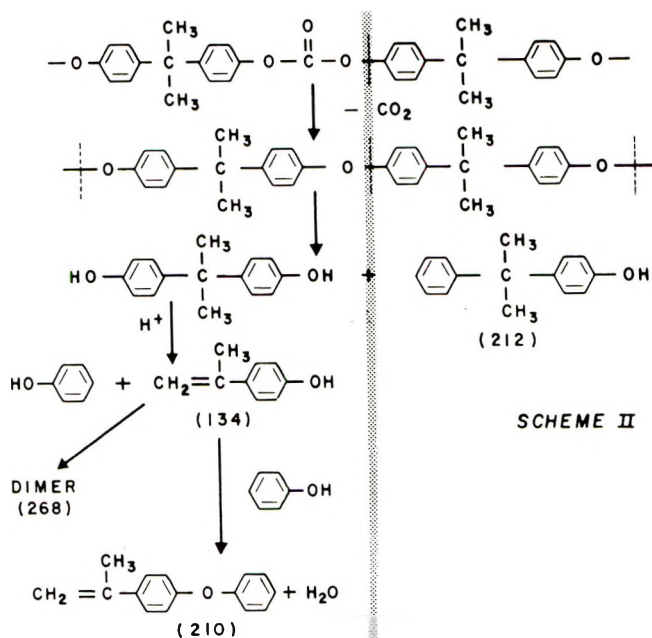


Fig. 10. Scheme II for the thermal decomposition of polycarbonate.

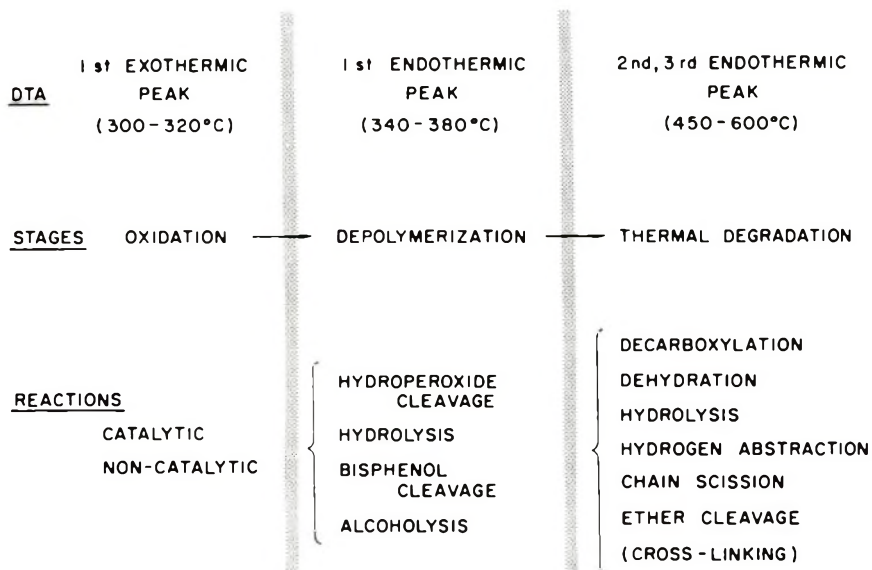


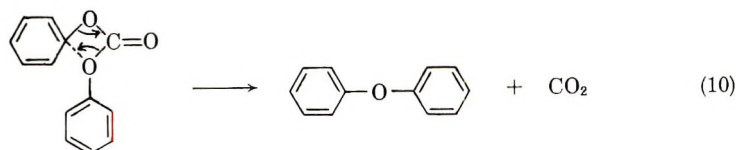
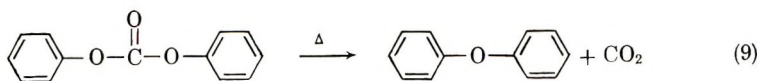
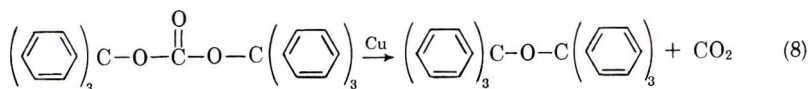
Fig. 11. Degradation of polycarbonate.

trometry and infrared spectrophotometry. The soluble decomposition products of bisphenol-A and polycarbonate are listed in Table II. Since about 40% of the soluble pyrolyzed products of polycarbonate is bisphenol-A, this comparison helps clarify the multiple schemes of decomposition.



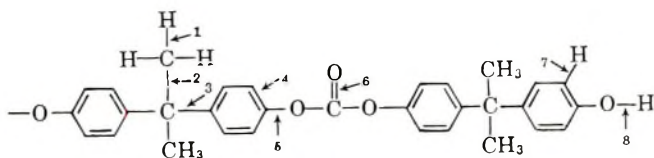
For those fractions occurring in trace amounts, identification was not pursued.

One of the important thermal degradation paths is presumably the decarboxylation of carbonate [eqs. (8) and (9)], which generally takes place over 450°C. for simple carbonic esters.<sup>14,15</sup> Recently another ether, *p*-cumenyl phenyl ether,  $[(\text{CH}_3)_2\text{CHC}_6\text{H}_4\text{OC}_6\text{H}_5]$ , was identified with the aid of NMR and infrared analysis. The fact that the quantity of this compound is equal to those of other phenols suggests that this ether is actually one of the primary products. The preceding would further substantiate the existence of the decarboxylation as the major step of degradation. The generally accepted mechanism for the decarboxylation is the concerted 1,3 shift [eq. (10)]. This mechanism is plausible as seen from the molecular model of a segment of bisphenol-A polycarbonate shown in Figure 8.



In Table III, the various bond energies are listed for reference. From these values, we could predict which bond, in preference to others, undergoes chain scission. However, the pure thermal degradation is unpredictable

TABLE III  
Bond Energies of Various Bonds of Polycarbonate



No.	Bond	Bond energy, kcal./mole
1	C—H	98.7
2	C—CH <sub>2</sub>	60.0
3	C—C	82.6
4	C=C	147.5
5	C—O	85.5
6	C=O	176.0–179.0
7	C=C—H	102.0
8	O—H	101.5

because it is the results of other reactions besides chain scission, such as decarboxylation, hydrolysis, dehydration, ether cleavage, hydrogen abstraction, and crosslinking. By a combination of these reactions, two concurrent schemes (Figs. 9 and 10) are tentatively proposed to account for most of the products described in Table II.

It should be noted that the soluble pyrolyzates obtained in vacuum are mostly the primary degradation products, while the pyrolyzates obtained in the presence of air are the mixture of the primary, the secondary and the oxidized products. The true reactions are highly complicated. The proposed schemes serve only as models for the idealized situation and, by no means, should be taken to represent the changeable degradation patterns.

The degradation of bisphenol-A polycarbonate is summarized in Figure 11. The three stages of degradation were found to be oxidative degradation, depolymerization, and thermal degradation. It has been shown that oxidation is the prelude to later degradations. The inhibition of oxidation should be the first step for the stabilization of polycarbonate. However, the pure thermal degradation can take place at elevated temperatures regardless of oxidation.

The author wishes to thank Messrs. J. G. Cobler and D. L. Miller of the Polymer Analysis Laboratory for the differential thermal and thermogravimetric analyses, and Mr. L. B. Westover of the Chemical Physics Research Laboratory for the mass spectrograph work.

## References

1. Fiedler, E. F., W. F. Christopher, and T. R. Calkins, *Modern Plastics*, **36**, 115 (April 1959).
2. Korshak, V. V., and S. V. Vinogradova, *Russ. Chem. Rev. (Engl. Transl.)*, **1960**, 171.
3. Thompson, R. J., and K. B. Goldblum, *Modern Plastics*, **35**, 131 (April 1958)
4. Karam, H. J., K. L. Cleereman, and J. L. Williams, *Modern Plastics*, **3.2**, 129 (March 1955).
5. Cobler, J. G., and D. L. Miller, paper presented to Division of Polymer Chemistry, 136th Meeting American Chemical Society, Atlantic City, N. J., September 1959.
6. Cobler, J. G., D. L. Miller, and E. P. Samsel, unpublished.
7. Janak, J., and R. Komers, *Z. Anal. Chem.*, **164**, 69 (1958).
8. DeCroes, G. C., and J. W. Tamblyn, *Natl. Bur. Std. Circ.* **525**, 171 (1953).
9. Wilson, J. E., *Ind. Eng. Chem.*, **47**, 2201 (1955).
10. Heron, G. F., *High Temperature Resistance and Thermal Degradation of Polymers*, Macmillan, New York, 1961, pp. 475-498.
11. Anderson, D. A., and E. S. Freeman, *J. Polymer Sci.*, **54**, 253 (1961).
12. Lee, L. H., and H. Keskkula, U. S. Pat. 3,026,298 (1962).
13. Lee, L. H., and H. Keskkula, U. S. Pat. 3,036,040 (1962).
14. Gomberg, M., *Ber.*, **46**, 226 (1913).
15. Richie, P. D., *J. Chem. Soc.*, **1935**, 1054.
16. Cottrell, T. L., *The Strengths of Chemical Bonds*, 2nd Ed., Butterworths, London, 1958.

### Résumé

Par analyse thermique différentielle on a découvert que le polycarbonate de bisphénol-A se dégrade progressivement aux températures dépassant 310°C. Le premier stade de la dégradation de la résine sèche et purifiée est induite par l'oxygène. En relation avec cette oxydation on remarque que le stéarate de zinc provoque une dégradation appréciable. Ce composé peut agir partiellement comme catalyseur d'oxydation. Le site initial attaqué par l'oxygène est sans doute le lien isopropylidène du polymère. La seconde étape de dégradation révèle un pic endothermique caractéristique entre 340°C et 380°C. Cette étape est principalement associée avec la dépolymérisation puisqu'on ne détecte qu'une petite quantité de matières volatiles. La dépolymérisation peut être causée par rupture d'hydroxyperoxydes, hydrolyse, alcoololyse et rupture des bisphénols. En présence d'acide le bisphénol-A peut se décomposer en phénol et en isopropénylphénol. Ce dernier composé est un matériau provoquant la coloration. Lorsque la température dépasse 400°C, la vitesse de volatilisation augmente progressivement. La dernière étape de dégradation devient incontrôlable au-dessus de 500°C; à ce stade, la décarboxylation, la déshydratation, l'hydrolyse, l'abstraction d'hydrogène, la rupture des liens éther, le pontage ainsi que la rupture des chaînes se produisent ensemble avec, comme conséquence, la formation d'hydrocarbures aromatiques, de composés phénoliques et de goudron. La quantité d'hydrocarbures aromatiques est déterminée par l'intensité de la dégradation thermique.

### Zusammenfassung

Die Differentialthermoanalyse zeigt, dass Bisphenol-A-Polykarbonat bei Temperaturen oberhalb 310°C schrittweise abgebaut wird. Die erste Abbaustufe des trockenen und gereinigten Harzes wird durch Sauerstoff induziert. Im Zusammenhang mit der Oxydation verursacht Zinkstearat einen merklichen Abbau. Diese Verbindung kann zum Teil als Oxydationskatalysator wirken. Der ursprüngliche Angriffspunkt des Sauerstoffs ist wahrscheinlich die Isopropylidenbindung des Polymeren. Die zweite Abbaustufe zeigt eine charakteristische endotherme Spitze zwischen 340°C und 380°C. Diese Stufe besteht vorwiegend in einer Depolymerisation, da nur eine kleine Menge an Flüchtigen nachweisbar ist. Depolymerisation kann durch Hydroperoxydspaltung, Hydrolyse, Alkoholyse und Bisphenolspaltung verursacht werden. Bisphenol-A kann sich in Gegenwart von Säure in Phenol und Isopropylphenol zersetzen. Letztere Verbindung ist ein farbbildender Stoff. Bei Temperaturerhöhung über 400°C nimmt die Verflüchtigungsgeschwindigkeit graduell zu. Die letzte Abbaustufe lässt sich oberhalb 500°C nicht mehr kontrollieren. Bei dieser Stufe treten Deacboxylierung, Dehydratisierung, Hydrolyse, Wasserstoffabspaltung, Atherspaltung, Vernetzung sowie Kettenspaltung auf und führen zu aromatischen Kohlenwasserstoffen, phenolischen Verbindungen und Teer. Die Menge der aromatischen Kohlenwasserstoffe wird durch die Intensität des thermischen Abbaus bestimmt.

Received October 5, 1962

Revised June 25, 1963

## Some Graft Copolymerizations at High Pressure

J. A. LAMB\* and K. E. WEALE, *Department of Chemical Engineering and Chemical Technology, Imperial College of Science and Technology, London, England*

### Synopsis

Some graft copolymerizations of monomers with substrates previously irradiated in air to form polymeric peroxides have been studied at pressures up to 8000 atm. In the heterogeneous system styrene-irradiated polyethylene, the rate of grafting increases considerably with pressure up to about 3000 atm. At higher pressures the reaction is retarded, and this is attributed to diffusion control of the propagation reaction. The rate of homopolymerization increases exponentially with pressure over the range 1-4000 atm. Irreproducible results were obtained when methyl methacrylate was used in place of styrene, possibly because the substrate is not swollen by this monomer. No grafting was observed between five different chloro-substituted ethylenes and irradiated polyethylene at pressures up to 5000 atm. The rate of grafting in the homogeneous system vinyl acetate-irradiated polystyrene increases considerably with pressure up to 8000 atm., and there is no indication of diffusion control of the propagation reaction.

### INTRODUCTION

The effect of pressure on the rate constant,  $k$ , of a homogeneous, liquid-phase reaction is given by

$$\partial(\ln k)/\partial P = -\Delta V^\ddagger/RT$$

where  $\Delta V^\ddagger$  is the volume change accompanying the formation of the transition state. Many free-radical polymerizations are considerably accelerated at high pressures<sup>1</sup> because  $\Delta V^\ddagger$  for the chain growth reaction is in the range  $-10$  to  $-20$  cc./mole. The rate constants for initiator dissociation and mutual chain termination (which is apparently diffusion-controlled) are reduced, but these effects are less important than the effect on chain growth. High pressures may also facilitate polymerization by increasing the thermodynamic ceiling temperature of the propagation reaction.

The object of the present work was to examine the effect of pressures up to 4000 atm. on the graft copolymerization of monomers with polyethylene and, in one case, polystyrene. The experiments included attempts to graft chloroethylenes onto polyethylene.

\* Present Address: Aysgarth Court, Sutton Common Rd., Sutton, Surrey, England.

## EXPERIMENTAL

### Materials

The substrates used for the reactions were low density polyethylene film 0.001 in. thick, free from antioxidant, and polystyrene film 0.002 in. thick. These materials were subjected to  $\gamma$ -radiation from a  $\text{Co}^{60}$  source in air to produce polymeric peroxides, after which they were stored for several weeks at room temperature to allow any free radical products in the amorphous regions to be destroyed. The radiation doses and dose rates were 8 Mrad at 0.09 Mrad/hr. for polyethylene and 58 Mrad at 0.155 Mrad/hr. for polystyrene. (The polystyrene was given a larger radiation dose because the  $G_R$  value for the initial radical formation, which leads to the formation of peroxides in air, is greater than that found with polyethylene.<sup>2</sup>)

Other reagents were commercial materials which were purified by standard techniques.

### Reactions

Conventional high pressure equipment, incorporating a hydraulic intensifier, was employed. About 0.13 g. of polyethylene film or 0.4 g. polystyrene film, and 5-6 ml. of monomer, were contained in a glass tube and pressure was transmitted to them via a mercury seal. The monomers styrene, methyl methacrylate, tetrachloroethylene, trichloroethylene, *cis*- and *trans*-dichloroethylene, and vinylidene chloride were each subjected to high pressure while in contact with irradiated polyethylene film. On removal from the reaction vessel the polyethylene film, which was not soluble in any of the monomers used under the experimental conditions, was extracted repeatedly with 1,2-epoxypropane to constant weight. After runs with styrene and methyl methacrylate, samples of the liquid phase were precipitated in methanol to isolate homopolymers.

High pressure experiments were also carried out with irradiated polystyrene film dissolved in vinyl acetate. As polystyrene is soluble in vinyl acetate, separation of the graft and homopolymers is more difficult. A mixture of irradiated polystyrene film and poly(vinyl acetate) homopolymer prepared at 2000 atm. and 60°C. was made up having the same composition as the product of the reaction at 2000 atm. described in Table III. It was found that almost complete separation of the two polymers could be achieved by precipitating the polystyrene from a solution of the polymer mixture in ethyl methyl ketone with three volumes of methanol. The products of the copolymerizations were treated in the same way. Further details are available elsewhere.<sup>3</sup>

## RESULTS AND DISCUSSION

The results of the above experiments together with those of controls carried out with nonirradiated films are given in Tables I-III.

### Characterization of Products

**Polyethylene Substrate.** The polyethylene films used in the experiments with styrene and methyl methacrylate showed large increases in weight, and the weights could not be reduced to their original values by prolonged extraction with 1,2-epoxypropane. Reprecipitation of the films from benzene also caused no significant change in their carbon content and it is concluded that graft copolymerisation had taken place. A comparable result to that obtained for grafting styrene onto irradiated polyethylene at 1 atm. was obtained by Ballantine et al.<sup>4</sup> These workers used a predose of 15.3 Mrad in air and obtained an hourly grafting rate of about 0.04 g./g. film at 53°C.

Some homopolymer was produced in the experiments with vinylidene chloride, and the films also increased in weight. However, successive

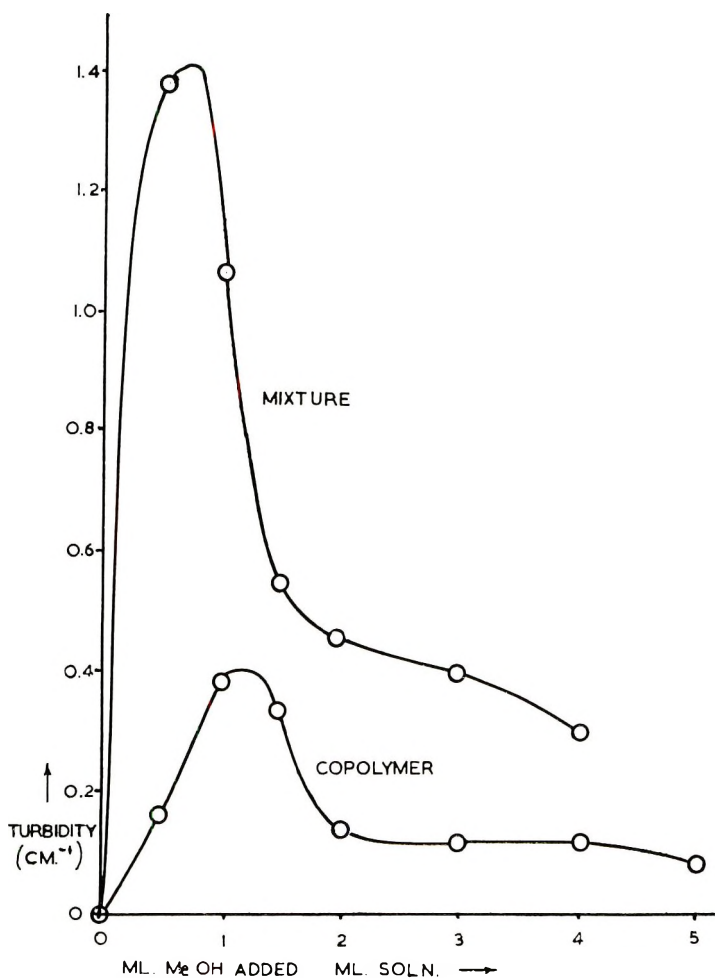


Fig. 1. Turbidities of solutions of vinyl acetate-polystyrene graft copolymer and a homopolymer mixture in ethyl methyl ketone solution on addition of methanol.

TABLE I  
Graft Copolymerization of Styrene onto Polyethylene at 60°C.

	Pressure, atm.	Time, hr.	Graft rate, g./g. hr. <sup>a</sup>	Homopolymer- ization rate, %/hr.
Irradiated substrate (predose 8 Mrad)	1	7	0.052	0.139
	1	17	0.070	0.199
	1000	5.5	0.276	0.386
	2000	3	0.626	0.890
	3000	1	1.2	1.9
	3000	1.5	1.1	1.3
	4000	0.67	0.77	3.3
	4000	1	0.67	2.9
Nonirradiated substrate	1	20.2	0.0036	0.149
	1000	18.3	0.0127	0.280
	1000	20.8	0.0146	0.284
	2000	21	0.0413	0.666
	3000	1.5	0.040	1.7
	3000	3.1	0.061	1.5
	3000	4.7	0.051	1.5
	4000	1	0.065	2.2
4000	2.8	0.044	2.5	

<sup>a</sup> Weight of monomer grafted onto unit weight of film per hour.

TABLE II  
Graft Copolymerization of Methyl Methacrylate onto Polyethylene at 60°C.

	Pressure, atm.	Time, hr.	Graft rate, g./g. hr. <sup>a</sup>	Homopolymer- ization rate, %/hr.
Irradiated substrate (predose 8 Mrad)	1	3.0	0.163	2.22
	1	1.0	Nil	Very low
	1	4.4	1.36	0.823
	1000	1.0	0.183	0.993
	1000	1.7	0.228	0.711
	1000	3.0	0.888	1.02
	2000	1.0	0.362	3.99
	2000	2.0	0.312	1.70
	3000	0.5	0.08	0.60
	3000	1.1	0.19	1.7
	3000	1.5	0.18	1.9
	4000	0.5	0.21	4.0
	4000	1.0	0.19	2.9
	Nonirradiated substrate	3000	0.5	Nil
3000		1.5	Nil	Nil
4000		3.0	Nil	Nil
4000		6.0	Nil	Nil

<sup>a</sup> Weight of monomer grafted onto unit weight of film per hour.

TABLE III  
Graft Copolymerization of Vinyl Acetate onto Irradiated Polystyrene at 60°C.

Pressure, atm.	Time, hr.	Wt. of monomer, g.	Wt. of film, g.	Total polymer, g.	Polymer in- soluble in MEK- MeOH, g.	Polymer- ization rate, %/hr.
1	47	5.828	0.4210	0.4355	0.3015	0.0053
2000	50	5.410	0.3909	0.5240	—	0.049
4000	22	5.390	0.3637	0.6451	Trace	0.24
8360 <sup>a</sup>	2	3.685	0.4092	0.6469	0.1838	3.22

<sup>a</sup> The temperature here was 68°C.

treatment with boiling methanolic potassium hydroxide, chlorine water and boiling methanol reduced the weights of the films to their original values, indicating that the poly(vinylidene chloride) was not chemically bound to the substrate. Films treated in the other chloroethylenes gave no evidence of grafting.

**Polystyrene Substrate.** The precipitation behavior of the polystyrene-vinyl acetate reaction products suggests that grafting has occurred. The figures in the fourth and sixth columns of Table III would be the same if the product were a mixture of homopolymers. Further evidence of graft copolymerization is given in Figure 1. In this the turbidities of a solution of the 2000 atm. grafted product in ethyl methyl ketone for successive additions of methanol is compared with turbidities of a physical mixture, in the same proportions, of irradiated polystyrene with poly(vinyl acetate) prepared at 2000 atm. and 60°C. The solubilizing effect of the grafted vinyl acetate on the polystyrene is apparent in Figure 1.

A second comparison between the 2000 atm. graft product and a physical mixture of the homopolymers was made by determining the Huggins constants of their solutions in benzene at 30°C. The value for the graft polymer was found to be 0.38 compared with 0.22 for the physical mixture with the same carbon content, 0.32 for the irradiated polystyrene alone, and 0.20 for the 2000 atm. vinyl acetate homopolymer. This marked difference in the solution properties indicates that a graft copolymerization has occurred.

Attempts to graft vinyl acetate onto polystyrene by polymerizing the monomer with benzoyl peroxide initiator in the presence of dissolved polystyrene have been unsuccessful.<sup>5,6</sup> This is probably due to the low reactivity of polystyryl radicals caused by resonance stabilization and the low reactivity of the vinyl acetate monomer, which gives rise to the very high (~55) reactivity ratio for styrene and the low (~0.01) value for vinyl acetate when these two monomers are copolymerized. When peroxidized polystyrene is used as substrate, resonance stabilization of the initiating radical does not occur, as the unpaired electron is not conjugated with the benzene ring. With this more reactive initiating species, grafting takes place at a measurable rate.



## Effect of Pressure

**Styrene-Polyethylene System.** The results of Table I are illustrated in Figure 2. The rate of homopolymer formation increases with pressure slightly more than in the benzoyl peroxide-initiated reaction, having an overall activation volume of around  $-20$  cc./mole compared with  $-18$  cc./mole. This may be because the activation volume for thermal initiation is less positive than for the peroxide-initiated reaction. The increase in the rate of homopolymerization at a given pressure when irradiated sub-

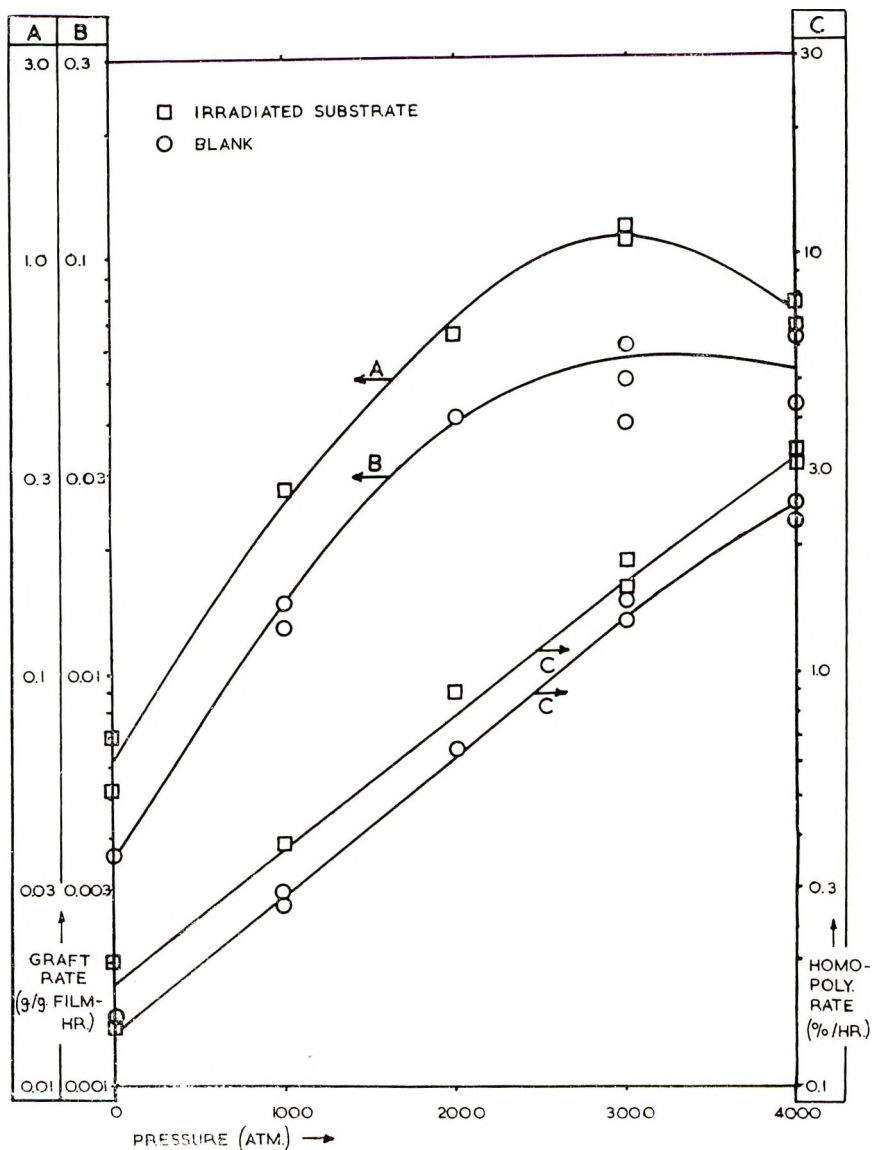


Fig. 2. Effect of pressure on the reaction of styrene with polyethylene at 60°C.

strate is used probably arises through monomer transfer from the growing graft copolymer radicals.<sup>7</sup>

The rate of grafting in the styrene-polyethylene system is approximately twenty times greater when irradiated substrate is used. The initial slope of the grafting rate versus pressure curves corresponds to an overall activation volume of about  $-35$  cc./mole, which is considerably higher than the range of values normally associated with liquid phase homopolymerizations. The value of  $\Delta V^\ddagger$  given here is probably affected by changes in the monomer's swelling power and hence its concentration in the substrate at different pressures. The decrease in the slope of the grafting rate curves at higher pressures until a negative slope is attained at pressures above 3000 atm. may be attributed to the effect of pressure on the propagation reaction so that the rate-controlling process changes from the chemical reaction to the diffusion of monomer through the substrate, a process which has a positive activation volume.

**Methyl Methacrylate-Polyethylene System.** This system yielded far less reproducible results than the above, (see Table II). A probable reason for this is that while styrene monomer swells polyethylene at 60°C., methyl methacrylate does not, so that if grafting does not occur on the surface of the substrate, and thus make it capable of imbibing more monomer, the monomer will not diffuse into the substrate to support further grafting in the manner suggested by Shinohara and Tomioka.<sup>8</sup> The results indicate that the grafting of methyl methacrylate onto the polyethylene is dependent upon local variations in the surface properties of the substrate, and this obscures the effect of pressure on the system.

**Chloroethylene-Polyethylene Systems.** Of the monomers vinylidene chloride, *cis*- and *trans*-dichloroethylene, trichloroethylene, and tetrachloroethylene only the first readily formed homopolymers, although the other monomers appeared to polymerize to some extent at high pressures. None of them formed graft copolymers with the polyethylene, although some runs were continued for 48 hr. at 5000 atm. The homopolymerization of vinylidene chloride was found to be accelerated by pressure.

**Vinyl Acetate-Polystyrene System.** The results of Table III show that the rate of polymerization of vinyl acetate in the presence of irradiated polystyrene increases considerably with pressure. There is no indication of a maximum in the grafting rate over the pressure range 1-8000 atm. This lends some support to the suggestion that the maximum in the two-phase system styrene-polyethylene is due to diffusion control.

One of us (J. A. L.) thanks the Department of Scientific and Industrial Research for the award of a Research Studentship during the tenure of which this work was carried out.

## References

1. Weale, K. E., *Quart. Revs.* **16**, 267 (1962).
2. Charlesby, A., *J. Polymer Sci.*, **11**, 513 (1953).
3. Lamb, J. A., Ph.D. Thesis, London University, 1961.

4. Ballantine, D., A. Glines, G. Adler, and D. J. Metz, *J. Polymer Sci.*, **34**, 419 (1959).
5. Smets, G., and M. Claisen, *J. Polymer Sci.*, **8**, 289 (1952).
6. Gaylord, N. G., *Interchem. Revs.*, **15**, 91 (1956-7).
7. Smets, G., *Pure Appl. Chem.*, **4**, 287 (1962).
8. Shinohara, Y., and K. Tomioka, *J. Polymer Sci.*, **44**, 195 (1960).

### Résumé

On a étudié à des pressions jusqu'à 8000 atm. les copolymérisations de monomères avec un substrat irradié antérieurement à l'air pour former des peroxydes polymériques. La vitesse de greffage pour le système styrolène-polyéthylène irradié augmente considérablement avec la pression jusqu'à 3000 atm. À des pressions plus élevées, la réaction est retardée. Ceci est dû au fait que la réaction de propagation devient elle-même contrôlée par la diffusion. La vitesse de l'homopolymérisation augmente exponentiellement avec la pression d'une à 4000 atm. Des résultats irreproductibles ont été obtenus en employant le méthacrylate de méthyle au lieu du styrolène, probablement parce que le substrat n'est pas gonflé dans ce monomère. On n'a pas observé de greffage entre cinq chloroéthylènes, et le polyéthylène irradié jusqu'à des pressions de 5000 atm. La vitesse de greffage dans le système homogène acétate de vinyle-polystyrène irradié augmente considérablement avec la pression jusqu'à 8.000 atm. et il n'y a aucune indication que la réaction de propagation soit contrôlée par la diffusion.

### Zusammenfassung

Einige Pfropfcopolymerisationsreaktionen von Monomeren mit vorher in Luft unter Bildung polymerer Peroxyde bestrahlten Substraten wurden bis zu Drucken von 8000 Atm untersucht. Im heterogenen System Styrol-bestrahltes Polyäthylen nimmt die Pfropfungsgeschwindigkeit mit steigendem Druck bis etwa 3000 Atm merklich zu. Bei höherem Druck wird die Reaktion verzögert. Dies wird der Diffusionskontrolle der Wachstumsreaktion zugeschrieben. Die Homopolymerisationsgeschwindigkeit nimmt im Bereich von 1 bis 4000 Atm exponentiell mit dem Druck zu. Die Verwendung von Methylmethacrylat statt Styrol führt zu nicht reproduzierbaren Ergebnissen, möglicherweise weil das Substrat in diesem Monomeren nicht quillt. Bei fünf verschiedenen chloersubstituierten Äthylenen tritt bis zu einem Druck von 5000 Atm keine Pfropfung auf bestrahltes Polyäthylen auf. Die Pfropfungsgeschwindigkeit im homogenen System Vinylacetat-bestrahltes Polystyrol nimmt mit steigendem Druck bis 8000 Atm merklich zu und es finden sich keine Hinweise auf eine Diffusionskontrolle der Wachstumsreaktion.

Received June 28, 1963

## Interaction of Poly(methacrylic Acid) and Bivalent Counterions. I

M. MANDEL and J. C. LEYTE, *Laboratorium voor Fysische Chemie der Rijksuniversiteit te Leiden, Netherlands*

### Synopsis

The calculation of formation curves of metal-polyacid complexes from titration curves is discussed. The interaction of bivalent ions of Cu, Cd, Zn, Ni, Co, and Mg with poly(methacrylic acid) is investigated by this method. These metals seem to form complexes involving two carboxylate groups for each ion in a large domain of pH values. Formation constants for these complexes are given which decrease according to the order indicated above.

### 1. INTRODUCTION

It has been shown that both poly(methacrylic acid)<sup>1-3</sup> (PMA) and poly(acrylic acid)<sup>1</sup> (PAA) form complexes with Cu(II) ions. Further, it has been stated<sup>2,3</sup> that the Cu-PMA chelate probably involves four carboxylate groups for every bound copper ion. This conclusion was drawn from spectrophotometric evidence in the visible and ultraviolet regions by a comparison of the Cu-PMA spectra with copper acetate spectra. In the visible region, it seems that an error was made in the interpretation of the copper acetate spectra, as may be seen on comparison of the cited source with the work of Klotz et al.<sup>5</sup> Regarding the ultraviolet region, the evidence was based on nonconclusive extrapolation from the measured absorption peaks of the acetate and the polymethacrylate (see appendix for detail).

On the other hand, for crosslinked copolymers of methacrylic acid and divinylbenzene, Gregor and co-workers<sup>1</sup> observed indications for the existence of a copper chelate involving two carboxylate groups.

Thus, from the published evidence, it is impossible to decide whether the copper (II) ion binds two or four carboxylate groups in the investigated concentration and pH regions.

The Cu-PMA complex and the interaction of PMA and some other bivalent ions was investigated by the present authors by means of potentiometric titrations.

For the interpretation of the potentiometric results the method of Gregor et al<sup>6</sup> was modified.

## 2. TRANSFORMATION OF TITRATION CURVES TO FORMATION CURVES

Gregor and co-workers<sup>6</sup> have shown that the method of Bjerrum for the evaluation of formation constants of complexes may be adapted to the specific characteristics of polyelectrolytes.

By defining a reaction which does not relate to any change of the charge on the polyion, Gregor uses an equilibrium constant which may be expected to be independent of the charge of the polymer. Thus the equilibrium



rather than



is chosen to describe the binding of  $M^+$  to the polyacid.

The successive formation of complexes of a central ion  $M$  of unspecified charge, and a singly charged ligand  $A$  related to the carboxylic acid group  $AH$  may be described with the help of equilibria analogous to eq. (1). The average coordination number  $\bar{j}$ , of the central ion may then be expressed as a function of  $[HA]$ ,  $[H^+]$ , and  $B_j$ , the last quantity being the overall stability constant for a complex involving  $j$  acid groups. The activity coefficients have been neglected throughout.

$$\bar{j} = \frac{\sum_{j=0}^{\infty} j B_j ([HA]/[H^+])^j}{\sum_{j=0}^{\infty} B_j ([HA]/[H^+])^j} \quad (3)$$

Here,  $B_0 = 1$  is introduced to achieve a compact formulation. If the successive equilibrium constants differ greatly, flat regions are observed in the formation curve that results from plotting  $\bar{j}$  against  $p([HA]/[H^+]) = -\log([HA]/[H^+])$ . Those parts of the formation curve having a low value of the slope of the curve correspond to regions in which one complex dominates. This may be concluded from the fact that the slope is proportional to the square of the standard deviation of  $j$ . If the formation curve exhibits such a wavelike shape, the equilibrium constants may be evaluated from the values of  $p([HA]/[H^+])$  at half integral values of  $\bar{j}$ . For example, the value of  $p([HA]/[H^+])$  at  $\bar{j} = 1$  is equal to  $1/2 \log B_2 = \log B_{av}$ , the logarithm of the average stability constant for a two-step process.

Another modification is introduced by Gregor in the calculation of  $\bar{j}$  from pH measurements. Consider a solution in which the total acid concentration (dissociated, undissociated and chelated) is  $[A_t]$  and the total concentration of metal ion  $[M_t]$ . Then  $\bar{j}$  is clearly given by

$$\bar{j} = ([A_t] - [HA] - [A])/[M_t] \quad (4)$$

The calculation of  $[A]$  presents a difficulty in the case of polyacids. Gregor and co-workers calculate  $[A]$  from the extended Henderson-Hasselbach equation:

$$pH = pK_a - n \log [(1 - \alpha)/\alpha] \quad (5)$$

which has been shown to give an empirical representation of the titration curve for many polyelectrolytes. Here,  $K_a$  and  $n$  are constants for a polyacid at a certain concentration and ionic strength while  $\alpha$  is the degree of dissociation of the polyacid. It is easily seen from eq. (5) that the  $\alpha$ -dependent part of the  $pK$ , which is defined as  $pH - \log [\alpha/(1 - \alpha)]$ , may be put equal to  $(n - 1) \log [\alpha/(1 - \alpha)]$ . From the assumption that the dependence of  $pK$  on  $\alpha$  has a principally electrostatic origin, it is a plausible step to interpret  $\alpha/(1 - \alpha)$  only as the ratio of charged and uncharged groups. Thus, if part of the carboxylic ions are bound to some metal ion,  $\alpha/(1 - \alpha)$  is replaced by  $[A]/([A_t] - [A])$ . The Henderson-Hasselbach equation for a polyacid in the presence of complexing ions then becomes:

$$\left( \frac{[A]}{[A_t] - [A]} \right)^{1-n} K_n = \frac{[H^+][A]}{[HA]} \quad (6)$$

If  $K_n$  and  $n$  are known for the titration curve in absence of the complexing ion,  $[A]$  may be calculated for a partially chelated polyacid by an iterative procedure from eq. (6) if  $[A_t]$ ,  $[HA]$ , and  $[H^+]$  are known.

In this method it is assumed, implicitly, that the interaction is between the metal ion and the individual carboxylate group (rather than with the polyion as a whole) and that this interaction always decreases the negative charge of the polyion. Further, it is assumed that the reaction of part of the carboxylic acid groups with metal ions does not influence the dissociation equilibrium of the other groups except by way of the charge of the polyion and by the occurring concentration changes. These assumptions, together with the omission of activity corrections, demand a cautious interpretation of the results that may be obtained with this transformation of potentiometric titrations.

In an investigation of the nature of the Cu(II)–PMA complex, Gregor's procedure for the calculation of  $[A]$  was used previously.<sup>7</sup> All results presented here, are, however, calculated by a more direct method.

The fact that in the described calculation of  $[A]$  use is made of an arbitrary, experimental representation of the titration behavior of a polyacid may give rise to the question whether the results of such a calculation will depend on the algebraic form of the Henderson-Hasselbach equation. As is known, other relations may be used to represent the experimental behavior of polyelectrolytes.<sup>3,9</sup>

Now, the essential assumption underlying the way the Henderson-Hasselbach equation is used here is that the  $\alpha$ -dependent portion of  $pK$  is only a function of the charge density of the polyion. Thus:

$$pK = G + \zeta_\alpha \quad (7)$$

where  $G$  is a constant and  $\zeta_\alpha$  a function depending on  $\alpha$ . Further

$$p([H^+]/[HA]) = G - p[A] + \zeta_\alpha \quad (8)$$

Equation (8) suggests the use of the following method to determine  $[A]$  in solutions where  $[H^+]$ ,  $[HA]$ , and  $[A_t]$  are known. A reference titration

curve of a polyacid (without complexing ion) is transformed to a plot of  $p([H^+]/[HA])$  against some function of  $[A]$ , for example,  $p[A]$ . After determination of  $p([H^+]/[HA])$  for a solution containing the same total amount of  $[A_t]$  and some salt, the concentration  $[A]$  in this solution may be conveniently found from the reference graph.

Thus this method uses the same physical basis as the former one without, however, depending on the algebraic form of the Henderson-Hasselbach equation. Further, the method is quicker and may be used in regions where the Henderson-Hasselbach equation does not represent the titration behavior adequately.

Some criticism has been directed<sup>10,11</sup> at Gregor's formulation of the association equilibrium of bivalent metal ions and polyacid molecules. Gregor defines an equilibrium constant:

$$B_2 = [MA_2][H^+]^2/[M][HA]^2 \quad (9)$$

It has been stated that the formulation of this constant is not consistent with the specific nature of polyacid solutions. Consider the formation of the chelate (both HA groups belong to the same polymer molecule) as a two step process. Then, for the first step, the overall concentration  $[HA]$  is the relevant quantity. The second step, it has been argued,<sup>10,11</sup> will occur independent of the overall concentration of carboxylic acid groups, as the central ion is already bound to the polymer chain and may, in fact, react with a neighboring group. Here, the local concentration should be used. It is assumed to be much larger than the overall concentration. Therefore, it has been proposed to formulate the second step as:



thus reducing the quadratic  $[HA]^2$  in eq. (9) to a linear factor. It seems however, that in the cited reasoning the argument has not been carried far enough. Although it may be accepted that the second step in the formation of the discussed chelate differs fundamentally from the first, the use of eq. (10) is not allowed as it violates the principle of conservation of mass. Instead, eq. (9) may be written:

$$B_2' = [MA_2][H^+]^2/[M][HA][HA'] \quad (11)$$

$[HA']$  reflects the different dependence on the concentration of carboxylic acid groups for the second step. It is useful to analyze  $[HA']$  in a qualitative way. Consider the central ion  $M$  bound to a reactive group  $A^i$  situated on a monomeric unit of an isolated polymer chain consisting of  $Z$  such units, each bearing a group  $A$ ,  $AM$ , or  $AH$ . Around  $AM^i$  we define a volume  $V$ , such that any group  $AH$  in  $V$  is within reacting distance of  $AM^i$ . Now, a distribution function  $f_i$  may be defined, giving the probability of the occurrence of any monomeric unit, other than the one on which  $AM^i$  is situated, within  $V$ . To a first approximation it may be further assumed that the distribution of  $AH$  groups is uniform; then the probability that

any monomeric unit bears a group AH is proportional to  $[AH]/[A_t]$ . Thus in the neighborhood of  $AM^+$  we have an effective concentration

$$[HA']^i = ([HA]/[A_t])f_i \quad (12)$$

If  $[HA']^i$  is averaged over all  $i$  we have

$$[HA'] = ([HA]/[A_t])f \quad (13)$$

where

$$f = \sum_{i=1}^z f_i/Z$$

If, to a first approximation, it is assumed that  $f_i$  does not depend on the density of  $AM$  groups along the chain, then  $f$  will also be independent of the degree of binding. From substituting eq. (13) into eq. (11) and comparing the result with eq. (9) it may be concluded that  $B_2 = B_2'f/[A_t]$ , which is a constant if no important changes in the dimensions of the polymer or in the total polymer concentration occur. Consequently Gregor's definition will be maintained hereafter.

A final remark concerning the adaption of Bjerrum's method to polyions is necessary. The value of  $j$  according to eq. (4) can only be calculated if it is assumed that the carboxylate groups that are bound to a chelating ion  $M^{2+}$  do not participate in the equilibrium between  $AH$  and  $A^-$ . This assumption is reasonable as long as the binding between  $A^-$  and  $M^+$  compensates the charge on the carboxylate groups, i.e., as long as the number of carboxylate groups bound per ion  $M^{2+}$  is smaller or equal to the total number of protonic charges borne by  $M^{2+}$ . It is not possible, however, to use this method when formation of complexes of the type  $M^{2+}(COO^-)_{2+i}$  ( $i > 0$ ) may occur as nothing can be said about the way in which these complexes may influence the dissociation equilibrium of the  $AH$  groups. Therefore when  $j$ , as calculated by eq. (4), becomes larger than 2, no definite conclusions may be drawn concerning the complexes existing under these circumstances.

### 3. THE PMA—Cu(II) SYSTEM

When the procedure which was outlined in the preceding section, is applied to study the interaction between PMA and bivalent metal ions, a complication arises. As has been shown elsewhere,<sup>7,8</sup> the potentiometric behavior of PMA may be discussed in terms of a configurational transition of the polyacid at low degrees of ionization ( $0.10 < \alpha < 0.30$ ). If the regions in which either or both structural forms exist may be assumed to depend only on the charge of the polyion, Gregor's method may be applied before and after the transition. As has already been indicated, the charge of the partly chelated polyion may be deduced from a reference titration curve (with the restrictions which have been mentioned), and this may be extended to the regions where the polyion exists completely in one of both



structural forms. This implies that the binding phenomena do not influence the region of  $\alpha$  values in which the transition occurs nor the conformation of the polyion after the transition. In the transition, however, the application of Gregor's method might be dangerous. Here, the general description of the reference curve may be written

$$p\left(\frac{[\text{H}^+]}{[\text{HA} + \text{HB}]}\right) = G' - p[\text{A} + \text{B}] + \zeta[\text{A} + \text{B}, \text{A}_t + \text{B}_t] + g\left[\frac{\text{A}}{\text{B}}, \frac{\text{A}_t}{\text{B}_t}\right] \quad (14)$$

Here A and B are used to represent the two conformational forms of PMA existing in equilibrium in the transition region. The last term of eq. (14) is introduced to account for the fact that  $p([\text{H}^+]/[\text{HA} + \text{HB}])$  is generally not determined by the total charge alone but also depends on the fractions of the polyacid in both forms and the degrees of dissociation of both forms.

From eq. (14) it may be seen that application of the procedure of section 2 in the transition region involves an extra assumption. In fact  $[\text{A} + \text{B}]$

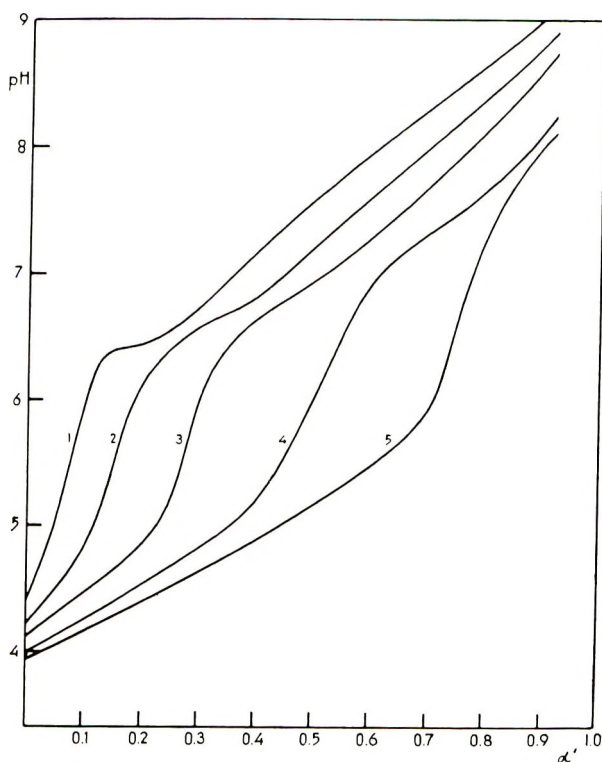


Fig. 1. Titration curves of PMA- $\text{Cu}(\text{NO}_3)_2$  solutions with sodium hydroxide at  $[\text{PMA}] = 1.73 \times 10^{-3}$  and varying  $[\text{Cu}(\text{NO}_3)_2]$ : (1) 0; (2)  $8.28 \times 10^{-5}M$ ; (3)  $2.07 \times 10^{-4}M$ ; (4)  $4.14 \times 10^{-4}M$ ; (5)  $6.21 \times 10^{-4}M$ .

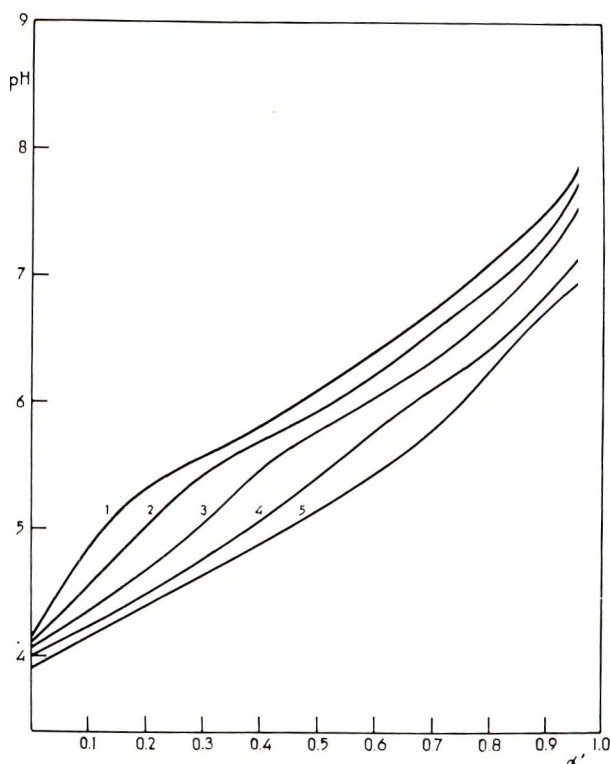


Fig. 2. Titration with sodium hydroxide of PMA- $\text{Cu}(\text{NO}_3)_2$  solutions in the presence of  $0.05M$   $\text{NaNO}_3$  and varying  $[\text{Cu}(\text{NO}_3)_2]$ : (1) 0; (2)  $8.28 \times 10^{-6}M$ ; (3)  $2.07 \times 10^{-4}M$ ; (4)  $4.14 \times 10^{-4}M$ ; (5)  $6.21 \times 10^{-4}M$ .

can only be determined with the help of the reference curve, eq. (14), if the binding of metal ions does not influence  $g[A/B, A_t/B_t]$ . This means that the binding of the metal ions by the polyacid should never interfere with the conformational transition of the polymer. As this may be a rather dangerous assumption the transition region of the reference curve will not be used here for the calculation of formation curves. Thus, only degrees of ionization which may be expected to fall outside the transition region ( $\alpha < 0.10$ ;  $\alpha > 0.30$ ) will be used to calculate the coordination numbers  $\bar{j}$ . This already involves the assumption that the transition takes place in approximately the same region of charge densities whether or not metal is bound.

In Figure 1 some titration curves of PMA with NaOH in the presence of several amounts of  $\text{Cu}(\text{NO}_3)_2$  are presented. It may be seen that the influence of  $\text{Cu}(\text{NO}_3)_2$  on the titration behavior of PMA differs greatly from that of salts like NaCl and  $\text{NaNO}_3$ . The depression of the titration curve and especially the dependence of the depressed region on the amount of  $\text{Cu}(\text{NO}_3)_2$  added indicates a specific binding of the copper ions to the PMA molecule. It is seen that the region in which the titration curve is depressed is roughly equivalent to the amount of  $\text{Cu}(\text{NO}_3)_2$  added.

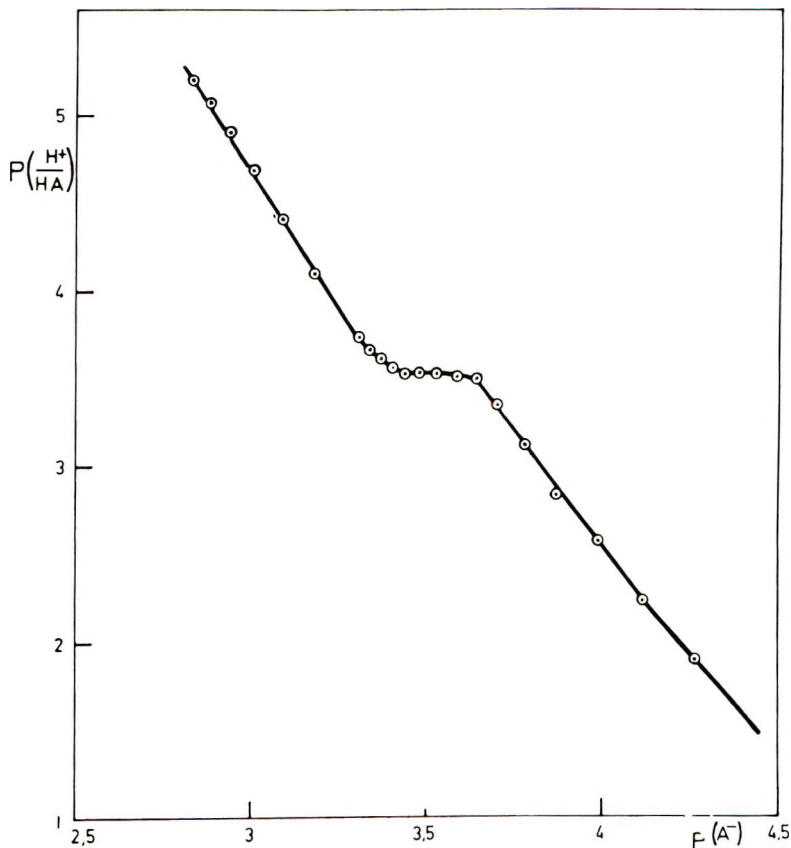


Fig. 3. Reference plot for calculation of formation curves,  $[PMA] = 1.73 \times 10^{-3}$  equiv./l.

Figure 2 demonstrates the persistence of the effect in the presence of sodium nitrate. Here, however, the effect is less visible. This may be ascribed to the lowering of the pH in the previously undepressed region of the curve. This lowering may be the result of the screening effect of the sodium nitrate on the electrostatic potential.

In Figure 3 a reference curve as defined by eq. (8) is shown. It consists of two more or less parallel parts separated by the transition region.

In Figures 4-9 formation curves of the Cu-PMA complex are given. These were calculated with the use of reference curves relating to equivalent PMA concentrations. For the transformation of titration curves of the PMA-Cu(NO<sub>3</sub>)<sub>2</sub> system in the presence of NaNO<sub>3</sub>, reference curves obtained with the same NaNO<sub>3</sub> concentration were used. In Figures 5 and 6 the uncertainty in the values of the mean coordination numbers is indicated to give an impression of the magnitude and variability of this uncertainty.

From, for example, Figure 4, it may be seen that points which were calculated from titration curves of PMA solutions, containing different amounts of Cu(NO<sub>3</sub>)<sub>2</sub>, conform to a common formation curve. No complex

with a coordination number equal to 1 seems to dominate over any appreciable  $p([\text{HA}]/[\text{H}^+])$  range. On the other hand, a two-coordinated complex seems to exist over a fairly large range of the variable. At low values of  $p([\text{HA}]/[\text{H}^+])$  this complex starts to disappear. From the formation

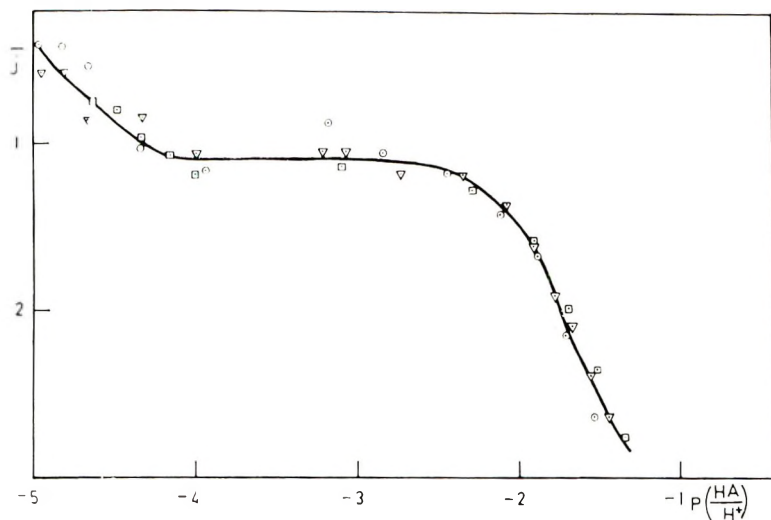


Fig. 4. Formation curve of copper-polymethacrylate at  $[\text{PMA}] = 2.78 \times 10^{-3}$  equiv./l. and varying  $[\text{Cu}(\text{NO}_3)_2]$ : (O)  $8.33 \times 10^{-5}M$ ; ( $\nabla$ )  $1.66 \times 10^{-5}M$ ; ( $\square$ )  $3.31 \times 10^{-4}M$ .

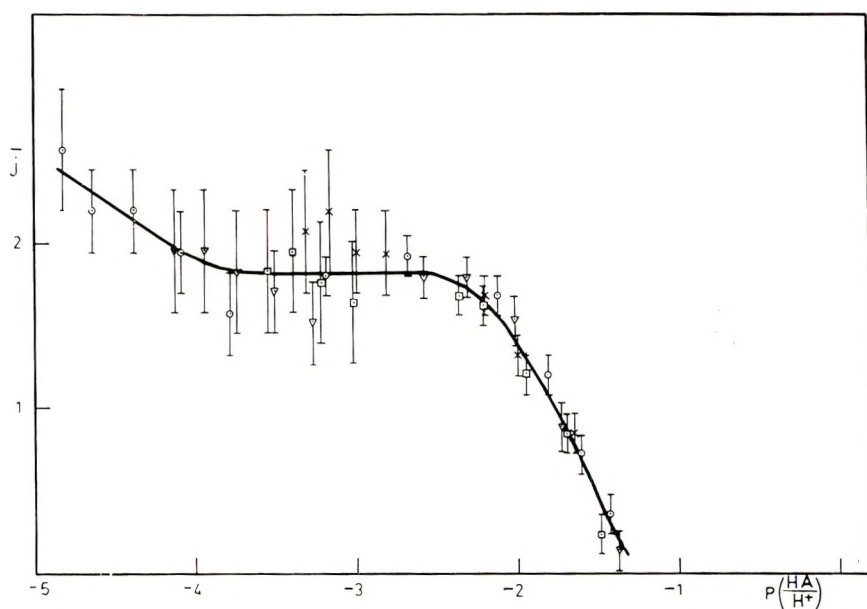


Fig. 5. Formation curves of copper-polymethacrylate at  $[\text{PMA}] = 1.73 \times 10^{-3}$  equiv./l.,  $[\text{Cu}(\text{NO}_3)_2] = 8.28 \times 10^{-5}M$ , and varying  $[\text{NaNO}_3]$ : (O) 0; ( $\nabla$ )  $0.01M$ ; ( $\square$ )  $0.05M$ ; ( $\times$ )  $0.1M$ .

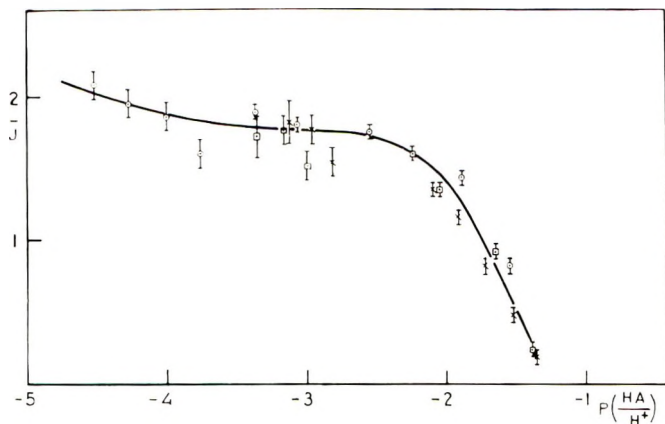


Fig. 6. Formation curve of copper-polymethacrylate at  $[PMA] = 1.73 \times 10^{-3}$  equiv./l.,  $[Cu(NO_3)_2] = 2.07 \times 10^{-4}M$ , and varying  $[NaNO_3]$ : (O) 0; (□) 0.05M; (X) 0.1M.

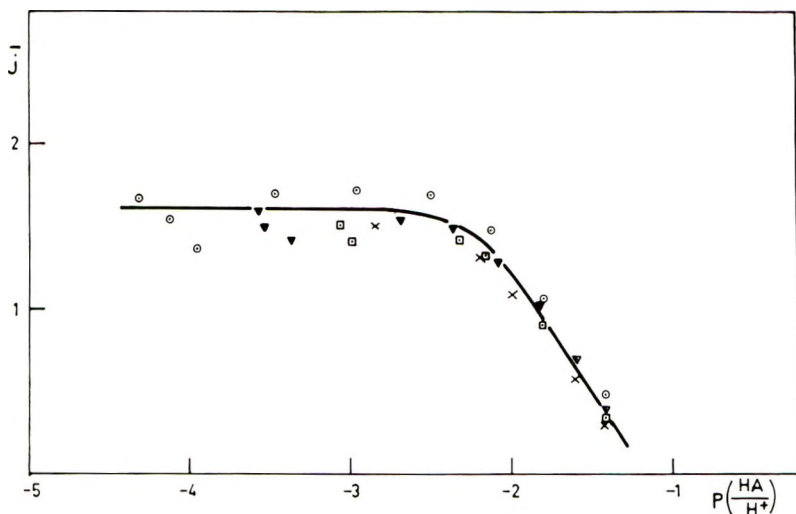


Fig. 7. Formation curve of copper-polymethacrylate at  $[PMA] = 1.73 \times 10^{-3}$  equiv./l.,  $[Cu(NO_3)_2] = 4.14 \times 10^{-4}M$ , and varying  $[NaNO_3]$ : (O) 0; (▽) 0.01M; (□) 0.05M; (X) 0.1M.

curve, no conclusion can be drawn as to the nature of the complex which replaces the two-coordinated one here. Also the disappearance of the complex always occurs in regions with charge densities corresponding to the conformationally transformed polymer, while the flat portion in the formation curves generally corresponds to low charge densities.

To investigate the influence of neutral electrolyte, formation curves have been evaluated from titration curves of PMA- $Cu(NO_3)_2$  solutions containing different amounts of sodium nitrate. Figures 5-8 present such formation curves for several  $Cu(NO_3)_2$  concentrations. These curves show

that in the presence of different amounts of sodium nitrate the calculated coordination numbers still conform to a common formation curve. In figure 8 the flat region of the formation curve falls outside the experimental region.

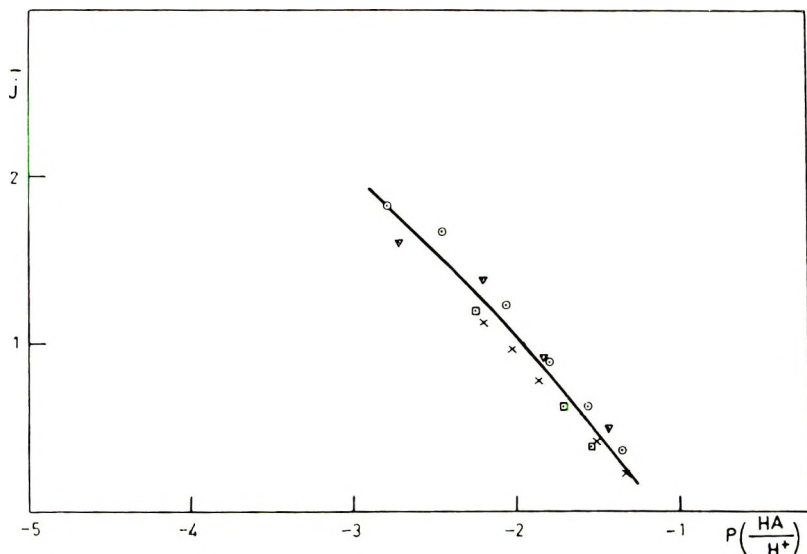


Fig. 8. Formation curve of copper-polymethacrylate at  $[PMA] = 1.73 \times 10^{-3}$  equiv./l.,  $[Cu(NO_3)_2] = 6.21 \times 10^{-4}M$ , and varying  $[NaNO_3]$ : (O) 0; ( $\nabla$ ) 0.01M; ( $\square$ ) 0.05M; ( $\times$ ) 0.1M.

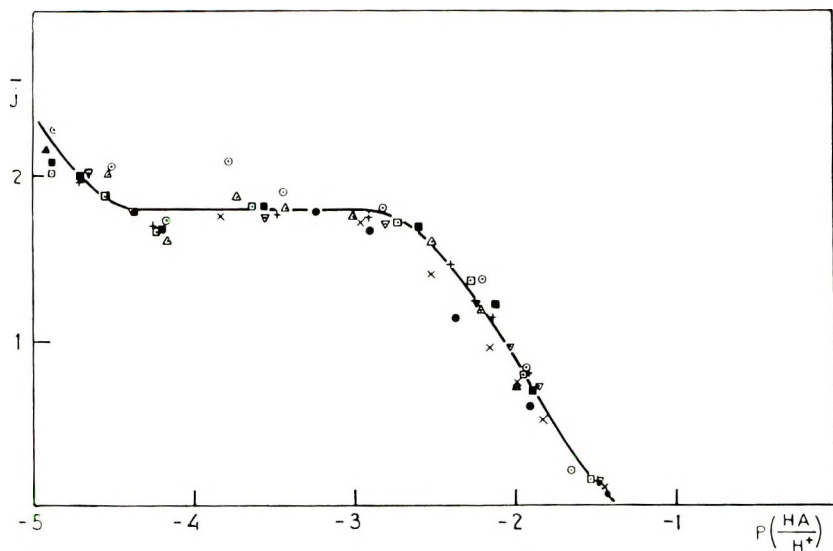


Fig. 9. Formation curve of copper-polymethacrylate at  $[PMA] = 1.197 \times 10^{-2}$  equiv./l., and varying  $[Cu(NO_3)_2]$ : ( $\Delta$ )  $4.14 \times 10^{-4}M$ ; (O)  $8.28 \times 10^{-4}M$ ; ( $\blacksquare$ )  $1.24 \times 10^{-3}M$ ; ( $\square$ )  $1.66 \times 10^{-3}M$ ; (+)  $2.08 \times 10^{-3}M$ ; ( $\nabla$ )  $2.51 \times 10^{-3}M$ ; ( $\times$ )  $3.31 \times 10^{-3}M$ ; ( $\bullet$ )  $4.14 \times 10^{-3}M$ .

TABLE I

Acid	Acid concn., equiv./l.	Cu(NO <sub>3</sub> ) <sub>2</sub> concn., mole/l.	NaNO <sub>3</sub> concn., mole/l.	log B <sub>av</sub>
PMA	$1.73 \times 10^{-3}$	$8.28 \times 10^{-5}$	(0-0.1)	-1.8
"	"	$2.07 \times 10^{-4}$	(0-0.1)	-1.8
"	"	$4.14 \times 10^{-4}$	(0-0.1)	-1.8
"	"	$6.21 \times 10^{-4}$	(0-0.1)	-1.9
"	$2.78 \times 10^{-3}$	$8.33 \times 10^{-5}$ - $3.31 \times 10^{-1}$	0	-1.8
"	$1.197 \times 10^{-2}$	$4.14 \times 10^{-4}$ - $4.14 \times 10^{-3}$	0	-2.1
PAA <sup>a</sup>	$10^{-2}$		0.2	-1.17
Malonic acid <sup>b</sup>	0		0	-1.46
Dimethylmalonic acid <sup>b</sup>	$10^{-3}$		0	-2.0
Glutaric acid <sup>a</sup>	$10^{-2}$		0.2	-2.8

<sup>a</sup> Data of Gregor.<sup>6</sup>

<sup>b</sup> Data of Martell and Calvin.<sup>12</sup>

From Table I it may be seen that  $p([HA]/[H^+])$  at  $\bar{j} = 1$  does not change much as a function of the copper concentration. For the highest copper concentration a small deviation may be observed. This is probably the result of the fact that the assumption that the binding phenomena only influence the hydrogen ion dissociation by way of the charge of the polyion is not valid at high copper concentrations. In fact, it is clear that this approximation will hold only if a relatively low number of carboxylic acid groups of the polyion is bound to copper ions.

For the highest PMA concentration investigated (Fig. 9), a small decrease in log B<sub>av</sub> may be observed with respect to the lower concentrations. This effect may be accounted for by the concentration dependence of B<sub>2</sub> which was discussed in the previous section.

As was mentioned before, the reference curves used relate to solutions which do not contain copper nitrate. Now it might be reasoned that, apart from its complex-forming tendencies, the copper nitrate also affects the titration curve by way of the ionic strength. On the one hand, the fact that  $\bar{j}$  values for solutions containing different amounts of sodium nitrate conform to a single formation curve indicates that the ionic strength of the copper nitrate is of secondary importance. On the other hand, the ionic strength of a PMA solution which is titrated with NaOH is not constant, and the binding phenomena in a PMA-Cu(NO<sub>3</sub>)<sub>2</sub> solution makes the estimate of an appropriate ionic strength difficult. For these reasons no correction is applied here. A correction procedure has been investigated however. Formation curves have been calculated using reference curves relating to PMA solutions to which an amount of NaNO<sub>3</sub> was added which was equivalent to the amount of Cu(NO<sub>3</sub>)<sub>2</sub> in the investigated solution. It was found that the portion of the formation curve relating to the transformed PMA is lowered without, however, changing the general shape of the curve.

As was pointed out the method of investigating complexes in solution applied here should be used with caution. Therefore it is important to confirm the principal result—the existence of a two-coordinated Cu(II)—PMA complex—by independent techniques. This was done, as will be reported in a subsequent communication.

#### 4. INTERACTION OF PMA AND Cd(II), Zn(II), Ni(II), Co(II), Mg(II)

In Figures 10–14 formation curves are given which were calculated in the same way as the curves for the Cu–PMA system. It is seen that, according to the formation curves, for all the investigated ions an appreciable region in which  $\bar{j} \approx 2$  is found. Except for Cd(II) and Zn(II), however, all points in the flat regions of these formation curves refer to charges on the polymer which fall in the region after the conformational transition in the pure

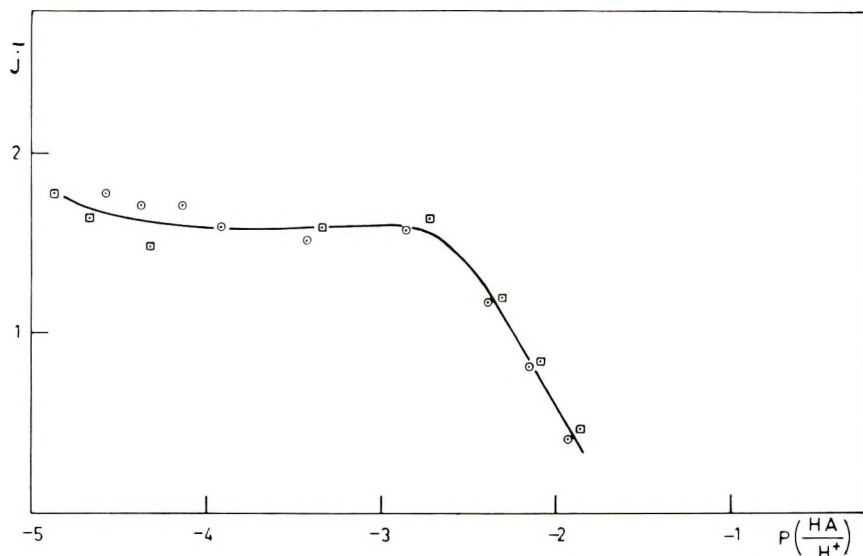


Fig. 10. Formation curve at [PMA]  $2.35 \times 10^{-3}$  equiv./l. and varying  $[\text{Cd}(\text{NO}_3)_2]$ : (O)  $1.72 \times 10^{-4}M$ ; (□)  $3.43 \times 10^{-4}M$ .

polyacid. As was pointed out before, calculations of  $\bar{j}$  in this region introduce an additional assumption. For this reason some doubt exists with respect to the region for which  $\bar{j} \approx 2$  for these ions. Irrespective of this,  $\log B_{av}$  may be found from these formation curves at  $\bar{j} = 1$ . The  $\log B_{av}$  values were determined for PMA concentrations of  $2.35 \times 10^{-3}$  equiv./l. except for  $\text{Cu}^{++}$ , where the PMA concentration was  $1.73 \times 10^{-3}$  equiv./l.

In Table II values of  $\log B_{av}$  are given. It is seen that all ions are bound less strongly by PMA than Cu(II), even if a correction is made for the difference in PMA concentrations. It is noted that the order of binding strength is:  $\text{Co(II)} < \text{Ni(II)} < \text{Cu(II)} > \text{Zn(II)}$ , as is usual for these ions.<sup>13</sup>



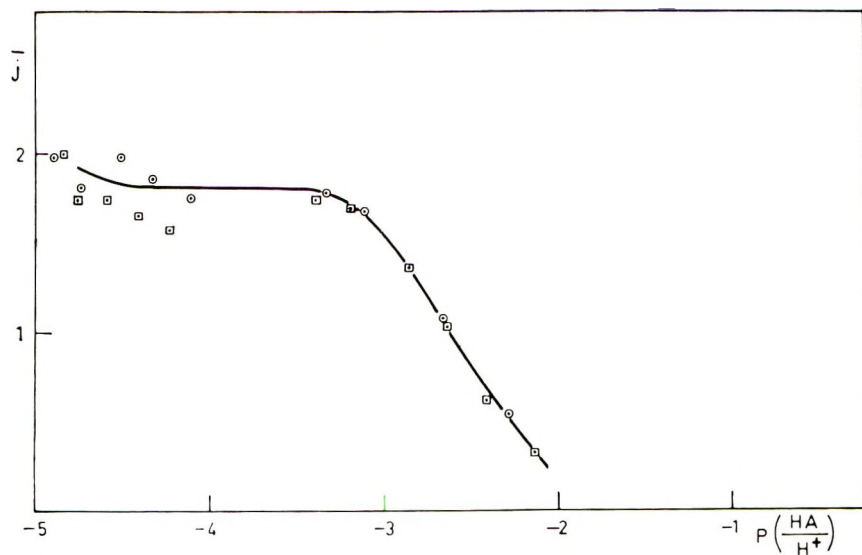


Fig. 11. Formation curve at  $[PMA] = 2.35 \times 10^{-3}$  equiv./l. and varying  $[Zn(NO_3)_2]$ : (O)  $1.85 \times 10^{-4}M$ ; (□)  $3.65 \times 10^{-4}M$ .

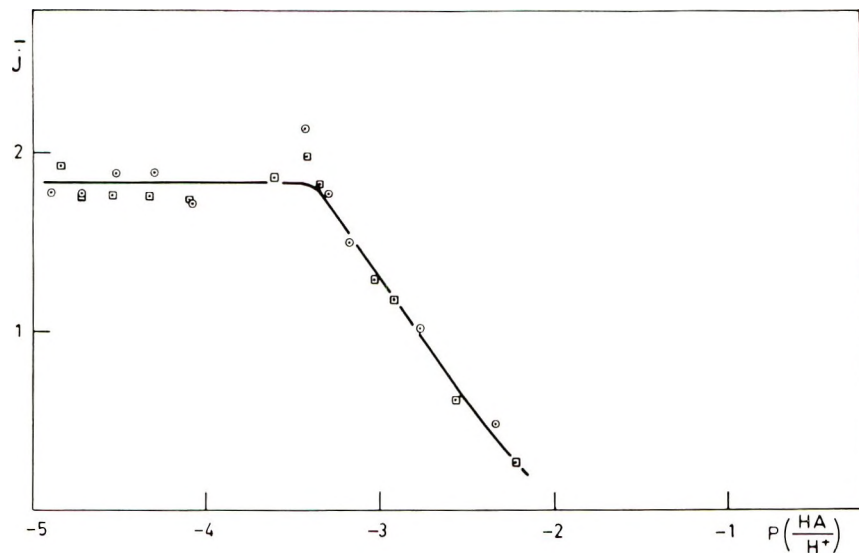


Fig. 12. Formation curve at  $[PMA] = 2.35 \times 10^{-3}$  equiv./l. and varying  $[Ni(NO_3)_2]$ : (O)  $1.88 \times 10^{-4}M$ ; (□)  $3.76 \times 10^{-4}M$ .

## 5. EXPERIMENTAL

### Materials

The molecular weight of the PMA used was  $8.7 \times 10^5$ . The synthesis and fractionation of the polymer are described elsewhere.<sup>7,8</sup>

TABLE II

Central ion	Concentration, mole/l.	$\log B_{av}$
Cu <sup>++</sup>		-1.8
Cd <sup>++</sup>	$1.72 \times 10^{-4}$ , $3.43 \times 10^{-4}$	-2.2
Zn <sup>++</sup>	$1.85 \times 10^{-4}$ , $3.70 \times 10^{-4}$	-2.6
Ni <sup>++</sup>	$1.88 \times 10^{-4}$ , $3.76 \times 10^{-4}$	-2.8
Co <sup>++</sup>	$1.82 \times 10^{-4}$ , $3.63 \times 10^{-4}$	-2.8 <sub>5</sub>
Mg <sup>++</sup>	$3.54 \times 10^{-4}$ , $7.07 \times 10^{-4}$	-3.1

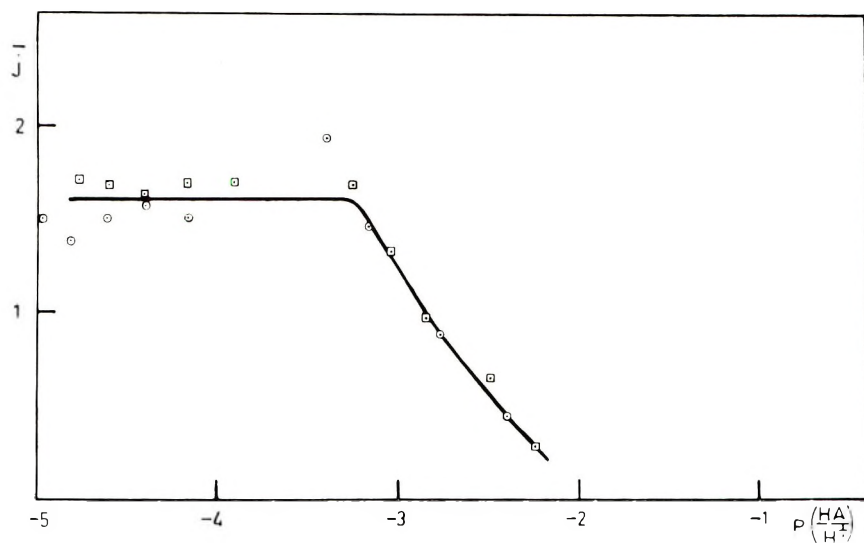


Fig. 13. Formation curve at  $[PMA] = 2.35 \times 10^{-3}$  equiv./l. and varying  $[Co(NO_3)_2]$ :  
 (O)  $1.82 \times 10^{-4}M$ ; (□)  $3.63 \times 10^{-4}M$ .

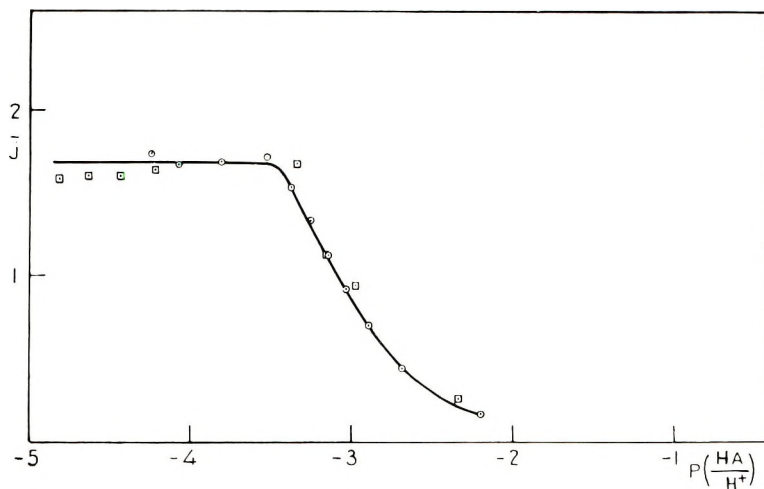


Fig. 14. Formation curve at  $[PMA] = 2.35 \times 10^{-3}$  equiv./l. and varying  $[Mg(NO_3)_2]$ :  
 (□)  $3.54 \times 10^{-4}M$ ; (O)  $7.07 \times 10^{-4}M$ .

The  $\text{Cu}(\text{NO}_3)_2$  solutions were obtained by dilution from a stock solution which was prepared by dissolving  $\text{Cu}(\text{NO}_3)_2$  (p.a. grade). The concentration of the stock solution was determined by electrolysis.

Sodium hydroxide solutions of 0.1 equiv./l. were obtained with the help of Fixanal ampullae. The usual precautions were taken to avoid contamination by carbonate. The concentration of the sodium hydroxide solutions was occasionally checked by titration of oxalic acid. It was always found that the NaOH concentration agreed with the nominal value.

The concentrations of the solutions of the nitrates of Mg, Zn, and Cd were determined by titration with the disodium salt of ethylenediaminetetraacetic acid (Titriplex III, Merck).<sup>14</sup> Eriochrome Black T (B. Siegfried) was used as indicator as a solution of 0.20 g. in 15 ml. triethanolamine and 5 ml. ethyl alcohol.

The solutions of the nitrates of Co and Ni were determined by back-titration of an added excess of Titriplex III with  $\text{Zn}(\text{NO}_3)_2$ .<sup>14</sup> Again Eriochrome Black T was used as indicator.

All duplicate titrations agreed within 0.5%.

$\text{Ni}(\text{NO}_3)_2$  and  $\text{Cd}(\text{NO}_3)_2$ , which could not be obtained in p.a. degree of purity, were recrystallized before use.

### Potentiometric Titrations

The potentiometric titrations were conducted with a Radiometer automatic titration apparatus as described before.<sup>7,8</sup>

## APPENDIX

The evidence for the formation of a Cu(II) chelate with four carboxylic groups of PMA has been advanced<sup>2,3</sup> on the basis of spectrophotometric results in the visible and ultraviolet regions.

**Visible Region.** Klotz et al.<sup>5</sup> are cited to have found that the absorption maximum of Cu(II) acetate solutions shifts from 770 to 750 and 730  $m\mu$  as the Cu(II) ion binds one, two, or three acetate groups. As the Cu(II)-PMA system absorbs with a maximum at about 700  $m\mu$ , this is interpreted as an indication that a copper chelate involving four carboxylate groups of PMA is formed over a wide range of conditions.

Comparison with the publication of Klotz,<sup>5</sup> however, shows that the order of the absorption maxima is 720 and 750  $m\mu$  for the acetates involving three and two acetate groups, respectively. This invalidates the mentioned interpretation.

**Ultraviolet Region.** Here evidence was advanced for the existence of a four-coordinated Cu(II)-PMA complex by comparing ultraviolet spectra of Cu(II) acetate, Cu(II)-PMA and Cu(II)-PAA solutions.

Although no evidence is given by Klotz<sup>5</sup> or by Morawetz<sup>2,3</sup> for the existence of a four-coordinated copper acetate under experimental conditions used, the existence of this complex was assumed and the absorption

maximum of this hypothetical complex was estimated with the help of a formation constant which was arbitrarily calculated from the constants for the one-, two-, and three-coordinated complexes.

On the other hand, the estimation of the position for the absorption peak of the four-coordinated copper acetate complex from the peaks of Cu-PMA and Cu-PAA solutions has not been carefully justified. Therefore the interpretation of the absorption curves as was done by the author, is not conclusive for the existing of a four-coordinated Cu-PMA complex. Using as another arbitrary hypothesis the absence of this four-coordinated complex, the same absorption curves could be interpreted as well.

### References

1. Gregor, H. P., L. B. Luttinger, and E. M. Loebel, *J. Phys. Chem.*, **59**, 366 (1955).
2. Kotliar, A. M., and H. Morawetz, *J. Am. Chem. Soc.*, **77**, 3692 (1955).
3. Morawetz, H., *J. Polymer Sci.*, **17**, 442 (1955).
4. Wall, F. T., and S. J. Gill, *J. Phys. Chem.*, **58**, 1128 (1954).
5. Klotz, J. M., J. L. Faller, and J. M. Urquhart, *J. Phys. Colloid Chem.*, **54**, 19 (1950).
6. Gregor, H. P., L. B. Luttinger, and E. M. Loebel, *J. Phys. Chem.*, **59**, 34 (1955).
7. Leyte, J. C., Thesis, Leiden, 1961; M. Mandel and J. C. Leyte, *J. Polymer Sci.*, **56**, S25 (1962).
8. Leyte, J. C., and M. Mandel, *J. Polymer Sci.*, **A2**, 1879 (1964).
9. Arnold, R., *J. Colloid Sci.*, **12**, 549 (1957).
10. Morawetz, H., *J. Polymer Sci.*, **23**, 247 (1957).
11. Zubay, G., *J. Phys. Chem.*, **61**, 377 (1957).
12. Martell, A. E., and M. Calvin, *Die Chemie der Metallchelateverbindungen*, Verlag Chemie, Weinheim 1958.
13. Irving, H. M. N. H., *International Conference on Coordinate Chemistry*, **1959**, Chemical Society Special Publication No. 13, London, 1959.
14. Schwarzenbach, G., *Die komplexometrische Titration*, F. Enke Verlag, Stuttgart, 1960.

### Résumé

On discute du calcul des courbes de formation des complexes métal-polyacide à partir des courbes de titration. On a étudié au moyen de cette méthode l'interaction entre les ions bivalents du Cu, Cd, Zn, Ni, Co et Mg et l'acide polyméthacrylique. Ces métaux semblent former des complexes impliquant deux groupements carboxylates pour chaque ion dans un large domaine de valeurs de pH. On donne les constantes de formation de ces complexes: elles décroissent suivant l'ordre indiqué ci-dessus.

### Zusammenfassung

Die Berechnung der Bildungskurven von Metall-Polysäure-Komplexen aus Titrationskurven wird diskutiert. Mittels dieser Methode wurde die Wechselwirkung der zweiwertigen Ionen von Cu, Cd, Zn, Ni, Co und Mg mit Polymethacrylsäure untersucht. Diese Metalle bilden offenbar in einem weiten pH-Bereich Komplexe unter Beteiligung zweier Carboxylatgruppen pro Ion. Die Bildungskonstanten dieser Komplexe werden angegeben. Sie nehmen in der oben dargestellten Reihenfolge ab.

Received July 1, 1963

## Vinyl Polymerization. LXXIX. Effect of the Alkyl Group on the Radical Polymerization of Alkyl Methacrylates

TAKAYUKI OTSU, TOSHIO ITO, and MINORU IMOTO,  
*Faculty of Engineering, Osaka City University, Osaka, Japan*

### Synopsis

The effect of the alkyl group on the rates of polymerization of alkyl methacrylates initiated by  $\alpha, \alpha'$ -azobisisobutyronitrile in benzene at 60°C. has been investigated. The rate of polymerization increased with increasing length of the alkyl group. This has already been attributed to the increased steric effect of the alkyl group in the termination process. In the present study, it was proved that the viscosities of alkyl methacrylate monomers increased with increasing length of the alkyl group, and that overall polymerization rate constants were inversely proportional to the viscosities. Accordingly, the above result might be explained by an increase in the contribution of the diffusion-controlled termination with increasing length of the alkyl group in alkyl methacrylate.

### INTRODUCTION

The effect of the alkyl group on the reactivity of alkyl methacrylate monomers in their radical copolymerizations has been investigated by many workers.<sup>1-3</sup> However, no detailed study of its effect on the rate of radical polymerization has appeared in the literature. In 1953, Burnett, Evans, and Melville<sup>1</sup> concluded that the propagation rate constant remains constant with increasing length of the alkyl (ester) group in alkyl methacrylate, whereas the termination rate constant decreases as the result of the increased steric effect of the alkyl group.

In the other hand, it is widely known that the termination in radical polymerizations of some alkyl acrylates<sup>4</sup> and methacrylates<sup>5</sup> is diffusion-controlled. Since the viscosities of alkyl methacrylate monomers increase with the number of carbon atoms in their alkyl groups, it might be possible to explain the results of Burnett and co-workers<sup>1</sup> for the series of alkyl methacrylates on the basis of the diffusion-controlled termination. More recently, North and Reed<sup>6</sup> have reported that the termination in polymerization of *n*-butyl, isobutyl, and nonyl methacrylates is diffusion-controlled. In the present paper, we prepare various kinds of alkyl methacrylates and deal with the effect of the alkyl group on the rate of their radical polymerizations.

In a previous paper,<sup>7</sup> we reported the steric effect of the endo- or exo-bornyl group on the rate and the reactivity of radical polymerizations of

bornyl (endo-bornyl) methacrylate (BMA) and isobornyl (exo-bornyl) methacrylate (IBMA), and found that the exo-bornyl group in IBMA showed a somewhat increased steric effect. The present paper will also discuss this point.

## EXPERIMENTAL

### Materials

Methyl methacrylate (supplied by Nihon Gas Co. Ltd.), and ethyl methacrylate, *n*-butyl methacrylate, and isobutyl methacrylate (supplied by Fujikura Kasei Co. Ltd.), were distilled twice in a stream of nitrogen under reduced pressure. The middle fraction was collected. Other alkyl methacrylates were synthesized by the alcoholysis of methyl methacrylate with corresponding alcohols and then distilled similarly. Boiling points and refractive indexes of all alkyl methacrylate monomers were in good agreement with the reported values. Viscosity of the 40 vol.-% monomer solution in benzene, which was the same as that of the polymerization mixture, was determined at 30°C. in an Ostwald viscometer.

$\alpha, \alpha'$ -Azobisisobutyronitrile (AIBN) was purified by recrystallization twice from ethanol. Benzene and other reagents were purified by usual methods.

### Polymerization Procedure

All polymerizations of alkyl methacrylates were carried out in sealed glass tubes at constant concentrations of monomer (40 vol.-% in benzene) and AIBN ( $5.5 \times 10^{-3}$  mole/l.) at 60°C. A solution of the monomer (4 ml.) and benzene (6 ml.) containing AIBN was charged into a polymerization tube which was degassed under vacuum by the usual freezing and thawing technique and then sealed off. Polymerizations were carried out with shaking the tube in a thermostat maintained at 60°C. After a given time, the tube was opened and the contents poured into a large amount of methanol to precipitate the polymer. Conversion was calculated from the weight of dry polymer obtained.

## RESULTS AND DISCUSSION

Time-conversion relations for radical polymerization of alkyl methacrylates in benzene initiated by AIBN at 60°C. are shown in Figure 1. As can be seen from this figure, the time-conversion relations for all monomers except *n*-octyl methacrylate showed straight lines up to 20% conversion with no induction period.

The rates of polymerization  $R_p$  were computed from the slopes of these straight lines. The results are shown in Table I. It is observed that  $R_p$  (or  $k$  values) increase with the number of carbon atoms of the alkyl group in alkyl methacrylates.

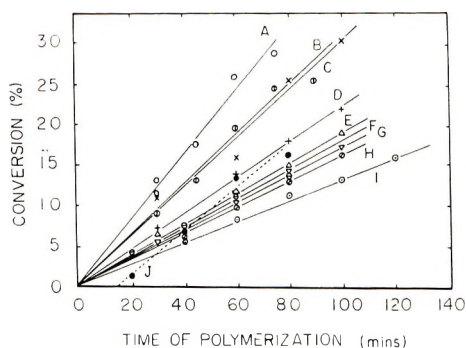


Fig. 1. Time-conversion relations for the polymerization of alkyl methacrylates at 60°C.,  $[AIBN] = 5.5 \times 10^{-3}$  mole/l.,  $[M] = 40$  vol.-% in benzene: (A) BMA: (B) IBMA: (C) CHMA: (D) *i*-AMA: (E) *n*-PMA: (F) *n*-BMA: (G) *s*-BMA: (H) EMA: (I) MMA: (J) *n*-OMA.

Although in the present work the rate equations for all monomers were not determined, several investigators derived the following rate eqs. (1) and (2) for radical polymerizations of some alkyl methacrylates:

For MMA,<sup>10</sup> *i*-BMA,<sup>9</sup> *n*-BMA<sup>9</sup>:

$$R_p = k[AIBN]^{0.5}[RMA]^{1.0} \quad (1)$$

for BMA,<sup>7</sup> IBMA<sup>7</sup>:

$$R_p = k[AIBN]^{0.5}[RMA]^{1.1} \quad (2)$$

where RMA stands for alkyl methacrylate and  $k$  is the overall polymerization rate constant, as given by eq. (3)

$$k = k_p(k_{df}/k_p)^{1/2} \quad (3)$$

TABLE I  
Kinetic Constants for the Polymerizations of Alkyl Methacrylates at 60°C.;  $[M] = 40$  vol.-% in Benzene

Monomer	R in monomer	Viscosity, cpoise	$R_p$ , %/hr. <sup>a</sup>	$k \times 10^4$	$k_p/k_t^{1/2}$
MMA	Methyl	0.527	8.3(8.8)	3.15(3.28) <sup>b</sup>	0.103(0.108) <sup>b</sup>
EMA	Ethyl	0.544	10.0(8.6)	3.54	0.116
<i>n</i> -PMA	<i>n</i> -Propyl	0.567	12.6(8.4)	4.02	0.132
<i>n</i> -BMA	<i>n</i> -Butyl	0.606	11.0(7.6)	4.06(4.41) <sup>c</sup>	0.134(0.145) <sup>c</sup>
<i>i</i> -BMA	<i>i</i> -Butyl	0.602		(4.61) <sup>c</sup>	(0.151) <sup>c</sup>
<i>s</i> -BMA	<i>sec</i> -Butyl	0.594	10.0(7.0)	3.76	0.123
<i>i</i> -AMA	<i>i</i> -Amyl	0.627	14.2(8.9)	5.26	0.173
CHMA	Cyclohexyl	0.806	17.0(11.7)	6.91	0.227
<i>n</i> -OMA	<i>n</i> -Octyl	0.770	15.6(8)	(6.0)	0.197
BMA	Bornyl	0.943	24.3(12.0)	8.71	0.286
IBMA	Isobornyl	0.943	18.3(9.2)	6.63	0.217

<sup>a</sup> Values in parentheses indicate  $R_p$  in units of mole/l. sec.  $\times 10^3$ .

<sup>b</sup> Data of Tobolsky and Mesrobian.<sup>8</sup>

<sup>c</sup> Data of Nair and Muthana.<sup>9</sup>

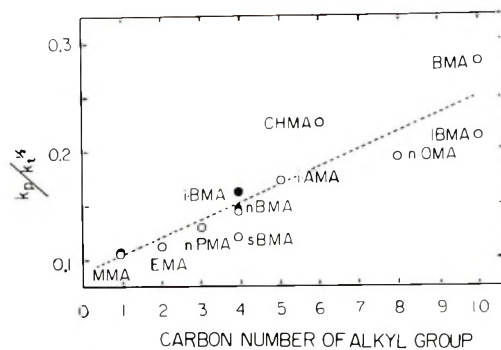


Fig. 2. Relationship between rate constant ratio ( $k_p/k_t^{1/2}$ ) and the number of carbon atoms in the alkyl group in alkyl methacrylates.

where  $k_d$ ,  $k_p$ , and  $k_t$  are rate constants for decomposition of AIBN, propagation, and termination, respectively, and  $f$  is the efficiency of initiator. By assuming that the rate equation, eq. (1), holds for other monomers and  $k_d = 1.33 \times 10^{-5} \text{ sec.}^{-1}$ ,  $f = 0.7$ , values of  $k_p/k_t^{1/2}$  for all monomers were calculated, as also shown in Table I.

Figure 2 shows the relationship between values of  $k_p/k_t^{1/2}$  for alkyl methacrylates and the number of carbon atoms in the alkyl group. As clearly seen from this figure, values of  $k_p/k_t^{1/2}$  for the series of alkyl methacrylates increase with increasing number of carbon atoms of the alkyl group.

Recently, in radical polymerization of alkyl methacrylates (MMA, *n*-PMA, *n*-BMA, and *t*-BMA), it was reported that  $k_p$  was kept constant, while  $k_t$  decreased with increasing of the carbon number in their alkyl group,<sup>1</sup> as shown in Table II.<sup>1,2,12-14</sup> Accordingly, it might be possible to explain the present results on the basis of an increase of the steric effect of the alkyl group.

TABLE II  
Rate Constants for Radical Polymerization of Alkyl Methacrylates

Monomer	Temp., °C.	$k_p$	$k_t \times 10^{-6}$	Reference
MMA	22.5	384	44	12
MMA	24	310	66	13
MMA	24	513	47	14
MMA	50	580	69	13
<i>n</i> -PMA	30	467	45	1
<i>n</i> -BMA	30	362	10	1
<i>t</i> -BMA	25	350	14	2

However, since the viscosities of alkyl methacrylates increase with increasing number of carbon atoms in the alkyl group as shown in Table I, a decrease in  $k_t$  may be explained by the diffusion-controlled termination. Recently, North and co-workers<sup>4-6,11</sup> reported that the termination in radical polymerization of methyl methacrylate was diffusion-controlled



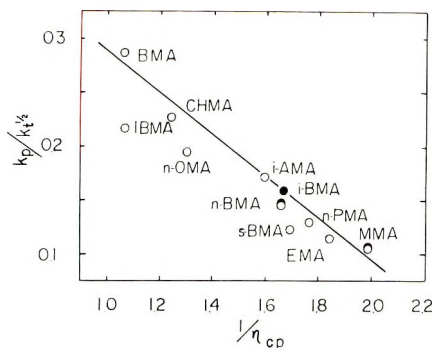


Fig. 3. Relationship between the rate constant ratio ( $k_p/k_t^{1/2}$ ) and the reciprocal viscosities of alkyl methacrylate-benzene solutions.

even in the initial stage of the polymerization and that the apparent termination rate constant was inversely proportional to the viscosity of the polymerization mixture.

Values of  $k_p/k_t^{1/2}$  obtained in the present work were plotted against the reciprocal viscosity of the polymerization mixture. The results are shown in Figure 3. It is clear that the translational diffusion-controlled termination in these radical polymerization becomes important with the increase in the number of carbon atoms of the alkyl group. Recently, in our laboratory, similar results were observed for the termination rate constants in radical polymerizations of *p*-substituted styrenes having  $\text{OCH}_3$ ,  $\text{CH}_3$ , F, Cl, Br, and CN groups;<sup>15</sup> their propagation rate constants are expressed by Hammett equation, while termination rate constants are inversely proportional to the viscosity of their monomers. Accordingly, it might be concluded that the contribution of such diffusion-controlled termination might not be eliminated in comparison with the rate constants for the series of the monomers which have similar structure.

In the previous paper,<sup>7</sup> we reported that the endo-bornyl group in BMA showed the same electric and steric effects as the methyl group, while the exo-bornyl group in IBMA showed a somewhat increased steric effect, even in the propagation process. In Figure 3, the value of  $k_p/k_t^{1/2}$  for BMA is located on the straight line, while that for IBMA deviates. This result might be also supported by our previous conclusion that the steric interaction of the exo-bornyl group is involved in the propagation process in the radical polymerization of BMA.

## References

1. Burnett, G. M., P. Evans, and H. W. Melville, *Trans. Faraday Soc.*, **49**, 1096, 1105 (1953).
2. Grant, D. H., and N. Grassie, *Trans. Faraday Soc.*, **55**, 1042 (1959).
3. Cameron, G. G., D. H. Grant, and N. Grassie, *J. Polymer Sci.*, **36**, 173 (1959).
4. Benson, S. W., and A. M. North, *J. Am. Chem. Soc.*, **81**, 1339 (1959).
5. North, A. M., and G. A. Reed, *Trans. Faraday Soc.*, **57**, 859 (1961).
6. North, A. M., and G. A. Reed, *J. Polymer Sci.*, **A1**, 1311 (1963).

7. Imoto, M., T. Otsu, K. Tsuda, and T. Ito, *J. Polymer Sci.*, **A2**, 1407 (1964).
8. Tobolsky, A. V., and R. B. Mesrobian, *J. Polymer Sci.*, **8**, 527 (1952).
9. Nair, A. S., and M. S. Muthana, *Makromol. Chem.*, **47**, 114 (1961).
10. Bamford, C. H., W. G. Barb, A. D. Jenkins, and P. F. Onyon, *The Kinetics of Vinyl Polymerization by Radical Mechanisms*, Butterworth, London, 1958, p. 76.
11. Benson, S. W., and A. M. North, *J. Am. Chem. Soc.*, **84**, 935 (1962).
12. Hyden, P., and H. W. Melville, *J. Polymer Sci.*, **43**, 201 (1960).
13. Mackay, M. H., and H. W. Melville, *Trans. Faraday Soc.*, **45**, 323 (1949).
14. Chinmayanadam, B. R., and H. W. Melville, *Trans. Faraday Soc.*, **50**, 73 (1954).
15. Kinoshita, M., and M. Imoto, paper presented at the 11th Meeting of the Society of High Polymers of Japan, November 1962; *Preprints*, p. 229.

### Résumé

On a étudié l'influence du groupe alcoyle sur la vitesse de polymérisation de méthacrylate d'alcoyle initiée par l'azobisisobutyronitrile à 60°C dans le benzène. La vitesse de polymérisation (%/hr) augmente en fonction de la longueur du groupe alcoyle. Ceci est dû à l'augmentation de l'effet stérique du groupe alcoyle dans le processus de terminaison. Le présent travail prouve que la viscosité des monomères de méthacrylate d'alcoyle augmente en fonction de la longueur du groupe alcoyle et que les constantes de vitesse de la polymérisation globale sont proportionnelles à leur viscosité. Le résultat obtenu peut être expliqué par l'importance croissante d'une réaction de terminaison contrôlée par la diffusion en fonction de la longueur du groupe alcoyle dans le méthacrylate d'alcoyle.

### Zusammenfassung

Der Einfluss der Alkylgruppe auf die Geschwindigkeit der mit  $\alpha, \alpha$ -Azobisisobutyronitril gestarteten Polymerisation von Alkylmethacrylaten in Benzol bei 60°C wurde untersucht. Die Polymerisationsgeschwindigkeit (%/Std.) nimmt bei Verlängerung der Alkylgruppe zu. Dies wurde früher durch den erhöhten sterischen Effekt der Alkylgruppe in der Abbruchreaktion erklärt. In der vorliegenden Arbeit wird gezeigt, dass die Viskosität der Alkylmethacrylatmonomeren bei Verlängerung der Alkylgruppe zunimmt und dass die Bruttopolymerisationsgeschwindigkeitskonstante dieser Viskosität umgekehrt proportional ist. Dementsprechend könnten die obigen Befunde durch eine Zunahme des Anteils der Diffusionskontrolle beim Abbruch durch Verlängerung der Alkylgruppe in Alkylmethacrylaten erklärt werden.

Received June 18, 1963

Revised July 16, 1963

## Some Aspects of the Photosensitivity of Poly(vinyl Cinnamate)

MINORU TSUDA, *Government Chemical Industrial Research Institute,  
Tokyo, Hiratsuka, Kanagawa, Japan*

### Synopsis

A theoretical investigation of the relationships between the photosensitivity of poly(vinyl cinnamate) and various factors—the degree of esterification, the average molecular weight, and the concentration of sensitizers—was made under the assumption that the main response of the polymer to light is the production of crosslinking by the dimerization of cinnamoyl groups. The obtained equations are  $S = k_{16}C^2$  for the degree of esterification,  $S = k_{22}\bar{M}$  for the average molecular weight, and  $S = k_{33}(1 - e^{-k_{31}c}) + k_{34}$  for the concentration of sensitizers, where  $S$  is the photosensitivity of the polymer,  $C$  is the degree of esterification,  $\bar{M}$  is the average molecular weight,  $c$  is the concentration of sensitizers, and  $k_{ij}$  is a constant. It was shown that these equations agree well with the experimental data obtained by other authors.

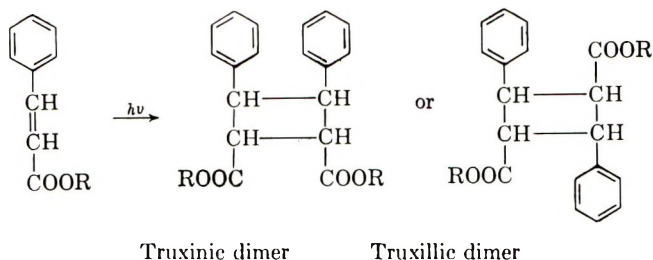
### 1. Introduction

Ultraviolet light irradiation of poly(vinyl cinnamate) reduces the solubility of the polymer according to the dose of light. This phenomenon has its application in the use of the polymer as a photosensitive resin.<sup>1</sup> Many experimental studies<sup>1-3</sup> were made on the photosensitivity of poly(vinyl cinnamate), but the interpretations of the experimental results were not satisfactory, and the mechanism of the photosensitivity of poly(vinyl cinnamate) remains obscure. This report contains the results obtained from theoretical investigations in which the dimerization of cinnamoyl groups was considered to be the main reaction occurring in the ultraviolet light irradiation of poly(vinyl cinnamate). These results agree well with the experimental results reported by other authors;<sup>1,3,4</sup> therefore, this may be considered to be at least one interpretation of the photosensitivity of poly(vinyl cinnamate).

### 2. Reaction Mechanism

The main response of cinnamic acid and its esters to photons is believed to be dimerization.<sup>5,6</sup> The response of cinnamoyl groups attached to polymer may not differ from the case of the low molecular weight substances. Indirect evidence of the mechanism, confirming the disappearance of the double bond from poly(vinyl cinnamate) in ultraviolet light irradiation, was obtained by infrared spectroscopy.<sup>7</sup> The dimerization of cinnamoyl

groups attached to a polymer molecule means the production of the cross-links in the polymer; the occurrence of crosslinking is followed by the insolubilization of the polymer.



The photosensitivity value  $S$  of photosensitive resins is defined as the reciprocal of the smallest dose  $\Delta E$  of energy of incident light required to insolubilize the polymer in a solvent under a standard set of conditions.<sup>1,3</sup> Thus, where  $k$  is a constant,

$$S = k/\Delta E \quad (1)$$

A polymer solution was coated on a glass plate or a paper printing plate and dried. A strip of this coating was exposed through a step tablet to the light in order to give a satisfactory image. The image was developed by rocking the exposed film in a tray immersed in a solvent for the polymer, drying, and inking. Ink is accepted by those areas covered by polymer and rejected elsewhere. The exposure time for the step midway between complete acceptance and complete rejection is proportional to  $\Delta E$ .<sup>1</sup> In another sensitometric method, the exposure time required to give the gel point was measured by extrapolating a series of gel fraction data which were obtained by weighing the glass strip produced by the same way as that stated above. (An exposure was made without a step tablet.)<sup>3</sup> The data obtained by these different methods may be considered to have the same meaning.

The dimerization reaction occurring is considered a topochemical reaction, because the polymer coating of poly(vinyl cinnamate) is dried. Many pairs of cinnamoyl groups adjacent may exist to be ready to dimerize in the coating. If the incident light is absorbed by such a pair of groups, dimerization will occur. Now we consider a small part  $dB$  of the coating and a number  $dA$  of pairs of cinnamoyl groups ready for dimerization in  $dB$ . In the process of coating the polymer may take any of the configurations; therefore, the production of the pairs is proportional to the number of combinations of two cinnamoyl groups belonging to different polymer molecules.

### 3. Effect of Degree of Esterification on the Photo-Response of Poly(vinyl Cinnamate)

The only variable is the content  $C$  of cinnamoyl groups of the polymer; other conditions, such as the molecular weight distribution, mean molecu-

lar weights, etc., are the same. The dispersion of cinnamoyl groups combined with polymers may be uniform. Therefore, for  $dA$ ,  $dB$  as defined above,

$$dA/dB = k_{11}C^2 \quad (2)$$

where  $k_{11}$  is a constant.

The number  $dy$  of dimerizations produced by a fixed dose  $dE$  of incident light is proportional to the number of pairs of cinnamoyl groups ready for dimerization. Thus, where  $k_{12}$  is a constant.

$$dy/dE = k_{12}dA/dB \quad (3)$$

Since the occurrence of one dimerization is followed by the consumption of two cinnamoyl groups,

$$dy/dE = -2dC/dE \quad (4)$$

Combining eqs. (2), (3), and (4) we obtain,

$$-dC/dE = k_{13}C^2 \quad (5)$$

where  $k_{13}$  is a constant. Integrating eq. (5), we obtain

$$E = (1/k_{13})(1/C) + k_{14} \quad (6)$$

where  $k_{14}$  is an integration constant. As discussed above, the dimerization involves crosslinking of the polymer. According to Charlesby<sup>8,9</sup> the number of crosslinks per molecule required to insolubilize polymer is a constant; and the value per the weight-average molecular weight is always one independent of the molecular weight distribution. We write here  $\Delta y$  for the number of crosslinks required to insolubilize poly(vinyl cinnamate) and  $\Delta E$  for the dose of light required to produce  $\Delta y$ .

Thus, from eq. (6)

$$\begin{aligned} \Delta E &= \frac{1}{k_{13}} \left( \frac{1}{c - 2\Delta y} - \frac{1}{C} \right) \\ &= \frac{1}{k_{13}} \frac{2\Delta y}{C(C - 2\Delta y)} \end{aligned} \quad (7)$$

where  $C \gg 2\Delta y$ , because the degree of polymerization of an ordinary photosensitive poly(vinyl cinnamate) is 1000-2000. Although the content of cinnamoyl groups is 10 mole-%,  $\Delta y$  is very small as compared with the number of cinnamoyl groups, since  $\Delta y$  is smaller than unity for the number-average molecular weight.<sup>8,9</sup>  $2\Delta y$  was used because one dimerization consumes two cinnamoyl groups. With those considerations, we obtain,

$$\Delta E = (1/k_{13})(2\Delta y/C^2) \quad (8)$$

Since  $2\Delta y/k_{13}$  is constant,

$$\Delta E = (1/k_{16})(1/C^2) \quad (9)$$

Combining eqs. (1) and (9), we obtain

$$\begin{aligned} S &= k k_{16} C^2 \\ &= k_{16} C^2 \end{aligned}$$

where

$$k_{16} = k k_{15} \quad (10)$$

Equation (10) expresses the relationship between the photosensitivity of poly(vinyl cinnamate) and its content of cinnamoyl groups. A graphical interpretation of this relation is given in Fig. 1.

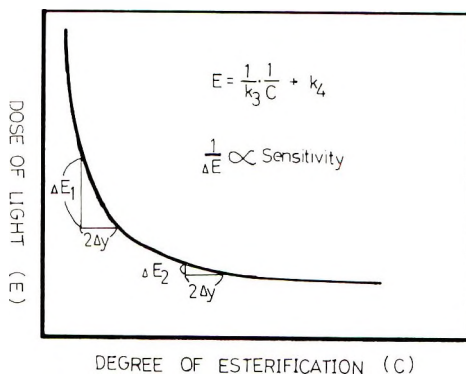
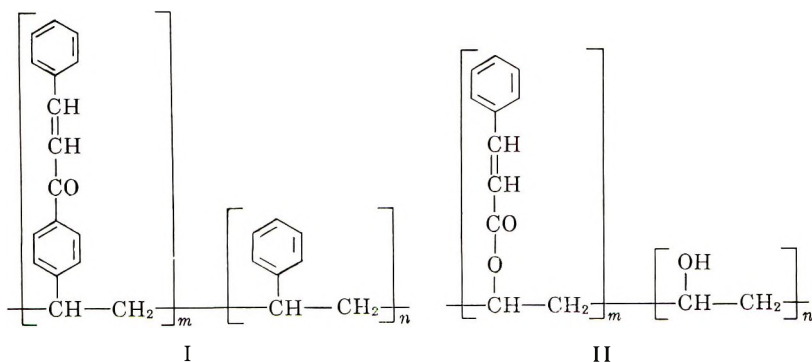


Fig. 1. A graphical interpretation of the relationship between the photosensitivity and the degree of esterification. A larger dose of light is required in order to produce the same amount of crosslinking in the region of the smaller content of cinnamoyl groups.

No experimental data have yet been obtained on the relationship between the photosensitivity of poly(vinyl cinnamate) and its cinnamoyl content. The reason is that poly(vinyl cinnamate) changes its solubility in a given developing solvent according to the cinnamoyl content, since the solubility characteristics of its components, vinyl cinnamate and vinyl alcohol, are extremely different; therefore, direct comparisons of partially esterified members in the same conditions are impossible.



Experimental results on poly(vinyl benzalacetophenone) (I) which is chemically similar to poly(vinyl cinnamate) (II), have been reported.<sup>4</sup>

Poly(vinyl benzalacetophenone) changes its solubility characteristics only slightly with its cinnamoyl content since its components, vinyl benzalacetophenone and styrene, have similar solubility characteristics. The chemical reaction produced by incident light may be the same in both cases of poly(vinyl cinnamate) and poly(vinyl benzalacetophenone), because their photosensitive groups have the same chemical structure. The results

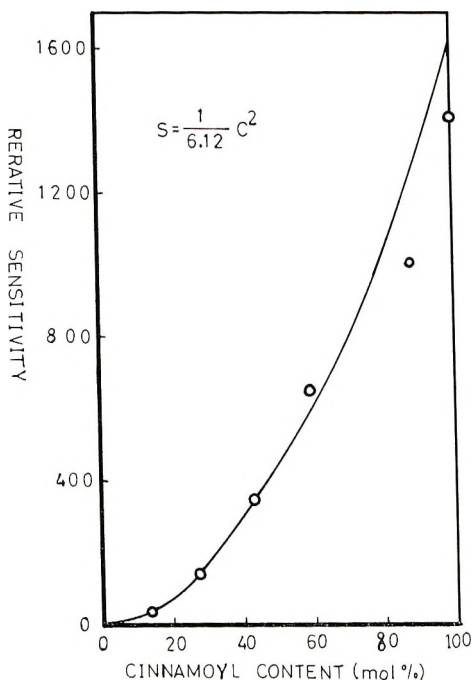


Fig. 2. Comparison between (—) theoretical curve and (O) experimental results<sup>4</sup> in the relationship between the photosensitivity and the content of cinnamoyl groups.

on the relationship between the mole fraction of polymerized vinyl benzalacetophenone units in the polymer and the photosensitometric response should, therefore, give fairly representative sensitometric data of the cinnamoyl-containing photosensitive polymers.<sup>4</sup>

The application of eq. (10) to the experimental data gives a better agreement than the straight line in the original paper<sup>4</sup> (Fig. 2).

#### 4. Effect of Molecular Weight on Sensitivity

The molecular weight of poly(vinyl cinnamate) may not affect the number  $dA$  of pairs of cinnamoyl groups ready for dimerization in a distinctive small part  $dB$ . The effect of the molecular weight is in the number  $n$  of  $dB$  which one polymer molecule, in the meaning of the average molecular

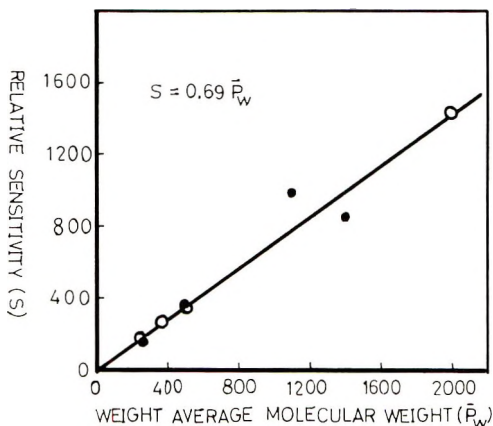


Fig. 3. Comparison between (—) theoretical curve and experimental results<sup>3</sup> in the relationship between the photosensitivity and the weight-average molecular weight: (O) 2,5-dinitrofluorene and (●) 5-nitroacenaphthene used as the sensitizers. The molecular weight was expressed by degree of polymerization.

weight, can occupy. The higher the molecular weight, the more the number of  $dB$  may be.

$$\bar{M} \propto n dB \quad (11)$$

If a fixed dose  $\Delta E$  of light is given each of the distinctive part  $dB$ , the probability of crosslinking  $P_{dB}$ , is equal in each part  $dB$ , and  $P_{dB}$  is proportional to the accepted energy in  $dB$ .

$$P_{dB} \propto \Delta E \cdot dB \quad (12)$$

The probability  $P_m$  of crosslinking of one molecule is proportional to the number  $n$  of  $dB$  which the molecule occupies, and  $P_{dB}$ .

$$P_m = n P_{dB} \quad P_m = n P_{dB} \quad (13)$$

The number  $\Delta y$  of crosslinks required to insolubilize<sup>2,3</sup> polymers is a constant per molecule for a given average molecular weight as discussed in section 3, which means that  $P_m$  is constant. Combining eqs. (11), (12), and (13) we obtain,

$$P_m = k_{21} \Delta E \bar{M} \quad (14)$$

where  $k_{21}$  is a constant. From eqs. (1) and (14)

$$\begin{aligned} S &= k / \Delta E = \frac{k k_{21}}{P_m} \bar{M} \\ &= k_{22} \bar{M} \end{aligned}$$

where

$$k_{22} = \frac{k k_{21}}{P_m} \quad (15)$$



Equation (15) expresses the relationship between the average molecular weight and the sensitivity of poly(vinyl cinnamate).

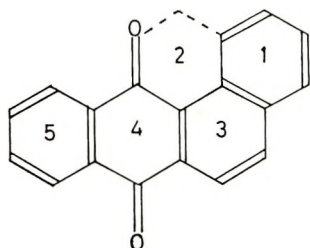
The experimental data have already been obtained on this problem.<sup>3</sup> The agreement between the theoretical result and the experimental data is satisfactory (Fig. 3).

### 5. Effect of Concentration of Sensitizer on Sensitivity

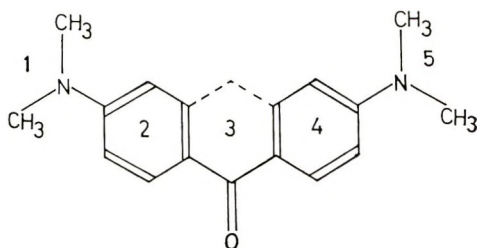
The photosensitivity of poly(vinyl cinnamate) increases on addition of various sensitizers.<sup>1,2</sup> The consideration that the addition of sensitizers does not change the number  $dA$  of a pair of cinnamoyl groups ready for dimerization and the area  $ndB$  occupied by one molecule of the polymer may be reasonable. The effect of sensitizers may be to increase the value of the constant  $k_{12}$  in eq. (3), the quantum efficiency.

There are two main causes for the increase in quantum efficiency; namely, the extension of the wavelength useful for photodimerizations by the sensitizer's absorption of light (optical sensitization) and the increase of the utilization of the absorbed energy at the same wavelength (chemical sensitization). The spectrograms of pure poly(vinyl cinnamate) and its combinations with various sensitizers showed that the effect of sensitizers involves the former only.<sup>2</sup>

The light absorbed by sensitizers is transferred to cinnamoyl groups, and then the cinnamoyl groups dimerize. There are three main steps in this process; namely, the absorption of light by sensitizers, the transfer of energy from the sensitizers to cinnamoyl groups, and the dimerization of cinnamoyl groups. A remarkable feature in the relationship between the concentration of a sensitizer and the sensitivity of the polymer is the experimental fact that the addition of ca. 10 wt.-% of a sensitizer to the polymer brings it to a limiting value of the sensitivity.<sup>1,3</sup> The molecular ratio of cinnamoyl groups to sensitizer is 16.32:1 in the case of Michler's ketone<sup>1</sup> and 14.81:1 in the case of 1,2-benzanthraquinone.<sup>3</sup> If the transfer of energy is the rate-determining stage, the higher concentration has to be more effective, because the transfer of energy may most effectively occur through the point of direct contact of sensitizer molecule and cinnamoyl group. Michler's ketone and 1,2-benzanthraquinone have planar structures, and the area occupied by each of these molecules is nearly equal.



1,2-benzanthraquinone



Michler's ketone

( $-\text{N}$  and  $-\text{CH}_3$  do not have plain structures.) The area occupied is as large as that of five benzene rings. The area of Michler's ketone is a little larger than that of 1,2-benzanthraquinone because of the spread of methyl groups. These considerations make us think that the rate-determining stage may be the absorption of light. The limiting value is attained when the entire area of the coating is occupied by the specific number of layers of sensitizer molecules. From this we can derive an equation which expresses the relationships between the concentration of sensitizers and the sensitivity of the polymer.

The intensity  $dI$  absorbed by small amounts  $dc$  of sensitizer molecules may be proportional to  $dc$  and the intensity  $I$  of the light attained by the sensitizer molecules.

$$dI = -k_{31}I dc \quad (16)$$

where  $k_{31}$  is the absorption coefficient of the sensitizer over the entire range of wavelengths effective for the dimerization of cinnamoyl groups. Integrating eq. (16) and rearranging, we obtain

$$I = I_0 e^{-k_{31}c}$$

where  $I_0$  is the intensity of the incident light. The energy absorbed by sensitizers is

$$\begin{aligned} \Delta\epsilon &= (I_0 - I)\Delta t \\ &= I_0\Delta t(1 - e^{-k_{31}c}) \end{aligned} \quad (17)$$

where  $\Delta t$  is the time of irradiation. Since  $\Delta E$  in the eq. (1) is the energy of the incident light,

$$\Delta E = I_0\Delta t \quad (18)$$

$$S = k/\Delta E \quad (19)$$

$$= (k/\Delta\epsilon)(1 - e^{-k_{31}c})$$

And where  $k_{32}$  is the efficiency of the absorbed light used for the dimerization of cinnamoyl groups, the net energy  $k_{32}\Delta\epsilon$  required for the production of the fixed number  $\Delta y$  of the dimerization is a constant; therefore,

$$S = k_{33}(1 - e^{-k_{31}c}) \quad (20)$$

$$k_{33} = k/\Delta\epsilon \quad (21)$$

When the incident light contains the wavelength for the inherent absorption of poly(vinyl cinnamate), the inherent sensitivity  $k_{34}$  is in the absence of sensitizers; so,

$$S = k_{33}(1 - e^{-k_{31}c}) + k_{34} \quad (22)$$

Equation (22) expresses the relationship between the concentration of sensitizers and the sensitivity of poly(vinyl cinnamate) containing them.

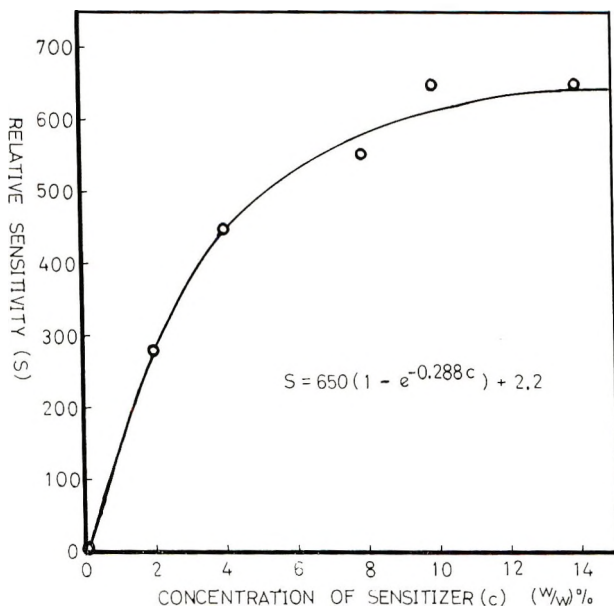


Fig. 4. Comparison between (—) theoretical curve and (O) experimental results<sup>1</sup> in the relationship between the photosensitivity and the concentration of sensitizer.

Equation (22) agrees well with the experimental data.<sup>1,3</sup> An example is shown in Figure 4.

It is supposed that the concentration of a sensitizer required for the saturation of the sensitivity may not always be 10 wt.-%, since  $k_{31}$  in eq. (22) is the absorption coefficient of the sensitizer. The concentration will depend on the absorbability of the sensitizer, which decides the number of the layers of sensitizer molecules required for the saturation.

### References

1. Minsk, L. M., J. G. Smith, W. P. Van Deusen, and J. F. Wright, *J. Appl. Polymer Sci.*, **2**, 302 (1959).
2. Robertson, E. M., W. P. Van Deusen, and L. M. Minsk, *J. Appl. Polymer Sci.*, **2**, 308 (1959).
3. Yoshinaga, T., Y. Chien, and S. Kikuchi, *Kogyo Kagaku Zasshi*, **66**, 665 (1963).
4. Unruh, C. C., *J. Appl. Polymer Sci.*, **2**, 358 (1959).
5. Stobbe, H., *Ber.*, **52B**, 666 (1919).
6. Mustafa, A., *Chem. Revs.*, **51**, 1 (1952).
7. Inami, A., and K. Morimoto, *Kogyo Kagaku Zasshi*, **65**, 293 (1962).
8. Charlesby, A., *Proc. Roy. Soc. (London)*, **A222**, 60, 542 (1954).
9. Charlesby, A., and S. H. Pinner, *Proc. Roy. Soc. (London)*, **A249**, 367 (1959).

### Résumé

Etudes théoriques sur la relation entre la photo-sensibilité de l'éther polyvinylique de l'acide cinnamique et les facteurs divers—le degré d'éthérisation, le poids moléculaire moyen, et la concentration des sensibilisateurs—ont été faites en supposant que le réponse principale du polymère vis-à-vis de la lumière est la formation de ponts par dimérisation des groupes cinnamoyles. Les équations obtenues sont  $S = k_{16}C^2$

pour le degré d'éthérisation,  $S = k_{22}\bar{M}$  pour le poids moléculaire moyen, et  $S = k_{33}(1 - e^{-k_{31}c}) + k_{34}$  pour la concentration en sensibilisateurs, où  $S$  est la photo-sensibilité du polymère,  $C$  le degré d'éthérisation,  $\bar{M}$  le poids moléculaire moyen,  $c$  la concentration des sensibilisateurs et  $k_{ij}$  est une constante. Il a été montré que les équations susdites sont bien d'accord avec les résultats expérimentaux qui sont obtenus par les autres auteurs.

### Zusammenfassung

Eine theoretische Untersuchung der Beziehung zwischen der Photosensibilität von Poly(vinyl cinnamat) und einigen Faktoren—dem Veresterungsgrad, dem mittleren Molekulargewicht und der Sensibilisatorkonzentration—wurde durchgeführt. Es wurde angenommen, dass die hauptsächlichste Lichtreaktion des Polymeren die Bildung von Vernetzungen durch Dimerisation der Cinnamoylgruppen ist. Die erhaltenen Formeln sind  $S = k_{16}C^2$  für den Veresterungsgrad,  $S = k_{22}\bar{M}$  für das mittlere Molekulargewicht und  $S = k_{33}(1 - e^{-k_{31}c}) + k_{34}$  für die Sensibilisatorkonzentration, worin  $S$  die Photosensibilität des Polymeren,  $C$  der Veresterungsgrad,  $\bar{M}$  das mittlere Molekulargewicht,  $c$  die Sensibilisatorkonzentration und  $k_{ij}$  eine Konstante ist. Es wurde gezeigt, dass die Formeln mit den Versuchsergebnissen anderer Autoren übereinstimmen.

Received July 8, 1963

## Tracer Diffusion, Electrical Conductivity, and Viscosity of Aqueous Solutions of Polystyrenesulfonates

R. FERNANDEZ PRINI and A. E. LAGOS, *Departamento de Química Inorgánica, Analítica y Química Física, Facultad de Ciencias Exactas y Naturales, Buenos Aires, Argentina*

### Synopsis

The variation of counterion mobilities in aqueous solutions of linear sodium polystyrenesulfonic acid over wide range of concentrations ( $10^{-2}$ – $0.7N$ ) was studied. The viscosities of these solutions were measured in order to calculate the reduced viscosities at different concentrations. From the data obtained it was possible to conclude that in the range of concentrations 0.08– $0.45N$ , an increase in  $D$  was observed. The enhancement of mobilities was attributed to an increase in the degree of apparent dissociation due to purely electrostatic interactions among neighboring chains. As concentration increased and chains approached each other, the above interactions should be accompanied by short-range interactions which would produce entanglements among neighbouring chains. This may be responsible for the appearance of a maximum in mobilities as the concentration increased. Evidence was found for a decrease of  $D_{Na}$  in solution when  $N > 0.45$ . The appearance of entanglements must produce an increase in the reduced viscosity which was observed. Tracer diffusion coefficients and reduced viscosities of the counterions  $Cs^+$ ,  $Ag^+$ , and  $Ca^{++}$  in the corresponding salts of polystyrenesulfonic acid all at the same normalities were also measured. It was observed that the counterions  $Cs^+$  had a slightly larger degree of association than  $Na^+$ . The behavior of  $Ca^{++}$  could be explained by the very strong association due to its double charge and for silver as partially due to the presence of complexes. For both counterions the reduced viscosity was much smaller than for the sodium salt.

Tracer diffusion and electrical conductivity of counterions in crosslinked and uncrosslinked polyelectrolytes have received considerable attention in recent years. Kitchener et al.<sup>1</sup> working with phenolsulfonic acid resins crosslinked with formaldehyde found that their conductivities in different ionic forms showed a maximum when represented as a function of their water content. A similar maximum was observed by the same authors<sup>2</sup> with the tracer diffusion rates of the counterions of the same resins, in which there is no electric field. Therefore they concluded that the phenomenon had to be related to the migration of the counterions and was not due to an electroosmotic effect. The same behavior was looked for with crosslinked polystyrenesulfonic acid-type resins,<sup>3</sup> but it was not possible to reach the range of water content at which the maximum was to be expected owing to their smaller swelling in water. As a consequence of this, a de-

crease in the tracer diffusion coefficients was observed when represented as a function of the water content. Some experiments were carried out by Kitchener et al.<sup>3</sup> concerning the electrical conductivity of aqueous solutions of linear sodium polystyrenesulfonate over a wide range of concentrations. A maximum very similar to that found previously with phenolsulfonic acid resins was observed. The assumption was made that significant migration of the polyelectrolyte chains is not likely, so that the transference number of the counterions should be near unity and the conductivity closely related to the mobility of these ions.

Wall et al.<sup>4</sup> measured the transference number of sodium and the polyanion in solution of polyacrylic acid of varying degree of neutralization. They obtained values between 0.4 and 0.6 for the transference numbers of the polyanion in solutions more than 60% neutralized. As this may also happen in solutions of sodium polystyrenesulfonate, the assumption that most of the current is transported by the counterions, i.e., that the equivalent conductivity shows the behavior of the counterion mobilities, may be abandoned.

Kitchener et al.<sup>1,2</sup> explain the maximum in the mobilities of the counterions as due to interactions between neighboring chains, and as these interactions must probably affect the average dimensions of the chains, it seems useful to study some properties which describes the variation of these dimensions. An equation which related the average dimensions of flexible chain polymers with their intrinsic viscosity has been given by Fox and Flory:<sup>5</sup>

$$[\eta] = 2.1 \times 10^{21} \langle h^2 \rangle^{3/2} / \bar{M} \quad (1)$$

where  $\langle h^2 \rangle$  is the average quadratic end-to-end distance of the chains and  $\bar{M}$  the average molecular weight of the polymer. Equation (1) has been used by several authors,<sup>6,7</sup> for concentrations different from zero in which case  $[\eta]$  has been replaced by the reduced viscosity,  $\eta_{sp}/C$ . The values for  $\langle h^2 \rangle$  obtained by the above authors using eq. (1) at concentrations different from zero are acceptable, although it has not been deduced for these conditions. In consequence it seems correct to use eq. (1) for comparative purposes in the present work.

Finally, it seems useful to analyze the values of the activity coefficients of counterions in polyelectrolyte solutions because they have a close relation with the apparent dissociation factor, and as we shall see below, with the counterion tracer diffusion coefficients. From the values of the counterions activity coefficients in solution ca.  $10^{-2}N$ , Rice and Nagasawa<sup>8</sup> arrived at some conclusions. One of them is that there must be some nonelectrostatic specific effect of the counterions on their activity coefficients. This is deduced from the different values of the ionic activities and their different variation with concentration, especially in the case of  $Ag^+$ . Therefore a specific effect of the counterions on their tracer diffusion coefficients may be expected.

For studying the influence of concentration on the mobility of the

counterions measurements of tracer diffusion of  $\text{Na}^+$ , equivalent conductivities, and reduced viscosity in aqueous solutions of sodium polystyrenesulfonate of different concentrations were measured. The specific effects of the counterions on their mobilities were studied by measuring the tracer diffusion coefficients of  $\text{Na}^+$ ,  $\text{Cs}^+$ ,  $\text{Ag}^+$ , and  $\text{Ca}^{2+}$  in aqueous solutions of the corresponding polystyrenesulfonates and at the same concentration.

## EXPERIMENTAL

### Preparation of Linear Polystyrenesulfonic Acid (HPSS)

Purified commercial polystyrene was ground and sulfonated according to Bachman<sup>9</sup> with concentrated  $\text{H}_2\text{SO}_4$  and 0.2 wt.-% of  $\text{Ag}_2\text{SO}_4$  as a catalyst at 95–105°C. for 7 hr. with stirring. The product was dissolved in ten times its weight of water and the solution thoroughly dialyzed against deionized water. The aqueous solution was dried from above with an infrared lamp at less than 100°C. to avoid crosslinking.<sup>6</sup> Two products with different degrees of sulfonation were obtained: HPSS I with an exchange capacity of 5.11 meq./g. of dry acid and HPSS II of 4.44 meq./g. of dry acid.

### Preparation of the Different Polystyrenesulfonates

The salts were: NaPSS I from HPSS I; NaPSS II, CsPSS, AgPSS, and CaPSS from HPSS II. They were prepared by exchange of the  $\text{H}^+$  by the different cations in a large excess of the solution of an appropriate salt, followed by dialysis. In all cases the absence of  $\text{H}^+$  was checked. Contamination due to glass leaching was avoided by keeping the solution in polyethylene vessels.<sup>6</sup>

### Determination of the Average Molecular Weight of NaPSS I

The average molecular weight of NaPSS I was determined by measuring sedimentation rates at  $20 \pm 0.5^\circ\text{C}$ . in 0.2M NaCl solutions and at different concentrations of polyelectrolytes. The results were extrapolated to infinite dilution. The equipment used consisted of Spinco analytical ultracentrifuge, Model E with schlieren optic system and flat cells. (These determinations were carried out in the Instituto Nacional de Microbiología, by courtesy of Drs. C. Milstein and R. Celis.) Sedimentation rate at infinite dilution was transformed into  $s_{20,w}$  and  $\bar{M}$  was obtained from Flory and Mandelkern's equation:<sup>10</sup>

$$s_{20,w} = \frac{[\eta]^{1/3}}{(\bar{M})^{2/3}} = \frac{2.6 \times 10^6 (1 - \bar{V}\delta)}{N\eta} \quad (2)$$

where  $[\eta]$  = intrinsic viscosity of NaPSS in 0.2M NaCl at 20°C.,  $\eta$  = solvent viscosity (0.2M NaCl solution) at 20°C.,  $\delta$  = solvent density (0.2M NaCl) at 20°C.,  $\bar{V}$  = partial specific volume of NaPSS in 0.2M NaCl solution at 20°C., and  $N$  = Avogadro's number.

A value of  $[\eta] = 1.071$  dl./g. was obtained with an Ostwald viscometer and from densities  $\bar{V} = 0.606$  ml./g. With  $s_{20,w} = 7.23 \times 10^{-13}$  sec., the value of  $\bar{M}$  is  $3.0 \times 10^6$ .

### Diffusion Technique

The same general procedure was employed as that of Anderson and Saddington.<sup>11</sup> A nonstirring technique was essential due to the high viscosity of the polystyrenesulfonate solution. Besides, this technique seemed more reliable than one employing stirring, according to Lengyel et al.,<sup>12</sup> because of the considerable change of viscosity of the solutions as the concentration varies. The diffusion vessel consisted of a Pyrex tube, 2.5 cm. in diameter and 25 cm. in length, in which the inactive solution was placed (40–60 ml.). A breather tube permitted slow submersion of the capillaries into the inactive solution avoiding convection movements. The diffusion capillaries used had a uniform internal diameters of about 0.78 mm. and were ca. 3 cm. long. One end of the capillaries was carefully sealed with a flat bottom. Before diffusion was started the capillaries were filled with a degassed, traced polyelectrolyte solution of known concentration using fine pipettes. The capillaries were held vertically inside the inactive solution of the same concentration with the open end at the top. The diffusion cell was supported on a separate framework from that of the thermostat and cushioned by rubber and lead mounts. When the capillaries were removed after diffusion took place, the excess of solution was carefully wiped off from their faces, and their contents centrifuged out, made up to a standard volume and counted with a suitable detector.

The following tracers were used: Na<sup>22</sup>, Cs<sup>134</sup>, and Ca<sup>45</sup> as chlorides and Ag<sup>110</sup> as nitrate; all were supplied by the Argentine Atomic Energy Commission. The  $\gamma$  emitters (Na<sup>22</sup>, Cs<sup>134</sup>, and Ag<sup>110</sup>) were counted in a well-type scintillation counter. The Ca<sup>45</sup> solutions were dried down on planchets and counted in a gas flow counter. The tracing of the polyelectrolyte solutions was done by placing a drop of the corresponding radioactive solution in a platinum dish and evaporating under an infrared lamp. The residue was dissolved in a volume of polystyrenesulfonate solution. This volume was such that the content of the capillary, when made up to a standard volume, would give an adequate number of counts per minute.

An approximate solution of Fick's law for the boundary conditions of our experiment as proposed by McKay<sup>14</sup> was used:

$$D = 0.78499 (1 - \gamma)^2 l^2/t \quad (3)$$

where  $D$  = the tracer diffusion coefficient,  $\gamma$  = the ratio of final and initial activities in the capillaries,  $l$  = length of the capillaries, and  $t$  = time of diffusion.

This equation is valid for  $\gamma \geq 0.5$ . As McKay states,<sup>14</sup> the error in  $D$  is never higher than 0.3% and decreases as  $\gamma$  increases, so that it is convenient that  $0.6 \leq \gamma \leq 0.7$ .



### Verification of the Method with NaCl Solutions

A series of five determinations was made on 1.44*M* NaCl solution using the method described above and eq. (3). Different authors<sup>15,16</sup> have found coincident values of *D* at this concentration; this is the reason for choosing such a concentration. The average value obtained for *D* was  $(1.152 \pm 0.017) \times 10^{-5} \text{ cm.}^2 \text{ sec.}^{-1}$ , and the deviation from the mean was 2%. The mean value of *D* was 4.2% below that of Mills and Godbole.<sup>15</sup> This is to be expected, since in our method stirring was not used.

The constancy of the deviation from the mean and the accuracy with varying concentration was verified by five determinations of *D* in 0.1*M* NaCl solutions. The mean value of *D* under these conditions was  $(1.217 \pm 0.017) \times 10^{-5} \text{ cm.}^2 \text{ sec.}^{-1}$ . This value was 4% below that of Mills and Godbole,<sup>17</sup> and the deviation from the mean was 1.4%. Accordingly, the error of *D* remains constant with varying concentration of the NaCl solution. The same constancy may be expected for the polyelectrolyte solution at different concentrations although in this case there is a large variation of viscosity. This fact has been reported by Lengyel et al.<sup>12</sup> working on electrolyte solutions of varying viscosity.

Equation (3) indicates that the main factor in limiting the precision in *D* is the determination of the activity of tracer solutions.

### Determination of Equivalent Conductivities

The equipment used consisted of a Solartron oscillator model G 546, a Tinsley conductivity bridge type 4896, a differential amplifier, and a Technitron oscillograph as zero detector. Over the whole range of concentration no frequency dependence of resistances was observed within experimental error (0.3%). The solutions were made up of twice-distilled water of specific conductivity about  $1\text{--}2 \times 10^{-6} \text{ ohm}^{-1} \text{ cm.}^{-1}$ .

### Determination of Viscosities

Viscosity measurements were made with a Fenske type viscometer. As the polyelectrolytes exhibit non-Newtonian behavior, the apparent viscosities depend on the flow rate. Eisenberg<sup>18</sup> measured viscosities of polymethacrylic acid solutions using both Ostwald and torsion viscometers. The latter allows an extrapolation of viscosity to zero flow rate. His work shows that in spite of the decrease in the viscosities with increasing flow rate and increasing molecular weight, the form of the variation of the viscosity with concentration does not depend on either of them. Thus it seems reasonable to use a capillary viscometer for the comparative study of the variation of viscosity with concentration.

## RESULTS

A summary of the final results is given in Tables I–III. Detailed results have been recorded elsewhere.<sup>19</sup>

TABLE I  
Tracer Diffusion Coefficients of  $\text{Na}^+$  in NaPSS I Aqueous Solutions at  $25 \pm 0.01^\circ\text{C}$ .

No.	$C$ , g./dl.	$N$ , eq./l.	$D \times 10^5$ , $\text{cm.}^2\text{sec.}^{-1}$	$D^0 \times 10^5$ , $\text{cm.}^2\text{sec.}^{-1}$	$\alpha$
1	0.2008	$0.922 \times 10^{-2}$	$0.512 \pm 0.012$	1.312	0.39
2	0.503	$2.310 \times 10^{-2}$	$0.502 \pm 0.012$	1.301	0.39
3	1.006	$4.62 \times 10^{-2}$	$0.528 \pm 0.012$	1.292	0.41
4	2.011	$9.24 \times 10^{-2}$	$0.605 \pm 0.017$	1.280	0.47
5	3.698	0.1699	$0.611 \pm 0.036$	1.280	0.48
6	6.350	0.2887	$0.628 \pm 0.032$	1.280	0.49
7	9.65	0.443	$0.676 \pm 0.023$	1.280	0.52
8	13.99	0.6428	0.614	1.280	0.48

TABLE II  
Tracer Diffusion Coefficients of  $\text{Na}^+$ ,  $\text{Cs}^+$ ,  $\text{Ag}^+$ , and  $\text{Ca}^{2+}$  in Aqueous Solutions of the Corresponding Polystyrenesulfonates II at  $25 \pm 0.01^\circ\text{C}$ .

Salt	$C$ , g./dl.	$N$ , eq./l.	$D \times 10^5$ , $\text{cm.}^2\text{sec.}^{-1}$	$D^0 \times 10^5$ , $\text{cm.}^2\text{sec.}^{-1}$	$\alpha$
NaPSS II	5.215	0.2107	$0.670 \pm 0.017$	1.333	0.50
CsPSS	7.465	0.2090	$0.913 \pm 0.034$	2.054	0.44
AgPSS	6.950	0.2092	$0.426 \pm 0.016$	1.647	0.26
CaPSS	5.105	0.2088	$0.191 \pm 0.003$	0.792	0.24

TABLE III  
Viscosities and Reduced Viscosities of Aqueous Solutions of Different Polystyrenesulfonates at  $25 \pm 0.01^\circ\text{C}$ .

Salt	$C$ , g./dl.	$N$ , eq./l.	$10^2\eta$ , poises	$\eta_{sp}/C$ , dl./g.
NaPSS II	0.1123	$4.54 \times 10^{-3}$	3.482	25.41
"	0.2246	$9.07 \times 10^{-3}$	4.980	20.41
"	0.518	$2.093 \times 10^{-2}$	7.285	13.86
"	1.035	$4.181 \times 10^{-2}$	10.286	10.20
"	2.070	$8.363 \times 10^{-2}$	15.39	7.869
"	4.580	0.1850	25.49	6.032
"	5.125	0.2071	31.79	6.773
"	8.530	0.3446	59.16	7.671
"	14.365	0.5803	159.8	12.43
CsPSS	7.365	0.2062	22.48	3.291
AgPSS	6.950	0.2092	22.19	3.442
CaPSS	5.105	0.2088	8.836	1.748

In Table I under the heading  $D$  are the mean values of three simultaneous determinations and their maximum deviation value from the mean. The value reported for solution 8 corresponds to only one determination.

In Table II are the tracer diffusion coefficients of the different counterions in solutions whose normalities were constant within 1%. The values of  $D$  in this table are the mean of at least two determinations with the corresponding deviations.

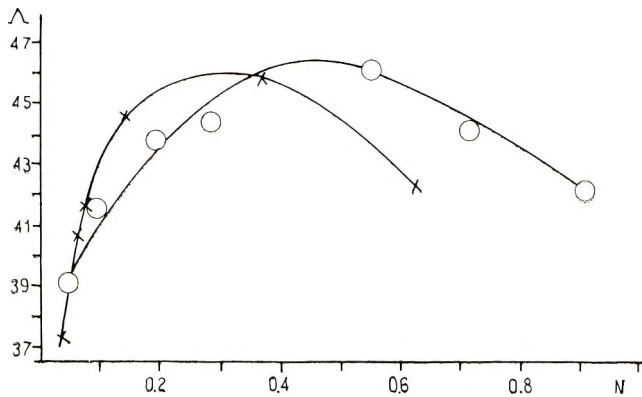


Fig. 1. Equivalent conductivities of aqueous solutions of (O) NaPSS I and (X) NaPSS II at  $25 \pm 0.01^\circ\text{C}$ .

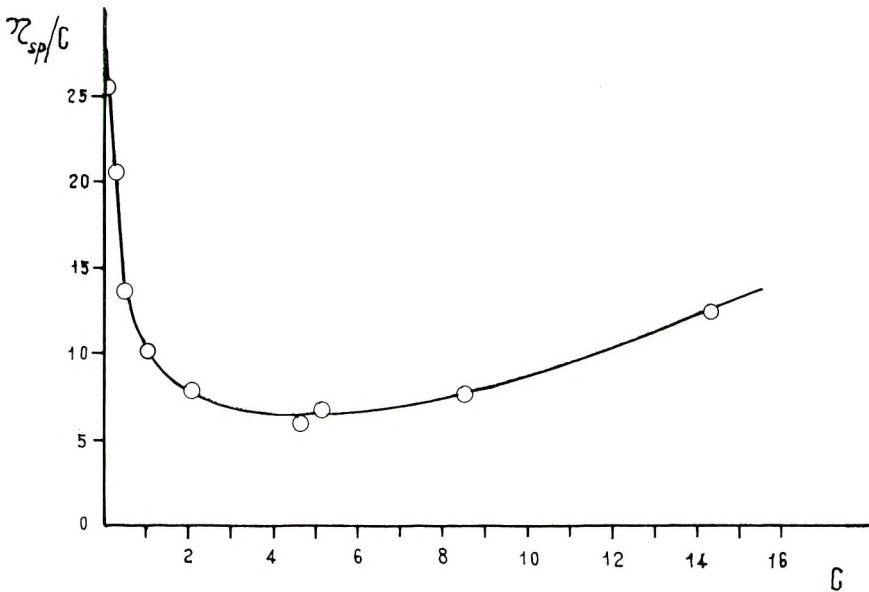


Fig. 2. Reduced viscosities of aqueous solutions of NaPSS II at  $25 \pm 0.01^\circ\text{C}$ .

Figure 1 represents the values  $\Lambda$  for NaPSS I and NaPSS II as a function of concentration. The errors in  $\Lambda$  were about 0.3%. It is evident from Figure 1 that although both polyelectrolytes have different degrees of sulfonation they show a similar variation of  $\Lambda$  with concentration. From this observation it seems possible to use the values of the reduced viscosity of NaPSS II to explain the behavior of  $D_{\text{Na}}$  in NaPSS I.

Figure 2 represents the variation of the reduced viscosity of NaPSS II as a function of  $C$ . Wall et al.<sup>4</sup> measuring transference numbers in polyelectrolyte solutions observed that a fraction of counterions is transported by the polyanion. From their observation it is clear that the diffusion of

$\text{Na}^+$  is due in part to the movement of the free counterions and in part to the movement of the polyanion which has a fraction of counterions associated with it. However, they concluded<sup>4b</sup> that the fraction of counterions carried by diffusion of the polyanion will be negligible, and so the tracer diffusion coefficient of  $\text{Na}^+$  will be a measure of counterion mobility. The same authors assumed that the differences of mobilities between the counterions in polyelectrolyte solutions and the same ions in electrolyte solutions is due solely to counterion association in the former. They were thus able to calculate dissociation factors of polyelectrolytes in aqueous solutions, by using Fick's second law and

$$D_{\text{Na}} = \alpha D^0_{\text{Na}} \quad (4)$$

where  $D_{\text{Na}}$  is the tracer diffusion coefficient of the counterion in a polyelectrolyte solution,  $D^0_{\text{Na}}$  is the tracer diffusion coefficient of the same ion in an electrolyte solution of the same concentration, and  $\alpha$  is the apparent degree of dissociation of the polyelectrolyte at that concentration.

Using these assumptions we have calculated the apparent degree of dissociation as shown in Table I from the observed counterion diffusion coefficients and using as  $D^0_{\text{Na}}$  Mills'<sup>20</sup> tracer diffusion coefficients of  $\text{Na}^+$  in  $\text{NaCl}$  aqueous solutions. In Table III  $\alpha$  has been calculated by using as  $D^0$  the values of tracer diffusion coefficients at infinite dilution due to the lack of experimental values for cations other than  $\text{Na}^+$  at adequate concentrations.

## DISCUSSION

### Influence of Concentration on $D$

Figure 3 shows an evident increase in  $D$  (i.e.,  $\alpha$ ) with increasing concentration (0.08–0.45*N* or 1.74–9.8 g./dl.). The same increase of  $\alpha$  was observed by several authors from measurements of activity coefficients in

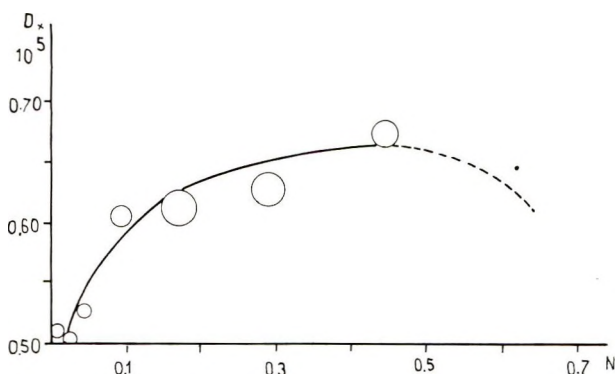


Fig. 3. Tracer diffusion coefficients of  $\text{Na}^+$  in aqueous solutions of NaPSS I at  $25 \pm 0.01^\circ\text{C}$ . (The radius of each circle is equal to the maximum deviation from the mean.)

dilute polyelectrolyte solutions<sup>7,21</sup> of concentrations around  $0.06N$ . In order to explain this increase in  $\alpha$  it is useful to remember that Wall's method for calculating the degree of dissociation is not based on a particular model but only on the assumption that the nonassociated counterions move freely as in an electrolyte solution. Nagasawa et al.<sup>22</sup> found that the counterion association of HPSS is only electrostatic. According to Jakubovic et al.<sup>1,2</sup> the increase of mobilities would have the meaning of a decrease of counterion density in the vicinity of the chains and an enhancement of it at larger distances from them. The simplified models for explaining the behavior of polyelectrolytes (rigid sphere<sup>7</sup>) and rigid cylinder<sup>23</sup> which accounts correctly for the values of  $\alpha$  in dilute solutions ( $< 0.04N$ ) assuming only intramolecular electrostatic interactions, are not able to explain the considerable increase of  $\alpha$  in more concentrated solutions. But on the other hand, it is difficult to accept in this range of concentration ( $0.08$ – $0.45N$ ) the existence of only intramolecular interactions. As concentration increases, the chains approach each other and some intermolecular interactions must start; these interactions which begin by being purely electrostatic will probably produce an increase of counterion density in the middle space between chains which will result in an increase of  $\alpha$ . It can be seen from Figure 2 that in the same range of concentrations in which  $D$  increases, the reduced viscosities indicate only minor variations on the average dimensions of the chains; this is in accordance with the above mentioned electrostatic interactions which modify only the internal distribution of counterions.

As concentration increases, chains approach each other, and the purely electrostatic intermolecular interactions must be accompanied by short-range interactions which would produce entanglements among neighboring chains. This effect is known to occur in ion-exchange resins<sup>2,3</sup> and its appearance produces a retardation in the mobilities of the counterions, (tortuosity effect). This effect offsets the increase in the counterion mobilities due to electrostatic interactions and is responsible for the appearance of a maximum in mobilities when the concentration increases.<sup>2</sup> Thus it seems reasonable to expect also in our case a decrease of  $\text{Na}^+$  mobility with concentration.

The tortuosity effect of the medium must start before the maximum in order to balance the previous enhancement in mobilities. On the other hand, the appearance of entanglements must produce an increase in the reduced viscosity, since now the average end-to-end distance of each entity has increased as actually they are not formed by only one macromolecule. It can be seen from Figure 1 for NaPSS II that the maximum is situated around  $0.32N$  (8 g./dl.), so the corresponding increase in  $\eta_{sp}/C$  may be expected at concentrations just below this. In Figure 2 an increase in the reduced viscosity is observed for concentrations above  $0.28N$  (7 g./dl.).

In Figure 3, the point at  $0.64N$  (14 g./dl.) is evidence of a decrease of  $D_{\text{Na}}$  in solutions with  $N > 0.45$ . Although this is poor evidence in itself, as it corresponds to only one determination, it actually supports the

arguments given above. The dashed line in Figure 3 represents the behavior of the system considering point 0.64*N*.

From Figures 1 and 3 it can be seen that there is a correlation between *D* and  $\Lambda$  for NaPSS I, i.e., that the variation of  $\Lambda$  is due to the change of the counterion mobility with concentration. This does not imply that the contribution of the electrical mobility of the polyanion is neglected, but rather that it is considered constant.

### Influence of Counterions

By determining the tracer diffusion coefficients of different counterions in the corresponding polystyrenesulfonate at equal normalities, as shown in Table III, it was possible to study the specific influence of the counterions in diffusion.

The strong association observed for  $\text{Ca}^{2+}$  is expected to be due to its higher charge; besides, from Table III it can be seen that the reduced viscosity of CaPSS solutions is much lower than that of the other salts. On analysis of eq. (1) this would mean that the average dimension is smaller, which could be explained considering that a smaller degree of dissociation would decrease the effective charge of the polyanion, favoring packed configurations: the average chain dimension would decrease, giving a smaller reduced viscosity.

$\text{Ag}^+$  shows a higher association than  $\text{Na}^+$ . This is also shown comparing the reduced viscosity of both polyelectrolytes. In this case, however, as  $\text{Ag}^+$  bears a simple charge and its hydrated radius is between that of  $\text{Na}^+$  and that of  $\text{Cs}^+$ , the strong association may be attributed to the partial formation of real covalent complexes. Another evidence of this is shown by the activity coefficient measurements<sup>8</sup> and the determination of formation constant of silver polyelectrolyte.<sup>24</sup>

The behavior of  $\text{Cs}^+$  is not so easily explained. Its association is slightly higher than that of  $\text{Na}^+$ , but its reduced viscosity decreases too much in comparison with NaPSS. It is possible to assume the existence of real association, since Frumkin et al.<sup>25</sup> showed that  $\text{Cs}^+$  is specifically absorbed on charged surfaces.

A shift on the characteristic lines of the  $-\text{SO}_3^-$  infrared spectrum<sup>26,27</sup> was looked for in order to verify the existence of association due in part to covalent bonds in CsPSS and specially in AgPSS with respect to NaPSS. The following results were observed: for NaPSS, lines appeared at 8.86 and 9.65  $\mu$ , for CsPSS at 8.89 and 9.66  $\mu$ , and for AgPSS at 8.92 and 9.69  $\mu$ . It may be seen that there is a slight shift, but its magnitude is not definite evidence for the existence of covalent bonds.

The authors wish to express their thanks to Dr. J. A. Kitchener for helpful advice and to the National Research Council of the Argentine Republic for financial support.

## References

1. Jakubovic, A. O., G. J. Hills, and J. A. Kitchener, *Trans. Faraday Soc.*, **55**, 1579 (1959).
2. Jakubovic, A. O., G. J. Hills, and J. A. Kitchener, *J. Chim. Phys.*, **62**, 263 (1958).
3. Lagos, A. E., and J. A. Kitchener, *Trans. Faraday Soc.*, **56**, 1245 (1960).
4. Huizenga, J. R., P. F. Grieger, and F. T. Wall, (a) *J. Am. Chem. Soc.*, **72**, 2636 (1950); (b) *ibid.*, **72**, 4228 (1950).
5. Fox, T. G., and P. J. Flory, *J. Am. Chem. Soc.*, **73**, 1904, 1909 (1951).
6. Butler, J. A. V., A. B. Robins, and K. V. Shooter, *Proc. Roy. Soc. (London)*, **A241**, 299 (1957).
7. Nagasawa, M., and I. Kagawa, *J. Polymer Sci.*, **25**, 61 (1957).
8. Rice, S., and M. Nagasawa, *Polyelectrolyte Solutions*, Academic Press, New York 1961.
9. Bachman, G. B., H. Hellman, K. R. Robinson, R. W. Finholt, E. H. Kahler, L. J. Filar, L. V. Heisey, L. L. Lewis, and D. D. Micucci, *J. Org. Chem.*, **12**, 108 (1947).
10. Flory, P. J., and L. Mandelkern, *J. Chem. Phys.*, **20**, 212 (1952).
11. Anderson, J. S., and K. Saddington, *J. Chem. Soc.*, **1949**, S381.
12. Lengyel, S., J. Tamás, J. Giber, A. Vértes, and J. Gergely, paper presented at International Conference on Electrochemistry, Rome, 1962.
13. Mills, R., and J. W. Kennedy, *J. Am. Chem. Soc.*, **75**, 5696 (1953).
14. McKay, R., *Proc. Phys. Soc.*, **42**, 547 (1930).
15. Mills, R., and E. W. Godbole, *Austral. J. Chem.*, **12**, 102 (1959).
16. Mills, R., *J. Am. Chem. Soc.*, **77**, 6116 (1955).
17. Mills, R., and E. W. Godbole, *Austral. J. Chem.*, **11**, 1 (1958).
18. Eisenberg, H., *J. Polymer Sci.*, **23**, 579 (1957).
19. Fernandez Prini, R., Thesis, Univ. de Buenos Aires, 1962.
20. Mills, R., *Rev. Pure Appl. Chem. Austral.*, **11**, 89 (1961).
21. Liquori, A. M., F. Ascoli, C. Broté, V. Crescensi, and A. Mele, *J. Polymer Sci.*, **40**, 169 (1959).
22. Kotin, L., and M. Nagasawa, *J. Am. Chem. Soc.*, **83**, 1026 (1961).
23. Oosawa, F., *J. Polymer Sci.*, **23**, 421 (1957).
24. Gregor, H. P., L. B. Luttinger, and E. M. Loebel, *J. Phys. Chem.*, **59**, 34 (1955).
25. Frumkin, A. N., B. B. Damaskin, and N. V. Nicolaeva Federovich, *Dokl. Akad. Nauk SSSR*, **121**, 493 (1958).
26. Bellamy, L. J., *The Infra Red Spectra of Complex Molecules*, Methuen, London, 1958.
27. Kidd, J. M., and R. N. Haszeldine, *J. Chem. Soc.*, **1954**, 4228.

## Résumé

On a étudié la variation des mobilités des contre-ions en solution aqueuse du sel sodique de l'acide polystyrène sulfonique linéaire, dans un large domaine de concentrations ( $10^{-2}$ -0,7 N). Les viscosités de ces solutions ont été mesurées en vue de calculer les viscosités réduites à différentes concentrations. Des résultats obtenus, il est possible de conclure que: (a) dans le domaine de concentrations 0,08-0,45 N, on observe une augmentation de  $D$ . L'augmentation des mobilités est attribuée à une augmentation dans le degré de dissociation apparent, du aux interactions purement électrostatiques parmi les chaînes voisines. (b) lorsque la concentration augmente et que les chaînes se rapprochent l'une de l'autre, les interactions ci-dessus peuvent s'accompagner d'interactions peu importantes qui produisent des empêchements parmi les chaînes voisines. Cela peut être responsable d'un maximum apparent dans les mobilités lorsque la concentration augmente. On a mis en évidence une diminution de  $D_{Na}$  en solution, lorsque  $N > 0,45$ . (c) l'apparition d'empêchements peut produire une augmentation de la viscosité réduite, ce que l'on a observé. On a également mesuré le coefficient de diffusion et la viscosité réduite des contre-ions  $Cs^+$ ,  $Ag^+$  et  $Ca^{++}$  dans les sels correspond-

ants de l'acide polystyrène sulfonique, tous aux mêmes normalités. On a observé que le contre-ion  $\text{Cs}^+$  possède un degré d'association légèrement plus grand que  $\text{Na}^+$ . Le comportement de  $\text{Ca}^{++}$  peut s'expliquer par une très forte association due à sa charge double et pour l'argent, le comportement est partiellement dû à la présence de complexes. Pour ces deux contre-ions, la viscosité réduite est beaucoup plus faible que pour le sel sodique.

### Zusammenfassung

Die Änderung der Gegenion-Beweglichkeit in wässrigen Lösungen von linearer Natrium-Polystyrolsulfosäure wurde über einen weiten Konzentrationsbereich ( $10^{-2}$ – $0,7N$ ) untersucht. Die Viskosität dieser Lösungen wurde gemessen und die reduzierte Viskosität bei verschiedenen Konzentrationen berechnet. Aus den erhaltenen Daten konnte der Schluss gezogen werden, dass: (a) Im Konzentrationsbereich von  $0,08$ – $0,45 N$  eine Zunahme von  $D$  auftritt. Die Erhöhung der Beweglichkeit wurde auf eine Zunahme des scheinbaren Dissoziationsgrades durch eine elektrostatische Wechselwirkung zwischen benachbarten Ketten zurückgeführt. (b) Bei Konzentrationszunahme und gegenseitiger Annäherung der Ketten diese Wechselwirkung von einer Wechselwirkung kurzer Reichweite begleitet sein sollte, die zu Verschlingungen zwischen benachbarten Ketten führt. Das könnte für das Auftreten eines Maximums der Beweglichkeit mit steigender Konzentration verantwortlich sein. Für  $N > 0,45$  wird eine Abnahme von  $D_{\text{Na}}$  in Lösung beobachtet. (c) Das Auftreten von Verschlingungen eine Zunahme der reduzierten Viskosität erzeugen muss, was dem tatsächlichen Verhalten entspricht. Weiters wurde der Diffusionskoeffizient nach der Tracer-Technik und die reduzierte Viskosität mit  $\text{Cs}^+$ ,  $\text{Ag}^+$  und  $\text{Ca}^{++}$  als Gegenion in den entsprechenden Salzen der Polystyrolsulfosäure, alle bei der gleichen Normalität, gemessen.  $\text{Cs}^+$  besass als Gegenion einen etwas grösseren Assoziationsgrad als  $\text{Na}^+$ . Das Verhalten von  $\text{Ca}^{++}$  konnte durch die durch seine doppelte Ladung bedingte sehr starke Assoziation und das von Silber zum Teil durch das Auftreten von Komplexen erklärt werden. Bei beiden Gegenionen war die reduzierte Viskosität bedeutend kleiner als beim Natriumsalz.

Received May 3, 1963

Revised July 1, 1963



## Radiation-Induced Post Polymerization of Trioxane in the Solid State\*

K. HAYASHI, H. OCHI,† and S. OKAMURA, *Osaka Laboratories,  
Japanese Association for Radiation Research on Polymers,  
Neyagawa, Osaka, Japan*

### Synopsis

Trioxane, the cyclic trimer of formaldehyde, is easily polymerized by ionizing radiation in the solid state at a temperature slightly below the melting point. It was found that this post-polymerization is analogous to the in-source polymerization, but its overall activation energy is more than 40 kcal./mole, which is much larger than for in-source polymerization. A kinetic scheme is proposed for the post-polymerization which accounts for the experimental results. In-source polymerization probably occurs by an ionic mechanism, but there co-exist two different mechanisms in the post-polymerization. One is probably initiated by the decomposition of a product produced by the ionizing radiation in the presence of oxygen. The other has not yet been clarified, but it does not seem to be due to trapped radical or ionic species. The thermal decomposition of the polymer formed and the influence of additives, such as methanol, and benzene, on post-polymerization were also studied.

It was previously reported that trioxane, the cyclic trimer of formaldehyde, was easily polymerized by ionizing radiation in the solid state and formed well oriented polyoxymethylene crystals.<sup>1,2</sup>

It was found that this monomer could be polymerized not only during irradiation, but also by a post-polymerization following low temperature preirradiation.

### EXPERIMENTAL

Commercial trioxane was purified by sublimation and was sealed in a glass tube. Preirradiation was carried out by  $\gamma$ -rays from a Co<sup>60</sup> source at Dry Ice-methanol temperature and the samples were then post-polymerized after warming to 40-60°C. With the exception of special cases, both preirradiation and post-polymerization were carried out in the presence of air.

The reaction mixture was washed with cold methanol to remove residual monomer, and the polymer yield was determined after drying *in vacuo*.

\* Presented in the Annual Meeting of the Chemical Society of Japan, Kyoto, April 1962.

† Present address: Polytechnic Institute of Brooklyn, Brooklyn, New York.

Qualitative analysis of peroxide was carried out by titration of  $I_2$  liberated from KI in mixtures with isopropanol and acetic acid.

A thermobalance was used for the measurement of the thermal decomposition of polymer formed.

## RESULTS AND DISCUSSION

### Kinetic Study of Post-Polymerization of Trioxane

#### Results

**Influence of the Preirradiation Dosage.** Trioxane preirradiated with various doses was post-polymerized at  $55^\circ\text{C}$ . Figure 1 shows that the post-polymerization of trioxane has a saturation yield just as in the case of in-source polymerization, and both this saturation yield and initial rate of polymerization increased on increasing the preirradiation dosage.

The saturation yield was proportional to the first power of the preirradiation dosage, as shown in Figure 2.

**Influence of the Crystalline State of the Monomer.** In the radiation-induced solid-state polymerizations of cyclic monomers, the initial polymerization rate and the saturation yield were generally affected by the crystalline

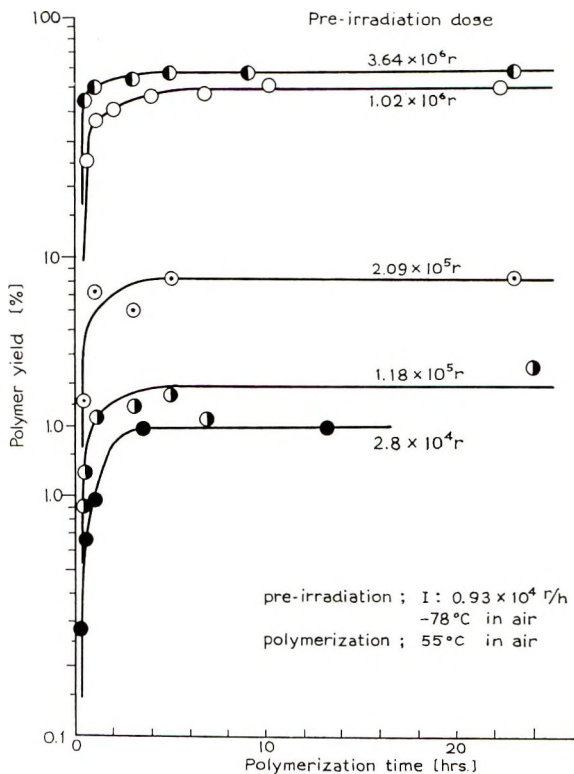


Fig. 1. Influence of preirradiation dose on polymer yield.

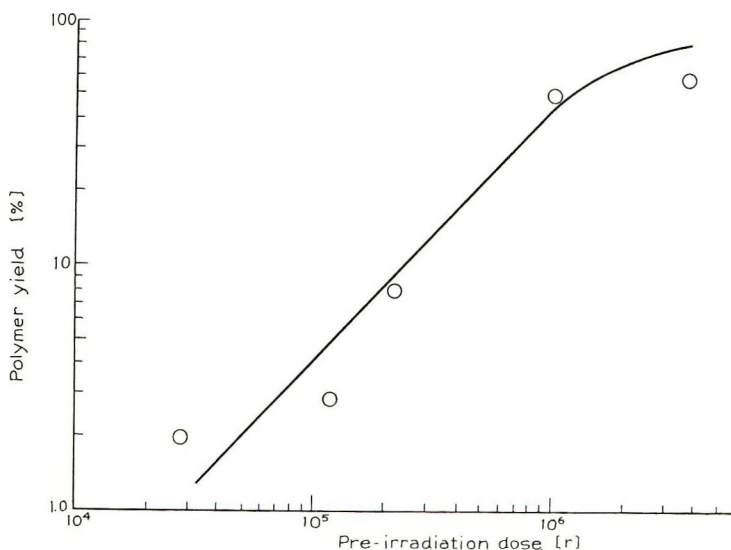


Fig. 2. Saturation polymer yield as a function of preirradiation dose.

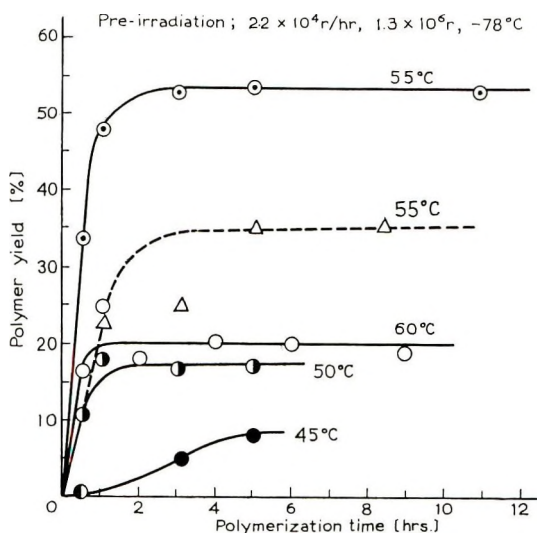


Fig. 3. Polymer yield as a function of polymerization temperature and effect of crystal size: ( $\odot$ ,  $\circ$ ,  $\bullet$ ,  $\bullet$ ) large crystals; ( $\Delta$ ) small crystal (quickly crystallized at  $-78^{\circ}\text{C}$ .).

state of the monomer.<sup>4</sup> The same phenomena are observed also in the post-polymerization of trioxane.

Figure 3 shows a comparison of the post-polymerization of relatively larger crystals obtained by sublimation and smaller crystals obtained by rapid cooling to  $-78^{\circ}\text{C}$ . from the molten state. Larger crystals clearly had a higher saturation yield and polymerization rate.

**Influence of the Temperature.** Figures 3 and 4 represent the results of the post-polymerization at various temperatures after preirradiation with a

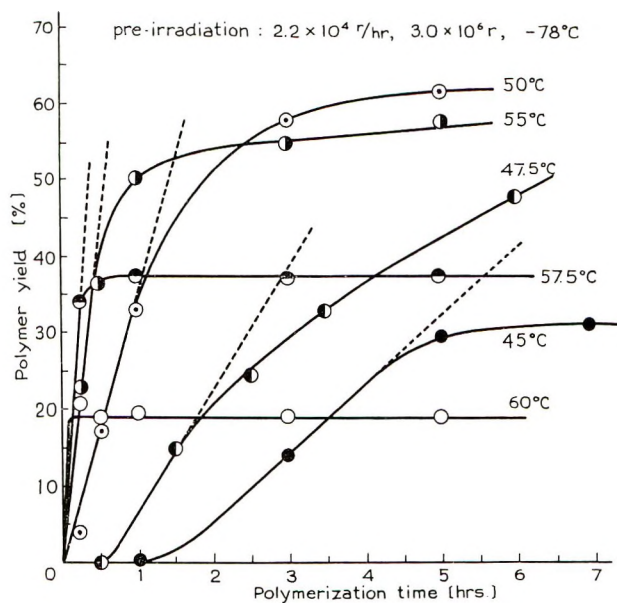


Fig. 4. Polymer yield as a function of polymerization temperature.

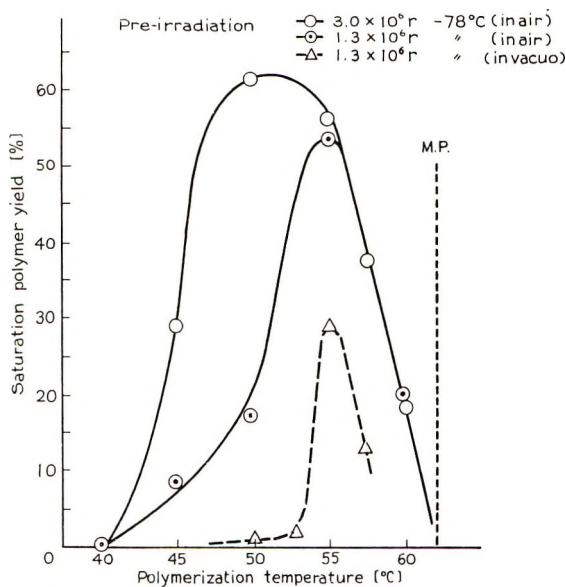


Fig. 5. Saturation yield as a function of polymerization temperature: (O,  $\odot$ ) preirradiated and post-polymerized in air; ( $\Delta$ ) preirradiated and post-polymerized *in vacuo*.

definite dose, and these results show that the initial rate of polymerization and saturation yield are both influenced by the temperature.

The relation between the saturation yield and post-polymerization temperature is shown in Figure 5. This relation is analogous to that found for

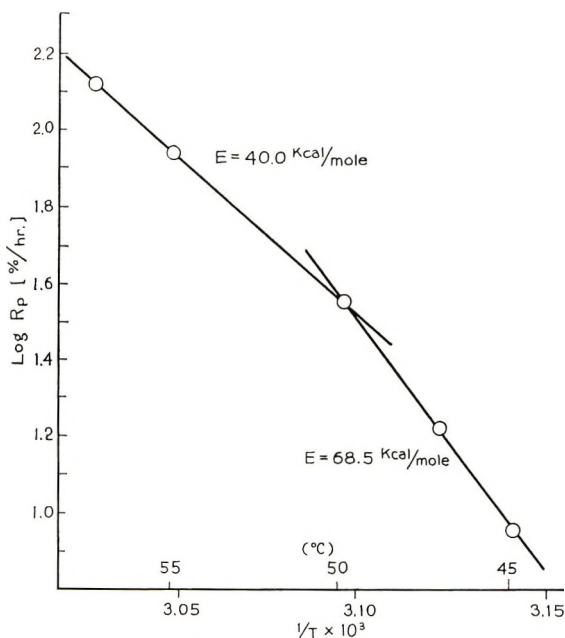


Fig. 6. Effect of polymerization temperature on post-polymerization ( $2.2 \times 10^4$  r/hr. for 60 hr. at  $-78^\circ\text{C}$ .).

in-source polymerization.<sup>1</sup> Three points should be noted. Firstly, the temperature which gives the maximum polymer yield, is slightly below that found for in-source polymerization, and this fall of the optimum temperature increased when the preirradiation dose increased. This phenomenon may be due to the disordering of monomer crystals caused by radiation damage. Secondly, the temperature range in which polymerization occurred became narrower. In the case of post-polymerization, this temperature range lies from about  $40^\circ\text{C}$ . to just below the melting point of monomer, whereas it extended to  $30^\circ\text{C}$ . in the case of in-source polymerization. Finally, an induction period was observed at low temperature in post-polymerization, but not during in-source polymerization.

The overall activation energy was calculated from the initial rates of polymerization in Figure 4, and this value is shown in Figure 6. It was found that for post-polymerization  $\Delta E^\ddagger > 40$  kcal./mole, very large compared with the value for in-source polymerizations of trioxane and other cyclic monomers.

**Influence of Additives.** Small amounts of methylene chloride, water, benzene, methanol and dioxane were added to trioxane crystals and their influence on the polymerization was investigated. (Fig. 7) The relation between the polymerization temperature and polymer yield in binary systems is shown in Figure 8.

These results show that relatively small amounts of additives affected strongly the post-polymerization, and the effectiveness of these additives

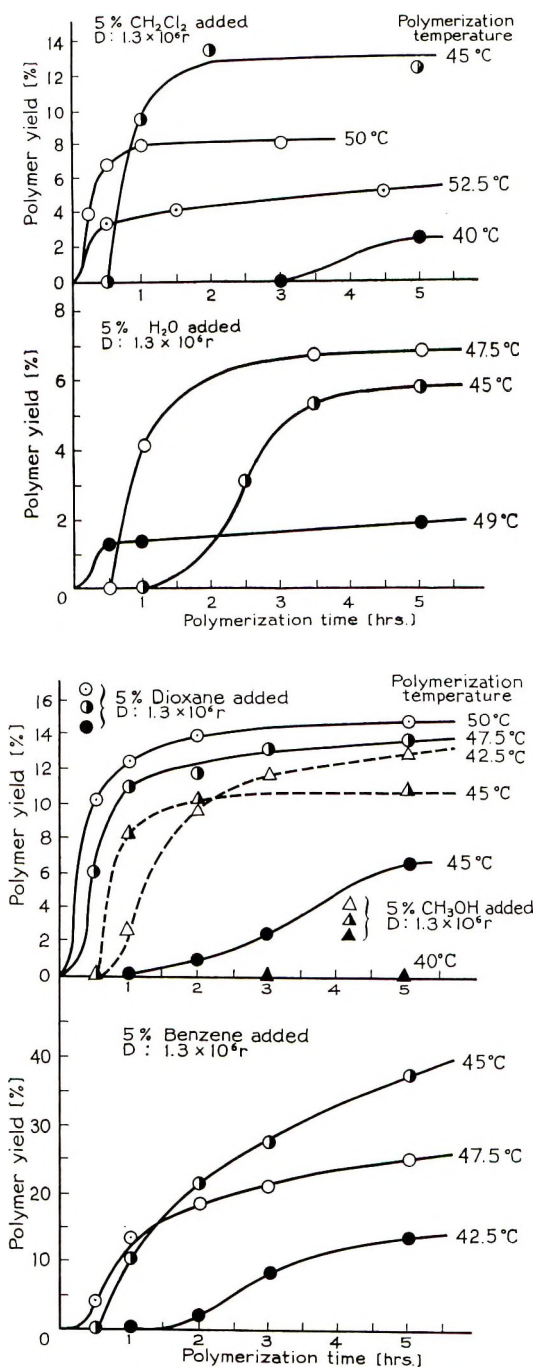


Fig. 7. Influence of additives.

as inhibitors was in the order: water > methanol > methylene chloride > dioxane > benzene. Due to the decrease of the melting point in the presence of additives, the temperature which gave the maximum polymer yield decreased, and the temperature range for polymerization became narrower compared with the polymerization of pure trioxane.

It is interesting that an induction period was observed in almost all cases.

It was not clear whether these influences of additives could be attributed to the disordering of crystals or a decreasing ability for the preservation of active species.

**Thermal Stability of Polymers.** The results of thermal stability determinations on the polymers at 200°C. in air are shown in Figures 9 and 10.

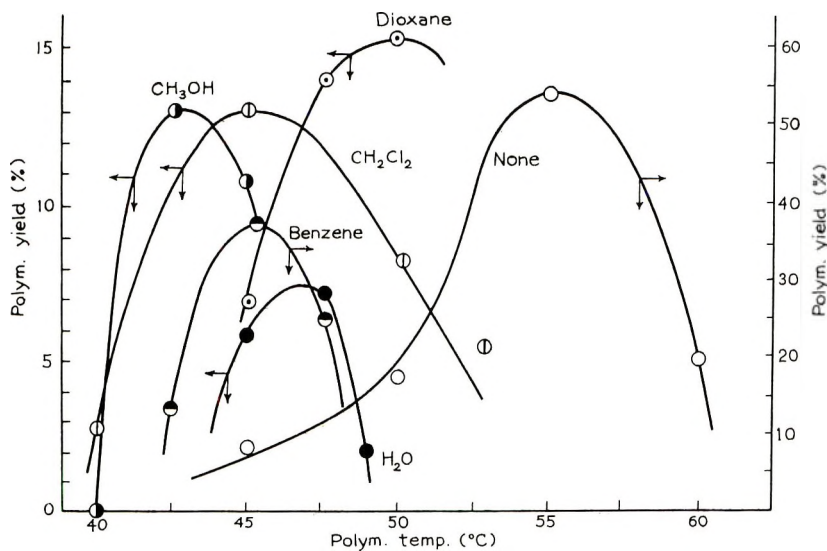


Fig. 8. Effect of additive in post-polymerization. Additives 5%,  $1.3 \times 10^6$  r; polymer yield at 5 hr. post-polymerization.

Polymers used for Figure 9a were obtained by polymerization at 55°C. after preirradiation with a dose of  $1.3 \times 10^6$  r. This figure shows a tendency for the thermal stability of polymers to improve with increasing post-polymerization time, that is, with decreasing of dose rate at a fixed dose.

The influence of the polymerization temperature on the thermal stability is shown in Figure 9b. The preirradiation dose was  $1.3 \times 10^6$  r. Figure 9b shows that the stability was improved by decreasing the polymerization temperature.

Figure 9c shows the influence of the total dose on the thermal decomposition of polymers which were polymerized at 55°C. It was expected that the stability might diminish with an increase of the preirradiation dose.

Figure 9d shows also the influence of additives. Samples used here were obtained at the temperature which gives the maximum yield in each case.

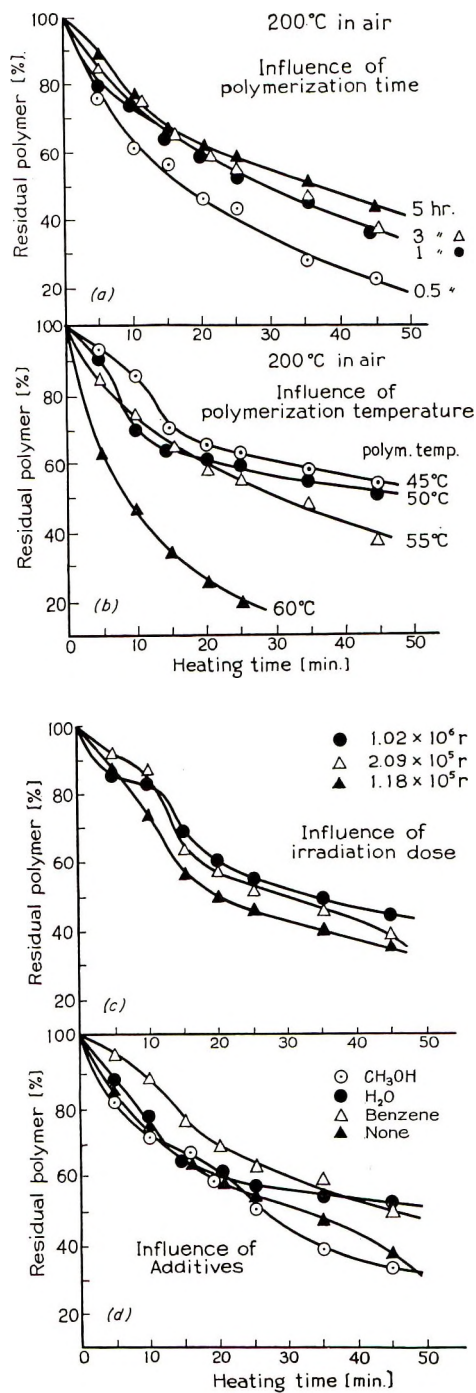


Fig. 9. Thermal stability of polymer.



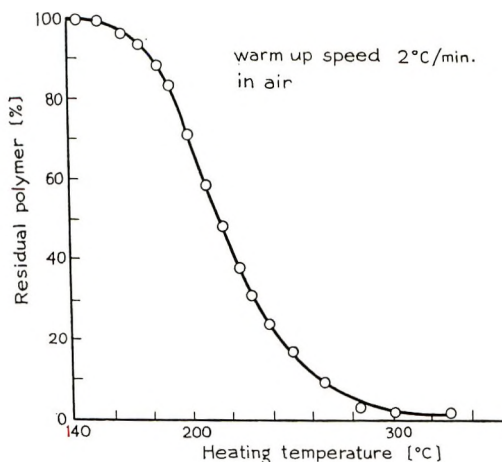


Fig. 10. Thermal stability of polymer at various temperatures.

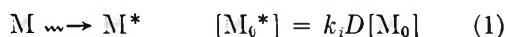
These are 45°C. for benzene, 42.5°C. for methanol, etc. It appears that thermal stability of polymers is not influenced by the presence of additives.

It was observed that almost in all cases the thermal decomposition curves showed sharp changes in slope. This phenomenon should be investigated further.

### Discussion

The following kinetic scheme accounts for the results obtained above.

#### 1. Formation of the Active Species (Initiation Reaction).



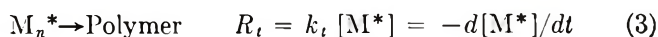
It is assumed that the formation of active species is proportional to the preirradiation dose,  $D$ , and the initial monomer concentration,  $[M_0]$ , and is not related to the dose rate.

#### 2. Propagation Reaction.



The active species is able to react only with the neighboring monomer because the reaction is carried out in the solid state and the chain must propagate in a fixed direction. Therefore, the polymerization rate is proportional only to the concentration of active species  $[M^*]$  and is independent of the monomer concentration.

#### 3. Termination Reaction.



Unimolecular termination by a crystal defect or irradiation damage is assumed. Here,  $k_i$ ,  $k_p$ , and  $k_t$  are the rate constants of initiation, propagation, and termination, respectively. From eq. (3)

$$[M^*] = [M_0^*]e^{-k_t t} \quad (4)$$

Combining eqs. (4) and (1) yields

$$[M^*] = k_i D [M_0] e^{-k_t t} \quad (5)$$

Denoting by  $x$  the polymer yield, we have

$$R_p = dx/dt = k_p k_i [M_0] D e^{-k_t t} \quad (6)$$

and

$$x = A (1 - e^{-k_t t}) \quad (7)$$

or

$$-\ln [1 - (x/A)] = k_t t \quad (8)$$

where

$$A = (k_p k_i / k_t) D [M_0]$$

The saturation yield of the polymer is obtained at infinite polymerization time so that

$$x_{t \rightarrow \infty} = A = \frac{k_p k_i}{k_t} [M_0] D \quad (9)$$

From eq. (9), it is evident that the saturation polymer yield is proportional to the preirradiation dose.

Figure 2 shows that this relation cannot be applied at higher doses, and there exists a maximum saturation yield independent of dosage. This phenomenon may be attributed to disruption of the monomer lattice by the formation of polymer and radiation damage, similar to that for the in-source polymerization of diketene,  $\beta$ -propiolactone, and 3,3-bis(chloromethyl)cyclohexane.

Equation (8) indicates that  $\ln [1 - (x/A)]$  must be linear in  $t$  with a slope  $k_t$ . This relation calculated from the initial values shown in Figure 3 is obtained as in Figure 11 and was shown to be well satisfied. Generally  $k_t$  is not greatly affected by temperature, but Figure 11 indicates a very different value of  $k_t$  at 45°C. compared to that at other temperatures. This may be due to a phase transition of the monomer crystals. The existence of a phase transition was confirmed by the change of the NMR peak width of trioxane crystal,<sup>3,8</sup> the change of the overall activation energy near this temperature, and the induction period in polymerization below the temperature of 47.5°C.

The degree of polymerization of the polytrioxane is, by eqs. (2) and (3),

$$DP = k_p / k_t = \text{const.} \quad (10)$$

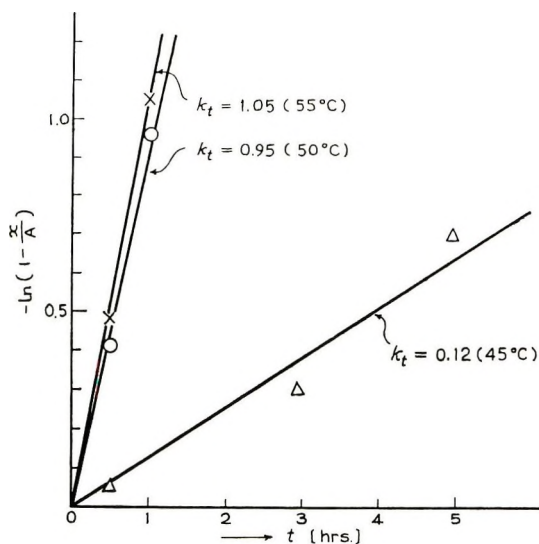


Fig. 11. Rate of polymerization.

Equation (10) shows that the polymerization degree is independent of the polymer yield. In fact, this relation is almost satisfied from the viscosity measurement of polymer in the solution of *p*-chlorophenol with  $\alpha$ -pinene as a stabilizer. However, measurements of thermal decomposition rates indicate that the thermal stability improves when the polymerization time and the degree of polymerization are increased, because the thermal stability is proportional to the degree of polymerization. The kinetic equation presented here is the treatment applicable only for the simplest case, and the situation may in fact be more complex. For example, there is the possibility of the successive addition propagation as in the case of the catalytic polymerization of cyclic monomers.

#### Attempt to Elucidate the Active Species

It has been assumed that in-source polymerization of trioxane was carried out by an ionic mechanism. However, it is completely unknown what mechanism is operative in post-polymerization, which could involve trapped ions, radicals, or unstable molecules which are apt to change into ions or radicals.

#### Results

**Influence of the Atmosphere.** Figure 12 indicates the influence of the atmosphere on the post-polymerization of trioxane. We cannot find any differences between the following three cases: (a) preirradiation and post-polymerization are both carried out in air; (b) after preirradiation *in vacuo* post-polymerization in air, (c) after irradiation in air, the sample is evacuated at  $-78^\circ\text{C}$ . and then post-polymerized. On the other

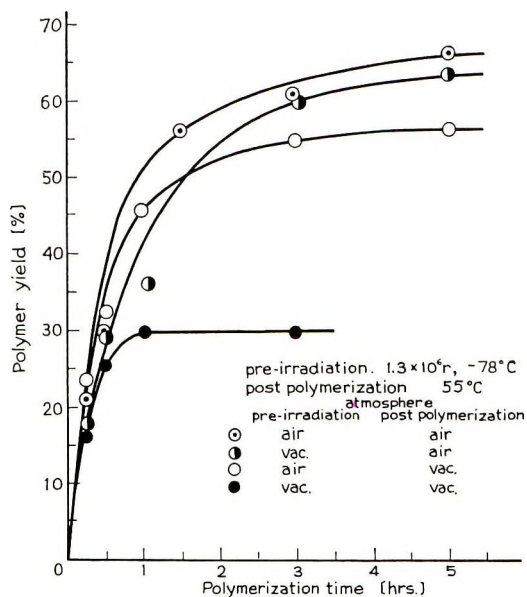


Fig. 12. Influence of atmosphere on post-polymerization.

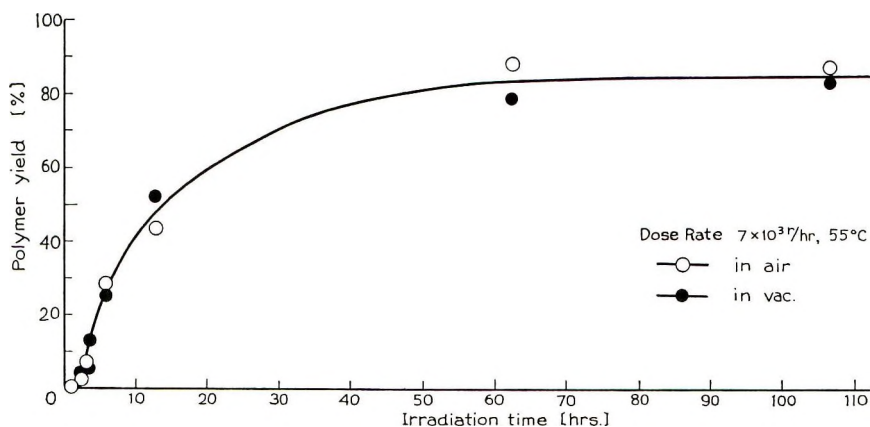


Fig. 13. Influence of atmosphere on in-source polymerization.

hand, the polymer yield falls to about a half if both irradiation and polymerization are carried out *in vacuo*.

By contrast, the influence of air cannot be observed in in-source polymerization. (Fig. 13)

These experiments show that oxygen has complicating effects on the polymerization of trioxane.

**Life of the Active Species.** When preirradiated trioxane was polymerized after being kept for various periods at temperatures at which no polymerization is observed, the subsequent polymerizability was found to decrease.

Figure 14 (broken line) indicates that there is no diminishing of the polymerizability if the sample is stored at  $-78^{\circ}\text{C}$ . in air under the same conditions used for preirradiation. Figures 14 and 15 (solid curves) the cases of storage at  $0^{\circ}\text{C}$ . in air and *in vacuo*, respectively, and Figure 15 (broken line) shows results on storage at  $40^{\circ}\text{C}$ . in air.

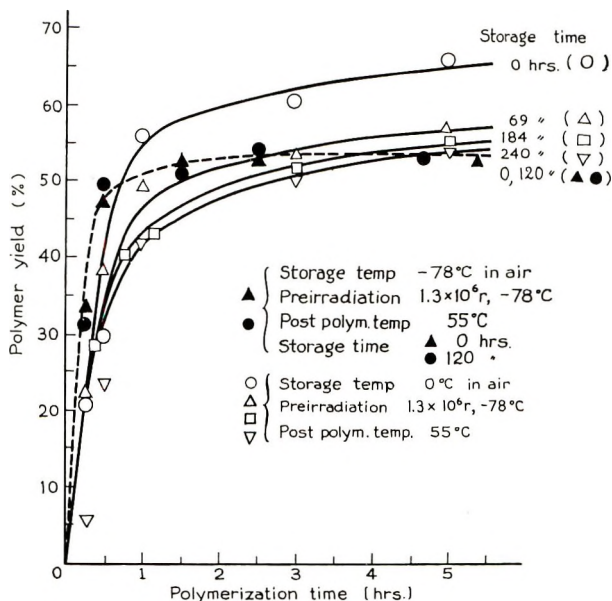


Fig. 14. Storage of active species.

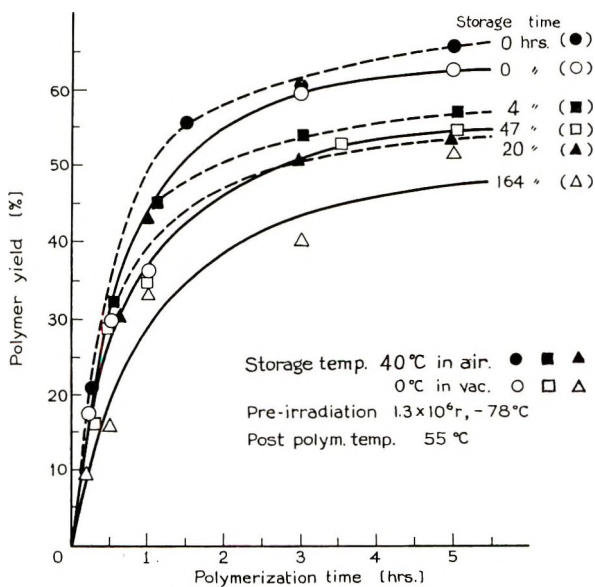


Fig. 15. Storage of active species.

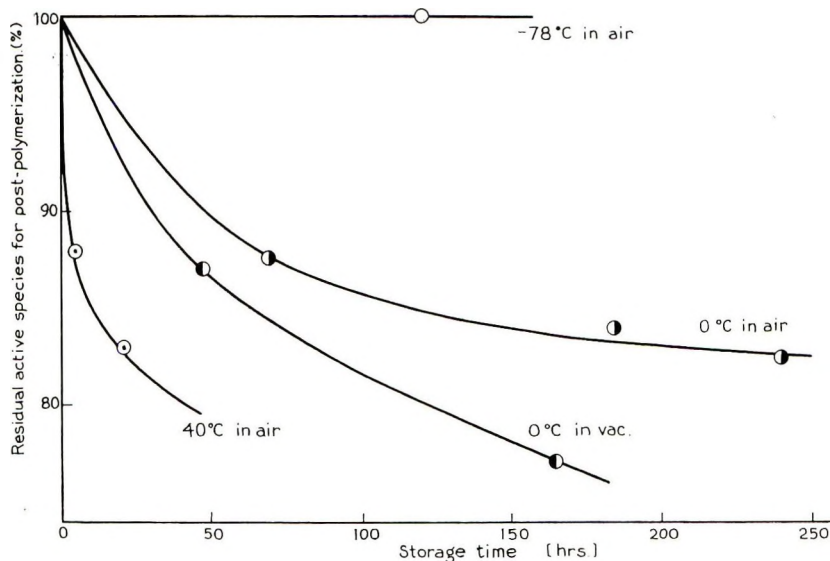


Fig. 16. Decay of active species.

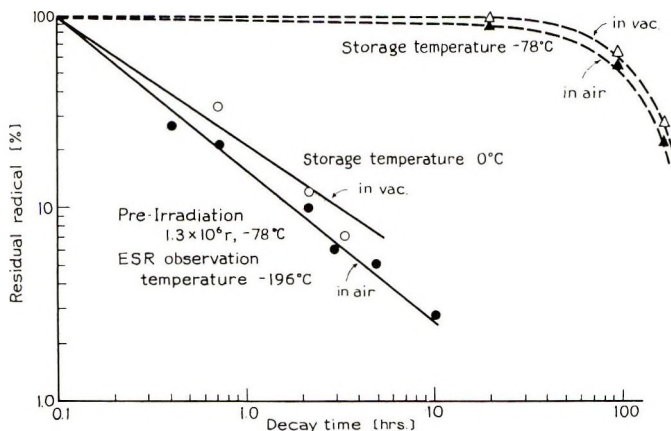


Fig. 17. Decay of radicals by ESR observation.

Except for cases where the irradiated crystals were stored at  $-78^{\circ}\text{C}.$ , it was found that the post-polymerizability falls with the storage period. The relation between the decreasing polymerizability and the storage period is shown in Fig. 16. The concentration of active species decreases faster with increasing storage temperature and the stability of active species in air is larger than *in vacuo*.

All of these results indicate that the life time of the active species may be very long and its stability is considerable.

**Decay of Trapped Radicals.** The decay of trapped radicals was measured by the ESR method. Figure 17 (broken line) shows the results for storage at  $-78^{\circ}\text{C}.$  The radical concentration falls to about 50% of the initial

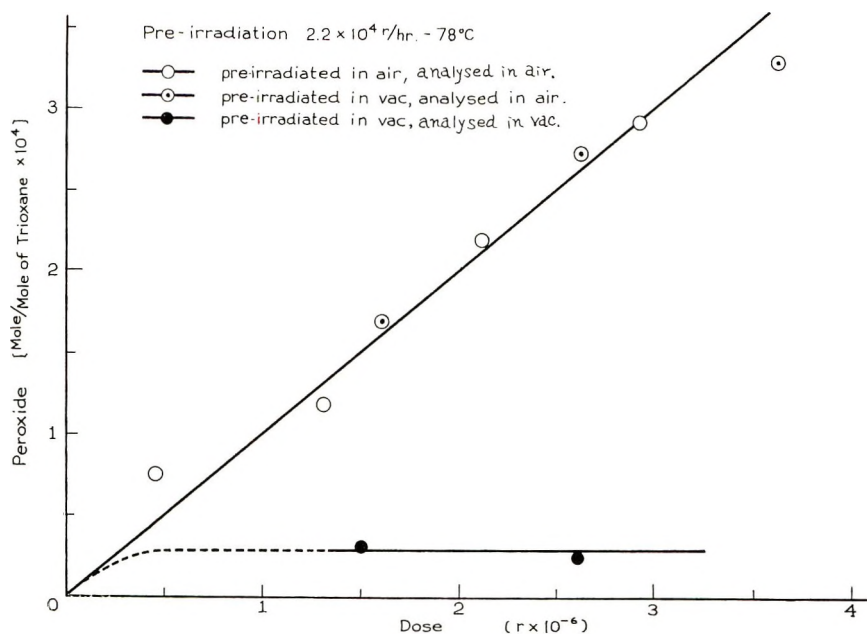


Fig. 18. Formation of peroxide by preirradiation.

value after storage for 120 hr., but the polymerizability remains constant at the same time. (cf. Figs. 14 and 16) In the same manner, Figure 17 (solid line) gives the results for storage at  $0^\circ\text{C}$ ., where the concentrations fall to about 10% after only 2 hr. Measurements cannot be carried out at  $40^\circ\text{C}$ ., since the decay is too rapid.

The decay of trapped radicals is more rapid in air than *in vacuo* both at  $-78$  and  $0^\circ\text{C}$ ., reversing the order of diminishing polymerizability. Therefore, there is no direct relation between the decay of radicals and the diminishing polymerizability.

**Formation of Peroxide.** Figure 18 shows the formation of peroxides by preirradiation. Formation of peroxide in air is proportional to total dose. However, the amount of peroxide obtained was the same when the trioxane preirradiated in *vacuo* was brought in contact with air by opening the glass tube. These results agree with the influence of air on the post-polymerization and indicate that the rate of peroxide formation is very rapid.

Peroxide is not found when trioxane is irradiated *in vacuo* and analyzed also *in vacuo* using degassed reagents.

It was confirmed that this peroxide decomposed rapidly at the temperature at which post-polymerization occurred. For instance, decomposition at  $55^\circ\text{C}$ . was so rapid that the peroxide almost disappeared after 5 min. of storage.

When the mixture of trioxane crystals and peroxide (benzoyl peroxide or cumene hydroperoxide) is heated at  $55^\circ\text{C}$ ., a small amount of polymer is obtained, in a yield of about 1%.

*Discussion*

As mentioned previously, radiation-induced polymerization of trioxane proceeds by an ionic mechanism (see also the answer in the discussion of the paper by Okamura et al.<sup>9</sup>). However, there arise many problems which are difficult to explain the post-polymerization by the ionic mechanism only. Although a conclusion has not yet been obtained, we shall try to consider the mechanism on the basis of the results obtained in this study.

In the first place, the following important differences are observed in a comparison of the in-source and post-polymerization. In-source polymerization is not affected by the presence of air but post-polymerization is strongly affected. There are large difference in the overall activation energy, that for in-source polymerization being  $\sim 5$  kcal./mole<sup>4</sup>, that for post-polymerization,  $\geq 40$  kcal./mole. Also, the possible temperature range for polymerization is for in-source polymerization, 20–62°C,<sup>4</sup> and for post-polymerization, 40–62°C. The above differences may be sufficient to suggest the possibility that these two processes are carried out by different mechanisms.

Furthermore, the following observations are inconsistent with an ionic mechanism for the post-polymerization. (a) The overall activation energy is very large. Generally, the overall molar activation energy for ionic polymerization is a few kilocalories. However, the value for post-polymerization is more than 40 kcal./mole, and it is difficult to attribute this large value to an ionic mechanism even in the solid phase. (b) The life time of the active species is very long. Usually the life time of ionic species is not very long, even at low temperature and in the solid state in which an ion is relatively stable. It is difficult to consider ionic species existing for as long as a few hours at the relatively high temperature of 40°C. (c) Trioxane, irradiated at low temperature, exhibits thermoluminescence with rising temperature due to the release of trapped electrons. If this luminescence is connected with post-polymerization, it is an important argument for an ionic mechanism. In fact, some relations were observed in the case of post-polymerization of  $\beta$ -propiolactone,<sup>5</sup> but with trioxane no such relation is indicated. Trioxane is polymerizable even when preirradiated samples are stored at a temperature at which all luminescence has disappeared. Moreover, almost as much polymer is obtained when preirradiation is carried out at this temperature.<sup>5</sup>

Arguments against a trapped radical mechanism are as follows. There is no direct relation between the decay of trapped radicals and lowering of the polymerizability when preirradiated samples are stored at a given temperature. The influence of oxygen on the rate of radical decay and the change of polymerizability are in opposite directions. Also, post-polymerization is not retarded by oxygen but accelerated. Further, trioxane polymerized easily only by ionic catalysts and it is difficult to initiate the reaction by radical catalysts or ultraviolet irradiation.

Let us now consider the peroxide produced by irradiation. If the assumption is made that the active species is the peroxide, and post-poly-



merization begins with the decomposition of peroxide, the following results may support these arguments. (a) Peroxide is produced by irradiation and is rapidly decomposed at the polymerization temperature. (b) The overall activation energy is larger than the value for ionic and radical polymerization and near the value for the decomposition of peroxides. (c) The polymer yield decreases *in vacuo*. (d) Influence of air on the polymer yield and on the formation of peroxide are in good agreement. (e) Trioxane can be polymerized by heating a sample mixed with peroxide, even though the yield is very small.

We believe, therefore, that post-polymerization of trioxane depends on an active species originating from the decomposition of peroxide and not on an ionic or trapped radical mechanism. However, the possibility of an ionic or trapped radical mechanism cannot be completely ruled out for the following reasons. (a) Trioxane can be polymerized only by the ionic catalyst in the case of liquid state catalytic polymerization. (b) Trioxane polymerizes easily with an ionic catalyst, even in the solid state.<sup>7</sup> (c) Polymerization occurs in spite of the absence of peroxides *in vacuo*. (d) There exists a possibility that the polymerization can be caused by very small amount of radicals which cannot be detected by ESR. (e) The formation of an acidic product was observed by means of pH measurement of the aqueous solution of irradiated trioxane,<sup>8</sup> which suggests an ionic mechanism by such acidic compounds.

The third reason is most important. This phenomenon may be attributed to very small amounts of peroxide due to the residual oxygen but it is more likely that there co-exist two different mechanisms in the post-polymerization of trioxane. A part of the trioxane polymerization in the presence of air may be caused by the decomposition of peroxide or peracid. Another part is polymerized even *in vacuo*, but the mechanism of this process is quite unknown at the present stage of the investigation.

### References

1. Okamura, S., K. Hayashi, and Y. Nakamura, *Isotopes Radiation*, **3**, 416 (1960).
2. Hayashi, K., and S. Okamura, *Makromol. Chem.*, **47**, 230, 237 (1961).
3. Hayashi, K., et al., paper presented at meeting of the Society of High Polymer, Japan, Kobe, June 1962.
4. Hayashi, K., Y. Nakase, and S. Okamura, paper presented at the annual meeting of the Chemical Society of Japan, Kyoto, April 1962.
5. Hayashi, K., S. Mori, and S. Okamura, *Makromol. Chem.*, **63**, 194 (1963).
6. Nakai, Y., S. Ohara, K. Hayashi, and S. Okamura, paper presented at the annual meeting of the Chemical Society of Japan, Kyoto, April 1962.
7. Okamura, S., T. Higashimura, and M. Tomikawa; *Kogyo Kagaku Zasshi*, **65**, 712 (1962).
8. Kawase, S., et al., paper presented at Symposium of High Polymer, Japan, Osaka, November 1962.
9. Okamura, S., K. Hayashi, and Y. Kitamishi, *J. Polymer Sci.*, **53**, 925 (1962).

### Résumé

Le trioxanne, le trimère cyclique du formaldéhyde est facilement polymérisable par radiation ionisante à l'état solide et à une température faiblement inférieure au point

de fusion. On a trouvé que cette post-polymérisation est analogue à la polymérisation première mais son énergie d'activation totale est supérieure à 40 Kcal/mole, et est plus grande que pour la polymérisation première. Un schéma cinétique a été proposé pour la post-polymérisation qui s'accorde avec les résultats expérimentaux. La polymérisation première se passe probablement par un mécanisme ionique mais pour la post-polymérisation il existe deux mécanismes différents. Le premier est probablement initié par la décomposition d'un corps produit par la radiation ionisante en présence d'oxygène. Le second n'a pas encore été clarifié mais semble être dû à un radical piégé ou une espèce ionique. La décomposition thermique du polymère formé et l'influence d'additifs tels que le méthanol, benzène . . . sur la post-polymérisation ont été étudiées.

### Zusammenfassung

Trioxan, das cyclische Trimere von Formaldehyd, wird durch ionisierende Strahlung im festen Zustand bei einer Temperatur knapp unterhalb des Schmelzpunktes leicht polymerisiert. Es zeigte sich, dass die Nachpolymerisation der Polymerisation während der Bestrahlung analog ist, nur ist ihre Bruttoaktivierungsenergie höher als 40 kcal/Mol und damit bedeutend grösser als die Polymerisation während der Bestrahlung. Für die Nachpolymerisation wird ein kinetisches Schema angegeben, das die Versuchsergebnisse befriedigend erklärt. Die Polymerisation während der Bestrahlung verläuft wahrscheinlich nach einem ionischen Mechanismus, während bei der Nachpolymerisation gleichzeitig zwei verschiedene Mechanismen wirksam sind. Einer wird wahrscheinlich durch die Zersetzung einer durch die ionisierende Strahlung in Gegenwart von Sauerstoff gebildeten Stoffes gestartet. Der andere wurde noch nicht aufgeklärt, scheint aber nichts mit eingeschlossenen Radikalen oder ionischen Produkten zu tun zu haben. Die thermische Zersetzung der gebildeten Polymeren, sowie der Einfluss von Zusätzen wie Methanol, Benzol . . . auf die Nachpolymerisation wurde untersucht

Received May 27, 1963

Revised July 22, 1963

## Origins of X-Ray Line Broadening in Polyethylene Single Crystals\*

H. G. THIELKE† and F. W. BILLMEYER, JR.,† *Department of  
Chemistry, University of Delaware, Newark, Delaware*

### Synopsis

If multiple orders of x-ray diffraction can be observed, the origins of line broadening in the diffraction pattern can be unambiguously assigned. In the absence of such data, rare in polymers, firm conclusions cannot be drawn. Line broadening data for single crystals of polyethylene, where multiple orders of diffraction were not observed, are consistent with the following origins: for planes with indices ( $hkl$ ), a size of 200 Å. and 1.3% strain; for the (002) plane, a size of 105 Å. (in good agreement with the lamellar thickness) if 1.3% strain is assumed, or 70 Å. (a lower limit) if no strain is assumed.

### INTRODUCTION

X-ray diffraction lines from the crystalline regions of polymers are typically broader than those from large single crystals of low molecular weight substances. This additional line broadening may arise from either small crystallite size or imperfect crystalline regions. A means of distinguishing between these possibilities would be helpful in assessing the relative merits of two current theories of the structure of crystalline polymers: the two-phase or fringed micelle theory,<sup>1</sup> in which the crystalline regions are considered small but perfect; and the single-phase or lamellar theory,<sup>2</sup> in which the crystalline regions are large in two dimensions but small in the third, and may contain many imperfections.

The cause of x-ray line broadening can be determined by assuming<sup>3</sup> that the broadening due to small crystal size and that due to imperfections are additive. The corrected line breadth  $B$  is given by

$$B \cos \theta/\lambda = 1/t + \epsilon \sin \theta/\lambda \quad (1)$$

where  $t$  is the apparent crystal size and  $\epsilon$  is the breadth of a strain distribution function characterizing the imperfections.

It does not appear to be generally recognized, however, that this equation is seriously restricted (for polymers) in that it is applicable only to successive orders of diffraction from a single crystal plane. The intensity

\* This research was performed by H. G. Thielke in partial fulfillment of the requirements for the degree of Master of Science at the University of Delaware.

† Mailing address: E. I. du Pont de Nemours and Company, Inc., Du Pont Experimental Station, Wilmington, Delaware.

of higher order diffraction is usually weak in polymers, and two or more orders of diffraction from the same plane seldom occur with high enough intensity for accurate measurements. The orders (110) and (220) were observed in highly oriented polyethylene filaments by Katayama,<sup>4</sup> however, and in metals multiple orders can readily be observed and the causes of line broadening assigned.<sup>5,6</sup>

In the absence of multiple orders, it is necessary to assume that the origins of line broadening are the same for a related group of crystal directions, such as those with indices ( $hk0$ ), to apply eq. (1). This assumption was made in the present study of line broadening in single crystals of polyethylene.

## EXPERIMENTAL

### Sample Preparation and Characterization

Single crystals were grown from polyethylene sample 85, an essentially linear polyethylene made in a low pressure synthesis using a transition metal halide-type catalyst. The crystals were grown by slow cooling of a dilute solution of the polymer in perchloroethylene. Examination by electron microscopy showed them to be typical dendritic single crystals,<sup>7</sup> presumably having the now-familiar folded chain conformation.

The crystals were allowed to settle into mats from which the solvent was removed by evaporation. Wide-angle x-ray diffraction experiments showed that the crystals were well oriented with the lamellae horizontal as the mat was laid down. A lamellar thickness of 105 Å. was calculated from the positions of first- and second-order diffraction maxima observed in small-angle x-ray diffraction.

### X-Ray Diffraction Techniques

X-ray diffraction patterns were recorded photographically with a Norelco diffraction unit, model 5001 (Philips Electronic Instruments Co.), and a 115-mm. Debye-Scherrer powder camera. The films were measured with a Knorr-Albers microphotometer (Leeds and Northrup Co). Film optical densities were related to exposure (x-ray intensity  $\times$  time) by means of characteristic curves determined from measurements of the diffraction patterns of sodium chloride. Experiments were made with x-ray tubes having molybdenum (wavelength 0.71 Å.), copper (1.54 Å.), cobalt (1.79 Å.), and chromium (2.29 Å.) targets.

A strip 0.020 in. square  $\times$  0.25 in. long, cut from the mat of polyethylene single crystals, was mounted in the powder camera with the surface of the mat perpendicular to the x-ray beam for observation of diffraction from ( $hk0$ ) planes. The sample was rotated 90° to place the beam parallel to the surface of the mat for observation of diffraction from the (002) plane.

### Measurement of Line Broadening

Line breadth was measured at the point of half maximum scattered intensity above the background, the intensities being determined from film optical densities by reference to the characteristic curves. For each x-ray wavelength, the instrumental line broadening (resulting from the divergence of the x-ray beam, the slit width of the camera and microphotometer, and other constant factors) was determined from diffraction patterns from single crystals of sodium chloride sufficiently large to introduce no small crystallite line broadening. The corrected line broadening from the polyethylene crystals was calculated as the square root of the difference between the squares of the observed and instrumental line broadening.<sup>8</sup>

### RESULTS AND DISCUSSION

Corrected line broadening is listed in Table I for several crystal planes of polyethylene. Weaker planes were located by their angular positions given by Bunn.<sup>10</sup> The instrumental line broadening is also indicated. Error figures, where included, are 95% confidence limits based on 7–10 measurements. Where no error figure is given, only one measurement was made.

TABLE I  
X-Ray Line Broadening for Polyethylene Single Crystals

Crystal plane	Line broadening, radians $\times 10^3$ , for various wavelengths			
	0.71 Å.	1.54 Å.	1.79 Å.	2.29 Å.
110	8.7 $\pm$ 1.9	11.2 $\pm$ 1.2	17.1 $\pm$ 0.9	15.1 $\pm$ 0.7
200	—	9.6	15.8	17.5
320/410	—	15.2	24.2	26.7
011	—	17.2	26.3	27.5
211	—	12.3	25.2	22.3
002	15.0	27.8	37.3	40.6
Instrumental	12.1 $\pm$ 0.7	11.6 $\pm$ 0.4	9.5 $\pm$ 0.6	7.2 $\pm$ 0.8

In a plot of eq. (1), the data for the  $(hk0)$  planes are reasonably consistent with the assumption that the line broadening of these planes has a common origin. The intercept and slope of the plot correspond to a crystallite size of 200 Å. and a strain of 1.3%, respectively. The value of the strain agrees with that found by Katayama<sup>4</sup> for the (110) plane in oriented polyethylene fibers. The observed crystallite size may imply that the perfect crystalline regions are much smaller than the overall dimensions of the single crystals, but it is difficult to draw a firm conclusion.

If the line broadening of the (002) plane results from a combination of 1.3% strain and small crystallite size, the size is calculated to be 105 Å., in good agreement with the lamellar thickness observed by low-angle x-ray diffraction. If the broadening of this line results entirely from small

crystallite size,<sup>9</sup> this size is calculated to be 70 Å. and is, of course, a lower limit. This value is still qualitatively of the correct order of magnitude, since the thickness of the perfect crystal regions must be somewhat smaller than the spacing between successive lamellae.

It was not possible to draw any conclusions about the origins of line broadening for the (011) and (211) planes, because of their complex relation to simple crystallographic directions.

General conclusions, however, are as follows. (1) Firm conclusions cannot be drawn about the origins of line broadening in polymer crystals unless two, or preferably more, successive orders of reflection can be observed. In the diffraction patterns of polymers, this is very rarely the case. (2) In the absence of multiple orders, it is virtually fruitless to attempt to assign the origins of line broadening to strain or imperfections, small crystallite size, or a combination of these factors.

### References

1. Bryant, W. M. D., *J. Polymer Sci.*, **2**, 547 (1947).
2. Keller, A., *Phil. Mag.*, [8] **2**, 1171 (1957).
3. Hall, W. H., *Proc. Phys. Soc. (London)*, **A62**, 741 (1949).
4. Katayama, K., *J. Phys. Soc. Japan*, **16**, 462 (1961).
5. Dehlinger, U., and A. Kochendorfer, *Z. Metallk.*, **31**, 231 (1939).
6. Smith, C. S., and E. E. Stickley, *Phys. Rev.*, **64**, 191 (1943).
7. Geil, P. H., and D. H. Reneker, *J. Polymer Sci.*, **51**, 569 (1961).
8. Warren, B. E., *J. Appl. Phys.*, **12**, 375 (1941).
9. Jones, F. W., *Proc. Roy. Soc. (London)*, **A166**, 16 (1938).
10. Bunn, C. W., *Trans. Faraday Soc.*, **35**, 482 (1939).

### Résumé

Si on peut observer des ordres multiples de diffraction par rayons-X, les origines des élargissements des lignes dans les figures de diffraction peuvent être déterminées sans ambiguïté. En absence de ces données, ce qui est rare pour des polymères, on ne peut pas tirer des conclusions définitives. Des résultats sur l'élargissement des lignes pour des cristaux uniques du polyéthylène, où on n'observe pas différents ordres de diffractions, sont compatibles avec les origines, suivantes: pour les plans possédant les indices ( $hk0$ ), une dimension de 200 Å et 1,3% de tension interne.

### Zusammenfassung

Wenn höhere Ordnungen bei Röntgenbeugung beobachtet werden können, so kann der Ursprung der Linienverbreiterung im Beugungsdiagramm eindeutig zugeordnet werden. In Ermangelung solcher bei Polymeren seltenen Daten können keine sicheren Schlüsse gezogen werden. Daten für die Linienverbreiterung für einzelne Polyäthyleneinkristalle, wo keine Beugung höherer Ordnung beobachtet wurde, lassen sich auf folgende Ursachen zurückführen: Für Ebenen mit den Indizes ( $hk0$ ), eine Grösse von 200 Å und 1,3% Verformung.

Received August 29, 1963

## Comparison of the Effects of Allylamine and *n*-Propylamine on Cellulose

LEON SEGAL, *Plant Fibers Pioneering Research Laboratory,\*  
New Orleans, Louisiana*

### Synopsis

Allylamine partially penetrates the cellulose crystal lattice and effects only partial transformation to the cellulose-amine complex. The 101 interplanar spacing of the allylamine complex is similar to that of the propylamine complex. Differences in amine interaction with cellulose are not explained by considerations of base strength of amines, stereochemistry, or degree of association of the amines. Cellulose treated with ethylamine, then allylamine is completely transformed to what seems to be the cellulose-allylamine complex. Slow evaporation of allylamine from the cellulose I complex seems to produce cellulose III; from the cellulose II complex, cellulose II. Fast evaporation of ethyl-, propyl-, or allylamine from amine-wet cellulose restores the initial cellulose lattice. Slow evaporation of ethylamine produces cellulose III; of propylamine a mixed lattice of cellulose I with little cellulose III and much of the complex.

Studies conducted at this laboratory on the interaction of cellulose with amines have shown that removal of ethylamine from the cellulose I-ethylamine complex with chloroform regenerates cellulose I with reduced crystallinity.<sup>1</sup> Removing ethylamine by evaporation under reduced pressure was shown to cause a lattice transformation, producing cellulose III.<sup>2</sup> There seems to be little in the literature to indicate whether cellulose III might be expected from the decomposition of complexes of cellulose with amines other than ethylamine, or what effect structural variations in the hydrocarbon portion of the amine might have on complex formation. This paper presents some results obtained from experiments designed for observing what effects amines of similar structure, allylamine ( $\text{CH}_2=\text{CH}-\text{CH}_2-\text{NH}_2$ ) and *n*-propylamine ( $\text{CH}_3-\text{CH}_2-\text{CH}_2-\text{NH}_2$ ) have on the cellulose crystal lattice, and for determining what lattice transformations result when either amine is removed from the corresponding amine-wet cellulose.

### MATERIALS AND METHODS

The allyl- and *n*-propylamines used were reagent-grade chemicals. Ethylamine when required was condensed from a supply cylinder in glass equipment cooled with ice water. For cellulose I a kiered, loose-twist,

\* One of the laboratories of the Southern Utilization Research and Development Division, Agricultural Research Service, U.S. Department of Agriculture.

combed cotton yarn was used. Cellulose II was prepared from the purified cotton by the usual mercerizing process using an 18% sodium hydroxide solution. Essentially complete lattice transformation was verified by x-ray diffractograms.

Cotton yarn for treatment with amine was ground in a Wiley mill to pass through a 20-mesh screen. Suitable quantities of the cut fiber were placed in glass-stoppered Erlenmeyer flasks, and the amines added until there was an excess of liquid. The stoppered flasks were usually set aside to stand overnight at room temperature. In some cases the cut fiber was allowed to soak as long as six days to establish that time of treatment longer than overnight did not influence the results. When treatment with ethylamine was required, the liquid amine was merely poured in quickly and the flask stored in a refrigerator for at least 16 hr. (overnight). When pretreatment by ethylamine was required to ensure lattice penetration by the higher amines, the procedure given by Davis and co-workers<sup>3</sup> was followed for the most part, except that several cycles of vacuum and amine were applied. A portion of the mat was removed for x-ray examination.

Removal of amine from the amine-wet samples was accomplished by fast and slow evaporation. In both cases excess amine was first decanted from the flask. For fast evaporation the opened flask containing the sample was placed on a steam bath. Within minutes all traces of liquid disappeared; the fiber was held on the bath for at least 30 min. longer. Slow evaporation was accomplished by applying house vacuum (35 mm. Hg pressure) for 6-7 hr.<sup>2</sup> If frost appeared on the flask, a water bath at room temperature was raised about the flask. Amine content was determined on weighed sample portions placed in distilled water and titrated to the endpoint electrometrically with standard hydrochloric acid.

X-ray diffractograms were obtained with a Philips, wide-range, precision, x-ray diffractometer (copper  $K\alpha$  radiation). A nickel filter mounted before the receiving slit eliminated the  $K\beta$  component. The diffractograms of amine-wet samples were taken with the sample held in a special holder designed for wet cellulosic materials.<sup>4</sup> Diffractograms of the dry fiber were obtained from 1 × 2 cm. plates, 0.150 g. in weight, pressed in a combination die and holder at a pressure of 25,000 lb./in.<sup>2</sup>

## RESULTS AND DISCUSSION

### Examination of Amine-Wet Specimens

The x-ray diffractograms obtained from allylamine- and propylamine-wet celluloses I and II are shown in Figure 1. It is immediately apparent in Figures 1A and 1C, the allylamine-wet samples, that the lattices of the original cellulose I and cellulose II have been markedly disrupted. For example, the cellulose I interferences at  $2\theta = 14.8^\circ$  and  $16.2^\circ$  have been shifted, while that of cellulose II at  $2\theta = 12.0^\circ$  has practically disappeared. Allylamine did not completely penetrate the crystalline lattice of either form of cellulose to effect lattice transformation to that of the complex



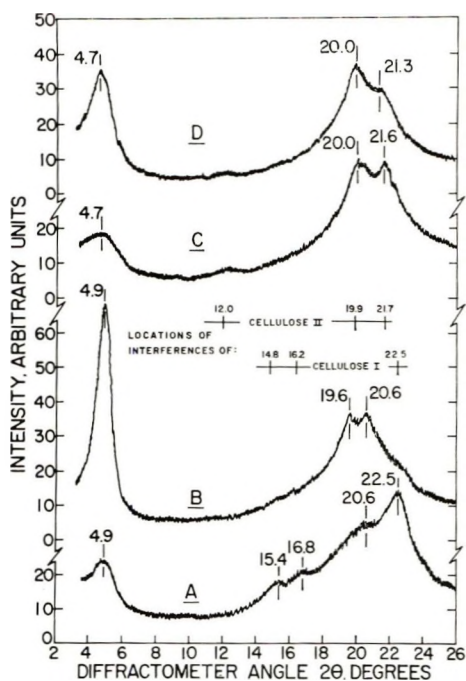


Fig. 1. X-ray diffractograms of allylamine- and propylamine-wet celluloses I and II: (A) allylamine and cellulose I; (B) propylamine and cellulose I; (C) allylamine and cellulose II; (D) propylamine and cellulose II.

alone. However, the new, broad interference in the region  $2\theta = 4.7\text{--}4.9^\circ$  of both tracings and the poorly resolved one at  $2\theta = 20.6^\circ$  in the cellulose I-amine tracing (Fig. 1A) indicate that some complex formation had occurred. Figures 1A and 1C bear some similarities, but one cannot expect any reasonable match of patterns when there remains so much of the initial interferences and such overlapping of the initial and the new interferences.

Allylamine ( $\text{CH}_2=\text{CH}-\text{CH}_2\text{NH}_2$ ) is related to propylamine ( $\text{CH}_3-\text{CH}_2-\text{CH}_2\text{NH}_2$ ), and, therefore, one should perhaps expect some similarity in the x-ray patterns of the cellulose complexes of the two amines. The diffractograms from the propylamine-wet celluloses given in Figures 1B and 1D indicate complete lattice penetration and complex formation. The observed differences between the diffractograms of the cellulose I and cellulose II complexes are not unexpected, as such an effect, but of somewhat different magnitude, has been reported previously.<sup>5</sup> The most prominent feature in the diffractograms of Figure 1 is the 101 interference ( $2\theta = 4.9^\circ$  for the cellulose I,  $4.7^\circ$  for the cellulose II complexes) which has the same location for the allyl- and the propylamine complexes of the two celluloses. The similar lattice distention indicated by the 101 peak would be expected from the similar chain length of the two amines. (Close comparison of Stuart-Briegleb molecular models of the molecules in the ex-

tended state shows only a very slightly longer length for propylamine; the two molecules are more similar when in the closest folded conformation.) Explanation is needed, however, for the incompleteness of the lattice transformation (or lack of appearance of the expected interferences) and the weakness of the intensities of such interferences of the cellulose-allylamine complex that do appear.

As the amine-cellulose complexes involve hydrogen bonding, amine base strength, which is related to the ease of sharing the lone electron pair of the amine nitrogen atom engaged in the bonding, might be a significant factor. Although base strength data are usually for an aqueous system which was not used here, Hall<sup>6</sup> and Mead<sup>7</sup> have shown that the base strength of amines in water is a good index of base strength in organic solvents. Hall<sup>6</sup> reports a  $pK_a$  of 10.59 for propylamine and 9.53 for allylamine. This lowered strength is the effect of the double bond predicted theoretically by Vexlearski and Rumpf.<sup>5</sup> Lowered base strength of allylamine, compared to propylamine, was also found in the electrometric half-neutralization values when amines were titrated in ethyl acetate with perchloric acid<sup>6</sup> and in the heats of neutralization for reaction in benzene with trichloroacetic acid.<sup>7</sup>

On the surface, then, lowered base strength seems sufficient to explain the difference in behavior of these amines toward cellulose. This seems to be supported, too, by the observation that monoethanolamine,  $\text{HO}-\text{CH}_2-\text{CH}_2-\text{NH}_2$ , which does not by itself penetrate the cellulose lattice and effect lattice transformation, has a  $pK_a$  of 9.45. On the other hand, *n*-butylamine which behaves similarly to monoethanolamine, has a  $pK_a$  of 10.61, comparable to that of propylamine. Di-*n*-butylamine,  $pK_a$  11.31, and diethylamine,  $pK_a$  11.00, amines more basic than propylamine, do not penetrate the cellulose crystal lattice as do propylamine, or ethylamine with a  $pK_a$  of 10.75.<sup>9</sup> Isopropylamine,  $pK_a$ , 10.63, also falls into the category of the secondary amines although it is not a secondary amine. So the proposition that base strength is highly significant does not seem to be the important factor.

Examination of the molecular models of allylamine and propylamine fail to show a difference in size or shape sufficient to account for their difference in behavior. The values of the molar volumes, 75.1 for allylamine and 82.2 for propylamine, as well as their parachors, 169.8 and 180.8, respectively, are in the wrong direction for bulk to be a factor. However, steric hindrance is the explanation offered by Davis and co-workers for the inability of *n*-butylamine (and the higher homologs) to penetrate the lattice. *n*-Butylamine adds only one  $-\text{CH}_2-$  group to the hydrocarbon portion of propylamine which is hardly sufficient to sterically hinder an interaction. Davis' explanation seems supported, though, by the greater molar volume, 98.8, and larger parachor, 219.8, of *n*-butylamine, but it fails with monoethanolamine and allylamine with molar volumes of 60.0 and 75.1 and parachors of 161.8 and 169.8. Be that as it may, pretreatment with liquid ammonia or ethylamine resulting in entrance of the

longer-chain amines into the lattice is evidence for a bulk factor that is difficult to refute. On the other hand, Creely, Segal, and Loeb<sup>10</sup> have shown that diamines from ethylene to heptamethylene easily penetrate the lattice and directly form diamine-cellulose complexes, all without pretreatment. This renders less clear-cut the role assigned to steric effects, and indicates that further study is required in this area.

TABLE I  
Interplanar Spacings for Propylamine-Cellulose Complexes

Assigned indices	Interplanar spacings, A.		
	Present work <sup>a</sup>		Davis and co-workers <sup>b</sup> cellulose I-amine
	Cellulose I-amine	Cellulose II-amine	
101	18.02 (4.9)	18.79 (4.7)	18.48 (4.8)
10 $\bar{1}$	4.53 (19.6)	4.44 (20.0)	4.35 (20.4)
002	4.31 (20.6)	4.17 (21.3)	—

<sup>a</sup> Figures in parentheses are the observed diffractometer angles  $2\theta$ .

<sup>b</sup> Figures in parentheses are diffractometer angles  $2\theta$  computed from the spacings given by Davis et al.<sup>3</sup>

Before passing, however, some comments should be made regarding the propylamine data reported here and those reported for the complex by Davis and co-workers.<sup>3</sup> Table I lists data reported by Davis et al., and those obtained in the present study. The principal discrepancies here, those involving assignment of interplanar spacings to the 10 $\bar{1}$  and 002 interferences, are considered to have arisen from certain limitations in the methods used by Davis and co-workers which could have influenced the interpretation of their data. Davis and co-workers have stated of propylamine: "This is the highest amine which will swell cellulose without pretreatment, hence the appearance of a few diffractions of normal cellulose is significant in that it indicates that the swelling in this case is not quite complete." Careful study of their work discloses the presence of several factors not readily apparent which possibly are highly contributory to this incomplete interaction and to the scantiness of the x-ray data. For example, the ramie fibers studied were held in bundles under tension. Tension in the cellulose structure has been shown to inhibit swelling (lattice penetration) and retard complete lattice transformation.<sup>11</sup> Copper radiation from the x-ray apparatus was unfiltered, allowing  $K\beta$  peaks to appear in the diagrams. This factor is important because interpretation of x-ray data becomes complicated when radiation is not monochromatic. One may now gather from studying Figure 1 and Table I of Davis' data that it is not the 10 $\bar{1}$  and 002 interferences that have merged or that the 002 peak has disappeared, but rather that the 10 $\bar{1}$  and  $K\beta$  peaks have merged. The interplanar spacing that Davis has listed for his assigned 10 $\bar{1}$  agrees with that assigned here to 002, while that of the presently assigned 10 $\bar{1}$  interference is of the right order of magnitude for a

peak in Davis' work that would be the above-mentioned combined  $10\bar{1} + K\beta$  interference. Davis and co-workers treated only cellulose I and so did not obtain verification of the effect of the amine on the cellulose lattice.

### Examination of Ethylamine-Pretreated, Allylamine-Wet Specimens

The diffractograms of ethylamine-pretreated, allylamine-wet celluloses (Fig. 2) are notably different from those of Figures 1A and 1C, and indicate complete lattice penetration and transformation. The tracings are quite close in appearance to that of propylamine-wet cellulose I (Fig. 1B) which is what was originally expected of allylamine-wet cellulose. If the products here are indeed the allylamine-cellulose complexes, their formation in this manner brings up more questions.

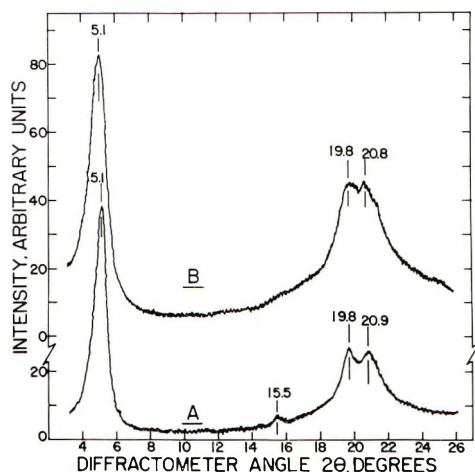


Fig. 2. X-ray diffractograms of ethylamine-pretreated, allylamine-wet celluloses: (A) cellulose I sample; (B) cellulose II sample.

With successful ethylamine-pretreatment (consistent with Davis' findings with other amines) suggesting that steric effects are involved, the observed behavior of allylamine might be attributable to bulkiness of the C=C grouping. The molecular model shows that the two carbon atoms of the  $-\text{CH}=\text{CH}_2$  group are broadened (compared to a single-bonded carbon atom) and are merged by the double bond into a doubly pinched discoid. But, again, comparison with the propylamine model fails to show spatial factors sufficiently great to exert such influence on the behavior of allylamine. Monoethanolamine, referred to earlier, is more closely comparable in dimensions and shape to propylamine than is allylamine, yet behaves like allylamine. Allylamine and monoethanolamine have this in common: the end of the chain, away from the amine group, terminates in other than  $-\text{CH}_3$ . Thus, for allylamine,  $=\text{CH}_2$ , and for monoethanolamine,  $-\text{OH}$ . But, ethylenediamine terminating in  $-\text{NH}_2$  does not behave like these two amines at all. Consideration of the amines

TABLE II  
Data on Amines and the 101 Interplanar Spacings of Amine-Wet Celluloses

Cellulose I wet with	Structure of amine	Boiling point of amine, °C.	101 interplanar spacing, Å.
Allylamine, pretreated with anhydrous ethylamine	$\text{CH}_2=\text{CH}-\text{CH}_2-\text{NH}_2$	53.2	17.66
Monoethanolamine, pretreated with liquid ammonia	$\text{HO}-\text{CH}_2-\text{CH}_2-\text{NH}_2$	172.2	11.32 <sup>a</sup>
Ethylenediamine	$\text{NH}_2-\text{CH}_2-\text{CH}_2-\text{NH}_2$	116.1	11.40 <sup>b</sup>
Propylamine	$\text{CH}_3-\text{CH}_2-\text{CH}_2-\text{NH}_2$	48.7	18.48

<sup>a</sup> Data of Davis and co-workers.<sup>3</sup>

<sup>b</sup> Data of Creely and co-workers.<sup>10</sup>

in this light does not begin to explain the differences in interplanar spacings shown in Table II, nor their behavior.

A glance at the boiling points of the amines seems to suggest that the degree of association of the amines might be related to their behavior with cellulose. Thus, there are two groups here—high boiling amines (highly associated) coupled with an 11 Å. spacing in the complex, and low boiling amines (low association) with an 18 Å. spacing. But on turning to the ability of the amines to directly penetrate the cellulose lattice and effect complete lattice transformation, one finds no relationship between this and the boiling point data.

So far, aspects of the amines have been discussed. Still to be studied are factors of cellulose itself which may reveal further information on the problem.

### Examination of Specimens after Removal of Amines by Evaporation

Fast evaporation of allylamine and of propylamine from amine-wet cellulose resulted in sharp, clear diffractograms of the original celluloses I and II. (Fig. 3C is the diffractogram, for example, of the product from propylamine and cellulose I.) Figure 3A, however, shows that fast evaporation applied to the ethylamine-wet sample also resulted in much cellulose I, and not the expected transformation to cellulose III. Slow evaporation of the ethylamine, however, gave the expected cellulose III (Fig. 3B).

Mann and Marrinan<sup>12</sup> reported production of cellulose I of reduced crystallinity, instead of cellulose III, from bacterial cellulose when the amine was evaporated. In a later work<sup>13</sup> they reported that the product obtained is dependent on the rate of evaporation of the amine. The present results confirm their statement that "If the ethylamine is evaporated slowly cellulose III is produced, but if evaporation is carried out quickly only a reduction in crystallinity occurs." The appearance of some cellulose III in Figure 3A does not contradict the statement, as the rate of evaporation from a mat of fibers would not be as rapid as that from a thin film of bacterial cellulose.

When propylamine was slowly evaporated from propylamine-wet cellulose I, the product gave a diffractogram (Fig. 3D) showing a mixture of cellulose I, cellulose I-propylamine complex, possibly some trace of cellulose III. There is no doubt, though, that evaporation of propylamine under the same conditions as for ethylamine fails to cause substantial conversion of cellulose I to cellulose III.

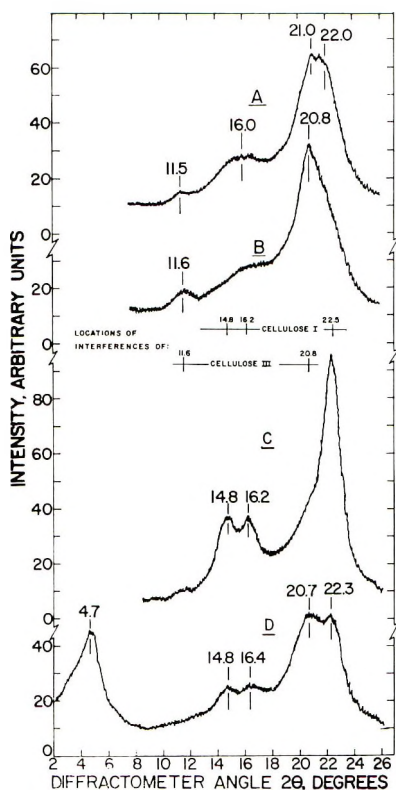


Fig. 3. X-ray diffractograms of the products obtained by evaporation of amine from amine-wet cellulose I: (A) fast evaporation of ethylamine; (B) slow evaporation of ethylamine; (C) fast evaporation of propylamine; (D) slow evaporation of propylamine.

Slow evaporation of allylamine from amine-wet cellulose led to different products, dependent on the pretreatment of the cellulose. With no ethylamine pretreatment, allylamine-wet cellulose I still returned to cellulose I, even after slow evaporation (Fig. 4A). Ethylamine pretreatment, however, changed the results as can be seen in Figure 4B. This diffractogram strongly resembles that of cellulose III, except for the broad interference at  $2\theta = 4.2^\circ$ . The interference is hardly likely to be a displacement of the peak found in allylamine-wet cellulose I at  $2\theta = 5.1^\circ$  as it represents a greater interplanar spacing than that of the amine-wet sample. Its origin is not clear, but it is most probably connected with the 15% amine content (as allylamine) found in the dry sample. Further investigation is required

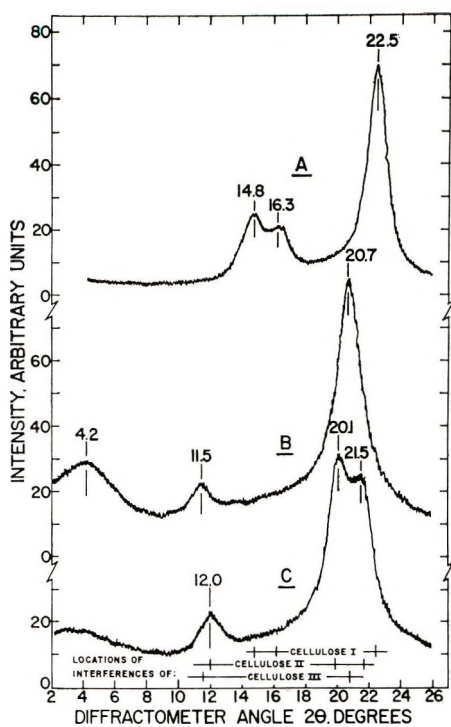


Fig. 4. X-ray diffractograms of samples after slow evaporative removal of allylamine from allylamine-wet celluloses: (A) cellulose I sample, no ethylamine pretreatment; (B) cellulose I sample, ethylamine pretreatment; (C) cellulose II sample, ethylamine pretreatment.

before any Miller index can be assigned. A similar interference appeared in the diffractogram (not shown here) obtained from a cellulose II sample with 23% amine content, where the remainder of the interferences were sharp, clear interferences of cellulose II. Further exposure of this sample to vacuum reduced the amine content to 10.5%, whereupon only a diffuse scattering was found at  $2\theta = 4.5\text{--}5^\circ$  (Fig. 4C). Except for the diffuse scattering, the diffractogram was definitely that of cellulose II.

## SUMMARY AND CONCLUSIONS

Allylamine only partially penetrates the cellulose crystal lattice and, therefore, effects only partial transformation to the cellulose-allylamine complex. Propylamine penetrates the lattice completely and forms the propylamine-cellulose complex. The 101 interplanar spacings of the two complexes are similar as would be expected from similar chain lengths of amines. Differences in interaction of the amines with cellulose, as shown by the extent of lattice transformation and intensity of interferences, are not explained by considerations of base strength, size, and degree of association of the amines.

Fast evaporation of amine—ethyl, propyl, or allyl—restores the initial cellulose crystal lattice. Slow evaporation of ethylamine, however, produces cellulose III; slow evaporation of propylamine, a mixed lattice of cellulose I, little of cellulose III, and much of the complex.

Treatment of cellulose with ethylamine, then with excess allylamine, completely transforms the cellulose crystal lattice to that of what seems to be the allylamine–cellulose complex. Upon removal of the amine by evaporation, structural changes occur. Slow evaporation of allylamine under the same conditions used with ethylamine gives what appears to be cellulose III if cellulose I is the starting material. If cellulose II is the starting material, then that lattice seems to be restored.

The author wishes to acknowledge the work of F. V. Eggerton who obtained the amine contents of the amine–cellulose complexes.

It is not the policy of the Department to recommend the products of one company over those of any others engaged in the same business.

### References

1. Segal, L., M. L. Nelson, and C. M. Conrad, *J. Phys. Colloid Chem.*, **55**, 325 (1951); *Textile Res. J.*, **23**, 428 (1953).
2. Segal, L., L. Loeb, and J. J. Creely, *J. Polymer Sci.*, **13**, 193 (1954).
3. Davis, W. E., A. J. Barry, F. C. Peterson, and A. King, *J. Am. Chem. Soc.*, **65**, 1294 (1943).
4. Segal, L., *Textile Res. J.*, **32**, 702 (1962).
5. Segal, L., and J. J. Creely, *J. Polymer Sci.*, **50**, 451 (1961).
6. Hall, H. K., *J. Phys. Chem.*, **60**, 63 (1956); *J. Am. Chem. Soc.*, **79**, 5441 (1957).
7. Mead, T. E., *J. Phys. Chem.*, **66**, 2149 (1962).
8. Vexlearschi, G., and P. Rumpf, *Compt. Rend.*, **236**, 939 (1953).
9. Segal, L., *J. Polymer Sci.*, **B1**, 241 (1963).
10. Creely, J. J., L. Segal, and L. Loeb, *J. Polymer Sci.*, **36**, 205 (1959).
11. Ziifle, H. M., F. V. Eggerton, and L. Segal, *Textile Res. J.*, **29**, 13 (1959); L. Segal and C. M. Conrad, *Am. Dyestuff Repr.*, **46**, 637 (1957).
12. Mann, J., and H. J. Marrinan, *Chem. Ind. (London)*, **1953** No. **41**, 1092.
13. Marrinan, H. J., and J. Mann, *J. Polymer Sci.*, **21**, 301 (1956).

### Résumé

L'allylamine pénètre partiellement dans le réseau cristallin de la cellulose et ne produit qu'une transformation partielle en complexe cellulose-amine. La distance interplanarie 101 du complexe d'allylamine est semblable à celle du complexe avec la propylamine. Les différences dans l'interaction de la cellulose avec l'amine ne sont pas expliquées par la basicité des amines, la stéréochimie ou le degré d'association des amines. La cellulose traitée avec l'éthylamine et ensuite à l'allylamine est complètement transformée dans ce qui semble être un complexe celluloseallylamine. Une évaporation lente d'allylamine du complexe cellulose I semble donner la cellulose III, la même expérience avec le complexe cellulose II donne la cellulose II. L'évaporation rapide de l'éthyl-, propyl-, ou allylamine de la cellulose inbibée d'amine refournit le cristal initial de la cellulose. L'évaporation lente de l'éthylamine donne la cellulose III, l'évaporation de la propylamine un réseau mixte de cellulose I avec un peu de cellulose III et beaucoup de complexe.



### Zusammenfassung

Allylamin dringt zum Teil in das Cellulosekristallgitter ein und bewirkt eine nur teilweise Umwandlung zum Cellulose-Aminkomplex. Der 101-Gitterebenenabstand des Allylaminokomplexes ist dem des Propylaminkomplexes ähnlich. Unterschiede in der Wechselwirkung zwischen Aminen und Cellulose können nicht durch die Basenstärke der Amine, ihre Stereochemie oder ihren Assoziationsgrad erklärt werden. Zuerst mit Äthylamin und dann mit Allylamin behandelte Cellulose wird vollständig zu einem offensichtlichen Cellulose-Allylaminokomplex umgewandelt. Langsame Verdampfung von Allylamin aus dem Cellulose-I-Komplex scheint zu Cellulose III zu führen; aus dem Cellulose-II-Komplex zu Cellulose II. Rasche Verdampfung von Äthyl-, Propyl- oder Allylamin aus aminfeuchten Cellulosen ergibt wieder das ursprüngliche Cellulosegitter. Langsame Verdampfung von Äthylamin erzeugt Cellulose III, von Propylamin ein Mischgitter aus Cellulose I mit ein wenig Cellulose III und viel Komplex.

Received June 20, 1963

Revised August 21, 1963

## Effects of Swelling on Proton Relaxation in Vinyl Polymers\*

G. BONERA, A. CHIERICO, and A. RIGAMONTI, *Istituto di Fisica  
dell'Università, Università di Pavia, Pavia, Italy*

### Synopsis

Polystyrene and poly(methyl methacrylate) were swelled with the respective monomers and with suitable organic solvents. By means of a special experimental arrangement the spin-lattice relaxation times of the protons of the swelling agent and of those of the swelled polymer were measured separately. Differences between the spin-lattice relaxation time of the polymer during polymerization and that of the polymer swelled by the monomer are revealed and seem to point out a different degree of mobility in the polymer chains. In some instances an indication of differences in the motions that produce the relaxation is gained from the observed differences in the behavior of a polymer obtained through thermal polymerization and that of the same polymer obtained by ultraviolet radiation-induced polymerization. With regard to the swelling agent there is also some experimental evidence pointing out the remarkable role taken by internal rotations of molecular groups in the mechanism of relaxation.

### Introduction

Nuclear magnetic resonance has been applied to some extent to investigating the swelling processes of polymers with organic solvents. Measurements of the spin-spin relaxation time  $T_2$  in dilute solutions of PIB in  $\text{CCl}_4$  performed by Nolle<sup>1,2</sup> show considerable movements of the polymer chains. Other measurements<sup>3</sup> on PIB swelled by  $\text{CCl}_4$  give resonance lines which are very narrow also for a limited amount of swelling agent. The spin-lattice relaxation time  $T_1$  in a polystyrene-tetrachloroethylene solution at 25°C. has been measured by McCall and Bovey;<sup>4</sup> with a special technique some differences between  $T_1$ 's of the aromatic and aliphatic protons have been pointed out. The behavior at low temperatures of polystyrene swelled by organic substances containing hydrogen has also been studied through the linewidth of the resonance signal.<sup>5,6</sup> The application of NMR to the study of polymers swelled by organic substances containing protons has until now found limitations due to the difficulties of separating the resonance signal of the polymer protons from that of the protons of the swelling liquid.

In a recent work<sup>7</sup> it was shown that, during the polymerization of some vinyl compounds, the relaxation time  $T_{1i}$  of the protons of the monomer

\* Supported in part by a research grant from the Consiglio Nazionale delle Ricerche.

still present in the syrup is much longer than the relaxation time  $T_{1s}$  of the protons of the polymer already formed. A special technique permitted the two relaxation times  $T_{1l}$  and  $T_{1s}$  to be measured separately; and thus information could be obtained on the mutual interactions among the monomer molecules and polymer molecules present in a partially polymerized sample.

By employing the same technique it should also be possible to obtain information on the process of swelling, in particular when the relaxation of the protons of the swelling agent is due to internal rotations, which are little affected by the presence of the polymer chains. In the present work this possibility is demonstrated, and some results obtained for vinyl polymers swelled by the monomer, by toluene, chloroform, and carbon tetrachloride are presented. The results obtained for the swelling by the monomer are then compared with those obtained during the polymerization process. Finally through the measurement of the relaxation time of the solvent protons in presence of polymer some information on the nature of the motions producing relaxation in such liquids is obtained.

### Experimental

The method of measurement of the relaxation time  $T_{1s}$  of the swelled polymer and the relaxation time  $T_{1l}$  of the swelling agent employs fast adiabatic passages and is analogous to that already described elsewhere.<sup>7</sup> In particular, the measurement of  $T_{1l}$  is accomplished by means of one pair of adiabatic passages through the resonance with the sample initially in thermal equilibrium; the experimental conditions are such that the passages are fast adiabatic for the protons of the swelling liquid, which have a longer relaxation time, while they are slow for the polymer protons, which have a shorter relaxation time. Under such conditions, if the time elapsed between the two passages is  $\tau' = T_{1l} \ln 2$ , then the signal due to the second passage is a pure slow-passage signal. By trial this condition can be found and  $T_{1l}$  easily measured.

The measurement of the relaxation time  $T_{1s}$  is accomplished by means of symmetric sweeps, the period  $\tau$  of which is of the order of  $T_{1s}$  and with such experimental conditions that the passages through the resonance are fast adiabatic for the protons of both the polymer and the swelling agent. In this case the stationary height attained by the nuclear signals is proportional to<sup>8</sup>

$$M_z(\tau) = M_{0s} \frac{1 - \exp \left\{ -\tau/2T_{1s} \right\}}{1 + \exp \left\{ -\tau/2T_{1s} \right\}} + M_{0l} \frac{1 - \exp \left\{ -\tau/2T_{1l} \right\}}{1 + \exp \left\{ -\tau/2T_{1l} \right\}} \quad (1)$$

where  $M_{0s}$  and  $M_{0l}$  are the nuclear magnetization at the thermal equilibrium due to the protons of the polymer and to those of the solvent respectively. If  $T_{1l}/T_{1s}$  is of the order of 100 or larger, the contribution of the protons of the swelling monomer to the signal is then negligible (e.g., for 50% of polymer and 50% of swelling agent and  $T_{1l}/T_{1s} = 100$ , for  $\tau = T_{1s}$  the contribution of the monomer protons to the signal at equilib-

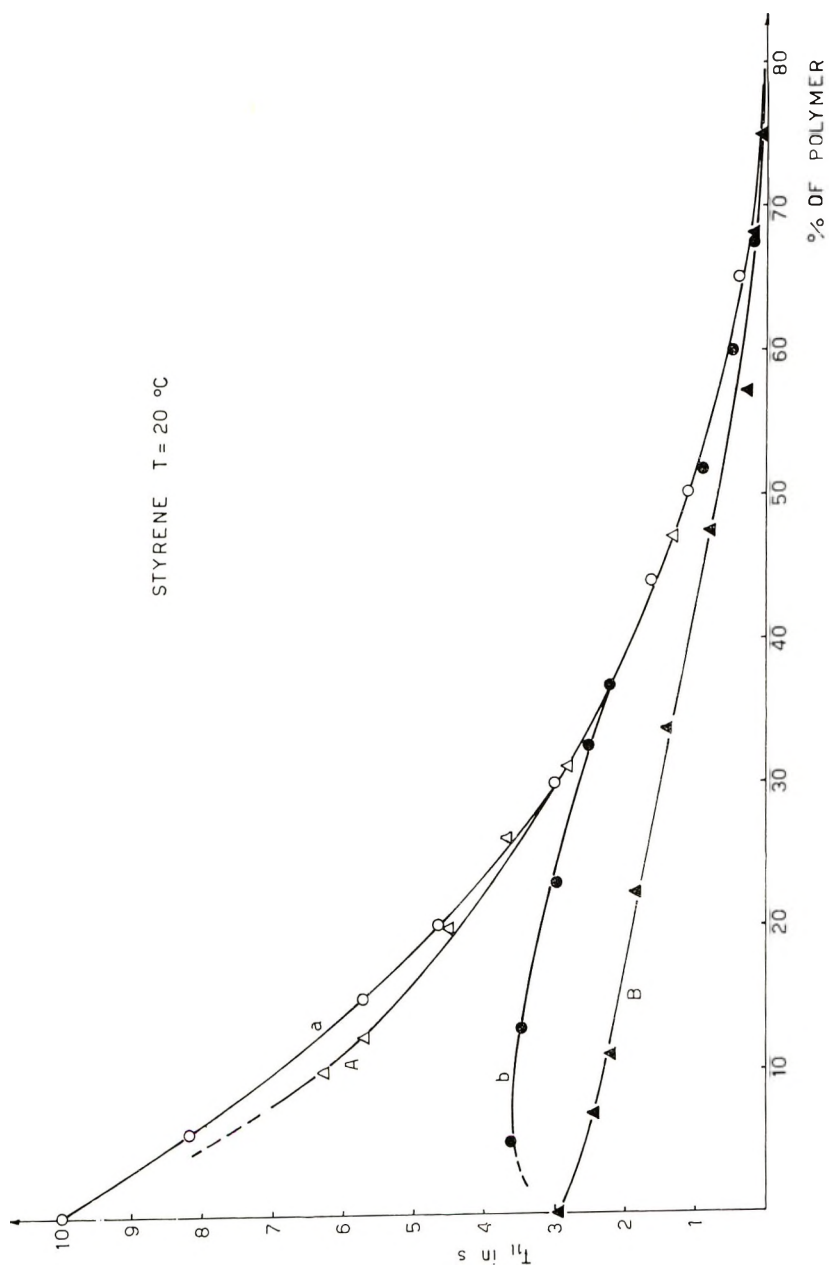


Fig. 1.  $T_{11}$  of styrene during thermal polymerization (a) in *vacuo*, and (b) in presence of atmospheric oxygen; and  $T_{11}$  during swelling of P<sub>1</sub>S (A) in *vacuo*; and (B) in presence of atmospheric oxygen, vs. per cent of polymer.

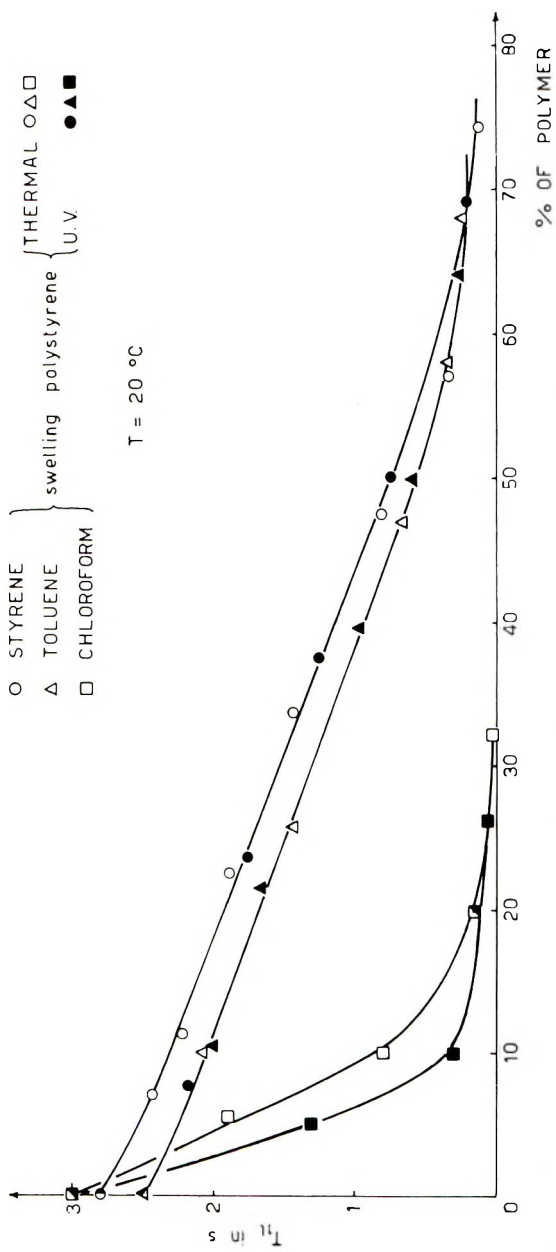


Fig. 2.  $T_{11}$  of styrene, toluene, and chloroform swelling of PS obtained (○, △, □) by thermal polymerization and by (●, ▲, ■) ultraviolet radiation vs. per cent of polymer.

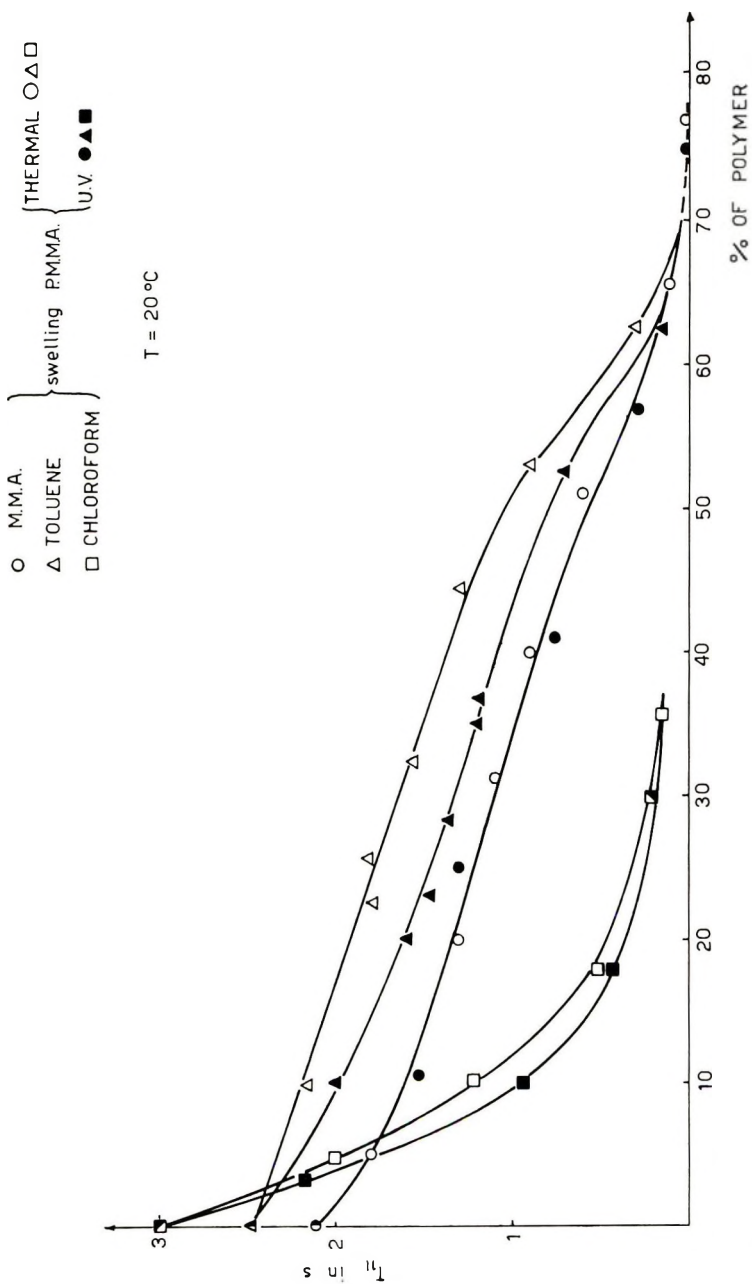


Fig. 3.  $T_{11}$  of meth methacrylate, toluene, and chloroform swelling of PMMA obtained (○, △, □) by thermal polymerization and (●, ▲, ■) by a ultraviolet vs. per cent of polymer.

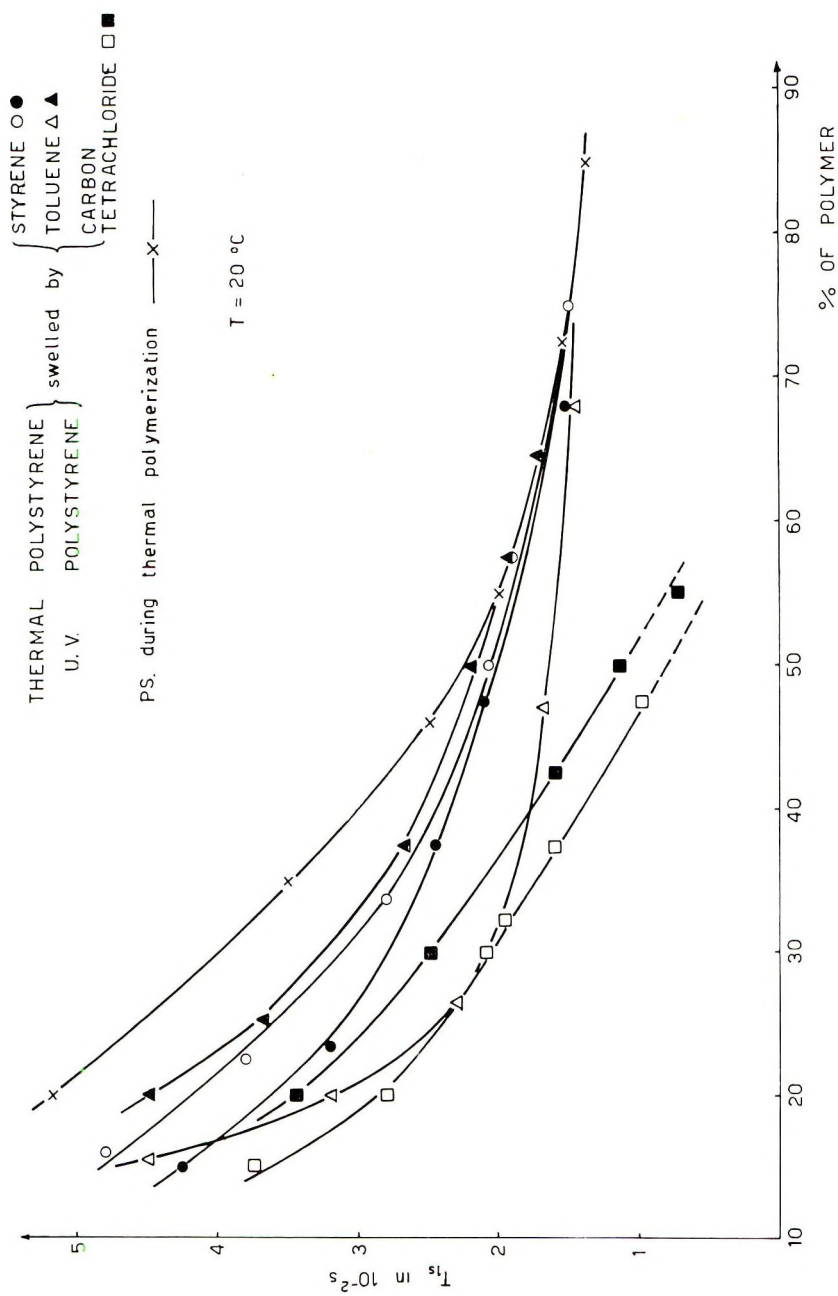


Fig. 4.  $T_{gs}$  of PS (both thermal and ultraviolet-induced polymerization) swelled by (○, ●) styrene, (△, ▲) toluene, and (□, ■) carbon tetrachloride vs. per cent of polymer.

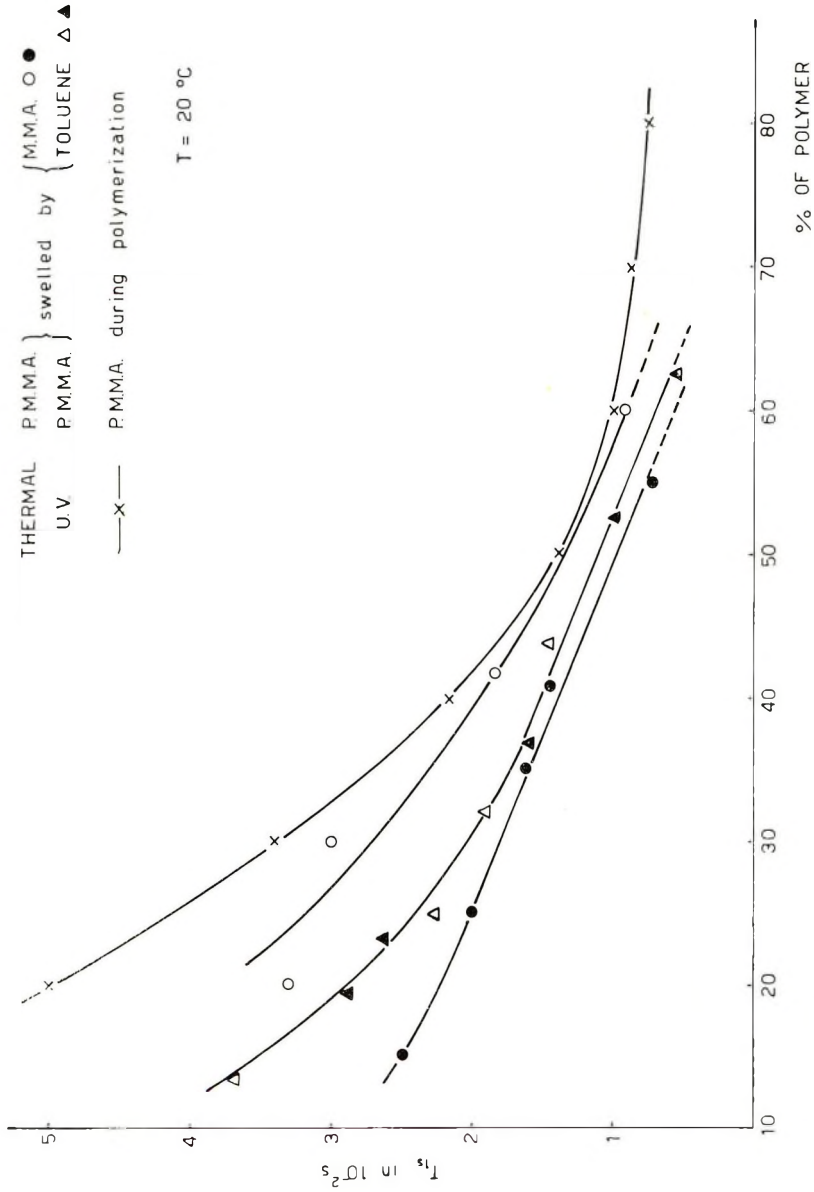


Fig. 5.  $T_{1\rho}$  of P.M.M.A. (both thermal and ultraviolet-induced polymerization) swelled by (O, ●) methyl methacrylate and (Δ, ▲) toluene vs. per cent of polymer.



rium is only 1%). Thus it is possible to evaluate  $T_{1s}$  by comparing the height of the signals which are obtained with two symmetrical sweeps of different frequencies. If  $T_{1l}/T_{1s}$  is of the order of 10 or less, the contribution of the solvent protons to the signal at equilibrium is no longer negligible, and an evaluation of  $T_{1s}$  on the basis of eq. (1) would be hazardous also because the measurement of  $T_{1l}$  is no longer accurate.

## Results

The polymers for which the swelling has been studied are polystyrene (PS) and poly(methyl methacrylate) (PMMA) polymerized both thermally (at 90°C.) and by ultraviolet-ray radiation. The swelling was obtained by absorption of toluene, chloroform, carbon tetrachloride, and the corresponding monomer. The relaxation time  $T_{1s}$  of the swelled polymer, from concentrations of 10–15% of polymer upward, and the relaxation time  $T_{1l}$  of the swelling agent, up to concentrations of about 80% of polymer, were measured with the technique previously discussed.

The relaxation time  $T_{1l}$  of styrene for various concentrations of PS during the polymerization process and for styrene swelling PS is shown in Figure 1. Curves *a* and *A* refer to polymerization and swelling without atmospheric oxygen; curves *b* and *B* refer to polymerization and swelling when atmospheric oxygen is present. Successful swelling of samples free from atmospheric oxygen is difficult to obtain, particularly at low concentration of swelling agent, and the experimental results seem also not to be reproducible with accuracy. Therefore, in general, it has been preferable to perform the swelling in presence of oxygen. The presence of atmospheric oxygen causes a contribution  $1/T_1^*$  to the nuclear magnetic relaxation, which is due to the paramagnetism of molecular oxygen. The spin-lattice relaxation time  $T_{1\text{exp}}$  which we measure is given by

$$1/T_{1\text{exp}} = (1/T_1) + (1/T_1^*)$$

The oxygen has little influence on the relaxation of the protons of the polymer chains because of the relatively short value of  $T_{1s}$ . The effect of the paramagnetism of oxygen is, on the contrary, important on the relaxation of the swelling agent; therefore the  $T_{1l}$  measured when oxygen is present is shorter than the real  $T_{1l}$ , thus accounting for the difference between curves *A* and *B* of Figure 1.

In Figures 2 and 3 the relaxation time  $T_{1l}$  of the swelling liquids is plotted against the concentration of PS and PMMA.

The results for the relaxation time  $T_{1s}$  of the protons of swelled PS and PMMA are shown in Figures 4 and 5. In these figures also the behavior of  $T_{1s}$  for PS and PMMA during polymerization<sup>7</sup> is reported for the sake of comparison.  $T_{1s}$  has been measured also for PS and PMMA swelled by chloroform. Because of the fast decrease of the relaxation time of the solvent causing  $T_{1l}/T_{1s} \simeq 10$  it was not possible to measure  $T_{1s}$  for concentrations of about 30–40%. The results are not shown; they do not show

marked departures from those obtained for the polymer swelled by the monomer itself.

### Discussion and Conclusions

As it is well known, from measurements of nuclear magnetic relaxation it is possible to gain information on the nature and magnitude of molecular motions. The spin-lattice relaxation time  $T_1$  is, in fact, strictly related to the correlation frequencies of the motions.

We consider at first the results obtained in the following conditions: (1) polymer in presence of its monomer during the polymerization process; (2) polymer swelled by the monomer with the same concentration of polymer. For polymer concentrations less than 70%, the relaxation time  $T_{1s}$  of the polymer in condition (2) is shorter than that obtained in condition (1) (see Fig. 4), showing that the polymer chains have greater mobility in condition (1): it may arise from molecular weight differences in some way. The experimental results seem to point out that the mobility of the monomer also is greater in condition (1) than in condition (2) (see Fig. 1, curves *a* and *A*). The difference between the relaxation time of the monomer in conditions (1) and (2) is much more relevant when atmospheric oxygen is present (see Fig. 1, curves *b* and *B*). This is to be attributed to the fact that during the thermal polymerization of styrene the atmospheric oxygen is disappearing from the sample because of oxidation reactions.<sup>9</sup> Moreover, this is substantiated by the fact that the relaxation time  $T_{1t}$  of the monomer (curve *b*, Fig. 1) seems to increase in the first stages of polymerization and, for concentrations of polymer greater than 35%, has the same value as that found for the samples polymerized *in vacuo* (curve *a*, Fig. 1). For concentrations greater than 65% the effects of both oxygen and a possible difference of mobility of the polymer chains are no longer recognizable, and the relaxation time measured for the swelling monomer, both in presence and absence of oxygen, is the same as that measured during the polymerization process.

We consider now the relaxation time  $T_{1s}$  of the swelled polymer. The rather high values of the relaxation time show that the polymer chains have great mobility even for low concentrations of swelling agent. The mobility is influenced by the nature of the swelling agent for low concentration of polymer. For PS swelled by liquids containing protons with polymer concentration greater than 70% the same spin-lattice relaxation time is found for the polymer protons, whatever the swelling agent.

The above independence of the correlation frequency for the hindered motions of the polymer chains from the choice of swelling agent is not found for PMMA; moreover, for this polymer a rather evident decrease of  $T_{1s}$  with respect to the values measured during the polymerization process is apparent. It is noteworthy that with regard to the relaxation of the protons of the swelling agent (Fig. 3) a fast decrease of the relaxation time  $T_{1t}$  seems to take place for concentrations greater than about 55%. This seems to be attributable to the fact that, for high concentrations of PMMA,

the swelling, instead of producing a separation of the polymer chains, brings about the formation of large clusters of macromolecules dispersed in the swelling liquid. This seems further substantiated by the fact that the samples look opalescent. An analogous behavior is offered by PS swelled by  $\text{CCl}_4$  for concentration greater than 60%; in this case, too, the relaxation time of the polymer is less than  $5 \times 10^{-3}$  sec.: at values less than this, accurate measurements with the technique of adiabatic fast passages, which we employ, becomes difficult.

Figures 2-5 reveal differences in the swelling of polymers whether polymerized thermally or by ultraviolet polymerized. Such differences are probably due to a difference in the molecular weight distributions of the macromolecules brought about by the different mechanism of polymerization. In order to obtain even qualitative information a systematic investigation on polymers obtained by different ways would be required, taking into account a possible difference in the degree of polymerization.

Last, we consider the effect of the presence of the polymer chains on the nuclear magnetic relaxation of the swelling agent. As it is seen from Figures 2 and 3, the relaxation time  $T_{1t}$  of toluene swelling of both PS and PMMA decreases slightly with increasing concentration of polymer, the behavior being similar to that of the monomer itself; in the case of chloroform, on the other hand, the decrease of  $T_{1t}$  is much sharper, and for a concentration of about 30% the relaxation time is already less than 0.1 sec. Such a difference between toluene and chloroform may be accounted for by assuming that for the toluene the motions that produce the relaxation are mainly internal rotations of molecular groups; these rotations are little affected by the presence of the polymer chains, which in turn cause the flow viscosity of the syrup to be very high. In chloroform, on the contrary, the absence of internal rotations produces a more marked dependence of  $T_{1t}$  on the polymer concentration. However, even if the real decrease of  $T_{1t}$  with increasing concentration of swelled polymer is much sharper than that shown in Figures 2 and 3 because of the effect of the paramagnetism of the oxygen molecules, it has however been verified that the decrease of  $T_{1t}$  with increasing viscosity of the sample is far from following a law of the form  $T_{1t} \propto K/\eta$ . This is in agreement with what one should expect, because the microviscosity relative to the tumbling and the translation of the molecules of the swelling agent may be much different from the flow viscosity.

The authors wish to thank Professor L. Giulotto for his interest in the work and valuable suggestions.

### References

1. Nolle, A. W., *Phys. Rev.*, **98**, 1560 (1955).
2. Nolle, A. W., *Bull. Am. Phys. Soc.*, **1**, 109 (1956).
3. Powles, J. G., *Arch. Sci. Genève*, **10**, 253 (1957).
4. McCall, P. W., and F. A. Bovey, *J. Polymer Sci.*, **45**, 530 (1960).
5. Kosfeld, R., and E. Jencker, *Z. Elektrochem.*, **63**, 1009 (1959).
6. Borsa, F., and G. Lanzi, *J. Polymer Sci.*, **A2**, 2623 (1964).

7. Bonera, G., P. De Stefano, and A. Rigamonti, *J. Chem. Phys.*, **37**, 1226 (1962).
8. Chiarotti, G., G. Cristiani, L. Giulotto, and G. Lanzi, *Nuovo Cimento*, **12**, 519 (1954).
9. Schildknecht, C. E., *Vinyl and Related Polymers*, Wiley, New York, 1952, p. 18.

### Résumé

Du polystyrène et du polyméthacrylate de méthyle ont été gonflés avec les monomères respectifs et des solvants organiques appropriés. Au moyen d'un assemblage expérimental spécial on a mesuré séparément les temps de relaxation spin-réseau de protons de l'agent de gonflement et ceux du polymère gonflé. Il est apparu des différences entre les temps de relaxation du polymère en cours de la polymérisation et ceux du polymère gonflé par le monomère; cela semble indiquer un degré de mobilité différent dans les chaînes polymériques. On obtient en quelque sorte une indication des différences dans les mouvements que produit la relaxation au départ des différences de comportement observées avec le polymère obtenu par polymérisation thermique et celui du même polymère mais dont la polymérisation est induite par irradiation ultra-violette. Il y a aussi quelques évidences expérimentales qui, au point de vue de l'agent de gonflement, mettent l'accent sur le rôle remarquable tenu par les rotations de groupes moléculaires dans le mécanisme de la relaxation.

### Zusammenfassung

Polystyrol und Polymethylmethacrylat wurde mit den entsprechenden Monomeren und mit geeigneten organischen Lösungsmitteln gequollen. Mit einer speziellen Versuchsanordnung wurde die Spin-Gitter-Relaxationszeit der Protonen des Quellungsmittels und des gequollenen Polymeren getrennt gemessen. Es bestehen Unterschiede zwischen der Spin-Gitter-Relaxationszeit des Polymeren während der Polymerisation und derjenigen des im Monomeren gequollenen Polymeren, was auf einen unterschiedlichen Beweglichkeitsgrad in den Polymerketten hinzuweisen scheint. In einigen Fällen wird ein Hinweis auf Unterschiede in den Bewegungsvorgängen, welche die Relaxation hervorrufen aus den beobachteten Unterschieden im Verhalten eines durch thermische Polymerisation erhaltenen Polymeren und des gleichen, durch ultraviolett-induzierte photochemische Polymerisation entstandenen Polymeren erhalten. Auch in Hinblick auf das Quellungsmittel bestehen gewisse Hinweise auf die bemerkenswerte Rolle, welche die innere Rotation von Molekülgruppen beim Relaxationsmechanismus spielt.

Received July 5, 1963

Revised September 16, 1963

## ERRATUM

### **Some Factors Affecting the Molecular Association of Poly(ethylene Oxide) and Poly(acrylic Acid) in Aqueous Solution**

(article in *J. Polymer Sci.*, **A2**, 845-851, 1964)

By F. E. BAILEY, JR., R. D. LUNDBERG, and R. W. CALLARD  
*Research and Development Department Union Carbide Chemicals Division  
South Charleston, West Virginia*

On p. 847, para. 2, line 12 should read: solution viscosities rather than reduced viscosities.

On p. 848, para. 1, line 2 should read: solution viscosity rather than reduced viscosity.